Natuurkundige Grondslagen van de Sterrenkunde A

An Introduction to Astrophysical (Magneto)hydrodynamics and Plasmas

Prof. Dr. A. Achterberg
Sterrenkundig Instituut, Universiteit Utrecht
and
Center for High Energy Astrophysics, Amsterdam

Revised Version, April 2005

Contents

1 Introduction **9**

1.1 Scope of these lecture notes 11

2 From Newton to Navier-Stokes **13**

2.1 The continuum description 13

2.2 Eulerian and Lagrangian derivatives 15

2.3 Pressure 17

2.4 Pressure and the internal energy of a gas 23

2.5 Gravity and self-gravity 24

2.6 Mass conservation and the continuity equation 26

2.7 The adiabatic gas law 31

2.7.1 The polytropic gas law, the specific heat coefficients and the isothermal gas 32

2.8 The isothermal sphere and globular clusters 37

2.8.1 The tidal radius 43

2.9 Dark matter halos 45

3 Conservative fluid equations and conservation laws **47**

3.1 Introduction 47

3.2 Conservative form of the fluid equations 51

3.2.1 Conservative momentum equation 51

3.2.2 Conservative form of the energy equation 53

4 Steady flows **59**

4.1 Basic equations 59

4.2 Application 1: the Parker model for a stellar wind 64

4.2.1 The critical point condition 68

4.2.2 Isothermal winds . . . 70
4.3 Application 2: Bondi accretion . . . 72
4.3.1 Why accretion? . . . 72
4.3.2 Bondi's solution . . . 75
4.4 Solutions Parker's equation: a graphical representation . . . 78

5 Jet flows **81**
5.1 Introduction . . . 81
5.1.1 A bit of history . . . 82
5.1.2 Superluminal motion . . . 86
5.2 A brief overview of jet sources . . . 89
5.2.1 Young Stellar Objects . . . 89
5.2.2 Microquasars . . . 89
5.2.3 Active galaxies and quasars . . . 94
5.2.4 Unification Models . . . 98
5.3 Equations for jet flow . . . 105
5.4 The Eddington limit: a brief derivation . . . 113

6 Linear waves **117**
6.1 Introduction . . . 117
6.1.1 Perturbation analysis of particle motion in a potential . . . 117
6.2 What constitutes a wave? . . . 121
6.3 The plane wave representation . . . 122
6.4 Lagrangian and Eulerian perturbations . . . 124
6.4.1 Velocity, density and pressure perturbations in a wave . . . 125
6.5 Sound waves . . . 139
6.5.1 Wave kinematics: phase- and group velocity . . . 146
6.6 Sound waves in a moving fluid . . . 150
6.7 Non-planar sound waves . . . 152
6.8 Some astrophysical applications of waves . . . 157
6.8.1 The Jeans instability . . . 157
6.8.2 The zero-frequency mode . . . 161
6.8.3 A simple physical explanation of the Jeans Instability . . . 164
6.8.4 Jeans' instability in an expanding universe . . . 168

6.9 The Jeans Instability in the Zeldovich Approximation . . . 182
6.10 Waves in a stratified atmosphere . . . 193
6.10.1 The Brunt-Väisälä frequency, buoyancy and convection . . . 203

7 Shocks 209
7.1 What are shocks, and why do they occur? . . . 209
7.1.1 Application to sound waves . . . 213
7.2 Plane Shock waves: an introduction . . . 218
7.3 A simple mechanical model: the marble-tube . . . 218
7.4 Shock waves in a simple fluid . . . 222
7.4.1 The Rankine-Hugoniot Relations . . . 229
7.5 The limit of a strong shock . . . 231
7.6 Dissipation in a shock and the entropy jump . . . 234
7.6.1 Shock thickness and the jump conditions . . . 235
7.7 An example: over- and underexpanded Jets . . . 236
7.8 Contact discontinuities . . . 241
7.9 Supernova remnants and stellar wind bubbles . . . 242
7.9.1 Blowing high-pressure bubbles into a uniform medium . . . 242
7.10 Supernova explosions and their remnants . . . 247
7.10.1 The Sedov-Taylor expansion law . . . 251
7.10.2 The pressure-driven and the momentum-conserving snowplow phases 254
7.10.3 Stellar wind bubbles . . . 259
7.10.4 Expansion into a non-uniform medium . . . 262

8 Rotating flows: rotation and vorticity 265
8.1 Introduction . . . 265
8.2 Vorticity . . . 266
8.2.1 Vortex stretching and vortex tubes . . . 269
8.3 Kelvin's circulation theorem . . . 271
8.4 Application to a thin vortex tube . . . 277
8.5 Cylindrical and rotating coordinates . . . 279
8.6 Distance recipe, gradient, rotation and divergence . . . 283
8.6.1 Distance, surface and volume . . . 283
8.6.2 gradient, rotation and divergence . . . 285

8.6.3 The directional derivative . . . 286
8.6.4 Application to cylindrical polar coordinates . . . 288
8.6.5 The acceleration field in polar coordinates . . . 291
8.6.6 Rotating coordinate systems . . . 293
8.6.7 Fluid equations in a rotating frame . . . 296
8.6.8 Planetary vorticity and the thermal wind equation . . . 299
8.6.9 A geophysical application: the global eastward circulation in the Zonal Wind . . . 302
8.7 The Shallow Water Approximation . . . 306
8.7.1 The Shallow Water Equations . . . 311
8.8 Water waves, cyclones and Jupiter's Great Red Spot . . . 317
8.8.1 Shallow water waves . . . 317
8.8.2 Cyclones . . . 319
8.8.3 Jupiter's Great Red Spot . . . 323

9 Theory of diffusion and viscosity 327
9.1 The one-dimensional random walk . . . 327
9.2 The isotropic three-dimensional random walk . . . 332
9.2.1 The diffusion tensor . . . 337
9.3 The diffusion equation . . . 339
9.3.1 Fundamental solutions of the diffusion equation . . . 344
9.3.2 Effects of a mean flow: the advection-diffusion equation . . . 345
9.4 Application I: diffusive radiation transport . . . 348
9.5 Diffusion and viscosity . . . 351
9.5.1 A simple example: shear flow . . . 352
9.5.2 The viscous stress tensor . . . 354
9.5.3 The Reynolds Number . . . 357
9.6 Viscous dissipation . . . 358
9.7 Conservative equations for a viscous fluid . . . 361

10 Axisymmetric, steady flows 363
10.1 Introduction . . . 363
10.2 Equations for a steady, axisymmetric flow . . . 365
10.2.1 Fundamental equations for a steady, axisymmetric flow . . . 368
10.3 An astrophysical example: Accretion Disks . . . 369

10.3.1 Sources powered by disk accretion: X-Ray Binaries and Cataclysmic Variables . . . 370
10.3.2 Modes of disk accretion . . . 373
10.4 Thin, quasi-Keplerian disks . . . 374
10.4.1 Force balance in a geometrically thin disk . . . 375
10.4.2 Mass flow and angular momentum loss . . . 378
10.5 Viscous angular momentum transport . . . 383
10.5.1 Viscous torque from the viscous stress tensor . . . 389
10.6 Angular momentum transport in a thin disk . . . 391
10.7 Disk energy balance . . . 393
10.7.1 The effective temperature of a thin disk . . . 397
10.7.2 The central temperature of the disk material . . . 400
10.7.3 The luminosity of an accretion disk . . . 403
10.8 Alpha-disks . . . 405
10.8.1 Turbulent viscosity and the alpha-parameter . . . 407

11 Fluid Instabilities 413
11.1 The Rayleigh-Taylor Instability . . . 415
11.1.1 A Physical explanation of the RT instability . . . 420
11.1.2 Astrophysical application of the RT instability . . . 422
11.2 The Kelvin-Helmholz instability . . . 422
11.2.1 A physical picture of the KH-instability . . . 427
11.2.2 Astrophysical example of the KH instability . . . 430
11.2.3 The KH instability in a compressible medium . . . 430
11.3 The Kelvin-Helmholz Instability of a cylindrical jet . . . 438
11.3.1 The compressible case . . . 444
11.4 Stability of a self-gravitating disk . . . 448
11.4.1 A steady, axisymmetric thin disk . . . 449
11.4.2 Perturbing a self-gravitating disk . . . 454
11.4.3 The self-gravitating sheet approximation . . . 458
11.4.4 Spiral density waves and the Lindblad Resonances . . . 469
11.5 Couette Flow and the Rayleigh Criterion . . . 478

Chapter 1

Introduction

Almost all matter in the Universe is in the gaseous state. The mean density of our universe corresponds to less than one hydrogen atom per cubic meter, and even the beautifully coloured emission nebulae that grace the pages of many popular astronomy books contain gas with a number density (number of atoms per unit volume) much less than can be achieved by the best vacuum pump on Earth.

The best description available for such tenous matter is one in terms of *fluid dynamics* or *gas dynamics*. The distinction between the two, at least in the context of astrophysics, is rather marginal. Even though most astrophysical applications deal with matter in the gaseous state rather than the fluid state (a notable exception: the superfluid interior of neutron stars), the term *astrophysical fluid dynamics* has stuck.

The common denominator of fluid and gas dynamics is the decription of fluids or gases in terms of a **continuum**, where the properties of the material (density, pressure, temperature etc.) are distributed *smoothly* over space. The continuum approximation neglects the details of the precise distribution of the constituent molecules or atoms and their individual properties, but rather works with an average density, temperature and velocity. The dynamics of the material (the equations of motion) is described in the terms of *fields:* quantities that depend on position and time, and which describe a limited number of properties of the system.

Although phenomenological studies of fluids date back to the well-known drawings of Leonardo Da Vinci of turbulent flows, the mathematical description used even today dates back to the work of Bernouilli and Euler[1]. The first modern textbooks appeared around the beginning of this century, perhaps the most famous one being the monograph by Horace Lamb[2]. Since then, many books on the subject have appreared. The most useful modern introductory text in my view is the one by Faber[3].

[1] *Principes généraux du mouvement des fluids*, Hist. de l'Acad. de Berlin, 1755
[2] Sir Horace Lamb, *Hydrodynamics*, Cambridge University Press, 1879
[3] T.E. Faber: *Fluid Dynamics for Physicists*, Cambridge University Press, 1995

The 'bible' of the subject, originally written in 1959, is still the 6^{th} volume of the well-known *Course of Theoretical Physics* by Russian phycisists Landau and Lifshitz[4].

Fluid dynamics makes full use of the dynamical laws formulated for ordinary mechanics by Newton. This approach is natural but, as we will see, it leads to an immediate complication: the decription in terms of fields yields equations of motion that are *non-linear*. This non-linearity is makes the subject more difficult, but (at least in the view of this author) more rich than ordinary dynamics. Exact solutions are more difficult to obtain than in simple mechanical systems. It therefore comes as no suprise that many approxation methods have been developed in the context of fluid dynamics. An example we will encounter in these lectures is *linearization* where one considers small perturbations on a equilibrium state.

A further complication in astrophysical gases is that a large portion of the tenuous matter between the stars or galaxies is *ionized* gas (HII), consisting (mostly) of protons and free electrons. The free charges in such gases support electromagnetic fields, whose dynamical influence (Coulomb- and Lorentz force) must be taken into account. This is the realm of *Plasma Physics* which, in a simplified description which neglects the rapid phenomena leading to strong electric fields, reduces to *Magnetohydrodynamics*. Good introductory text on these subjects are the books by Sturrock[5], Boyd & Sanderson[6], Goedbloed & Poedts[7], Gurnett & Bhattacharjee[8], Davidson[9], Kulsrud[10] and the (unfortunately out-of-print) text by Roberts[11].

A compromise between the detailed description of each individual particle as practised in Newtonian mechanics, an approach which is clearly impractical here given the huge number of particles involved, and the continuum description of (magneto)hydrodynamics, is *kinetic gas theory* where the motion of a gas is described in *phase-space*, keeping track of both position and velocity (momentum) of a (representative) group of particles using the 'single-particle' equations of motion. This is the point-of-view usually taken in plasma physics, which will also be of use to us when we consider the motion of stars in stellar systems (globular clusters or galaxies).

---

[4] L.D. Landau & E.M. Lifshitz, *Fluid Mechanics*, Pergamon Press, 1959

[5] P.A. Sturrock, *Plasma Physics*, Cambridge University Press, 1994.

[6] T.J.M. Boyd and J.J. Sanderson: *The Physics of Plasmas*, Cambridge University Press, 2003.

[7] H. Goedbloed & S. Poedts, *Principles of Magnetohydrodynamics*, Cambridge University Press, 2004

[8] D.A. Gurnett & A. Bhattacharjee, *Introduction to Plasma Physics with Space and Laboratory Applications*, Cambridge University Press, 2005.

[9] P.A. Davidson, *An Introduction to Magnetohydrodynamics*, Cambridge University Press, 2001.

[10] R.M. Kulsrud, *Plasma Physics for Astrophysics*. Princeton University Press, 2005.

[11] P.H. Roberts: *An Introduction to Magnetohydrodynamics*, Longmans, Green and Co. Ltd, London, 1967.

1.1 Scope of these lecture notes

The aim of these lectures is to develop the understanding of fluids and gases in the context of astrophysics. This means that a number of subjects typically covered in textbooks (engineering applications, incompressible fluids, boundary layers at solid surfaces, aerodynamics, combustion etc.) will not be found here. On the other hand, the theory of *self-gravitating fluids*, and the theory of the interaction of a gas with radiation which are usually neglected in the mainstream of fluid dynamics, will be covered here. Also, since the effects of internal friction (viscosity) in astrophysical fluids is almost always small, our discussion of these effects will be cursory. In addition, we will consider the theory of propagation of 'contaminants' in a fluid, a subject also of interests to geophysicists.

A notable exception to this difference in emphasis between mainstream hydrodynamics books and the more astrophysically oriented literature is the book by noted astrophysicist Frank Shu[12]. Shu's book covers most of the subjects treated in these notes, albeit at a somewhat lower level of exposition. A recent and very useful addition to the astrophysically oriented literature on the subject is the book by Michael Thomson[13]. This book covers much the same ground as these Lecture Notes, at a slighly more basic level.

We will also give a 'preview' of the effects of relativity which become important at velocities close to the speed of light and in strong gravitational fields: relativistic fluid dynamics.

The principles will be applied to astrophysical systems, such as:

- Magnetic structures on the Sun;
- Solar and Stellar Winds;
- Cosmic Rays;
- Accretion disks in X-ray binaries and Active Galactic Nuclei (AGNs);
- Stellar convection and stability
- Jets in Proto-stars, Active Galaxies and Quasars;
- Cosmic Rays and the Interstellar Medium;
- Supernova explosions and Gamma Ray Bursts;
- Thermodynamics and orbit theory of galaxies and globular clusters

My hope is that, at the end of this course, you will have gained sufficient understanding of the subject to move on to the 'real' stuff: the modern research literature.

[12] F.H. Shu, *The Physics of Astrophysics*, Vol. II: Gas Dynamics, University Science Books, 1992

[13] M.J. Thomson, *An Introduction to Astrophysical Fluid Dynamics*, Imperial College Press, London, 2006

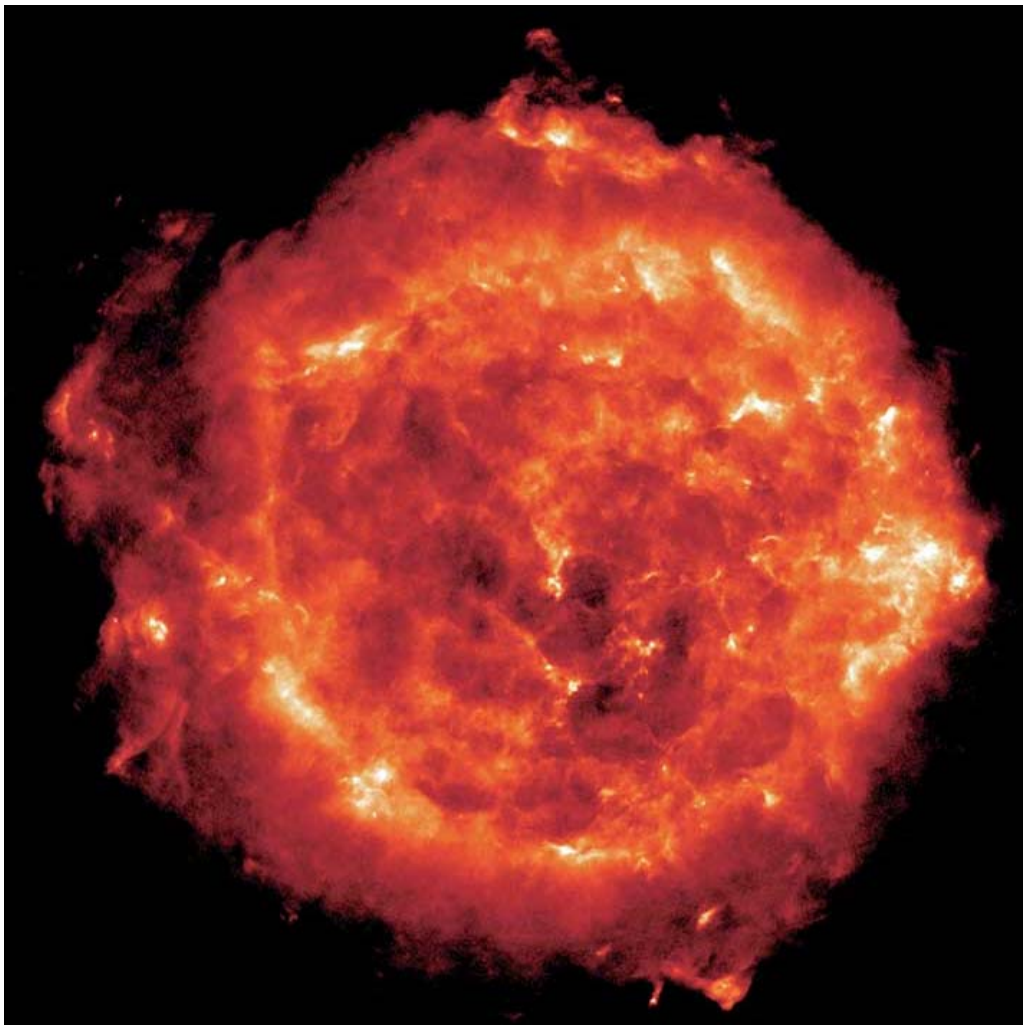

Figure 1.1: *The supernova remnant Cassiopeia A as seen with the Very Large Array radio observatory in the United States. This is a cloud of expanding hot gas several hundred light years across. Remnants like these are born when the core of a massive star runs out of nuclear fuel, and collapses under its own weight: a Type II supernova. Perhaps paradoxally at first sight, this implosion is followed by an explosion in which the star expells its outer layers. The expelled stellar material sweeps up interstellar gas, and forms a supernova remnant. The observed radio emission is synchrotron radiation of relativistic (typical energy: 1 GeV) electrons in a weak ($B \sim 10^{-6} - 10^{-5}$ G) magnetic field.*

Chapter 2

From Newton to Navier-Stokes

2.1 The continuum description

In ordinary dynamics, as 'invented' by Isaac Newton, the motion of a single particle of mass m under the influence of some force $\boldsymbol{F}$ is described by the simple equation of motion, linking the acceleration $\boldsymbol{a} = \mathrm{d}\boldsymbol{V}/\mathrm{d}t$ to the force:

$$m\,\frac{\mathrm{d}\boldsymbol{V}}{\mathrm{d}t} = \boldsymbol{F}\ . \tag{2.1.1}$$

A fluid (or gas) consists in principle of a large number of particles (ions, atoms or molecules), each of which satisfies an equation like (2.1.1). However, the expression for the force $\boldsymbol{F}$ is horribly complicated since it has to take account of all the interactions between the individual particles. Consider for instance a gas of identical particles with mass m which interact through mutual forces, such as the gravitational interaction or the Coulomb force between charged particles If we were to number the particles with some index α, the equation of motion of the α-th particle would look something like

$$m\,\frac{\mathrm{d}\boldsymbol{V}_\alpha}{\mathrm{d}t} = \sum_{\alpha\neq\beta} \boldsymbol{F}_{\alpha\beta}\ . \tag{2.1.2}$$

Here $\boldsymbol{F}_{\alpha\beta}$ is the force on particle α excerted by particle β. For instance, in a gas of electrons with mass m_e and charge $-e$ the electron-electron force would be the repulsive electrostatic Coulomb force:

$$\boldsymbol{F}_{\alpha\beta} = \frac{e^2\,(\boldsymbol{x}_\alpha - \boldsymbol{x}_\beta)}{|\boldsymbol{x}_\alpha - \boldsymbol{x}_\beta|^3}\ . \tag{2.1.3}$$

Taking the plasma in the Solar Corona as an example: one cubic centimeter of gas contains about 10^6 electrons. This means that one would have to calculate $\sim 10^{12}$ interactions to describe the dynamics of these electrons, clearly an impractical approach.

The power of the fluid description is that it dispenses with a detailed consideration of the constituent individual particles in some volume $\mathcal{V}$, and replaces the point particles by a smeared-out distribution of mass. To that end one introduces a mass density ρ, defined as:

$$\rho(\boldsymbol{x}\ ,\ t) = \frac{\text{total mass in small volume}}{\text{volume}} = \lim_{\Delta\mathcal{V}\to 0} \frac{\Delta m}{\Delta\mathcal{V}}\ , \tag{2.1.4}$$

and an average velocity which is essentially the center-of-mass velocity of the collection of particles residing inside the small volume $\Delta\mathcal{V}$:

$$\boldsymbol{V}(\boldsymbol{x}\ ,\ t) = \frac{1}{\Delta m} \sum_{\Delta\mathcal{V}} m_\alpha \boldsymbol{v}_\alpha\ . \tag{2.1.5}$$

Here $\Delta m = \sum_{\Delta\mathcal{V}} m_\alpha$ is the total mass of the particles in the volume-element $\Delta\mathcal{V}$ and $\boldsymbol{v}_\alpha$ is the velocity of particle α.

This *continuum description* of a fluid leads to an equation analogous to (2.1.1). For a fluid with mass*density* ρ, subject to forces with a force*density* (the net force per unit volume) $\boldsymbol{f}$, the equation of motion reads

$$\rho\, \frac{\mathrm{d}\boldsymbol{V}}{\mathrm{d}t} = \boldsymbol{f}\ . \tag{2.1.6}$$

This deceivingly simple-looking equation of motion hides two difficulties. The obvious difficulty is the definition of the precise form of the force density $\boldsymbol{f}$. We will consider that question in more detail below. The less obvious (but mathematically rather more intricate) problem is the correct interpretation of the time-derivative $\mathrm{d}/\mathrm{d}t$.

In Newtonian dynamics this problem never explicitly arises: there it is obvious that one has to calculate the time-derivative $\mathrm{d}\boldsymbol{V}/\mathrm{d}t$ and the force $\boldsymbol{F}$ in the equation of motion (2.1.1) while following the particle along its orbit. We will show that this interpretation still holds in fluid mechanics, but that the fact that we are dealing with a continuum rather than a single particle complicates things. This complication stems from the fact that the velocity $\boldsymbol{V}$ also has to be interpreted as a *distribution* of velocities over space: a *velocity field*, which changes with time.

$$\boldsymbol{V}(\boldsymbol{x}\ ,\ t) = (V_x\ ,\ V_y\ ,\ V_z) = V_x\, \hat{\boldsymbol{x}} + V_y\, \hat{\boldsymbol{y}} + V_z\, \hat{\boldsymbol{z}}\ . \tag{2.1.7}$$

The magnitude and direction of the vector $\boldsymbol{V}$ is determined by the three functions $V_x(\boldsymbol{x}\,,\,t)$, $V_y(\boldsymbol{x}\,,\,t)$ and $V_z(\boldsymbol{x}\,,\,t)$, which are the three components of the velocity vector at each point in space-time in cartesian (rectangular) coordinate system with unit vectors $\hat{\boldsymbol{x}}$, $\hat{\boldsymbol{y}}$ and $\hat{\boldsymbol{z}}$.

The velocity $\boldsymbol{V}$ is the *local average* over some small volume of the velocities of the constituent particles at position $\boldsymbol{x}$ and point in time t, c.f. Eqn. (2.1.5). The velocity of any individual particles is never precisely the average velocity. As we will see below, the influence of the deviations from that average (the so-called *velocity dispersion* of the particles) is taken into account by introducing the *fluid pressure* and the associated pressure force.

2.2 Eulerian and Lagrangian derivatives

Let us consider the precise interpretation of the time derivative $\mathrm{d}/\mathrm{d}t$. As already discussed above, the interpretation of the time derivative $\mathrm{d}/\mathrm{d}t$ is obvious in Newtonian mechanics: it is the change in time, as measured by an observer moving with the particle along its orbit. The same interpretation should hold for the time-derivative $\mathrm{d}/\mathrm{d}t$ in fluid mechanics. It is the time derivative seen by an observer moving along with the flow. Therefore, $\mathrm{d}/\mathrm{d}t$ is often called the *co-moving* or *Lagrangian* time-derivative.

This is *not* the only time-derivative one can think of in a fluid description where all physical quantities are *fields* that depend on both $\boldsymbol{x}$ and t. Let us assume that some quantity $Q(\boldsymbol{x}\,,\,t)$ is measured by two observers. One observer is at some fixed position $\boldsymbol{x}$ in space, while the second observer moves with the fluid at a (variable) velocity $\boldsymbol{V}(\boldsymbol{x},t)$. We calculate the change in Q as seen by both observers in a small time interval Δt. The first (stationary) observer measures a change

$$\begin{aligned} \delta Q &= Q(t+\Delta t\,,\,\boldsymbol{x}) - Q(t\,,\,\boldsymbol{x}) \\ &\approx \left(\frac{\partial Q}{\partial t}\right)\,\Delta t\,, \end{aligned} \tag{2.2.1}$$

assuming $\Delta t \ll t$. The change seen by the second (co-moving) observer in the same time interval is influenced by his change in position, which amounts to

$$\Delta\boldsymbol{x} = \boldsymbol{V}\,\Delta t = (V_x\,\Delta t\,,\,V_y\,\Delta t\,,\,V_z\,\Delta t) \tag{2.2.2}$$

during the time interval Δt.

The observer moving with the fluid therefore measures a change in Q equal to:

$$\begin{aligned} \Delta Q &= Q(t+\Delta t\ ,\ \boldsymbol{x}+\Delta\boldsymbol{x}) - Q(t\ ,\ \boldsymbol{x}) \\ &\approx \frac{\partial Q}{\partial t}\,\Delta t + (\Delta\boldsymbol{x}\cdot\boldsymbol{\nabla})Q \\ &= \left[\frac{\partial Q}{\partial t} + (\boldsymbol{V}\cdot\boldsymbol{\nabla})Q\right]\Delta t \\ &\equiv \left(\frac{\mathrm{d}Q}{\mathrm{d}t}\right)\,\Delta t\ . \end{aligned} \tag{2.2.3}$$

Here $\boldsymbol{\nabla} = (\partial/\partial x\ ,\ \partial/\partial y\ ,\ \partial/\partial z)$ is the gradient operator, and the short-hand notation

$$\boldsymbol{V}\cdot\boldsymbol{\nabla} \equiv V_x\frac{\partial}{\partial x} + V_y\frac{\partial}{\partial y} + V_z\frac{\partial}{\partial z}\ , \tag{2.2.4}$$

valid in cartesian coordinates, has been used.

This derivation shows that the *Eulerian* time derivative $\partial/\partial t$, as measured by the first observer at a fixed position, and the comoving (or *Lagrangian*) time derivative, as measured by the second observer moving with velocity $\boldsymbol{V}$, are related by:

$$\boxed{\frac{\mathrm{d}}{\mathrm{d}t} = \frac{\partial}{\partial t} + (\boldsymbol{V}\cdot\boldsymbol{\nabla})\ .} \tag{2.2.5}$$

This means that the equation of motion for a fluid, which involves the total time derivative, can also be written as:

$$\rho\left[\frac{\partial\boldsymbol{V}}{\partial t} + (\boldsymbol{V}\cdot\boldsymbol{\nabla})\,\boldsymbol{V}\right] = \boldsymbol{f} \tag{2.2.6}$$

This form of the equation of motion for a fluid explicitly shows the reason why fluid dynamics is so much more difficult than the Newtonian dynamics of a single particle.

The term $(\boldsymbol{V}\cdot\boldsymbol{\nabla})\boldsymbol{V}$ introduces a non-linearity into the equation of motion. This is the price one has to pay for having to deal with a velocity*field*.

By combining relations 2.2.1 and 2.2.3 one can also see that the Eulerian change δQ at a fixed position, and the Lagrangian change ΔQ of some quantity Q given a position shift $\Delta\boldsymbol{x}$, are related by:

$$\boxed{\Delta Q = \delta Q + (\Delta\boldsymbol{x}\cdot\boldsymbol{\nabla})\,Q\ .} \tag{2.2.7}$$

This relation is valid for small $\Delta\boldsymbol{x}$ regardless the precise nature of Q (scalar function, vector, tensor, $\cdots$).

2.3 Pressure

The precise form of the force density $\boldsymbol{f}$ of course depends on the circumstances. Generally speaking, it consists of contributions that are *internal* to the fluid, such as the pressure force or the force due to internal friction, and forces that are applied by external sources, for example the gravitational pull of a star (or the Earth) on its outer atmosphere.

The most important internal force density of a gas or fluid is the pressure force[1]. The pressure force takes account of the spread of velocities of the constituent particles around the mean velocity $\boldsymbol{V}$. This velocity spread means that the exact momentum of an individual particle, and the mean momentum of the fluid differ. This momentum difference leads ultimately to a force. The spread in velocities is due to the thermal motion of the particles. The precise derivation of fluid pressure in terms of the microscopic physics of the constituent particles will have to wait until we discuss kinetic gas theory. However it is possible to give an approximate derivation of the pressure force which gives some insight into its nature.

Consider a collection of particles of identical mass m in some local volume $\mathcal{V}$. The individual velocity of particle α[2] is given by

$$\boldsymbol{v}_\alpha = \boldsymbol{V}(\boldsymbol{x}\ ,\ t) + \boldsymbol{\sigma}_\alpha(\boldsymbol{x}\ ,\ t)\ . \tag{2.3.1}$$

Here the velocity has been written as the sum of the *mean* velocity $\boldsymbol{V}$ of the whole set of particles, and the deviation $\boldsymbol{\sigma}_\alpha$ from the mean of particle α. If there are in total N particles in the volume this definition implies, using a notation $\overline{\cdots}$ for the average,

[1] I will follow the general convention to speak of 'forces' even though, technically speaking, one should speak of force densities.

[2] Greek indices are used to distinguish particles

$$\overline{\boldsymbol{v}} \equiv \frac{1}{N} \sum_{\alpha=1}^{N} \boldsymbol{v}_\alpha = \boldsymbol{V}(\boldsymbol{x}\ ,\ t) \tag{2.3.2}$$

and

$$\overline{\boldsymbol{\sigma}} = \overline{\boldsymbol{v}} - \boldsymbol{V} = \boldsymbol{0}\ . \tag{2.3.3}$$

Here I have used that $\boldsymbol{V}$ already is an average, and must therefore satisfy $\overline{\boldsymbol{V}} = \boldsymbol{V}$. Let us write down the equation of motion of each particle. We do this in the 'fluid mechanics' form:

$$m\,\frac{\mathrm{d}\boldsymbol{u}_\alpha}{\mathrm{d}t} = m\,\left[\frac{\partial \boldsymbol{u}_\alpha}{\partial t} + (\boldsymbol{u}_\alpha \cdot \boldsymbol{\nabla})\boldsymbol{u}_\alpha\right] = \boldsymbol{F}_\alpha \tag{2.3.4}$$

Substituting Eqn. (2.3.1) for $\boldsymbol{u}_\alpha$ and summing over all N particles, using the above definition (2.3.2) for the average, yields an average equation of motion:

$$Nm\,\left[\frac{\partial \boldsymbol{V}}{\partial t} + (\boldsymbol{V}\cdot\boldsymbol{\nabla})\,\boldsymbol{V} + \overline{(\boldsymbol{\sigma}\cdot\boldsymbol{\nabla})\boldsymbol{\sigma}}\right] = N\overline{\boldsymbol{F}}\ . \tag{2.3.5}$$

One sees that the only term involving the deviations from the mean velocity that survives this averaging procedure is a term that is *quadratic* in $\boldsymbol{\sigma}$:

$$Nm\,\overline{(\boldsymbol{\sigma}\cdot\boldsymbol{\nabla})\boldsymbol{\sigma}}\ . \tag{2.3.6}$$

This term will in general *not* vanish. All terms that are linear in $\boldsymbol{\sigma}$ are averaged out because of (2.3.3). This procedure assumes implicitly that the averaging process is not influenced by the action of time- and space derivatives.

The mean number density (number of particles per unit volume) equals $n = N/\mathcal{V}$, while the external (mean) force density is $\boldsymbol{f}_{\rm ext} = N\overline{\boldsymbol{F}}/\mathcal{V}$. Dividing (2.3.5) by $\mathcal{V}$ and re-ordering terms one can write:

$$\rho\,\left[\frac{\partial \boldsymbol{V}}{\partial t} + (\boldsymbol{V}\cdot\boldsymbol{\nabla})\,\boldsymbol{V}\right] = -\rho\,\overline{(\boldsymbol{\sigma}\cdot\boldsymbol{\nabla})\boldsymbol{\sigma}}\ +\ \boldsymbol{f}_{\rm ext}\ , \tag{2.3.7}$$

with $\rho \equiv nm$ the mass density.

We now use a result from tensor analysis[3]. Consider the *dyadic tensor*, which is obtained from the *direct product* of two vectors $\boldsymbol{A}$ and $\boldsymbol{B}$:

$$\boldsymbol{A} \otimes \boldsymbol{B} \equiv A_i B_j \, \boldsymbol{e}_i \otimes \boldsymbol{e}_j \; . \tag{2.3.8}$$

The $\boldsymbol{e}_i$ with $i = 1 \, , \, 2 \, , \, 3$ are the three unit vectors employed in the coordinate system. For instance, in a standard cartesian coordinate system one has $\boldsymbol{e}_1 \equiv \hat{\boldsymbol{x}} = (1 \, , \, 0 \, , \, 0)$, $\boldsymbol{e}_2 \equiv \hat{\boldsymbol{y}} = (0 \, , \, 1 \, , \, 0)$ and $\boldsymbol{e}_3 \equiv \hat{\boldsymbol{z}} = (0 \, , \, 0 \, , \, 1)$. A vector $\boldsymbol{A}$ can be represented as a column vector,

$$\boldsymbol{A} = A_x \, \hat{\boldsymbol{x}} + A_y \hat{\boldsymbol{y}} + A_z \, \hat{\boldsymbol{z}} = \begin{pmatrix} A_x \\ \\ A_y \\ \\ A_z \end{pmatrix} \; ,$$

and the direct procuct $\boldsymbol{M} \equiv \boldsymbol{A} \otimes \boldsymbol{B}$ as a 3×3 matrix with components $M_{ij} = A_i B_j$:

$$\boldsymbol{A} \otimes \boldsymbol{B} = \begin{pmatrix} A_x B_x & A_x B_y & A_x B_z \\ \\ A_y B_x & A_y B_y & A_y B_z \\ \\ A_z B_x & A_z B_y & A_z B_z \end{pmatrix} \; .$$

In (2.3.8) we employ the *Einstein summation convention* where one sums over all *repeated* indices, in this case over $i = 1, 2, 3$ and $j = 1, 2, 3$. One can show that the following relation holds generally if one takes the *divergence* of such a dyadic tensor, This mathematical operation yields a *vector* in a manner that, for now, may be employed as recipe:

$$\boldsymbol{\nabla} \cdot \, (\boldsymbol{A} \otimes \boldsymbol{B}) = (\boldsymbol{\nabla} \cdot \boldsymbol{A}) \; \boldsymbol{B} + (\boldsymbol{A} \cdot \boldsymbol{\nabla}) \, \boldsymbol{B} \; . \tag{2.3.9}$$

Here

$$\boldsymbol{\nabla} \cdot \boldsymbol{A} = \frac{\partial A_x}{\partial x} + \frac{\partial A_y}{\partial y} + \frac{\partial A_z}{\partial z} \tag{2.3.10}$$

is the divergence of the vector $\boldsymbol{A}$.

[3]For a good introduction see: G.B. Arfken & H.J. Weber, *Mathematical Methods for Physicists*, 4^{th} Edition, Academic Press, 1995, Chapters 1 and 2
Additional information is available in the Mathematical Appendix on Internet

The operator $(\boldsymbol{A}\cdot\boldsymbol{\nabla})\,\boldsymbol{B}$ is defined as[4].

$$(\boldsymbol{A}\cdot\boldsymbol{\nabla})\,\boldsymbol{B}=\left(A_x\frac{\partial}{\partial x}+A_y\frac{\partial}{\partial y}+A_z\frac{\partial}{\partial z}\right)\boldsymbol{B}\ . \tag{2.3.11}$$

This allows us to write:

$$(\rho\,\boldsymbol{\sigma}\cdot\boldsymbol{\nabla})\boldsymbol{\sigma}=\boldsymbol{\nabla}\cdot\,(\rho\,\boldsymbol{\sigma}\otimes\boldsymbol{\sigma})-(\boldsymbol{\nabla}\cdot(\rho\boldsymbol{\sigma}))\ \boldsymbol{\sigma}\ . \tag{2.3.12}$$

If the detailed microscopic physics is in equilibrium, and if there is no preferred direction so that the fluid is *isotropic*, the second term must vanish upon averaging as $\boldsymbol{\nabla}\cdot\boldsymbol{\sigma}$ is a scalar (not influenced by rotations) but $\boldsymbol{\sigma}$ is a vector. For a gas or fluid where the molecular velocities are distributed isotropically we must therefore have:

$$\rho\,\overline{(\boldsymbol{\sigma}\cdot\boldsymbol{\nabla})\boldsymbol{\sigma}}=\boldsymbol{\nabla}\cdot\,(\rho\,\overline{\boldsymbol{\sigma}\otimes\boldsymbol{\sigma}})\ .$$

The assumption of isotropy also implies that the following relations must be valid:

$$\overline{\sigma_x^2}=\overline{\sigma_y^2}=\overline{\sigma_z^2}=\tfrac{1}{3}\overline{\sigma^2}\ , \tag{2.3.13}$$

and

$$\overline{\sigma_x\sigma_y}=\overline{\sigma_x\sigma_z}=\overline{\sigma_y\sigma_z}=\cdots=0\ . \tag{2.3.14}$$

The first relationship says that all three coordinate directions on average contribute equally to $\sigma^2=\sigma_x^2+\sigma_y^2+\sigma_z^2$. The second relation follows from the fact that products like $\sigma_x\sigma_y$ change if one rotates the coordinate system, but that such a rotation can have no effect if the *physics* is isotropic. This is only possible if all these cross-terms vanish identically.

To see this explicitly how this comes about, consider a rotation of the coordinate system in the $x-y$ plane over an angle θ. The new unit vectors are

$$\hat{\boldsymbol{e}}_1=\cos\theta\,\hat{\boldsymbol{x}}+\sin\theta\,\hat{\boldsymbol{y}}\ \ ,\ \ \hat{\boldsymbol{e}}_2=-\sin\theta\,\hat{\boldsymbol{x}}+\cos\theta\,\hat{\boldsymbol{y}}\ \ ,\ \ \hat{\boldsymbol{e}}_3=\hat{\boldsymbol{z}}\ . \tag{2.3.15}$$

[4]These last two definitions are *only* valid in cartesian (rectangular) coordinates. More detailed expressions, valid for general (curvilinear) coordinate systems, can be found in the Mathematical Appendix available on Internet.

The new components of any vector $\boldsymbol{A}$ follow from the projection of that vector on the unit vectors, which can be expressed as a scalar product:

$$A_i = \boldsymbol{A} \cdot \hat{\boldsymbol{e}}_i \ . \tag{2.3.16}$$

Using (2.3.15) one calculates the velocity components in the rotated coordinate system:

$$\sigma_1 = \sigma_x \ \cos\theta + \sigma_y \ \sin\theta \quad , \quad \sigma_2 = -\sigma_x \sin\theta + \sigma_y \ \cos\theta \ . \tag{2.3.17}$$

From this one immediately finds:

$$\begin{aligned} \sigma_1^2 &= \sigma_x^2 \cos^2\theta + \sigma_y^2 \ \sin^2\theta + 2\sigma_x\sigma_y \ \cos\theta\sin\theta \ . \\ \sigma_2^2 &= \sigma_x^2 \sin^2\theta + \sigma_y^2 \ \cos^2\theta \ - 2\sigma_x\sigma_y \ \cos\theta\sin\theta, \\ \sigma_1\sigma_2 &= \left(\sigma_y^2 - \sigma_x^2\right) \ \sin\theta\cos\theta + \sigma_x\sigma_y \ \left(\cos^2\theta - \sin^2\theta\right) \ . \end{aligned} \tag{2.3.18}$$

If one now averages over the isotropic velocity distribution one should find that the averages do not change. To an observer rotating with the coordinate system the gas has rotated over an angle $-\theta$. However, an isotropic velocity distribution has (by definition) the same statistical properties when rotated over *any angle*, and should there have the same statistics regardless the value of θ. This means that one must have:

$$\begin{aligned} \overline{\sigma_1^2} = \overline{\sigma_2^2} &= \overline{\sigma_x^2} = \overline{\sigma_y^2} \ , \\ \overline{\sigma_1\sigma_2} &= \overline{\sigma_x\sigma_y} \ . \end{aligned} \tag{2.3.19}$$

With $\overline{\sigma_x^2} = \overline{\sigma_y^2} = \overline{\sigma^2}/3$ one immediately finds that $\overline{\sigma_1^2} = \overline{\sigma_2^2} = \overline{\sigma^2}/3$, for any θ, *provided* that the cross term satisfies $\overline{\sigma_x\sigma_y} = 0$, simply because $\sin^2\theta + \cos^2\theta = 1$. In that case one also immediately finds $\overline{\sigma_1\sigma_2} = \overline{\sigma_x\sigma_y} = 0$. The set of rules (2.3.13) and (2.3.14) is the only set of rules that is consistent with an isotropic distribution of thermal velocities.

These two sets of relations, (2.3.13) and (2.3.14), can be summarized in a single equation, using the *Kronecker symbol* δ_{ij}, which has the properties $\delta_{ij} = 1$ when $i = j$ and $\delta_{ij} = 0$ when $i \neq j$:

$$\overline{\sigma_i\sigma_j} = \tfrac{1}{3} \, \overline{\sigma^2} \, \delta_{ij} \ . \tag{2.3.20}$$

Using the above representation of a dyadic tensor together with (2.3.20), this means that one can write

$$\rho\,\overline{\boldsymbol{\sigma}\otimes\boldsymbol{\sigma}} = \rho \begin{pmatrix} \frac{1}{3}\overline{\sigma^2} & 0 & 0 \\ 0 & \frac{1}{3}\overline{\sigma^2} & 0 \\ 0 & 0 & \frac{1}{3}\overline{\sigma^2} \end{pmatrix} = \frac{\rho\overline{\sigma^2}}{3}\,\boldsymbol{I}\;, \tag{2.3.21}$$

with $\boldsymbol{I} = \mathrm{diag}(1,1,1)$ the 3×3 unit tensor which has components $I_{ij} = \delta_{ij}$. Defining the *scalar pressure* P as

$$P = \tfrac{1}{3}nm\,\overline{\sigma^2} = \tfrac{1}{3}\rho\,\overline{\sigma^2}\;, \tag{2.3.22}$$

one can write

$$\rho\,\overline{(\boldsymbol{\sigma}\cdot\boldsymbol{\nabla})\boldsymbol{\sigma}} = \boldsymbol{\nabla}\cdot\,(\rho\,\overline{\boldsymbol{\sigma}\otimes\boldsymbol{\sigma}}) = \boldsymbol{\nabla}\cdot\,(P\,\boldsymbol{I})\;. \tag{2.3.23}$$

The definition, valid in cartesian coordinates, for the divergence of a rank 2 tensor $\boldsymbol{T}$ (i.e. a 3×3 matrix with components T_{ij}) can be represented by the column vector with components

$$\boldsymbol{\nabla}\cdot\boldsymbol{T} = \begin{pmatrix} \dfrac{\partial T_{xx}}{\partial x} + \dfrac{\partial T_{yx}}{\partial y} + \dfrac{\partial T_{zx}}{\partial z} \\ \dfrac{\partial T_{xy}}{\partial x} + \dfrac{\partial T_{yy}}{\partial y} + \dfrac{\partial T_{zy}}{\partial z} \\ \dfrac{\partial T_{xz}}{\partial x} + \dfrac{\partial T_{yz}}{\partial y} + \dfrac{\partial T_{zz}}{\partial z} \end{pmatrix}\;. \tag{2.3.24}$$

If one substitutes expression (2.3.21) written in the form

$$\rho\,\overline{\sigma_i\sigma_j} \equiv P_{ij} = P\,\delta_{ij} \tag{2.3.25}$$

into this definition one finds:

$$\boldsymbol{\nabla} \cdot (P\,\boldsymbol{I}) = \begin{pmatrix} \dfrac{\partial P}{\partial x} \\ \dfrac{\partial P}{\partial y} \\ \dfrac{\partial P}{\partial z} \end{pmatrix} = \boldsymbol{\nabla} P \ . \tag{2.3.26}$$

This means that the equation of motion (2.3.7) for a frictionless fluid or gas can be written as

$$\rho \left[\frac{\partial \boldsymbol{V}}{\partial t} + (\boldsymbol{V} \cdot \boldsymbol{\nabla})\, \boldsymbol{V} \right] = -\boldsymbol{\nabla} P + \boldsymbol{f}_{\rm ext} \ . \tag{2.3.27}$$

Here $\boldsymbol{f}_{\rm ext}$ is the force density applied externally to the fluid. Friction (called viscosity in fluid dynamics) will be treated later.

2.4 Pressure and the internal energy of a gas

The thermal motion of the particles, which is the source of the velocity dispersion around the mean velocity $\boldsymbol{V}$, leads to a force proportional to the gradient in the pressure P. The minus sign in this pressure force $-\boldsymbol{\nabla} P$ can be understood intuitively: material tends to move away from a region of high pressure, or into a region of low pressure as any meteorologist will tell you.

Thermodynamics[5] tells us that the energy of a system in thermal equilibrium at temperature T is $\frac{1}{2} k_{\rm b} T$ per degree of freedom, with $k_{\rm b}$ Boltzmann's constant. In the case of an isotropic gas in three dimensions, consisting of point particles with no *internal* degrees of freedom, this means

$$\tfrac{1}{2} m \overline{\sigma_x^2} = \tfrac{1}{2} m \overline{\sigma_y^2} = \tfrac{1}{2} m \overline{\sigma_z^2} = \tfrac{1}{2} k_{\rm b} T \ , \tag{2.4.1}$$

or equivalently

$$\sigma_x^2 = \sigma_y^2 = \sigma_z^2 = v_{\rm th}^2 \text{ with } v_{\rm th} = \sqrt{k_{\rm b} T / m} \ . \tag{2.4.2}$$

[5] A good introduction: D. ter Haar, *Elements of Thermostatistics*, Holt, Rinehart and Winston, 1966

This thermodynamic relationship implies that the pressure is related to the density $\rho = nm$ and temperature T by

$$\boxed{P(\rho\,,\,T) = nk_{\rm b}T = \frac{\rho\mathcal{R}T}{\mu}\,.} \tag{2.4.3}$$

In this expression $\mathcal{R} = k_{\rm b}/m_{\rm H}$ is the universal gas constant, and $\mu = m/m_{\rm H}$ is the mass of the particles in units of the hydrogen mass $m_{\rm H}$. The thermal energy density of the gas (i.e. the kinetic energy of the thermal motions per unit volume) equals:

$$\frac{U}{\mathcal{V}} = \tfrac{1}{2}nm\left(\overline{\sigma_x^2+\sigma_y^2+\sigma_z^2}\right) = \tfrac{3}{2}nk_{\rm b}T = \tfrac{3}{2}\frac{\rho\mathcal{R}T}{\mu}\,. \tag{2.4.4}$$

2.5 Gravity and self-gravity

A gravitational force on the fluid due to a gravitational field with potential $\Phi(\boldsymbol{x}\,,\,t)$ leads to a force density

$$\boldsymbol{f}_{\rm gr} = \rho\,\boldsymbol{g} = -\rho\,\boldsymbol{\nabla}\Phi\,. \tag{2.5.1}$$

Here the gravitational acceleration has been written in terms of the gradient of the gravitational potential $\Phi(\boldsymbol{x}\,,\,t)$:

$$\boldsymbol{g}(\boldsymbol{x},t) = -\boldsymbol{\nabla}\Phi(\boldsymbol{x},t) = -\begin{pmatrix} \dfrac{\partial\Phi}{\partial x} \\ \\ \dfrac{\partial\Phi}{\partial y} \\ \\ \dfrac{\partial\Phi}{\partial z} \end{pmatrix}\,. \tag{2.5.2}$$

If gravity is the only additional force working on the fluid, the equation of motion becomes:

$$\boxed{\rho \left[\frac{\partial \boldsymbol{V}}{\partial t} + (\boldsymbol{V} \cdot \boldsymbol{\nabla}) \, \boldsymbol{V} \right] = -\boldsymbol{\nabla} P - \rho \, \boldsymbol{\nabla} \Phi \; .} \tag{2.5.3}$$

In astrophysical applications, one has to allow for the possiblity of *self-gravitation*, where the mass of the fluid generates (part of) the gravitational field. In that case we must add Poissons equation to the system of equations:

$$\boxed{\boldsymbol{\nabla}^2 \Phi(\boldsymbol{x}, t) = 4\pi G \, \rho(\boldsymbol{x}, t) \; .} \tag{2.5.4}$$

Poisson's equation relates the gravitational potential $\Phi(\boldsymbol{x} \; , \; t)$ to the mass distribution $\rho(\boldsymbol{x} \; , \; t)$ that acts as a source of gravity. This equation can be solved formally by the integral expression:

$$\Phi(\boldsymbol{x}, t) = -\int \mathrm{d}^3 \boldsymbol{x'} \, \frac{G \, \rho(\boldsymbol{x'}, t)}{|\boldsymbol{x} - \boldsymbol{x'}|} \; . \tag{2.5.5}$$

Note that Newtons potential works *instantaneously*, and is therefore only valid for 'slowly varying' gravitational fields. Here 'slow' is defined with respect to the light travel time across the system one is considering. To properly describe the effects of a time-varying gravitational field one has to turn to General Relativity, where the action of gravity is described by tensor fields rather than by a scalar potential Φ. In particular, it is *not* correct to replace Newtons potential by a *retarded* potential to take account of relativistic effects, such as the light travel-time between the mass that is the source of the potential, and the position where one tries to determine the value of the gravitational potential. A similar procedure works in electromagnetism, but not in General Relativity.

2.6 Mass conservation and the continuity equation

In order to solve the equation of motion we need to know how the fluid mass density $\rho(\boldsymbol{x}\,,\,t)$ behaves. Consider a droplet of fluid at position $\boldsymbol{x}$ with infinitesimal volume $\Delta\mathcal{V}$ and mass $\Delta M = \rho\,\Delta\mathcal{V}$. Due to the motion of the fluid the droplet will be deformed, as a simple observation of milk in a stirred cup of coffee will immediately show. However, as long as there are no processes that create particles (e.g. pair creation by high-energy photons) or destroy them, the mass of the droplet is conserved, regardless its shape:

$$\Delta M = \rho\,\Delta\mathcal{V} = \text{constant}\ . \tag{2.6.1}$$

This means that in principle it is sufficient to calculate the change in the droplet volume $\Delta\mathcal{V}$. In order to properly calculate the deformation of a small volume-element in a flow, we must first consider the concept of *material curves*: curves connecting points where each individual point is carried along passively by the flow with a velocity equal to the speed of the flow, see the figure below.

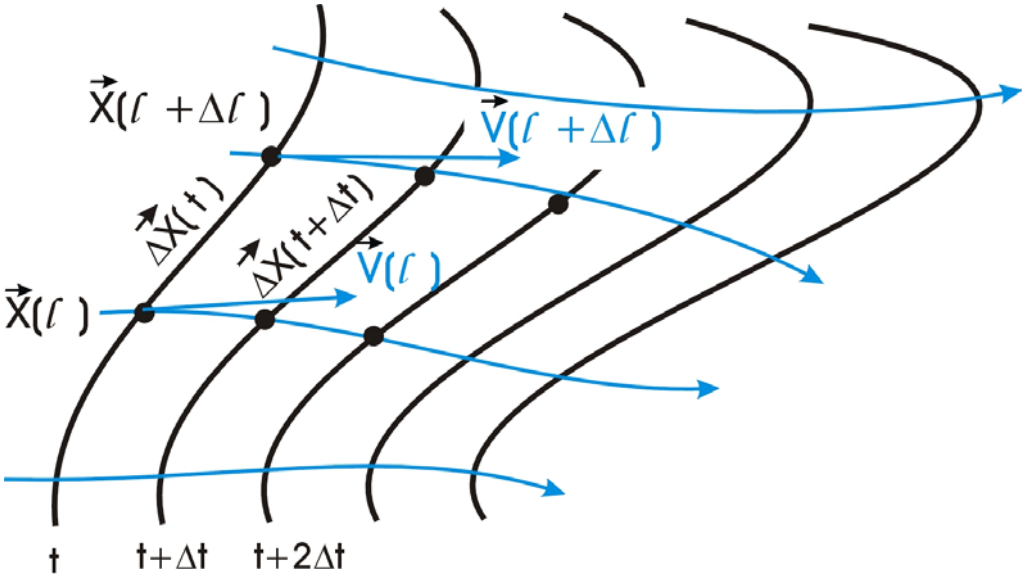

Figure 2.1: *Flow lines are carried passively by the flow. The figure shows how a given flow line is deformed as time progresses.*

Take a material curve $\boldsymbol{X}(\ell)$, with ℓ measuring the length along the curve. It is carried along by the flow so that the velocity at the position $\boldsymbol{X}(\ell)$ is given by the local value of the fluid velocity:

$$\frac{\mathrm{d}\boldsymbol{X}}{\mathrm{d}t} = \boldsymbol{V}(\boldsymbol{x} = \boldsymbol{X}, t)\ . \tag{2.6.2}$$

Consider a small section of the curve with length $\Delta\ell$, between ℓ and $\ell+\Delta\ell$. For $\Delta\ell \to 0$ the section of curve can be approximated by the tangent vector,

$$\Delta \boldsymbol{X} = \boldsymbol{X}(\ell + \Delta\ell) - \boldsymbol{X}(\ell) \approx \frac{\partial \boldsymbol{X}}{\partial \ell}\, \Delta\ell \,. \tag{2.6.3}$$

The vector $\Delta\boldsymbol{X}$ changes in time according to

$$\frac{\mathrm{d}(\Delta \boldsymbol{X})}{\mathrm{d}t} = \boldsymbol{V}(\boldsymbol{X}(\ell) + \Delta\boldsymbol{X}, t) - \boldsymbol{V}(\boldsymbol{X}(\ell), t) \,. \tag{2.6.4}$$

In the limit $|\Delta\boldsymbol{X}| \to 0$ one can write:

$$\boxed{\frac{\mathrm{d}(\Delta \boldsymbol{X})}{\mathrm{d}t} = (\Delta\boldsymbol{X} \cdot \boldsymbol{\nabla})\boldsymbol{V} \,.} \tag{2.6.5}$$

Any small volume in a flow can be defined by three infinitesimal (tangent) vectors $\Delta\boldsymbol{X}$, $\Delta\boldsymbol{Y}$ and $\Delta\boldsymbol{Z}$. These vectors need not be orthogonal (see figure), and form the 'edges' of the infinitesimal volume. If one takes these three edges to be sections of material curves, the volume moves with the flow. This means that it contains a *fixed* amount of mass: no material can flow *across* a material curve, and therefore the mass flux across the outer surfaces of the volume, defined by material curves, vanishes. The vectors $\Delta\boldsymbol{X}$, $\Delta\boldsymbol{Y}$ and $\Delta\boldsymbol{Z}$ are carried passively by the flow and, as a result, are stretched and rotated according to Eqn. (2.6.5). According to the results of vector algebra[6], the *oriented* volume spanned by these three infinitesimal vectors equals

$$\Delta\mathcal{V} = \Delta\boldsymbol{X} \cdot (\Delta\boldsymbol{Y} \times \Delta\boldsymbol{Z}) = \begin{Vmatrix} \Delta X_x & \Delta X_y & \Delta X_z \\ \Delta Y_x & \Delta Y_y & \Delta Y_z \\ \Delta Z_x & \Delta Z_y & \Delta Z_z \end{Vmatrix} . \tag{2.6.6}$$

[6] e.g. G.B. Arfken & H.J. Weber, *Mathematical Methods for Physicists*, 4^{th} Edition, Academic Press, 1995: Ch. 1.5

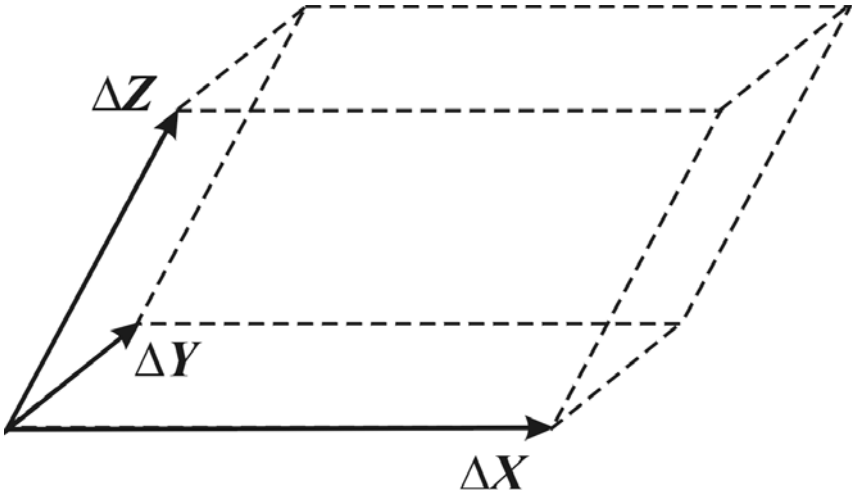

Figure 2.2: *The volume defined by three arbitrary vectors $\Delta\boldsymbol{X}$, $\Delta\boldsymbol{Y}$ and $\Delta\boldsymbol{Z}$.*

Taking the time-derivative $\mathrm{d}/\mathrm{d}t$ of this definition using the chain rule for differentiation,

$$\frac{\mathrm{d}\Delta\mathcal{V}}{\mathrm{d}t} = \frac{\mathrm{d}\Delta\boldsymbol{X}}{\mathrm{d}t} \cdot (\Delta\boldsymbol{Y} \times \Delta\boldsymbol{Z}) + \Delta\boldsymbol{X} \cdot \left(\frac{\mathrm{d}\Delta\boldsymbol{Y}}{\mathrm{d}t} \times \Delta\boldsymbol{Z} + \Delta\boldsymbol{Y} \times \frac{\mathrm{d}\Delta\boldsymbol{Z}}{\mathrm{d}t} \right) , \quad (2.6.7)$$

and using the result (2.6.5) for material curves one finds:

$$\begin{aligned} \frac{\mathrm{d}\Delta\mathcal{V}}{\mathrm{d}t} = \quad & (\Delta\boldsymbol{X} \cdot \boldsymbol{\nabla})\boldsymbol{V} \cdot (\Delta\boldsymbol{Y} \times \Delta\boldsymbol{Z}) \\ + \quad & (\Delta\boldsymbol{Y} \cdot \boldsymbol{\nabla})\boldsymbol{V} \cdot (\Delta\boldsymbol{Z} \times \Delta\boldsymbol{X}) \\ + \quad & (\Delta\boldsymbol{Z} \cdot \boldsymbol{\nabla})\boldsymbol{V} \cdot (\Delta\boldsymbol{X} \times \Delta\boldsymbol{Y}) \end{aligned} \quad (2.6.8)$$

Here I have used the cyclic permutation rule (see the mathematical appendix on Internet):

$$\boldsymbol{A} \cdot (\boldsymbol{B} \times \boldsymbol{C}) = \boldsymbol{B} \cdot (\boldsymbol{C} \times \boldsymbol{A}) = \boldsymbol{C} \cdot (\boldsymbol{A} \times \boldsymbol{B}) . \quad (2.6.9)$$

The algebra can be simplified considerably if one makes a special choice for the vectors $\Delta\boldsymbol{X}$, $\Delta\boldsymbol{Y}$ and $\Delta\boldsymbol{Z}$. Let us take the three infinitesimal vectors to be *orthogonal* and aligned with the three coordinate axes of a cartesian coordinate system:

$$\Delta\boldsymbol{X} = \begin{pmatrix} \Delta X \\ 0 \\ 0 \end{pmatrix} , \; \Delta\boldsymbol{Y} = \begin{pmatrix} 0 \\ \Delta Y \\ 0 \end{pmatrix} , \; \Delta\boldsymbol{Z} = \begin{pmatrix} 0 \\ 0 \\ \Delta Z \end{pmatrix} . \tag{2.6.10}$$

It is easily checked that for this particular choice the volume-element (2.6.6) reduces to $\Delta\mathcal{V} = \Delta X\, \Delta Y\, \Delta Z$, as should be expected. This assumption simplifies the algebra considerably but, as will be argued below, does not constrain the generality of the final result.

The first term on the right-hand side of (2.6.8) can be written in determinant form as

$$\Delta X \begin{Vmatrix} \partial V_x/\partial x & \partial V_y/\partial x & \partial V_z/\partial x \\ 0 & \Delta Y & 0 \\ 0 & 0 & \Delta Z \end{Vmatrix} = \Delta X \left(\frac{\partial V_x}{\partial x}\right) \Delta Y\, \Delta Z \; . \tag{2.6.11}$$

The remaining two terms can be calculated in a similar fashion, and give $(\partial V_y/\partial y)\Delta X\Delta Y\Delta Z$ and $(\partial V_z/\partial z)\, \Delta X\, \Delta Y\, \Delta Z$. Therefore expression (2.6.8) reduces to the simple form

$$\begin{aligned} \frac{\mathrm{d}\Delta\mathcal{V}}{\mathrm{d}t} &= \Delta X\, \Delta Y\, \Delta Z \left(\frac{\partial V_x}{\partial x} + \frac{\partial V_y}{\partial y} + \frac{\partial V_z}{\partial z}\right) \\ &= \Delta\mathcal{V}\, (\boldsymbol{\nabla}\cdot\boldsymbol{V}) \; . \end{aligned} \tag{2.6.12}$$

Since any volume, regardless its shape, can always be constructed using much smaller rectangular cubes as 'building blocks'[7], with each small cube individually satisfying relation (2.6.12), this relationship must be true *regardless* the shape of the volume, provided that this total volume remains infinitesimally small.

[7] The 'Lego Principle'

Mass conservation, $\rho\Delta\mathcal{V} =$ constant, implies that

$$\frac{\mathrm{d}(\rho\Delta\mathcal{V})}{\mathrm{d}t} = \Delta\mathcal{V}\,\frac{\mathrm{d}\rho}{\mathrm{d}t} + \rho\,\frac{\mathrm{d}\Delta\mathcal{V}}{\mathrm{d}t} = 0\ . \tag{2.6.13}$$

Using the change-of-volume law (2.6.12), one finds:

$$\frac{\mathrm{d}\rho}{\mathrm{d}t} \equiv \frac{\partial\rho}{\partial t} + (\boldsymbol{V}\cdot\boldsymbol{\nabla})\rho = -\rho\,\left(\frac{1}{\Delta\mathcal{V}}\,\frac{\mathrm{d}\Delta\mathcal{V}}{\mathrm{d}t}\right) = -\rho\,(\boldsymbol{\nabla}\cdot\boldsymbol{V})\ . \tag{2.6.14}$$

Reordering terms in this equation and employing the vector identity

$$\boldsymbol{\nabla}\cdot(f\boldsymbol{A}) = f(\boldsymbol{\nabla}\cdot\boldsymbol{A}) + (\boldsymbol{A}\cdot\boldsymbol{\nabla})f\ , \tag{2.6.15}$$

one can write this differential version of the mass conservation law as

$$\boxed{\frac{\partial\rho}{\partial t} + \boldsymbol{\nabla}\cdot(\rho\,\boldsymbol{V}) = 0\ .} \tag{2.6.16}$$

This equation is known as the **continuity equation**.

2.7 The adiabatic gas law

The final missing element in our description of fluids is a recipe describing the behaviour of the pressure $P = \rho\mathcal{R}T/\mu$. I will defer a full treatment of this problem to the discussion of heating and cooling processes, limiting the discussion here to the case of an *adiabatic gas*.

An adiabatic proces in thermodynamics is a process where (in a closed system) no energy is added by irreversible heating, or extracted by irreversible cooling. The *first law of thermodynamics* states that the amount of heat $\mathrm{d}Q$ added to a gas in some volume $\mathcal{V}$ is related to the change in the energy $\mathrm{d}U$ and/or the volume-change $\mathrm{d}\mathcal{V}$ by

$$\mathrm{d}Q \equiv T\,\mathrm{d}S = \mathrm{d}U + P\,\mathrm{d}\mathcal{V}\ . \tag{2.7.1}$$

Here S is the *entropy*, T the gas temperature and P the gas pressure. We already calculated the energy of an ideal gas in thermal equilibrium:

$$U = \tfrac{3}{2}\,\frac{\rho\mathcal{R}T\mathcal{V}}{\mu}\ . \tag{2.7.2}$$

The pressure satisfies the ideal gas law (Eqn. 2.4.3): $P = \rho\mathcal{R}T/\mu$. An adiabatic process satisfies by definition

$$\mathrm{d}Q = T\,\mathrm{d}S = 0\ , \tag{2.7.3}$$

so that the first law of thermodynamics reduces to:

$$\mathrm{d}\left(\frac{3\rho\mathcal{R}T\mathcal{V}}{2\mu}\right) + \left(\frac{\rho\mathcal{R}T}{\mu}\right)\,\mathrm{d}\mathcal{V} = 0\ . \tag{2.7.4}$$

Writing out the first differential, using the chain rule $\mathrm{d}(f\,g) = (\mathrm{d}f)\,g + f\,(\mathrm{d}g)$, one finds:

$$\left(\frac{5\rho\mathcal{R}T}{2\mu}\right)\,\mathrm{d}\mathcal{V} + \mathcal{V}\,\mathrm{d}\left(\frac{3\rho\mathcal{R}T}{2\mu}\right) = 0. \tag{2.7.5}$$

Using $P = \rho\mathcal{R}T/\mu$ and multiplying by $2/3$ leads to

$$\tfrac{5}{3}\,P\,\mathrm{d}\mathcal{V} + \mathcal{V}\,\mathrm{d}P = 0\ . \tag{2.7.6}$$

This can be written as

$$\frac{\mathrm{d}P}{P} + \tfrac{5}{3}\,\frac{\mathrm{d}\mathcal{V}}{\mathcal{V}} = \mathrm{d}\log\left(P\,\mathcal{V}^{5/3}\right) = 0\;, \tag{2.7.7}$$

or equivalently in the form

$$P \times \mathcal{V}^{5/3} = \text{constant}\;. \tag{2.7.8}$$

Here I have used that $\mathrm{d}x/x = \mathrm{d}\ln x$. As long as the volume $\mathcal{V}$ is small, we can apply this law *locally*. Take an infinitesimal volume $\Delta\mathcal{V}$, containing a fluid of density ρ and pressure P. As the gas expands (or contacts) the volume changes, and the pressure adjusts according to (2.7.8). The conservation of mass implies that $\rho\,\Delta\mathcal{V} =$ constant. This implies $\Delta\mathcal{V} \propto 1/\rho$, and relation (2.7.8) can be rewritten in terms of the density:

$$\boxed{P\,\rho^{-5/3} = \text{constant}\;.} \tag{2.7.9}$$

2.7.1 The polytropic gas law, the specific heat coefficients and the isothermal gas

Relation (2.7.9) is a special case of a *polytropic gas law*, which generally takes the form

$$P = \text{constant} \times \rho^{\gamma}\;. \tag{2.7.10}$$

The value of the exponent γ ($= 5/3$ for an ideal classical gas) depends on the circumstances. For an ideal gas γ is related to the ratio of *specific heat* at constant volume, c_{v}, and at constant pressure, c_{p}: $\gamma = c_{\mathrm{p}}/c_{\mathrm{v}}$ as we will now prove.

Let us introduce the *specific volume* $\overline{\mathcal{V}}$, the volume containing a *unit* mass:

$$\overline{\mathcal{V}} \equiv \frac{1}{\rho} \tag{2.7.11}$$

In terms of this quantity, relation (2.7.1) can be written as

$$\mathrm{d}Q = T\,\mathrm{d}s = \mathrm{d}e + P\,\mathrm{d}\left(\frac{1}{\rho}\right)\ , \tag{2.7.12}$$

by applying the general relation (2.7.1) to the specific volume $\overline{\mathcal{V}}$. Here s is the entropy per unit mass, and e the energy per unit mass,

$$e \equiv \tfrac{3}{2}\,\frac{\mathcal{R}T}{\mu} = \tfrac{3}{2}\,\frac{k_{\mathrm{b}}T}{m}\ . \tag{2.7.13}$$

The quantity c_{v} is simply defined by the relation

$$(\mathrm{d}Q)_{\overline{\mathcal{V}}\,=\,\mathrm{cnst}} = c_{\mathrm{v}}\,\mathrm{d}T\ . \tag{2.7.14}$$

It determines the amount of energy needed to raise the temperature of a unit mass of gas by an amount $\mathrm{d}T$, keeping the volume (and, because of mass conservation, the density) constant. Using (2.7.12) with $\mathrm{d}(1/\rho) = 0$ this definition implies

$$\boxed{c_{\mathrm{v}} = \frac{\partial e}{\partial T} = \tfrac{3}{2}\,\frac{k_{\mathrm{b}}}{m}\ .} \tag{2.7.15}$$

The quantity c_{p} can be found by writing (2.7.12) in the form

$$\mathrm{d}Q = \mathrm{d}\left(e + \frac{P}{\rho}\right) - \frac{\mathrm{d}P}{\rho}\ ,$$

and defining c_{p} by

$$(\mathrm{d}Q)_{P\,=\,\mathrm{cnst}} = c_{\mathrm{p}}\,\mathrm{d}T\ . \tag{2.7.16}$$

The coefficient c_{p} determines the amount of energy needed to raise the temperature of a unit mass by an amount $\mathrm{d}T$ while the pressure is kept constant so that $\mathrm{d}P = 0$. This means that the gas is allowed to expand if it is heated, or will contract as it cools

Definition (2.7.16) implies

$$\boxed{c_{\rm p} = \frac{\partial(e + P/\rho)}{\partial T} = \tfrac{5}{2}\,\frac{k_{\rm b}}{m}\,.} \tag{2.7.17}$$

One must have $c_{\rm p} > c_{\rm v}$ because part of the energy supplied goes into the work done by the gas during the expansion. From (2.7.15) and (2.7.16) one immediately finds

$$c_{\rm p} - c_{\rm v} = \frac{k_{\rm b}}{m} = \frac{\mathcal{R}}{\mu}\,. \tag{2.7.18}$$

The first law of thermodynamics can be rewritten in terms of $c_{\rm p}$ and $c_{\rm v}$. Using relations (2.7.15) to (2.7.18) one finds:

$$\begin{aligned} {\rm d}Q &= c_{\rm v}\,{\rm d}T + \left(\frac{\rho\mathcal{R}T}{\mu}\right)\,{\rm d}\left(\frac{1}{\rho}\right) \\ &= c_{\rm v}\,{\rm d}T - \left(\frac{\mathcal{R}T}{\rho\mu}\right)\,{\rm d}\rho \\ &= c_{\rm v}T\,\left[\frac{{\rm d}T}{T} - \left(\frac{c_{\rm p}}{c_{\rm v}} - 1\right)\,\frac{{\rm d}\rho}{\rho}\right]\,. \end{aligned} \tag{2.7.19}$$

Putting ${\rm d}Q = 0$ as required for an adiabatic process, the resulting equation is solved by

$$\log T - (\gamma - 1)\,\log\rho = \text{constant}\,, \tag{2.7.20}$$

with

$$\gamma \equiv \frac{c_{\rm p}}{c_{\rm v}} = \frac{5}{3}\,. \tag{2.7.21}$$

Relation (2.7.20) can be written as the adiabatic temperature-density relation:

$$T\rho^{-(\gamma-1)} = \text{constant}\,. \tag{2.7.22}$$

It is easily checked that this relation is equivalent with the adiabatic gas law: since $P = \rho\mathcal{R}T/\mu \propto \rho T$ relation (2.7.22) implies $P \propto \rho^\gamma$. This proves the relationship between the index γ in the polytropic gas law (2.7.10) and the specific heat ratio in the case of an adiabatic gas.

As a by-product of this derivation we can derive the specific entropy s (entropy per unit mass) for an ideal gas directly from Eqn. (2.7.19). Using $\mathrm{d}Q = T\,\mathrm{d}s$ and (2.7.21) one has

$$T\,\mathrm{d}s = c_\mathrm{v} T\,\left[\frac{\mathrm{d}T}{T} - (\gamma - 1)\,\frac{\mathrm{d}\rho}{\rho}\right]\,.$$

Dividing out the common factor T, the resulting equation for $\mathrm{d}s$ can be integrated to

$$s = c_\mathrm{v}\,\log\left(\frac{T}{\rho^{\gamma-1}}\right) + \mathrm{constant}\,. \tag{2.7.23}$$

An alternative expression follows from $P = \rho\mathcal{R}T/\mu$:

$$\boxed{s = c_\mathrm{v}\,\log\left(P\,\rho^{-\gamma}\right) + \mathrm{constant}\,.} \tag{2.7.24}$$

A special case, often used in astrophysical models, is the assumption of an **isothermal gas** satisfying the relation

$$T = \mathrm{constant}\,. \tag{2.7.25}$$

In that case the pressure $P = \rho\mathcal{R}T/\mu$ becomes a function of density only, and the polytropic index γ in (2.7.10) takes the special value

$$\gamma_\mathrm{iso} = 1\,.$$

Note that for an ideal gas this can only be true if there exists some mechanism which acts as a 'thermostat' that keeps the temperature constant by supplying (extracting) exactly the right amount of energy to the gas if it expands (contracts). A gas embedded in a strong black-body radiation field of fixed temperature often behaves in this manner.

The radiation acts as a heat reservoir with such a large capacity that any changes in the internal energy of the the gas are immediately compensated by the radiation, forcing the gas to remain in temperature equilibrium with the radiation field.

2.8 The isothermal sphere and globular clusters

As a first astronomical application we will consider a simple model for a spherically-symmetric, self-gravitating stellar system: the *isothermal sphere*. The isothermal sphere is a crude model for a globular cluster, for the quasi-spherical central region ('bulge') of a disk galaxy or for the nucleus of an elliptical galaxy.

Figure 2.3: *The globular cluster NGC 5139*

Consider a large number of stars with a density distribution that only depends on the distance r from the center of the sphere. If all the stars have a mass m_* and the number density at radius r equals $n(r)$, the mass density equals

$$\rho(r) = n(r)m_* \, . \tag{2.8.1}$$

If the number of stars is large enough we can describe it as a 'gas' of stars with a 'temperature' T which is determined by the velocity dispersion according Eqn. (2.4.1):

$$\overline{\sigma_x^2} = \overline{\sigma_y^2} = \overline{\sigma_z^2} \equiv \tilde{\sigma}^2 = \frac{k_{\rm b} T}{m_*} \ . \tag{2.8.2}$$

This definition implies that $\sigma^2 = 3\tilde{\sigma}^2$. Typically, a globular cluster contains 100,000 stars and has a mass between 10^4 and $10^6\ M_\odot$, with an average mass of $10^5\ M_\odot$.

The velocity dispersion of the stars in a globular cluster can be measured by looking at the Doppler broadening of the absorption lines in the spectrum of a globular cluster: one observes the 'average' spectrum of a large number of stars with velocity dispersion $\tilde{\sigma}$ along the line-of-sight, leading to a line-width $\Delta\lambda$ given by

$$\frac{\Delta\lambda}{\lambda} \simeq \frac{\tilde{\sigma}}{c} \ . \tag{2.8.3}$$

In the isothermal sphere model the cluster is treated as a self-gravitating ball of gas. The pressure of this gas, where the stars play the role of 'molecules', equals

$$P(r) = n(r) k_{\rm b} T = \rho(r) \tilde{\sigma}^2 \ . \tag{2.8.4}$$

The isothermal assumption means that the temperature, and therefore $\tilde{\sigma}$, does not depend on the radius r. All other quantities are assumed to depend only on the radial coordinate r, the distance to the center of the globular cluster.

The consequences of the isothermal sphere model were first investigated exhaustively by Chandrasekhar[8]. A good modern account of this (and related) models can be found in the book by Binney and Tremaine[9].

Since there is only velocity dispersion, and no *bulk* motion of the stars we have $\boldsymbol{V} = 0$, and the equation of motion becomes the *hydrostatic equilibrium equation* where the gravitational force in the radial direction is balanced by the pressure gradient:

$$\frac{{\rm d}P}{{\rm d}r} = \tilde{\sigma}^2 \left(\frac{{\rm d}\rho}{{\rm d}r}\right) = -\rho \, \frac{G\, M(r)}{r^2} \ . \tag{2.8.5}$$

[8] S. Chandrasekhar, *Principles of Stellar Dynamics*, University of Chicago Press, 1942, reprinted by Dover Publications Inc.

[9] J. Binney & S. Tremaine, *Galactic Dynamics*, Princeton University Press, 1987, Ch. 4.4

Here we use the fact that for a spherically symmetric mass distribution the gravitational acceleration at some radius r depends only on the amount of mass $M(r)$ contained *within* that radius. Because of this symmetry, the mass outside r does not excert a net force.

The amount of mass contained in a spherical shell between r and $r + \mathrm{d}r$ equals

$$\mathrm{d}M = 4\pi r^2 \, \rho(r) \, \mathrm{d}r \; .$$

Therefore the mass contained within a radius r is given by the integral

$$M(r) = \int_0^r \mathrm{d}r' \, 4\pi r'^2 \, \rho(r') \; . \tag{2.8.6}$$

The gravitational potential $\Phi(r)$ is defined by the equation

$$g_r = -\frac{G \, M(r)}{r^2} = -\frac{\mathrm{d}\Phi}{\mathrm{d}r} \; . \tag{2.8.7}$$

The isothermal assumption together with $P(r) = \rho(r)\tilde{\sigma}^2$ imply that the equation of hydrostatic equilibrium (2.8.5) can be written as

$$\tilde{\sigma}^2 \, \left(\frac{1}{\rho} \, \frac{\mathrm{d}\rho}{\mathrm{d}r} \right) = -\frac{\mathrm{d}\Phi}{\mathrm{d}r} \; . \tag{2.8.8}$$

This equation has a formal solution in terms of the gravitational potential:

$$\rho(r) = \rho_0 \, e^{-\Phi(r)/\tilde{\sigma}^2} \; . \tag{2.8.9}$$

Here ρ_0 is the mass density at $r = 0$, assuming that $\Phi(0) = 0$.

The potential $\Phi(r)$ must be calculated by solving Poissons equation. Because of the use of the radial coordinate r it takes the form (see the mathematical appendix on Internet)

$$\frac{1}{r^2} \frac{\mathrm{d}}{\mathrm{d}r} \left(r^2 \, \frac{\mathrm{d}\Phi}{\mathrm{d}r} \right) = 4\pi G \, \rho(r) = 4\pi G \rho_0 \, e^{-\Phi(r)/\tilde{\sigma}^2} \; . \tag{2.8.10}$$

One can introduce the following *dimensionless* variables for the radial distance and gravitational potential:

$$\xi = \frac{r}{r_{\rm K}} \quad , \quad \Psi = \frac{\Phi}{\tilde{\sigma}^2} = \frac{m_* \Phi}{k_{\rm b} T} \; . \tag{2.8.11}$$

The radius $r_{\rm K}$ a normalizing length scale, the so-called *King radius*, which is defined in terms of the central density ρ_0 and the velocity dispersion $\tilde{\sigma}$ of the cluster:

$$r_{\rm K} = \left(\frac{\tilde{\sigma}^2}{4\pi G \rho_0} \right)^{1/2} = \left(\frac{k_{\rm b} T}{4\pi G m_* \rho_0} \right)^{1/2} \; . \tag{2.8.12}$$

In terms of these variables Poisson's equation takes the following simple form:

$$\boxed{\frac{1}{\xi^2} \frac{\rm d}{{\rm d}\xi} \left(\xi^2 \, \frac{{\rm d}\Psi}{{\rm d}\xi} \right) = e^{-\Psi} \; .} \tag{2.8.13}$$

This dimensionless form of Poisson's equation displays **no** explicit information about the properties of the cluster. In particular all reference to the central density ρ_0 and the velocity dispersion $\tilde{\sigma}$ has disappeared. The interpretation of this result is as follows. All isothermal spheres are *self-similar*. If one plots the density relative to the central density $\rho(r)/\rho_0$ as a function of the dimensionless radius $\xi = r/r_{\rm K}$, all globular clusters that behave as an isothermal sphere have exactly the same density profile!

In order to solve this equation one must add two boundary conditions:

$$\Psi(\xi = 0) = 0 \quad , \quad \left(\frac{{\rm d}\Psi}{{\rm d}\xi} \right)_{\xi = 0} = 0 \; .$$

The first boundary condition corresponds to our earlier assumption that $\Phi(0) = 0$, and is not special as the gravitational potential Φ is determined *up to a constant*: this choice is always possible. The second condition is a consequence of the symmetry of the problem: at the center of the sphere *all* the mass is at larger radii, and there can be no net gravitational force: $g_r(0) = -({\rm d}\Phi/{\rm d}r)_{r=0} = 0$.

There is no analytical solution of this equation for these boundary conditions in closed form. Near $\xi = 0$ one can solve by a power series, using the fact that for $\Psi \ll 1$ the exponential can be expanded:

$$e^{-\Psi} = 1 - \Psi + \tfrac{1}{2} \Psi^2 + \cdots \; .$$

Assuming a solution of the form

$$\Psi(\xi) = a_1 \, \xi^2 + a_2 \, \xi^4 + \cdots \; ,$$

and using the above expansion of the exponential, one determines the coefficients a_1, a_2 $\cdots$ by equating powers of ξ on both sides of the equation. One finds:

$$\Psi(\xi) \simeq \frac{\xi^2}{6} - \frac{\xi^4}{120} + \cdots \quad (\text{for } \xi \ll 1) \, . \tag{2.8.14}$$

The corresponding density follows from $\rho = \rho_0 e^{-\Psi}$, using the expansion $\exp(-\Psi) \approx 1 - \Psi + \frac{1}{2}\Psi^2 + ...$:

$$\rho(\xi) \simeq \rho_0 \left(1 - \frac{\xi^2}{6} + \frac{\xi^4}{45} + \cdots\right) \, . \tag{2.8.15}$$

For large values of ξ, the solution goes asymptotically to

$$\Psi(\xi) \simeq \log\left(\frac{\xi^2}{2}\right) \quad (\text{for } \xi \gg 1) \, . \tag{2.8.16}$$

The density for large values of $\xi = r/r_{\rm K}$ is therefore

$$\rho(\xi) \approx \rho_0 \left(\frac{2}{\xi^2}\right) \, . \tag{2.8.17}$$

Expressing the density in terms of the radius, this solution is known as the *singular isothermal sphere* solution as the density goes to infinity at $r = 0$:

$$\rho(r) = \frac{\tilde{\sigma}^2}{2\pi G r^2} \, . \tag{2.8.18}$$

The singular isothermal sphere is in fact the only *analytic* solution known to the isothermal sphere equation, as can be checked by substitution. Note that the density in this solution depends only on the velocity dispersion and radius, but is independent of the central density ρ_0. It can be shown that *any* solution of the isothermal sphere equation takes this form asymptotically at large radii: $r \gg r_{\rm K}$. The full solution for the density of an isothermal sphere is plotted in the figure below.

The density in a singular isothermal sphere decays with radius as $\rho(r) \propto r^{-2}$, which means that the mass within a sphere of radius r grows for large radii as $M(r) \propto r$:

$$M(r) = \int_0^r {\rm d}r' \, 4\pi r'^2 \, \rho(r') \longrightarrow 8\pi\rho_0 \, r_{\rm K}^2 \, r \quad \text{for } r \gg r_{\rm K} \, . \tag{2.8.19}$$

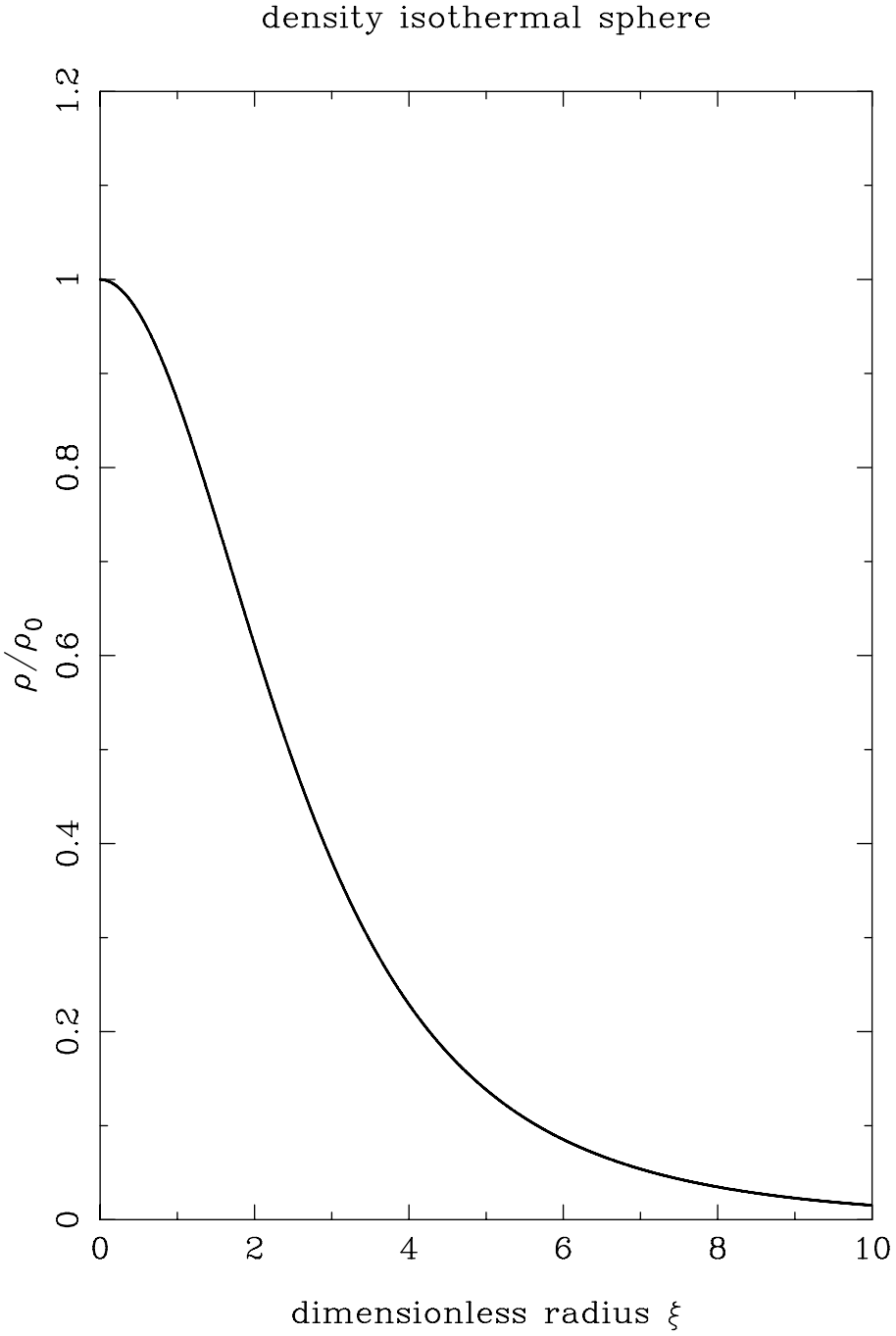

Figure 2.4: *The mass density in an isothermal sphere relative to the central density ρ_0 as a function of the dimensionless radius $\xi = r/r_{\rm K}$. The density profile of all globular clusters in hydrostatic equilibrium look the same if one scales the radius in terms of the King radius $r_{\rm K} = \sqrt{\tilde{\sigma}^2/4\pi G\rho_0}$, and the density with the central density ρ_0.*

Such behaviour is clearly unacceptable as a description for a real globular cluster: the mass of an isothermal sphere grows without bound as $r \to \infty$. This means that the isothermal sphere can only be an approximate model which fails at large radii.

2.8.1 The tidal radius

Observations show that clusters have a well-defined edge beyond which the stellar density rapidly goes to zero. The relatively sharp edge of globular clusters can be explained if one takes account of *tidal forces*: the variation of the gravitational pull of the Galaxy across the globular cluster[10]. If the cluster has a radius $r_{\rm t}$ and is located at a distance R from the galactic center, the typical magnitude of the tidal acceleration for $r_{\rm t} \ll R$ is

$$g_{\rm t} \approx r_{\rm t} \frac{\partial}{\partial r}\left(-\frac{GM_{\rm gal}}{R^2}\right) = \frac{2GM_{\rm gal}\, r_{\rm t}}{R^3} \,, \tag{2.8.20}$$

with $M_{\rm gal}$ the mass of the Galaxy. This is essentially the difference between the Galactic gravitational force at the center, and at the outer edge of the globular cluster. The value of $r_{\rm t}$, the so-called *tidal radius*, can be estimated by equating the tidal force to the gravitational pull of the cluster itself: around $r_{\rm t}$ tidal forces are able to pull stars from the cluster. If the cluster mass is $M_{\rm c}$ this balance reads:

$$\frac{GM_{\rm c}}{r_{\rm t}^2} \approx \frac{2GM_{\rm gal}\, r_{\rm t}}{R^3} \,, \tag{2.8.21}$$

or equivalently:

$$\frac{r_{\rm t}}{R} \approx \left(\frac{M_{\rm c}}{2M_{\rm gal}}\right)^{1/3} \,. \tag{2.8.22}$$

This defines the maximum size of the cluster where the stars in the clusters are still marginally bound by the gravitational pull of the cluster mass.

[10] For a full discussion see: L. Spitzer, *Dynamical Evolution of Globular Clusters*, Princeton University Press, 1987.

If one uses estimate (2.8.19) for the mass contained within $r_{\rm t}$,

$$M_{\rm c} \approx 8\pi\rho_0 r_{\rm K}^2\, r_{\rm t}\ , \tag{2.8.23}$$

one finds from (2.8.20):

$$r_{\rm t} = \left(\frac{4\pi\rho_0 R^3}{M_{\rm gal}}\right)^{1/2} r_{\rm K} = \left(\frac{\tilde\sigma^2 R^3}{GM_{\rm gal}}\right)^{1/2}\ . \tag{2.8.24}$$

Using typical values for the distance, observed velocity dispersion and central mass density of globular clusters and for the mass of our Galaxy,

$$\tilde\sigma \simeq 5\ {\rm km/s}\ \ ,\ \ \rho_0 \simeq 10^4\ M_\odot\ {\rm pc}^{-3}\ \ ,\ \ R \simeq 10\ {\rm kpc}\ \ ,\ \ M_{\rm gal} \simeq 10^{11}\ M_\odot\ ,$$

one finds a tidal radius equal to

$$r_{\rm t} \approx 200\ \left(\frac{\tilde\sigma}{5\ {\rm km/s}}\right)\ \left(\frac{R}{10\ {\rm kpc}}\right)^{3/2}\ {\rm pc}\ .$$

The tidal radius is much larger than the King radius, which equals for typical parameters

$$r_{\rm K} \approx 0.2\left(\frac{\tilde\sigma}{5\ {\rm km/s}}\right)\ \left(\frac{\rho_0}{10^4\ M_\odot\ {\rm pc}^{-3}}\right)^{-1/2}\ {\rm pc}\ .$$

The King radius yields a good estimate for the size of the dense central core of the cluster: the density in an isothermal sphere drops to $\frac{1}{2}\rho_0$ at $r \sim 3r_{\rm K} \sim 1$ pc.

From these estimates one finds from (2.8.23) the typical mass of a globular cluster,

$$M_{\rm c} \sim \frac{2\tilde\sigma^2}{G}\ \left(\frac{\tilde\sigma^2 R^3}{GM_{\rm gal}}\right)^{1/2} \approx 2.5\times 10^6\ \left(\frac{\tilde\sigma}{5\ {\rm km/s}}\right)^3\ \left(\frac{R}{10\ {\rm kpc}}\right)^{3/2}\ M_\odot\ .$$

This estimate compares well with the masses of globular clusters that are inferred from observations.

2.9 Dark matter halos

The singular isothermal sphere is often used as a model for the mass distribution in the *dark halo* believed to be present around many galaxies and clusters. As such it is often used to calculate the effect if *gravitational lenzing* by galaxies and clusters[11].

The existence of dark matter was first noted by the Swiss astronomer Bernard Zwicky in 1942. In his observations of one of the close, rich clusters of Galaxies, the *Coma Cluster*, he found that the individual galaxies were moving so fast that the cluster could not be gravitationally bound by the mass associated with visible matter. It should have flown apart long ago. He postulated that there was an unseen mass present whose gravitional pull is able to confine the cluster, keeping it from flying apart. Although his suggestion was initially ridiculed, we now know that about 80% of all matter in the Universe is invisible.

Some of the most persuasive evidence for dark matter comes from the *rotation curves* of disk galaxies (spiral galaxies). There one measures the rotation speed $V_{\rm rot}$ of hydrogen clouds around the galactic center as a function of the distance to the center. Assuming a circular orbit of radius R in the plane of the galaxy this rotation speed is of order

$$V_{\rm rot} \sim \sqrt{\frac{GM(<R)}{R}}\,. \tag{2.9.1}$$

Here $M(<R)$ is the mass contained *within* the orbit. The gravitational pull of all mass outside the orbit cancels.

On the basis of relation (2.9.1) one expects that the rotation speed decays as

$$V_{\rm rot} \sim \sqrt{\frac{GM_{\rm gal}}{R}} \propto R^{-1/2} \tag{2.9.2}$$

in the outer reaches of the galaxy where almost all of the visible mass is inside the radius R. The observations show something different: rather than the velocity law (2.9.2) one finds for large radii:

$$V_{\rm rot} \sim \text{constant}. \tag{2.9.3}$$

An example of such a rotation curve is shown in the figure below. Using relation (2.9.1) this behaviour implies

$$M(<R) \propto R\,. \tag{2.9.4}$$

[11] e.g. J.A. Peacock, *Cosmological Physics*, Cambridge Univ. Press, 1999, Ch. 4 and Ch. 12

This is exactly the behaviour of an isothermal sphere at large radii, see Eqn. (2.8.19). The observations suggest that each galaxy is sitting inside an invisible dark matter sphere, the *dark halo*, with an extent considerably larger than the size of the visible galaxy. Apparently this dark matter halo obeys the density law of an isothermal sphere at sufficiently large radius.

It is as yet unclear what the composition of this dark matter sphere is. The prejudice of many theorists is that we are dealing with some weakly-interacting, massive particle (WIMP) left over from the early phases of the Big Bang that created our Universe.

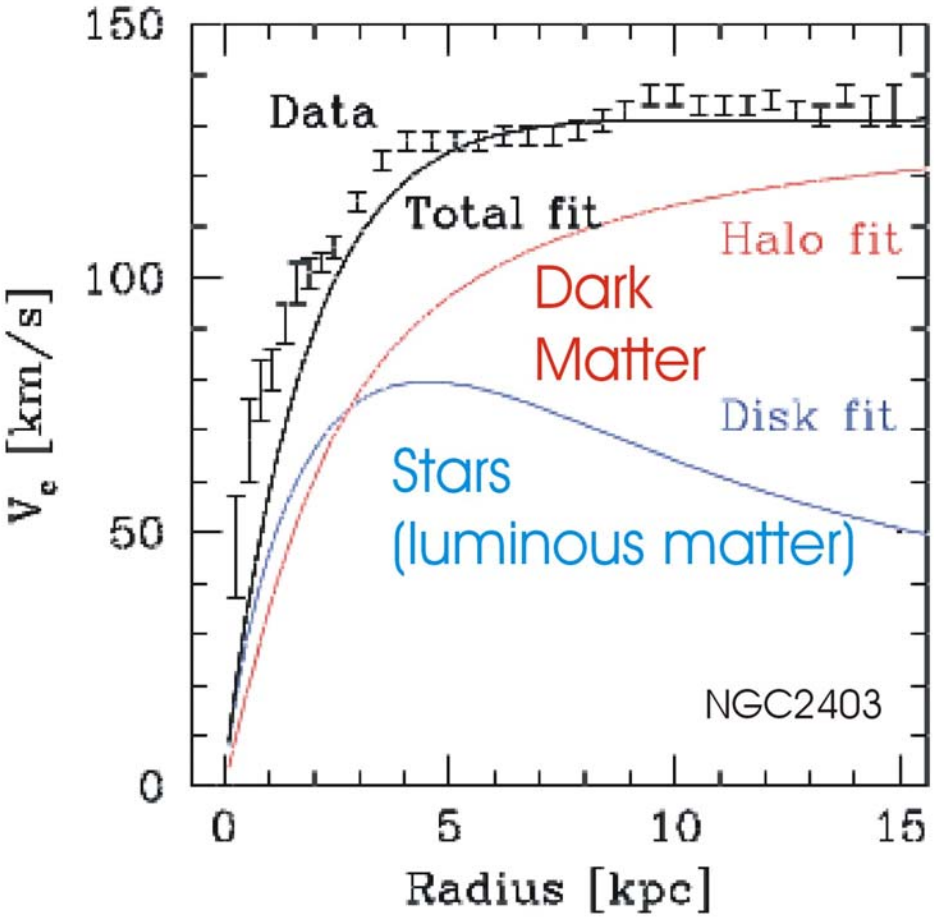

Figure 2.5: *The rotation curve of a spiral galaxy. Note the almost constant rotational speed at large radii. The blue and the red curve give the rotational speed expected from the visible (luminous) matter alone, and the rotation velocity due to the extra mass of the Dark Halo needed to explain the observations. Note that the net rotation speed depends on the total mass, which is dominated by the halo mass at large radii.*

Chapter 3

Conservative fluid equations and conservation laws

3.1 Introduction

There is a formulation of the hydrodynamic equations which is useful for isolating constants of motion in stationary flows, and for the determination of jump conditions at discontinuities such as a shock, or the interface between two different fluids: a contact discontinuity. This formulation forms the basis for most modern numerical codes in computational fluid dynamics and magnetohydrodynamics. This so-called *conservative formulation* takes the following generic form:

$$\frac{\partial}{\partial t}\left(\begin{array}{c}\text{density of}\\ \\ \text{quantity}\end{array}\right)+\boldsymbol{\nabla}\cdot\left(\begin{array}{c}\text{flux of that}\\ \\ \text{quantity}\end{array}\right)=\left(\begin{array}{c}\text{external sources of that}\\ \\ \text{quantity per unit volume}\end{array}\right). \tag{3.1.1}$$

The flux in the divergence term is defined in such a manner that the amount of a quantity passing an oriented infinitesimal surface $\mathrm{d}\boldsymbol{O}$ (a vector!) in a time interval Δt equals

$$\Delta\left(\begin{array}{c}\text{quantity}\\ \\ \end{array}\right)=\left[\left(\begin{array}{c}\text{flux of that}\\ \\ \text{quantity}\end{array}\right)\cdot\mathrm{d}\boldsymbol{O}\right]\times\Delta t\,. \tag{3.1.2}$$

This definition determines what form (vector, tensor, $\cdots$) the flux takes.

If the quantity to be transported is some *scalar field* S, such as the number- or mass density or the concentration of some contaminant, the associated flux must be a *vector field* $\boldsymbol{F}$ so that the quantity $\boldsymbol{F} \cdot \mathrm{d}\boldsymbol{O}$ once again is a scalar. Therefore, in the case of a scalar field the conservative equation takes the form

$$\boxed{\frac{\partial S}{\partial t} + \boldsymbol{\nabla} \cdot \boldsymbol{F} = q(\boldsymbol{x}\ ,\ t)\ ,} \tag{3.1.3}$$

where the source term (the amount added per unit volume and unit time by external sources) has been designated by q. In component-notation, and for cartesian coordinates, equation (3.1.3) reads

$$\frac{\partial S}{\partial t} + \left(\frac{\partial F_x}{\partial x} + \frac{\partial F_y}{\partial y} + \frac{\partial F_z}{\partial z} \right) = q\ . \tag{3.1.4}$$

If the quantity involved is a vector field $\boldsymbol{M}$, such as the momentum density $\rho \boldsymbol{V}$ of a fluid, the flux must be a (rank two) tensor field $\boldsymbol{T}$ so that

$$\boldsymbol{T} \cdot \mathrm{d}\boldsymbol{O} \equiv \sum_{j=1}^{3} T_{ij} \mathrm{d}O_j$$

is once again a vector (meaning: has one free index!). In this case the conservative equation must look like

$$\boxed{\frac{\partial \boldsymbol{M}}{\partial t} + \boldsymbol{\nabla} \cdot \boldsymbol{T} = \boldsymbol{Q}(\boldsymbol{x}\ ,\ t)\ .} \tag{3.1.5}$$

Here the source term $\boldsymbol{Q}$ must be a vector field.

The fact that the flux of a vector field is a rank-2 tensor can be understood as follows. The transported quantity is a vector with three arbitrary components. Each of these vector components can be transported in three independent directions, for instance the directions along the three unit vectors $\hat{\boldsymbol{x}}$, $\hat{\boldsymbol{y}}$ and $\hat{\boldsymbol{z}}$. So, in total, there are 3×3 independent quantities. This is exactly the number of components of a rank-2 tensor in three-dimensional space. For example: a fluid with density ρ and flow velocity $\boldsymbol{V}$ has momentum density $\boldsymbol{M} = \rho \boldsymbol{V}$, which is transported with velocity $\boldsymbol{V}$. Therefore, the momentum flux associated with the mean flow equals $\boldsymbol{T} = \rho \boldsymbol{V} \otimes \boldsymbol{V}$.

This momentum flux tensor has the components

$$T_{ij} = \rho\, V_i V_j \ , \tag{3.1.6}$$

with $i, j = x\,,\ y\,,\ z$. As we will see below, there is also a contribution to the momentum flux of a gas or fluid that is associated with the thermal motion of the molecules or atoms in the fluid.

The divergence of a rank two tensor (i.e. a tensor with two free indices) is defined in cartesian coordinates as

$$\boldsymbol{\nabla}\cdot\boldsymbol{T} = \begin{pmatrix} \dfrac{\partial T_{xx}}{\partial x} + \dfrac{\partial T_{yx}}{\partial y} + \dfrac{\partial T_{zx}}{\partial z} \\ \dfrac{\partial T_{xy}}{\partial x} + \dfrac{\partial T_{yy}}{\partial y} + \dfrac{\partial T_{zy}}{\partial z} \\ \dfrac{\partial T_{xz}}{\partial x} + \dfrac{\partial T_{yz}}{\partial y} + \dfrac{\partial T_{zz}}{\partial z} \end{pmatrix} . \tag{3.1.7}$$

This means that the component-form of (3.1.5) reads

$$\frac{\partial}{\partial t}\begin{pmatrix} M_x \\ M_y \\ M_z \end{pmatrix} + \begin{pmatrix} \dfrac{\partial T_{xx}}{\partial x} + \dfrac{\partial T_{yx}}{\partial y} + \dfrac{\partial T_{zx}}{\partial z} \\ \dfrac{\partial T_{xy}}{\partial x} + \dfrac{\partial T_{yy}}{\partial y} + \dfrac{\partial T_{zy}}{\partial z} \\ \dfrac{\partial T_{xz}}{\partial x} + \dfrac{\partial T_{yz}}{\partial y} + \dfrac{\partial T_{zz}}{\partial z} \end{pmatrix} = \begin{pmatrix} Q_x \\ Q_y \\ Q_z \end{pmatrix} . \tag{3.1.8}$$

The strength of this form of the equations lies in *Stokes theorem*, an integral relation between the volume integral of a divergence and the integral of the flux over the surface bounding that volume. Let $\mathcal{V}$ be some volume, and $\mathrm{d}\boldsymbol{O} \equiv \mathrm{d}O\ \hat{\boldsymbol{n}}$ an element of the surface $\partial\mathcal{V}$ of that volume, defined in such a way that the unit vector $\hat{\boldsymbol{n}} \equiv (n_x\,,\ n_y\,,\ n_z)$ is pointing outwards. Stokes law, valid for both vectors and tensors, then reads:

$$\int_{\mathcal{V}} \mathrm{d}\mathcal{V} \begin{pmatrix} \boldsymbol{\nabla}\cdot\boldsymbol{F} \\ \boldsymbol{\nabla}\cdot\boldsymbol{T} \end{pmatrix} = \oint_{\partial\mathcal{V}} \mathrm{d}\boldsymbol{O}\cdot \begin{pmatrix} \boldsymbol{F} \\ \boldsymbol{T} \end{pmatrix} . \tag{3.1.9}$$

In cartesian coordinates the surface integrals should be interpreted as

$$\begin{aligned} \int \mathrm{d}\boldsymbol{O}\cdot\boldsymbol{F} &= \int \mathrm{d}O\,(\hat{\boldsymbol{n}}\cdot\boldsymbol{F}) \\ &= \int \mathrm{d}O\;(n_xF_x+n_yF_y+n_zF_z) \end{aligned} \tag{3.1.10}$$

if the transported quantity is a scalar, and as

$$\int \mathrm{d}\boldsymbol{O}\cdot\boldsymbol{T} = \int \mathrm{d}O\,(\hat{\boldsymbol{n}}\cdot\boldsymbol{T}) \tag{3.1.11}$$

if the transported quantity is a vector. Here $\hat{\boldsymbol{n}}\cdot\boldsymbol{T}$ is a vector, with components

$$(\hat{\boldsymbol{n}}\cdot\boldsymbol{T}) \equiv \begin{pmatrix} n_xT_{xx}+n_yT_{yx}+n_zT_{zx} \\ n_xT_{xy}+n_yT_{yy}+n_zT_{zy} \\ n_xT_{xz}+n_yT_{yz}+n_zT_{zz} \end{pmatrix} . \tag{3.1.12}$$

Here $\mathrm{d}O$ is the magnitude of the surface element, and $\hat{\boldsymbol{n}}$ is the oriented unit vector normal to that surface element, which always points *outwards* (i.e away from the volume).

For instance, if one takes the volume integral of the scalar conservative equation (3.1.3) and applies Stokes' theorem, one finds that

$$\frac{\partial}{\partial t}\left(\int_{\mathcal{V}} \mathrm{d}\mathcal{V}\,S\right) = \int_{\mathcal{V}} \mathrm{d}\mathcal{V}\,q(\boldsymbol{x}\,,\,t) - \oint_{\partial\mathcal{V}} \mathrm{d}\boldsymbol{O}\cdot\boldsymbol{F}\,. \tag{3.1.13}$$

This integral relation states that the amount of quantity S in a volume can only change due to sources contained within that volume (first term on the right-hand side), or by a flux of that quantity into the volume (when $\boldsymbol{F}\cdot\mathrm{d}\boldsymbol{O} < 0$) or out of the volume (when $\boldsymbol{F}\cdot\mathrm{d}\boldsymbol{O} > 0$) across its outer surface, as described by the second term on the right-hand side.

3.2 Conservative form of the fluid equations

In the preceding Chapter, the equations of motion for an ideal fluid have been derived by analogy with Newtonian dynamics, with the help of mass conservation and some simple thermodynamics. With a considerable amount of algebra the fluid equations can be cast into the special *conservative* form discussed above.

The equation of mass conservation,

$$\frac{\partial \rho}{\partial t} + \boldsymbol{\nabla} \cdot (\rho \boldsymbol{V}) = 0 \, , \tag{3.2.1}$$

already has the required form (3.1.3) for a scalar field (in this case ρ), without external sources and with flux vector equal to the mass flux $\rho \boldsymbol{V}$. I now will derive conservative equations for the momentum and energy of a fluid.

3.2.1 Conservative momentum equation

The momentum equation (2.5.3),

$$\rho \left[\frac{\partial \boldsymbol{V}}{\partial t} + (\boldsymbol{V} \cdot \boldsymbol{\nabla}) \, \boldsymbol{V} \right] = -\boldsymbol{\nabla} P - \rho \, \boldsymbol{\nabla} \Phi \, , \tag{3.2.2}$$

can also be cast in conservative form. First we use the chain rule, together with (3.2.1), to rewrite the time derivative of the velocity in the form

$$\begin{aligned} \rho \frac{\partial \boldsymbol{V}}{\partial t} &= \frac{\partial (\rho \boldsymbol{V})}{\partial t} - \boldsymbol{V} \, \frac{\partial \rho}{\partial t} \\ &= \frac{\partial (\rho \boldsymbol{V})}{\partial t} + \boldsymbol{V} \, (\boldsymbol{\nabla} \cdot (\rho \boldsymbol{V})) \, . \end{aligned} \tag{3.2.3}$$

Substituting this into the equation of motion one finds:

$$\frac{\partial (\rho \boldsymbol{V})}{\partial t} + (\boldsymbol{\nabla} \cdot (\rho \boldsymbol{V})) \, \boldsymbol{V} + \rho (\boldsymbol{V} \cdot \boldsymbol{\nabla}) \boldsymbol{V} = -\boldsymbol{\nabla} P - \rho \boldsymbol{\nabla} \Phi \, . \tag{3.2.4}$$

By applying relation (2.3.9) for the divergence of a dyadic tensor $\boldsymbol{A} \otimes \boldsymbol{B}$, with $\boldsymbol{A} = \rho \boldsymbol{V}$ and $\boldsymbol{B} = \boldsymbol{V}$, we can combine the second and third term on the left-hand side of this equation.

One finds:

$$(\boldsymbol{\nabla}\cdot(\rho\boldsymbol{V}))\,\boldsymbol{V}+\rho\,(\boldsymbol{V}\cdot\boldsymbol{\nabla})\boldsymbol{V}=\boldsymbol{\nabla}\cdot\,(\rho\boldsymbol{V}\otimes\boldsymbol{V})\ . \tag{3.2.5}$$

In addition, one can write the pressure force as a divergence:

$$\boldsymbol{\nabla}P=\boldsymbol{\nabla}\cdot(P\,\boldsymbol{I})\ . \tag{3.2.6}$$

Using these relations, one finds the conservative form for the equation of motion:

$$\boxed{\frac{\partial(\rho\boldsymbol{V})}{\partial t}+\boldsymbol{\nabla}\cdot\,(\rho\boldsymbol{V}\otimes\boldsymbol{V}+P\,\boldsymbol{I})=-\rho\boldsymbol{\nabla}\Phi\ .} \tag{3.2.7}$$

By defining the *momentum density vector* $\boldsymbol{M}$ of the fluid, and the *stress tensor* $\boldsymbol{T}$ as

$$\boldsymbol{M}\equiv\rho\boldsymbol{V}\quad,\quad\boldsymbol{T}\equiv\rho\boldsymbol{V}\otimes\boldsymbol{V}+P\,\boldsymbol{I}\ , \tag{3.2.8}$$

this equation assumes the standard form (3.1.5) for the tranport of a vector:

$$\frac{\partial\boldsymbol{M}}{\partial t}+\boldsymbol{\nabla}\cdot\boldsymbol{T}=-\rho\,\boldsymbol{\nabla}\Phi\ . \tag{3.2.9}$$

The gravitational force on the fluid acts as the momentum source in this case.

The term $\rho\,\boldsymbol{V}\otimes\boldsymbol{V}$ in the definition (3.2.8) of the momentum flux tensor $\boldsymbol{T}$ is what one expects naively. The second term involving the pressure P is the momentum flux associated with the thermal motions. Using the definitions of the previous Chapter this flux is equal to

$$\rho\,\overline{\boldsymbol{\sigma}\otimes\boldsymbol{\sigma}}=\frac{\rho\overline{\sigma^2}}{3}\,\boldsymbol{I}=P\,\boldsymbol{I}\ . \tag{3.2.10}$$

Here I have used $\overline{\sigma_i\sigma_j}=(\overline{\sigma^2}/3)\,\delta_{ij}$ and the definitions of the pressure and the unit rank-2 rensor $\boldsymbol{I}$.

It is easily checked, using the rules of averaging outlined in the previous chapter in our derivation of the pressure force, that the total momentum flux tensor is exactly what one expects if one averages the momentum flux of all particles:

$$\boldsymbol{T} = \rho\,\overline{\boldsymbol{u}_\alpha \otimes \boldsymbol{u}_\alpha} = \rho\,\left(\boldsymbol{V}\otimes\boldsymbol{V} + \overline{\boldsymbol{\sigma}\otimes\boldsymbol{\sigma}}\right) = \rho\,\left(\boldsymbol{V}\otimes\boldsymbol{V}\right) + P\,\boldsymbol{I}\,. \tag{3.2.11}$$

3.2.2 Conservative form of the energy equation

Starting point for the derivation of an equation for the total energy of the fluid is the equation of motion:

$$\rho\left(\frac{\partial \boldsymbol{V}}{\partial t} + (\boldsymbol{V}\cdot\boldsymbol{\nabla})\boldsymbol{V}\right) = -\boldsymbol{\nabla}P - \rho\boldsymbol{\nabla}\Phi\,. \tag{3.2.12}$$

First we derive an equation for the kinetic energy. Using the vector identity

$$(\boldsymbol{V}\cdot\boldsymbol{\nabla})\boldsymbol{V} = \boldsymbol{\nabla}(\tfrac{1}{2}V^2) - \boldsymbol{V}\times(\boldsymbol{\nabla}\times\boldsymbol{V}) \tag{3.2.13}$$

and taking the scalar product of Eqn. (3.2.12) with $\boldsymbol{V}$ one finds:

$$\rho\,\frac{\partial}{\partial t}\left(\tfrac{1}{2}V^2\right) + \rho(\boldsymbol{V}\cdot\boldsymbol{\nabla})\left(\tfrac{1}{2}V^2\right) = -(\boldsymbol{V}\cdot\boldsymbol{\nabla})P - \rho(\boldsymbol{V}\cdot\boldsymbol{\nabla})\Phi\,. \tag{3.2.14}$$

Using the equation of mass conservation once again,

$$\begin{aligned}\rho\,\frac{\partial}{\partial t}\left(\tfrac{1}{2}V^2\right) &= \frac{\partial}{\partial t}\left(\tfrac{1}{2}\rho V^2\right) - \tfrac{1}{2}V^2\,\left(\frac{\partial\rho}{\partial t}\right)\\ &= \frac{\partial}{\partial t}\left(\tfrac{1}{2}\rho V^2\right) + \tfrac{1}{2}V^2\,\boldsymbol{\nabla}\cdot(\rho\boldsymbol{V})\,,\end{aligned} \tag{3.2.15}$$

together with the vector identity

$$\rho(\boldsymbol{V}\cdot\boldsymbol{\nabla})\left(\tfrac{1}{2}V^2\right) + \tfrac{1}{2}V^2\,\boldsymbol{\nabla}\cdot(\rho\boldsymbol{V}) = \boldsymbol{\nabla}\cdot\left[\rho\boldsymbol{V}\,\left(\tfrac{1}{2}V^2\right)\right]\,, \tag{3.2.16}$$

Eqn. (3.2.14) becomes an equation for the kinetic energy density $\frac{1}{2}\rho V^2$ of the fluid:

$$\frac{\partial}{\partial t}\left(\frac{\rho V^2}{2}\right) + \boldsymbol{\nabla}\cdot\left(\rho\boldsymbol{V}\,\frac{V^2}{2}\right) = -(\boldsymbol{V}\cdot\boldsymbol{\nabla})P - \rho(\boldsymbol{V}\cdot\boldsymbol{\nabla})\Phi\,. \tag{3.2.17}$$

This equation shows how the kinetic energy of the fluid changes due to work done by pressure forces (first term on the right-hand side) and by the gravitational force (second term on the right-hand side). The pressure force and gravitational force act as sources of kinetic energy. The kinetic energy flux $\rho\boldsymbol{V}\,(\frac{1}{2}V^2)$ merely redistributes the kinetic energy over space.

To derive an equation for the *total* energy one must use the thermodynamic relation 2.7.12:

$$\begin{aligned} \mathrm{d}Q = T\,\mathrm{d}s &= \mathrm{d}e + P\,\mathrm{d}\left(\frac{1}{\rho}\right) \\ &= \mathrm{d}\left(e + \frac{P}{\rho}\right) - \frac{\mathrm{d}P}{\rho}\,. \end{aligned} \tag{3.2.18}$$

Defining the *enthalpy* per unit mass as

$$h \equiv e + \frac{P}{\rho}\,, \tag{3.2.19}$$

one has for an ideal fluid with adiabatic index $\gamma = c_\mathrm{p}/c_\mathrm{v}$:

$$\begin{aligned} e &= c_\mathrm{v}\,T = \frac{1}{\gamma-1}\,\frac{k_\mathrm{b}T}{m} = \frac{P}{(\gamma-1)\rho} \\ h &= c_\mathrm{p}\,T = \frac{\gamma}{\gamma-1}\,\frac{k_\mathrm{b}T}{m} = \frac{\gamma P}{(\gamma-1)\rho}\,. \end{aligned} \tag{3.2.20}$$

The second relation in (3.2.18) allows one to write the pressure gradient as

$$\boldsymbol{\nabla}P = \rho\boldsymbol{\nabla}h - \rho T\boldsymbol{\nabla}s\,. \tag{3.2.21}$$

In addition, the first relation in (3.2.18) implies

$$\begin{aligned} \rho \frac{\partial e}{\partial t} &= \rho T \frac{\partial s}{\partial t} + \frac{P}{\rho^2} \frac{\partial \rho}{\partial t} \\ &= \rho T \frac{\partial s}{\partial t} - \frac{P}{\rho} \boldsymbol{\nabla} \cdot (\rho \boldsymbol{V}) \, . \end{aligned} \tag{3.2.22}$$

Here I employed the now well-known trick of using mass conservation to eliminate $\partial\rho/\partial t$.

Adding equation (3.2.22) for the internal energy e to equation (3.2.17) for the kinetic energy, eliminating the pressure gradient using (3.2.21), one finds after some rearrangement of terms:

$$\begin{aligned} \frac{\partial}{\partial t}\left(\tfrac{1}{2}\rho V^2 + \rho\, e\right) &+ \boldsymbol{\nabla} \cdot \left[\rho \boldsymbol{V}\left(\tfrac{1}{2}V^2 + h\right)\right] = \\ &= \rho T \left(\frac{\partial s}{\partial t} + (\boldsymbol{V} \cdot \boldsymbol{\nabla}) s\right) - \rho\, (\mathbf{V} \cdot \boldsymbol{\nabla})\Phi \, . \end{aligned} \tag{3.2.23}$$

The first term on the right-hand side corresponds to the irreversible changes in the internal energy of the fluid. This can be can be seen by using the first law of thermodynamics in the form

$$\rho T \left(\frac{\partial s}{\partial t} + (\boldsymbol{V} \cdot \boldsymbol{\nabla}) s\right) = \mathcal{H} \, , \tag{3.2.24}$$

where $\mathcal{H}$ is the amount of heat irreversibly added (or removed) from the gas *per unit volume* by *external* agents[1]. The second term corresponds to the work done by the gravitational field. It can be rewritten using the definition of $\mathrm{d}/\mathrm{d}t$ together with mass conservation:

$$\begin{aligned} \rho(\boldsymbol{V} \cdot \boldsymbol{\nabla})\Phi &= \rho \frac{\mathrm{d}\Phi}{\mathrm{d}t} - \rho \frac{\partial \Phi}{\partial t} \\ &= \frac{\partial(\rho\Phi)}{\partial t} + \boldsymbol{\nabla} \cdot (\rho \boldsymbol{V}\, \Phi) - \rho \frac{\partial \Phi}{\partial t} \, . \end{aligned} \tag{3.2.25}$$

[1] In this derivation I assume that internal friction (viscosity) is not present in the gas. That case will be treated later.

Substituting relations (3.2.24) and (3.2.25) into (3.2.23) yields the final form of the energy conservation law:

$$\boxed{\frac{\partial}{\partial t}\left(\tfrac{1}{2}\rho\, V^2 + \rho e + \rho\Phi\right) + \boldsymbol{\nabla}\cdot\left[\rho \boldsymbol{V}\left(\tfrac{1}{2}V^2 + h + \Phi\right)\right] = \mathcal{H}_{\rm eff}\ .} \tag{3.2.26}$$

Here the 'net heating rate' per unit volume is given by:

$$\mathcal{H}_{\rm eff} \equiv \mathcal{H} + \rho\,\frac{\partial\Phi}{\partial t}\ . \tag{3.2.27}$$

The first term in $\mathcal{H}_{\rm eff}$ is the *true* heating (or cooling) due to 'external' irreversible processes such as radiation losses. The second 'gravitational heating' term $\propto \partial\Phi/\partial t$ corresponds to the process known as *violent relaxation* in a time-varying gravitational potential.

This violent relaxation term is formally completely analogous to the non-conservation of energy of a single particle in a time-dependent gravitational field. A particle of mass m moving in a gravitational field with potential $\Phi(\boldsymbol{x}\ ,\ t)$ obeys the equation of motion:

$$m\,\frac{{\rm d}\boldsymbol{v}}{{\rm d}t} = -m\,\boldsymbol{\nabla}\Phi\ . \tag{3.2.28}$$

A simple example is the motion of a single star in a galaxy or globular cluster. The star feels the fluctuating gravitational field due to all other stars. These stars themselves all move around in the galaxy or globular cluster, leading to a very 'granular' and strongly time-dependent gravitational potential.

Taking the scalar product with the velocity $\boldsymbol{v} = {\rm d}\boldsymbol{x}/{\rm d}t$ yields:

$$m\,\boldsymbol{v}\cdot\frac{{\rm d}\boldsymbol{v}}{{\rm d}t} = \frac{\rm d}{{\rm d}t}\left(\tfrac{1}{2}mv^2\right) = -m(\boldsymbol{v}\cdot\boldsymbol{\nabla})\Phi\ . \tag{3.2.29}$$

The kinetic energy of the particle changes due to the work done by the gravitational field. Now, the total time derivative of the potential along the particle orbit is

$$\frac{{\rm d}\Phi}{{\rm d}t} = \frac{\partial\Phi}{\partial t} + (\boldsymbol{v}\cdot\boldsymbol{\nabla})\Phi\ . \tag{3.2.30}$$

This means that we can rewrite (3.2.29) as

$$\frac{\mathrm{d}}{\mathrm{d}t}\left(\tfrac{1}{2}mv^2 + m\Phi\right) = m\,\frac{\partial\Phi}{\partial t}\,. \tag{3.2.31}$$

This shows that the total particle energy,

$$\mathcal{E} \equiv \tfrac{1}{2}mv^2 + m\,\Phi\,, \tag{3.2.32}$$

is *not* conserved in a gravitational field that *explicitly* depends on time so that $\partial\Phi/\partial t \neq 0$. In that case the gravitational field is not a conservative force field.

Violent relaxation plays an important role in the dynamics of galaxies, where it acts in a way analogous to a heating mechanism.

Chapter 4

Steady flows

4.1 Basic equations

The conservative form of the fluid equations are a powerful tool in the case of *steady flows*: flows where the relation

$$\frac{\partial}{\partial t}\,(\text{any flow quantity}) = 0 \tag{4.1.1}$$

is satisfied. We will limit most of the discussion to the case of *adiabatic flows* where there is no net heating: $\mathcal{H} = 0$.

The basic equations for a steady adiabatic flow read:

$$\text{mass conservation:} \qquad \boldsymbol{\nabla} \cdot (\rho \boldsymbol{V}) = 0 \; ; \tag{4.1.2}$$

$$\text{momentum conservation:} \qquad \boldsymbol{\nabla} \cdot (\rho\, \boldsymbol{V} \otimes \boldsymbol{V} + P\, \boldsymbol{I}) = -\rho \boldsymbol{\nabla} \Phi \; ; \tag{4.1.3}$$

$$\text{energy conservation:} \qquad \boldsymbol{\nabla} \cdot \left[\rho \boldsymbol{V} \left(\tfrac{1}{2} V^2 + h + \Phi\right)\right] = 0 \; . \tag{4.1.4}$$

In addition, the adiabatic gas law holds:

$$P\, \rho^{-\gamma} = \text{constant.} \tag{4.1.5}$$

By combining the mass conservation equation and the energy conservation law, using

the vector relation

$$\boldsymbol{\nabla} \cdot (f\boldsymbol{A}) = f\,(\boldsymbol{\nabla} \cdot \boldsymbol{A}) + (\boldsymbol{A} \cdot \boldsymbol{\nabla}) f\ ,$$

it follows that the energy conservation law can also be written as

$$(\boldsymbol{\nabla} \cdot \rho \boldsymbol{V})\ \left(\tfrac{1}{2}V^2 + h + \Phi\right) + \rho(\boldsymbol{V} \cdot \boldsymbol{\nabla})\left(\tfrac{1}{2}V^2 + h + \Phi\right) = 0\ . \tag{4.1.6}$$

Because of the mass conservation law the first term vanishes, and one is left with

$$(\boldsymbol{V} \cdot \boldsymbol{\nabla})\left(\tfrac{1}{2}V^2 + h + \Phi\right) = 0\ . \tag{4.1.7}$$

This alternative form of the energy conservation law has a simple interpretation. Consider the **flowlines** or streamlines of a flow field (see figure), defined as a trajectory $\boldsymbol{x} = \boldsymbol{X}(\ell)$ such that the *tangent vector* to the line is always parallel to the local flow velocity:

$$\frac{\mathrm{d}\boldsymbol{X}}{\mathrm{d}\ell} \parallel \boldsymbol{V}(\boldsymbol{X})\ . \tag{4.1.8}$$

Here ℓ is a length parameter along the flow line, which can always be chosen such that the tangent vector has unit length:

$$\left|\frac{\mathrm{d}\boldsymbol{X}}{\mathrm{d}\ell}\right| = 1. \tag{4.1.9}$$

In that case the a fluid element courses along the flow line with velocity $V = |\boldsymbol{V}|$ so that

$$\frac{\mathrm{d}\ell}{\mathrm{d}t} = V\ . \tag{4.1.10}$$

In the case of a steady flow, the flow lines are an infinite set of fixed curves through space. The coordinates of points on a given flow line satisfy the (rather obvious) difference relation

$$\mathrm{d}\boldsymbol{X} = \boldsymbol{V}(\boldsymbol{x} = \boldsymbol{X})\,\mathrm{d}t\ . \tag{4.1.11}$$

Writing this definition in cartesian components, e.g. $\boldsymbol{X} = (X\ ,\ Y\ ,\ Z)$ and $\mathrm{d}X = V_x(\boldsymbol{X})\,\mathrm{d}t$ etc., this definition can be written as a set of difference equations:

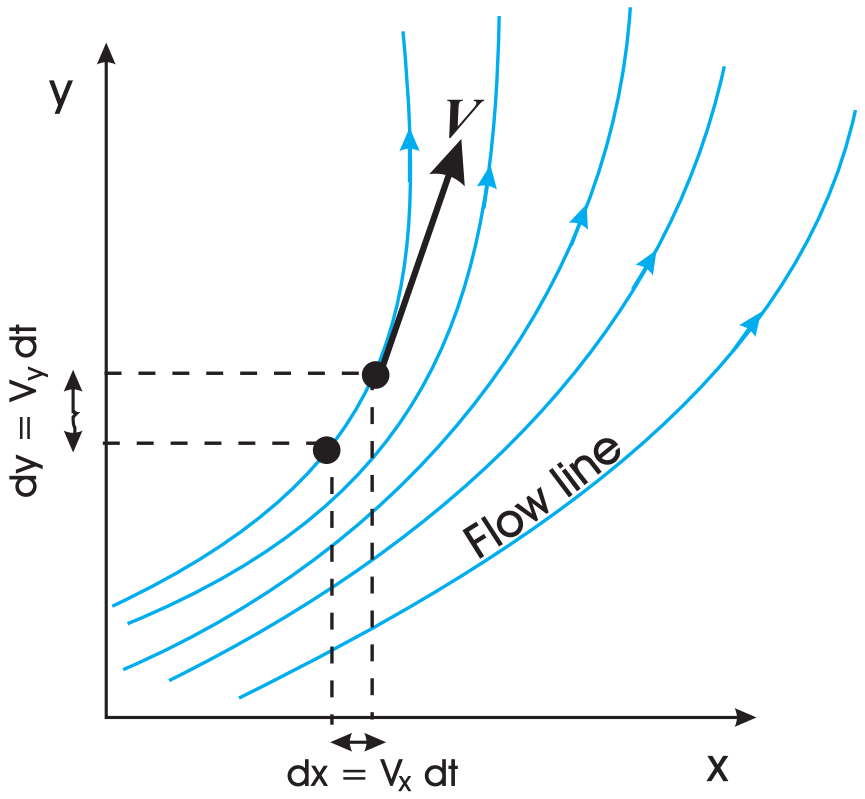

Figure 4.1: *Flow lines in the $x-y$ plane for a steady flow. At each point along a flow line, the flow velocity is tangent to the line. The coordinates $(x\ ,\ y)$ along a given flow line therefore satisfy the relation $\mathrm{d}x = V_x\ \mathrm{d}t$ and $\mathrm{d}y = V_y\ \mathrm{d}t$.*

$$\frac{\mathrm{d}X}{V_x(\boldsymbol{X})} = \frac{\mathrm{d}Y}{V_y(\boldsymbol{X})} = \frac{\mathrm{d}Z}{V_z(\boldsymbol{X})} = \frac{\mathrm{d}\ell}{|\boldsymbol{V}|} = \mathrm{d}t \ . \tag{4.1.12}$$

Let us assume that some quantity $f(\boldsymbol{x})$ is *constant* along the flowlines $\boldsymbol{x} = \boldsymbol{X}(\ell)$. This implies

$$\frac{\mathrm{d}f}{\mathrm{d}\ell} = \frac{\mathrm{d}X}{\mathrm{d}\ell}\,\frac{\partial f}{\partial x} + \frac{\mathrm{d}Y}{\mathrm{d}\ell}\,\frac{\partial f}{\partial y} + \frac{\mathrm{d}Z}{\mathrm{d}\ell}\,\frac{\partial f}{\partial z} = 0 \ . \tag{4.1.13}$$

This relation essentially defines for any function $f(x\ ,\ y\ ,\ z)$ the quantity

$$\mathrm{d}f \equiv \mathrm{d}x\,\frac{\partial f}{\partial x} + \mathrm{d}y\,\frac{\partial f}{\partial y} + \mathrm{d}z\,\frac{\partial f}{\partial z} \tag{4.1.14}$$

for infinitesimally small $\mathrm{d}x$, $\mathrm{d}y$ and $\mathrm{d}z$, see the Mathematical Appendix on Internet.

One can express relation (4.1.13) in terms of the displacement vector $\mathrm{d}\boldsymbol{X} = (\mathrm{d}X, \mathrm{d}Y, \mathrm{d}Z)$ along a flow line and the gradient $\boldsymbol{\nabla} f$ (also a vector!) of the function $f(\boldsymbol{x})$:

$$(\mathrm{d}\boldsymbol{X} \cdot \boldsymbol{\nabla}) f(\boldsymbol{x}) = 0 \ . \tag{4.1.15}$$

Using definition $\mathrm{d}\boldsymbol{X} = \boldsymbol{V}\ \mathrm{d}t$ it is easily seen that this requirement is equivalent with

$$(\boldsymbol{V} \cdot \boldsymbol{\nabla}) f(\boldsymbol{x}) = 0 \ . \tag{4.1.16}$$

Note that all explicit reference to the streamlines (e.g. ℓ) has disappeared. Condition (4.1.16) ensures that the function $f(\boldsymbol{x})$ is constant along *any* streamline in a steady flow. However, a variation of $f(\boldsymbol{x})$ *across* streamlines is still allowed by this relation, and the value of f will in general vary from streamline to streamline.

The energy conservation law (4.1.7) in a steady flow can now be represented by a constraint equation known as *Bernoulli's law*:

$$\boxed{\tfrac{1}{2}V^2 + \frac{\gamma P}{(\gamma - 1)\,\rho} + \Phi = \text{constant along flowlines} \ .} \tag{4.1.17}$$

The quantity

$$\mathcal{E} \equiv \tfrac{1}{2}V^2 + \frac{\gamma P}{(\gamma-1)\,\rho} + \Phi \tag{4.1.18}$$

is the *total energy per unit mass*. This quantity which contains the following contributions: [1] the kinetic energy per unit mass $V^2/2$ of the mean flow, [2] the thermodynamic energy per unit mass due to thermal motions and [3] the gravitational potential energy Φ per unit mass. Here I have used the definition of the enthalpy per unit mass for an ideal gas, $h = \gamma P/(\gamma-1)\rho$.

It is important to realize that Bernouilli's law only states that the $\mathcal{E}$ does not vary *along* a flow line. It says nothing about the variation of $\mathcal{E}$ *across* flowlines! Therefore, $\mathcal{E}$ constant may differ from flowline to flowline, which implies that in general it is not a **global** constant over all of space.

Our assumption of no heating implies, according to (4.1.5) that for each fluid element the relation

$$\frac{\mathrm{d}}{\mathrm{d}t}\left(P\,\rho^{-\gamma}\right) = (\boldsymbol{V}\cdot\boldsymbol{\nabla})\left(P\,\rho^{-\gamma}\right) = 0 \tag{4.1.19}$$

must hold. If we use definition (2.7.24) for the specific entropy S of an ideal gas this can be written as:

$$(\boldsymbol{V}\cdot\boldsymbol{\nabla})s = (\boldsymbol{V}\cdot\boldsymbol{\nabla})\left[c_{\mathrm{v}}\ln\left(P\,\rho^{-\gamma}\right)\right] = 0\ .\ , \tag{4.1.20}$$

The flow is *isentropic* along a given flowline. This leads to a second constraint on the flow:

$$\boxed{s = c_{\mathrm{v}}\ln\left(P\rho^{-\gamma}\right) = \text{constant along flowlines}\ .} \tag{4.1.21}$$

This relation could also have been derived from the entropy equation Eqn. (3.2.24) with $\mathcal{H} = 0$ (no irreversibe heating) and $\partial s/\partial t = 0$ (steady flow).

4.2 Application 1: the Parker model for a stellar wind

The constraint equations derived in the previous Section are sufficient to derive flow properties in those cases where the flow lines are known *a priori*. Invariably, these are cases where the physical situation has a high degree of symmetry.

The simplest example of relevance for astrophysical applications are *spherically symmetric flows*. There the flowlines are radial lines, and if the flow is steady the velocity vector takes the form

$$\boldsymbol{V}(\boldsymbol{x}) = V(r)\,\hat{\boldsymbol{e}}_r\ . \tag{4.2.1}$$

Here $\hat{\boldsymbol{e}}_r$ is a unit vector in the radial direction. All flow quantities depend only on the radial distance r to the origin.

In this case the mass conservation equation, $\boldsymbol{\nabla}\cdot(\rho\boldsymbol{V}) = 0$, reads

$$\frac{1}{r^2}\,\frac{\partial}{\partial r}\,\Big[r^2\rho(r)V(r)\Big] = 0\ . \tag{4.2.2}$$

The factors r^2 appearing in this equation arise because of the use of the spherical coordinate r: the radial flow lines diverge! The area $\mathcal{A}$ of a bundle of radial flowlines increases with radius as $\mathcal{A}\propto r^2$. Equation (4.2.2) can be integrated immediately:

$$\rho(r)\,V(r)\,r^2 = \text{constant} \equiv \frac{\dot{M}}{4\pi}\ . \tag{4.2.3}$$

Here the constant $\dot{M}$ is the amount mass that crosses a spherical surface at arbitrary r with area $4\pi r^2$ each second.

The other two constraints are Bernouilli's law (conservation of the energy per unit mass),

$$\tfrac{1}{2}V^2(r) + \frac{\gamma P(r)}{(\gamma-1)\,\rho(r)} + \Phi(r) = \text{constant} \equiv \mathcal{E}\ , \tag{4.2.4}$$

and the condition for an adiabatic (isentropic) flow:

$$P(r) = \text{constant} \times \rho^{\gamma}(r) \ . \tag{4.2.5}$$

In this highly-symmetric case the conserved quantities $\dot{M} = 4\pi\ r^2 \rho V$, $\mathcal{E}$ and $s = c_{\rm v}\ \log(P\rho^{-\gamma})$ are in fact *global* constants of the flow: they take the same value at any radius.

We will limit the discussion to the case of flows near a star of mass M_*, which determines the Newtonian gravitational potential:

$$\Phi(r) = -\frac{GM_*}{r} \ . \tag{4.2.6}$$

The mass conservation law (4.2.3) implies the following relation for the infinitesimal density change $\mathrm{d}\rho$ along a radial flowline:

$$\mathrm{d}\dot{M} = 4\pi\ \left\{ (r^2\ V)\ \mathrm{d}\rho + (\rho\, r^2)\ \mathrm{d}V + (2\rho\, V)\ r\mathrm{d}r \right\} = 0 \ . \tag{4.2.7}$$

This relation can be written as:

$$\frac{\mathrm{d}\rho}{\rho} = -\left(\frac{\mathrm{d}V}{V} + 2\,\frac{\mathrm{d}r}{r} \right) \ . \tag{4.2.8}$$

Energy flux conservation, $\mathrm{d}\mathcal{E} = 0$, implies

$$V\ \mathrm{d}V + \mathrm{d}\left[\frac{\gamma P}{(\gamma-1)\ \rho} \right] + \frac{GM_*}{r^2}\ \mathrm{d}r = 0 \ . \tag{4.2.9}$$

Here I have used the Newtonian potential (4.2.6) so that

$$\mathrm{d}\Phi = \frac{\mathrm{d}\Phi}{\mathrm{d}r}\ \mathrm{d}r = \frac{GM_*}{r^2}\ \mathrm{d}r \ . \tag{4.2.10}$$

The second term in (4.2.9) can be rewritten, using condition (4.2.5) for an isentropic flow:

$$\mathrm{d}\left[\frac{\gamma P}{(\gamma-1)\ \rho} \right] = \mathrm{d}h = \frac{\mathrm{d}P}{\rho} = \left(\frac{\partial P}{\partial \rho} \right)\ \frac{\mathrm{d}\rho}{\rho} \ . \tag{4.2.11}$$

The *adiabatic sound speed* $c_{\rm s}$ is defined as[1]

$$c_{\rm s} \equiv \sqrt{\frac{\partial P}{\partial \rho}} = \sqrt{\frac{\gamma P}{\rho}} = \sqrt{\frac{\gamma \mathcal{R} T}{\mu}} \; . \tag{4.2.12}$$

Using this definition one has $\mathrm{d}h = c_{\rm s}^2(\mathrm{d}\rho/\rho)$, and the energy conservation constraint becomes

$$V \, \mathrm{d}V + c_{\rm s}^2 \, \frac{\mathrm{d}\rho}{\rho} + \frac{GM_*}{r^2} \, \mathrm{d}r = 0 \; . \tag{4.2.13}$$

Substituting (4.2.8) for $\mathrm{d}\rho/\rho$ and re-ordering the resulting equation one finds:

$$\left(V^2 - c_{\rm s}^2 \right) \, \frac{\mathrm{d}V}{V} = \left(2c_{\rm s}^2 - \frac{GM_*}{r} \right) \, \frac{\mathrm{d}r}{r} \; . \tag{4.2.14}$$

This equation can be written as a differential equation. Using the relations $\mathrm{d}r/r = \mathrm{d}\ln r$ and $\mathrm{d}V/V = \mathrm{d}\ln V$ we find an equation that is known as the *Parker equation*, named after the American astrophysicist Gene Parker:

$$\boxed{\left(V^2 - c_{\rm s}^2 \right) \, \frac{\mathrm{d}\ln V}{\mathrm{d}\ln r} = 2c_{\rm s}^2 - \frac{GM_*}{r} \; .} \tag{4.2.15}$$

Parker proposed this equation for the *Solar Wind*[2], a tenuous stream of particles emanating form the Sun with a net mass loss of

$$\dot{M}_\odot \approx 10^{-14} \;\; M_\odot/\mathrm{yr} \; .$$

The possible existence of a Solar Wind was the subject of much discussion in the 1950/60's. It had been noted in the 1950's by German astrophysicist Biermann that the most plausible explanation for the behaviour of the tails of comets (known from their spectra to contain ionized matter) was the existence of a stream or wind of ionized matter from the Sun. It had also been noted that the activity of the Sun, and the occurence of such geophysical phenomena such as the Northern Lights (*Aurora Borealis*) are related, which hints at an agent propagating from the Sun to the Earth.

[1] As we will show in the next Chapter this is the propagation speed for sound waves in an adiabatic gas.

[2] E.N. Parker: *Phys. Fluids* **1**, 171, 1958

The existence of such a wind is also plausible for another reason: the outer layer of the Solar atmosphere, the *Corona*, has a temperature $T \sim 2 \times 10^6$ K. This was known from observations of the Corona during a solar eclipse. At such temperatures, the proton thermal velocity is of order

$$v_{\rm p} = \sqrt{\frac{3k_{\rm b}T}{m_{\rm p}}} \sim 200 \ {\rm km/s} \ ,$$

fairly close to the escape velocity of the Sun:

$$v_\odot^{\rm esc} \sim \sqrt{\frac{2GM_\odot}{r_\odot}} \sim 620 \ {\rm km/s} \ .$$

This would mean that protons in the tail of the thermal maxwellian distribution, with a velocity some three times the mean thermal velocity, could in principle escape from the Sun.

Such considerations (among others) led Parker to his hypothesis. His prediction of the existence of the Solar Wind and of its velocity near Earth (~ 400 km/s) was convincingly demonstrated to be correct by the first satellite measurements around 1960. The history of the subject can be found in the book by Brandt[3]

We now know that the Sun is not unique: many stars show signs of mass loss, some much stronger than the Sun [4]. Bright young stars (O-B-stars), Wolf Rayet and Be-stars and the stars on the *Asymptotic Giant Branch* have strong winds, some with velocities up to 3000 km/s. Given the large mass-loss rate in some of these cases ($\dot{M} \sim 10^{-8} - 10^{-5} \ M_\odot/{\rm yr}$) the existence of such a *stellar wind* can have a distinct influence on the evolution of the star concerned. It is also believed that *Young Stellar Objects*, stars in the evolutionary phase immediately after the ignition of stellar nucleosynthesis in their core, have strong outflows. In some cases the stellar winds have a visible influence on their surroundings: they blow a hot bubble of tenuous gas in the much colder surrounding interstellar medium.

The manner in which the wind material is accelerated away from the star is not always the same. In cool stars, such as our Sun, the wind is the result of the presence of the hot corona. Such corona's are probably the result of the magnetic activity of the star, which requires the presence of a *convection zone* just below the visible stellar surface. In this case pressure forces are ultimately responsible for the wind. In hot stars on the other hand the wind is driven by radiation forces which result from the absorption of photons by metals in the wind material.

[3] J.C. Brandt, *Introduction to the Solar Wind*, W.H. Freeman and Company, San Francisco, 1970

[4] For a wide-ranging introduction: H.J.G.L.M. Lamers & J.P. Cassinelli, *Introduction to Stellar Winds*, Cambridge Univ. Press, 1999, Ch. 2.

4.2.1 The critical point condition

In the case of Parker's wind model the wind is 'driven' by the large pressure (and the associated thermal energy) of the material in the Solar Corona. In the wind, the thermal energy is converted into the kinetic energy of the outward motion. This means that the flow must accelerate away from the star, $\mathrm{d}V/\mathrm{d}r > 0$, and must also go from subsonic flow ($V < c_\mathrm{s}$) to a supersonic flow ($V > c_\mathrm{s}$).

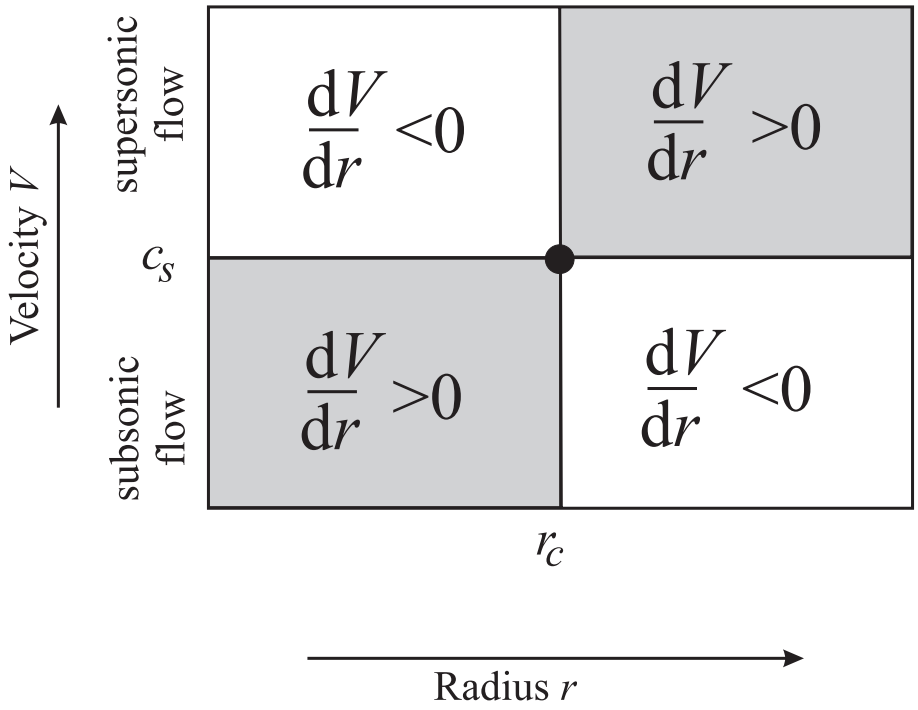

Figure 4.2: *A schematic representation of the solution plane of the Parker equation. The radius varies in the horizontal direction, and the flow velocity V in the vertical direction. The solution plane can be divided into four regions, depending on $V < c_\mathrm{s}$ (subsonic flow) or $V > c_\mathrm{s}$ (supersonic flow), and on the conditions $r < r_\mathrm{c}$ and $r > r_\mathrm{c}$. The* **critical point** *is located intersection of the boundaries of these regions, at $V = c_\mathrm{s}$ and $r = r_\mathrm{c} = GM_*/2c_\mathrm{s}^2$. In the lower left and upper right panes of this diagram the flow accelerates so that $\mathrm{d}V/\mathrm{d}r > 0$. In the lower right and upper left panes the flow decelerates so that $\mathrm{d}V/\mathrm{d}r < 0$.*

If one tries to solve Parker's equation,

$$\left(V^2 - c_\mathrm{s}^2\right) \frac{\mathrm{d}\ln V}{\mathrm{d}\ln r} = 2c_\mathrm{s}^2 - \frac{GM_*}{r}\,, \tag{4.2.16}$$

one is faced with a difficulty: the term in front of $\mathrm{d}\ln V/\mathrm{d}\ln r$ vanishes if the flow velocity equals the local sound speed so that $V(r) = c_{\rm s}(r)$. At that radius where this occurs the velocity derivative $\mathrm{d}V/\mathrm{d}r$ will go to infinity, *unless* the right-hand side of equation (4.2.16) vanishes simultaneously:

$$2c_{\rm s}^2(r) - \frac{GM_*}{r} = 0 \; . \tag{4.2.17}$$

The requirement that infinities in the solution should be avoided leads to the **critical point conditions**. These relate the flow speed V, the sound speed $c_{\rm s}$ and the value of the critical radius $r_{\rm c}$:

$$V(r = r_{\rm c}) = c_{\rm s}(r = r_{\rm c}) = \sqrt{\frac{GM_*}{2r_{\rm c}}} \; . \tag{4.2.18}$$

The critical point (also called *sonic point*) occurs at a radius

$$r_{\rm c} = \frac{GM_*}{2c_{\rm sc}^2} \; , \tag{4.2.19}$$

with $c_{\rm sc} \equiv c_{\rm s}(r = r_{\rm c})$. These conditions plays a central role in the Parker wind theory.

The reason for this behaviour is easily seen if one considers a schematic representation of the solution plane of Parker's equation, shown in the figure above. The solution must inevitably go through the critical point, where $V = c_{\rm s}$ and $r = GM_*/2c_{\rm s}^2 = r_{\rm c}$, if the wind starts subsonically ($V < c_{\rm s}$) at small radii near the stellar surface, becomes supersonic ($V > c_{\rm s}$) at some distance from the star, and continues to accelerate so that $\mathrm{d}V/\mathrm{d}r > 0$ throughout the flow: the true wind solutions.

Note that condition (4.2.19) is an implicit equation if the sound speed varies with radius. Once this the location of the critical point is determined, the mass loss can be calculated immediately:

$$\dot{M} = 4\pi r_{\rm c}^2 \rho_c c_{\rm sc} = \frac{\pi \rho_{\rm c} (GM_*)^2}{c_{\rm sc}^3} \tag{4.2.20}$$

Here $\rho_{\rm c}$ and $c_{\rm sc}$ are the density and sound speed at the critical point. This critical point condition defines a **unique** solution: there are **no** other admissable solutions which can make a smooth transition from a subsonic outward flow to a supersonic outward flow.

4.2.2 Isothermal winds

A special case is the *isothermal wind* where one assumes

$$P = nk_{\rm b}T_0 = \frac{\rho\mathcal{R}T_0}{\mu} \qquad (\mathcal{R} = k_{\rm b}/m_{\rm H})\,, \tag{4.2.21}$$

with a *constant* temperature T_0. Formally for a pressure-density relation of the form $P \propto \rho^\gamma$ this corresponds with $\gamma = 1$, and the above expressions are no longer valid: the enthalpy $h = \gamma P/(\gamma-1)\,\rho$ becomes infinite!

This problem can be circumvented by defining the enthalpy as the '$P{\rm d}\mathcal{V}$'-work done per unit mass:

$$h(\rho) \equiv \int_{\rho_0}^{\rho} \frac{{\rm d}P}{\rho} = \begin{cases} \dfrac{\mathcal{R}T_0}{\mu}\,\ln\left(\dfrac{\rho}{\rho_0}\right) & \text{isothermal gas with } \gamma = 1 \\ \\ \dfrac{\gamma P}{(\gamma-1)\,\rho} & \text{polytropic gas with } \gamma > 1 \end{cases}. \tag{4.2.22}$$

Here ρ_0 is an arbitrary reference density which is put equal to zero for $\gamma > 1$. Note that this definition reduces for $\gamma > 1$ to the case already discussed above.

The sound speed in this case, called the *isothermal sound speed*, is constant as it depends only on temperature:

$$c_{\rm si} = \sqrt{\frac{\partial P}{\partial \rho}} = \sqrt{\frac{\mathcal{R}T_0}{\mu}} = \text{constant}. \tag{4.2.23}$$

This fact allows a direct calculation of the location of the critical point. In an isothermal wind it occurs at a radius

$$r_{\rm ci} = \frac{GM_*}{2c_{\rm si}^2} = \frac{GM_*}{2(\mathcal{R}T_0/\mu)}\,, \tag{4.2.24}$$

determined only by the assumed temperature T_0 and the mass M_* of the star. The conserved energy per unit mass along flowlines now equals

$$\mathcal{E} = \tfrac{1}{2}V^2 + c_{\rm si}^2\,\ln\left(\frac{\rho}{\rho_*}\right) - \frac{GM_*}{r}\,. \tag{4.2.25}$$

Here the reference density is chosen to be the density ρ_* at the stellar surface.

Evaluating $\mathcal{E}$ twice, once at the stellar surface $r = r_*$, assuming that the velocity is much less than the escape velocity (i.e. $V(r_*) \ll \sqrt{2GM_*/r_*}$), and once at the critical point $r = r_{\rm ci}$ where $V = c_{\rm si}$, one can derive a relation for the density at the critical point, given the density at the stellar surface:

$$\ln\left(\frac{\rho_{\rm c}}{\rho_*}\right) \approx \frac{3}{2} - \frac{2r_{\rm ci}}{r_*} \,, \tag{4.2.26}$$

where I have used $\rho_* \equiv \rho(r_*)$. Given the temperature T_0 in the wind this determines the density at the critical point, and the total mass loss $\dot{M}$:

$$\dot{M} = \frac{\pi\rho_{\rm c}(GM_*)^2}{(\mathcal{R}T_0/\mu)^{3/2}} \,. \tag{4.2.27}$$

Such an isothermal solution applies whenever there is a mechanism that acts as a 'thermostat' to keep the wind temperature constant. An example of such a mechanism is a strong radiation field which forces the material to remain at a temperature equal to the effective temperature of the radiation.

Let us apply this model to the Sun. Assuming T_0 to be the typical coronal temperature derived from observations, $T_0 = 2 \times 10^6$ K, the isothermal sound speed equals

$$c_{\rm si} \approx 138 \ {\rm km/s} \,,$$

and the critical radius is[5]

$$r_{\rm ci} \approx 3.5 \times 10^{11} \ {\rm cm} \simeq 5 \ R_\odot \,.$$

This implies a density at the critical point equal to

$$\rho_{\rm c} \approx e^{-8.5}\rho_* \approx 3.4 \times 10^{-20} \ {\rm g/cm^3} \,,$$

and a mass loss rate[6]

$$\dot{M} \simeq 6.7 \times 10^{11} \ {\rm g/s} = 1.1 \times 10^{-14} \ M_\odot/{\rm yr} \,.$$

Here I used relation (4.2.26) with the observed *number* density $n_* \sim 10^8$ cm^{-3} at the base of the Solar Corona, corresponding to $\rho_* \sim n_* m_{\rm p} \approx 1.6 \times 10^{-16}$ g/cm^3. This crude estimate of the Solar mass loss rate is suprisingly close to the observed value, even though the Solar Wind is not isothermal or spherically symmetric.

[5] The Solar radius is equal to $R_\odot = 6.96 \times 10^{10}$ cm.

[6] $1 \ M_\odot/{\rm yr} = 6.3 \times 10^{25}$ g/s

4.3 Application 2: Bondi accretion

There is another solution of the Parker equation, which corresponds to a flow towards a star, so that matter *accretes* onto the star. This is the case of *Bondi accretion*.

The velocity is still in the radial direction, but it is directed *inward*. In order to keep V positive we write:

$$\boldsymbol{V}(\boldsymbol{x}) = -V(r)\,\hat{\boldsymbol{e}}_r \tag{4.3.1}$$

with $V(r) > 0$. The equation of mass conservation looks exactly the same as in the case of an outflowing wind, but now refers to the amount of mass accreting on the star per second:

$$4\pi r^2\,\rho(r)\,V(r) = \text{constant} = \dot{M}\ , \tag{4.3.2}$$

The same goes for the energy constraint and the condition of an adiabatic (or isothermal) flow:

$$\tfrac{1}{2}V^2(r) + h(\rho) + \Phi(r) = \text{constant} = \mathcal{E}\ , \tag{4.3.3}$$

and

$$P(\rho) = \text{constant} \times \rho^\gamma\ . \tag{4.3.4}$$

As long as the enthalpy $h(\rho)$ is defined according to Eqn. (4.2.22) the isothermal case $\gamma = 1$ is included in these equations. This means that Parker's equation (4.2.15) for $V(r)$ also describes this inward accretion flow.

4.3.1 Why accretion?

The most powerful sources known in the astronomical 'zoo' are powered by accretion: the infall of matter on a compact object under the influence of gravity. Accreting sources include *close binaries* in our Galaxy, where tidal forces due to the companion star pull mass from a normal star after which this mass accretes on the compact companion star (white dwarf, neutron star or even a stellar-mass black hole), and the 'central engines' powering *active galaxies* and *quasars*, which involve massive black holes with a mass between $10^6 - 10^8\ M_\odot$.

A full account of accretion phenomena can be found in the book of Frank, King and Raine[7]. The reason why accretion is so important can be summarized in one word: *efficiency*. Accretion is the most efficient way of liberating energy in astrophysical sources.

Let us define the efficiency ϵ of *any* energy-generating process in terms of the amount of mass processed per second, $\dot{M}$, and the power (luminosity) L produced by this process, by writing the latter as:

$$L = \epsilon \times \dot{M}c^2 \ . \tag{4.3.5}$$

A 'maximally efficient' process ($\epsilon = 1$) would convert an amount of energy equal to the rest energy of the accreting material into some form of radiation.

The efficiency of accretion as a power source can be estimated by a simple argument. Assume that a particle falls towards a compact object with mass M_* and radius R_*. If it starts out at an infinite distance with zero velocity, the velocity at radius R equals the *free-fall velocity*:

$$V_{\rm ff}(R) = \sqrt{\frac{2GM_*}{R}} \tag{4.3.6}$$

Now suppose all the kinetic energy of the free fall is converted into energy when the particle reaches the surface of the star at radius $R = R_*$. The total amount of energy liberated per second for a mass flow $\dot{M}$ equals in that case:

$$\boxed{L = \frac{1}{2}\,\dot{M}V_{\rm ff}^2 = \frac{GM_*\dot{M}}{R_*}\ .} \tag{4.3.7}$$

The associated efficiency follows from its definition in Eqn. (4.3.5):

$$\epsilon_{\rm acc} = \frac{L}{\dot{M}c^2} = \frac{GM_*}{R_*c^2}\ . \tag{4.3.8}$$

This expression can be written in a form which makes it immediately obvious why especially *compact* sources shine most brightly.

[7] J. Frank, A. King & D. Raine, *Accretion Power in Astrophysics*, second edition, Cambridge University Press, 1992

The *Schwarzschild radius* for a mass M_* is defined as

$$R_{\rm s} = \frac{2GM_*}{c^2} \ . \tag{4.3.9}$$

Classically it corresponds to the radius where the escape velocity (equal to the free-fall velocity) equals the velocity of light (c). In General Relativity the Schwarzschild radius corresponds to the 'radius' of a non-rotating *black hole*: no signal originating from within the sphere bounded by the Schwarzschild radius $R_{\rm S}$ can reach an outside observer at infinity. In terms of the Schwarzschild radius the efficiency of accretion can be written as:

$$\epsilon_{\rm acc} \sim R_{\rm s}/2R_* \ . \tag{4.3.10}$$

The reason I have put a $\sim$ sign here is to emphasize that this must be interpreted as a rough (order-of-magnitude) estimate. Of course, near a black hole one should use fully relativistic expressions. As an order-of-magnitude estimate however equation (4.3.10) is sufficiently accurate.

The following table gives the typical parameters for a number of accreting objects.

Object	**Mass**	**Radius** R_* (m)	$R_{\rm s}/R_*$
White Dwarf	$\leq 1.4\ M_\odot$	$\sim 10^7$	$\sim 3\times10^{-4}$
Neutron Star	$\sim 1.4\ M_\odot$	$\sim 10^4$	~ 0.3
Black Hole	$M_{\rm bh}$	$3\ 10^3(M_{\rm bh}/M_\odot)$	1

One can compare the efficiency of accretion as a power source with nuclear burning. The proton-proton cycle, which powers our Sun, has an efficiency of nuclear burning which can be calculated from the energy liberated per hydrogen nucleus lost in the fusion reactions:

$$\Delta E_{\rm pp} = 6.55\ {\rm MeV} \ . \tag{4.3.11}$$

The efficiency for the proton-proton cycle simply follows as[8]

$$\epsilon_{\rm pp} = \frac{\Delta E_{\rm pp}}{m_{\rm p}c^2} \sim 7 \times 10^{-3} \; . \tag{4.3.12}$$

Comparing this value with the efficiency of accretion $\epsilon_{\rm acc}$ in the above table, one sees that the yield of nuclear burning of a similar amount of mass can only be competitive with accretion in the case of accretion onto a white dwarf. Accretion on a neutron star and a black hole is far more efficient than the nuclear burning.

4.3.2 Bondi's solution

Consider a star embedded in a cloud of interstellar gas with density ρ_∞ and temperature T_∞, both at large ('infinite') distance from the star. The associated sound speed is $c_\infty = \sqrt{\gamma \mathcal{R} T_\infty/\mu}$.

If we assume that the flow at $r \longrightarrow \infty$ satisfies $V_\infty \approx 0$, Bernouilli's law, $\mathcal{E} =$ constant, tells us that

$$\tfrac{1}{2}V^2 + \frac{c_{\rm s}^2}{\gamma - 1} - \frac{GM_*}{r} = h_\infty = \frac{c_\infty^2}{\gamma - 1} \; . \tag{4.3.13}$$

Here h_∞ is the enthalpy per unit mass of the interstellar gas, and I have used that for $\gamma \neq 1$ one can write the enthalpy h in terms of the adiabatic sound speed $c_{\rm s} = \sqrt{\gamma P/\rho}$:

$$h = \frac{c_{\rm s}^2}{\gamma - 1} \; . \tag{4.3.14}$$

A true accretion flow must go from a subsonic flow far from the star, to supersonic flow close to the stellar surface. The flow speed close to the star will be close to the free-fall velocity. In view of our definition (4.3.1) this implies that $\mathrm{d}V/\mathrm{d}r < 0$ throughout the flow: V increases as r decreases! This means that the accretion flow, like a Parker wind, has to go through the critical point of the Parker equation such that

$$V(r_{\rm c}) = c_{\rm s}(r_{\rm c}) \equiv c_{\rm sc} \;\; \text{at} \;\; r_{\rm c} = \frac{GM_*}{2c_{\rm sc}^2} \; . \tag{4.3.15}$$

For an ideal gas with $P \propto \rho^\gamma$ with $\gamma > 1$ one can actually find a solution.

[8] Proton rest energy equals $E_0 = m_{\rm p}c^2 = 938.27$ MeV

Applying (4.3.13) at the critical radius yields

$$c_{\rm sc}^2 \left[\tfrac{1}{2} + \frac{1}{\gamma-1} - 2 \right] = \frac{c_\infty^2}{\gamma-1} \ . \tag{4.3.16}$$

From this one immediately finds the value of the sound speed at the critical radius:

$$c_{\rm sc} = c_\infty \left(\frac{2}{5-3\gamma} \right)^{1/2} \ . \tag{4.3.17}$$

For $P \propto \rho^\gamma$ the sound speed scales with density as $c_{\rm s} = \sqrt{\gamma P/\rho} \propto \rho^{(\gamma-1)/2}$. One can use this to find the density $\rho_{\rm c}$ at the critical radius:

$$\rho_{\rm c} = \rho_\infty \left(\frac{c_{\rm sc}}{c_\infty} \right)^{2/(\gamma-1)} \ . \tag{4.3.18}$$

This finally yields the mass accretion rate:

$$\boxed{\dot{M} = 4\pi r_{\rm c}^2 \, \rho_{\rm c} \, c_{\rm sc} = 4\pi\kappa \, \rho_\infty c_\infty \left(\frac{GM_*}{c_\infty^2} \right)^2 \ .} \tag{4.3.19}$$

Here κ is a numerical constant of order unity,

$$\kappa = 2^{-(\gamma+1)/2(\gamma-1)} \left(\frac{5-3\gamma}{4} \right)^{-(5-3\gamma)/2(\gamma-1)} \ .$$

The quantity

$$\frac{GM_*}{c_\infty^2} \equiv r_{\rm acc} \tag{4.3.20}$$

which appears in this expression is the so-called *accretion radius*. In terms of this accretion radius the critical radius is located at

$$r_{\rm c} = \left(\frac{5-3\gamma}{4} \right) r_{\rm acc} \ , \tag{4.3.21}$$

where I used Eqns. (4.3.15) and (4.3.17). The value of the constant κ is tabulated below for different values of γ, including the isothermal case $\gamma = 1$:[9]

Values of the accretion constant κ

γ	κ
1	1.120
4/3	0.707
7/4	0.625
3/2	0.500
5/3	0.250

Let us calculate the Bondi accretion rate for a star accreting from the interstellar medium. One believes that the interstellar medium (outside the dense molecular clouds) can roughly be thought of as consisting of two phases, the *cold phase* where most hydrogen is in HI (neutral atoms) and the *hot phase* where hydrogen is (partially) ionized (HII). One believes these two phases coexist roughly in pressure equilibrium, with most of the volume in the cold phase. The properties of the ISM are tabulated below.

Properties of the general ISM

phase	**number density** (in cm^{-3})	**temperature** (in K)	**sound speed** (in km/s)
Cold phase gas (HI)	10^2	$\sim 10^4$	10
Hot phase gas (HII)	~ 1	$\sim 10^6$	100
Molecular Clouds	3×10^2	~ 30	2

[9] From: S.L. Shapiro & S.A. Teukolsky, *Black Holes, White Dwarfs and Neutron Stars*, J. Wiley & Sons, 1983, p. 415

From this one can calculate the Bondi accretion rate for a star with mass M_*. Assuming $\gamma \approx 5/3$ and using $\rho_\infty \sim n_\infty\, m_{\rm p}$, with $m_{\rm p} \approx 1.67 \times 10^{-24}$ g the protons mass, one finds:

$$\dot{M} \approx 1.5 \times 10^{-15} \left(\frac{M_*}{M_\odot}\right)^2 \left(\frac{n_\infty}{1\ {\rm cm}^{-3}}\right) \left(\frac{c_\infty}{10\ {\rm km/s}}\right)^{-3} M_\odot/{\rm yr}\ . \tag{4.3.22}$$

Although Bondi accretion is an interesting exercise in hydrodynamics, it is difficult to realize in nature. The reason is simple: *angular momentum*. The assumption of radial flow lines means that the accretion flow carries no angular momentum. In most cases, and in particular in accretion processes in close binaries, the angular momentum is all-important: one needs some form of friction to get rid of it so that the material can actually reach the star. Without friction, the centrifugal force associated with the rotation of the material prevents accretion, essentially forcing the gas into quasi-Keplerian orbits.

In the case where a significant amount of angular momentum is carried by the flow, accretion proceeds in an entirely different fashion: **disk accretion**, a process which we will consider in the Chapter on rotating flows.

4.4 Solutions Parker's equation: a graphical representation

The two fundamental solutions to the Parker equation presented above, a pressure-driven stellar wind and the spherical accretion on a star, are not the only solutions. Figure 4.4 gives a graphical representation of all solutions to the equation for an isothermal flow ($\gamma = 1$), represented in terms of the isothermal Machnumber $\mathcal{M}_i = V/c_{\rm si}$ of the flow as a function of the dimensionless radius $\xi \equiv r/r_{\rm ci} = 2c_{\rm si}^2 r/GM_*$. Here $V \equiv |\boldsymbol{V}|$ is the magnitude of the flow velocity. There are four different classes of solution curves:

- The Parker wind solution and the Bondi accretion solution, two unique solutions which go through the critical point at $\xi = 1$. There they make the transition from subsonic ($\mathcal{M}_{\rm i} < 1$) to supersonic ($\mathcal{M}_{\rm i} > 1$) flow. They are the *only* solutions that make this transition. In the figure they are represented by thick solid lines.

- The *Solar breeze* solutions, represented by the thick dashed lines. These solutions remain subsonic ($\mathcal{M}_i < 1$) for all radii, and the flow speed has a maximum at the critical radius ($\xi = 1$). These solutions where proposed by Chapman for the outflow of material from the Sun, hence the name. Observations clearly show that this not the case: the solar wind at Earth is supersonic.

- A branch of supersonic solutions with $\mathcal{M}_i > 1$ at all radii. These are represented by a thick dash-dot curve in the figure. These solutions are unphysical because they do not satisfy sensible boundary conditions: the flow has to *start* supersonically!

- Two sets of unphysical, double-valued solutions which remain entirely within or outside the critical radius ($\xi < 1$ and $\xi > 1$ respectively). These solutions are represented by thin dash-dot curves, and can not be realized since there are two possible velocities, one subsonic and one supersonic, for a given radius.

One thing about these solutions should be realized: we have assumed throughout that the flow velocity is a *continuous* function of radius, without sudden jumps, such as *shocks* where the flow makes a sudden transition from supersonic to subsonic flow. One could imagine that, by inserting such jumps into the flow, one could connect one solution branch to another, while still satisfying mass- and energy conservation. It turns out that the constraints set by the conservation laws are so stringent that the insertion of a shock in a spherical accretion flow is only possible if one gives up the assumption of an adiabatic flow by introducing heating processes.[10] The physics of shocks will be considered in Chapter 6.

[10]For a review: S.K. Chakrabarti, *Accretion Processes on a Black Hole*, Phys. Rep. **266**, 229, 1996, Chapter 2

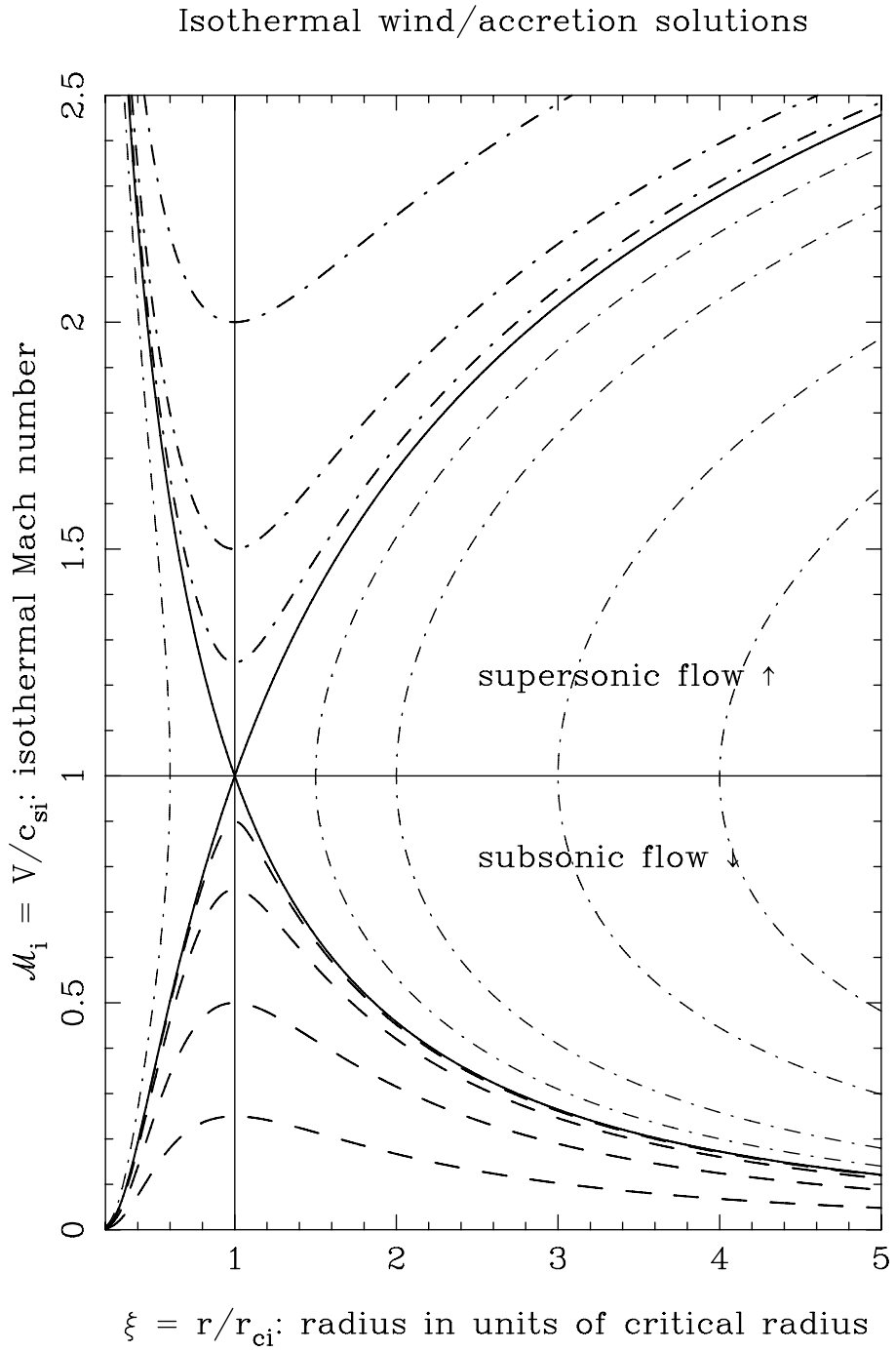

Figure 4.3: *Diagram showing the possible solutions to Parker's equation, assuming an isothermal wind with* $T = \text{constant}$, $\gamma = 1$. *Only the Parker wind solution and Bondi solution (solid lines) can make the transition from subsonic to supersonic flow at the critical point. All solution curves which are represented by dash-dot lines are unphysical.*

Chapter 5

Jet flows

5.1 Introduction

There is a class of stationary flows of great importance to astrophysics: *jet flows*. These are flows which can be considered as almost one-dimensional in the sense: the streamlines are confined to quasi-cylindrical surfaces with a small opening angle. Jets are highly collimated streams of matter, not unlike the exhaust of hot gas from a jet engine, or the water stream from a high-pressure firehose.

Jets are observed in a number of astrophysical objects, as summarized in the table below:

Astrophysical jets

Object	**jet length** (in pc)	**jet power** (in W)	**opening angle** (in degrees)	**flow speed** (in units of c)
Gamma Ray Bursts	0.01	10^{43}	~ 0.01	1
Young stellar objects	$0.01 - 1$	$10^{28} - 10^{30}$	$1 - 10$	0.01
Microquasars in X-ray binaries	~ 1	10^{31} (?)	small	$0.3 - 1$
Radio galaxies and quasars	$10^3 - 10^6$	$10^{35} - 10^{40}$	$1 - 10$	$0.2 - 1$

The jets associated Young Stellar Objects and microquasars are associated with stellar-mass objects, in the case of microquasars neutron stars of black holes. Radio galaxies and quasars contain massive black holes with a mass of $10^6 - 10^8\ M_\odot$. The jets associated with *Gamma Ray Bursts* are special: they are formed *inside* a massive star when the core of this star collapses directly into a black hole: a so-called *hypernova*. The Gamma Ray Burst phenomenon produces short-lived, very powerful jets where an energy of $\sim 10^{52}$ ergs (1% of the rest-energy of one solar mass) is liberated in 10-100 seconds. The jets produced in this manner are *ultra-relativistic*, with a speed $V_{\rm j}$ corresponding to a Lorentz factor $\Gamma_{\rm j} = 1/\sqrt{1 - V_{\rm j}^2/c^2} \sim 100 - 300$.

The common denominator of all these sources is that they derive their power from the accretion of matter, probably through an accretion disk. Some process associated with this accretion disk is capable of accelerating a small fraction of the accreted material to high velocities, expelling it from the system in a narrowly collimated flow.

5.1.1 A bit of history

Historically, the need for the existence of such flows was first realized in the context of powerful double radio galaxies. Double radio sources consist of two radio-emitting clouds on either side of the parent galaxy. The archetypical example is the radio galaxy Cygnus A (see figure), one of the strongest radiosources in the sky, which Baade and Minkowski identified in 1954 as being associated with an elliptical galaxy.

The radio emission is *synchrotron radiation* from relativistic electrons spiralling in a magnetic field of $1 - 100\ \mu$G. This can be inferred from the observed properties of the radiation: its spectrum and the polarization. Radio telescopes operate on wavelengths of the cm-meter range, corresponding to frequencies of order MHz-GHz. The theory of synchrotron radiation [1] gives the typical frequency of the radiating electron (charge e and mass $m_{\rm e}$) in terms of its energy E and the magnetic field strength B as

$$\nu_{\rm s} \simeq \frac{3}{4\pi}\,\frac{eB}{m_{\rm e}c}\,\left(\frac{E}{m_{\rm e}c^2}\right)^2 = \frac{3}{4\pi}\,\frac{eB}{m_{\rm e}c}\,\gamma^2\ , \tag{5.1.1}$$

with γ the Lorentz-factor of an electron with energy $E = \gamma m_{\rm e}c^2$. In practical units this frequency corresponds to:

$$\nu = 16.1\ B_{\mu{\rm G}}\ E^2_{\rm GeV}\ {\rm MHz}\ . \tag{5.1.2}$$

[1] e.g. G.B. Rybicki & A.P. Lightman: *Radiative Processes in Astrophysics*, J. Wiley & Sons, 1979, Ch. 6

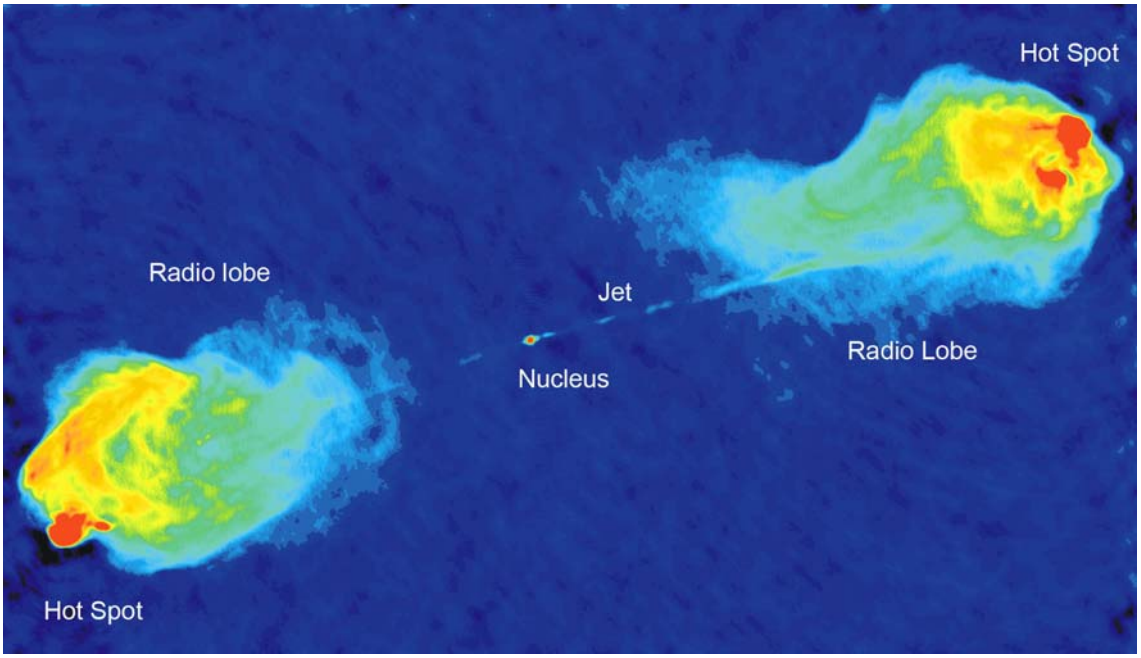

Figure 5.1: *The radio galaxy* **Cygnus A**, *one of the most powerful radio galaxies in the sky. This shows a false-color map of the synchrotron emission at a wavelength* $\lambda = 6$ *cm* ($\nu = 5$ *Ghz). The location of the nucleus of the active galaxy, the one visible jet and of the Hot Spots (red) is indicated. Around the hot spots, extensive* radio lobes *(yellow) are formed. These lobes are clouds of relativistic, synchrotron-emitting electrons that have been accelerated in the shocks that form the hot spots. The electron clouds are then left behind as the jets push further into the surrounding intergalactic medium. The galaxy that hosts the massive Black Hole, which is responsible for the jets, is invisible in this radio image, as the stars that make up the galaxy emit very little power at radio frequencies. The distance between the two Hot Spots is* ~ 150 *kpc.* Image credit: R. Perley, C. Carilli & J. Dreher, NRAO/AUI/NSF.

So, given the typical field strengths in many sources, which ranges from 10^{-6} to 10^{-4} G, one observes the radio emission from electrons with energies of order $E \simeq 10$ MeV - 10 GeV, corresponding to Lorentz-factors of order $\gamma \simeq 10^2 - 10^5$.

The electrons loose their energy as a result of the emitted synchrotron radiation. The typical loss-time of an electron of energy E in a magnetic field B is

$$\tau_{\rm loss}(E,B) \simeq 8 \times 10^9 \, B_{\mu\rm G}^{-2} \, E_{\rm GeV}^{-1} \ {\rm yr} \ . \tag{5.1.3}$$

Combining Eqns. (5.1.2) and (5.1.3), one can express the loss time in terms of the observing frequency ν and the fieldstrength B in the source:

$$\tau_{\rm loss}(\nu,B) \simeq 2 \times 10^9 \, B_{\mu\rm G}^{-3/2} \, \nu_{\rm MHz}^{-1/2} \ {\rm yr} \ . \tag{5.1.4}$$

This quantity gives the typical time a source will be able to maintain its synchrotron power before fading out due to energy losses. So a powerful source with $B \sim 10$ μG, observed at a wavelength of 21 cm (the famous wavelength for observing neutral hydrogen, which corresponds with a frequency of $\nu \sim 1.4$ Ghz), will fade away in a few million years *unless* it is continuously resupplied with energy.

Many of the observed powerful radio galaxies must be older than the synchrotron loss time: their linear size is larger than (loss time) $\times$ (velocity of light)! This observation led Roger Blandford and Martin Rees[2] to the conclusion that the older models, which proposed that the radio clouds are expelled from the parent galaxy in a *single* explosive event, can not be correct. They argued that there must be a *continuous* supply of energy from the 'central engine' in the nucleus of the active galaxy or quasar to the clouds of radio emission which lie at a distance up to several Mpc. They proposed that a strongly collimated flow of matter,[3] a so-called *jet*, furnishes this supply. It was not long before advances in radio astronomy made it possible to observe these jets. The figure below shows a modern radio observation of the jet in the elliptical galaxy M87.

Around 1985 it became obvious that the synchrotron emission from some sources extends into the optical ($\nu \sim 400$ THz). Electrons at these frequencies have a synchrotron loss time of only $\sim$ 1000-100,000 years! This radiation can only be maintained if the radiating electrons are continuously resupplied *in situ*.

[2] R.D. Blandford & M.J. Rees: *Mon. Not. Roy. astr. Soc.* **169**, 395, 1974; one of the most-quoted papers in modern astrophysics

[3] They also left open the possibility that the 'jet' consists almost purely of radiation. This idea has gone out of fashion in view of some theoretical difficulties, and the modern observations which clearly show the jets as sources of synchrotron radiation, for which one needs a copious supply of electrons (or positrons) in addition to magnetic fields.

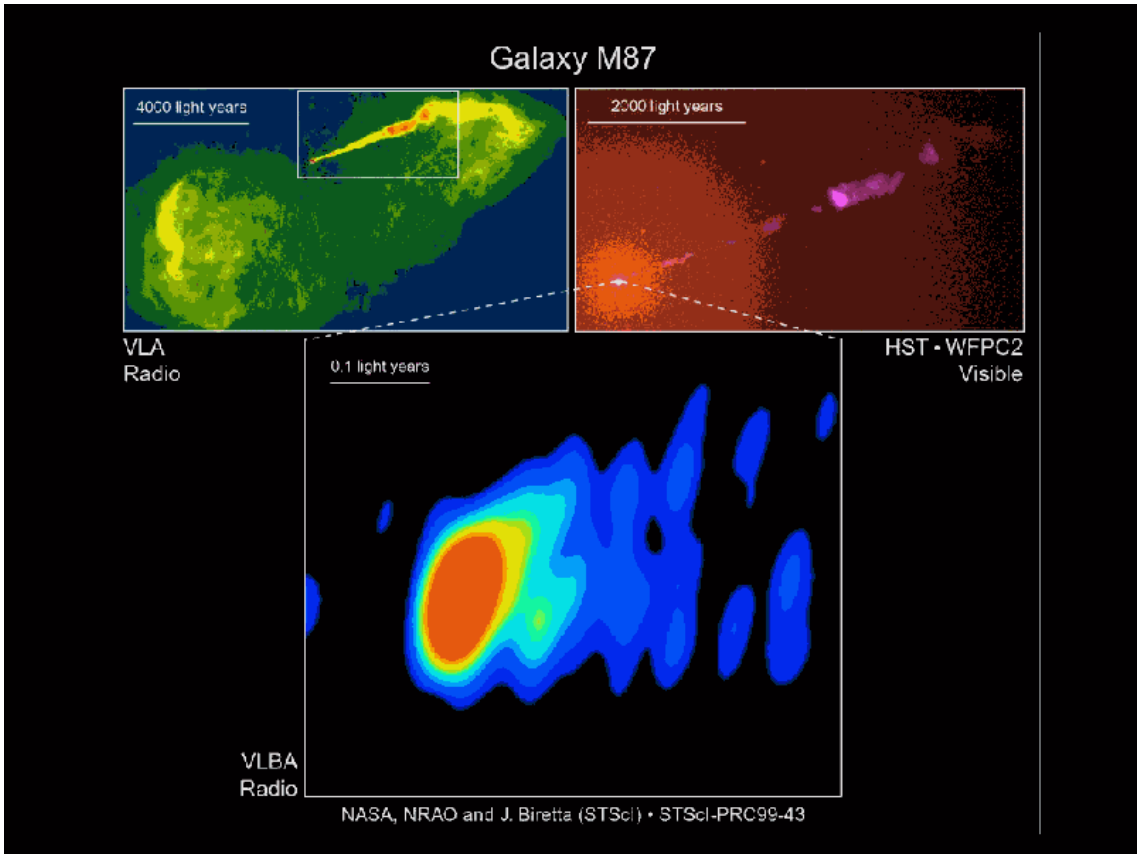

Figure 5.2: *Radio maps and a* Hubble Space Telescope *picture of the jet of radio galaxy M87 (= Virgo A). The scale of the maps ranges from* ~ 1 *pc to* ~ 1.5 *kpc. This jet was discovered in 1917 by American astronomer Curtis, who noticed a faint optical extension of the galaxy. Its true nature was only realised with the advent of radio astronomy around 1960.*

5.1.2 Superluminal motion

In the case of microquasars and poweful radio galaxies, the flow speeds are estimated to be close to the velocity of light, $c \approx$ 300,000 km/s. In the microquasars associated with a few luminous X-ray binaries our galaxy, and in some powerful radio galaxies, the fact that the material must move at a velocity close to light speed has been inferred from the observation of *superluminal motion*. Superluminal motion is a kinematic consequence of *special relativity:* the fact that light always propagates at c *regardless* the velocity of source or observer. The figure below shows the observed superluminal motion of the 'knots' (bright spots) in the jet of M87.

Consider a source which creates a cloud of radio-emitting plasma at $t = 0$, which moves with a constant velocity $V = \beta c$ at an angle θ with respect to the line-of-sight to the observer (see figure). For $\theta = 0$ the cloud moves exactly along the line-of-sight towards the observer. In a time interval $\mathrm{d}t$ the cloud moves distance $\mathrm{d}D = \beta c\,\mathrm{d}t$, with components along and perpendicular to the line-of-sight respectively equal to

$$\mathrm{d}D_\parallel = \beta c\,\cos\theta\,\mathrm{d}t \quad , \quad \mathrm{d}D_\perp = \beta c\,\sin\theta\,\mathrm{d}t\ . \tag{5.1.5}$$

Two fotons, foton 1 emitted at time $t = t_0$ and foton 2 at $t = t_0 + \mathrm{d}t$, reach the observer, given a source distance equal to d, at times

$$\begin{aligned} t_1 &= t_0 + \frac{d}{c} \\ t_2 &= t_0 + \frac{d}{c} + \mathrm{d}t - \frac{\mathrm{d}D_\parallel}{c} \\ &= t_0 + \frac{d}{c} + (1 - \beta\,\cos\theta)\ \mathrm{d}t\ . \end{aligned} \tag{5.1.6}$$

The second expression takes account of the fact that the distance the second foton has to travel differs by an amount $\mathrm{d}D_\parallel = \beta c\,\mathrm{d}t\,\cos\theta$, and is less than the distance travelled by the first photon provided that $\theta < \pi/2$. In that case the reception of the two photons is separated by a time interval $\mathrm{d}t_{\rm obs} = t_2 - t_1$ equal to

$$\mathrm{d}t_{\rm obs} = (1 - \beta\,\cos\theta)\ \mathrm{d}t\ , \tag{5.1.7}$$

which is smaller than the time interval $\mathrm{d}t$ separating the emission. For clouds moving away from the observer (i.e. $\theta > \pi/2$) the arrival time interval is *larger* that the time interval between the emission of the two photons.

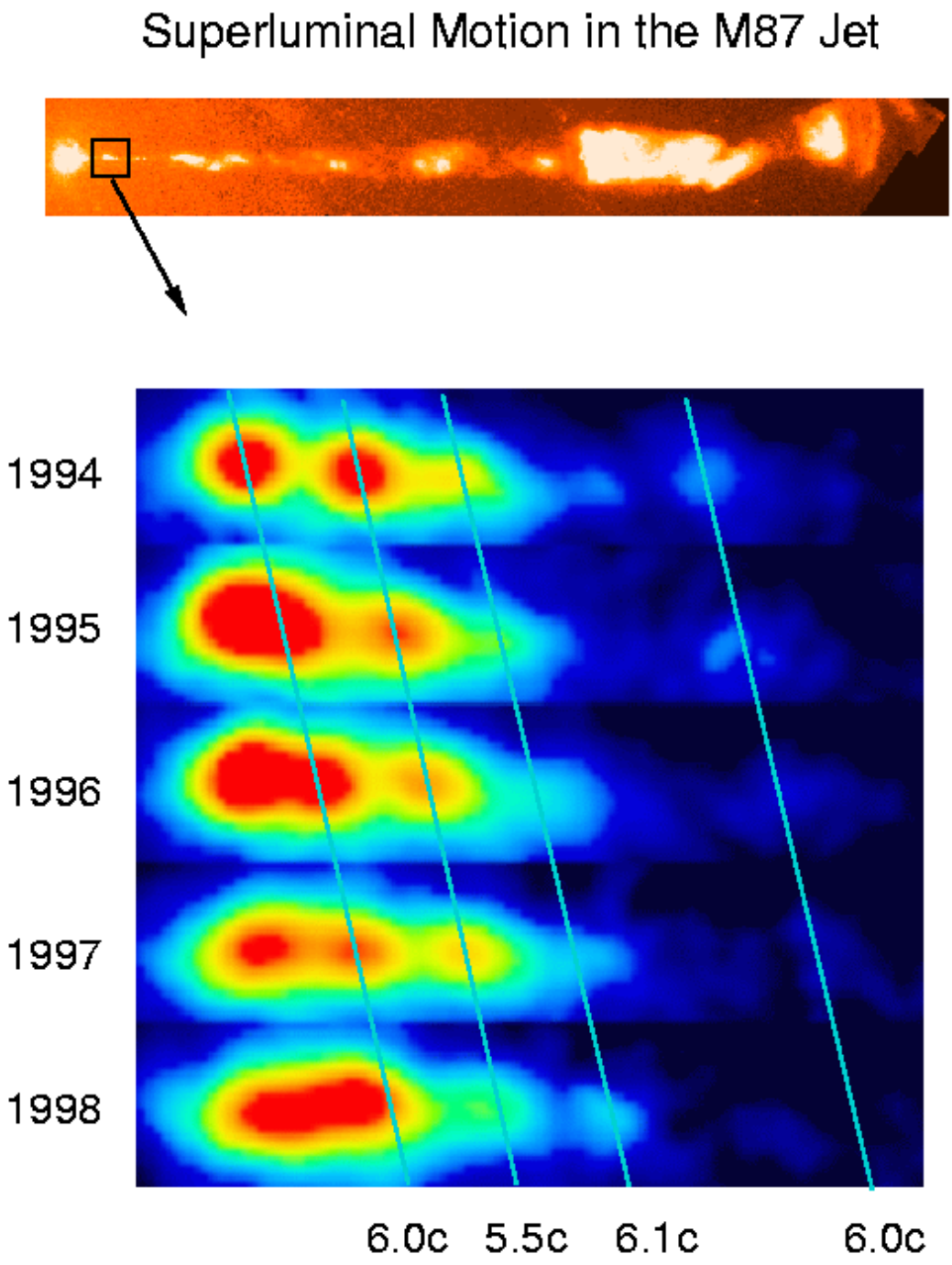

Figure 5.3: *The apparent superluminal motion in the jet of the powerful radio galaxy M87, as derived from repeated observations over a four-year period.*

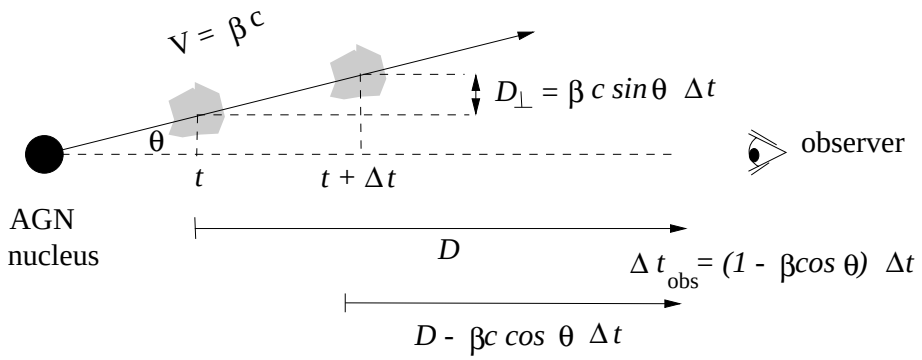

Figure 5.4: *A simple diagram explaining superluminal motion. A radio cloud (gray) moving with velocity $V = \beta c$ at an angle θ with the line-of-sight is observed at time t and time $t + \Delta t$. For a distant observer, it has travelled a distance $D_\perp = \beta c \, \sin\theta \, \Delta t$ perpendicular to the line-of-sight. The photons from the second observation arrive a time $\Delta t_{\rm obs} = (1 - \beta \cos\theta) \, \Delta t$ after the photons of the first observation due to the decrease in distance to the observer. The apparent perpendicular velocity is $V_\perp = D_\perp / \Delta t_{\rm obs} = \beta c \, \sin\theta / (1 - \beta \cos\theta)$.*

This compression of reception times implies that an observer who follows the motion of the radio cloud in the plane of the sky will associate an *apparant* velocity $\beta_{\perp \rm app} c$ with the source, perpendicular to the line-of-sight, with $\beta_{\perp \rm app}$ equal to

$$\boxed{\beta_{\perp \rm app} = \frac{1}{c} \, \frac{{\rm d}D_\perp}{{\rm d}t_{\rm obs}} = \frac{\beta \, \sin\theta}{1 - \beta \, \cos\theta} \; .} \tag{5.1.8}$$

It is easily checked that this apparent velocity (in units of c) will be larger that the actual cloud speed ($\beta_{\perp \rm app} > \beta$) provided the angle θ lies in the range

$$0 < \cos\theta < \frac{2\beta}{1 + \beta^2} \; . \tag{5.1.9}$$

The apparant velocity has a maximum possible value $\beta_{\rm m}$ if the cloud travels at an angle $\theta_{\rm m}$ with respect to the line of sight, with $\beta_{\rm m}$ and $\theta_{\rm m}$ given by:

$$\beta_{\rm m} = \frac{\beta}{\sqrt{1 - \beta^2}} = \Gamma\beta \;\; \text{at an angle} \;\; \theta_{\rm m} = \sin^{-1}\left(\frac{1}{\Gamma}\right) \; . \tag{5.1.10}$$

Here $\Gamma = (1 - \beta^2)^{-1/2}$ is the Lorentz factor associated with the cloud velocity.

5.2 A brief overview of jet sources

5.2.1 Young Stellar Objects

Although the theory of star formation in the galaxy is far from complete, the observations seem to indicate that proto-stars and young stellar objects (YSOs) are often surrounded by a massive disk. This in it self is not suprising: a little amount of angular momentum in a contracting and/or accreting gas cloud naturally leads to the formation of such a disk. One can speculate that the dust disks which are now observed around some stars (e.g. Vega, β-pictoris), which contain a mass $\sim 0.01 - 1\ M_\odot$, could be the remnants of these massive disks. Such a disk would contain mostly dust and small rocks as most the gaseous material has been removed when the hydrogen fusion ignited in the proto-star, while the heavier dust has remained. Dust disks have indeed been observed (e.g. the famous β-Pictoris disk or the disk around Vega). In some cases the presence of such disk could lead of the formation of a planetary system.

The observational evidence for the existence of disks in YSOs comes mostly from disk-associated phenomena, e.g. strong winds and jets. The observational evidence includes *bipolar flows* of molecular gas with large opening angles ($> 45^o$), best observed in the lines of such molecules as CO at millimeter wavelengths. These flows consist of cold gas ($T \sim 10 - 20$ K) moving at speeds of $V = 5 - 100$ km/s. The mass flux in these bipolar flows is of order $\dot{M} \sim 10^{-7} - 10^{-5}\ M_\odot/\mathrm{yr}$.

Furthermore, narrowly collimated jets with an opening angle $1 - 10^o$ have been observed from high-luminosity sources, $L > 1000\ L_\odot$. These jets have a length of about 0.01-0.5 pc, see the figure below for an example. In these jets one finds dense clumps of gas, the so-called *Herbig-Haro Objects* which have been accelerated to speeds up to 100 km/s by the ram pressure (intercepted momentum flux) of the jet material. The speed of the material of the jet itself lies in the range $V \simeq 100 - 450$ km/s, and these jets carry a mass flux of order $\dot{M} \sim 10^{-10} - 10^{-8}\ M_\odot/\mathrm{yr}$.

5.2.2 Microquasars

In recent years, it has become obvious that some galactic X-ray sources exhibit some of the same phenomena as Active Galactic Nuclei (AGN): bulk mass outflow in the form of strong winds or narrowly collimated streams (jets).

The most famous (and first recognized) case of course is the source **SS433**. The name refers to object 433 of the Stephenson-Sandulaek catalogue for stars exhibiting emission lines. In a number of spectra taken in 1978 it became obvious that these emission lines are at a variable position in the spectrum. It had already been noticed that SS433 resides in a supernova remnant which has an 'odd' elongated shape, and which contains a radio point source.

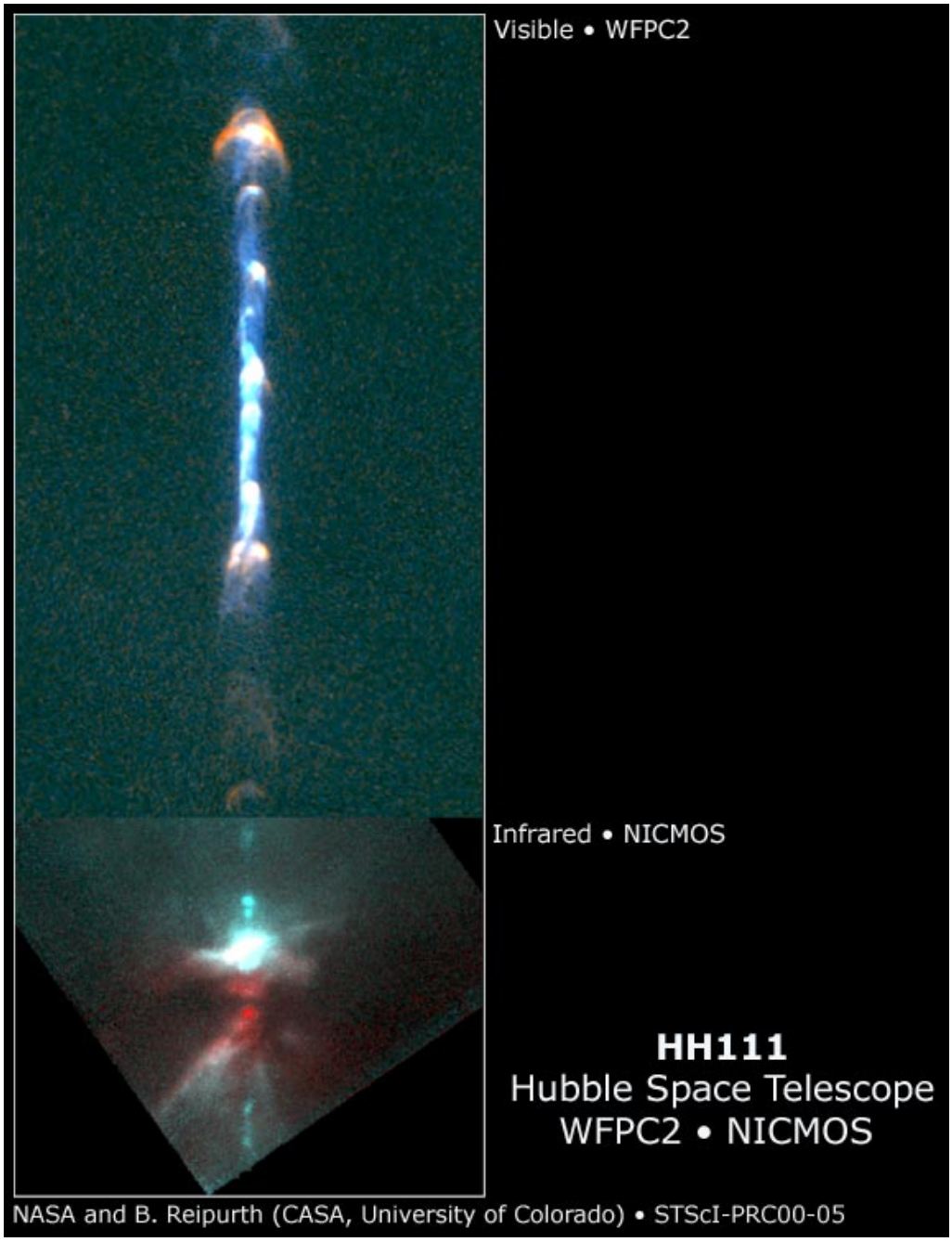

Figure 5.5: *The two jets emanating from the Herbig-Haro object H111, as seen by the* Hubble Space Telescope. *The jet contains many bright spots, not unlike what is observed in the much larger jets from active galaxies. Note that both jets end in a 'hot spot'. This is where the head of the jet is located, and where it hits the undisturbed interstellar gas. Further back, the jet has already cleared a channel.*

The optical emission lines occur in blue- and redshifted pairs. The explanation for this phenomenon is that the emitting material occurs in 'blobs' or condensations which stream out from the central object in a precessing jet. This precession is probably associated with a precessing accretion disk, where the jet flow is collimated and directed.

From the relativistic Doppler formula for the blue- and redshifted wavelengths, which are located asymmetrically on either side of the rest wavelength λ_0,

$$\frac{\lambda_{\rm b}}{\lambda_0} = \frac{1-\beta\ \cos\theta}{\sqrt{1-\beta^2}} \quad , \quad \frac{\lambda_{\rm r}}{\lambda_0} = \frac{1+\beta\ \cos\theta}{\sqrt{1-\beta^2}} \ ,$$

one can infer both the streaming velocity and the angle θ with respect to the line-of-sight. For SS433 one finds a flow speed in the jets (or a speed of the 'blobs' in the jet) equal to $V = 0.26c$. This jet precesses with a period of 164 days.

This picture has been confirmed dramatically by radio observations. These show twin sets blobs of synchrotron emitting material, located in a corkscrew pattern on either side of the central object, with an outward proper motion of about 3 arcseconds/year. Each set of blobs is associated with an outburst, and can be followed for a few years. Their position on the sky is in complete agreement with the ballistic model where these blobs are shot out in the direction of the jet at the moment of the outburst.

The odd elongation ('ears') of the supernova remnant associated with SS533, known as W50, lies exactly on the line defined by the precession axis of the twin jets. It is believed that the material of the jets pushes out the material of the supernova remnant. Recent radio observations show something of a spiral structure in one of the 'ears' which follows the trajectory of the precessing jet. This is illustrated in the figure below.

We now know that a number of other binary X-ray sources exhibit similar outflows. I will list a few of the most famous ones, except for SS433.

- **Cygnus X-3**
  Cygnus X-3 is one of the brightest X-ray sources in the sky. It is thought to be a close binary with a luminosity $L_{\rm X} \simeq 10^{38}$ erg/s at a distance of about 10 kpc. At radio frequencies, it shows strong, irregular bursts where the radio flux rises by a factor $10^2 - 10^3$. The spectrum of the radio emission is consistent with synchrotron emission from relativistic electrons in a rapidly expanding cloud. VLBI observations show an elongated source, expanding at $V_{\rm exp} \simeq 0.3 - 0.4$ c for the assumed distance of 10 kpc. This could be interpreted as blobs in a (transient?) jet. In 1989 it was discovered with the WSRT that there is extended radio emission reminiscent of the radio lobes of some radio galaxies. These lobes have a linear size of about 0.3 pc and a luminosity of about 3×10^{30} erg/s.

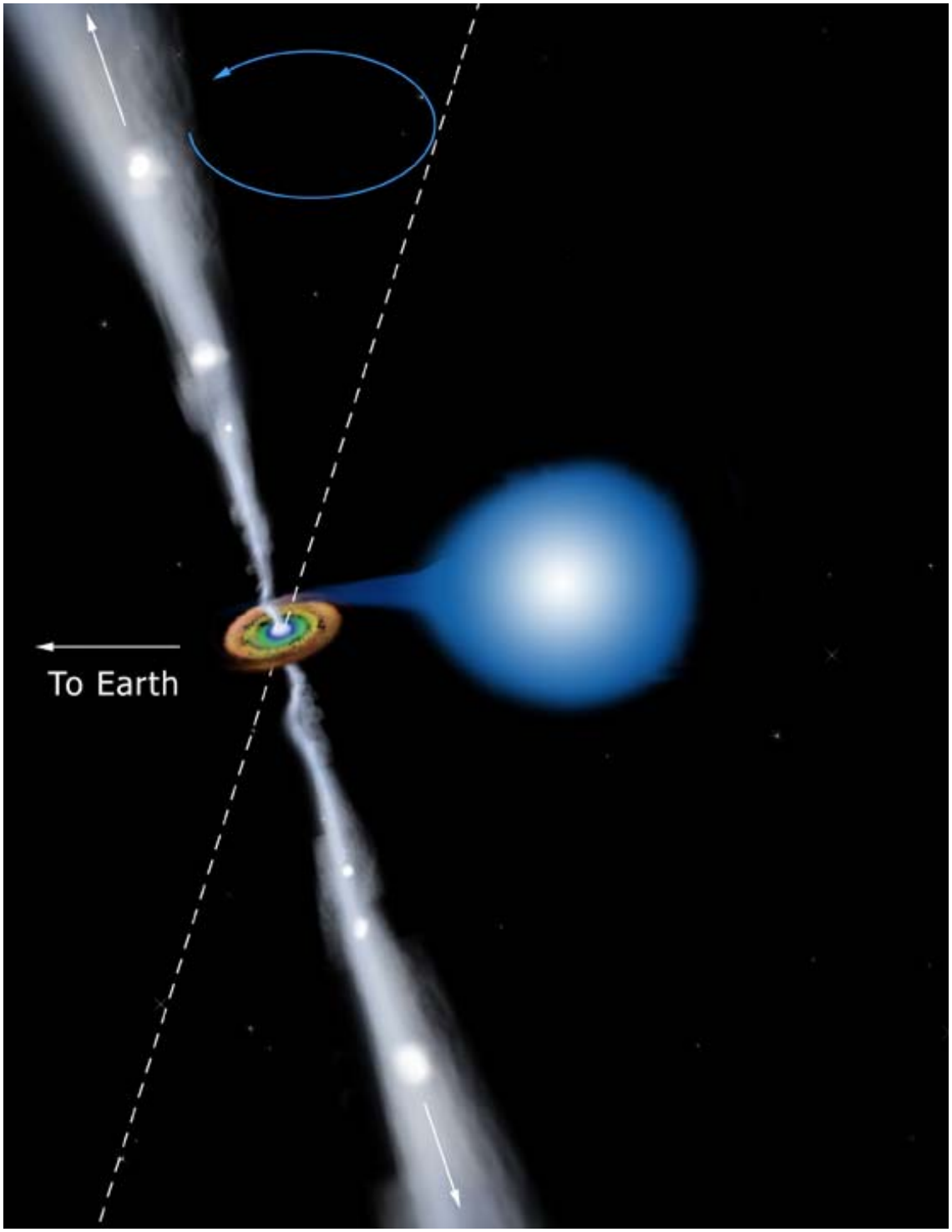

Figure 5.6: *An illustration of the geometry of SS433. Twin jets emanate from a precessing accretion disk around the compact object orbiting a normal star. Tidal forces rip the material from the star, which gathers into the accretion disk. The precession changes the angle between the line-of-sight to Earth and each of the two jets*

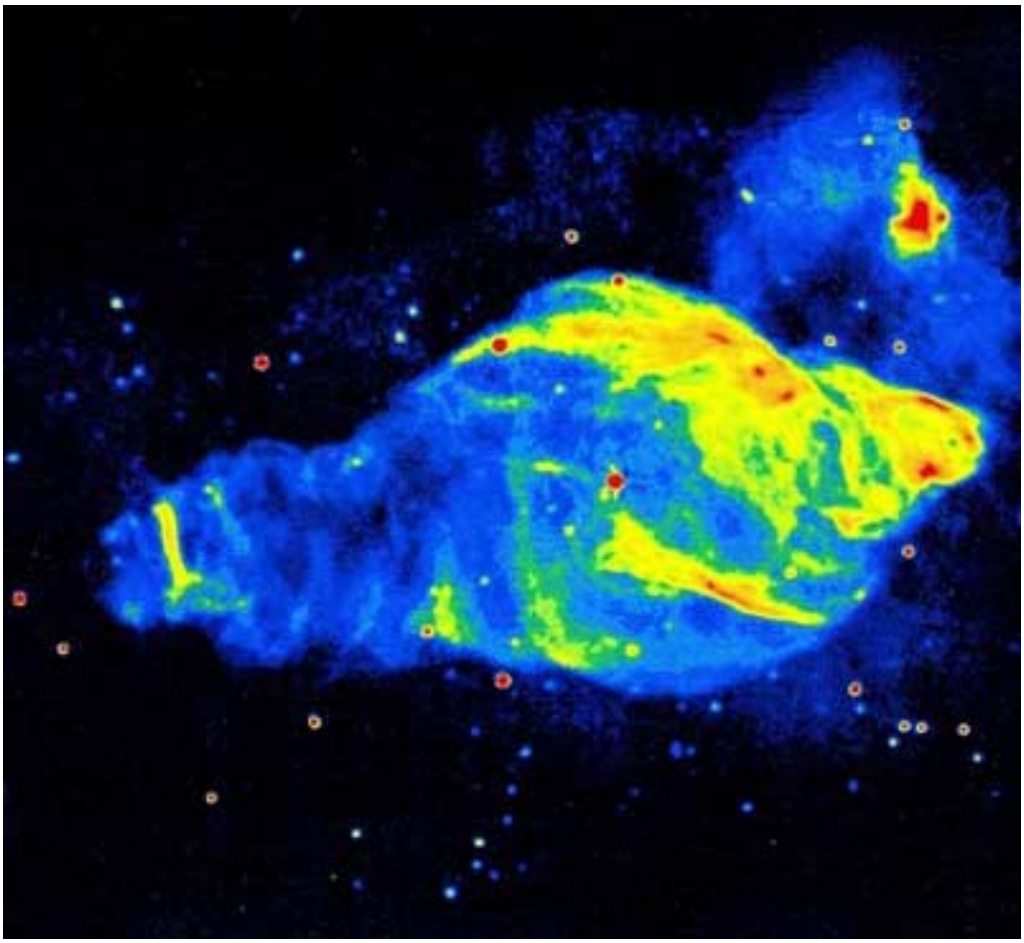

Figure 5.7: *Radio map of the supernova remnant W50 associated with the microquasar SS433. Rather than a roughly circular shape the remnant has two distinctive ears whose position angle coincides with the direction of the axis around which the two jets of the binary SS433 precess. These observations where obtained with the* Very Large Array *synthesis telescope located near Socorro, New Mexico in the US.*
From: Dubner, G.M., Holdaway, M., Goss, W.M. & Mirabel, I.F., 1998: *Astron. J.* **116**, 1842.

- **GRS 1915+105 and J1655-40**[4]
  The source GRS 1915+105 is a so-called Hard X-Ray Transient. During an outburst, it is one of the brightest sources in the X-ray sky. For an assumed distance of 12.5 kpc, the X-ray luminosity during outbursts is of the order $L_{\rm X} \simeq 3 \times 10^{38}$ erg/s. It was discovered in 1994 using the VLA radio interferometer that the associated radio source shows superluminal motion: the blobs of radio emission show a proper motion on the sky which corresponds to a linear velocity exceeding the speed of light. The observations of this object are consistent with a jet velocity $V \geq 0.32$ c and an angle of the jet with the line-of-sight of order $\theta \leq 71^o$, with the most probable value of $V \simeq 0.92$c.

  GRO J1655-40 is another bright galactic X-ray source showing X-ray and radio bursts. It was discovered in 1994 that this source also exhibits superluminal motion, where radio clouds separate at a rate of $\mu \simeq 0.065$ arcseconds/day! The large proper motion is probably due to the relatively small distance ($d \simeq 3 - 5$ kpc). The inferred streaming velocity equals $V \simeq 0.5 - 0.8$ c. The optical counterpart of this source has been identified. Its optical characteristics are similar to Black Hole Candidate binary systems.

5.2.3 Active galaxies and quasars

With the advent of radio astronomy in the years immediately following the Second World War it was found that the radio sky does not simply refect the distribution of souces in the visible sky. Many strong radio sources are very faint (or even invisible) optically. To some extent this reflects the fact that radio telescopes can be built with enormous collecting areas. For instance, the *Westerbork Synthesis Radio Telescope*, consisting of 14 mirrors with a diameter of 25 m, has a collecting area of about $7000\ {\rm m}^2$. The largest optical telescope, the *Keck Telescope*, has a mirror with a diameter of 10 m, and a collecting area of about $300\ {\rm m}^2$. The huge collecting area of radio telescopes allows the detection of many 'faint' radio sources, even though usually only a tiny fraction of the total luminosity of these sources is actually emitted at radio frequencies.

Some of the radio sources found were quickly identified with galactic objects. In particular, young supernova remnants such as the *Crab Nebula*, *Cas A*, *Tycho's remnant* (supernova A.D. 1572) and *Keplers remnant* (supernova A.D. 1604) are prominent radio sources. As already discussed, the radiation mechanism is mostly synchrotron radiation by relativistic electrons in a magnetic field.

[4]For a recent review: I.F. Mirabel & L.F. Rodriguez, *Microquasars in our Galaxy*, *Nature* **392**, 673, 1998

Early radio surveys contained also many sources without an immediately obvious optical counterpart. The identification (in 1954) of the radio source *Cygnus A* with an optical galaxy confirmed for the first time the extragalactic nature of some of the strong radio sources. As we explained above, the energy powering this emission is supplied continuously by jets. Historically, the first jet was discovered by Curtis in 1917, as an optical extension of the elliptical galaxy M87.

Radio galaxies can be roughly divided into two classes, Fanaroff-Riley class I and Fanaroff-Riley class II, on the basis of their power (monochromatic luminosity L_ν at a frequency $\nu = 178$ MHz) and their morphological properties. The figure below shows two typical representatives. The properties of these two classes can be summarized as follows:

Fanaroff-Riley Class I sources

- Power $(\nu L_\nu)_{178\ \mathrm{MHz}} < 10^{34}$ W;
- Diffuse, *edge darkened* radio clouds;
- No prominent Hot Spots;
- Two-sided Jets.

Fanaroff-Riley Class II sources

- Power $(\nu L_\nu)_{178\ \mathrm{MHz}} > 10^{34}$ W;
- Compact radio clouds, which are brightest at their outer edge;
- Prominent Hot Spots due of the impact of the jets on the intergalactic gas;
- One-sided (visible) jets due to Doppler-boosting of approaching, and Doppler-fading of the receding jet.

Some spiral galaxies also show signs of activity, be it on a smaller scale and at a reduced power. A study by Seyfert in the 1940's showed that some spirals have an anomalously bright and blue nucleus.

These *Seyfert galaxies* emit continuum radiation, and have spectral characteristics (optical and UV emission lines) which are non-stellar in nature. Seyfert galaxies usually contain weak, compact non-thermal radio sources in their nucleus.

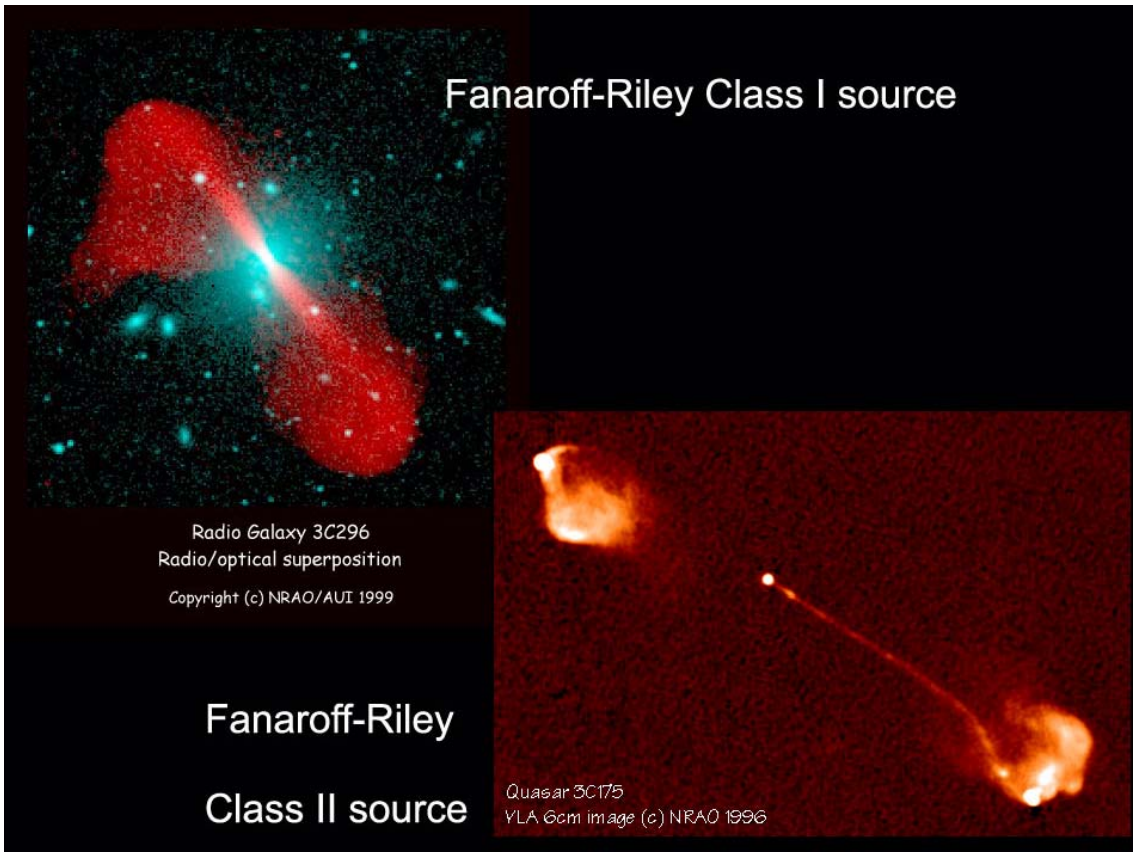

Figure 5.8: *Two typical examples of class FRI (top left) and FRII (bottom right) radio galaxies*

Quasars were discovered in 1963 in Maarten Schmidt as very distant objects that appeared star-like (unresolved) in the optical telescopes available at that time. The radiation from quasars is strongly redshifted, as evidenced by the position of the emission lines in their optical spectrum. This implies (at least according to a strong majority of astrophysicists) that quasars are at cosmological distances, and one is seeing the effects of the global expansion of the universe in the spectrum of quasars.

Quasars are now believed to be the high-luminosity counterparts of Seyfert galaxies. They are the most luminous objects in the universe with a power up to $10^{40}\ W$. A typical quasar could provide Earth's energy supply for 10^9 years if its power source was tapped for only 10^{-9} seconds! Only a few percent of quasars are *radio loud*, and show extended radio structure reminiscent of powerful radio galaxies such as Cygnus A. Radio quiet quasars usually also contain a (weak), compact radio source.

The whole class of *Active Galactic Nuclei*, which includes the parent objects of Seyfert galaxies, radio galaxies and quasars, are believed to derive their power from accretion on a massive ($10^6 - 10^8\ M_\odot$) black hole in the nucleus of a galaxy. Part of this energy is apparently converted into relativistic particles which in turn are responsible for the observed radiation.

The argument that supports this idea is one of efficiency: apart from somehow directly tapping the rotational energy of a rapidly rotating black hole, accretion is the only mechanism that can deliver the required power. The non-thermal emission from AGN's spans some 14 decades in energy (from gamma rays to radio frequencies) with a radiation flux which scales roughly as $L_\nu \sim \nu^{-1}$.

The observational signatures of Active Galactic Nuclei (including quasars) are the following:

1. **Continuum radiation** over a wide range of frequencies with nearly constant flux per logarithmic bandwidth: $\nu\, L_\nu \sim$ constant.

2. **Emission lines** at optical and UV wavelengths. These lines come in two varieties: *narrow lines* with a width $\Delta\lambda/\lambda \leq 0.002$ and *broad lines* with a width $\Delta\lambda/\lambda \sim 0.05$. This line emission is caused by *photo-ionization* by strong continuum radiation at wavelengths $\lambda \leq 912$ $\mathring{\mathrm{A}}$. Since lines from ions with widely different ionization potential are observed this continuum must be broad-banded.

   The *Broad Line Region* (BLR) where the broad emission lines originate must be small (size $\sim$ 10 light days - few light years) because of the observed rapid variability, and relatively dense (electron) density $n_\mathrm{e} \geq 10^8\ \mathrm{cm}^{-3}$, which can be deduced from the presence of strong forbidden lines.

   The *Narrow Line Region* (NRL), where the narrow emission lines are formed, must be much larger (size $R \sim$ a few parsec) since narrow line emission does not mirror the rapid variations of the *nuclear* continuum: these variations are smeared out by the light travel time, $t \sim R/c \sim 3 - 10\ \mathrm{yr}$, across the NRL.

3. **Variability** on timescales ranging from days to years. This variability is seen at different wavelengths, and is sometimes accompanied by a high percentage of (also variable) polarization.

4. **Large-scale radio emission.** As already discussed, some of these objects show radio clouds and jets on kpc-Mpc scales. In some quasars and strong radio galaxies one has been able to detect radioblobs on parsec scales, and track their motion in the plane of the sky using *Very Long Baseline Interferometry* (VLBI). This motion often exhibits the superluminal motion discussed above.

It should be realized that these observational characteristics need not all be present simultaneously in any given source[5]

[5]. A review of theory and observations of AGN, still relevant after more than a decade, can be found in M.C. Begelman, R.D Blandford & M.J. Rees, *Rev. Mod. Phys* **56**, 255, 1984.
A recent good introduction to AGNs is: B.M. Peterson: *An Introduction to Active Galactic Nuclei*, Cambridge Univ. Press, 1997.
An extensive up-to-date book on AGNs is: J.H. Krolik, *Active Galactic Nuclei*, Princeton University Press, 1999.
Superluminal expansion is covered in: J.A. Zensus & T.J. Pearson (Eds.), *Superluminal Radio Sources*, Cambridge Univ. Press, 1987

5.2.4 Unification Models

In recent years a point of view has become popular where the variety in the phenomenological appearance of AGN is not so much due to *intrinsic* differences between the sources (type of host galaxy, source size, luminosity, black hole mass, accretion rate etc.), but is largely due to an *external* factor: the position of the observer [6]!

These *Unification Schemes* postulate that the appearance of the source, and the observable phenomena it exhibits, is largely due to its orientation. In particular this is true for galaxies exhibiting broadened *permitted* lines (Broad Line Radio Galaxies, BLRG and Seyfert 1 galaxies) and those showing only narrow permitted lines (Narrow Line Radio Galaxies, NLRG and Seyfert 2 galaxies).

The basic idea is simple (see the figures below). One assumes that the 'Central Engine' powering all energetic phenomena in the galactic nucleus is surrounded by a 'torus' or 'doughnut' of dusty material. Depending on the orientation of that torus with respect to the line-of-sight, an outside observer can see further into the galactic nucleus. At right angles, the torus obscures the nucleus, and an outside observer sees only the large-scale manifestations such as the NLR, radio clouds and jets. As the angle between the line-of-sight and the axis of the torus decreases, the observer sees deeper into the nucleus, and will start to see the BLR and, ultimately, will directly observe the ionizing radiation coming from the 'central engine' (accretion disk?) and its surroundings. If one looks directly into the 'mouth of the monster', an additional effect may become important: *relativistic beaming* of the radiation. If one of the by-products of the central engine is a collimated, relativistic jet which provides a significant fraction of the emission, emission from the material in the jet pointing in our direction will be strongly blue-shifted, and material from the other (receding) jet is strongly red-shifted. The blue-shifted radiation seems enormously brightened and, conversely, the red-shifted emission is strongly weakened. This may explain why so many powerful radio galaxies, such as Cygnus A, seem to have only one jet, even though there are radio clouds on both sides of the galaxy. The receding jet is simply too faint to observe due to relativistic doppler effects. The fact that some one-sided radio galaxies also exhibit superluminal motion, hinting at a bulk velocity near the speed of light, supports this idea.

In extreme versions of such unification schemes one also attributes the difference between powerful radio galaxies and quasars to orientation: one sees a quasar whenever one looks directly into the nucleus of an active galaxy. In this point-of-view a powerful radio galaxy is simply a quasar seen from the side.

There is now some indirect observational evidence to support this overall picture. These observations can be summarized as follows:

1. In a few galaxies (notably NGC 4261) a gaseous disk is observed in the nucleus, oriented at right angles with respect to the large-scale radio structure.

[6] A review of unification models can be found in: R. Antonucci: *Ann. Rev. Astron. Astrophys.* **31**, 473, 1993

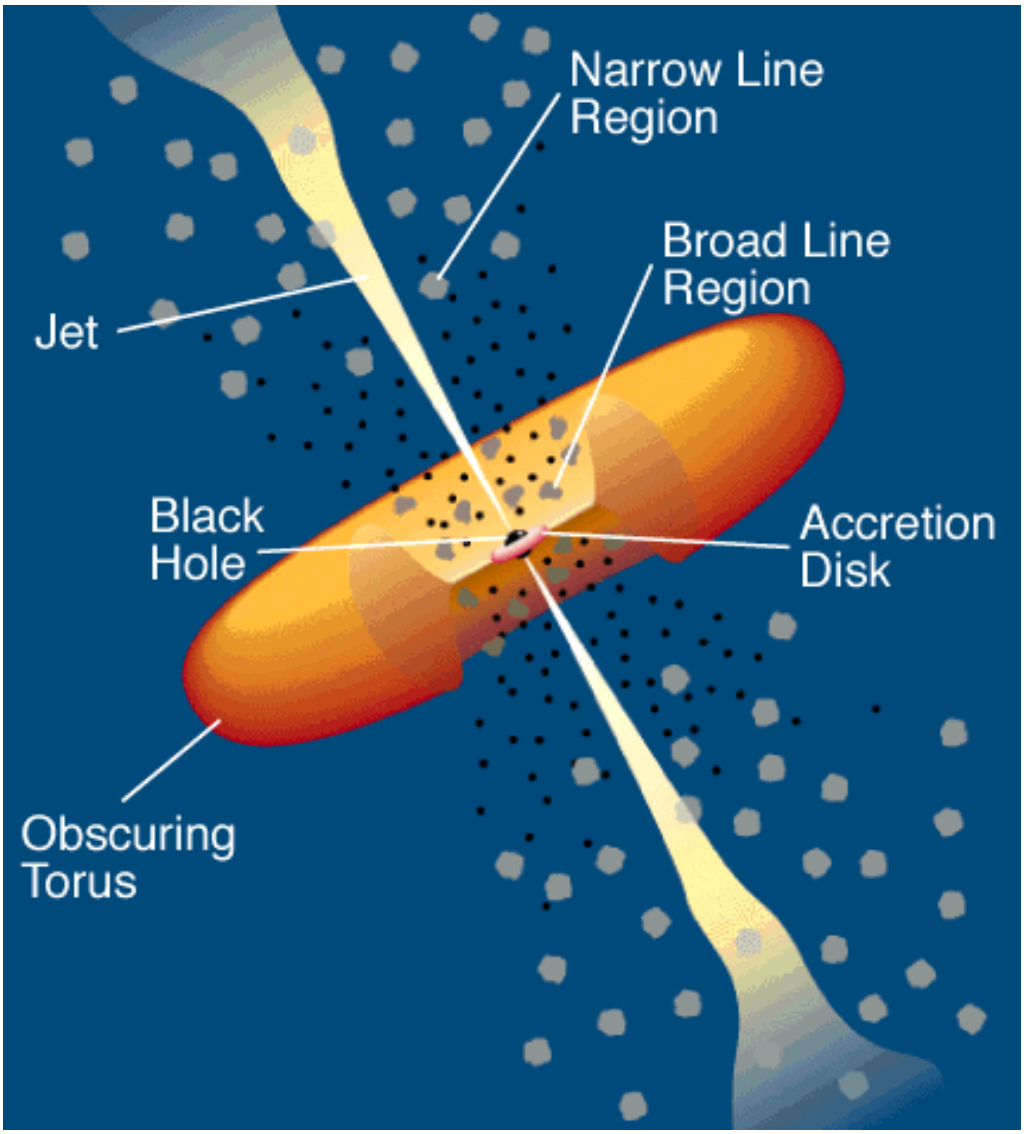

Figure 5.9: *Schematic representation of an AGN in unified models. Shown are the obscuring dust torus, the jet, the clouds responsible for the Broad Line Region (black dots) and the clouds at larger distances (gray clouds) responsible for the Narrow Line emission.* From: C.M. Urry & P. Padovani, *Publ. Astron. Soc. Pac.* **107**, 803, 1995

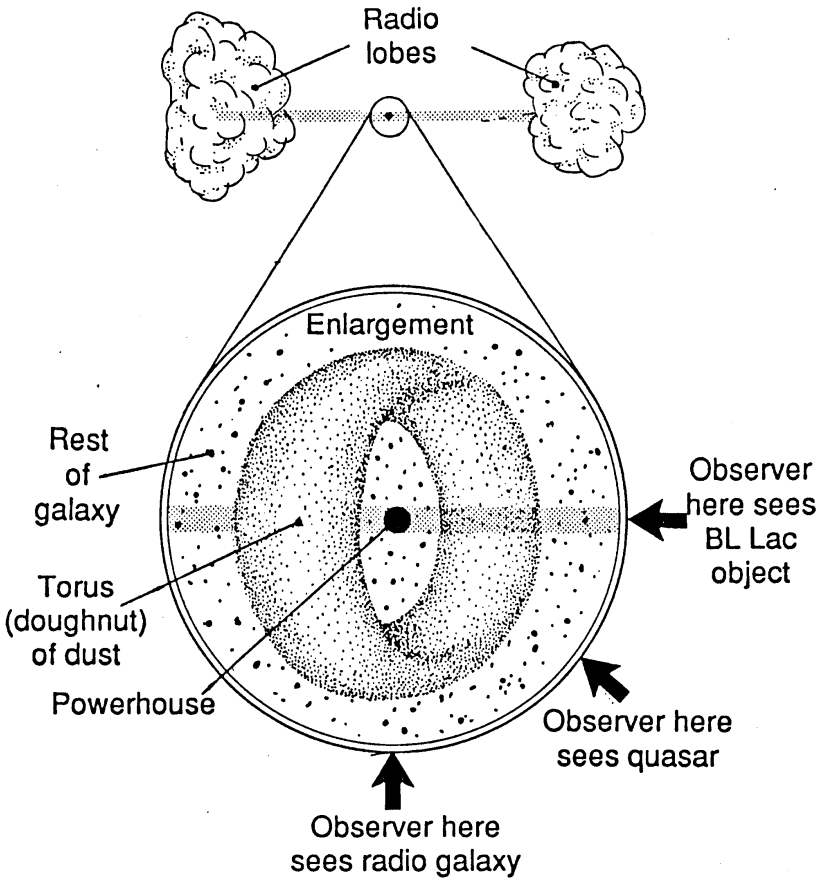

Figure 5.10: *Unification scheme for Quasars and powerful radio galaxies based on the position of the observer (From New Scientist)*

2. In the Seyfert 2 galaxy NGC 1068 polarized light appears to have the characteristics of the radiation from a BLR characteristic of a Seyfert 1. The explanation is that the polarized light is reflected light, originating in the obscured BLR and scattered into the line of sight by material at larger distances. This polarized emission is distributed in a conical region (see figure 5.12), which is consistent with the idea of an obscuring torus. Such a conical structure, usually called an *ionization cone*, has now been observed in a number of galaxies containing AGN.

3. In the powerful radio galaxy Cygnus A infra-red observations show a small source, coincident with the nuclear radio source. This could be the radiation from the nucleus, which is intercepted by a dusty torus, reprocessed by the dust and re-emitted as infra-red radiation.

4. X-ray observations of the active galaxy MCG-6-30-15 show the $K\alpha$-line of Iron (rest wavelength corresponding to $h\nu = 6.4$ keV) in emission. The profile of this emission line (see figure 5.11) is consistent with the emission from a rapidly rotating disk close to a black hole. The line width corresponds to a velocity $\simeq$ 100.000 km/s (0.3 c!) and its asymmetric redshifted profile seems to show the effect of the relativistic transverse Doppler shift (time dilatation). The shape of the line profile is roughly consistent with models for line emission from an accretion disk close to a black hole.

Although such unification schemes are attractive from a theoretical point-of-view, they will never unify all sources powered by AGN. For instance: powerful radio galaxies supporting long jets and radio clouds are found exclusively in elliptical galaxies, whereas Seyferts are associated with spiral (disk-)galaxies. This shows that the 'environment' of AGN *does* play a role in determining the way the nuclear activity manifests itself.

The idea that accretion on a Black Hole with a mass of $10^6 - 10^8\ M_\odot$ is the powersource for active galaxies and quasars is largely based on an energy argument. As we will see later, accretion of matter onto a mass M_* can be characterized by a typical luminosity, the *Eddington Luminosity* $L_{\rm edd} \propto M_*$, given by:

$$L_{\rm edd} = \frac{4\pi G m_{\rm p} M_* c}{\sigma_{\rm T}} \simeq 10^{39} \left(\frac{M_*}{10^8\ M_\odot} \right)\ {\rm W}\ . \qquad (5.2.1)$$

Only the very efficient process of accretion, involving objects with such large masses, seems to be capable to generate the required power.

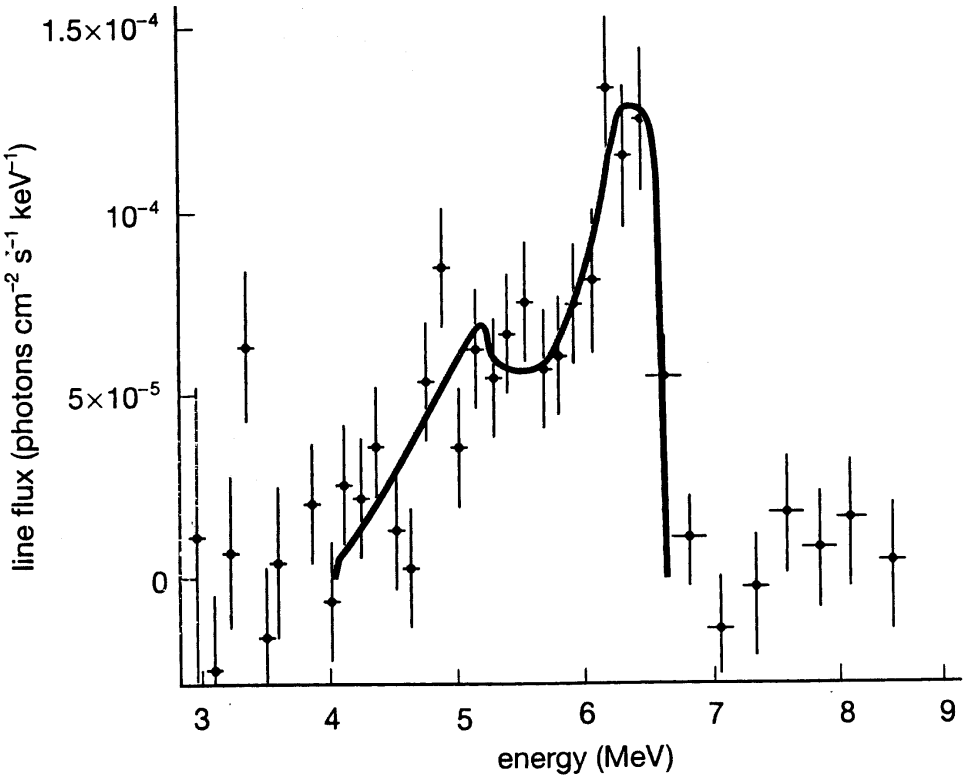

Figure 5.11: *Fluoresence line of Iron, observed in the active galaxy MCG-6-30-15. The solid curve gives the line profile expected for emission from a differentially rotating disk.* From: Y. Tanaka *et al.* , *Nature* **375**, 659, 1995)

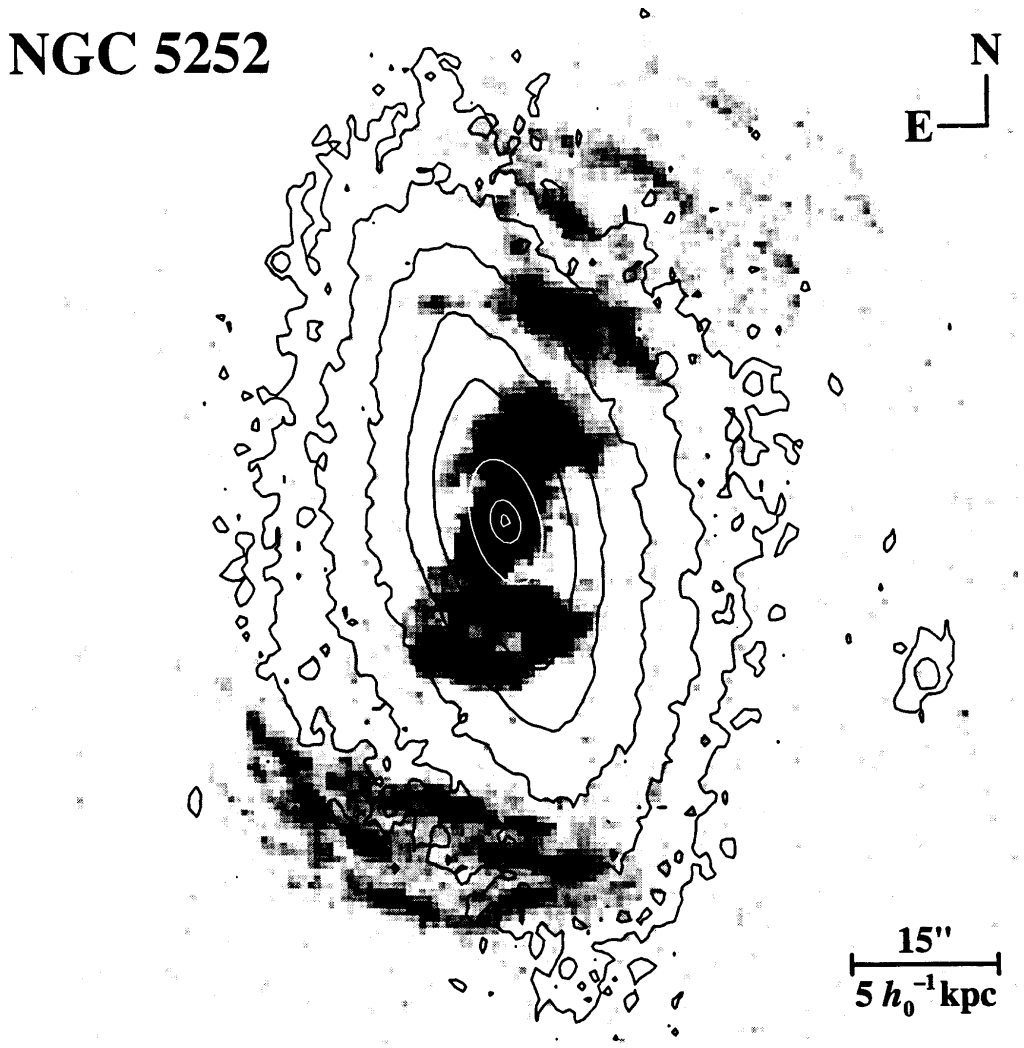

Figure 5.12: *Cone of line-emission from the [O III] λ5007 line of oxygen, produced in the obscured nucleus of the Seyfert galaxy NGC 5252, and scattered into the line-of-sight by free electrons in the interstellar gas of this galaxy. The contours give the optical isophotes of the galaxy, the dark blotches the scattered line radiation. The cone-like distribution of the scattered radiation can be explained if the nucleus is surrounded by a thick torus of dust so that the scattered line radiation is confined to a cone around the axis through the central hole in of the torus.* From: B.M.Peterson: *Active Galactic Nuclei*, p. 108, Cambridge Univ. Press, 1996.

One has sought to find *direct* observational evidence for the existence of these massive black holes. A tell-tale indication for the presence of a massive black hole is the motion of stars and gas in the nucleus of a galaxy. If the total mass contained within a radius R equals $M_{\rm tot}(R)$, the rotation speed $V_{\rm rot}$ (or stellar velocity dispersion σ) at that radius will be roughly the Keplerian rotation speed

$$V_{\rm rot} \text{ or } \sigma \simeq \sqrt{\frac{GM_{\rm tot}(R)}{R}} \ . \tag{5.2.2}$$

The mass of the stars contained in the nucleus can be estimated form the (optical) luminosity and the mass-to-light ratio for the stellar population. The remaining 'dark' mass would then be indicative of a massive black hole.

The problem of course is that this method only works reliably relatively close to the black hole. The typical mass-density in a galactic nucleus is

$$\rho_{\rm c} \simeq 5 \times 10^6 \ M_\odot \ {\rm pc}^{-3} \ . \tag{5.2.3}$$

So, in order to reliably establish the presence of a black hole of mass $M_{\rm bh}$ one has to resolve a radius of order

$$R \sim \left(\frac{3M_{\rm bh}}{4\pi \ \rho_{\rm c}} \right)^{1/3} \simeq 1.8 \ \left(\frac{M_{\rm bh}}{10^8 \ M_\odot} \right)^{1/3} \ {\rm pc} \ . \tag{5.2.4}$$

This corresponds to an angular size[7] at a distance D of order

$$\Delta\theta \simeq \frac{R}{D} \approx 0.04 \ \left(\frac{M_{\rm bh}}{10^8 \ M_\odot} \right)^{1/3} \ \left(\frac{D}{10 \ {\rm Mpc}} \right)^{-1} \ {\rm arcsecond} \ . \tag{5.2.5}$$

Earth-based optical telescopes rarely achieve a resolution exceeding $0.5''$, so one needs either a close-by galaxy, or a very massive black hole. With the advent of the *Hubble Space Telescope* (HST) one can resolve about $0.1''$. In 1994, Holland Ford and his collegues measured a molecular disk in the nucleus of M87 (distance $D \sim 13$ Mpc). Using the Doppler shift of OII emission lines, they established a rotation speed of about 550 km/s at a distance of 20 pc from the nucleus. This gives a mass of about $2 - 3 \times 10^9 \ M_\odot$ within 20 pc, much more than what the optical luminosity of the nucleus would seem to indicate.

[7] $1'' =$ one arcsecond $= 4.818 \times 10^{-6}$ radian

An even more spectacular measurement, using VLBI, has been done by Miyoshi *et al.* [8] They measured the rotation speed of *water masers* in the central 0.13 pc of the galaxy NGC4258 (distance $D \sim 6.4$ Mpc). The observed rotation speed of $V_{\rm rot} \simeq 900$ km/s indicates a mass $M_* \simeq 4 \times 10^6\ M_\odot$ in the central region of this galaxy.

5.3 Equations for jet flow

Consider a quasi-cylindrical jet with its axis oriented along the z-axis. We assume that the cross-section of the jet equals $\mathcal{A}(z) = \pi R^2$ and that all fluid variables (density, pressure, velocity $\cdots$) depend *only* on the coordinate z along the axis, and are constant over the cross-section.

These assumptions can be justified provided the expansion of the jet radius is sufficiently slow. This condition means that the jet must be able to adjust rapidly to pressure changes in the direction perpendicular to its axis. If the flow speed in the jet equals $V(z)$, a fluid element 'feels' a pressure change

$$\frac{{\rm d}P}{{\rm d}t} = V(z)\,\frac{{\rm d}P}{{\rm d}z}\ , \tag{5.3.1}$$

as it travels along the jet. This pressure change must be communicated to all points over the jet's cross-section, which will take a time of order $t_\perp \sim R(z)/c_{\rm s}$ since pressure changes propagate as sound waves. The jet will be able to adjust smoothly to pressure changes provided

$$\frac{{\rm d}P}{{\rm d}t} \ll \frac{P}{t_\perp} = \left(\frac{c_{\rm s}}{R}\right)\ P\ . \tag{5.3.2}$$

Using the above expression (5.3.1) for the pressure change, it is easily seen that this condition corresponds to

$$\frac{1}{P}\,\frac{{\rm d}P}{{\rm d}z} \ll \frac{1}{\mathcal{M}_{\rm s} R}\ , \tag{5.3.3}$$

with $\mathcal{M}_{\rm s} \equiv V/c_{\rm s}$ the sound Mach number of the flow. If the jet changes its properties on a scale $\Delta z = L$ so that ${\rm d}P/{\rm d}z \approx P/L$, this condition implies

$$R \ll L/\mathcal{M}_{\rm s}\ . \tag{5.3.4}$$

[8] M. Miyoshi *et al.*:, *Nature* **373**, 127, 1995

As jets are strongly supersonic at large distances from the source region ($\mathcal{M}_{\rm s} \gg 1$), this implies that the opening angle α of the jet must be small:

$$\alpha \approx \frac{{\rm d}R}{{\rm d}z} \approx \frac{R}{L} \ll \frac{1}{\mathcal{M}_{\rm s}} \ll 1 \; . \tag{5.3.5}$$

Here I use the approximation $\tan\alpha \approx \alpha$. If this condition is satisfied the equations for the jet flow simplify considerably. The equations are:

$$\begin{aligned}
\dot{M} \equiv \rho V \, \mathcal{A} = \text{constant} \qquad & \text{(mass conservation)} \\
\mathcal{E} \equiv \tfrac{1}{2} V^2 + \frac{\gamma P}{(\gamma-1)\,\rho} + \Phi(z) = \text{constant} \qquad & \text{(Bernouilli's law)} \\
P = P_0 \left(\frac{\rho}{\rho_0} \right)^{\gamma} \qquad & \text{(isentropic flow)} \\
P(z) = P_{\rm e}(z) \qquad & \text{(pressure balance)}
\end{aligned} \tag{5.3.6}$$

The first equation makes use of the fact that the flowlines are almost perpendicular to the jet cross-section as long as the opening angle $\alpha \ll 1$. In that case the amount of mass flowing through the jet (mass flux $\times$ area) equals $\dot{M} = \rho V \mathcal{A}$. The other two equations should be familiar by now.

The pressure P_0 and the density ρ_0 are simply reference values, which we can choose to be the pressure and density of the gas at the beginning of the jet in the nucleus of the active galaxy.

The last equation is an additional condition that must be imposed for a steady jet. At the outer edge of the jet (at cylindrical radius R) there must be balance between the pressure P inside the jet and the pressure $P_{\rm e}$ of the surrounding medium. If this was not the case, the interface would start to move radially outwards in attempt to equalize the force acting on both sides. If the jet expands slowly in the sense of Eqn. (5.3.5), pressure equilibrium is established quickly over the *whole* jet cross-section. Therefore, the interior jet pressure must equal the pressure of the surrounding gas.

The interface between the jet and the surrounding gas is a so-called *contact discontinuity*. Note that (by definition) there is no mass flux across this cylindrical surface. If the gas surrounding the jet is the atmosphere of some galaxy, and if this atmosphere is in hydrostatic equilibrium with a density $\rho_{\rm e}$, the exterior (atmospheric) pressure satisfies the

$$\frac{{\rm d}P_{\rm e}}{{\rm d}z} = \rho_{\rm e}\, g_z \ , \tag{5.3.7}$$

with $g_z = -\partial\Phi/\partial z$ the local z-component of the gravitational acceleration due to the galaxy.

The pressure constraint, $P(z) = P_{\rm e}(z)$, together with the condition of an isentropic flow, immediately fixes the internal density:

$$\rho(z) = \rho_0 \left(\frac{P_{\rm e}(z)}{P_0}\right)^{1/\gamma} \ . \tag{5.3.8}$$

Bernouilli's law can be rewritten into an equation for the flow speed in a way similar to the Parker wind (Chapter 4.2):

$$V\,{\rm d}V + \frac{{\rm d}P}{\rho} + \left(\frac{\partial\Phi}{\partial z}\right)\,{\rm d}z = 0 \ . \tag{5.3.9}$$

From mass conservation one finds

$$\frac{{\rm d}\rho}{\rho} = -\left(\frac{{\rm d}V}{V} + \frac{{\rm d}\mathcal{A}}{\mathcal{A}}\right) \ . \tag{5.3.10}$$

If the external gas satisfies the equation (5.3.7) for hydrostatic equilibrium one has

$$\left(\frac{\partial\Phi}{\partial z}\right) = -g_z = -\frac{1}{\rho_{\rm e}}\,\frac{{\rm d}P_{\rm e}}{{\rm d}z} \ . \tag{5.3.11}$$

This, together with the pressure equilibrium condition $P = P_{\rm e}$ allows us to write the equation of motion as

$$V\,\frac{{\rm d}V}{{\rm d}z} = -\frac{1}{\rho}\,\frac{{\rm d}P}{{\rm d}z} + g_z = -\left(\frac{\rho_{\rm e}}{\rho} - 1\right)\,g_z \ . \tag{5.3.12}$$

This means that the increase in the outward velocity of the jet can be understood as the effect of *buoyancy*[9]: the rise of a light material in a denser fluid or gas against the direction of gravity. In this case $g_z < 0$ and the jet velocity increases towards positive z provided the jet material is less dense than the surroundings: $\rho < \rho_{\rm e}$. No jet can be formed if $\rho > \rho_{\rm e}$: the material would fall back onto the nucleus.

This is the essential ingredient of the Blandford-Rees model of jet formation. Here one assumes that the 'central engine' in the nucleus of the AGN produces a hot, tenuous gas with a high pressure and low density compared with the surrounding interstellar gas. This material becomes buoyant in the gravitational field of the galaxy hosting the massive black hole and its entourage, and the material escapes in the direction where the gravitational acceleration is largest, usually the rotational axis of the central part of the galaxy. The material accelerates until it reaches the maximum velocity allowed by Bernouilli's law.

An illuminating analogy (due to Martin Rees) is the following: put a hose discharging air at the bottom of a lake. If the gas discharge is small, individual air bubbles will rise to the surface. When the discharge rate of the air hose is cranked up there will ultimately come a point where so much air will rise to the surface that the air bubbles merge and a jet of air propagates to the surface, confined by the pressure of the surrounding water. At each depth, there will be (roughly) pressure equilibrium between the water pressure and the air pressure in the jet. The internal jet velocity near the lake surface will be larger if we put the air hose in a deeper lake so that the pressure at the mouth of the hose is larger, and the jet is (by necessity) longer.

An alternative form for the equation of motion uses Eqn. (5.3.10) to write a close analogue of the Parker wind equation[10]:

$$\left(V^2 - c_{\rm s}^2\right) \frac{{\rm d}\ln V}{{\rm d}z} = c_{\rm s}^2 \frac{{\rm d}\ln \mathcal{A}}{{\rm d}z} + g_z \,, \tag{5.3.13}$$

with $c_{\rm s}^2 = \gamma P/\rho = \gamma P_{\rm e}/\rho$. We can use (5.3.11) once again to eliminate g_z from this equation,

$$g_z = \frac{1}{\rho_{\rm e}} \frac{{\rm d}P_{\rm e}}{{\rm d}z} = \frac{1}{\rho_{\rm e}} \frac{{\rm d}P}{{\rm d}z} = \frac{\rho}{\rho_{\rm e}} \left[c_{\rm s}^2 \left(\frac{1}{\rho} \frac{{\rm d}\rho}{{\rm d}z} \right) \right] \,. \tag{5.3.14}$$

[9] Also known as *Archimedes' law*; The word buoyancy comes from the Dutch *boei*, a floating object used to mark shipping lanes.

[10] One recovers the Parker wind equation exactly if one puts $\mathcal{A} \propto z^2$ and $g_z = -GM_*/z^2$.

Using mass conservation in the form (5.3.10) to eliminate the density derivative term $(1/\rho)\mathrm{d}\rho/\mathrm{d}z$, one finds a third version of the equation:

$$\boxed{\left(V^2 - c_*^2\right) \frac{\mathrm{d}\ln V}{\mathrm{d}z} = c_*^2 \frac{\mathrm{d}\ln \mathcal{A}}{\mathrm{d}z} \ .} \tag{5.3.15}$$

Here the velocity c_* is defined by

$$c_*^2 = \frac{\gamma P}{\rho} - \frac{\gamma P}{\rho_\mathrm{e}} \ . \tag{5.3.16}$$

Note that this quantity is positive as $\rho < \rho_\mathrm{e}$. If the adiabatic index γ_e of the external medium equals that of the jet material one has simply $c_*^2 = c_\mathrm{s}^2 - c_\mathrm{se}^2$.

This second version of Parker's equation for jet flow clearly shows that there is a critical point in the jet flow where the two conditions

$$V = c_* \quad , \quad \frac{\mathrm{d}\mathcal{A}}{\mathrm{d}z} = 0 \tag{5.3.17}$$

must be satisfied *simultaneously*. This is illustrated in the figure below. Inside the critical point (close to the central engine) the flow will be 'subsonic' with respect to c_* and the jet cross-section must diminish: $\mathrm{d}\mathcal{A}/\mathrm{d}z < 0$. Once the material passes through the critical point and becomes supersonic with respect to c_*, the jet expands again as $\mathrm{d}\mathcal{A}/\mathrm{d}z > 0$.

This situation, with a constriction of the jet at the critical point, is analogous to the so-called *Laval-nozzle* that is present in jet- and rocket engines (see figure). In that case the combustion products of the engine squirt out of the constriction at the sound speed, and are accelerated in the flaring ($\mathrm{d}\mathcal{A}/\mathrm{d}z > 0$) exhaust tube to high speeds so that most of the chemical energy released in the engine ends up in the associated (highly supersonic) momentum discharge. This momentum discharge delivers the engine thrust needed to power the rocket. Since there is no gravity in this situation, the velocity of the gas in a Laval nozzle satisfies

$$\left(V^2 - c_\mathrm{s}^2\right) \frac{\mathrm{d}\ln V}{\mathrm{d}z} = c_\mathrm{s}^2 \frac{\mathrm{d}\ln \mathcal{A}}{\mathrm{d}z} \ . \tag{5.3.18}$$

It is relatively simple to write down the *asymptotic behaviour* of the jet at large distances from the nucleus, say when the jet flow has left the optical galaxy hosting the AGN.

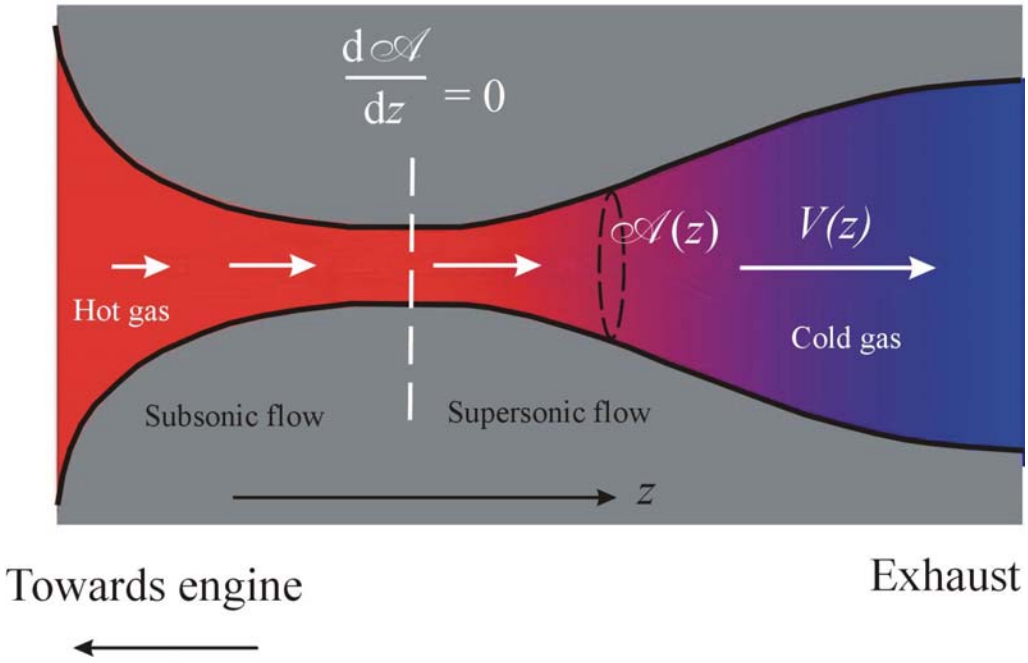

Figure 5.13: *A Laval Nozzle is a tube with a constriction, which is generally used in rocket engines. High-pressure gas coming from the combustion chamber enters the nozzle, and flows into a region where the nozzle cross section declines:* $\mathrm{d}\mathcal{A}/\mathrm{d}z < 0$. *The thermal energy is converted into kinetic energy of the flow, and the flow accelerates. It can only keep accelerating if the flow goes through a sonic point (where* $V = c_\mathrm{s}$*) at the critical point* z_**, where* $\mathrm{d}\mathcal{A}/\mathrm{d}z = 0$. *The cross section increases again after the critical point,* $\mathrm{d}\mathcal{A}/\mathrm{d}z > 0$*, and the gas is accelerated further. The two critical point conditions,* $V = c_\mathrm{s}(z_*)$ *and* $\mathrm{d}\mathcal{A}/\mathrm{d}z = 0$ *at* $z = z_*$*, are analogous to those encountered in the Parker model of the Solar Wind.*

It is then safe to assume that the external pressure (that of the intergalactic medium) is much less than the pressure P_0 close to the central engine, and that the gravitational potential becomes negligible. Assuming that the velocity $V \ll c_{\rm s}$ near the central engine, but that $V \gg c_{\rm s}$ and $V \gg \sqrt{\Phi}$ at large z, Bernouilli's equation yields

$$V(z) \longrightarrow V_\infty = \sqrt{2\mathcal{E}} \approx \left(\frac{2c_{\rm s0}^2}{(\gamma-1)} \right)^{1/2} = \text{constant} \; . \tag{5.3.19}$$

This shows that the jet velocity will never be much larger than the *internal* sound speed $c_{\rm s0} = \sqrt{\gamma P_0/\rho_0}$ of the jet material near the central engine. Mass conservation together with density law (5.3.8) then gives the variation of cross-section of the jet:

$$\mathcal{A} = \pi R^2 \propto \rho^{-1} \propto P_{\rm e}^{-1/\gamma} \; . \tag{5.3.20}$$

If the pressure in the intergalactic gas becomes constant at large distances from the galaxy the jet cross-section and jet radius also become constant, and the jet shape asymptotically becomes a pure cylinder.

In this derivation we have not paid much attention to the precise details of jet formation near the central engine, or the question whether this formation mechanism ever leads to a 'slender' jet satisfying the constraint (5.3.5) on the degree of collimation of the bundle of flowlines that constitute the jet. We will discuss these issues in more detail when we consider one of the most promising mechanisms for the collimation of high-speed jets: *magnetic collimation*.

We have not considered the case where the flow speed approaches the velocity of light. For that we need the relativistic flow equations which we will consider later. We have also not asked the question about what happens at the *end point* of a jet, where the jet material impacts on the intergalactic medium. Since the jet velocity is supersonic, it is reasonable to expect that strong shocks occur at that point. These shocks are in fact seen to be present in the radio lobes of FRII radio galaxies as the *hot spots* of increased surface brightness. The question of shocks, both internal and at the end point of jets, the associated question of the advance of the jet into the intergalactic medium and the disposition of the material that 'squirts' out of the jet at its endpoint will be discussed in the next chapter as one of the applications of shock physics.

Finally, we have assumed that a jet propagating over a large distance remains *stable* in the sense that the flow is not disrupted by some hydrodynamical instability. An instability in a supersonic jet generally will lead to the formation of internal shocks, the associated rapid heating of the jet material and finally to deconfinement of the jet where jet material mixes strongly with the surrounding gas (*turbulent mixing*).

It is not at all obvious that jets *should* be stable: experimental jets in Earth-bound experiments are easily disrupted by what is known as the *Kelvin-Helmholtz instability*, an instability that occurs at the interface between two fluids moving at different speeds. If magnetic fields are allowed to play a role, the question of stability becomes even more complicated. This issue will be considered when we treat the most important dynamical instabilities for astrophysical flows. One of the conclusions will be that a strongly supersonic jet with a flow speed $V \gg c_{\rm s}$ is more stable than a subsonic jet with $V \ll c_{\rm s}$.

5.4 The Eddington limit: a brief derivation

I briefly mentioned the Eddington limit, the typical luminosity one expects an accreting source to have. In fact, this luminosity is the *maximum* luminosity allowed for a spherically accreting source which converts all the kinetic energy of the infalling matter into radiation.
Historically, Eddington calculated this quantity as the maximum luminosity a star could have, long before it was known what actually powers a star. Consider a star, radiating a total luminosity L_*. If the radiation is emitted isotropically, so that it is evenly distributed over a sphere, the radiative energy flux at a distance r of the star is

$$F_* = \frac{L_*}{4\pi r^2} \ . \tag{5.4.1}$$

This is the amount of energy carried by photons that passes per unit area per second.

A photon of energy $E = h\nu$ has a momentum $p = E/c$. This implies that a net energy flux in the radial direction corresponds with a net momentum flux carried by the photons in the radial direction (with corresponding unit vector $\hat{\boldsymbol{e}}_r$) equal to

$$\boldsymbol{S} = \frac{F_*}{c}\,\hat{\boldsymbol{e}}_r = \frac{L_*}{4\pi r^2 c}\,\hat{\boldsymbol{e}}_r \ . \tag{5.4.2}$$

Suppose that the outer layers of the star are composed of ionized hydrogen: free electrons and protons. Free electrons are capable of scattering light in a process known as *Thomson scattering*. The scattered light is emitted in such a way that -on average- it carries no net momentum. The original photons on the other hand *do* carry a net momentum flux. This means that there is a net radially directed force on the electrons, which equals *per electron*

$$\boldsymbol{F}_{\rm e} = \sigma_{\rm T}\boldsymbol{S} = \frac{\sigma_{\rm T} L_*}{4\pi r^2 c}\,\hat{\boldsymbol{e}}_r \ . \tag{5.4.3}$$

Here $\sigma_{\rm T} = 6.625 \times 10^{-25}$ cm^2 is the *Thomson cross section*, the relevant cross section for this process. If the density of electrons equals $n_{\rm e}$, the corresponding force density, sometimes somewhat misleadingly called radiation pressure, is:

$$\boldsymbol{f}_{\rm e} = n_{\rm e}\,\boldsymbol{F}_{\rm e} = \frac{n_{\rm e}\sigma_{\rm T} L_*}{4\pi r^2 c}\,\hat{\boldsymbol{e}}_r \ . \tag{5.4.4}$$

The negatively charged electrons and the positively charged protons couple strongly to each other. They can not move independently because of the electrostatic attraction. This means that the radiation force on the electrons is mediated to the protons by electric forces, and the force density (5.4.4) is in fact the radiation force on the *whole* gas and is also felt by the protons.

Now let us asume that the hydrogen gas is at rest, and in hydrostatic equilibrium so that the pressure force balances both the gravitational force of the star and the radiation force due to Thomson scattering by the electrons. The force balance in the radial direction then becomes:

$$\frac{\mathrm{d}P}{\mathrm{d}r} = -\frac{GM_*\rho}{r^2} + \frac{n_\mathrm{e}\sigma_\mathrm{T}L_*}{4\pi r^2 c} \ . \tag{5.4.5}$$

The electrons are much lighter than the protons ($m_\mathrm{p}/m_\mathrm{e} = 1836.2$). Assuming that the gas is electrically neutral we have equal numbers of protons and electrons, $n_\mathrm{p} = n_\mathrm{e} \equiv n$, and the mass density of the hydrogen plasma equals to a good approximation $\rho = nm_\mathrm{p}$.

Now note that both the gravity term and the radiation force term on the right-hand side of (5.4.5) drop of with radius as $1/r^2$. This allows us to write the equation of hydrostatic equilibrium in the following way:

$$\frac{\mathrm{d}P}{\mathrm{d}r} = -\frac{GM_*\rho}{r^2}\left(1 - \frac{L_*}{L_\mathrm{edd}}\right) \ , \tag{5.4.6}$$

where the Eddington luminosity L_edd is defined as

$$L_\mathrm{edd} = \frac{4\pi GM_*\, m_\mathrm{p} c}{\sigma_\mathrm{T}} \ . \tag{5.4.7}$$

Eddington now argued that star can only exist if the net force in the radial direction due to gravity and radiation is directed *inwards*, i.e. the right-hand side of Eqn. (5.4.6) should remain *negative*. Since the energy in a star is generated in its nucleus, the above calculation holds everywhere outside the nucleus, even well inside the star! This means that stars can only exist if their luminosity is less than the Eddington luminosity:

$$L_* < L_\mathrm{edd} \approx 10^{38}\left(\frac{M_*}{M_\odot}\right) \ \mathrm{erg/s}. \tag{5.4.8}$$

If a star would somehow magically acquire a luminosity exceeding the Eddington limit, it would blow itself apart.

Eddington's argument holds irrespective of the power source fueling the radiation. When matter accretes onto a compact object with mass M_* and radius R_*, such as a neutron star or white dwarf, the free-fall energy of the accreting material is converted into radiation, with a typical luminosity (see Chapter 4):

$$L_{\rm acrr} \approx \frac{GM_*\dot{M}}{R_*} \ . \tag{5.4.9}$$

Here $\dot{M}$ is the mass accretion rate.
If this luminosity exceeds the Eddington limit, the outward radiation force acting on the infalling material will be larger than the inward gravitational force, and accretion will stop. As a result, the condition $L_{\rm accr} < L_{\rm edd}$ sets an upper limit on the mass accretion rate:

$$\dot{M} < \dot{M}_{\rm edd} = \frac{4\pi R_* m_{\rm p} c}{\sigma_{\rm T}} \ . \tag{5.4.10}$$

This limit is, for a stellar-mass compact object,

$$\dot{M}_{\rm edd} = 1.5 \times 10^{-8} \left(\frac{R_*}{10 \ {\rm km}}\right) \ M_\odot/{\rm yr} \ . \tag{5.4.11}$$

Of course there are ways around this argument. We have assumed that the mass is distributed spherically and falls in radially, and therefore *must* encounter all the radiation. In a systems such as accreting binaries this is obviously not the case: there the angular momentum of the accreting material forces it to form an accretion disk. If the disk is not to thick, most of the matter could avoid the radiation coming from the immediate vicinity of the compact object, and super-Eddington accretion rates with $\dot{M} > \dot{M}_{\rm edd}$ are possible. Nevertheless, the most luminous accreting sources seem to have a typical luminosity close to the Eddington luminosity. Super-Eddington luminosities are usually observed in sources which emit *bursts* of radiation rather than a persistent radiation flux.

A further complication, neglected in this derivation, is the influence of radiation forces due to spectral lines. Astrophysical plasmas are never pure hydrogen plasmas. There are always traces of heavier materials mixed in: everything heavier than Helium is called a 'metal' by astrophysicists. These metals can be *partially* ionized, making it possible for photons to be absorbed in a standard atomic transition. The momentum transfer from the photons to the gas that is associated with the spectral lines of these metals can be much larger than the transfer due to Thomson scattering, even though the mass fraction of these heavier elements is small. Such radiation forces play an important role in the theory of *line-driven stellar winds*. This also implies that the effects of radiative forces associated with spectral lines becomes important at luminosities much smaller that the Eddington luminosity.

Chapter 6

Linear waves

6.1 Introduction

One of the main difficulties of fluid mechanics is its intrinsic non-linearity. This makes it difficult to find exact solutions except in cases where there is a lot of symmetry. An example of such a situation is the Solar Wind model treated in Chapter 4: it is a steady flow ($\partial/\partial t = 0$) and in addition the flow is spherically symmetric so that the direction of the flow lines is known in advance: the radial direction.

Another way to simplify the equations is to look at small perturbations. One assumes that there is an equilibrium state that is a solution of the fluid equations. One then looks at small deviations from that equilibrium, assuming that the changes in velocity, density and pressure remain small. If that is the case, nonlinear terms can be neglected when describing the evolution of these small perturbations. As an illustration of this technique, known as *perturbation analysis*, I will look at an analogous situation in classical mechanics.

6.1.1 Perturbation analysis of particle motion in a potential

Consider a particle of mass m moving in one dimension x under the influence of a potential $V(x)$. The equation of motion reads

$$m\,\frac{\mathrm{d}^2x}{\mathrm{d}t^2} = F(x) = -\frac{\mathrm{d}V}{\mathrm{d}x}\ . \tag{6.1.1}$$

Now let's assume that there is an equilibrium position x_0 where the force $F(x)$ vanishes. This implies that the potential satisfies

$$\left(\frac{\mathrm{d}V}{\mathrm{d}x}\right)_{x=x_0} = 0 \; . \tag{6.1.2}$$

Consider a particle at rest at the equilibrium position $x = x_0$. We now perturb the particle, shifting its position from $x = x_0$ to $x = x_0 + \xi$. How will the particle move?

In the immediate vicinity of x_0 (i.e. for *small* ξ) the potential can be expanded in powers of $\xi = x - x_0$ as:

$$V(x_0 + \xi) \approx V_0 + \left(\frac{\mathrm{d}V}{\mathrm{d}x}\right)_{x=x_0} \xi + \frac{1}{2}\left(\frac{\mathrm{d}^2V}{\mathrm{d}x^2}\right)_{x=x_0} \xi^2 + \cdots \tag{6.1.3}$$

Here $V_0 \equiv V(x_0)$. If we break off the expansion for the potential at the quadratic term, and use the equilibrium condition (6.1.2) we get

$$V(x_0 + \xi) \approx V_0 + \frac{1}{2} k\, \xi^2 \; , \tag{6.1.4}$$

where $k \equiv (\mathrm{d}^2V/\mathrm{d}x^2)_{x=x_0}$. Now substituting

$$x(t) = x_0 + \xi(t) \tag{6.1.5}$$

into the equation of motion (6.1.1), and using $\xi = x - x_0$ so that for constant x_0 one has

$$\frac{\mathrm{d}V}{\mathrm{d}x} = \frac{\mathrm{d}\xi}{\mathrm{d}x}\,\frac{\mathrm{d}V}{\mathrm{d}\xi} = \frac{\mathrm{d}V}{\mathrm{d}\xi} \; , \tag{6.1.6}$$

one finds:

$$m\,\frac{\mathrm{d}^2\xi}{\mathrm{d}t^2} = -\frac{\mathrm{d}V}{\mathrm{d}\xi} = -k\xi \; . \tag{6.1.7}$$

By breaking off the expansion (6.1.3) of the potential at the quadratic term in ξ, we get a *linear* equation of motion for the dispacement $\xi(t)$ of the particle. Had we included terms proportional to ξ^3, there would be a corresponding term $\propto \xi^2$ in the equation of motion for ξ. By making this choice we have *linearized* the problem, and must therefore assume that $|\xi|$ remains sufficiently small so that our approximation remains valid.

The equation of motion (6.1.7) looks like the equation of motion for a linear oscillator if $k > 0$. In that case the force is directed back towards the equilibrium position x_0, and the solution is a harmonic oscillation around the equilibrium position:

$$\xi(t) = \xi_0 \, \cos(\omega t + \alpha) \, , \tag{6.1.8}$$

where ξ_0 is the amplitude of the oscillation and the oscillation frequency equals

$$\omega = \sqrt{\frac{k}{m}} = \sqrt{\frac{1}{m} \left(\frac{\mathrm{d}^2 V}{\mathrm{d}x^2} \right)_{x=x_0}} \, . \tag{6.1.9}$$

The amplitude ξ_0 and phase angle α follow directly from initial conditions: the displacement $\xi(0) = \xi_0 \, \cos\alpha$ and the velocity $(\mathrm{d}\xi/\mathrm{d}t)_0 = -\omega\xi_0 \, \sin\alpha$ at $t = 0$.

The condition $k > 0$ corresponds to:

$$\left(\frac{\mathrm{d}^2 V}{\mathrm{d}x^2} \right)_{x=x_0} > 0 \, . \tag{6.1.10}$$

Condition (6.1.10) is simply that the position x_0 must correspond with a *minimum* in the potential. In that case the equilibrium is *stable* since a small perturbation from the equilibrium position leads to a harmonic oscillation of the particle around that position. The stable case is illustrated below.

If the equilibrium position is at a *maximum*, so that $k < 0$ and

$$\left(\frac{\mathrm{d}^2 V}{\mathrm{d}x^2} \right)_{x=x_0} < 0 \, , \tag{6.1.11}$$

the force is always directed away from equilibrium position x_0. In that case the solution of the equation of motion for ξ reads

$$\xi(t) = \xi_+ \exp(\sigma t) + \xi_- \exp(-\sigma t) \, . \tag{6.1.12}$$

The term proportional to ξ_+ grows exponentially in time, and will dominate the solution when $\sigma t \gg 1$.

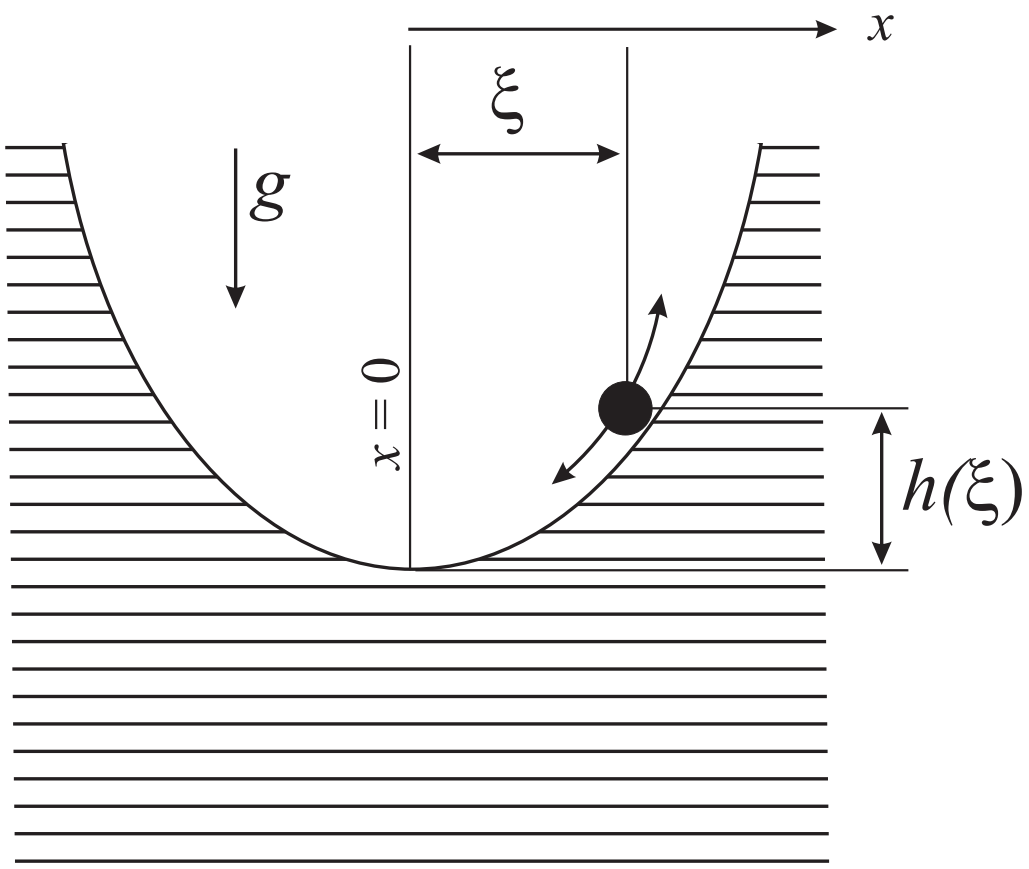

Figure 6.1: *A simple example of a stable oscillation is the motion of a spherical ball in a bowl under the influence of gravity. The gravitational potential energy equals* $V(\xi) = mg\,h(\xi)$*, with* g *acceleration of gravity and where* ξ *is the horizontal distance to the point where the bottom of the bowl reaches its lower level. This point coincides with* $x = 0$*. Also,* $h(\xi)$ *is the height above the lowest point at distance* ξ*. The minimum of the potential occurs in this example at* $x = 0$*, and the constant* k *in this case equals* $k = mg\,(\mathrm{d}^2h/\mathrm{d}x^2)_{x=0}$*.*

The *growth rate* σ is

$$\sigma \equiv \sqrt{\frac{|k|}{m}} = \sqrt{\frac{1}{m}\left|\frac{\mathrm{d}^2 V}{\mathrm{d}x^2}\right|_{x=x_0}} \,. \tag{6.1.13}$$

The amplitude of the term $\propto \xi_+$ doubles in a time interval $\Delta t = \tau = \ln 2/\sigma = 0.693/\sigma$, and grows without bound. This exponential growth of $\xi(t)$ (in the linear approximation) implies that the equilibrium is *unstable*: the particle will move further and further away from the equilibrium position. This means that our assumption that linearization is allowed must inevitably break down when the displacement becomes sufficiently large.

This example of perturbation anaysis illustrates the main features of an approach that is also valid in fluid mechanics. There we will also perturb an equilibrium, and derive a linear equation of motion for a small displacement $\Delta \boldsymbol{x} = \boldsymbol{\xi}$ from that equilibrium. If the equilibrium is stable we will find the linear waves (oscillations) the fluid is able to support. If the equilibrium turns out to be unstable, we will find the linear growth rate of the instability. Like in the case of ordinary mechanics, the perturbation approach allows us to determine the stability of an equilibrium state.

6.2 What constitutes a wave?

In an ideal fluid in a *stable* equilibrium, small pertubations in pressure, density and temperature propagate as waves. The qualification 'small' in this context means that a number of conditions must be satisfied:

- The amplitude of the pressure perturbation ΔP, density perturbation $\Delta\rho$ and the temperature perturbation ΔT are all small compared with the average pressure, density, and temperature:

$$|\Delta P| \ll P \quad , \quad |\Delta\rho| \ll \rho \quad , \quad |\Delta T| \ll T \,. \tag{6.2.1}$$

- The displacement $\Delta \boldsymbol{x} \equiv \boldsymbol{\xi}$ of a fluid element must be small compared with the wavelength λ of the wave, and the wavelength is small compared with the scale length L on which the average pressure, density or temperature of the fluid change:

$$|\boldsymbol{\xi}| \ll \lambda \ll L \,. \tag{6.2.2}$$

If these conditions are not fulfilled, a description in terms of simple linear and purely harmonic waves is not possible.

In a wave it is assumed that ΔP, $\Delta\rho$, ΔT and $\boldsymbol{\xi}$ all vary harmonically in space and time. Such harmonic behaviour is to be expected. Consider for example what happens in a sound wave, which is simply a periodic train of alternating regions of slightly higher and slightly lower pressure than the average pressure. When the gas is locally compressed so that the density increases, the associated local pressure increase will lead to a pressure force directed away from the compression region. This presure force induces a motion of the gas away from the compression which, by virtue of mass conservation, decreases the density. This density decrease can not stop instantaneously due to the inertia of the material. Therefore it continues until the region becomes *less* dense than its surroundings. The region is now under-pressurized and the direction of the pressure force reverses. As a result, the material flows back into the region. Without some form of friction, this cycle will continue indefinitely.

6.3 The plane wave representation

The displacement of a fluid element in a harmonic wave can be represented as

$$\boxed{\boldsymbol{\xi}(\boldsymbol{x}\ ,\ t) = \boldsymbol{a}\exp\left(i\boldsymbol{k}\cdot\boldsymbol{x} - i\omega t\right) + \mathrm{cc}\ .} \tag{6.3.3}$$

Here $\boldsymbol{a}$ is a complex amplitude, $\boldsymbol{k}$ the *wave vector*, which is related to the wavelength λ by

$$\boldsymbol{k} = \frac{2\pi}{\lambda}\,\hat{\boldsymbol{n}} \tag{6.3.4}$$

with $\hat{\boldsymbol{n}}$ a unit vector perpendicular to the wave front, ω is the wave frequency and the notation 'cc' denotes the *complex conjugate*. The complex conjugate must be included to keep $\boldsymbol{\xi}$ (an observable quantity!) real-valued. Such a representation is equivalent (but much more convenient, as we will see) to a representation in sines and cosines. In fact it is equivalent with

$$\boldsymbol{\xi}(\boldsymbol{x}\ ,\ t) = 2|a|\ \hat{\boldsymbol{e}}_a\ \cos\left(\boldsymbol{k}\cdot\boldsymbol{x} - \omega t + \alpha\right)\ , \tag{6.3.5}$$

if we write $\boldsymbol{a} = a\hat{\boldsymbol{e}}_a$ where $\hat{\boldsymbol{e}}_a$ is a (real) unit vector.

The phase angle α is related to the real and imaginary parts of the complex amplitude $\boldsymbol{a}$:

$$\alpha = \tan^{-1}\left(\mathrm{Im}(a)/\mathrm{Re}(a)\right) \equiv \tan^{-1}\left(a_{\mathrm{i}}/a_{\mathrm{r}}\right) \ , \tag{6.3.6}$$

and $|a|$ is

$$|a| = \sqrt{a_{\mathrm{r}}^2 + a_{\mathrm{i}}^2} \ . \tag{6.3.7}$$

Note that the displacement $\boldsymbol{\xi}(\boldsymbol{x} \ , \ t)$ is a *field* on space-time, just as the fluid velocity. The velocity perturbation associated with this displacement is

$$\Delta \boldsymbol{V} = \frac{\mathrm{d}\boldsymbol{\xi}}{\mathrm{d}t} \ . \tag{6.3.8}$$

For the other quantities that vary as a result of the presence of the waves a similar expressions can be written down. For instance, one can write for the density and pressure variations

$$\begin{aligned} \Delta\rho &= \tilde{\rho} \exp\left(i\boldsymbol{k} \cdot \boldsymbol{x} - i\omega t\right) + \mathrm{cc} \ , \\ \Delta P &= \tilde{P} \exp\left(i\boldsymbol{k} \cdot \boldsymbol{x} - i\omega t\right) + \mathrm{cc} \ . \end{aligned} \tag{6.3.9}$$

The fundamental equations of the flow will provide the relation between $\Delta\rho$ or ΔP and the displacement $\boldsymbol{\xi}$.

This description will be valid provided the wave number and wave frequency satisfy

$$\omega \mathrm{T} \gg 1 \quad , \quad |\boldsymbol{k}| L \gg 1 \ . \tag{6.3.10}$$

Here L is the lengthscale of the spatial variation of the properties of the fluid, and T the timescale on which the fluid changes its properties.

6.4 Lagrangian and Eulerian perturbations

In Chapter 2.1 we already noted the two different time derivatives that play a role in fluid mechanics: the partial (or *Eulerian*) time derivative $\partial/\partial t$ which gives the change at a fixed coordinate position, and the total (or *Lagrangian*) time derivative $\mathrm{d}/\mathrm{d}t$ which is the derivative following the flow. We also noted there the difference between the Eulerian perturbation δQ of some quantity (field) $Q(\boldsymbol{x}\,,\,t)$ at some fixed position, and the Lagrangian perturbation ΔQ, given a small change in position $\Delta\boldsymbol{x}$:

$$\Delta Q = \delta Q + (\Delta\boldsymbol{x}\cdot\boldsymbol{\nabla})\,Q\;. \tag{6.4.1}$$

These definitions can be given a precise mathematical meaning. If the flow field is well-behaved, it is possible to assign to each fluid element a label that will identify it unambiguously. A simple choice for such a label is the position the fluid element has at some arbitrary reference time t_0:

> Lagrangian label: the position $\boldsymbol{x}(t_0)\equiv\boldsymbol{x}_0$ of each fluid element at $t=t_0$.

One can think of the position of a fluid element as a function of time t *and* of the label $\boldsymbol{x}_0$,

$$\boldsymbol{x} = \boldsymbol{x}(\boldsymbol{x}_0\,,\,t)\;, \tag{6.4.2}$$

with 'initial condition' $\boldsymbol{x}(t_0)=\boldsymbol{x}_0$. Evaluating this function $\boldsymbol{x}(\boldsymbol{x}_0\,,\,t)$ at *fixed* $\boldsymbol{x}_0$ as a function of t gives you the trajectory of a given fluid element: a flow line. Changing the value of $\boldsymbol{x}_0$ at fixed t takes you to a different fluid element, jumping from flowline to flowline. The label $\boldsymbol{x}_0$ is carried along by a flow element, is constant along a given flowline and must therefore satisfy

$$\frac{\mathrm{d}\boldsymbol{x}_0}{\mathrm{d}t} = 0\;. \tag{6.4.3}$$

The Lagrangian time derivative can be re-interpreted in these terms as

$$\frac{\mathrm{d}}{\mathrm{d}t} \equiv \left(\frac{\partial}{\partial t}\right)_{\boldsymbol{x}_0}\;. \tag{6.4.4}$$

In contrast, the partial (Eulerian) time derivative is taken with the coordinate position $\boldsymbol{x}$ fixed:

$$\frac{\partial}{\partial t} \equiv \left(\frac{\partial}{\partial t}\right)_{\boldsymbol{x}} \ . \tag{6.4.5}$$

In the same manner one can define the Lagrangian perturbation ΔQ and its Eulerian counterpart δQ for any fluid quantity $Q(\boldsymbol{x}\ ,\ t)$ as

$$\begin{aligned} \Delta Q &= \text{perturbation of } Q \text{ with } \boldsymbol{x}_0 \text{ fixed} \ , \\ \delta Q &= \text{perturbation of } Q \text{ with } \boldsymbol{x} \text{ fixed} \ . \end{aligned} \tag{6.4.6}$$

This definition ensures that ΔQ is the change as seen by an observer moving with the flow.

There is an important set of relations between these variations, spatial derivatives and the Eulerian and Lagrangian time derivatives, which follow directly from the formal definitions (6.4.4), (6.4.5) and (6.4.6):

$$\delta\left(\frac{\partial Q}{\partial t}\right) = \frac{\partial\, \delta Q}{\partial t} \quad , \quad \delta(\boldsymbol{\nabla} Q) = \boldsymbol{\nabla}(\delta Q) \quad , \quad \Delta\left(\frac{\mathrm{d}Q}{\mathrm{d}t}\right) = \frac{\mathrm{d}\ \Delta Q}{\mathrm{d}t} \ . \tag{6.4.7}$$

These results will prove useful when we derive the wave properties below.

6.4.1 Velocity, density and pressure perturbations in a wave

The displacement field (wave amplitude) $\boldsymbol{\xi}(\boldsymbol{x}\ ,\ t)$ as defined above corresponds to the change of the fixed coordinates as seen by a hypothetical observer moving with the oscillating motion of the fluid in the wave: the sloshing motion. A fixed observer is by definition always at the same coordinate position. This implies for a small-amplitude wave that the following relations must be valid:

$$\Delta \boldsymbol{x} = \boldsymbol{\xi}(\boldsymbol{x}\ ,\ t) \quad , \quad \delta \boldsymbol{x} = \boldsymbol{0} \ . \tag{6.4.8}$$

We can use the unperturbed position $\boldsymbol{x}$ of the fluid as Lagrangian labels to identify different fluid elements[1].

[1] From this point onwards, I will write $\boldsymbol{x}$ rather than $\boldsymbol{x}_0$ for the unperturbed position of a fluid element.

Each fluid element is then displaced according to the simple prescription

$$\boldsymbol{x} \longrightarrow \overline{\boldsymbol{x}} = \boldsymbol{x} + \boldsymbol{\xi}(\boldsymbol{x}\ ,\ t)\ . \tag{6.4.9}$$

If we use the definition (6.4.6) and relation (6.4.1), which give the relation between the Lagrangian and Eulerian variations in some quantity Q, one finds:

$$\Delta Q = \delta Q + (\boldsymbol{\xi}\cdot\boldsymbol{\nabla})Q\ . \tag{6.4.10}$$

This is the connection between the Lagrangian and Eulerian variation in a small-amplitude wave, neglecting terms of order $|\boldsymbol{\xi}|^2$ and higher. The quantity Q can be a scalar, vector or tensor.

We can apply the relations derived in the previous Section immediately to calculate the velocity perturbation induced by the wave. The Lagrangian velocity perturbation equals

$$\begin{aligned} \Delta\boldsymbol{V} &\equiv \Delta\left(\frac{\mathrm{d}\boldsymbol{x}}{\mathrm{d}t}\right) = \frac{\mathrm{d}\,\Delta\boldsymbol{x}}{\mathrm{d}t} \\ &= \frac{\mathrm{d}\boldsymbol{\xi}}{\mathrm{d}t} \equiv \frac{\partial\boldsymbol{\xi}}{\partial t} + (\boldsymbol{V}\cdot\boldsymbol{\nabla})\boldsymbol{\xi}\ . \end{aligned} \tag{6.4.11}$$

The Eulerian velocity variation seen by a fixed observer now follows from (6.4.1) as:

$$\begin{aligned} \delta\boldsymbol{V} &= \Delta\boldsymbol{V} - (\boldsymbol{\xi}\cdot\boldsymbol{\nabla})\boldsymbol{V} \\ &= \frac{\partial\boldsymbol{\xi}}{\partial t} + (\boldsymbol{V}\cdot\boldsymbol{\nabla})\boldsymbol{\xi} - (\boldsymbol{\xi}\cdot\boldsymbol{\nabla})\boldsymbol{V}\ . \end{aligned} \tag{6.4.12}$$

These relations simplify considerably in the case where the fluid is globally at rest so that $\boldsymbol{V} = \boldsymbol{0}$. In that case one has $\Delta\boldsymbol{V} = \delta\boldsymbol{V} = \partial\boldsymbol{\xi}/\partial t$. Note that we consistently neglect all higher order terms $\propto |\boldsymbol{\xi}|^2\ ,\ |\boldsymbol{\xi}|^3\ \cdots$.

The density change follows from a simple argument of mass conservation quite similar to the one used to derive the continuity equation in Chapter 2.6. Consider different fluid elements, their unperturbed position separated by an infinitesimal vector $\mathrm{d}\boldsymbol{x}$, which we write in component form as

$$\mathrm{d}\boldsymbol{x} \equiv (\mathrm{d}x_1\ ,\ \mathrm{d}x_2\ ,\ \mathrm{d}x_3)\ . \tag{6.4.13}$$

The wave motion (6.4.9) transports each fluid element to a new position according to

$$x_i \longrightarrow \overline{x}_i = x_i + \xi_i(\boldsymbol{x}\ ,\ t) \quad \text{for } i = 1\ ,\ 2\ ,\ 3\ . \tag{6.4.14}$$

This means that the vector $\mathrm{d}\boldsymbol{x}$ is stretched and tilted according to the prescription

$$\mathrm{d}x_i \longrightarrow \mathrm{d}\overline{x}_i = \frac{\partial \overline{x}_i}{\partial x_1}\,\mathrm{d}x_1 + \frac{\partial \overline{x}_i}{\partial x_2}\,\mathrm{d}x_2 + \frac{\partial \overline{x}_i}{\partial x_3}\,\mathrm{d}x_3 \tag{6.4.15}$$

By using the *Einstein summation convention*, where a summation is implied whenever an index is repeated, we can write $\mathrm{d}\overline{x}_i$ as

$$\mathrm{d}\overline{x}_i = \frac{\partial \overline{x}_i}{\partial x_j}\,\mathrm{d}x_j \equiv D_{ij}\,\mathrm{d}x_j\ . \tag{6.4.16}$$

In this expression the summation is over the index j for $j = 1\ ,\ 2\ ,\ 3$. The quantity $D_{ij} \equiv \partial\overline{x}_i/\partial x_j$ is a tensor, the so-called *deformation tensor*. This tensor contains in principle all the information needed to calculate how the vector $\mathrm{d}\boldsymbol{x}$ connecting two neighbouring points is changed as a result of the fluid motion. Using (6.4.14) one can calculate the components of this tensor:

$$D_{ij} = \frac{\partial \overline{x}_i}{\partial x_j} = \delta_{ij} + \frac{\partial \xi_i}{\partial x_j}\ . \tag{6.4.17}$$

In matrix form this corresponds to

$$\boldsymbol{D} = \begin{pmatrix} 1+\dfrac{\partial \xi_1}{\partial x_1} & \dfrac{\partial \xi_1}{\partial x_2} & \dfrac{\partial \xi_1}{\partial x_3} \\ \dfrac{\partial \xi_2}{\partial x_1} & 1+\dfrac{\partial \xi_2}{\partial x_2} & \dfrac{\partial \xi_2}{\partial x_3} \\ \dfrac{\partial \xi_3}{\partial x_1} & \dfrac{\partial \xi_3}{\partial x_2} & 1+\dfrac{\partial \xi_3}{\partial x_3} \end{pmatrix} . \tag{6.4.18}$$

This tensor generally is a function of position and time.

Now consider the infinitesimal volume $\mathrm{d}\mathcal{V}$ defined by the three infinitesimal vectors $\mathrm{d}\boldsymbol{X} \equiv (\mathrm{d}X\ ,\ 0\ ,\ 0)$, $\mathrm{d}\boldsymbol{Y} \equiv (0\ ,\ \mathrm{d}Y\ ,\ 0)$ and $\mathrm{d}\boldsymbol{Z} \equiv (0\ ,\ 0\ ,\ \mathrm{d}Z)$ that all connect to neighbouring fluid elements. The infinitesimal volume enclosed by these three vectors is given by the general rule (2.6.6):

$$\mathrm{d}\mathcal{V} = \mathrm{d}\boldsymbol{X} \cdot (\mathrm{d}\boldsymbol{Y} \times \mathrm{d}\boldsymbol{Z}) = \mathrm{d}X\,\mathrm{d}Y\,\mathrm{d}Z\ . \tag{6.4.19}$$

Each of these three vectors changes as a result of the wave motion, in a manner described by recipe (6.4.16).

For instance, the infinitesimal vector $\mathrm{d}\boldsymbol{X} = (\mathrm{d}X\ ,\ 0\ ,\ 0)$ becomes:

$$\mathrm{d}\overline{\boldsymbol{X}} = \boldsymbol{D} \cdot \mathrm{d}\boldsymbol{X} = \left(1+\frac{\partial \xi_1}{\partial x_1}\ ,\ \frac{\partial \xi_2}{\partial x_1}\ ,\ \frac{\partial \xi_3}{\partial x_1}\right)\ \mathrm{d}X\ . \tag{6.4.20}$$

The first component, along the unperturbed vector, corresponds to the stretching of the vector, increasing its length. The other two components correspond to a rotation of the vector $\mathrm{d}\boldsymbol{X}$. This is illustrated in the figure below. Similar expressions can be written down for $\mathrm{d}\overline{\boldsymbol{Y}}$ and $\mathrm{d}\overline{\boldsymbol{Z}}$:

$$\mathrm{d}\overline{\boldsymbol{Y}} = \left(\frac{\partial \xi_1}{\partial x_2}\ ,\ 1+\frac{\partial \xi_2}{\partial x_2}\ ,\ \frac{\partial \xi_3}{\partial x_2}\right)\ \mathrm{d}Y\ \ ,\ \ \mathrm{d}\overline{\boldsymbol{Z}} = \left(\frac{\partial \xi_1}{\partial x_3}\ ,\ \frac{\partial \xi_2}{\partial x_3}\ ,\ 1+\frac{\partial \xi_3}{\partial x_3}\right)\ \mathrm{d}Z\ . \tag{6.4.21}$$

The volume enclosed by the new separation vectors $\mathrm{d}\overline{\boldsymbol{X}}$, $\mathrm{d}\overline{\boldsymbol{Y}}$ and $\mathrm{d}\overline{\boldsymbol{Z}}$ is

$$\mathrm{d}\overline{\mathcal{V}} = \mathrm{d}\overline{\boldsymbol{X}} \cdot \left(\mathrm{d}\overline{\boldsymbol{Y}} \times \mathrm{d}\overline{\boldsymbol{Z}}\right)\ . \tag{6.4.22}$$

Let us write this in component form, using the totally anti-symmetric *Levi-Cevita tensor* ϵ_{ijk} which is defined by:

$$\epsilon_{ijk} = \begin{cases} +1 & \text{for } i\,j\,k \text{ an even permutation of } 1\,2\,3; \\ -1 & \text{for } i\,j\,k \text{ an uneven permutation of } 1\,2\,3; \\ 0 & \text{if any of the } i\,j\,k \text{ have the same value} \end{cases} . \tag{6.4.23}$$

This definition implies $\epsilon_{123} = \epsilon_{312} = \epsilon_{231} = +1$, $\epsilon_{132} = \epsilon_{213} = \epsilon_{321} = -1$, and all other components vanish. In terms of this tensor, the components of the cross product of two vectors $\boldsymbol{A}$ and $\boldsymbol{B}$ can be written as (remember the summation convention!)

$$(\boldsymbol{A} \times \boldsymbol{B})_i = \epsilon_{ijk}\, A_j B_k \, . \tag{6.4.24}$$

The volume-element (6.4.22) expressed in component notation is

$$\mathrm{d}\overline{\mathcal{V}} = \epsilon_{ijk}\, \mathrm{d}\overline{X}_i\, \mathrm{d}\overline{Y}_j\, \mathrm{d}\overline{Z}_k \, . \tag{6.4.25}$$

Using (6.4.20) for $\mathrm{d}\overline{\boldsymbol{X}}$ in component form, $\mathrm{d}\overline{X}_i = D_{i1}\, \mathrm{d}X$, and the corresponding expressions $\mathrm{d}\overline{Y}_i = D_{i2}\, \mathrm{d}Y$, $\mathrm{d}\overline{Z}_i = D_{i3}\, \mathrm{d}Z$, one finds:

$$\mathrm{d}\overline{\mathcal{V}} = \epsilon_{ijk}\, D_{i1}\, D_{j2}\, D_{k3}\, \mathrm{d}X\, \mathrm{d}Y\, \mathrm{d}Z \, . \tag{6.4.26}$$

The product involving the Levi-Cevita tensor and three factors of D_{ij} is the determinant of the deformation tensor:

$$\epsilon_{ijk}\, D_{i1}\, D_{j2}\, D_{k3} \equiv \det(\boldsymbol{D}) \equiv D(\boldsymbol{x}\,,\, t) = \left\| \begin{array}{ccc} 1 + \dfrac{\partial \xi_1}{\partial x_1} & \dfrac{\partial \xi_1}{\partial x_2} & \dfrac{\partial \xi_1}{\partial x_3} \\ \dfrac{\partial \xi_2}{\partial x_1} & 1 + \dfrac{\partial \xi_2}{\partial x_2} & \dfrac{\partial \xi_2}{\partial x_3} \\ \dfrac{\partial \xi_3}{\partial x_1} & \dfrac{\partial \xi_3}{\partial x_2} & 1 + \dfrac{\partial \xi_3}{\partial x_3} \end{array} \right\| . \tag{6.4.27}$$

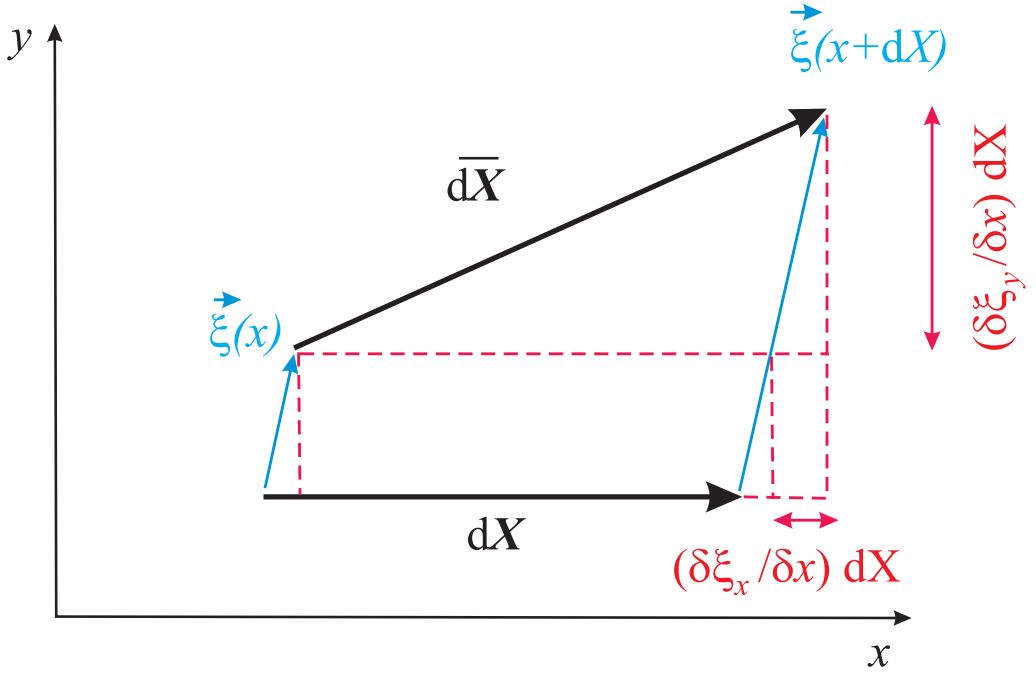

Figure 6.2: *The stretching and rotation of the infinitesimal vector* $\mathrm{d}\boldsymbol{X} = (\mathrm{d}X\ ,\ 0\ ,\ 0)$ *in two dimensions. The change of the vector is characterized by a displacement vector* $\boldsymbol{\xi}(x\ ,\ y\ ,\ t)$ *at its root, and by a displacement vector* $\boldsymbol{\xi}(x + \mathrm{d}X\ ,\ y\ ,\ t)$ *at its tip. The difference between the* x*-components of these two displacement vectors leads to stretching of the vector* $\mathrm{d}\boldsymbol{X}$ *by an amount* $\propto (\partial\xi_x/\partial x)\mathrm{d}X$*, while the difference between the* y*-components,* $\xi_y(x + \mathrm{d}X) - \xi_y(x) \approx (\partial\xi_y/\partial x)\ \mathrm{d}X$*, rotates the vector away from its original orientation parallel to the* x*-axis, with a rotation angle* $\propto (\partial\xi_y/\partial x)\ \mathrm{d}X$*, all to first order in* $|\boldsymbol{\xi}|$*.*

This means that expression (6.4.26) for the volume $\mathrm{d}\overline{\mathcal{V}}$ is simply

$$\mathrm{d}\overline{\mathcal{V}} = D(\boldsymbol{x}\ ,\ t)\,\mathrm{d}\mathcal{V}\ . \tag{6.4.28}$$

Writing out the determinant of the deformation tensor one finds:

$$D(\boldsymbol{x}\ ,\ t) = 1 + \frac{\partial \xi_1}{\partial x_1} + \frac{\partial \xi_2}{\partial x_2} + \frac{\partial \xi_3}{\partial x_3} + \text{terms of order } |\boldsymbol{\xi}|^2 \text{ and } |\boldsymbol{\xi}|^3. \tag{6.4.29}$$

Using the definition[2]

$$\frac{\partial \xi_1}{\partial x_1} + \frac{\partial \xi_2}{\partial x_2} + \frac{\partial \xi_3}{\partial x_3} = \boldsymbol{\nabla}\cdot\boldsymbol{\xi}\ , \tag{6.4.30}$$

one has

$$D(\boldsymbol{x}\ ,\ t) = 1 + \boldsymbol{\nabla}\cdot\boldsymbol{\xi} + \text{terms of order } |\boldsymbol{\xi}|^2 \text{ and } |\boldsymbol{\xi}|^3. \tag{6.4.31}$$

The perturbed volume (6.4.28) therefore equals

$$\boxed{\mathrm{d}\overline{\mathcal{V}} = (1 + \boldsymbol{\nabla}\cdot\boldsymbol{\xi})\ \mathrm{d}\mathcal{V}\ .} \tag{6.4.32}$$

Once again we neglect all non-linear terms in the wave amplitude $|\boldsymbol{\xi}|$.

The density change follows from mass conservation,

$$\mathrm{d}m = \rho\,\mathrm{d}\mathcal{V} = \overline{\rho}\,\mathrm{d}\overline{\mathcal{V}} = \text{constant}\ , \tag{6.4.33}$$

or equivalently

$$\overline{\rho} = \rho\,\left(\frac{\mathrm{d}\mathcal{V}}{\mathrm{d}\overline{\mathcal{V}}}\right)\ . \tag{6.4.34}$$

[2]Simply associate x_1 with the x-coordinate, x_2 with the y-coordinate and x_3 with the z-coordinate.

Using (6.4.32) one has

$$\overline{\rho} = \frac{\rho}{(1 + \boldsymbol{\nabla} \cdot \boldsymbol{\xi})} \approx \rho \ (1 - \boldsymbol{\nabla} \cdot \boldsymbol{\xi}) \ . \tag{6.4.35}$$

Here I have used the approximation $(1 + \eta)^{-1} \approx 1 - \eta$ for $|\eta| \ll 1$.

The Lagrangian variation of the density is by definition

$$\Delta\rho = \overline{\rho} - \rho = -\rho \ (\boldsymbol{\nabla} \cdot \boldsymbol{\xi}) \ . \tag{6.4.36}$$

The Eulerian density perturbation follows from Eqn. (6.4.10): [3]

$$\begin{aligned} \delta\rho &= -\rho \ (\boldsymbol{\nabla} \cdot \boldsymbol{\xi}) - (\boldsymbol{\xi} \cdot \boldsymbol{\nabla}) \, \rho \\ &= -\boldsymbol{\nabla} \cdot (\rho \boldsymbol{\xi}) \ . \end{aligned} \tag{6.4.37}$$

We consider an adiabatic gas without external heat sources. This means that the pressure must follow the adiabatic gas law $P \propto \rho^\gamma$ *along a given flowline*. Therefore, the Lagrangian pressure perturbation $\Delta P = \overline{P} - P$ equals

$$\Delta P = \left(\frac{\partial P}{\partial \rho} \right) \ \Delta\rho = -\gamma P \ (\boldsymbol{\nabla} \cdot \boldsymbol{\xi}) \ . \tag{6.4.38}$$

The Eulerian pressure perturbation follows in the now familiar fashion:

$$\delta P = -\gamma P \ (\boldsymbol{\nabla} \cdot \boldsymbol{\xi}) - (\boldsymbol{\xi} \cdot \boldsymbol{\nabla}) \, P \ . \tag{6.4.39}$$

The table on the following page collects all the results we have derived in this Section for the perturbations associated with a small-amplitude wave.

[3] Here I use the vector identity $f(\boldsymbol{\nabla} \cdot \boldsymbol{A}) + (\boldsymbol{A} \cdot \boldsymbol{\nabla}) f = \boldsymbol{\nabla} \cdot (f \boldsymbol{A})$.

Perturbed quantities in a linear adiabatic wave

Quantity	**Lagrangian perturbation**	**Eulerian perturbation**
Position $\boldsymbol{x}$	$\Delta \boldsymbol{x} = \boldsymbol{\xi}(\boldsymbol{x}\,,\,t)$	$\delta \boldsymbol{x} = \mathbf{0}$ (by definition!)
Velocity $\boldsymbol{V}(\boldsymbol{x}\,,\,t)$	$\Delta \boldsymbol{V} = \dfrac{\partial \boldsymbol{\xi}}{\partial t} + (\boldsymbol{V} \cdot \boldsymbol{\nabla})\boldsymbol{\xi}$	$\delta \boldsymbol{V} = \dfrac{\partial \boldsymbol{\xi}}{\partial t} + (\boldsymbol{V} \cdot \boldsymbol{\nabla})\boldsymbol{\xi} - (\boldsymbol{\xi} \cdot \boldsymbol{\nabla})\boldsymbol{V}$
Density $\rho(\boldsymbol{x}\,,\,t)$	$\Delta \rho = -\rho\,(\boldsymbol{\nabla} \cdot \boldsymbol{\xi})$	$\delta \rho = -\rho\,(\boldsymbol{\nabla} \cdot \boldsymbol{\xi}) - (\boldsymbol{\xi} \cdot \boldsymbol{\nabla})\,\rho$ $\equiv -\boldsymbol{\nabla} \cdot (\rho \boldsymbol{\xi})$
Pressure $P(\boldsymbol{x}\,,\,t)$	$\Delta P = -\gamma P\,(\boldsymbol{\nabla} \cdot \boldsymbol{\xi})$	$\delta P = -\gamma P\,(\boldsymbol{\nabla} \cdot \boldsymbol{\xi}) - (\boldsymbol{\xi} \cdot \boldsymbol{\nabla})\,P$

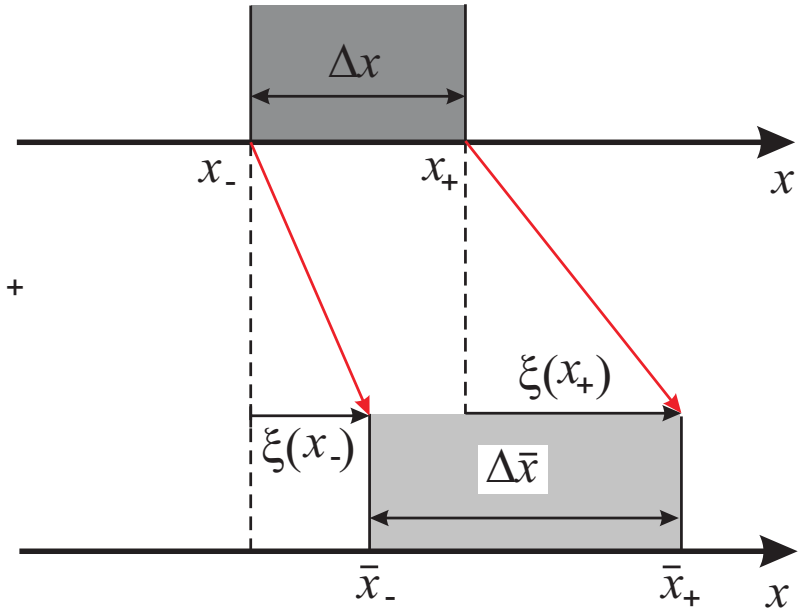

Figure 6.3: *A volume-element with width Δx is stretched as a result of the difference between the displacement $\xi(x_-)$ at the trailing edge, and the displacement $\xi(x_+)$ at the leading edge. Due to these displacements, the new width equals $\Delta\bar{x}$. The example shown is for the case of expansion where $\partial\xi/\partial x > 0$ so that $\Delta\bar{x} > \Delta x$. The opposite case (where $\partial\xi/\partial x < 0$, not shown) would compress the volume-elements so that $\Delta\bar{x} < \Delta x$.*

The one-dimensional case

The derivation of the Lagrangian density change $\Delta\rho$ and the pressure change ΔP (and their Eulerian counterparts $\delta\rho$ and δP) given above is quite general, but also rather complicated. Some insight can be gained from the one-dimensional case, where one does not have to worry about the vector-character of the displacement. Consider a one-dimensional fluid with density $\rho(x\,,\,t)$ and pressure $P(x\,,\,t)$. The position of all fluid elements changes as a result of a perturbation (sound wave). If we label this position with an x-coordinate, we can represent the effect of the perturbation by:

$$x \longrightarrow \bar{x} \equiv x + \xi(x\,,\,t)\;. \tag{6.4.40}$$

This defines the displacement $\xi(x\,,\,t)$ for the one-dimensional case. The role of the small 'volume' is now played by the interval Δx, see the figure above.

Consider the fluid element with its trailing edge at $x_- \equiv x$ and the leading edge at $x_+ = x_- + \Delta x$. The mass of the fluid element is

$$\Delta m = \rho \, \Delta x \; . \tag{6.4.41}$$

Due to the perturbation (6.4.40) the trailing edge of the volume changes its position from x_- to $\bar{x}_- = x_- + \xi(x_- \, , \, t)$, whereas the leading edge changes its position from x_+ to $\bar{x}_+ = x_+ + \xi(x_+ \, , \, t)$. The width of the fluid element is now equal to:

$$\begin{aligned} \Delta \bar{x} &= \bar{x}_+ - \bar{x}_- \\ &= x_+ + \xi(x_+ \, , \, t) - (x_- + \xi(x_- \, , \, t)) \; . \end{aligned} \tag{6.4.42}$$

Now using $x_- = x$ and $x_+ = x + \Delta x$ one finds:

$$\begin{aligned} \Delta \bar{x} &= \Delta x + \xi(x + \Delta x \, , \, t) - \xi(x \, , \, t) \\ &\approx \Delta x + \frac{\partial \xi}{\partial x} \, \Delta x \; . \end{aligned} \tag{6.4.43}$$

Here I have used the fact that Δx is infinitesimally small. One concludes that the new and the old 'volume' are related by

$$\Delta \bar{x} = \left(1 + \frac{\partial \xi}{\partial x} \right) \Delta x \; . \tag{6.4.44}$$

This is the one-dimensional analogue of relation (6.4.32). Note that the fluid element is compressed (so that $\Delta \bar{x} < \Delta x$) when $\partial \xi / \partial x < 0$, and expands (so that $\Delta \bar{x} > \Delta x$) in the case $\partial \xi / \partial x > 0$.

Mass conservation ($\Delta m =$ constant) now reads $\rho \, \Delta x = \bar{\rho} \, \Delta \bar{x}$, so the new density is

$$\bar{\rho} = \rho \, \frac{\Delta x}{\Delta \bar{x}} \; . \tag{6.4.45}$$

Using (6.4.44) one has

$$\bar{\rho} = \frac{\rho}{1 + \dfrac{\partial \xi}{\partial x}} \approx \rho \left(1 - \frac{\partial \xi}{\partial x}\right) , \tag{6.4.46}$$

where I have assumed that $|\xi|$ is small compared with the wavelength λ of the perturbation, which implies that $|\partial \xi / \partial x| \sim |\xi|/\lambda$ is much smaller than unity.

The new density $\bar{\rho}$ is the density in the displaced fluid element, which is now at a position $\bar{x} = x + \xi$. So we should write relation (6.4.46) more precisely as:

$$\bar{\rho}(x + \xi \, , \, t) = \rho(x \, , \, t) \left(1 - \frac{\partial \xi}{\partial x}\right) . \tag{6.4.47}$$

This defines the *Lagrangian* density perturbation as

$$\Delta\rho = \bar{\rho}(x + \xi \, , \, t) - \rho(x \, , \, t) = -\rho(x \, , \, t) \left(\frac{\partial \xi}{\partial x}\right) . \tag{6.4.48}$$

This is the one-dimensional version of relation (6.4.36).

The density at the old (unperturbed) position follows from using (for small ξ)

$$\bar{\rho}(x + \xi \, , \, t) \approx \bar{\rho}(x \, , \, t) + \xi \left(\frac{\partial \rho}{\partial x}\right) . \tag{6.4.49}$$

Note that I have replaced $\partial \bar{\rho} / \partial x$ by $\partial \rho / \partial x$, which is allowed since the difference between ρ and $\bar{\rho}$ (and the two density derivatives) is of order $|\xi|$, and can be neglected since we are only considering terms *linear* in ξ in relation (6.4.49).

Substituting this into relation (6.4.47) and re-ordering terms one finds:

$$\bar{\rho}(x\ ,\ t) = \rho(x\ ,\ t)\ \left(1 - \frac{\partial \xi}{\partial x}\right) - \xi\ \left(\frac{\partial \rho}{\partial x}\right)\ . \tag{6.4.50}$$

This defines the *Eulerian* density perturbation, the difference between the new and the old density at the old (unperturbed) position:

$$\delta\rho = \bar{\rho}(x\ ,\ t) - \rho(x\ ,\ t) = -\rho\ \left(\frac{\partial \xi}{\partial x}\right) - \xi\ \left(\frac{\partial \rho}{\partial x}\right)\ . \tag{6.4.51}$$

This result can be written more compactly as

$$\delta\rho = -\frac{\partial}{\partial x}\left(\rho\,\xi\right)\ . \tag{6.4.52}$$

This is the one-dimensional version of Eqn. (6.4.37).

In the special case of a *uniform* mass density, where $\partial\rho/\partial x = 0$ everywhere in the unperturbed fluid, there is no difference between the Eulerian and Lagrangian density perturbations:

$$\delta\rho = \Delta\rho = -\rho\ \left(\frac{\partial \xi}{\partial x}\right) \quad (\textbf{uniform}\ \text{fluid only!}) \tag{6.4.53}$$

But in the general case the two do not coincide.

The pressure perturbation due to the displacement can be calculated in much the same manner. For an adiabatic gas, where

$$P(\rho) \propto \rho^{\gamma}\ , \tag{6.4.54}$$

we can use (6.4.45) to write:

$$\bar{P}(x + \xi\ ,\ t) = P(x\ ,\ t)\ \left(\frac{\bar{\rho}}{\rho}\right)^{\gamma} = P(x\ ,\ t)\ \left(\frac{\Delta x}{\Delta \bar{x}}\right)^{\gamma}\ . \tag{6.4.55}$$

Using (6.4.44) we have

$$\bar{P}(x+\xi\ ,\ t) = P(x\ ,\ t)\ \left(1+\frac{\partial\xi}{\partial x}\right)^{-\gamma}\ . \tag{6.4.56}$$

Using $|\partial\xi/\partial x| \ll 1$ we can approximate this by:

$$\bar{P}(x+\xi\ ,\ t) = P(x\ ,\ t)\ \left(1-\gamma\frac{\partial\xi}{\partial x}\right)\ . \tag{6.4.57}$$

The Lagrangian perturbation of the pressure follows immediately:

$$\Delta P \equiv \bar{P}(x+\xi\ ,\ t) - P(x\ ,\ t) = -\gamma P\ \left(\frac{\partial\xi}{\partial x}\right)\ . \tag{6.4.58}$$

The Eulerian perturbation can be found using (compare Eqn. 6.4.49)

$$\bar{P}(x+\xi\ ,\ t) \approx \bar{P}(x\ ,\ t) + \xi\ \left(\frac{\partial P}{\partial x}\right)\ . \tag{6.4.59}$$

Upon substitution of this relation into (6.4.57), and after a re-arrangement of terms, one finds:

$$\delta P \equiv \bar{P}(x\ ,\ t) - P(x\ ,\ t) = -\gamma P\ \left(\frac{\partial\xi}{\partial x}\right) - \xi\ \left(\frac{\partial P}{\partial x}\right)\ . \tag{6.4.60}$$

Only if the pressure gradient vanishes in the unperturbed fluid, so that $\partial P/\partial x = 0$ everywhere, do the Lagrangian and the Eulerian pressure perturbations coincide:

$$\Delta P = \delta P = -\gamma P\ \left(\frac{\partial\xi}{\partial x}\right) \quad (\textbf{uniform}\ \text{fluid only!}) \tag{6.4.61}$$

In three dimensions Eqn. (6.4.58) becomes Eqn. (6.4.38), and (6.4.60) becomes (6.4.39).

6.5 Sound waves

The results derived in the previous Section allow us to calculate the properties of an adiabatic sound wave propagating in a stationary, homogeneous fluid. We assume that $\boldsymbol{V} = 0$ everywhere and that avarage density ρ and average pressure P are are independent of position. Because of that assumption, and the fact that the unperturbed fluid is stationary, there is no difference between the linear Lagrangian variations and the Eulerian variations:

$$\text{homogeneous fluid: } \Longleftrightarrow \delta Q = \Delta Q, \tag{6.5.1}$$

a relation that is valid for any quantity $Q(\boldsymbol{x}\ ,\ t)$ in the fluid.

We introduce the small displacement $\Delta\boldsymbol{x} \equiv \boldsymbol{\xi}(\boldsymbol{x}\ ,\ t)$ of a fluid element, due to the presence of a sound wave, that takes the form (6.3.3),

$$\boldsymbol{\xi}(\boldsymbol{x}\ ,\ t) = \boldsymbol{a}\exp\left(i\boldsymbol{k}\cdot\boldsymbol{x} - i\omega t\right) + \text{cc}\ . \tag{6.5.2}$$

Pressure and density fluctuations induced by this wave satisfy

$$\Delta\rho = \delta\rho = -\rho\left(\boldsymbol{\nabla}\cdot\boldsymbol{\xi}\right) \quad , \quad \Delta P = \delta P = -\gamma P\left(\boldsymbol{\nabla}\cdot\boldsymbol{\xi}\right)\ . \tag{6.5.3}$$

The velocity induced by the wave equals

$$\delta\boldsymbol{V} = \Delta\boldsymbol{V} = \frac{\partial\boldsymbol{\xi}}{\partial t}\ . \tag{6.5.4}$$

From the properties of the exponential function,

$$\begin{aligned} \frac{\partial}{\partial t}\left[\exp\left(i\boldsymbol{k}\cdot\boldsymbol{x} - i\omega t\right)\right] &= -i\omega\exp\left(i\boldsymbol{k}\cdot\boldsymbol{x} - i\omega t\right)\ , \\ \frac{\partial}{\partial x_i}\left[\exp\left(i\boldsymbol{k}\cdot\boldsymbol{x} - i\omega t\right)\right] &= ik_i\exp\left(i\boldsymbol{k}\cdot\boldsymbol{x} - i\omega t\right)\ , \end{aligned} \tag{6.5.5}$$

we can calculate the velocity perturbation and the density- and pressure perturbations in terms of $\boldsymbol{\xi}$ by using (6.5.3) and (6.5.2):

$$\boxed{\begin{pmatrix} \delta\boldsymbol{V}(\boldsymbol{x}\ ,\ t) \\ \\ \delta\rho(\boldsymbol{x}\ ,\ t) \\ \\ \delta P(\boldsymbol{x}\ ,\ t) \end{pmatrix} = \begin{pmatrix} -i\omega\boldsymbol{a} \\ \\ -\rho\, i(\boldsymbol{k}\cdot\boldsymbol{a}) \\ \\ -\gamma P\, i(\boldsymbol{k}\cdot\boldsymbol{a}) \end{pmatrix} \times \exp\left(i\boldsymbol{k}\cdot\boldsymbol{x} - i\omega t\right) + \mathrm{cc}\ .} \tag{6.5.6}$$

The only missing ingredient is an equation of motion which links the velocity $\delta\boldsymbol{V} = \partial\boldsymbol{\xi}/\partial t$ to the density and pressure perturbations. Consider the equation of motion for the gas:

$$\frac{\mathrm{d}\boldsymbol{V}}{\mathrm{d}t} = -\frac{1}{\rho}\,\boldsymbol{\nabla}P\ . \tag{6.5.7}$$

From the Lagrangian perturbation of the left-hand-side of this equation we obtain the acceleration of the fluid elements due to the wave. For this acceleration term we can use the fact that taking the Lagrangian variation Δ and the comoving time derivative $\mathrm{d}/\mathrm{d}t$ commute. Using (6.5.4) one finds:

$$\Delta\left(\frac{\mathrm{d}\boldsymbol{V}}{\mathrm{d}t}\right) = \frac{\mathrm{d}\,\Delta\boldsymbol{V}}{\mathrm{d}t} = \frac{\mathrm{d}^2\boldsymbol{\xi}}{\mathrm{d}t^2} = \frac{\partial^2\boldsymbol{\xi}}{\partial t^2}\ . \tag{6.5.8}$$

In the last equality I have used that the *unperturbed* velocity vanishes: $\boldsymbol{V} = 0$.

The Lagrangian perturbation of the right-hand-side gives the pressure force per unit mass due to the waves. This term can be evaluated using [1] the fact that we have assumed that both the unperturbed pressure P and the unperturbed density ρ are constant everywhere, and [2] by applying (6.5.1) and the properties listed in Eqn. (6.4.7):

$$\begin{aligned} \Delta\left(\frac{1}{\rho}\,\boldsymbol{\nabla}P\right) &= \frac{1}{\rho}\,\Delta\left(\boldsymbol{\nabla}P\right) \quad (\text{as } \boldsymbol{\nabla}P = 0 \text{ in the } \textit{unperturbed} \text{ fluid}) \\ &= \frac{1}{\rho}\,\delta\left(\boldsymbol{\nabla}P\right) \quad (\text{as } \Delta = \delta \text{ in a homogeneous fluid}) \\ &= \frac{1}{\rho}\,\boldsymbol{\nabla}\,\delta P \qquad (\text{as } \delta(\boldsymbol{\nabla}P) = \boldsymbol{\nabla}\delta P.) \end{aligned} \tag{6.5.9}$$

The steps taken in this last derivation are only true for the *linear* perturbations.

The perturbed version of the equation of motion obtained in this fashion is the equation governing the perturbations due to the presence of sound waves:

$$\begin{aligned} \frac{\partial^2 \boldsymbol{\xi}}{\partial t^2} &= -\frac{1}{\rho} \boldsymbol{\nabla} \, \delta P \\ &= \frac{\gamma P}{\rho} \boldsymbol{\nabla} \left(\boldsymbol{\nabla} \cdot \boldsymbol{\xi} \right) \, . \end{aligned} \tag{6.5.10}$$

Here I have substituted expression (6.5.3) for δP. The relation

$$\frac{\gamma P}{\rho} \equiv c_{\rm s}^2 \tag{6.5.11}$$

defines the *adiabatic sound speed*. One can write (6.5.10) as a *wave equation* in three dimensions:

$$\boxed{\frac{\partial^2 \boldsymbol{\xi}}{\partial t^2} - c_{\rm s}^2 \, \boldsymbol{\nabla} \left(\boldsymbol{\nabla} \cdot \boldsymbol{\xi} \right) = 0 \, .} \tag{6.5.12}$$

In conclusion: in order to find the equation of motion for the perturbation amplitude $\boldsymbol{\xi}(\boldsymbol{x} \, , \, t)$ one has to perturb the equation of motion, expressing all quantities (such as the velocity and pressure perturbations) in terms of $\boldsymbol{\xi}$ and its derivatives.

If we now substitute (6.5.2) for $\boldsymbol{\xi}$ and make use of the properties of the exponential factor, this equation is converted into a set of linear *algebraic* equations for the amplitude $\boldsymbol{a}$: [4]

$$\omega^2 \, \boldsymbol{a} - c_{\rm s}^2 \left(\boldsymbol{k} \cdot \boldsymbol{a} \right) \boldsymbol{k} = 0 \, . \tag{6.5.13}$$

In order to simplify the algebra, assume that the sound wave propagates in the $x - y$ plane so that $\boldsymbol{k} = (k_x \, , \, k_y \, , \, 0)$. In that case we have

$$\boldsymbol{k} \cdot \boldsymbol{a} = k_x a_x + k_y a_y \, .$$

[4] There is a similar equation for the complex conjugate $\boldsymbol{a}^*$, but that equation does not contain any new information: it is simply the complex conjugate of the equation for $\boldsymbol{a}$. We can therefore safely ignore it in what follows, as I show in more detail below.

It is always possible to define your coordinate system in such a way that this choice is valid, as long as one is dealing with *plane* waves.

By writing out the three spatial components of equation (6.5.13) explicitly we put this system of equations in matrix form:

$$\begin{pmatrix} \omega^2 - k_x^2 c_{\rm s}^2 & -k_x k_y\, c_{\rm s}^2 & 0 \\ -k_y k_x\, c_{\rm s}^2 & \omega^2 - k_y^2 c_{\rm s}^2 & 0 \\ 0 & 0 & \omega^2 \end{pmatrix} \begin{pmatrix} a_x \\ a_y \\ a_z \end{pmatrix} = 0\ . \tag{6.5.14}$$

Matrix algebra[5] tells us that there are only non-trivial solutions, i.e. solutions where the a_i do not vanish identically, when the determinant of the 3×3 matrix in (6.5.14),

$$M_{ij} \equiv \omega^2\, \delta_{ij} - c_{\rm s}^2 k_i k_j\ , \tag{6.5.15}$$

vanishes. This determinant equals

$$\det\left(M_{ij}\right) = \omega^2 \left\{ \left(\omega^2 - k_x^2 c_{\rm s}^2\right) \left(\omega^2 - k_y^2 c_{\rm s}^2\right) - \left(k_x k_y\, c_{\rm s}^2\right)^2 \right\}\ . \tag{6.5.16}$$

Re-ordering terms, and putting the determinant equal to zero, yields a relation between wave frequency ω and the wave number $\boldsymbol{k}$, the so-called *dispersion relation*. For sound waves in a stationary fluid or gas this dispersion relation is

$$\boxed{\omega^4 \left(\omega^2 - k^2\, c_{\rm s}^2\right) = 0\ ,} \tag{6.5.17}$$

with $k^2 = k_x^2 + k_y^2$.

There are two types of solutions: the solution $\omega = 0$ does not really correspond with a wave: the corresponding amplitude does not vary in time. Strictly speaking, this solution should be discarded for this reason.

[5] e.g. G.B. Arfken & H.J. Weber, *Mathematical Methods for Physicists*, Fourth Edition, Academic Press, 1995, Chapter 3.

The remaining two solutions correspond to a positive- and a negative frequency sound wave:

$$\omega(\boldsymbol{k}) = +kc_{\rm s} \quad , \quad \omega(\boldsymbol{k}) = -kc_{\rm s} \; , \tag{6.5.18}$$

with $k = |\boldsymbol{k}| = \sqrt{k_x^2 + k_y^2}$. The frequency of the sound waves depends only on the sound speed and the magnitude of the wave vector, but **not** on the direction of $\boldsymbol{k}$! This means that sound waves in a stationary fluid propagate with equal velocity in all directions. There is no preferred direction. We will see below that this is no longer true for sound waves in a *moving* fluid. In that case, the direction of the fluid velocity $\boldsymbol{V}$ introduces a preferred direction.

Using the three possible solutions for ω in the original equations one can determine the corresponding *eigenvectors*. It is easily checked that the solution $\omega = 0$ must have $a_x = a_y = 0$ and $a_z \neq 0$ or $a_x/a_y = -k_y/k_x$ and $a_z = 0$. In both cases $\boldsymbol{a} \perp \boldsymbol{k}$. This can also be seen directly from (6.5.13): if we substitute $\omega = 0$ it reduces to $c_{\rm s}^2(\boldsymbol{k} \cdot \boldsymbol{a})\,\boldsymbol{k} = 0$, which has the solution $\boldsymbol{k} \cdot \boldsymbol{a} = 0$.

Sound waves on the other hand must have

$$a_x/a_y = k_x/k_y \quad , \quad a_z = 0 \; . \tag{6.5.19}$$

This implies that the sound wave amplitude and the wave vector must be parallel:

$$\boldsymbol{a}_{\rm sound} \parallel \boldsymbol{k} \; . \tag{6.5.20}$$

Sound waves are compressive *longitudinal waves*. The main properties of a sound wave are illustrated in the figure below.

Now that we know the both the frequency and the polarization of the sound wave, we can immediately write down the relation between the amplitude $|\boldsymbol{\xi}| = \sqrt{2\boldsymbol{a} \cdot \boldsymbol{a}^*}$ of the wave, and the velocity, density and pressure perturbations. From (6.5.6) and (6.5.20) one finds:

$$\begin{aligned} |\delta \boldsymbol{V}| &= c_{\rm s}\, k |\boldsymbol{\xi}| \; , \\ |\delta\rho| &= \rho\, k |\boldsymbol{\xi}| = \rho\, \frac{|\delta \boldsymbol{V}|}{c_{\rm s}} \; , \\ |\delta P| &= \gamma P\, k |\boldsymbol{\xi}| = \gamma P\, \frac{|\delta\rho|}{\rho} \; . \end{aligned} \tag{6.5.21}$$

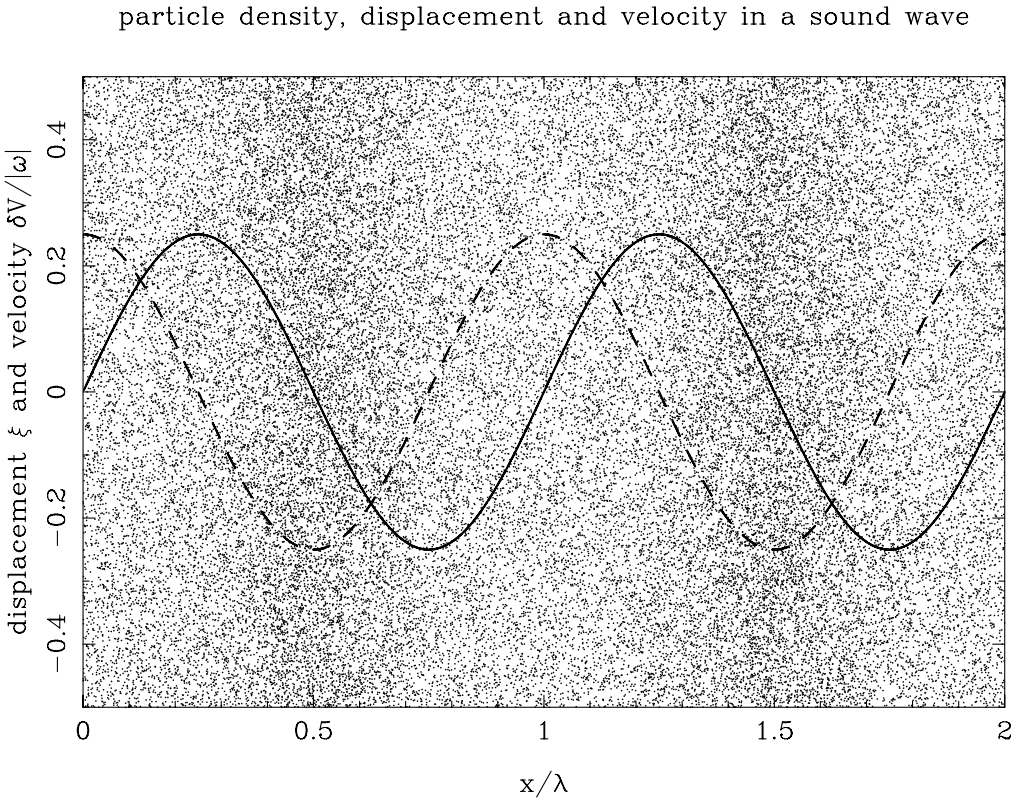

Figure 6.4: *The density ρ, displacement ξ and velocity δV in a sound wave of wavelength λ and frequency ω propagating in the x-direction. This figure shows a 'snapshot' of the wave, the density represented by the position of a large number of 'test-particles' carried passively along by the flow, the displacement by a solid sinusoidal curve, and the velocity is represented by $\delta V/|\omega|$: the dashed curve. Note that with this scaling, the velocity curve has the same amplitude as the displacement curve, (see Eqn. 6.5.6) but is shifted by $\lambda/2$, i.e. the velocity curve is 90^o out of phase. Note that the density is largest where the displacement derivative $\partial\xi/\partial x < 0$ and $\xi = 0$.*

What about the complex conjugate?

This derivation treats the algebra resulting from the plane wave assumption,

$$\boldsymbol{\xi}(\boldsymbol{x}\ ,\ t) = \boldsymbol{a}\exp\left(i\boldsymbol{k}\cdot\boldsymbol{x} - i\omega t\right) + \text{cc}\ ,$$

in a rather cavalier fashion. To justify the approach taken, i.e. converting differential equations for $\boldsymbol{\xi}$ to an algebraic equation for the amplitude $\boldsymbol{a}$, I will look at this approach in more detail, taking the case of sound waves as an example.
The partial differential equation (wave equation) for sound waves reads

$$\frac{\partial^2\boldsymbol{\xi}}{\partial t^2} - c_{\text{s}}^2\,\boldsymbol{\nabla}\left(\boldsymbol{\nabla}\cdot\boldsymbol{\xi}\right) = 0\ .$$

Now writing the plane-wave assumption as

$$\boldsymbol{\xi}(\boldsymbol{x}\ ,\ t) = \boldsymbol{a}\,e^{+iS} + \boldsymbol{a}^*e^{-iS}$$

with

$$S(\boldsymbol{x}\ ,\ t) \equiv \boldsymbol{k}\cdot\boldsymbol{x} - \omega t$$

the phase of the wave and $\boldsymbol{a}^*$ the complex conjugate of the (complex) wave amplitude, substitution of this expression into the wave equation yields:

$$\left[\omega^2\boldsymbol{a} - c_{\text{s}}^2\,\boldsymbol{k}\left(\boldsymbol{k}\cdot\boldsymbol{a}\right)\right]\ e^{+iS} + \left[\omega^2\boldsymbol{a}^* - c_{\text{s}}^2\,\boldsymbol{k}\left(\boldsymbol{k}\cdot\boldsymbol{a}^*\right)\right]\ e^{-iS} = 0\ .$$

This equation should be satisfied for *all* values of $\boldsymbol{x}$ and t, meaning for all values of the phase $S(\boldsymbol{x}\ ,\ t)$. Since

$$e^{\pm iS} = \cos S \pm i\sin S\ ,$$

the above equation can only be satisfied for all $\boldsymbol{x}$ and t if the two factors in the square brackets are **both** zero:

$$\begin{aligned}\omega^2\boldsymbol{a} - c_{\text{s}}^2\,\boldsymbol{k}\left(\boldsymbol{k}\cdot\boldsymbol{a}\right) &= 0\ ,\\ &\textbf{and}\\ \omega^2\boldsymbol{a}^* - c_{\text{s}}^2\,\boldsymbol{k}\left(\boldsymbol{k}\cdot\boldsymbol{a}^*\right) &= 0\ .\end{aligned}$$

However, the second equation is simply the complex conjugate of the first equation (assuming that ω and $\boldsymbol{k}$ are real quantities), so it contains no new information (as $0^* = 0$). Therefore it is sufficient to solve only one of then, the equation for $\boldsymbol{a}$. If the wave frequency becomes complex, the story is a bit more complicated, but the final conclusion is the same: **in the algebraic equations resulting from the plane wave assumption we can forget the phase factor $e^{\pm iS}$ after differentiation, and the complex conjugate. In effect you only need to solve a set of equations for the components of the amplitude vector $\boldsymbol{a}$.**

6.5.1 Wave kinematics: phase- and group velocity

The propagation of the waves is characterized by two velocities: the *phase velocity* $\boldsymbol{v}_{\rm ph}$ and the *group velocity* $\boldsymbol{v}_{\rm gr}$. The phase velocity is the velocity at which points or surfaces of *constant* phase move. This phase is defined by writing Eqn. (6.5.2) as

$$\boldsymbol{\xi}(\boldsymbol{x}\ ,\ t) = \boldsymbol{a}\exp\left[iS(\boldsymbol{x}\ ,\ t)\ \right] + \mathrm{cc}\ , \tag{6.5.22}$$

where, for waves in a uniform steady fluid, the phase S is simply

$$S(\boldsymbol{x}\ ,\ t) \equiv \boldsymbol{k}\cdot\boldsymbol{x} - \omega t\ .$$

The phase velocity $\boldsymbol{v}_{\rm ph}$ is defined by the requirement that an observer moving with this velocity stays on a surface of constant wave phase:

$$\left(\frac{\mathrm{d}S}{\mathrm{d}t}\right)_{\rm ph} = \frac{\partial S}{\partial t} + (\boldsymbol{v}_{\rm ph}\cdot\boldsymbol{\nabla})S = 0\ . \tag{6.5.23}$$

Since we have

$$\frac{\partial S}{\partial t} = -\omega \quad , \quad \frac{\partial S}{\partial x_i} = k_i\ , \tag{6.5.24}$$

this condition means that the phase velocity must satisfy

$$\omega(\boldsymbol{k}) - \boldsymbol{k}\cdot\boldsymbol{v}_{\rm ph} = 0\ . \tag{6.5.25}$$

The obvious choice is[6]

$$\boxed{\boldsymbol{v}_{\rm ph} = \frac{\omega(\boldsymbol{k})}{k}\,\hat{\boldsymbol{\kappa}}\ ,} \tag{6.5.26}$$

with $\hat{\boldsymbol{\kappa}} \equiv \boldsymbol{k}/k$ the unit vector along the wave vector.

[6] One can always add an arbitrary velocity $\boldsymbol{v}_\perp \perp \boldsymbol{k}$ to $\boldsymbol{v}_{\rm ph}$ and still satisfy this condition. The only sensible and non-arbitrary choice however is to put this perpendicular velocity to zero.

The group velocity $\boldsymbol{v}_{\rm gr}$ is defined as the velocity with which the *wave amplitude* propagates. Its value can be determined by the following argument. For simplicity, I use a one-dimensional example.

Consider a *wave packet*, containing waves of different wavelengths, centered in a small bandwidth $\Delta k \ll k$ around some central wave number k. In that case, the displacement can be represented as an integral counting all wave numbers present in the packet[7]

$$\xi(x\ ,\ t) = \int_{-\infty}^{+\infty} \frac{\mathrm{d}k'}{2\pi}\, \mathcal{A}(k')\, e^{ik'x - i\omega(k')t}\ . \tag{6.5.27}$$

An example of such a superposition of waves is shown below. The typical spatial extent of the wavepacket equals $\Delta x \approx 1/\Delta k$. The differential wave amplitude (the so-called Fourier amplitude) $\mathcal{A}(k)$ satisfies

$$\mathcal{A}(k') = 0 \ \text{ for } |k' - k| \gg \Delta k\ , \tag{6.5.28}$$

i.e. $\mathcal{A}(k')$ is strongly peaked around wave number k.

The wave packet will evolve in time as the waves propagate. Everywhere along the path of the wavepacket (and at each wave number) the local dispersion relation $\omega = \omega(k)$ must be satisfied. This determines the wave frequency at some wave number $k + \Delta k$ near k as

$$\omega(k + \Delta k) \approx \omega(k) + \Delta k \left(\frac{\partial \omega}{\partial k}\right)\ . \tag{6.5.29}$$

Using this expansion, together with the fact that the Fourier amplitude is strongly peaked around wave number k, one can write:

$$\xi(x,t) \approx e^{ikx - i\omega(k)t} \times \underbrace{\int_{-\infty}^{+\infty} \frac{\mathrm{d}k'}{2\pi}\, \mathcal{A}(k')\, e^{i\Delta k\,[x - (\partial\omega/\partial k)t\,]}}_{\text{effective amplitude}}\ . \tag{6.5.30}$$

Here $\Delta k \equiv k' - k$. The integral over k' defines what can be considered as the effective amplitude of the wave packet.

[7] This is an example of a so-called *Fourier representation*. It is needed to represent a wave packet with a finite spatial size $L \sim 1/\Delta k$. In contrast, a monochromatic wave ($\Delta k = 0$) always has an **infinite** spatial extent.

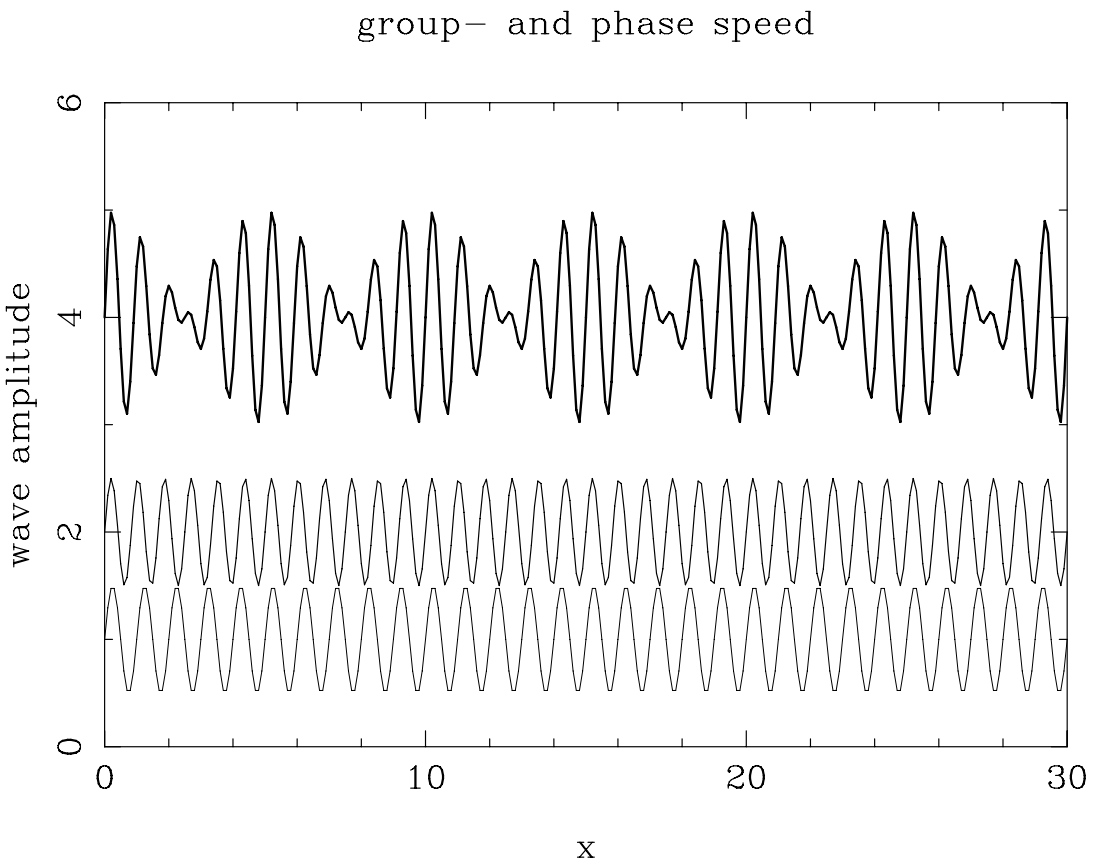

Figure 6.5: *The wave pattern that results from adding two sinusiodal waves, with a slightly different wave number k and frequency ω. These two waves are the two sinus-like curves at the bottom of the figure. Here the relation between the frequency and wave number is chosen to be of the form $\omega(k) = \sqrt{k^2c^2 + \omega_0^2}$. The two waves together interfere to form the wave shown at top. The resulting amplitude modulation in this wave travels at the group velocity. The rapid sinusoidal variation on the other hand travels at the phase speed.*

This effective amplitude will be vanishingly small due to the sinusoidal behaviour of the exponential factor in the integrand, the result of **destructive interference**, **except** at those positions where the phase factor in that exponential term vanishes:

$$x - \left(\frac{\partial \omega}{\partial k}\right) \, t = 0 \; . \tag{6.5.31}$$

At those points the different Fourier amplitudes add up, a case of **constructive interference**. Condition (6.5.31) therefore determines the position of the wave packet, and defines the group velocity in this one-dimensional example as

$$v_{\rm gr} = \left(\frac{{\rm d}x}{{\rm d}t}\right)_{\rm packet} = \frac{\partial \omega}{\partial k} \; . \tag{6.5.32}$$

In three dimensions this generalizes to:

$$\boxed{\boldsymbol{v}_{\rm gr} = \frac{\partial \omega(\boldsymbol{k})}{\partial \boldsymbol{k}} = \left(\frac{\partial \omega}{\partial k_x} \, , \, \frac{\partial \omega}{\partial k_y} \, , \, \frac{\partial \omega}{\partial k_z}\right) \; .} \tag{6.5.33}$$

For sound waves, the phase and group velocity are equal:

$$\boldsymbol{v}_{\rm ph} = \boldsymbol{v}_{\rm gr} = c_{\rm s} \hat{\boldsymbol{\kappa}} \; . \tag{6.5.34}$$

Such waves are said to show *no dispersion*: the amplitude and phase propagate with the same velocity, regardless the wavelength or frequency. If the sound waves in our atmosphere were not almost dispersionless, human hearing would have to be much more sophisticated to discern intelligible signals from human speech, which covers a frequency range of ~ 100 Hz to ~ 1 kHz, or to enjoy music which covers a range ~ 10 Hz to ~ 20 kHz.

6.6 Sound waves in a moving fluid

Now consider sound waves propagating in a moving medium with velocity $\boldsymbol{V}$. If we assume that the wavelength of the waves concerned is much smaller than the scale on which this velocity changes, and that the wave period is much shorter than the timescale on which the temporal variation of $\boldsymbol{V}$ occurs, we may treat this situation (to lowest order) as a case where the fluid velocity is constant and uniform. In that approximation, the relation between the displacement vector and Lagrangian velocity perturbation is

$$\Delta \boldsymbol{V} = \left(\frac{\partial}{\partial t} + (\boldsymbol{V} \cdot \boldsymbol{\nabla}) \right) \boldsymbol{\xi} \, ,$$

while the Lagrangian perturbation of the acceleration is

$$\frac{\mathrm{d}\Delta \boldsymbol{V}}{\mathrm{d}t} = \left(\frac{\partial}{\partial t} + (\boldsymbol{V} \cdot \boldsymbol{\nabla}) \right)^2 \boldsymbol{\xi} \, .$$

The only difference with the case treated above, where the fluid was at rest, is a consistent replacement of the time derivatives:

$$\frac{\partial}{\partial t} \implies \frac{\mathrm{d}}{\mathrm{d}t} = \frac{\partial}{\partial t} + (\boldsymbol{V} \cdot \boldsymbol{\nabla}), \tag{6.6.1}$$

The ordinary time derivative is replaced by the comoving derivative in the unperturbed flow. The density- and pressure variations depend only on the spatial derivatives of $\boldsymbol{\xi}$, and remain unchanged, e.g.

$$\Delta P = \delta P = -\gamma P \, (\boldsymbol{\nabla} \cdot \boldsymbol{\xi}) \, .$$

Therefore, we can immediately write down the wave equation in a moving fluid which corresponds to Eqn. (6.5.12) which is valid in a stationary fluid:

$$\left(\frac{\partial}{\partial t} + (\boldsymbol{V} \cdot \boldsymbol{\nabla}) \right)^2 \boldsymbol{\xi} - c_{\mathrm{s}}^2 \, \boldsymbol{\nabla} \, (\boldsymbol{\nabla} \cdot \boldsymbol{\xi}) = 0 \, . \tag{6.6.2}$$

If we now again assume a plane wave solution,

$$\boldsymbol{\xi}(\boldsymbol{x} \, , \, t) = \boldsymbol{a} \exp \left(i \boldsymbol{k} \cdot \boldsymbol{x} - i \omega t \right) + \mathrm{cc} \, , \tag{6.6.3}$$

it is easily checked that we find essentially the same dispersion relation as before,

$$\left(\omega - \boldsymbol{k} \cdot \boldsymbol{V} \right)^2 \, \boldsymbol{a} - c_{\mathrm{s}}^2 \, (\boldsymbol{k} \cdot \boldsymbol{a}) \, \boldsymbol{k} = 0 \, . \tag{6.6.4}$$

except for the replacement

$$\omega \implies \omega - \boldsymbol{k}\cdot\boldsymbol{V} \equiv \tilde{\omega}, \tag{6.6.5}$$

i.e. the wave frequency ω is replaced by the *Doppler-shifted* frequency $\tilde{\omega}$, which corresponds to the frequency of the wave seen by an observer moving with the fluid, i.e. the frequency in the *fluid rest frame*. This is a simple consequence of replacement rule (6.6.1), which implies that the time derivative of the displacement vector $\boldsymbol{\xi}(\boldsymbol{x}\ ,\ t)$ is:

$$\begin{gathered}\left(\frac{\partial}{\partial t} + (\boldsymbol{V}\cdot\boldsymbol{\nabla})\right)\ \boldsymbol{a}\exp\left(i\boldsymbol{k}\cdot\boldsymbol{x} - i\omega t\right) = \\ -i\left(\omega - \boldsymbol{k}\cdot\boldsymbol{V}\right)\ \boldsymbol{a}\exp\left(i\boldsymbol{k}\cdot\boldsymbol{x} - i\omega t\right)\end{gathered} \tag{6.6.6}$$

This allows us to immediately write down the dispersion relation for sound waves in a moving fluid:

$$\tilde{\omega} = \omega - \boldsymbol{k}\cdot\boldsymbol{V} = \pm|\boldsymbol{k}|c_{\rm s}\ , \tag{6.6.7}$$

or equivalently:

$$\boxed{\omega(\boldsymbol{k}) = \boldsymbol{k}\cdot\boldsymbol{V} \pm |\boldsymbol{k}|c_{\rm s}\ .} \tag{6.6.8}$$

If we now calculate the *group* velocity, the velocity with which signals can propagate, we find in this case

$$\boxed{\boldsymbol{v}_{\rm gr} = \frac{\partial\omega}{\partial\boldsymbol{k}} = \boldsymbol{V} \pm c_{\rm s}\,\hat{\boldsymbol{\kappa}}\ ,} \tag{6.6.9}$$

with $\hat{\boldsymbol{\kappa}} = \boldsymbol{k}/|\boldsymbol{k}|$ as before. This result simply says that sound waves are *dragged along* by the moving fluid at velocity $\boldsymbol{V}$, and propagate *with respect to the fluid* at the (local) sound speed in the direction of $\boldsymbol{k}$.

6.7 Non-planar sound waves

The previous two Sections could leave the impression that all sound waves are plane waves, where the displacement vector $\boldsymbol{\xi}(\boldsymbol{x}\ ,\ t)$ is given by relation (6.5.2). This is not the case. As a counter-example I will briefly consider the case of spherical sound waves.

Let us assume that we place a spherical membrane of radius R at the origin. This membrane acts as a loudspeaker: its radius varies harmonically in time with a prescribed frequency ω:

$$R(t) = R_0 + \delta R\ \cos(\omega t)\ . \tag{6.7.10}$$

We will assume that the amplitude of this vibration is small: $\delta R \ll R_0$.

The gas surrounding this vibrating sphere must respond: at the surface of the vibrating sphere the gas must move in concert. There the displacement vector of the fluid is given by:

$$\boldsymbol{\xi}(r = R_0\ ,\ t) = \delta R\ \cos(\omega t)\ \hat{\boldsymbol{e}}_r\ . \tag{6.7.11}$$

These radial motions induce density- and pressure fluctuations, which in turn lead to the emission of spherical sound waves.

In order to derive the equation for these spherical waves I will use a different form of the wave equation for sound waves. The original equation (6.5.12) reads

$$\frac{\partial^2 \boldsymbol{\xi}}{\partial t^2} - c_{\rm s}^2\ \boldsymbol{\nabla}\left(\boldsymbol{\nabla}\cdot\boldsymbol{\xi}\right) = 0\ . \tag{6.7.12}$$

Sound waves are the compressive solutions of this equations with

$$\Delta \equiv \frac{\delta\rho}{\rho} = -\left(\boldsymbol{\nabla}\cdot\boldsymbol{\xi}\right) \neq 0\ . \tag{6.7.13}$$

We can 'isolate' the sound waves in the wave equation by taking the divergence on both sides. Using the relations

$$\boldsymbol{\nabla}\cdot\left(\frac{\partial^2\boldsymbol{\xi}}{\partial t^2}\right) = \frac{\partial^2(\boldsymbol{\nabla}\cdot\boldsymbol{\xi})}{\partial t^2} = -\frac{\partial^2\Delta}{\partial t^2} \quad , \quad \boldsymbol{\nabla}\cdot\left[\boldsymbol{\nabla}\left(\boldsymbol{\nabla}\cdot\boldsymbol{\xi}\right)\right] = -\boldsymbol{\nabla}^2\Delta \tag{6.7.14}$$

one finds the following equation that *exclusively* describes sound waves:

$$\left\{\frac{\partial^2}{\partial t^2} - c_{\rm s}^2\,\boldsymbol{\nabla}^2\right\}\Delta(\boldsymbol{x}\ ,\ t) = 0\ . \tag{6.7.15}$$

If the waves are spherical, meaning that the surfaces of constant phase are expanding spheres since the waves are outgoing waves that propagate away from the origin, the function $\Delta(\boldsymbol{x}\ ,\ t)$ can only depend on the distance r to the origin, and on time. The resulting wave equation reads in spherical coordinates:

$$\left\{\frac{\partial^2}{\partial t^2} - \frac{c_{\rm s}^2}{r^2}\,\frac{\partial}{\partial r}\left(r^2\,\frac{\partial}{\partial r}\right)\right\}\Delta(r\ ,\ t) = 0\ . \tag{6.7.16}$$

The frequency ω is fixed: it must equal the vibration frequency of the sphere. This means we can put

$$\Delta(r\ ,\ t) = \tilde{\Delta}(r)\,e^{-i\omega t} + {\rm cc}\ , \tag{6.7.17}$$

and use

$$\frac{\partial^2\Delta}{\partial t^2} = -\omega^2\,\Delta\ . \tag{6.7.18}$$

The wave equation (6.7.16) can be then written as an equation for $\tilde{\Delta}(r)$[8]:

$$\frac{1}{r^2}\,\frac{\rm d}{{\rm d}r}\left(r^2\,\frac{{\rm d}\tilde{\Delta}}{{\rm d}r}\right) = -\frac{\omega^2}{c_{\rm s}^2}\,\tilde{\Delta}\ . \tag{6.7.19}$$

Note that the partial derivatives with respect to r have been replaced by ordinary derivatives. This is allowed since $\tilde{\Delta}$ only depends on r.

This equation must be solved subject to sensible boundary conditions. At the surface of the vibrating sphere one has condition (6.7.11). We will deal with this condition later. At large distances the wave should die out, meaning that $\Delta \downarrow 0$ when $r \to \infty$. Equation (6.7.19) can be cast in the form

$$r^2\,\frac{{\rm d}^2\tilde{\Delta}}{{\rm d}r^2} + 2r\,\frac{{\rm d}\tilde{\Delta}}{{\rm d}r} + k^2r^2\,\tilde{\Delta} = 0\ , \tag{6.7.20}$$

[8]Once again, you can forget about the complex conjugate for the time being.

Here k is defined as

$$k \equiv \frac{\omega}{c_{\rm s}} \ , \tag{6.7.21}$$

and essentially plays the role of the wave number. The solution to this equation is

$$\tilde{\Delta}(r) = A\, j_0(kr) + B\, n_0(kr) \ . \tag{6.7.22}$$

Here $j_0(x)$ and $n_0(x)$ are the *spherical Bessel functions* of order zero[9], and A and B are arbitrary constants, to be determined from the boundary conditions. The two functions j_0 and h_0 can be given in closed form:

$$j_0(x) = \frac{\sin x}{x} \quad , \quad n_0(x) = -\frac{\cos x}{x} \ . \tag{6.7.23}$$

Both functions satisfly the boundary condition $\tilde{\Delta} \rightarrow 0$ as $r \rightarrow \infty$. We are forced to use another argument to decide which Bessel function (or what combination of the two functions) to use.

The form of these spherical Bessel functions shows that we are truly dealing with waves: the density $\delta\rho(r\ ,\ t) = \rho\, \Delta(r\ ,\ t)$ varies harmonically in time, and the spherical ripples due to $\sin(kr)$ and $\cos(kr)$ have a wavelength $\Delta r = \lambda = 2\pi/k = 2\pi c_{\rm s}/\omega$. This is exactly the same wavelength one would assign to a plane sound wave with the same frequency. There is a major difference however: the typical amplitude of the spherical waves scales as $1/r$, as both $j_0(kr)$ and $n_0(kr)$ have a factor $1/kr$ in front of the sine and cosine term. In a plane wave (without damping) on the other hand the amplitude is constant. This reflects the different geometry of a spherical wave.

We can decide which combination of the two spherical Bessel functions to use by employing the following argument. Far from the vibrating sphere, at a distance that is large compared to both R_0 and λ, the wave should look like an *outgoing* (almost) plane wave to a local observer. Assuming without loss of generality that $\omega > 0$, this means that $\Delta(r\ ,\ t)$ should vary like:

$$\Delta_{\rm out}(r\ ,\ t) \sim \cos(kr - \omega t + \alpha) \ . \tag{6.7.24}$$

In contrast, an *ingoing* spherical wave propagating towards the origin would behave like

$$\Delta_{\rm in}(r\ ,\ t) \sim \cos(-kr - \omega t + \alpha) \ . \tag{6.7.25}$$

[9]see for instance: Arfken & Weber, *Mathematical Methods for Physicists*, Ch. 11.7.

This argument implies that the solution should be chosen to be equal to:

$$\tilde{\Delta}(r) = A\ (j_0(kr) + in_0(kr)) \equiv A\, h_0^{(1)}(kr)\ . \tag{6.7.26}$$

The function

$$h_0^{(1)}(x) = j_0(x) + in_0(x) = \frac{1}{ix}\exp(ix) \tag{6.7.27}$$

is the zero-th order spherical Hankel function of the first kind.

The remaining constant A can only be found by considering the boundary condition at the surface of the vibrating sphere (i.e. at $r = R_0$). Because of the spherical symmetry of the problem, the motion of the fluid induced by the sphere will be in the radial direction:

$$\boldsymbol{\xi}(\boldsymbol{x}\ ,\ t) = \xi(r\ ,\ t)\ \hat{\boldsymbol{e}}_r\ . \tag{6.7.28}$$

Consequently, the linearized equation of motion only has a radial component,

$$\rho\,\frac{\partial^2\xi}{\partial t^2} = -\frac{\partial \delta P}{\partial r}\ , \tag{6.7.29}$$

compare Eqn. (6.5.10). The associated pressure perturbation is

$$\delta P = \gamma P\,\Delta(r\ ,\ t)\ . \tag{6.7.30}$$

and because of the harmonic time dependence we can rewrite (6.7.29) as:

$$\frac{\partial^2\xi}{\partial t^2} = -\omega^2\,\xi = -c_{\rm s}^2\,\frac{\partial\Delta}{\partial r}\ . \tag{6.7.31}$$

Here I have used $c_{\rm s}^2 = \gamma P/\rho$. This gives the amplitude of the motion as

$$\xi(r\ ,\ t) = \left(\frac{c_{\rm s}^2}{\omega^2}\right)\frac{\partial\Delta}{\partial r} = \frac{1}{k^2}\,\frac{\partial\Delta}{\partial r}\ . \tag{6.7.32}$$

Substituting the solution

$$\Delta(r\ ,\ t) = Ah_0^{(1)}(kr)\exp(-i\omega t) + \mathrm{cc} \tag{6.7.33}$$

One finds:

$$\xi(r\ ,\ t) = \frac{A}{k}h_0'^{(1)}(kr)\exp(-i\omega t) + \mathrm{cc} \tag{6.7.34}$$

Here $h_0'^{(1)}(x) \equiv \mathrm{d}h_0^{(1)}/\mathrm{d}x$ is the first derivative of the Hankel function. At the surface of the sphere we must satisfy the condition that the velocity, and therefore the amplitude ξ matches the motion of the surface, $\xi(R_0\ ,\ t) = \delta R\ \cos(\omega t)$. This condition fixes A:

$$A = \frac{k\,\delta R}{2h_0'^{(1)}(kR_0)}\ . \tag{6.7.35}$$

This solves the problem of spherical sound waves generated by a vibrating sphere. Note that the coefficient A is proportional to the amplitude δR of the vibration on the spherical membrane.

The full solution of the sound waves emitted by a vibrating spherical membrane now reads, for $r > R_0$:

$$\xi(r\ ,\ t) = \tfrac{1}{2}\delta R\ \left(\frac{h_0'^{(1)}(kr)}{h_0'^{(1)}(kR_0)}\right)\ \exp(-i\omega t) + \mathrm{cc}. \tag{6.7.36}$$

6.8 Some astrophysical applications of waves

6.8.1 The Jeans instability

Around 1902, Sir James Jeans investigated the stability of a self-gravitating fluid. This calculation considers the fate of small-amplitude waves ('sound waves') in a fluid which generates its own gravity. This means one one has to solve the equation of motion and the continuity equation in concert with Poisson's equation for the gravitational potential:

$$\begin{aligned} \frac{\mathrm{d}\boldsymbol{V}}{\mathrm{d}t} &= -\frac{1}{\rho}\,\boldsymbol{\nabla}P - \boldsymbol{\nabla}\Phi\;, \\ \frac{\mathrm{d}\rho}{\mathrm{d}t} &= -\rho\,(\boldsymbol{\nabla}\cdot\boldsymbol{V})\;, \\ \boldsymbol{\nabla}^2\Phi &= 4\pi G\,\rho\;, \end{aligned} \tag{6.8.1}$$

together with the adiabatic gas law $P(\rho) \propto \rho^\gamma$. The unperturbed state on which these waves are superposed is sometimes referred to as *Jeans' swindle*: a fluid with uniform density ρ, pressure P and no gravity: $\boldsymbol{g} = -\boldsymbol{\nabla}\Phi = 0$. There can be no gravitational acceleration in a uniform fluid: the gravitational acceleration $\boldsymbol{g}$ is a vector. Its direction would introduce a *preferred* direction, which can not be present in an infinite homogeneous medium that looks the same everywhere and in every direction. One must therefore conclude that $\boldsymbol{g} = -\boldsymbol{\nabla}\Phi = 0$, which implies $\Phi =$ constant. However, according to Poisson's equation one has $\boldsymbol{\nabla}^2\Phi = 4\pi G\,\rho$. This will only give a constant Φ if $\rho = 0$. This inconsistency is glossed over by assuming that Poisson's equation only applies to the density *fluctuations* induced by the waves.

The results derived for the velocity, density and pressure perturbations in sound waves remain valid in this case:

$$\delta\boldsymbol{V} = \frac{\partial\boldsymbol{\xi}}{\partial t} \quad , \quad \delta\rho = -\rho\,(\boldsymbol{\nabla}\cdot\boldsymbol{\xi}) \quad , \quad \delta P = -\gamma P\,(\boldsymbol{\nabla}\cdot\boldsymbol{\xi}) = c_{\mathrm{s}}^2\,\delta\rho\;. \tag{6.8.2}$$

The equation of motion for the perturbations must be modified in order to take the effect of gravity into account. It now reads:

$$\frac{\partial^2\boldsymbol{\xi}}{\partial t^2} = -\frac{1}{\rho}\,\boldsymbol{\nabla}\delta P - \boldsymbol{\nabla}\delta\Phi\;. \tag{6.8.3}$$

Here I have used that, according to Jean's Swindle, the gravitational acceleration acting on a fluid element is

$$\delta \boldsymbol{g} = -\boldsymbol{\nabla}\delta\Phi \; . \tag{6.8.4}$$

This acceleration is caused by the gravitational action of the density fluctuations: density enhancements in the waves tend to attract the surrounding matter. Poisson's equation links the potential perturbations to the fluctuations in the density:

$$\boldsymbol{\nabla}^2 \, \delta\Phi = 4\pi G \, \delta\rho \; . \tag{6.8.5}$$

Let us define the relative density perturbation:

$$\Delta \equiv \frac{\delta\rho}{\rho} = -(\boldsymbol{\nabla} \cdot \boldsymbol{\xi}) \; . \tag{6.8.6}$$

Substituting for the pressure perturbation δP from (6.8.2), the equation of motion becomes:

$$\frac{\partial^2 \boldsymbol{\xi}}{\partial t^2} = c_{\rm s}^2 \, \boldsymbol{\nabla}(\boldsymbol{\nabla} \cdot \boldsymbol{\xi}) - \boldsymbol{\nabla}\delta\Phi \; . \tag{6.8.7}$$

Using the fact that $c_{\rm s} = \sqrt{\gamma P/\rho}$ is constant, we can take the divergence of both sides of the equation, effectively isolating the compressive ($\boldsymbol{\nabla} \cdot \boldsymbol{\xi} \neq 0$) 'sound-like' solutions:

$$\begin{aligned} \frac{\partial^2}{\partial t^2}(\boldsymbol{\nabla} \cdot \boldsymbol{\xi}) &= c_{\rm s}^2 \, \boldsymbol{\nabla}^2(\boldsymbol{\nabla} \cdot \boldsymbol{\xi}) - \boldsymbol{\nabla}^2\delta\Phi \\ &= c_{\rm s}^2 \, \boldsymbol{\nabla}^2(\boldsymbol{\nabla} \cdot \boldsymbol{\xi}) + 4\pi G\rho \, (\boldsymbol{\nabla} \cdot \boldsymbol{\xi}) \; . \end{aligned} \tag{6.8.8}$$

Here I have used $\boldsymbol{\nabla} \cdot \boldsymbol{\nabla}(\cdots) = \boldsymbol{\nabla}^2 \cdots$, and I have employed Poisson's equation (6.8.5) to eliminate $\boldsymbol{\nabla}^2 \, \delta\Phi$ in terms of the density perturbation:

$$\boldsymbol{\nabla}^2\delta\Phi = 4\pi G \, \delta\rho = 4\pi G\rho \, \Delta \; . \tag{6.8.9}$$

Equation (6.8.8) is a linear equation for $\Delta = \delta\rho/\rho$:

$$\boxed{\left[\frac{\partial^2}{\partial t^2} - c_{\rm s}^2\,\boldsymbol{\nabla}^2 - 4\pi G\,\rho\right]\,\Delta = 0\;.} \tag{6.8.10}$$

The rest of the analysis proceeds along the same lines as for sound waves. Consider a plane wave solution, where the relative density perturbation $\Delta = \delta\rho/\rho$ takes the form[10]

$$\Delta(\boldsymbol{x}\;,\;t) = \tilde{\Delta}\,\exp\left(i\boldsymbol{k}\cdot\boldsymbol{x} - i\omega t\right) + {\rm cc}\;. \tag{6.8.11}$$

A substitution of this assumption for $\Delta(\boldsymbol{x}\,,\,t)$ into (6.8.10) yields the dispersion relation for compressive (sound) waves in a self-gravitating fluid:

$$\boxed{\omega^2 = k^2 c_{\rm s}^2 - 4\pi G\,\rho\;.} \tag{6.8.12}$$

The last term on the right-hand-side gives the modification of sound waves due to gravity. The solution of this equation,

$$\omega(\boldsymbol{k}) = \pm\sqrt{k^2 c_{\rm s}^2 - 4\pi G\,\rho}\;, \tag{6.8.13}$$

describes fundamentally different behaviour at short and long wavelengths.

The dividing line between these two types of behaviour is at the wavelength $\lambda_{\rm J}$, the so-called *Jeans length*, where the wave frequency $\omega(\boldsymbol{k})$ vanishes. Defining $k_{\rm J} = 2\pi/\lambda_{\rm J}$ one must have $k_{\rm J}^2 c_{\rm s}^2 = 4\pi G\,\rho$, and one finds:

$$\lambda_{\rm J}^2 = \left(\frac{2\pi}{k_{\rm J}}\right)^2 = \frac{\pi c_{\rm s}^2}{G\rho}\;. \tag{6.8.14}$$

For waves with a wavelength $\lambda < \lambda_{\rm J}$ the argument of the square root in (6.8.13) is positive, and the wave frequency is real.

[10] In terms of the plane-wave expression (6.5.2) for $\boldsymbol{\xi}(\boldsymbol{x}\;,\;t)$ the amplitude $\tilde{\Delta}$ is related to the displacement amplitude $\boldsymbol{a}$ by $\tilde{\Delta} = -i(\boldsymbol{k}\cdot\boldsymbol{a})$, see Eqn. (6.5.6).

However, for wavelengths $\lambda > \lambda_{\rm J}$ the argument of the square root is *negative*, and the wave frequency becomes purely imaginary. The solution (6.8.13) for $\lambda > \lambda_{\rm J}$ can be written in terms of the Jeans length:

$$\omega = \pm ikc_{\rm s}\sqrt{\frac{\lambda^2}{\lambda_{\rm J}^2} - 1}\ . \tag{6.8.15}$$

Imaginary frequencies, where $\omega = i\sigma$, lead to exponentially growing or decaying perturbations. Solution (6.8.15) always has one exponentially growing mode and one decaying mode. The decaying mode is not very important as it dies away. The assumed time-dependence together with $\omega = i\sigma$ means that the relative density perturbation behaves as

$$\Delta(\boldsymbol{x}\ ,\ t) \propto e^{-i\omega t} = e^{\sigma t}\ . \tag{6.8.16}$$

If $\mathrm{Im}(\omega) = \sigma > 0$ the perturbation grows exponentially in time. This means that the wave amplitude gets larger and larger, and our assumption that the pressure, density and velocity perturbations associated with the wave all remain small will ultimately break down. When such a situation arises, the equilibrium state used to calculate the wave properties is said to be **linearly unstable** against suitable perturbations:

If $\mathrm{Im}\ \omega(\boldsymbol{k}) \equiv \sigma(\boldsymbol{k}) > 0$ a linear instability arises	(6.8.17)

The importance of the Jeans length $\lambda_{\rm J}$ as the wavelength that separates stable from unstable oscillations can be illustrated in another way. The pressure force and the gravitational force due to the perturbation are

$$\begin{aligned} \boldsymbol{F}_{\rm p} &= -\boldsymbol{\nabla}\delta P = -\gamma P\, k^2 \boldsymbol{a}\, \exp\left(i\boldsymbol{k}\cdot\boldsymbol{x} - i\omega t\right) + \mathrm{cc}\ , \\ \boldsymbol{F}_{\rm g} &= -\rho\, \boldsymbol{\nabla}\delta\Phi = 4\pi G\, \rho^2\, \boldsymbol{a}\, \exp\left(i\boldsymbol{k}\cdot\boldsymbol{x} - i\omega t\right) + \mathrm{cc}\ . \end{aligned} \tag{6.8.18}$$

Here I have used the plane wave assumption, and the fact that $\boldsymbol{a} \parallel \boldsymbol{k}$. One sees that the pressure force and the gravitational force are 180 degrees out of phase: they work in opposite directions.

Comparing the amplitude of these two forces one has:

$$\frac{|\boldsymbol{F}_{\rm g}|}{|\boldsymbol{F}_{\rm p}|} = \frac{4\pi G\,\rho}{k^2 c_{\rm s}^2} = \left(\frac{\lambda}{\lambda_{\rm J}}\right)^2 \ . \tag{6.8.19}$$

In the stable case ($\lambda < \lambda_{\rm J}$) the amplitude of pressure force is larger than the amplitude of the gravitational force, and the system is stable. In the case $\lambda > \lambda_{\rm J}$ the amplitude of the gravitational force is larger than the amplitude of the pressure force. In that case the system is unstable, and the density enhancements in the wave will continue to grow.

This is illustrated in the two figures above. It shows the displacement ξ, the velocity $\delta v = \partial\xi/\partial t$, the pressure force and the gravitational force in a plane wave propagating in the x-direction. The first figure considers the stable case $\lambda = \lambda_{\rm J}/\sqrt{2}$, the second figure considers the unstable case with $\lambda = \sqrt{2}\,\lambda_{\rm J}$.

We encountered a similar unstable situation in our simple perturbation analysis of a single particle moving in a potential well. In that case, it turned out that an equilibrium is unstable if $\mathrm{d}^2V/\mathrm{d}x^2 < 0$ at the equilibrium point. The example of the Jeans' instability shows that in fluid dynamics you can have a situation where there are stable as well as unstable solutions to the equations of motion. However, if there is an unstable solution, the system is unstable and can not persist.

6.8.2 The zero-frequency mode

For completeness sake, I mention the fact that the zero-frequency waves present in our discussion of sound waves are also present in Jeans' problem. This can be seen by taking

$$\boldsymbol{\nabla} \times \text{ (Equation of motion 6.8.7)} \ .$$

Using the vector identity

$$\boldsymbol{\nabla} \times \boldsymbol{\nabla} f = 0 \ , \tag{6.8.20}$$

valid for an arbitrary function $f(\boldsymbol{x}\ ,\ t)$, this leads to

$$\frac{\partial^2}{\partial t^2}\left(\boldsymbol{\nabla} \times \boldsymbol{\xi}\right) = 0 \ . \tag{6.8.21}$$

Note that this equation does not show any coupling to gravity since $\boldsymbol{\nabla} \times \boldsymbol{\nabla}\delta\Phi = 0$. Substituting a plane wave solution for $\boldsymbol{\xi}(\boldsymbol{x}\ ,\ t)$ (c.f. 6.5.2) one immediately finds

$$\omega^2\ \left(\boldsymbol{k} \times \boldsymbol{a}\right) = 0 \ . \tag{6.8.22}$$

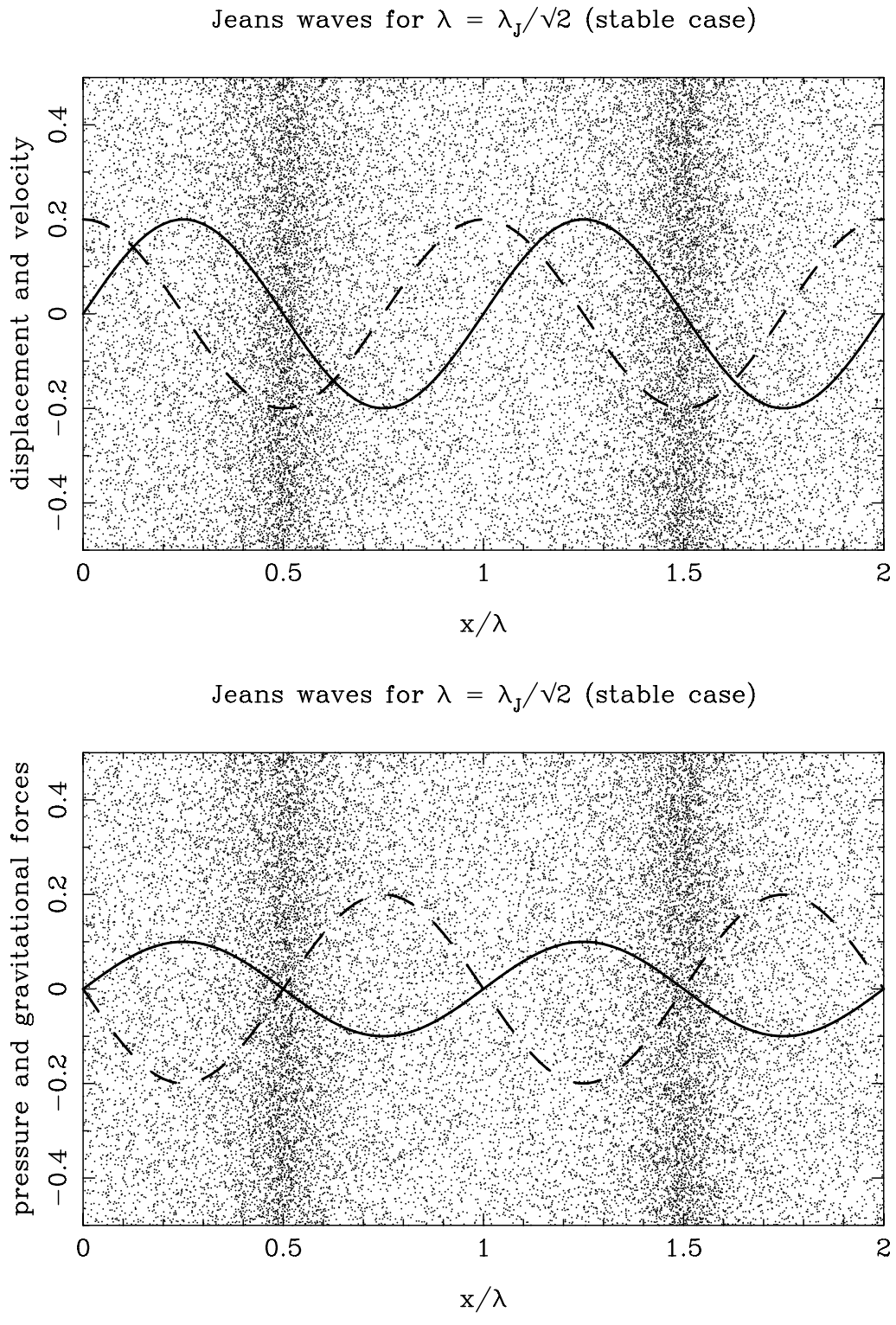

Figure 6.6: *The displacement (top panel, solid curve), velocity (top panel, dashed curve) gravitational force (bottom panel, solid curve) and pressure force(bottom panel, dashed curve) in a linear sound wave in a self-gravitating fluid. Shown is the stable case with wavelength* $\lambda = \lambda_{\rm J}/\sqrt{2}$. *In this case the amplitude of the pressure force is twice that of the gravitational force. The small dots are test particles moving with the fluid, and show where the compressions and rarefactions are located.*

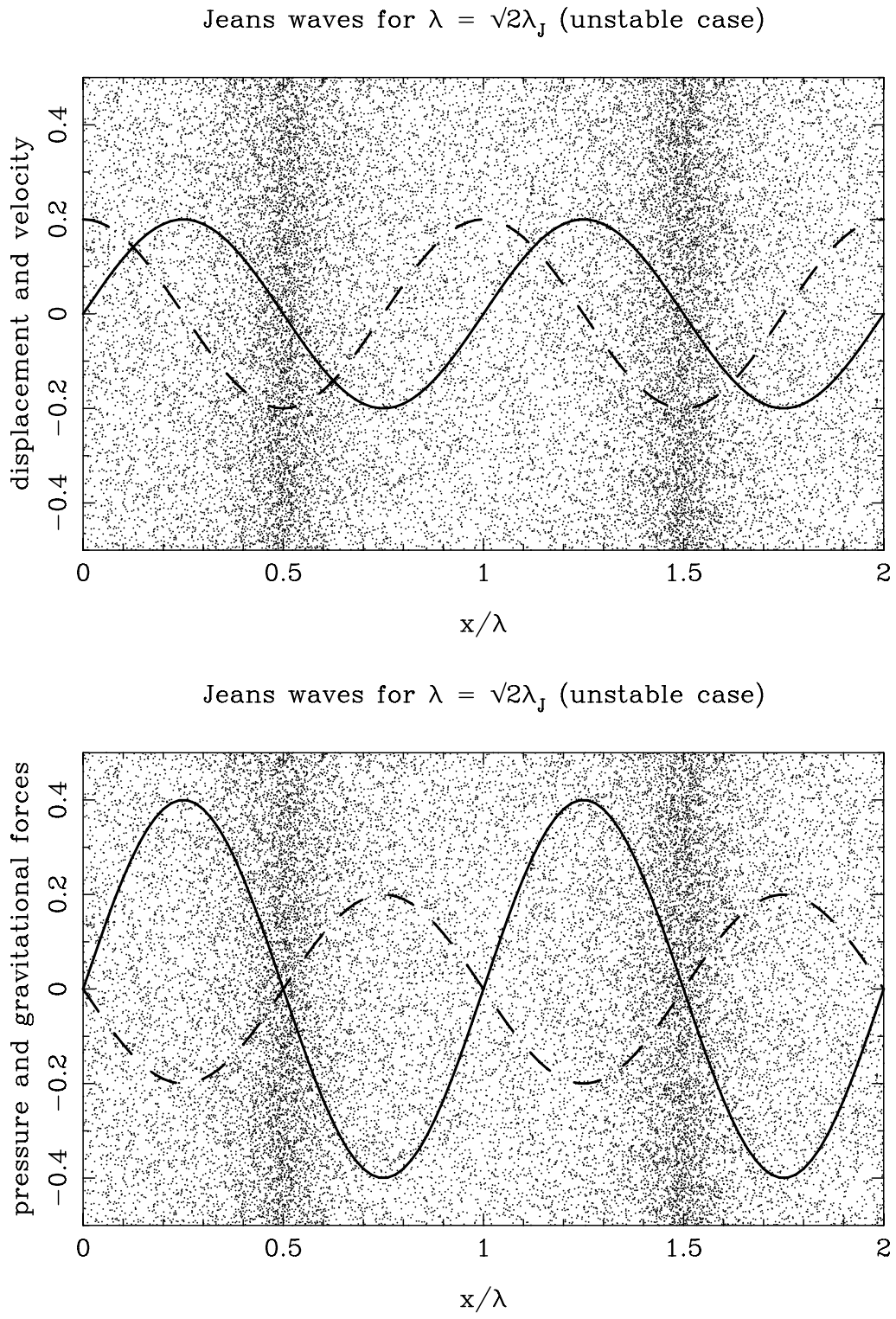

Figure 6.7: *The displacement (top panel, solid curve), velocity (top panel, dashed curve) gravitational force (bottom panel, solid curve) and pressure force(bottom panel, dashed curve) in a linear sound wave in a self-gravitating fluid. Shown is the unstable case with wavelength* $\lambda = \sqrt{2}\,\lambda_{\rm J}$. *In this case the amplitude of the pressure force is half that of the gravitational force.*

The only non-trivial solution where $\boldsymbol{k} \times \boldsymbol{a} \neq 0$ must have $\omega = 0$. The compressive (longitudinal) waves which play a role in the Jeans Instability have $\boldsymbol{k} \parallel \boldsymbol{a}$, just like ordinary sound waves.

6.8.3 A simple physical explanation of the Jeans Instability

The physics behind the Jeans Instability can be understood in a different manner without referring to waves and their stability. This alternative approach uses a stability criterion based on an energy argument. Consider a spherical cloud of hydrogen gas ($\mu \approx 1$) with radius a, uniform density ρ, temperature T and pressure $P = \rho \mathcal{R} T$. The total energy $W(a)$ of this cloud is

$$W(a) = \int_0^M \mathrm{d}m(r) \left[\frac{3}{2} \mathcal{R} T - \frac{G m(r)}{r} \right] \equiv U_{\rm th} + U_{\rm gr} \, . \tag{6.8.23}$$

Here

$$\mathrm{d}m(r) = 4\pi r^2 \, \rho \, \mathrm{d}r \quad , \quad m(r) = \frac{4\pi}{3} \, \rho \, r^3 \tag{6.8.24}$$

are the mass contained in a spherical shell between r and $r + \mathrm{d}r$, and the mass contained within a radius r respectively. The total mass of the cloud is

$$M = \frac{4\pi}{3} \, \rho \, a^3 \, . \tag{6.8.25}$$

The term $3\mathcal{R}T/2$ in integral (6.8.23) is the thermal energy per unit mass in an ideal gas with adiabatic index $\gamma = 5/3$. The term involving $\Phi(r) = -Gm(r)/r$ is the gravitational binding energy per unit mass at radius r. Integrating these quantities over all mass elements in the cloud yields the total cloud energy W.

The integration of this expression is relatively straightforward. One finds:

$$W(a) = \tfrac{3}{2} \, M \mathcal{R} T - \tfrac{3}{5} \, \frac{G M^2}{a} \, . \tag{6.8.26}$$

I now consider the effect of a change $-\Delta a$ (with $\Delta a > 0$) in the radius of the cloud, so that the radius decreases from a to $a - \Delta a$. Let us assume that this change occurs adiabatically, so that no heat is added to, or extracted from the gas.

In that case, the thermodynamical equations of Chapter 2.5 tell us that the thermal energy changes according to $\mathrm{d}U_{\rm th} = -P\,\mathrm{d}\mathcal{V}$. The volume change is $\Delta\mathcal{V} = -4\pi a^2\,\Delta a$. This means that the thermal energy of the cloud changes by an amount

$$\Delta U_{\rm th} = -P\,\Delta\mathcal{V} \approx \rho\mathcal{R}T\,4\pi a^2\,\Delta a\,. \tag{6.8.27}$$

The change of the gravitational binding energy due to the change in radius from a to $a - \Delta a$ is

$$\Delta U_{\rm gr} \approx \left(\frac{\partial U_{\rm gr}}{\partial a}\right) \times (-\Delta a) = -\frac{3}{5}\,\left(\frac{GM^2}{a^2}\right)\,\Delta a\,. \tag{6.8.28}$$

Here I have used that the total mass M of the cloud is conserved. Adding these two contributions yields the change of the total energy, $\Delta W = \Delta U_{\rm th} + \Delta U_{\rm gr}$, of the cloud:

$$\Delta W \approx \left(3M\mathcal{R}T - \frac{3}{5}\,\frac{GM^2}{a}\right) \times \left(\frac{\Delta a}{a}\right)\,. \tag{6.8.29}$$

Now there are two possibilites:

- If $\Delta W > 0$ the change *costs* energy since the increase in the inward gravitational force is smaller than the increase of the outward pressure force that resists the volume change. In this case the cloud is **stable**.
- If $\Delta W < 0$, the change *liberates* energy! The inward gravitational force increases faster than the outward pressure force. This implies that, once started, the contraction of the cloud will continue, leading to *gravitational collapse*. The cloud is **unstable**, which can be interpreted as a consequence of the fact that physical systems tend to evolve towards a minimum-energy state.

Using $M = 4\pi\rho a^3/3$ expression (6.8.29) can be rewritten as

$$\Delta W = 3M\mathcal{R}T\left(1 - \frac{a^2}{\overline{\lambda}_{\rm J}^2}\right) \times \left(\frac{\Delta a}{a}\right)\,. \tag{6.8.30}$$

The characteristic length $\overline{\lambda}_{\rm J}$ in this expression is defined by:

$$\overline{\lambda}_{\rm J} = \sqrt{\frac{15}{4\pi}} \left(\frac{\mathcal{R}T}{G\rho} \right)^{1/2} . \tag{6.8.31}$$

This characteristic length is almost the same as the Jeans length introduced in the previous Section when we discussed the Jeans Instability. Using $c_{\rm s} = (5\mathcal{R}T/3)^{1/2}$ one finds

$$\overline{\lambda}_{\rm J} = \left(\frac{3}{2\pi} \right) \lambda_{\rm J} \approx 0.5 \, \lambda_{\rm J} .$$

The above criterion for (in)stability leads to the following conclusion: if the cloud has a radius $a > \overline{\lambda}_{\rm J}$ (and therefore the cloud diameter is larger than $2\overline{\lambda}_{\rm J} \sim \lambda_{\rm J}$) it will be unstable against gravitational collapse since $\Delta W < 0$. Smaller clouds, with $a < \overline{\lambda}_{\rm J}$, are stable as $\Delta W > 0$.

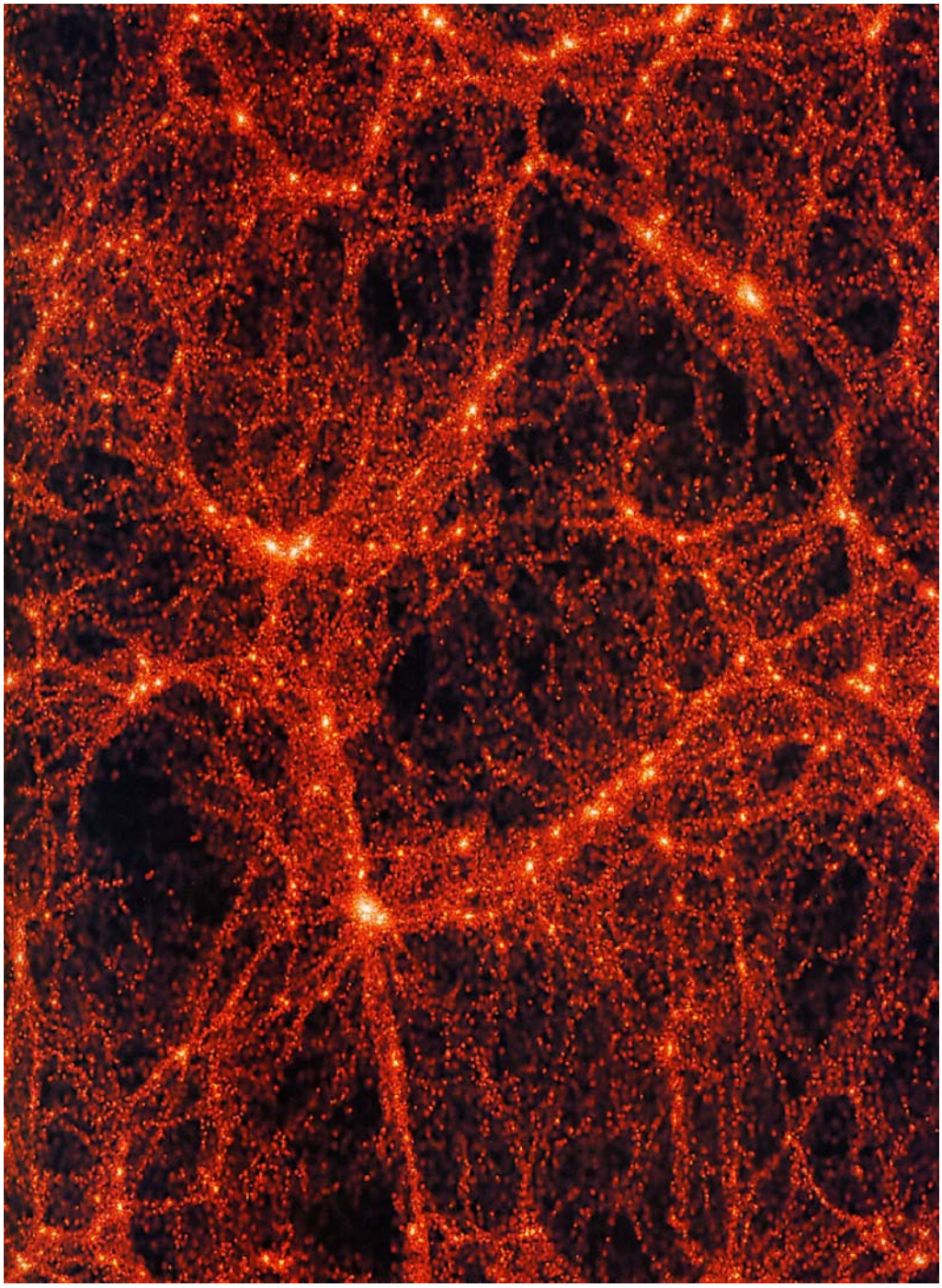

Figure 6.8: *The matter distribution calculated using a numerical simulation of the Jeans instability in an expanding universe. Here the instability has long entered the non-linear phase, where the matter collects in thin filaments.*
Figure: the Virgo Consortium.

6.8.4 Jeans' instability in an expanding universe

In an expanding universe, the exponential growth of unstable waves with wavelength $\lambda > \lambda_{\rm J}$ is slowed down to an algebraic growth. This effect can be illustrated using a simple (quasi-Newtonian) model for the universal expansion, without recourse to the equations of general relativity [11].

Consider a flow where the unperturbed position of fluid elements is given by the prescription

$$\boldsymbol{x}(t) = \frac{R(t)}{R_0} \times \boldsymbol{r} \ . \tag{6.8.32}$$

Here $R(t)$ is the so-called *scale factor*, $R_0 \equiv R(t_0)$ is its value at some reference time $t = t_0$ and $\boldsymbol{r}$ is a set of constant *comoving coordinates*:

$$\boldsymbol{r} \equiv (r_1 \ , \ r_2 \ , \ r_3) = (x_1(t_0) \ , \ x_2(t_0) \ , \ x_3(t_0)) \ . \tag{6.8.33}$$

These comoving coordinates are the perfect illustration of the concept of Lagrangian labels introduced in Chapter 6.2. This is illustrated in the cartoon below.

The unperturbed velocity in this flow is

$$\begin{aligned} \boldsymbol{V}(\boldsymbol{x} \ , \ t) &= \frac{{\rm d}\boldsymbol{x}}{{\rm d}t} = \left(\frac{1}{R_0} \, \frac{{\rm d}R}{{\rm d}t} \right) \boldsymbol{r} \\ &\equiv H(t) \, \boldsymbol{x} \ , \end{aligned} \tag{6.8.34}$$

where the *Hubble 'constant'* equals

$$H(t) = \frac{1}{R} \, \frac{{\rm d}R}{{\rm d}t} \ . \tag{6.8.35}$$

The kinematics of this flow, and in particular the 'Hubble law' (6.8.34), is the same as the kinematics of the Friedmann model for an expanding universe. In particular, the distance of any fluid element to the origin increases in time as $D(t) \propto R(t)$.

[11] e.g. J.A. Peacock, *Cosmological Physics*, Cambridge Univ. Press, 1998, Ch. 15;
M.S. Longair, *Galaxy Formation*, Springer Verlag, Heidelberg, Ch. 11;
T. Padmanabhan, *Structure Formation in the Universe*, Cambridge University Press, 1993, Ch. 4.3

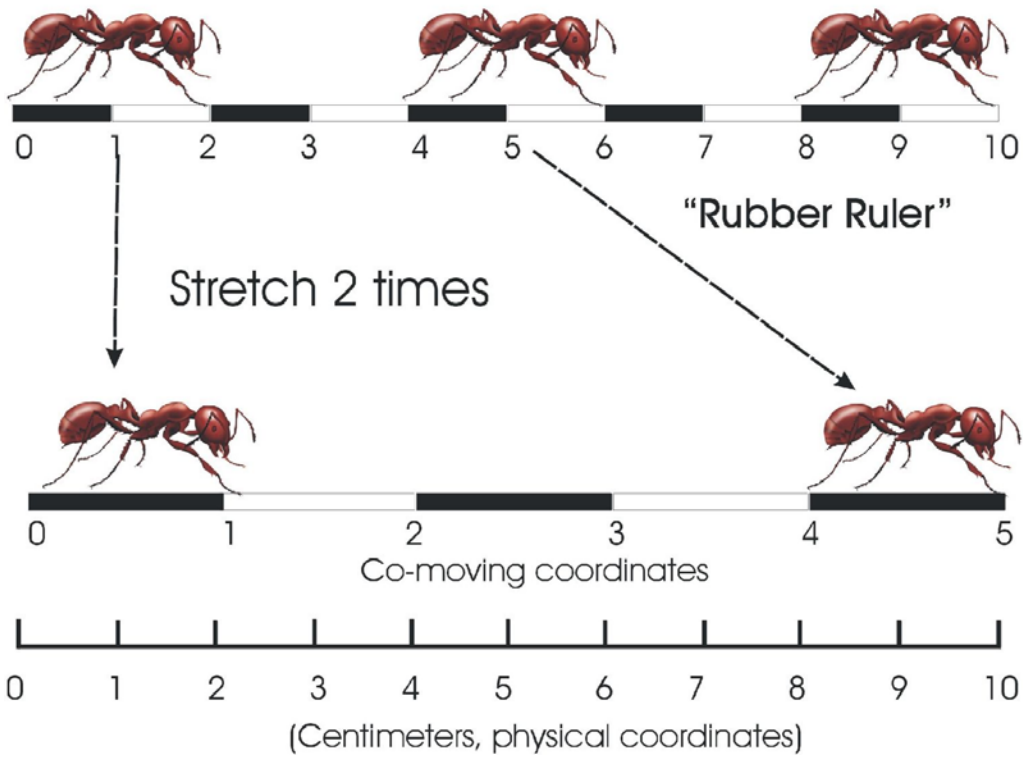

Figure 6.9: *An illustration of physical and comoving coordinates in the one-dimensional 'Ant Universe'. The ants live on a rubber ruler that stretches uniformly as time progresses. The black and white coordinate intervals painted on the rubber ruler are stretched, and define the comoving coordinates. The physical coordinates on the other hand do not change, and have fixed length intervals. As the Ant Universe expands, the relation between a physical distance and the comoving distance intervals is* $\Delta x_{\rm phys} = R(t)\,\Delta x_{\rm cm}$*, with* $R(t) \geq 1$ *the scale factor that measures the amount of stretch.*

An unphysical property of this model is that the origin of the coordinate system is singled out: it plays a special role as the center of expansion. In cosmology, it is usually assumed that the *Copernican Principle* applies, which states that there is no preferred position in the Universe. General relativity solves this problem in a simple fashion: there *space itself* expands, and the recession of distant galaxies from us (and each other) which results from this expansion has no center, as it does not correspond to a *true* physical velocity.

The *Hubble flow*, defined by equations (6.8.32) and (6.8.34), leads to a density decrease. The continuity equation (2.6.14) reads in this case:

$$\frac{\mathrm{d}\rho}{\mathrm{d}t} = -\rho\,(\boldsymbol{\nabla}\cdot\boldsymbol{V}) = -3\rho\,H(t)\;. \tag{6.8.36}$$

Here I have used that

$$\boldsymbol{\nabla}\cdot\boldsymbol{V} = H(t)\,\left(\frac{\partial x}{\partial x}+\frac{\partial y}{\partial y}+\frac{\partial z}{\partial z}\right) = 3H(t)\;. \tag{6.8.37}$$

With the definition (6.8.35) for the Hubble constant this equation for the density can be solved immediately. Assuming a homogeneous density at time t_0, $\rho(\boldsymbol{x}\,,\,t_0)=\rho_0$, one has

$$\rho(t) = \rho_0\,\left(\frac{R(t)}{R_0}\right)^{-3}\;. \tag{6.8.38}$$

This is the density law for a homogeneous universe filled with 'cold' (i.e. non-relativistic) matter where the pressure satisfies $P \ll \rho c^2$.

To complete this model, we have to prescribe the behaviour of the scale factor $R(t)$ as a function of time. For this we use Friedmann's equation valid for a flat universe[12]:

$$H^2 = \left(\frac{1}{R}\,\frac{\mathrm{d}R}{\mathrm{d}t}\right)^2 = \frac{8\pi G}{3}\,\rho(t)\;. \tag{6.8.39}$$

It is easily checked that the following expansion law results:

$$R(t) = R_0\left(\frac{t}{t_0}\right)^{2/3}\quad,\quad t_0 = \frac{1}{\sqrt{6\pi G\,\rho_0}}\;. \tag{6.8.40}$$

[12] e.g. J.A. Peacock, *Cosmological Physics*, Cambridge University Press, 1998, Ch. 3.

One can always scale the coordinates in such a way that $R_0 = 1$. This means that the comoving coordinates correspond to the physical coordinates at time t_0. We adopt this convention, so the relation between physical (= Eulerian) and comoving (= Lagrangian) coordinates, the expansion law and the density law become

$$\boldsymbol{x} = R(t)\,\boldsymbol{r} \quad , \quad R(t) = (t/t_0)^{2/3} \quad , \quad \rho(t) = \rho_0\,R^{-3}\,. \tag{6.8.41}$$

We now perturb this model universe. Since the unperturbed motion corresponds to *constant* comoving coordinates r_i it seems natural to separate out the universal expansion by writing:

$$\Delta\boldsymbol{x} \equiv \boldsymbol{\xi}(\boldsymbol{x}\,,\,t) = R(t)\,\boldsymbol{\eta}(\boldsymbol{r}\,,\,t)\,. \tag{6.8.42}$$

By introducing the *comoving perturbation vector* $\boldsymbol{\eta}(\boldsymbol{r}\,,\,t)$ we achieve this separation cleanly. In addition we have changed the position variable from $\boldsymbol{x}$ to $\boldsymbol{r}$, i.e. to the Lagrangian coordinate labels of the Hubble expansion. This means we have to rewrite our derivatives. The gradient operator $\boldsymbol{\nabla}$ can be expressed in terms of the r_i by using the general rule for a change of variables,

$$\frac{\partial}{\partial x_i} = \left(\frac{\partial r_j}{\partial x_i}\right)_t \frac{\partial}{\partial r_j} = \left(\frac{\partial [x_j/R(t)]}{\partial x_i}\right)_t \frac{\partial}{\partial r_j} = \frac{\delta_{ij}}{R(t)}\,\frac{\partial}{\partial r_j} = \frac{1}{R(t)}\,\frac{\partial}{\partial r_i}\,.$$

Here I have used relation (6.8.33) and the fact that the x-deriavtives are taken at constant t. From this one can immediately write

$$\boxed{\boldsymbol{\nabla} = \frac{1}{R(t)}\,\boldsymbol{\nabla}_{\rm cm}\,,} \tag{6.8.43}$$

where $\boldsymbol{\nabla}_{\rm cm} \equiv (\partial/\partial r_1\,,\,\partial/\partial r_2\,,\,\partial/\partial r_3)$ is the *comoving gradient*.

The interpretation of the partial time-derivative $\partial/\partial t$ must be considered carefully in this case. If we employ '$\boldsymbol{x} - t$ language', where the independent variables are $\boldsymbol{x}$ and t, we must use the standard convention that the partial time derivative is taken while the position $\boldsymbol{x}$ is fixed. But once we employ the $\boldsymbol{r} - t$ representation, where the independent variables of the problem are $\boldsymbol{r}$ and t, one should keep $\boldsymbol{r}$ fixed when taking the partial time-derivative. As I will demonstrate below, this means that in '$\boldsymbol{r} - t$ language' $\partial/\partial t$ corresponds with the comoving time derivative in the Hubble flow. This is in agreement with definition (6.4.4) given earlier, with $\boldsymbol{r}$ playing the role of $\boldsymbol{x}_0$.

These two time derivatives are therefore related by:

$$\begin{aligned}\left(\frac{\partial}{\partial t}\right)_{\boldsymbol{x}} &= \left(\frac{\partial}{\partial t}\right)_{\boldsymbol{r}} + \left(\frac{\partial \boldsymbol{r}}{\partial t}\right)_{\boldsymbol{x}} \cdot \frac{\partial}{\partial \boldsymbol{r}} \\ &= \left(\frac{\partial}{\partial t}\right)_{\boldsymbol{r}} + \left(\frac{\partial [\boldsymbol{x}/R(t)]}{\partial t}\right)_{\boldsymbol{x}} \cdot \frac{\partial}{\partial \boldsymbol{r}} \\ &= \left(\frac{\partial}{\partial t}\right)_{\boldsymbol{r}} - \left(\frac{\mathrm{d}R}{\mathrm{d}t}\right)\left(\frac{\boldsymbol{x}}{R^2(t)}\right) \cdot \frac{\partial}{\partial \boldsymbol{r}} \\ &= \left(\frac{\partial}{\partial t}\right)_{\boldsymbol{r}} - H\,\boldsymbol{x}\cdot\boldsymbol{\nabla}\ .\end{aligned} \tag{6.8.44}$$

Here I have used (6.8.43) again, together with the definition of Hubble's constant. This relation can be written as

$$\boxed{\left(\frac{\partial}{\partial t}\right)_{\boldsymbol{r}} = \left(\frac{\partial}{\partial t}\right)_{\boldsymbol{x}} + H\boldsymbol{x}\cdot\boldsymbol{\nabla}\ .} \tag{6.8.45}$$

The partial time derivative at fixed $\boldsymbol{r}$ is seen to correspond with the co-moving derivative in the unperturbed Hubble flow $\boldsymbol{V} = H\boldsymbol{x}$. This is not suprising: the comoving coordinates are defined in such a way that an observer with *fixed* comoving coordinates $\boldsymbol{r} = \boldsymbol{r}_0$ passively moves with the Hubble flow.

One can apply these relations to calculate the perturbed quantities in terms of the comoving coordinates and the comoving perturbation $\boldsymbol{\eta}$ From (6.8.42) and (6.8.43) one finds immediately:

$$\boldsymbol{\nabla}\cdot\boldsymbol{\xi}(\boldsymbol{x}\ ,\ t) = \frac{1}{R(t)}\,\boldsymbol{\nabla}_{\rm cm}\cdot\ (R(t)\boldsymbol{\eta}(\boldsymbol{r}\ ,\ t)) = \boldsymbol{\nabla}_{\rm cm}\cdot\boldsymbol{\eta}(\boldsymbol{r}\ ,\ t)\ .$$

This means that the density- and pressure perturbations can be expressed as

$$\Delta\rho = -\rho\,(\boldsymbol{\nabla}_{\rm cm}\cdot\boldsymbol{\eta}) \quad , \quad \Delta P = -\gamma P\,(\boldsymbol{\nabla}_{\rm cm}\cdot\boldsymbol{\eta}) = c_{\rm s}^2\,\Delta\rho\ , \tag{6.8.46}$$

where we have simply used Eqns. (6.5.3) which are generally valid, and substituted the above relation for $\boldsymbol{\nabla}\cdot\boldsymbol{\xi}$. Note that our 'model universe' is homogeneous (no density or pressure gradients) so that $\delta\rho = \Delta\rho$ and $\delta P = \Delta P$.

We must be careful when we calculate the velocity perturbation: there are velocity gradients in the Hubble flow, $\boldsymbol{V} = H\,\boldsymbol{x}$. The flow velocity is **not** uniform, unlike the pressure or the density. As a result, the Lagrangian velocity perturbation $\Delta\boldsymbol{V}$ and Eulerian velocity perturbation $\delta\boldsymbol{V}$ do **not** coincide. They are related according to the general rule (6.4.10), which in this particular case reduces to

$$\Delta\boldsymbol{V} = \delta\boldsymbol{V} + (\boldsymbol{\xi}\cdot\boldsymbol{\nabla})(H\boldsymbol{x}) = \delta\boldsymbol{V} + H\,\boldsymbol{\xi}\;. \tag{6.8.47}$$

Here I have used the relation $(\boldsymbol{\xi}\cdot\boldsymbol{\nabla})(H\boldsymbol{x}) = H\boldsymbol{\xi}$. This relation is easily proven in cartesian coordinates[13]: the j-th component of $(\boldsymbol{\xi}\cdot\boldsymbol{\nabla})(H\boldsymbol{x})$ equals

$$(\boldsymbol{\xi}\cdot\boldsymbol{\nabla})(Hx_j) = H\,\left(\xi_i\frac{\partial x_j}{\partial x_i}\right) = H\;(\xi_i\,\delta_{ij}) = H\,\xi_j\;. \tag{6.8.48}$$

The Lagrangian velocity perturbation is given as before by

$$\Delta\boldsymbol{V} \equiv \frac{\mathrm{d}\boldsymbol{\xi}}{\mathrm{d}t} = \frac{\mathrm{d}}{\mathrm{d}t}\,[R(t)\,\boldsymbol{\eta}\,] = \left(\frac{\mathrm{d}R}{\mathrm{d}t}\right)\,\boldsymbol{\eta} + R(t)\,\left(\frac{\mathrm{d}\boldsymbol{\eta}}{\mathrm{d}t}\right)\;. \tag{6.8.49}$$

For the first term on the right-hand-side we can use

$$\left(\frac{\mathrm{d}R}{\mathrm{d}t}\right)\,\boldsymbol{\eta} = \left(\frac{\mathrm{d}R}{\mathrm{d}t}\right)\,\frac{\boldsymbol{\xi}}{R} = H\,\boldsymbol{\xi}\;. \tag{6.8.50}$$

We therefore find:

$$\Delta\boldsymbol{V} = R(t)\,\left(\frac{\mathrm{d}\boldsymbol{\eta}}{\mathrm{d}t}\right) + H\,\boldsymbol{\xi}\;. \tag{6.8.51}$$

Comparing this expression with relation (6.8.47) one immediately finds the Eulerian velocity perturbation:

$$\delta\boldsymbol{V} = \Delta\boldsymbol{V} - H\,\boldsymbol{\xi} = R(t)\,\left(\frac{\mathrm{d}\boldsymbol{\eta}}{\mathrm{d}t}\right)\;. \tag{6.8.52}$$

[13] Since the final relation can be written in vector form, $(\boldsymbol{\xi}\cdot\boldsymbol{\nabla})(H\boldsymbol{x}) = H\boldsymbol{\xi}$, the fact that cartesian coordinates are used for the intermediate steps in the calculation is **not** important! This is an example of the **covariance** of physics: physical laws are *independent* of the coordinates used to represent the vectors, tensors etc. that are involved. If the final result can be written in vector or tensor form, the relation is *generally* valid.

Here $\mathrm{d}/\mathrm{d}t$ is the comoving derivative in $\boldsymbol{x} - t$ language in the *unperturbed flow*: we are only interested in terms to first order in the perturbations. This means that we can use Eqn. (6.8.45) and write:

$$\boxed{\delta \boldsymbol{V} = R(t)\, \frac{\partial \boldsymbol{\eta}(\boldsymbol{r}\ ,\ t)}{\partial t} \equiv R(t)\, \boldsymbol{u}(\boldsymbol{r}\ ,\ t)\ ,} \tag{6.8.53}$$

where the partial time-derivative is now taken at constant $\boldsymbol{r}$ and $\boldsymbol{u} \equiv \partial \boldsymbol{\eta}/\partial t$. One sees that in the expression for the Eulerian velocity perturbation $\delta \boldsymbol{V}$ the effect of the universal expansion once again shows up as an overal scaling factor $R(t)$.

We now must derive the equation of motion for the perturbations. In this case the best strategy is to start with the equation of motion in the form

$$\frac{\partial \boldsymbol{V}}{\partial t} + (\boldsymbol{V} \cdot \boldsymbol{\nabla})\boldsymbol{V} = -\frac{\boldsymbol{\nabla} P}{\rho} - \boldsymbol{\nabla}\Phi\ , \tag{6.8.54}$$

together with Poisson's equation for the gravitational potential,

$$\boldsymbol{\nabla}^2 \Phi = 4\pi G\, \rho\ . \tag{6.8.55}$$

We make use of the fact that in the unperturbed state there are no pressure gradients, $\boldsymbol{\nabla} P = 0$, and that the Eulerian variation δ commutes with spatial and time derivatives, c.f. Eqn. (6.4.7). The Eulerian variation of the total time derivative of the velocity (the acceleration) on the left-hand-side of the equation of motion follows from

$$\begin{aligned} \delta\left(\frac{\partial \boldsymbol{V}}{\partial t} + (\boldsymbol{V} \cdot \boldsymbol{\nabla})\boldsymbol{V}\right) \ &\equiv\ \left(\frac{\partial [\boldsymbol{V} + \delta \boldsymbol{V}\,]}{\partial t} + ([\boldsymbol{V} + \delta \boldsymbol{V}] \cdot \boldsymbol{\nabla})[\boldsymbol{V} + \delta \boldsymbol{V}]\right) - \\ &-\ \left(\frac{\partial \boldsymbol{V}}{\partial t} + (\boldsymbol{V} \cdot \boldsymbol{\nabla})\boldsymbol{V}\right) \qquad (6.8.56) \\ &=\ \frac{\partial \delta \boldsymbol{V}}{\partial t} + (\boldsymbol{V} \cdot \boldsymbol{\nabla})\delta \boldsymbol{V} + (\delta \boldsymbol{V} \cdot \boldsymbol{\nabla})\boldsymbol{V} + \mathcal{O}\left(|\delta \boldsymbol{V}|^2\right)\ . \end{aligned}$$

Note that the term $(\delta \boldsymbol{V} \cdot \boldsymbol{\nabla})\delta \boldsymbol{V}$ (which is quadratic in $\delta \boldsymbol{V}$) has been neglected.

We now use the relationships (6.8.43), (6.8.45) and (6.8.53) derived above, together with Hubble's law $\boldsymbol{V} = H\boldsymbol{x}$:

$$\begin{aligned}\frac{\partial \delta\boldsymbol{V}}{\partial t} + (\boldsymbol{V}\cdot\boldsymbol{\nabla})\delta\boldsymbol{V} &= \frac{\partial \delta\boldsymbol{V}}{\partial t} + (H\boldsymbol{x}\cdot\boldsymbol{\nabla})\delta\boldsymbol{V} = \frac{\partial}{\partial t}\left(R(t)\,\frac{\partial \boldsymbol{\eta}(\boldsymbol{r}\,,\,t)}{\partial t}\right)_{\boldsymbol{r}} \\ &= R(t)\,\frac{\partial^2\boldsymbol{\eta}}{\partial t^2} + \left(\frac{\mathrm{d}R}{\mathrm{d}t}\right)\,\frac{\partial\boldsymbol{\eta}}{\partial t}\;;\end{aligned} \tag{6.8.57}$$

$$\begin{aligned}(\delta\boldsymbol{V}\cdot\boldsymbol{\nabla})\boldsymbol{V} &= (\delta\boldsymbol{V}\cdot\boldsymbol{\nabla})[H\,\boldsymbol{x}\,] = H\,\delta\boldsymbol{V} \\ &= \left(\frac{\mathrm{d}R}{\mathrm{d}t}\right)\,\frac{\partial\boldsymbol{\eta}}{\partial t}\,.\end{aligned}$$

In the second expression I have used $(\delta\boldsymbol{V}\cdot\boldsymbol{\nabla})\boldsymbol{x} = \delta\boldsymbol{V}$. Combining these terms one finds the effective acceleration associated with the perturbed motion:

$$\boxed{\delta\left(\frac{\partial\boldsymbol{V}}{\partial t} + (\boldsymbol{V}\cdot\boldsymbol{\nabla})\boldsymbol{V}\right) = R(t)\,\left(\frac{\partial^2\boldsymbol{\eta}}{\partial t^2} + 2H\,\frac{\partial\boldsymbol{\eta}}{\partial t}\right)\,.} \tag{6.8.58}$$

The pressure and gravity term on the right-hand-side follow more simply:[14]

$$\begin{aligned}\delta\left(\frac{\boldsymbol{\nabla}P}{\rho}\right) &= \frac{\boldsymbol{\nabla}\delta P}{\rho} = \frac{\boldsymbol{\nabla}_{\rm cm}\delta P}{\rho R} = \frac{c_{\rm s}^2\,(\boldsymbol{\nabla}_{\rm cm}\delta\rho)}{\rho R}\,, \\ \delta\,(\boldsymbol{\nabla}\Phi) &= \boldsymbol{\nabla}\,(\delta\Phi) = \frac{\boldsymbol{\nabla}_{\rm cm}\,(\delta\Phi)}{R}\,.\end{aligned} \tag{6.8.59}$$

Here I have used Eqn. (6.8.46).

[14]Strictly speaking one has $\delta(\boldsymbol{\nabla}P/\rho) = \boldsymbol{\nabla}(\delta P)\times(1/\rho) + \boldsymbol{\nabla}P\times\delta(1/\rho)$, but $\boldsymbol{\nabla}P = 0$ in this case.

The perturbed gravitational potential follows from Poisson's equation as

$$\boldsymbol{\nabla}^2\,\delta\Phi = \frac{1}{R^2}\,\boldsymbol{\nabla}^2_{\rm cm}\delta\Phi = 4\pi G\,\delta\rho\ . \tag{6.8.60}$$

This yields the following equation of motion for the perturbations:

$$\frac{\partial^2\boldsymbol{\eta}}{\partial t^2} + 2H\,\frac{\partial\boldsymbol{\eta}}{\partial t} = -\frac{1}{R^2}\,\left(c_{\rm s}^2\,\frac{\boldsymbol{\nabla}_{\rm cm}\delta\rho}{\rho} + \boldsymbol{\nabla}_{\rm cm}\delta\Phi\right)\ . \tag{6.8.61}$$

These results are summarized in the table on the next page.

We now use a trick similar to the one employed in our discussion of the Jeans Instability in a stationary medium. We define the quantity

$$\Delta \equiv \frac{\delta\rho}{\rho} = -\boldsymbol{\nabla}_{\rm cm}\cdot\boldsymbol{\eta}\ , \tag{6.8.62}$$

and make use of the fact that Poisson's equation, which links the perturbations in the gravitational potential to the density perturbations, can be written as

$$\boldsymbol{\nabla}^2_{\rm cm}\delta\Phi = 4\pi G\,\rho\,R^2\Delta\ . \tag{6.8.63}$$

Now we take the comoving divergence[15], $\boldsymbol{\nabla}_{\rm cm}\cdot$, of both sides of the equation of motion (6.8.61). We can use

$$\begin{aligned}
\boldsymbol{\nabla}_{\rm cm}\cdot\left(\frac{\partial\boldsymbol{\eta}}{\partial t}\right) &= \frac{\partial(\boldsymbol{\nabla}_{\rm cm}\cdot\boldsymbol{\eta})}{\partial t} = -\frac{\partial\Delta}{\partial t}\ , \\
\boldsymbol{\nabla}_{\rm cm}\cdot\left(\frac{\partial^2\boldsymbol{\eta}}{\partial t^2}\right) &= \frac{\partial^2(\boldsymbol{\nabla}_{\rm cm}\cdot\boldsymbol{\eta})}{\partial t^2} = -\frac{\partial^2\Delta}{\partial t^2}\ ,
\end{aligned} \tag{6.8.64}$$

together with

$$\boldsymbol{\nabla}_{\rm cm}\cdot\left(c_{\rm s}^2\,\frac{\boldsymbol{\nabla}_{\rm cm}\delta\rho}{\rho}\right) = c_{\rm s}^2\boldsymbol{\nabla}^2_{\rm cm}\Delta\ . \tag{6.8.65}$$

[15]This defined in cartesian comoving coordinates as $\boldsymbol{\nabla}_{\rm cm}\cdot\boldsymbol{\eta} = \partial\eta_1/\partial r_1 + \partial\eta_2/\partial r_2 + \partial\eta_3/\partial r_3$.

Perturbed quantities in a linear adiabatic wave in an expanding universe

Quantity	**In '$\boldsymbol{x}-t$' language**	**In '$\boldsymbol{r}-t$' language**
Position (physical and comoving)	$\boldsymbol{x}(t) = R(t)\,\boldsymbol{r}$	$\boldsymbol{r}$
Unperturbed velocity (Hubble flow)	$\boldsymbol{V}(\boldsymbol{x}\,,\,t) = H(t)\,\boldsymbol{x}$	$\boldsymbol{V} = \left(\dfrac{\mathrm{d}R}{\mathrm{d}t}\right)\,\boldsymbol{r} \quad , \quad \dfrac{\partial \boldsymbol{r}}{\partial t} = \boldsymbol{0}$
Co-moving derivative in unperturbed flow	$\dfrac{\mathrm{d}}{\mathrm{d}t} = \left(\dfrac{\partial}{\partial t}\right)_{\boldsymbol{x}} + H(\boldsymbol{x}\cdot\boldsymbol{\nabla})$	$\left(\dfrac{\partial}{\partial t}\right)_{\boldsymbol{r}}$
Physical gradient	$\boldsymbol{\nabla} = \left(\dfrac{\partial}{\partial x_1}\,,\,\dfrac{\partial}{\partial x_2}\,,\,\dfrac{\partial}{\partial x_3}\right)$	$\dfrac{1}{R(t)}\,\boldsymbol{\nabla}_{\mathrm{cm}} = \dfrac{1}{R(t)}\,\left(\dfrac{\partial}{\partial r_1}\,,\,\dfrac{\partial}{\partial r_2}\,,\,\dfrac{\partial}{\partial r_3}\right)$
Displacement vector	$\Delta\boldsymbol{x} = \boldsymbol{\xi}(\boldsymbol{x}\,,\,t)$	$R(t)\,\Delta\boldsymbol{r} \equiv R(t)\,\boldsymbol{\eta}(\boldsymbol{r}\,,\,t)$
Lagrangian velocity perturbation $\Delta\boldsymbol{V}$	$\dfrac{\mathrm{d}\boldsymbol{\xi}}{\mathrm{d}t} = \dfrac{\partial\boldsymbol{\xi}}{\partial t} + H(\boldsymbol{x}\cdot\boldsymbol{\nabla})\boldsymbol{\xi}$	$\left(\dfrac{\mathrm{d}R}{\mathrm{d}t}\right)\,\boldsymbol{\eta} + R(t)\,\left(\dfrac{\partial\boldsymbol{\eta}}{\partial t}\right)$
Eulerian velocity perturbation $\delta\boldsymbol{V}$	$\dfrac{\partial\boldsymbol{\xi}}{\partial t} + H(\boldsymbol{x}\cdot\boldsymbol{\nabla})\boldsymbol{\xi} - H\,\boldsymbol{\xi}$	$R(t)\,\dfrac{\partial\boldsymbol{\eta}}{\partial t}$
Eulerian acceleration in wave $\delta\boldsymbol{a}$	$\dfrac{\partial\delta\boldsymbol{V}}{\partial t} + H\,(\boldsymbol{x}\cdot\boldsymbol{\nabla})\delta\boldsymbol{V} + H\,\delta\boldsymbol{V}$	$R(t)\,\left(\dfrac{\partial^2\boldsymbol{\eta}}{\partial t^2} + 2H\,\dfrac{\partial\boldsymbol{\eta}}{\partial t}\right)$

Poisson's equation (6.8.63)allows us to eliminate the gravitational potential $\delta\Phi$ in terms of Δ. This yields the following equation for $\Delta(\boldsymbol{r}\ ,\ t) = \delta\rho/\rho$:

$$\boxed{\left[\frac{\partial^2}{\partial t^2} + 2H\,\frac{\partial}{\partial t} - \left(\frac{c_{\rm s}^2}{R^2}\right)\,\boldsymbol{\nabla}_{\rm cm}^2 - 4\pi G\,\rho\right]\,\Delta(\boldsymbol{r}\ ,\ t) = 0} \tag{6.8.66}$$

This is the 'wave equation' for density fluctuations in an expanding universe.

We can compare this equation with the one derived in the previous Section: Eqn. (6.8.10). If we assume a *static*, non-expanding universe we can always put $R = 1$, $H = 0$ and $\boldsymbol{\nabla}_{\rm cm} = \boldsymbol{\nabla}$. In that case, the above equation reduces to Eqn. (6.8.10). So the case of the ordinary Jeans Instability in an unchanging (static) self-gravitating medium is contained in Eqn. (6.8.66).

Equation (6.8.66) has two new features: the first is the term $2H(\partial\Delta/\partial t)$ proportional to the Hubble-constant. This term acts as a kind of 'friction term' if $H > 0$: it is proportional to the *first-order* time derivative $\partial\Delta/\partial t$, which is the velocity of the density change.

The second new feature is the fact that the coefficients in this wave equation depend *explicitly* on time. This reflects the fact that the background in which the perturbations evolve is itself evolving in time due to the expansion of the Universe. For a cold universe with $R(t) \propto t^{2/3}$ the Hubble constant equals

$$H(t) = \left(\frac{1}{R}\,\frac{{\rm d}R}{{\rm d}t}\right) = \frac{2}{3t}\ . \tag{6.8.67}$$

Furthermore, if the gas in in the universe behaves as an ideal gas with $P \propto \rho^\gamma$, the density decrease due to the universal expansion (see Eqn. 6.8.41) implies a pressure decrease,

$$\rho(t) = \rho_0\,\left(\frac{t}{t_0}\right)^{-2}\quad ,\quad P = P_0\,\left(\frac{\rho}{\rho_0}\right)^\gamma = P_0\,\left(\frac{t}{t_0}\right)^{-2\gamma}\ , \tag{6.8.68}$$

and an associated change in the sound speed:

$$c_{\rm s} \equiv \sqrt{\frac{\gamma P}{\rho}} = c_{\rm s0}\,\left(\frac{t}{t_0}\right)^{-(\gamma-1)}\ . \tag{6.8.69}$$

This time-dependence of the coefficients is the reason that it is no longer possible to find solutions in the form of waves with a harmonic behaviour in time (i.e. solutions where $\Delta \propto e^{-i\omega t}$). Since we assumed a homogeneous Universe, there is *no* explicit dependence on position $\boldsymbol{r}$. Therefore, we *can* still look for plane wave solutions of the form

$$\Delta(\boldsymbol{r}\ ,\ t) = \tilde{\Delta}(t)\,\exp(i\boldsymbol{q}\cdot\boldsymbol{r}) + \mathrm{cc}\ . \tag{6.8.70}$$

Here $\boldsymbol{q}$ is the *comoving wave number*, which means that the maxima in the waves are separated by a comoving distance (or comoving wavelength)

$$|\Delta\boldsymbol{r}| \equiv \lambda_{\mathrm{cm}} = \frac{2\pi}{|\boldsymbol{q}|}\ . \tag{6.8.71}$$

The *physical* wavelength follows from the general recipe for converting comoving coordinate differences into physical distances (see Eqn. 6.8.41):

$$\lambda(t) = R(t)\,\lambda_{\mathrm{cm}} = \frac{2\pi R(t)}{|\boldsymbol{q}|}\ . \tag{6.8.72}$$

The physical wavelength of the perturbation is proportional to the scale factor of the universe. This is exactly the same behaviour as exhibited by photons in an expanding Universe: like photons, the 'acoustic' waves of self-gravitating linear perturbations in an expanding universe are *redshifted* to longer and longer wavelengths.

If we substitute the trial solution (6.8.70) into the equation 6.8.66 one finds the following equation for the wave amplitude $\tilde{\Delta}(t)$:

$$\boxed{\left[\frac{\mathrm{d}^2}{\mathrm{d}t^2} + 2H(t)\,\frac{\mathrm{d}}{\mathrm{d}t} + \left(\frac{|\boldsymbol{q}|^2 c_{\mathrm{s}}^2}{R^2} - 4\pi G\,\rho(t)\right)\right]\ \tilde{\Delta}(t) = 0\ .} \tag{6.8.73}$$

As was the case for the Jeans Instability in a static universe, the solutions of this equation behave in a fundamentally different manner for short and for long wavelengths. The criterion separating these two regimes is the same as in the static case. Let us define the *physical* wave number $\boldsymbol{k}$ as

$$\boldsymbol{k}(t) = \frac{\boldsymbol{q}}{R(t)} \iff \lambda(t) = \frac{2\pi}{|\boldsymbol{k}(t)|}\ . \tag{6.8.74}$$

We can then write

$$\begin{aligned} \frac{|\boldsymbol{q}|^2 c_{\rm s}^2}{R^2} - 4\pi G\,\rho(t) &= |\boldsymbol{k}(t)|^2 c_{\rm s}^2 - 4\pi G\,\rho(t) \\ &= |\boldsymbol{k}(t)|^2 c_{\rm s}^2 \left(1 - \frac{\lambda^2}{\lambda_{\rm J}^2}\right) , \end{aligned} \tag{6.8.75}$$

with $\lambda_{\rm J} = \sqrt{\pi c_{\rm s}^2/G\rho}$ the Jeans length defined above. Equation (6.8.73) leads to the following possible solutions:

$$\begin{aligned} &\text{if } \lambda < \lambda_{\rm J}\text{: wave-like acoustic solutions} \\ &\text{if } \lambda > \lambda_{\rm J}\text{: damped } \textit{and} \text{ growing (unstable) solutions} \end{aligned} \tag{6.8.76}$$

In an expanding Universe both the physical wavelength of the perturbation and the Jeans length depend explicitly on time:

$$\lambda \propto R(t) \propto t^{2/3} \quad , \quad \lambda_{\rm J} \propto c_{\rm s}/\sqrt{\rho} \propto t^{2-\gamma} \, . \tag{6.8.77}$$

If the specific heat ratio satisfies $\gamma > 4/3$ the wavelength ratio $\lambda/\lambda_{\rm J}$ grows in time. This means that in an expanding matter-dominated Universe the wavelength of acoustic waves in a cold gas (which has $\gamma = 5/3$) grows more rapidly in time than the Jeans length. Therefore perturbations which start out as 'sound waves' with $\lambda < \lambda_{\rm J}$ which are stable against gravitational collapse, will ultimately be redshifted into a wavelength range where $\lambda > \lambda_{\rm J}$, so that the perturbations become unstable according to the Jeans' criterion.

Let us consider the limiting case $\lambda \gg \lambda_{\rm J}$ so that we can neglect the acoustic term $\propto c_{\rm s}^2$ in the equation for $\tilde{\Delta}(t)$. We use the properties of the universal expansion for a flat universe:

$$H(t) = \frac{2}{3t} \quad , \quad H^2 = \frac{8\pi G\,\rho}{3} \iff 4\pi G\,\rho = \tfrac{3}{2} H^2 = \frac{2}{3t^2} \, . \tag{6.8.78}$$

Using these relations we can write (6.8.73) in the long-wavelength limit as

$$\left[\frac{{\rm d}^2}{{\rm d}t^2} + \frac{4}{3t}\,\frac{\rm d}{{\rm d}t} - \frac{2}{3t^2} \right] \tilde{\Delta}(t) = 0 \, . \tag{6.8.79}$$

Let us try a power-law solution in time t:[16]

$$\tilde{\Delta}(t) = At^{\alpha} \ . \tag{6.8.80}$$

Substituting this into (6.8.79) one finds that the following equation must be satisfied:

$$\left[\alpha\left(\alpha-1\right)+\tfrac{4}{3}\alpha-\tfrac{2}{3}\right]At^{\alpha-2}=0 \ . \tag{6.8.81}$$

This is only possible if the term in the square brackets vanishes identically:

$$\alpha^2+\tfrac{1}{3}\alpha-\tfrac{2}{3}=0 \ . \tag{6.8.82}$$

There are two possible solutions for the exponent α of the power-law (6.8.80):

$$\alpha=\begin{cases}\frac{2}{3} & \text{growing solution}\\ \\ -1 & \text{decaying solution}\end{cases} \ . \tag{6.8.83}$$

Since this corresponds to two independent solutions of a *linear* equation for $\tilde{\Delta}$, the most general solution is a superposition of a growing and a decaying solution:

$$\tilde{\Delta}(t) = A_{+}t^{2/3} + A_{-}t^{-1} \ . \tag{6.8.84}$$

As time progresses, the growing solution $\propto t^{2/3}$ will always dominate, and the density perturbation will grow as

$$\frac{\delta\rho}{\rho} \propto t^{2/3} \propto R(t) \ . \tag{6.8.85}$$

So we see that in an expanding Universe the exponential growth of the Jeans Instability that we found in a static (non-evolving) Universe is slowed down to an algebraic growth, where the relative density perturbation ultimately becomes proportional to the scale factor. This growth will continue until the perturbation becomes so strong (i.e. when $\tilde{\Delta} \sim 1$) that the linear analysis, on which this conclusion is based, becomes invalid.

[16] You can guess this trial solution by observing that the equation for $\tilde{\Delta}(t)$ contains only time derivatives and powers of t with the total number of factors of t in each term the same, counting $\partial/\partial t$ as a factor $1/t$.

6.9 The Jeans Instability in the Zeldovich Approximation

Around 1970 the Russian astrophysicist Zeldovich devised an ingenious method for treating the intial stages of the non-linear Jeans Instability. He assumed that the motion of fluid elements takes the form:

$$\boldsymbol{x}(t) = R(t)\ [\boldsymbol{r} + b(t)\ \boldsymbol{f}(\boldsymbol{r})\ ]\ . \tag{6.9.86}$$

The first term in this expression is the unperturbed Hubble flow, $\boldsymbol{x}(t) = R(t)\ \boldsymbol{r}$, with $\boldsymbol{r}$ the comoving position vector whose components define the comoving coordinates: $\boldsymbol{r} = (r_1\ ,\ r_2\ ,\ r_3)$. The second term is the perturbation due to the instability. Note that the displacement vector takes a special form: a (function of time) $\times$ (a vector $\boldsymbol{f}$) that only depends on the comoving coordinates $\boldsymbol{r}$. The linear (comoving) displacement $\boldsymbol{\eta}$ introduced in Eqn. (6.8.42) is related to the vector $\boldsymbol{f}$ by

$$\boldsymbol{\eta}(\boldsymbol{r}\ ,\ t) = b(t)\boldsymbol{f}(\boldsymbol{r})\ . \tag{6.9.87}$$

This form of the displacement means that the fluid elements move on *straight* trajectories in comoving coordinates: the displacement vector $\boldsymbol{\eta}$ never changes its direction. That direction is fixed by the direction of the vector $\boldsymbol{f}(\boldsymbol{r})$, and for a given fluid element the Lagrangian label $\boldsymbol{r}$ is fixed. Only the magnitude of the displacement changes!

Now let us assume that we choose our units in such a way that $R(t) = 1$ at $t = t_0$. We start the instability by perturbing the flow at $t = t_0$. Initially, the perturbations are very small. We can use a result from Chapter 2.6. The mass in an infinitesimal volume $\mathrm{d}\mathcal{V}$ is conserved if the volume expands (or contracts) with the flow. This is automatically true if we construct this volume using the tangent vectors to material lines. In this particular case this means that the density satisfies

$$\rho(\boldsymbol{x}\ ,\ t)\ \mathrm{d}^3\boldsymbol{x} = \text{constant.} \tag{6.9.88}$$

If the initial unperturbed density (i.e. for $\boldsymbol{f} = 0$) at t_0 equals ρ_0, which is independent of position, the density at an arbitrary later time in the presence of the perturbations is:

$$\rho(\boldsymbol{x}\ ,\ t) = \frac{\rho_0}{R^3(t)\ D(\boldsymbol{r}\ ,\ t)}\ . \tag{6.9.89}$$

Here $D(\boldsymbol{r}\ ,\ t)$ is the Jacobian determinant of the deformation tensor

$$D_{ij} = \delta_{ij} + b(t)\ \frac{\partial f_i}{\partial r_j} \tag{6.9.90}$$

for the comoving coordinates, which is

$$D(\boldsymbol{r}\ ,\ t) = \left\| \begin{array}{ccc} 1 + b(t)\ \dfrac{\partial f_1}{\partial r_1} & b(t)\ \dfrac{\partial f_1}{\partial r_2} & b(t)\ \dfrac{\partial f_1}{\partial r_3} \\ b(t)\ \dfrac{\partial f_2}{\partial r_1} & 1 + b(t)\ \dfrac{\partial f_2}{\partial r_2} & b(t)\ \dfrac{\partial f_2}{\partial r_3} \\ b(t)\ \dfrac{\partial f_3}{\partial r_1} & b(t)\ \dfrac{\partial f_3}{\partial r_2} & 1 + b(t)\ \dfrac{\partial f_3}{\partial r_3} \end{array} \right\| . \tag{6.9.91}$$

This quantity is the ratio $D = \mathrm{d}^3\boldsymbol{r}/\mathrm{d}^3\boldsymbol{r}_0$ of the perturbed and unperturbed *comoving* volume, and is the analogue in comoving coordinates of the determinant D defined in Eqn. (6.4.27). If one switches off the perturbations by putting $b(t) = 0$ one has $D(\boldsymbol{r}\ ,\ t) = 1$, and one recovers the usual density law in an expanding Universe: $\rho(t) = \rho_0/R^3$. Therefore we can also write (6.9.89) as

$$\rho(\boldsymbol{x}\ ,\ t) = \frac{\rho(t)}{D(\boldsymbol{r}\ ,\ t)}\ , \tag{6.9.92}$$

with $\rho(t)$ the unperturbed density at time t. This result reproduces the linear theory of the previous Section: if the perturbation is small so that $b(t)|\partial f_i/\partial r_j| \ll 1$ one has (compare Eqns. 6.4.31):

$$D(\boldsymbol{r}\ ,\ t) = 1 + b(t)\ (\boldsymbol{\nabla}_{\rm cm} \cdot \boldsymbol{f}) = 1 + \boldsymbol{\nabla}_{\rm cm} \cdot \boldsymbol{\eta}\ . \tag{6.9.93}$$

so that

$$\rho(\boldsymbol{r}\ ,\ t) = \frac{\rho(t)}{1 + \boldsymbol{\nabla}_{\rm cm} \cdot \boldsymbol{\eta}} \approx \rho(t)\ \ (1 - \boldsymbol{\nabla}_{\rm cm} \cdot \boldsymbol{\eta})\ \ . \tag{6.9.94}$$

This is in accordance with Eqn. (6.8.46). In the linear regime, the amplitude of the waves follows from Eqn. (6.8.61):

$$\frac{\partial^2 \boldsymbol{\eta}}{\partial t^2} + 2H\,\frac{\partial \boldsymbol{\eta}}{\partial t} = -\frac{1}{R^2}\,\left(c_{\rm s}^2\,\frac{\boldsymbol{\nabla}_{\rm cm}\delta\rho}{\rho} + \boldsymbol{\nabla}_{\rm cm}\delta\Phi\right)\,, \tag{6.9.95}$$

with $\boldsymbol{\eta} = b(t)\boldsymbol{f}(\boldsymbol{r})$. Since the coefficients in equation (6.9.95) depend on time, but not on position, it is possible to introduce a function $\psi(\boldsymbol{r})$ such that

$$\boldsymbol{f}(\boldsymbol{r}) = \boldsymbol{\nabla}_{\rm cm}\psi\,. \tag{6.9.96}$$

In terms of the function $\psi(\boldsymbol{r})$ the deformation tensor (6.9.90) is

$$D_{ij} = \delta_{ij} + b(t)\,\frac{\partial^2\psi}{\partial r_i \partial r_j} \tag{6.9.97}$$

This is an obviously symmetric tensor: $D_{ij} = D_{ji}$. The quantity

$$S_{ij} \equiv \frac{\partial^2\psi}{\partial r_i \partial r_j} \tag{6.9.98}$$

is usually called the *strain tensor*. A symmetric tensor such as this always has three *real* eigenvalues and three associated (mutually orthogonal) eigenvectors. If we call the first eigenvalue at comoving position $\boldsymbol{r}$ $-\alpha_1(\boldsymbol{r})$ (the minus sign is convention) and the corresponding eigenvector $\boldsymbol{A^{(1)}}$, the eigenvalue and eigenvector satisfy:

$$S_{ij}\,A_j^{(1)} = -\alpha_1\,A_i^{(1)}\,. \tag{6.9.99}$$

The other two eigenvectors and eigenvalues satisfy an analogous relation. The three eigenvectors $\boldsymbol{A}^{(1)}$, $\boldsymbol{A}^{(2)}$ and $\boldsymbol{A}^{(3)}$ of the strain tensor can be normalized to unit length, and must be orthogonal. If we use these three vectors as the unit vectors in a cartesian coordinate system, the deformation tensor (6.9.97) takes a particularly simple form:

$$D_{ij} = \begin{pmatrix} 1-\alpha_1\,b(t) & 0 & 0 \\ 0 & 1-\alpha_2\,b(t) & 0 \\ 0 & 0 & 1-\alpha_3\,b(t) \end{pmatrix}\,. \tag{6.9.100}$$

This is an example of a *principle axes transformation*[17]. This form of the deformation tensor immediately yields the determinant of the deformation tensor:

$$D(\boldsymbol{r}\ ,\ t) = [1 - \alpha_1(\boldsymbol{r})\, b(t)\,]\,[1 - \alpha_2(\boldsymbol{r})\, b(t)\,]\,[1 - \alpha_3(\boldsymbol{r})\, b(t)\,]\ . \tag{6.9.101}$$

The function $b(t)$ increases with time (as a power of t in the linear regime). Therefore, factors in (6.9.101) with $\alpha_i > 0$ lead to a decrease of D and an increase of $\rho(\boldsymbol{r}\ ,\ t)$, as $\rho(\boldsymbol{r}\ ,\ t) = \rho(t)/D$. Factors in (6.9.101) with $\alpha_i < 0$ on the other hand increase the value of D as $b(t)$ grows, and decrease the density.

The behaviour of the function $b(t)$ can be derived using the *linear* equations[18]. Substituting

$$\boldsymbol{\eta}(\boldsymbol{r}\ ,\ t) = b(t)\ \boldsymbol{\nabla}_{\rm cm}\psi(\boldsymbol{r}) = b(t)\ \left(\frac{\partial\psi}{\partial r_1}\ ,\ \frac{\partial\psi}{\partial r_2}\ ,\ \frac{\partial\psi}{\partial r_3}\right) \tag{6.9.102}$$

into (6.9.95) one has

$$\left(\frac{{\rm d}^2 b}{{\rm d}t^2} + 2H\,\frac{{\rm d}b}{{\rm d}t}\right)\ \boldsymbol{\nabla}_{\rm cm}\psi = -\frac{1}{R^2}\ \left(c_{\rm s}^2\ \frac{\boldsymbol{\nabla}_{\rm cm}\delta\rho}{\rho} + \boldsymbol{\nabla}_{\rm cm}\delta\Phi\right)\ . \tag{6.9.103}$$

Taking the comoving divergence $\boldsymbol{\nabla}_{\rm cm}\,\cdot$ on both sides of the equation, and using the relations

$$\delta\rho = -\rho\ \boldsymbol{\nabla}_{\rm cm}\cdot\boldsymbol{\eta}\ \ ,\ \ \ \boldsymbol{\nabla}^2_{\rm cm}\delta\Phi = 4\pi G R^2\ \delta\rho\ , \tag{6.9.104}$$

one finds:

$$\left(\frac{{\rm d}^2 b}{{\rm d}t^2} + 2H\,\frac{{\rm d}b}{{\rm d}t}\right)\ \boldsymbol{\nabla}^2_{\rm cm}\psi = \left[\left(\frac{c_{\rm s}^2}{R^2}\right)\ \boldsymbol{\nabla}^4_{\rm cm}\psi + 4\pi G\rho\ \boldsymbol{\nabla}^2_{\rm cm}\psi\right]\ b(t)\ . \tag{6.9.105}$$

If one assumes that the gas is so cold that the acoustic term $\propto c_{\rm s}^2$ can be neglected, this becomes

$$\left(\frac{{\rm d}^2 b}{{\rm d}t^2} + 2H(t)\,\frac{{\rm d}b}{{\rm d}t} - 4\pi G\rho(t)\ b(t)\right)\ \boldsymbol{\nabla}^2_{\rm cm}\psi = 0\ . \tag{6.9.106}$$

[17] e.g. G.B. Arfken & H.J. Weber, *Mathematical Methods for Physicists*, Fourth Edition, p. 202.

[18] In fact this is the main assumption that Zeldovich made!

This can be satisfied for *any* $\psi(\boldsymbol{r})$ provided that the function $b(t)$ is a solution of

$$\frac{\mathrm{d}^2 b}{\mathrm{d}t^2} + 2H(t)\,\frac{\mathrm{d}b}{\mathrm{d}t} - 4\pi G\rho(t)\,b(t) = 0\ . \tag{6.9.107}$$

This means that the Zeldovich approximation is *not* limited to plane wave solutions where $\psi(\boldsymbol{r}) = \psi_0\,\exp(i\boldsymbol{q}\cdot\boldsymbol{r}) + \mathrm{cc}$, unlike the linear theory of the previous Section. We have already derived the solutions to Eqn. (6.9.107) for a matter-dominated flat Universe. Retaining only the growing mode of the solution (see Eqn. 6.8.84) one has:

$$b(t) \propto R(t) \propto t^{2/3}\ . \tag{6.9.108}$$

If we put $c_{\rm s} = 0$ in Eqn. (6.9.95) and substitute $\boldsymbol{\eta}(\boldsymbol{r}\ ,\ t) = b(t)\ \boldsymbol{f}(\boldsymbol{r})$, one finds:

$$\left(\frac{\mathrm{d}^2 b}{\mathrm{d}t^2} + 2H(t)\,\frac{\mathrm{d}b}{\mathrm{d}t}\right)\ \boldsymbol{f}(\boldsymbol{r}) = -\frac{1}{R^2}\,\boldsymbol{\nabla}_{\rm cm}\delta\Phi\ . \tag{6.9.109}$$

Since $b(t)$ satisfies (6.9.107) and $\boldsymbol{f}$ can be written as $\boldsymbol{f} = \boldsymbol{\nabla}_{\rm cm}\psi(\boldsymbol{r})$, this is equivalent with:

$$4\pi G\,\rho(t)\,b(t)\,\boldsymbol{\nabla}_{\rm cm}\psi = -\frac{1}{R^2}\,\boldsymbol{\nabla}_{\rm cm}\delta\Phi\ . \tag{6.9.110}$$

This means that ψ and $\delta\Phi$ are related by

$$\psi(\boldsymbol{r}) = -\frac{\delta\Phi}{4\pi G\rho\ R^2(t)b(t)} = -\frac{\delta\Phi}{4\pi G\rho_0}\ \frac{R(t)}{b(t)}\ . \tag{6.9.111}$$

This relation also implies that

$$\boldsymbol{\eta}(\boldsymbol{r}\ ,\ t) = b(t)\ \boldsymbol{\nabla}\psi = \frac{\boldsymbol{g}_{\rm cm}}{4\pi G\ \rho R^2}\ , \tag{6.9.112}$$

with

$$\boldsymbol{g}_{\rm cm} = -\boldsymbol{\nabla}_{\rm cm}\delta\Phi \tag{6.9.113}$$

the 'gravitational acceleration' associated with $\delta\Phi$ in comoving coordinates.

These relations allow us to predict the behaviour of a collapsing cloud. Let us assume that we perturb the density locally, in such a way that the *equipotential surfaces* of the resulting gravitational potential $\delta\Phi$ are a set of nested perfect spheres. In that case, the vector $\boldsymbol{g}_{\rm cm}$ is always directed to the center of these spheres, and has a constant magnitude everywhere on an equipotential surface. The displacement vector $\boldsymbol{\eta}$ and velocity $\boldsymbol{u} = \partial\boldsymbol{\eta}/\partial t$ are also radially directed, and (at fixed time) have a constant magnitude on a equipotential surface. The resulting gravitational collapse is spherically symmetric, and remains so as the collapse progresses. The fact that the equipotential surfaces are spheres implies that the eigenvalues of the strain tensor introduced in Eqns. (6.9.98) and (6.9.100) are all equal,

$$\alpha_1 = \alpha_2 = \alpha_3 \ , \tag{6.9.114}$$

explicitly showing the 'isotropy' of a spherically symmetric gravitational collapse.

Because of relation (6.9.111) the strain tensor and the so-called *tidal tensor* of the gravitational field are proportional to each other:

$$S_{ij} = \frac{\partial^2\psi}{\partial r_i \partial r_j} = -\frac{1}{4\pi G\rho\, R^2 b}\ \underbrace{\left(\frac{\partial^2\delta\Phi}{\partial r_i \partial r_j}\right)}_{\text{tidal tensor}} \ . \tag{6.9.115}$$

The proportionality factor only depends on time. The principle axes of the strain tensor and the tidal tensor coincide, and the eigenvalues of the two tensors differ only by a constant factor. This explains why spherical equipotential surfaces lead to three equal eigenvalues of the strain tensor, c.f. Eqn. (6.9.114). The tidal tensor gives the variations of the gravitational acceleration $\boldsymbol{g}_{\rm cm} = -\boldsymbol{\nabla}_{\rm cm}\delta\Phi$ with position. These variations lead to tidal forces, which explains the name.

Let us now consider a more complicated case, where the equipotential surfaces form a set of nested, three-axial ellipsoids (see the figure below). The three principle axes are the coordinate axis x, y and z. The cross section in the $x-y$ plane is an ellipse with

$$\frac{x^2}{a^2} + \frac{y^2}{b^2} = 1 \ , \tag{6.9.116}$$

while the cross-section in the $y-z$ plane is the ellipse defined by

$$\frac{x^2}{a^2} + \frac{z^2}{c^2} = 1 \ . \tag{6.9.117}$$

The material inside the ellipsoid has a (slighly) larger density, and the gravitational acceleration $\boldsymbol{g}_{\rm cm}$ is pointing inwards. The vector $\boldsymbol{g}_{\rm cm}$ is everywhere perpendicular to an equipotential surface. Let us now assume that the length parameters a, b and c satisfy:

$$c < b < a \; . \tag{6.9.118}$$

In that case, the gravitational acceleration $\boldsymbol{g}_{\rm cm}$ is the largest along the z-axis, simply because the equipotential surfaces are crowded together the most along that axis. If one has to close equipotential surfaces, one with $\delta\Phi = \Phi_1$ and one with $\delta\Phi = \Phi_1 + \Delta\Phi$ the magnitude of the gravitational acceleration is simply

$$|\boldsymbol{g}_{\rm cm}| = \frac{\Delta\Phi}{|\Delta\boldsymbol{r}|} \; , \tag{6.9.119}$$

with $|\Delta\boldsymbol{r}|$ the distance between the two surfaces measured along the normal to the surface. A similar conclusion holds for the tidal tensor: the zz-component

$$\frac{\partial^2\delta\Phi}{\partial z^2} \tag{6.9.120}$$

is the largest, and in fact assumption (6.9.118) implies:

$$\frac{\partial^2\delta\Phi}{\partial z^2} > \frac{\partial^2\delta\Phi}{\partial y^2} > \frac{\partial^2\delta\Phi}{\partial x^2} \; . \tag{6.9.121}$$

Zeldovich's analysis as outlined above implies that the collapse proceeds most rapidly along the z-axis. The collapse along the y-axis is slower, and along the x-axis the collapse proceeds at the slowest rate.

This means that the cloud, and with it the equipotential surfaces, will deform in such a way that it becomes flatter and flatter in the z-direction, etc. The deviation of the equipotential surfaces $\delta\Phi =$ constant from a sphere is *amplified* as the collapse proceeds further and further. Because of relation (6.9.111) between the tidal tensor and the strain tensor relation (6.9.121) implies that the three eigenvalues of the strain tensor satisfy

$$\alpha_3 > \alpha_2 > \alpha_1 \; . \tag{6.9.122}$$

Expression (6.9.101) then immediately shows that the largest density increase ($\rho \propto 1/D!$) is due to the factor involving α_3 in the determinant, i.e. due to the collapse in the z-direction.

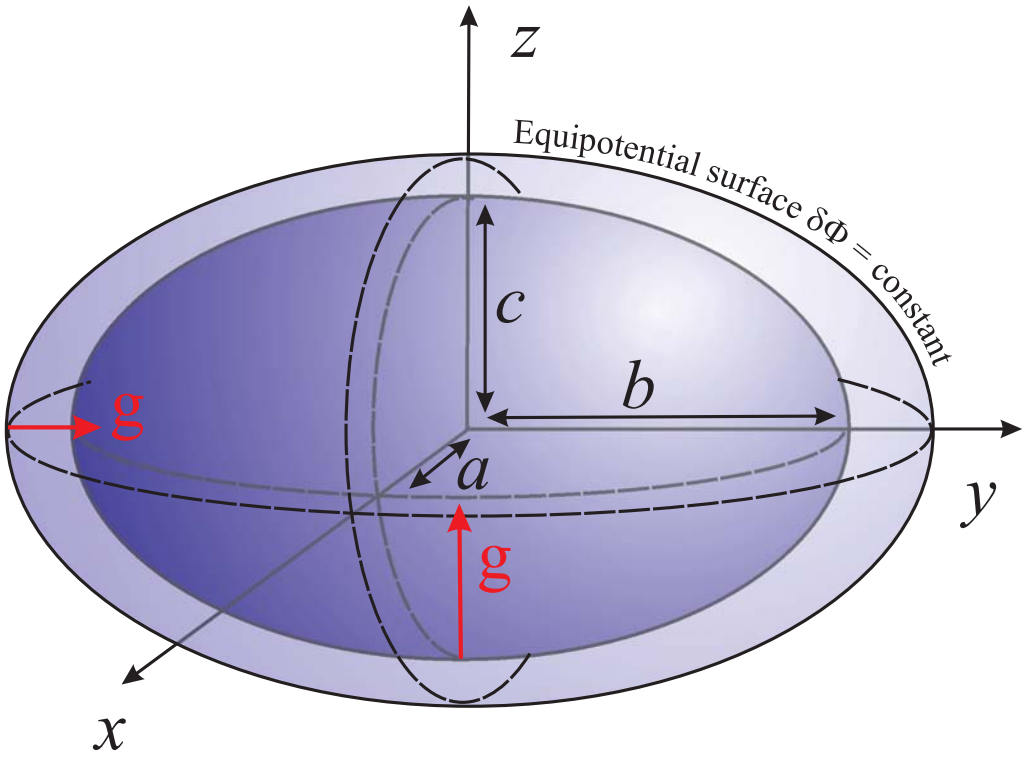

Figure 6.10: *The equipotential surfaces* $\delta\Phi = \text{constant}$ *of an ellipsoidal mass distribution. The three principle axes coincide with the three coordinate axes of a cartesian system. The gravitational acceleration* $\boldsymbol{g}_{\rm cm}$ *(the red arrows) is* **largest** *along the* z*-axis where the equipotential surfaces are crowded together the most.*

Zeldovich called the objects that ultimately result from such an anisotropic collapse *pancakes*, for obvious reason. The formation of such a pancake is illustrated schematically below. Of course Zeldovich's analysis breaks down long before the simple expressions predict an *infinite* density, which happens as

$$1 - \alpha_3\, b(t) \downarrow 0\ . \tag{6.9.123}$$

Long before that happens, the compression in the collapsing cloud becomes so large that the effects of pressure (neglected in this analysis when we put $c_{\rm s} = 0$) must be taken into account. Nevertheless, Zeldovich's approach shows results that closely resemble more sophisticated numerical simulations. In particular, it explains why the matter tends to collect into thin filaments and sheets, as is observed.

Interestingly enough, exactly the opposite happens in an ellipsoidal region that is less dense than its surroundings. There the gravitational acceleration $\boldsymbol{g}_{\rm cm}$ is directed towards the exterior of the region, and it *expands* rather than contracts. In that case the region becomes more and more spherical as it expands. This explains why the large 'voids' observed in the large-scale distribution of galaxies (or in the simulation shown at the beginning of this Chapter) are mode-or-less circular: see the result from the 2DF Galaxy Survey below.

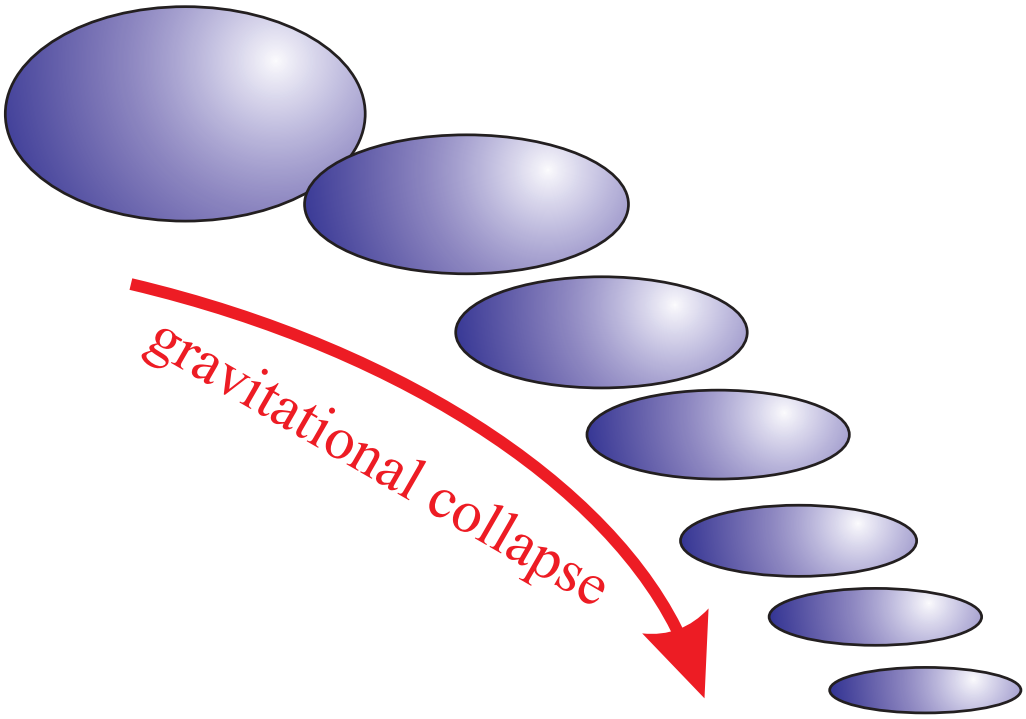

Figure 6.11: *The gravitational collapse of an overdense ellipsoidal cloud. The deviations of the equipotential surfaces from a perfect sphere are amplified during the collapse, and the cloud gets flatter and flatter as the collapse proceeds.*

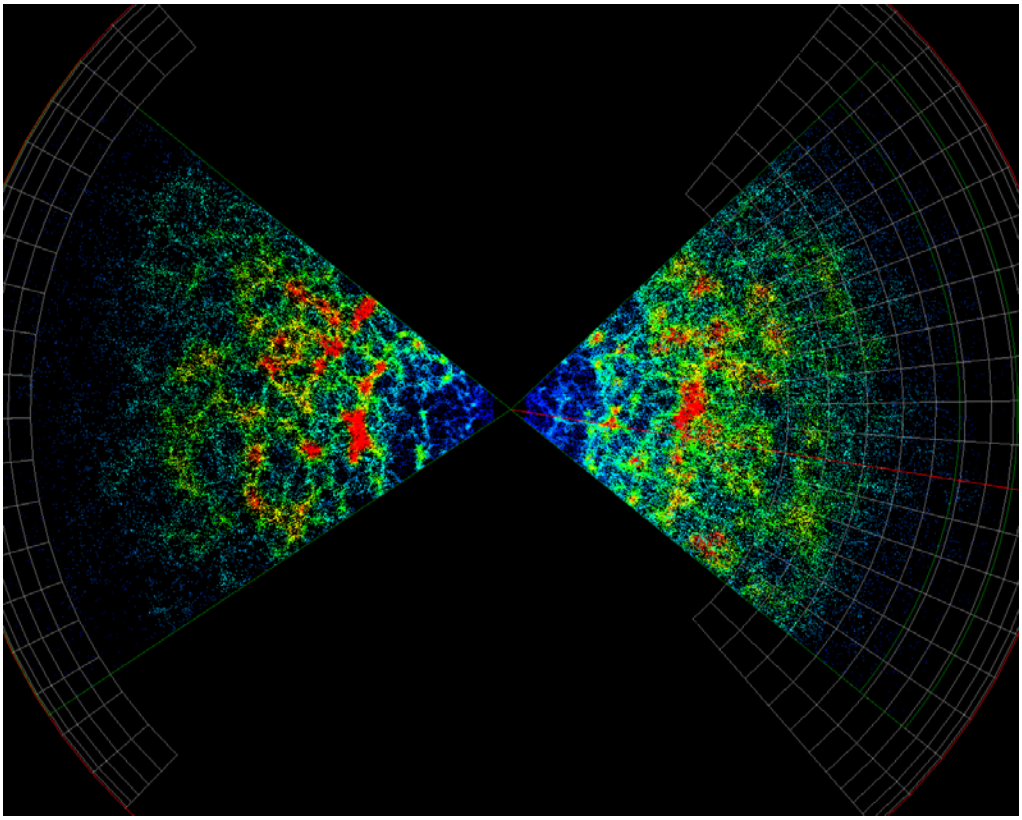

Figure 6.12: *The 2DF Redshift Survey of galaxies. Shown are two 'pie slices' which correspond with two thin sections of the sky. The distance from the middle, where the slices meet, is proportional to the redshift, and therefore the distance of the galaxies.*

6.10 Waves in a stratified atmosphere

In the photosphere of the Sun, or in the Earth's atmosphere and oceans, long-wavelength waves are influenced by the presence of gravity, and the associated stratification of the atmosphere. This stratification leads to the occurence of *acoustic-gravity waves* or *internal gravity waves*[19], where buoyancy plays a role in determining wave properties.

I will consider the simplest case: that of a plane-parallel, isothermal atmosphere at rest ($\boldsymbol{V} = 0$), with a *constant* gravitational acceleration and a constant temperature. Assume that the vertical direction is along the z-axis, so that the gravitational acceleration equals

$$\boldsymbol{g} = -\boldsymbol{\nabla}\Phi = -g\,\hat{\boldsymbol{e}}_z\ . \tag{6.10.1}$$

The equation of hydrostatic equilibrium then reduces to

$$\frac{\mathrm{d}P(z)}{\mathrm{d}z} = -g\,\rho(z)\ . \tag{6.10.2}$$

Given the constant temperature ($\partial T/\partial z = 0$), and using the ideal gas law,

$$P(z) = \frac{\rho(z)\mathcal{R}T}{\mu}\ ,$$

hydrostatic equilibrium can be written as

$$\left(\frac{\mathcal{R}T}{\mu}\right)\,\frac{\mathrm{d}\rho}{\mathrm{d}z} = -\rho\,g\ . \tag{6.10.3}$$

The solution of this equation is simple, and one finds that the pressure and density decay exponentially with increasing height z:

$$\boxed{P(z) = P_0 e^{-z/\mathcal{H}} \quad , \quad \rho(z) = \rho_0\,e^{-z/\mathcal{H}}\ .} \tag{6.10.4}$$

Here ρ_0 and $P_0 = \rho_0\mathcal{R}T/\mu$ are the density and pressure at $z = 0$.

[19]For a discussion of these waves in the Solar atmosphere see: E.R. Priest, 1982, *Solar Magnetohydrodynamics*, Kluwer Academic Press, Ch. 4;
For a discussion of internal gravity waves in the ocean see: P.H. LeBlond & L.A. Mysak, 1978, *Waves in the Ocean*, Elsevier Scientific Publ. Co., Ch. 2.10

The quantity $\mathcal{H}$ is the constant *pressure scale height* of an isothermal atmosphere that is given by:

$$\mathcal{H} = \frac{\mathcal{R}T}{\mu g} \; . \tag{6.10.5}$$

I will now calculate the properties of small-amplitude waves in this stratified atmosphere. Since the unperturbed atmosphere is at rest, the velocity perturbation associated with the waves satisfies

$$\Delta \boldsymbol{V} = \delta \boldsymbol{V} = \frac{\partial \boldsymbol{\xi}}{\partial t} \; ,$$

with $\boldsymbol{\xi}$ the displacement vector of the wave motion. The linearized equation of motion for the perturbations becomes

$$\rho \, \frac{\partial^2 \boldsymbol{\xi}}{\partial t^2} = -\boldsymbol{\nabla} \delta P + \delta \rho \, \boldsymbol{g} \; . \tag{6.10.6}$$

This equation can be easily derived by taking the Eulerian perturbation δ of the full equation of motion for the gas, using $\boldsymbol{V} = 0$ and $\delta \boldsymbol{g} = 0$ as we are neglecting self-gravity, and neglecting the non-linear terms. The density- and pressure perturbations follow from the general expressions derived in Chapter 6.2:

$$\begin{aligned} \delta \rho &= -\rho \, (\boldsymbol{\nabla} \cdot \boldsymbol{\xi}) - (\boldsymbol{\xi} \cdot \boldsymbol{\nabla}) \rho \\ \delta P &= -\gamma P \, (\boldsymbol{\nabla} \cdot \boldsymbol{\xi}) - (\boldsymbol{\xi} \cdot \boldsymbol{\nabla}) P \; . \end{aligned} \tag{6.10.7}$$

Here I have assumed that the pressure variations in the waves are adiabatic so that $\Delta P = (\gamma P / \rho) \, \Delta \rho$. One can combine these two expressions by eliminating $\boldsymbol{\nabla} \cdot \boldsymbol{\xi}$ from the equations:

$$\begin{aligned} \delta P &= \frac{\gamma P}{\rho} \, (\delta \rho + (\boldsymbol{\xi} \cdot \boldsymbol{\nabla}) \rho) - (\boldsymbol{\xi} \cdot \boldsymbol{\nabla}) P \\ &= c_{\rm s}^2 \, \delta \rho - P \, (\boldsymbol{\xi} \cdot \boldsymbol{\nabla}) \ln \left[\, P \rho^{-\gamma} \, \right] \end{aligned} \tag{6.10.8}$$

Note that the sound speed $c_{\rm s} = \sqrt{\gamma \mathcal{R} T / \mu}$ is constant in an isothermal atmosphere. Using $P(z) = \rho(z) \mathcal{R} T / \mu$ one has (see Eqn. 6.10.4):

$$\begin{aligned} \boldsymbol{\nabla} \ln\left[\, P\rho^{-\gamma}\,\right] &= \left[\frac{1}{P}\,\frac{\mathrm{d}P}{\mathrm{d}z} - \gamma\left(\frac{1}{\rho}\frac{\mathrm{d}\rho}{\mathrm{d}z}\right)\right]\hat{\boldsymbol{e}}_z \\ &= \left(\frac{\gamma-1}{\mathcal{H}}\right)\hat{\boldsymbol{e}}_z\,. \end{aligned} \tag{6.10.9}$$

Using this in (6.10.8) we find:

$$\delta P = c_{\rm s}^2\,\delta\rho - \frac{\gamma-1}{\mathcal{H}}\,\xi_z\,P\,. \tag{6.10.10}$$

The first term on the right-hand side of this relation is the same as in a sound wave: it is the *acoustic* response of the pressure to small density perturbations. The second term, involving the scaleheight $\mathcal{H}$, is new: this term is due to the stratification of the unperturbed gas. The displacement of the gas in the z direction over a distance ξ_z means that an observer at a *fixed* position $z = z_0$ finds himself surrounded by gas that used to sit at $z_0 - \xi_z$. Since the gas is stratified in the z-direction he will measure a different density and pressure. The stratification term in (6.10.10) takes account of the effect of this pressure change.

We can use relation (6.10.10) together with the expression for $\delta\rho$ in (6.10.7) to solve the equation of motion (6.10.6). First we make a change of variables, defining

$$\boldsymbol{\zeta}(\boldsymbol{x}\,,\,t) \equiv \rho(z)\,\boldsymbol{\xi}(\boldsymbol{x}\,,t)\,. \tag{6.10.11}$$

In terms of this variable the inertial term in the equation of motion becomes

$$\rho\,\frac{\partial^2\boldsymbol{\xi}}{\partial t^2} = \frac{\partial^2\boldsymbol{\zeta}}{\partial t^2}\,, \tag{6.10.12}$$

and the density and pressure perturbations are

$$\begin{aligned} \delta\rho &= -(\boldsymbol{\nabla}\cdot\boldsymbol{\zeta})\,, \\ \delta P &= -c_{\rm s}^2\left[(\boldsymbol{\nabla}\cdot\boldsymbol{\zeta}) + \frac{\gamma-1}{\gamma\mathcal{H}}\,\zeta_z\right]\,. \end{aligned} \tag{6.10.13}$$

Substituting these relations into the equation of motion (6.10.6), one finds a single partial differential equation (wave equation) for $\boldsymbol{\zeta}(\boldsymbol{x},t)$ with *constant* coefficients (which motivates this variable change):

$$\boxed{\frac{\partial^2\boldsymbol{\zeta}}{\partial t^2} = c_{\rm s}^2\,\boldsymbol{\nabla}\left[(\boldsymbol{\nabla}\cdot\boldsymbol{\zeta}) + \frac{\gamma-1}{\gamma\mathcal{H}}\,\zeta_z\right] + (\boldsymbol{\nabla}\cdot\boldsymbol{\zeta})g\;\hat{\boldsymbol{e}}_z\;.} \tag{6.10.14}$$

The exponential z-dependence of pressure and density in the atmosphere has been hidden, or rather it has been 'absorbed' into $\boldsymbol{\zeta}$. Because of the constant coefficients in (6.10.14) we can once again look for a plane wave solution of the form

$$\boldsymbol{\zeta}(\boldsymbol{x}\;,\;t) = \boldsymbol{a}\;e^{ik_x x + ik_z z - i\omega t} + \text{cc.} \tag{6.10.15}$$

Here I have assumed that there is no dependence on the y-coordinate. This does not restrict the the validity of the solution as one can always rotate around the z-axis, in effect choosing new x and y coordinates, without changing the physics. In that way you can align the x-axis with the component of $\boldsymbol{k}$ in the horizontal plane so that plane waves show no dependence on y.

Substituting the plane-wave assumption into the equation of motion yields a set of three algebraic relations between a_x, a_y and a_z which can be written in matrix form as:

$$\begin{pmatrix} \omega^2 - k_x^2 c_{\rm s}^2 & 0 & ik_x(\gamma-1)g - k_x k_z\,c_s^2 \\ 0 & \omega^2 & 0 \\ ik_x g - k_x k_z\,c_{\rm s}^2 & 0 & \omega^2 - k_z^2\,c_{\rm s}^2 + ik_z\gamma g \end{pmatrix} \begin{pmatrix} a_x \\ a_y \\ a_z \end{pmatrix} = 0\;. \tag{6.10.16}$$

In deriving these relations I have made use of the definitions of the pressure scale height $\mathcal{H}$ and of the adiabatic sound speed $c_{\rm s}$ to write:

$$\mathcal{H} = \frac{c_{\rm s}^2}{\gamma g} \quad , \quad \frac{(\gamma-1)\,c_{\rm s}^2}{\gamma\mathcal{H}} = (\gamma-1)\,g \tag{6.10.17}$$

There is only a non-trivial solution to these equations if the determinant of the of the 3×3 matrix in Eqn (6.10.16) vanishes.

After some algebra this condition leads to the following dispersion relation for the waves:

$$\omega^2 \left\{ \omega^4 - \left[\left(k_x^2 + k_z^2 \right) c_{\rm s}^2 - i k_z \gamma g \right] \omega^2 + (\gamma - 1) k_x^2 g^2 \right\} = 0 \; . \tag{6.10.18}$$

The solution $\omega = 0$ is not a wave in the true sense of the word: it does not vary in time. This solution corresponds to $a_x = a_z = 0$, $a_y \neq 0$.

The term in the curly brackets contains both a real and an imaginary part. This means that either the wave frequency, or the wave vector $\boldsymbol{k} = (k_x \, , \, k_z)$ must be complex. We choose the latter possibility, keeping the wave frequency ω real-valued in order to avoid waves that grow (or decay) as a function of time.

Let us write

$$k_z = \tilde{k}_z + i\kappa \; , \tag{6.10.19}$$

with $\tilde{k}_z = {\rm Re}(k_z)$ and $\kappa = {\rm Im}(k_z)$. Substituting this into (6.10.18) one finds that the term in the curly brackets splits into a purely real and a purely imaginary term, *both* of which must vanish simultaneously. This leads to two solution conditions:

$$\begin{aligned} \text{real part:} \quad & \omega^4 - \left(k_x^2 + \tilde{k}_z^2 - \kappa^2 \right) c_{\rm s}^2 \omega^2 - \kappa \gamma g \omega^2 + (\gamma - 1) k_x^2 g^2 = 0 \; ; \\ \text{imaginary part:} \quad & \omega^2 \left(\gamma g \tilde{k}_z - 2 \tilde{k}_z \kappa c_{\rm s}^2 \right) = 0 \; . \end{aligned} \tag{6.10.20}$$

The second equation immediately determines the value of κ:

$$\kappa = \frac{\gamma g}{2 c_{\rm s}^2} = \frac{1}{2\mathcal{H}} \; . \tag{6.10.21}$$

This result implies that the z-dependence of $\boldsymbol{\zeta}$ and of the displacement $\boldsymbol{\xi}$ is

$$\begin{aligned} \boldsymbol{\zeta}(\boldsymbol{x} \, , \, t) \propto e^{i k_z z} \quad &= \quad e^{i \tilde{k}_z z} \times e^{-z/2\mathcal{H}} \\ \boldsymbol{\xi}(\boldsymbol{x} \, , \, t) \equiv \frac{\boldsymbol{\zeta}(\boldsymbol{x} \, , \, t)}{\rho(z)} \quad &\propto \quad e^{i \tilde{k}_z z} \times e^{z/2\mathcal{H}} \; . \end{aligned} \tag{6.10.22}$$

This exponential behaviour of the displacement vector $\boldsymbol{\xi}$ is a direct consequence of the exponential pressure-and density profiles in the atmosphere.

Substituting the above value for κ back into the real term yields the dispersion relation for acoustic-gravity waves in an isothermally stratified atmosphere:

$$\omega^4 - \left(\tilde{k}^2 c_{\rm s}^2 + \frac{\gamma^2 g^2}{4 c_{\rm s}^2} \right) \, \omega^2 + (\gamma - 1) \, k_x^2 g^2 = 0 \; . \tag{6.10.23}$$

Here $\tilde{k}^2 \equiv k_x^2 + \tilde{k}_z^2$.

Let us define the following two frequencies:

$$N_{\rm s} \equiv \frac{\gamma g}{2 c_{\rm s}} = \frac{c_{\rm s}}{2 \mathcal{H}} \; . \quad , \quad N_{\rm BV} \equiv \frac{(\gamma - 1)^{1/2} \, g}{c_{\rm s}} = \left(\frac{\sqrt{\gamma - 1}}{\gamma} \right) \, \frac{c_{\rm s}}{\mathcal{H}} \tag{6.10.24}$$

The second frequency is known as the *Brunt Väisälä frequency*. Its general definition (valid also in non-isothermal atmospheres) is:

$$N_{\rm BV}^2 \equiv - \left(\frac{\boldsymbol{\nabla} P}{\gamma \rho} \right) \cdot \left(\boldsymbol{\nabla} \left\{ \ln \left[P \rho^{-\gamma} \right] \right\} \right) \; . \tag{6.10.25}$$

It is easily checked that this definition reduces to $N_{\rm BV}^2 = (\gamma - 1) g^2 / c_{\rm s}^2$ in an isothermal atmosphere, where the pressure satisfies the equation of hydrostatic equilibrium. One has $N_{\rm s} \geq N_{\rm BV}$ for $\gamma < 2$, with equality at $\gamma = 2$.

Expressed in terms of the two characteristic buoyancy frequencies $N_{\rm s}$ and $N_{\rm BV}$, the above dispersion relation can be written as:

$$\boxed{\omega^4 - \left(N_{\rm s}^2 + \tilde{k}^2 c_{\rm s}^2 \right) \, \omega^2 + \tilde{k}^2 c_{\rm s}^2 \, N_{\rm BV}^2 \, \sin^2 \theta = 0 \; .} \tag{6.10.26}$$

The angle θ in this expression is the angle between the *real* part of the wavevector and the vertical direction, i.e.

$$k_x = \tilde{k} \, \sin \theta \quad , \quad \tilde{k}_z = \tilde{k} \, \cos \theta \; .$$

Waves propagating in the horizonthal plane have $\theta = \pi/2$, and waves propagating along the vertical have $\theta = 0$.

This dispersion relation for acoustic-gravity waves is a quadratic equation for ω^2, with the formal solution

$$\omega^2 = \tfrac{1}{2}\left(N_{\rm s}^2 + \tilde{k}^2 c_{\rm s}^2\right) \pm \tfrac{1}{2}\sqrt{\left(N_{\rm s}^2 + \tilde{k}^2 c_{\rm s}^2\right)^2 - 4\tilde{k}^2 c_{\rm s}^2\, N_{\rm BV}^2\, \sin^2\theta}\ . \tag{6.10.27}$$

We can look this solution in a number of limiting cases:

- **Purely vertical propagation:** $k_x = \tilde{k}\, \sin\theta = 0$.
  In this case the solution of (6.10.26)is easily obtained:

  $$\omega = \pm\sqrt{\tilde{k}^2 c_{\rm s}^2 + N_{\rm s}^2}\ .$$

- **The high-frequency/short wavelength limit:** $\omega \gg N_{\rm s}\ ,\ N_{\rm BV}$ and $\tilde{k} \gg 1/\mathcal{H}$.
  Here the terms due to the stratification of the atmosphere are unimportant, dispersion relation (6.10.26) can be approximated by $\omega^2(\omega^2 - \tilde{k}^2 c_{\rm s}^2) \approx 0$. This is the dispersion relation for sound waves with solution

  $$\omega \approx \pm\tilde{k} c_{\rm s}\ .$$

  In this limit, the acoustic effects are much stronger than the effects due to the stratification of the atmosphere, and the waves behave as sound waves.

- **The low-frequency/short wavelenth limit:** $\omega \ll \tilde{k} c_{\rm s}$ and $N_{\rm s}\ ,\ N_{\rm BV} \ll \tilde{k} c_{\rm s}$.
  In this limit we can neglect the ω^4 term in the the dispersion relation altogether, and neglect $N_{\rm s}^2$ with respect to $\tilde{k}^2 c_{\rm s}^2$ in the second term of (6.10.26). The dispersion relation can therefore be approximated by $\tilde{k}^2 c_{\rm s}^2(\omega^2 - N_{\rm BV}^2\, \sin^2\theta) \approx 0$, and we find pure *internal gravity waves* as solutions:

  $$\omega \approx \pm N_{\rm BV}\, \sin\theta\ .$$

  This limit is valid when $\tilde{k}\mathcal{H} \gg 1$, corresponding to (horizontal) wavelengths much *smaller* than the pressure scale height. In this low-frequency limit, the effects of the stratification of the atmosphere determine the pressure perturbation, and the behaviour of the waves.

We can also rewrite the dispersion relation as an equation for $\tilde{k}^2$:

$$\tilde{k}^2 = \left(\frac{\omega}{c_{\rm s}}\right)^2 \times \frac{\omega^2 - N_{\rm s}^2}{\omega^2 - N_{\rm BV}^2\, \sin^2\theta}\ . \tag{6.10.28}$$

Since we have assumed that $\tilde{k}$ and ω are real, the quantities $\tilde{k}^2$ and ω^2 are both positive. Equation (6.10.28) can therefore only be satisfied if

$$\frac{\omega^2 - N_{\rm s}^2}{\omega^2 - N_{\rm BV}^2 \, \sin^2\theta} > 0 \; . \tag{6.10.29}$$

For an ideal mono-atomic gas with $\gamma = 5/3$ one has $N_{\rm BV} \approx 0.98 \, N_{\rm s}$, so this means that **no** waves can propagate in the frequency range

$$N_{\rm BV} \, \sin\theta < \mid \omega \mid < N_{\rm s} \; . \tag{6.10.30}$$

In this frequency range waves are *evanescent* since $\tilde{k}$ must become purely imaginary in order to satisfy Eqn. (6.10.28). The 'forbidden region' in frequency shrinks as $\theta \rightarrow \pi/2$, in the direction towards purely horizontal propagation.

The figure below shows the solution curves $\omega = \omega(k_x \, , \, k_z)$ for acoustic-gravity waves are shown for propagation angles equal to $\theta = 0$ (vertical propagation), $\theta = \pi/4$ and for $\theta = \pi/2$ (horizontal propagation). By defining the following dimensionless frequency and wavenumber,

$$\nu = \omega \mathcal{H}/c_{\rm s} \quad , \quad \ell = \tilde{k} \mathcal{H} \; , \tag{6.10.31}$$

the dispersion relation (6.10.26) can be written as

$$\nu^4 - \left(\tfrac{1}{4} + \ell^2 \right) \, \nu^2 + \frac{\gamma - 1}{\gamma^2} \, \ell^2 \, \sin^2\theta = 0 \; . \tag{6.10.32}$$

and the solution to the dispersion relation is

$$\nu^2 = \frac{\ell^2 + 1/4}{2} \pm \frac{1}{2} \left\{ \left(\ell^2 + \frac{1}{4} \right)^2 - \frac{4(\gamma - 1)}{\gamma^2} \, \ell^2 \sin^2\theta \right\}^{1/2} \; . \tag{6.10.33}$$

Note that all *explicit* references to the physical conditions in the atmosphere, such as the sound speed $c_{\rm s}$, the gravitational acceleration g and the pressure scale height $\mathcal{H}$, have been scaled away.

Expressed in terms of these dimensionless varaiables for the frequency and the wavenumber, sound waves (the high-frequency/short wavelength limit) and internal gravity waves (the low-frequency/short wavelength limit) correspond to:

$$\begin{aligned} \nu &= \pm\ell \\ &\quad \text{(sound waves; the limit } \ell \gg 1 \text{ and } |\nu| \gg 1) \\ \nu &= \pm\frac{\sqrt{\gamma-1}}{\gamma}\,\sin\theta \\ &\quad \text{(internal gravity waves; the limit } |\nu| \ll \ell \text{ and } \ell \gg 1.)\ . \end{aligned} \tag{6.10.34}$$

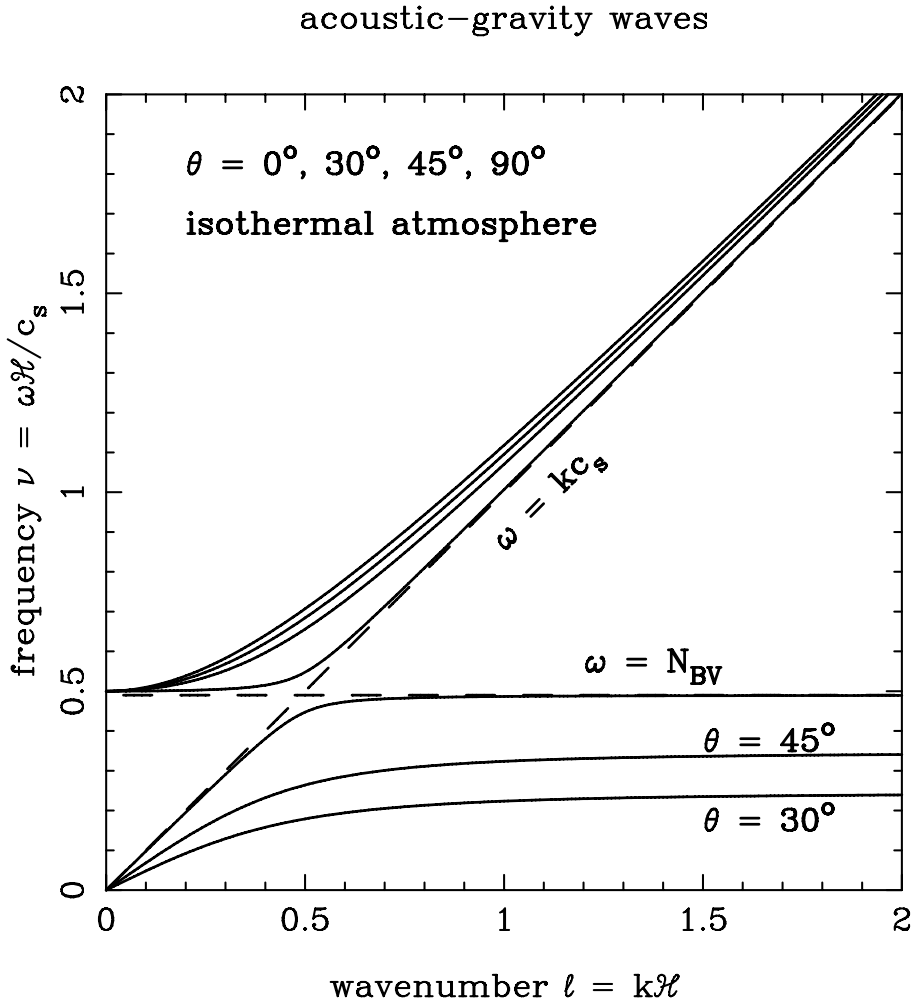

Figure 6.13: *Diagram showing the solutions of the dispersion relation (6.10.26) in terms of the dimensionless frequency ν and wave number ℓ. Dispersion curves are shown for propagation angles with respect to the vertical direction equal to $\theta = 0$, 30^o , 45^o and 90^o. Note that the low-frequency modes all stay below the horizontal (dashed) line $\omega = N_{\rm BV}$, and asymptotically go to $\omega = N_{\rm BV} sin\theta$ for $\ell = \tilde{k}\mathcal{H} \gg 1$. The high-frequency solutions all stay above the sound line $\omega = \tilde{k}c_{\rm s}$ (the diagonal dashed line) and the line $\omega = N_{\rm s}$ (not shown, but $N_{\rm s} \approx N_{\rm BV}$), and approach the diagonal sound line closely for large values of ℓ. The region between the Brunt-Väisälä frequency $N_{\rm BV}$ and the sound frequency $\tilde{k}c_{\rm s}$ is 'forbidden' as no propagating waves are allowed there* **regardless** *the propagation angle. With increasing propagation angle θ the low- and high-frequency curves approach these two limiting lines more closely.*

6.10.1 The Brunt-Väisälä frequency, buoyancy and convection

The Brunt-Väisälä frequency $N_{\rm BV}$, which plays such a prominent role in the properties of acoustic-gravity waves, has a simple physical interpretation. Consider a spherical bubble of fluid in a gravitationally stratified atmosphere. Initially, the bubble is located at some height z. The material in the fluid bubble has the same properties as its surroundings: the internal pressure and density equal

$$P = P_{\rm e}(z) \quad , \quad \rho = \rho_{\rm e}(z) \; . \tag{6.10.35}$$

I use a subscript 'e' to denote the properties of the fluid surrounding the bubble. We now displace the fluid bubble in the vertical direction, from its initial position z to a new position $\bar{z} \equiv z + \xi_z$. The fluid must remain in pressure equilibrium with its surroundings.

If the bubble rises ($\xi_z > 0$) it finds itself in a environment with lower pressure, and will expand until pressure equilibrium is re-established. The pressure at the new position of the bubble equals

$$\bar{P} = P_{\rm e}(\bar{z}) \approx P + \xi_z \left(\frac{{\rm d}P_{\rm e}}{{\rm d}z} \right) \; . \tag{6.10.36}$$

Here I have used the initial pressure balance (6.10.35) and assumed that ξ_z is small. If the fluid in the bubble behaves adiabatically, the density change $\Delta\rho$ the pressure change ΔP must be related by

$$\Delta P = \frac{\gamma P}{\rho} \, \Delta\rho \equiv c_{\rm s}^2 \, \Delta\rho \; , \tag{6.10.37}$$

with $c_{\rm s}$ the speed of sound in the bubble. The pressure change is

$$\Delta P = \bar{P} - P = \xi_z \left(\frac{{\rm d}P_{\rm e}}{{\rm d}z} \right) \; . \tag{6.10.38}$$

This implies that the density inside the bubble after displacement equals

$$\begin{aligned} \bar{\rho} &= \rho + \frac{\Delta P}{c_{\rm s}^2} \\ &= \rho_{\rm e}(z) \left[1 + \xi_z \left(\frac{1}{\gamma P_{\rm e}} \frac{{\rm d}P_{\rm e}}{{\rm d}z} \right) \right] \; . \end{aligned} \tag{6.10.39}$$

Here I have used that $\rho = \rho_{\rm e}(z)$ initially, and $c_{\rm s}^2 = \gamma P/\rho \approx \gamma P_{\rm e}/\rho_{\rm e}$.

The density in the surrounding medium at the new position $\bar{z}$ equals

$$\rho_{\rm e}(\bar{z}) = \rho + \xi_z \left(\frac{{\rm d}\rho_{\rm e}}{{\rm d}z}\right) . \tag{6.10.40}$$

In general, there will be a density difference between the fluid in the bubble and the surrounding fluid:

$$\bar{\rho} - \rho_{\rm e}(\bar{z}) = \rho_{\rm e}\, \xi_z \left[\frac{1}{\gamma P_{\rm e}} \left(\frac{{\rm d}P_{\rm e}}{{\rm d}z}\right) - \frac{1}{\rho_{\rm e}} \left(\frac{{\rm d}\rho_{\rm e}}{{\rm d}z}\right)\right] . \tag{6.10.41}$$

This density difference leads according to Archimedes' law to a vertical buoyancy force, which equals

$$\begin{aligned} \boldsymbol{f}_{\rm buoy} &\equiv (\bar{\rho} - \rho_{\rm e}(\bar{z}))\ \boldsymbol{g} \\ &= -\left[\frac{1}{\gamma P_{\rm e}} \left(\frac{{\rm d}P_{\rm e}}{{\rm d}z}\right) - \frac{1}{\rho_{\rm e}} \left(\frac{{\rm d}\rho_{\rm e}}{{\rm d}z}\right)\right] g\rho_{\rm e}\, \xi_z\, \hat{\boldsymbol{e}}_z . \end{aligned} \tag{6.10.42}$$

If the fluid inside the bubble is lighter than the surrounding fluid at the new position, this force is in the direction opposite to the direction of gravity, and the bubble will float further upwards. If on the other hand the material in the bubble has a larger density than the surrounding fluid, the bubble will sink.

The atmosphere as a whole must satisfy the equation of hydrostatic equilibrium,

$$\frac{{\rm d}P_{\rm e}}{{\rm d}z} = -\rho_{\rm e}\, g . \tag{6.10.43}$$

Using this to eliminate g from the above expression for the buoyancy force one finds:

$$\begin{aligned} \boldsymbol{f}_{\rm buoy} &= \frac{1}{\gamma} \left(\frac{{\rm d}P_{\rm e}}{{\rm d}z}\right) \left[\frac{1}{P_{\rm e}} \left(\frac{{\rm d}P_{\rm e}}{{\rm d}z}\right) - \frac{\gamma}{\rho_{\rm e}} \left(\frac{{\rm d}\rho_{\rm e}}{{\rm d}z}\right)\right] \xi_z \hat{\boldsymbol{e}}_(z) \\ &= -\rho\, N_{\rm BV}^2\, \xi_z\, \hat{\boldsymbol{e}}_z . \end{aligned} \tag{6.10.44}$$

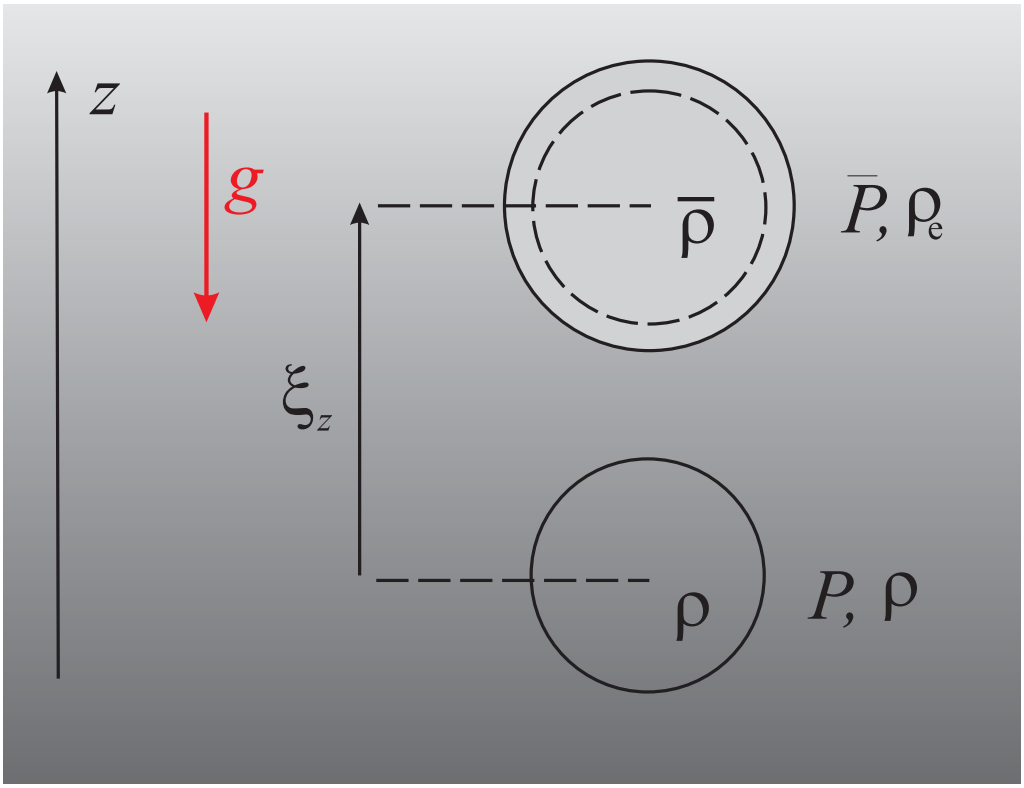

Figure 6.14: *A simple model used to demonstate the Schwarzschild criterion for convection. A small bubble rises vertically along the z-axis over a distance ξ_z. The surrounding atmosphere is stratified in the z-direction due to gravity (the red arrow). As the bubble rises it expands in order to maintain pressure equilibrium with the falling pressure in the surrounding gas. Even when the density inside the bubble is the same as in the surrounding fluid (equal to $\rho = \rho_e$) initially, this is generally no longer the case after the bubble has expanded.*

Here $N_{\rm BV}$ is the Brunt-Väisälä frequency of the external medium,

$$N_{\rm BV}^2 = -\frac{1}{\gamma\rho}\left(\frac{{\rm d}P}{{\rm d}z}\right)\left(\frac{\rm d}{{\rm d}z}\left\{\ln\left[P\rho^{-\gamma}\,\right]\right\}\right)\ . \tag{6.10.45}$$

Here I have dropped the subscript 'e'.

The equation of motion for the bubble which results as a consequence of this buoyancy force reads

$$\rho\,\frac{\partial^2\xi_z}{\partial t^2} = -\rho\,N_{\rm BV}^2\,\xi_z\ . \tag{6.10.46}$$

The solutions of this equation behave differently, depending on the sign of $N_{\rm BV}^2$:

- If $N_{\rm BV}^2 > 0$ the solution corresponds to harmonic motion, $\xi_z \propto e^{-i\omega t}$, with frequency $\omega = \pm N_{\rm BV}$. This corresponds to pure internal gravity waves.
- If $N_{\rm BV}^2 < 0$ there is a solution where the vertical displacement grows exponentially with time, $\xi_z \propto e^{\sigma t}$, with $\sigma = \sqrt{-N_{\rm BV}^2}$. This corresponds to an *instability* of the atmosphere against *convection*, where bubbles will rise spontaneously.

An atmosphere is **stable** against convection if the **Schwarzschild criterion** [20] $N_{\rm bv}^2 > 0$ is fulfilled. Since ${\rm d}P/{\rm d}z < 0$ the condition $N_{\rm BV}^2 > 0$ corresponds to

$$\frac{\rm d}{{\rm d}z}\left\{\ln\left[\frac{P}{\rho^\gamma}\,\right]\right\} = \frac{\rm d}{{\rm d}z}\left\{\ln\left[\frac{T^\gamma}{P^{\gamma-1}}\,\right]\right\} > 0\ . \tag{6.10.47}$$

Here I have used the ideal gas law $P = \rho\mathcal{R}T/\mu$ to write

$$\ln\left[P\,\rho^{-\gamma}\,\right] = \ln\left[P\,(\mu P/\mathcal{R}T)^{-\gamma}\,\right] = \ln\left[T^\gamma\,P^{-(\gamma-1)}\right] + \text{constant}\ , \tag{6.10.48}$$

assuming for simplicity that μ is constant.

[20] For a full discussion see:
R. Kippenhahn & A. Weigert, 1990, *Stellar Structure and Evolution*, Springer Verlag, Ch. 6;
R.Q. Huang & K.N. Yu, 1998, *Stellar Astrophysics*, Springer Verlag, Ch. 3.

Writing out the logarithm in (6.10.47) one finds that this corresponds to

$$\gamma \left(\frac{1}{T}\,\frac{\mathrm{d}T}{\mathrm{d}z}\right) > (\gamma - 1)\,\left(\frac{1}{P}\,\frac{\mathrm{d}P}{\mathrm{d}z}\right)\,. \tag{6.10.49}$$

Using the equation for hydrostatic equilibrium once again, $\mathrm{d}P/\mathrm{d}z = -\rho\, g < 0$, this condition becomes

$$\boxed{\left(\frac{\mathrm{d}\ln T}{\mathrm{d}\ln P}\right) < \left(\frac{\mathrm{d}\ln T}{\mathrm{d}\ln P}\right)_{\mathrm{s=constant}} = \frac{\gamma - 1}{\gamma}\,.} \tag{6.10.50}$$

One can reformulate the Schwarzschild criterion in terms of the specific entropy s of the gas. This specific entropy is given by (Eqn. 2.7.24) for an ideal polytropic gas:

$$s = c_{\mathrm{v}}\,\ln\left(P\rho^{-\gamma}\right) + \text{constant}\,. \tag{6.10.51}$$

The Brunt-Väisälä frequency can be expressed in terms of the specific entropy and the gravitational acceleration $\boldsymbol{g}$ for an atmosphere in hydrostatic equilibrium:

$$N^2_{\mathrm{BV}} = -\frac{1}{\gamma\rho\, c_{\mathrm{v}}}(\boldsymbol{\nabla}P\cdot\boldsymbol{\nabla}s) = -\frac{(\boldsymbol{g}\cdot\boldsymbol{\nabla}s)}{\gamma c_{\mathrm{v}}}\,. \tag{6.10.52}$$

Schwarzschild's criterion for stability, $N^2_{\mathrm{BV}} > 0$, shows that a plane-parallel atmosphere with gravitational acceleration $\boldsymbol{g} = -g\,\hat{\boldsymbol{e}}_z$ is stable provided

$$\boxed{g\,\frac{\mathrm{d}s}{\mathrm{d}z} > 0\,.} \tag{6.10.53}$$

The entropy of the gas must increase with height. In an atmosphere where s decreases with height, bubbles will rise spontaneously.

The figure below shows a high-resolution image of the Solar photosphere, with the pattern of *granulation* around a Sun Spot. This granulation is the top of the Solar convection zone. The small cells are colums of rising, hot material that penetrates into the visible surface of the Sun, the *photosphere*. Once the hot material cools, it sinks back into the convection zone around the edges of the granular convection cells, which are darker in this image.

Figure 6.15: *A photograph of the granulation (the irregular cell-like pattern) at the top of the Solar Convection Zone. The dark spot near the middle is a* Sun Spot*, a region of strong magnetic field (fieldstrength* ~ 1000 *G) that is cooler than the surroundings. This temperature difference leads to the large brightness contrast, which makes the Sun Spot seem black, even though the material in the Sun Spot is actually quite bright.*
This photograph was taken with the Dutch Open Telescope*, a special-purpose 1-meter solar telescope that is capable of making diffraction-limited images of the Sun, with a resolution of* $\sim$ *0.1 arc-second (*~ 75 *km on the Sun).*

Chapter 7

Shocks

7.1 What are shocks, and why do they occur?

In the previous Chapter we discussed the propagation of *small-amplitude* disturbances, and showed that they take the form of linear waves. It was easy to find wave solutions by using the fluid equations in the linearized version, which neglects the non-linearities stemming from terms like $(\boldsymbol{V}\cdot\boldsymbol{\nabla})\boldsymbol{V}$ in the equation of motion. In this Chapter I will condider the opposite limit of *strong* disturbances, where the fluid properties change rapidly. In this case the *intrinsic non-linearity* of the fluid equations plays an essential role. In particular I will discuss sudden transitions: shock waves and contact discontinuities which, in the limit of an ideal fluid, are infinitesimally thin.

Shock waves occur *supersonic* flows where the flow velocity exceeds the (adiabatic) sound speed. In a shock material flows across the discontinuity surface. A different type of discontinuity is the so-called *contact discontinuity* that can occur at any flow speed. A contact discontinuity is a surface separating two fluids or gases with different physical properties. Unlike a shock, there is *no* flow of mass across a contact discontinuity[1].

The simplest illustration for the reasons that lead to the formation of shock waves is a one-dimensional,isentropic (the specific entropy s is constant so that $P\propto\rho^{\gamma}$) flows[2]. Consider the equations for a one-dimensional flow in the x-direction, with a velocity $u(x\,,\,t)$, a density $\rho(x\,,\,t)$ and a pressure $P(x\,,\,t)$. The set of equations governing such a flow will be rewritten in a form that allows the identification of invariants.

[1] We neglect for the moment the effects of the thermal motion

[2] For a full discussion of the results of this paragraph see:
F.H. Shu: *The Physics of Astrophysics, Vol. II, Gas Dynamics*, University Science Books, Mill, Valley, CA, USA, Ch. 15;
L.D. Landau & E.M. Lifshitz: *Fluid Mechanics*, Course of Theoretical Physics Vol. 6, Pergamon Press, Oxford, 1959, Chapter IX

The relevant equations can be written as

$$\begin{aligned} \frac{\partial \rho}{\partial t} + u\,\frac{\partial \rho}{\partial x} &= -\rho\left(\frac{\partial u}{\partial x}\right) ; \\ \frac{\partial u}{\partial t} + u\,\frac{\partial u}{\partial x} &= -\frac{1}{\rho}\left(\frac{\partial P}{\partial x}\right) ; \\ \frac{\partial P}{\partial t} + u\,\frac{\partial P}{\partial x} &= c_{\rm s}^2\left(\frac{\partial \rho}{\partial t} + u\,\frac{\partial \rho}{\partial x}\right) . \end{aligned} \tag{7.1.1}$$

The last equation is a simple consequence of the assumption of constant entropy,

$$P\,\rho^{-\gamma} = \text{constant}, \tag{7.1.2}$$

with the isentropic sound speed defined as before by

$$c_{\rm s}^2 = \left(\frac{\partial P}{\partial \rho}\right)_s = \frac{\gamma P}{\rho} . \tag{7.1.3}$$

By algebraic manipulation of these equations one can eliminate the density from these equations. By using the relation

$$\frac{{\rm d}\rho}{\rho} = \frac{2}{\gamma - 1}\,\frac{{\rm d}c_{\rm s}}{c_{\rm s}} , \tag{7.1.4}$$

the system reduces to a set of two partial differential equations of the form

$$\begin{aligned} \left[\frac{\partial}{\partial t} + (u + c_{\rm s})\,\frac{\partial}{\partial x}\right]\left(u + \frac{2}{\gamma - 1}\,c_{\rm s}\right) &= 0 ; \\ \left[\frac{\partial}{\partial t} + (u - c_{\rm s})\,\frac{\partial}{\partial x}\right]\left(u - \frac{2}{\gamma - 1}\,c_{\rm s}\right) &= 0 . \end{aligned} \tag{7.1.5}$$

These equations can be written in short-hand notation as

$$\mathcal{D}_+\,\mathcal{C}_+ = 0 \quad \text{and} \quad \mathcal{D}_-\,\mathcal{C}_- = 0 , \tag{7.1.6}$$

where

$$\mathcal{C}_{\pm} = u \pm \frac{2}{\gamma - 1}\, c_{\rm s} \quad , \quad \mathcal{D}_{\pm} = \frac{\partial}{\partial t} + (u \pm c_{\rm s})\, \frac{\partial}{\partial x} \, . \tag{7.1.7}$$

These two equations can be interpreted as follows: the two *characteristic variables*[3] $\mathcal{C}_+$ and $\mathcal{C}_-$ are constant on curves in the $x-t$ plane which are the two trajectories defined by the (implicit) equations

$$\left(\frac{{\rm d}x}{{\rm d}t}\right)_{\pm} = u \pm c_{\rm s} \, . \tag{7.1.8}$$

These two sets of trajectories are known as the *plus-characteristic* and *minus-characteristic*. The trajectories of the plus-characteristic can be found by tracing the path in space-time $x-t$ of a hypothetical observer, which moves with a velocity equal to the sum of the *local* flow speed and the sound speed. This is exactly the speed of sound waves propagating in the same direction as the (one-dimensional) flow. In a similar fashion, the trajectory associated with the minus-characteristic has can be found by moving at a velocity equal to the speed of sound waves propagating in the direction opposite to the flow direction. This is illustrated in the figure below. These characteristic equations are true *regardless* the amplitude of the perturbations, and not just for (weak) sound waves. They have been derived using the full (non-linear) set of fluid equations.

One can prove a number of interesting general properties with the theory of characteristics, for instance:

- At any point P in the flow, only the space-time region contained between the plus- and minus characteristic originating from that point can be influenced by the physical conditions at P;
- Conversely, at any point P in the flow, only the physical conditions in the region contained within the plus- and minus characteristics *arriving* at P can influence the conditions at P

The variation of the orinary fluid variables along the characteristics can be derived directly from the isentropic gas law $P \propto \rho^{\gamma}$ and the associated relation

$$\frac{{\rm d}P}{\rho} = c_{\rm s}^2\, \frac{{\rm d}\rho}{\rho} = \frac{2 c_{\rm s}}{\gamma - 1}\, {\rm d}c_{\rm s} \, . \tag{7.1.9}$$

[3]Usually called the **Riemann Invariants** in the context of fluid mechanics.

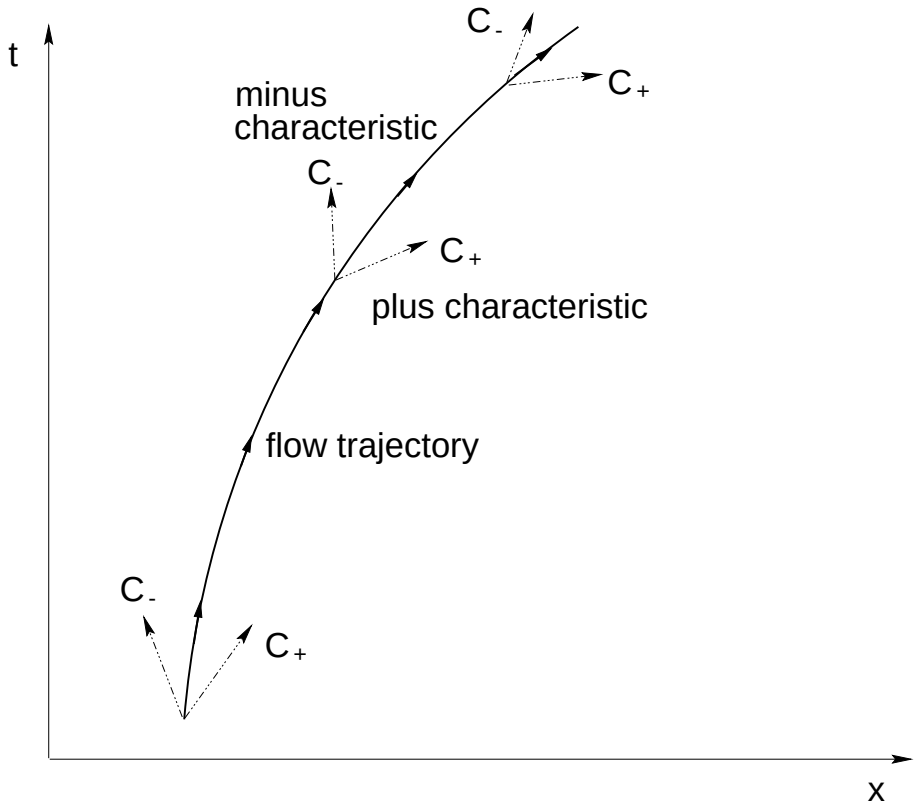

Figure 7.1: *Diagram showing the space-time flow line, defined by* $\mathrm{d}x = u\,\mathrm{d}t$*, and the two characteristics* $\mathcal{C}_+$ *and* $\mathcal{C}_-$ *defined by* $\mathrm{d}x = (u + c_\mathrm{s})\,\mathrm{d}t$ *and* $\mathrm{d}x = (u - c_\mathrm{s})\,\mathrm{d}t$*. From each point in the flow two characteristics originate along which* $\mathcal{C}_+$ *and* $\mathcal{C}_-$ *are constant respectively. Note that the value of* $\mathcal{C}_\pm$ *can be different on the different characteristics so that the characteristic variables* $\mathcal{C}_+$ *and* $\mathcal{C}_-$ *are* **not** *global constants!*

This relation allows one to write the condition that $\mathcal{C}_\pm$ remain constant along their respective characteristic trajectories as:

$$\mathrm{d}\mathcal{C}_\pm = \mathrm{d}u \pm \frac{2}{\gamma-1}\,\mathrm{d}c_\mathrm{s} = 0 \iff \mathrm{d}u \pm \frac{\mathrm{d}P}{\rho c_\mathrm{s}} = 0\ . \tag{7.1.10}$$

Here I have used Eqn. (11.4.21). This means that the two Riemann invariants $\mathcal{C}_+$ and $\mathcal{C}_-$ can also be expressed as

$$\mathcal{C}_\pm = u \pm \int \frac{\mathrm{d}P}{\rho c_\mathrm{s}}\ , \tag{7.1.11}$$

up to an arbitrary integration constant.

7.1.1 Application to sound waves

Let us apply this to a simple small-amplitude sound wave propagating along the x-axis in the positive x-direction, with a wave vector $\boldsymbol{k} = k\,\hat{\boldsymbol{e}}_x$. In absence of the wave the fluid is at rest ($u = 0$). Using the relations (6.5.6) derived in the previous Chapter, together with the sound wave frequency that follows from the dispersion relation

$$\omega = |\boldsymbol{k}| c_\mathrm{s}\ , \tag{7.1.12}$$

it is easily checked that the velocity induced by the presence of the wave equals

$$u = \delta V = \frac{\delta P}{\rho c_\mathrm{s}}\ . \tag{7.1.13}$$

Here I have used that both the wave vector $\boldsymbol{k}$ and the amplitude $\boldsymbol{a}$ of the wave are along the x-axis.

Without the wave, the Riemann invariants $\mathcal{C}_\pm$ have constant values in the uniform, stationary gas:

$$\mathcal{C}_+^0 = -\mathcal{C}_-^0 = 2c_\mathrm{s}/(\gamma-1) \equiv \mathcal{C}_0\ . \tag{7.1.14}$$

Here c_s is the sound speed in the unperturbed uniform gas. The presence of the small-amplitude sound wave changes the Riemann constants.

They now equal (compare Eqn. 7.1.10)

$$\mathcal{C}_{\pm} = \pm\mathcal{C}_0 + \delta V \pm \frac{\delta P}{\rho c_{\rm s}} \ . \tag{7.1.15}$$

It is easily seen form (7.1.13) that a forward propagating wave changes $\mathcal{C}_+$ to

$$\mathcal{C}_+ = \mathcal{C}_0 + \frac{2\delta P}{\rho c_{\rm s}} = \mathcal{C}_0 + 2c_{\rm s}\,\frac{\delta\rho}{\rho} \ . \tag{7.1.16}$$

Here I have used that $\delta P = c_{\rm s}^2\,\delta\rho$ in a sound wave. The second invariant $\mathcal{C}_-$ on the other hand remains unchanged: the term involving δV cancels the term involving δP. We conclude that the Riemann invariant with the characteristic trajectory running in the direction opposite to the propagation direction of the sound wave (the characteristic: $\mathrm{d}x = (u - c_{\rm s})\,\mathrm{d}t$) is not influenced by the wave, at least in the linear limit. Therefore $\mathcal{C}_- = -2c_{\rm s0}/(\gamma-1)$ remains a global constant in this case. The other Riemann invariant $\mathcal{C}_+$ varies sinusoidally around $\mathcal{C}_0$ due to the presence of the sound wave, and will therefore take different values on the different plus-characteristics that originate along the wave.

As the wave propagates it **must** develop non-linearities in the long run as the underlying *exact* fluid equations are non-linear. This means that the displacement vector $\boldsymbol{\xi}(\boldsymbol{x}\ ,\ t)$, $\delta\rho(\boldsymbol{x}\ ,\ t)$ and $\delta P(\boldsymbol{x}\ ,\ t)$ can no longer be described as simple sinusoidal variations in space and time. If one thinks in terms of a Fourier sum of waves with different frequencies and wavenumbers, this means that a monochromatic wave with a given frequency and wavenumber (related by the dispersion relation) will exite higher harmonics in the long run, and does not remain monochromatic.

The development of these non-linearities can be traced using the theory of characteristics. Let the density at the nodes of the wave where $\delta V \propto |\boldsymbol{a}| = 0$ be ρ_0, the unperturbed density, and the associated sound speed be equal to $c_{\rm s}(\rho_0) \equiv c_{\rm s0}$. The sound speed varies with density as

$$c_{\rm s}(\rho) = c_{\rm s0}\left(\frac{\rho}{\rho_0}\right)^{(\gamma-1)/2} \ . \tag{7.1.17}$$

The fact that $\mathcal{C}_-$ is a global constant implies that

$$\mathcal{C}_- = u - \frac{2c_{\rm s}}{\gamma-1} = -\frac{2c_{\rm s0}}{\gamma-1} \ . \tag{7.1.18}$$

Solving for the velocity u one finds that on the minus-characteristic x_- one must have:

$$u(x_-) = \frac{2c_{\rm s0}}{\gamma - 1} \left[\left(\frac{\rho(x_-)}{\rho_0} \right)^{(\gamma-1)/2} - 1 \right] \tag{7.1.19}$$

Regions with a density surplus ($\rho > \rho_0$) have $u > 0$ and $c_{\rm s} > c_{\rm s0}$, and those with a density deficit ($\rho < \rho_0$) must have $u < 0$ and $c_{\rm s} < c_{\rm s0}$. This means that the plus characteristics $\mathrm{d}x = (u + c_{\rm s})\,\mathrm{d}t$ emanating from an overdense region travel at a larger velocity than average, but those emanating from a region of density deficit are traveling slower than average, as illustrated in figure 7.2. As a result, a sinusoidal wave must steepen as it propagates (see figure 7.3): the wave crests (regions with a density surplus) catch up with the wave throughs (regions with a lower than average density) and an acoustic wave will steepen into a saw-tooth form. The plus-characteristics from overdense and underdense regions must ultimately cross, leading to an unphysical situation: there can not be two different values for the variant $\mathcal{C}_+$ at the same space-time position. The same happens to the minus-characteristics. Therefore, something drastic must happen that prevents such an unphysical situation, in this case the formation of a shock. Sound waves in the absence of dissipation will steepen into compressive shocks!

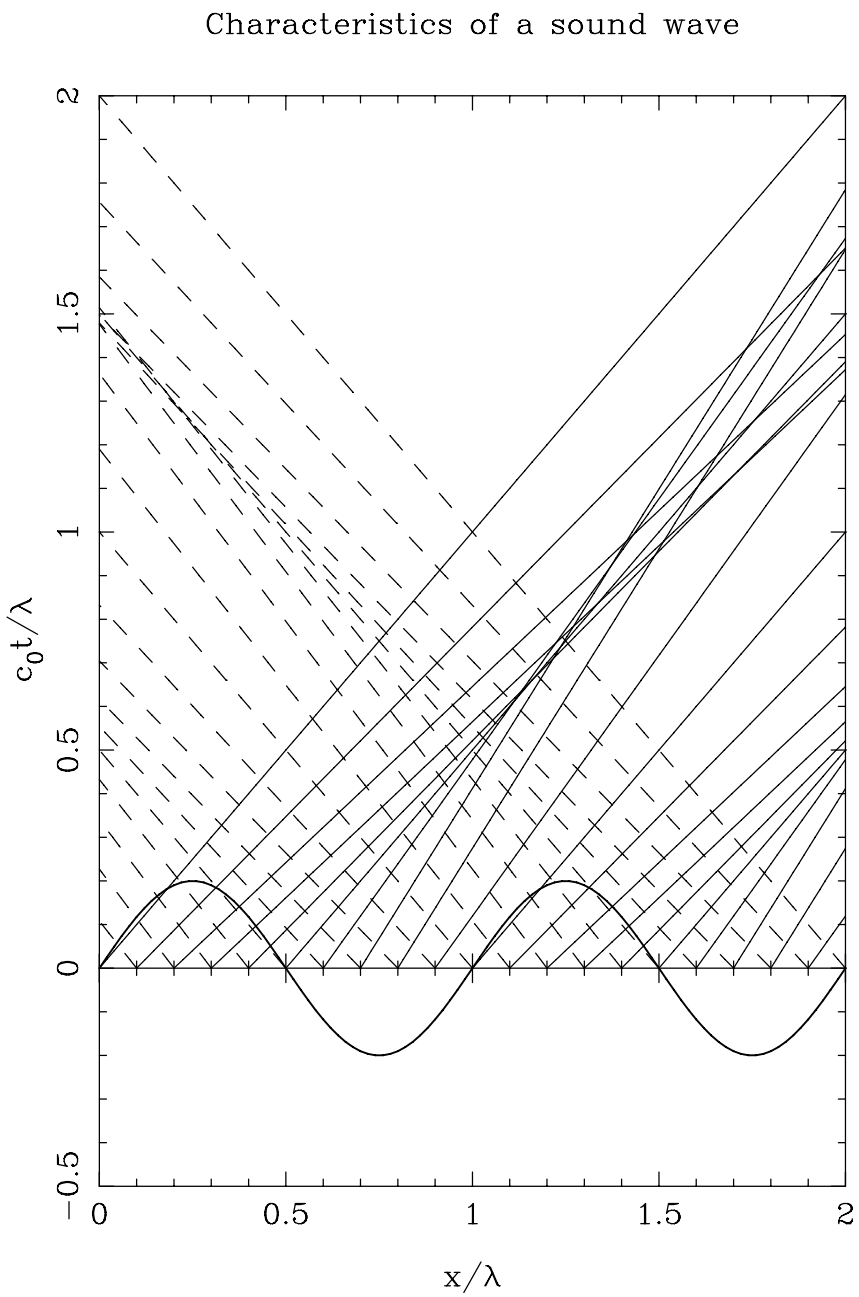

Figure 7.2: *The plus characteristics (solid lines) and minus characteristics (dashed lines) emanating from a small-amplitude sinusoidal sound wave of wavelength λ. The density amplitude of the wave is indicated (arbitrary units). The characteristics in a* **uniform** *flow with sound speed $c_{\rm s0}$ would correspond in this figure to lines at an inclination of ± 45 degrees with respect to the time axis. Note the crossing of the characteristics which signals that something drastic, i.e. the formation of shocks, is inevitable as the non-linearities build up.*

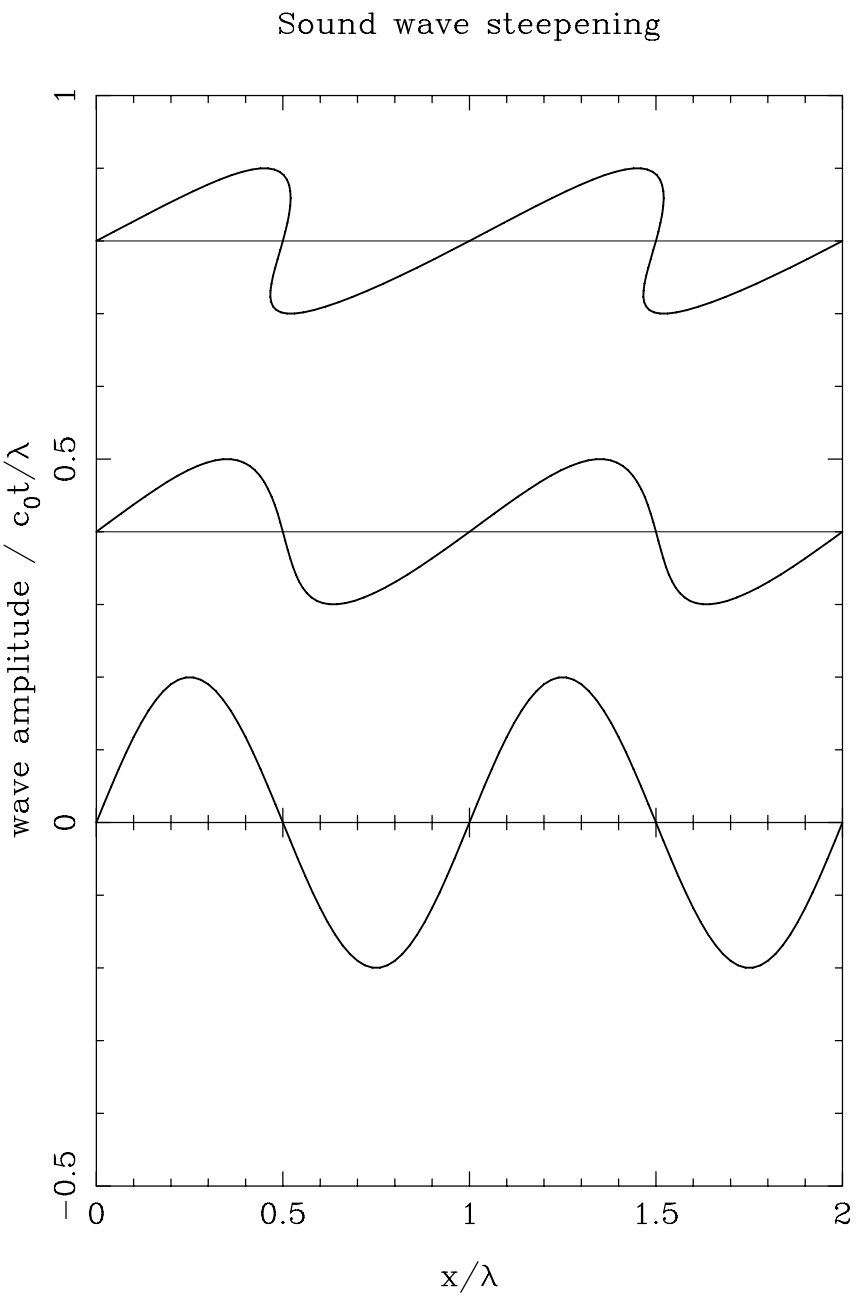

Figure 7.3: *The shape of an initially sinusoidal sound wave at* $t = 0$, $c_{\rm s0}t/\lambda = 0.4$ *and* $c_{\rm s0}t/\lambda = 0.8$. *The sound wave steepens. Before the plus-characteristics cross at* $c_{\rm s0}t/\lambda = 0.4$ *it has a saw tooth-like shape. After the crossing of the characteristics at* $c_{\rm s0}t/\lambda = 0.8$ *the shape is double-valued, and hence unphysical near the nodes at* $x/\lambda = 0.5$ *and* 1.5. *Before that, a shock will form at these nodes.*

7.2 Plane Shock waves: an introduction

Shock waves are a feature of supersonic flows with a Machnumber exceeding unity:

$$\mathcal{M}_{\rm s} = \frac{|\boldsymbol{V}|}{c_{\rm s}} > 1 \; . \tag{7.2.1}$$

They occur when a supersonic flow encounters an obstacle which forces it to change its velocity. For instance: a bowshock forms around the Earth in the tenuous Solar Wind where the ionized wind material 'hits' the strongly magnetized Earth's magnetosphere.

We have seen in Chapter 6.4 that small-amplitude sound waves in a flow propagate with a velocity

$$\boldsymbol{v}_{\rm gr} = \boldsymbol{V} + c_{\rm s}\,\hat{\boldsymbol{\kappa}} \; , \tag{7.2.2}$$

with $\hat{\boldsymbol{\kappa}} = \boldsymbol{k}/|\boldsymbol{k}|$ the direction of propagation. Sound waves act as an 'messenger': they carry density and pressure fluctuations that in some sense alert the incoming flow when an obstacle is present. For low-Machnumber flows ($\mathcal{M}_{\rm s} < 1$) waves can propagate against the flow, getting ahead of the obstacle.

However, in a supersonic flow with $\mathcal{M}_{\rm s} > 1$ the *net* velocity of the waves given by (7.2.2) is *always* directed downstream, and no waves can reach the flow upstream from the obstacle. In this situation a shock forms. In the shock, there is a sudden transition where the density, pressure and temperature of the flow increases. *Behind* the shock the temperature is so high that the component of the flow normal to the shock becomes *subsonic*. In that post-shock region, sound waves are once again able to communicate the presence of an obstacle to the flow so that pressure forces can deflect the flow, steering it around the obstacle. The figure below gives the Earth's bow shock as an example.

7.3 A simple mechanical model: the marble-tube

As a simple mechanical model for shock formation, consider the figure below. In a hollow (semi-infinite) tube, spherical marbles with a diameter D, separated by a distance $L > D$ roll with velocity V. The end of the tube is plugged, forming an obstacle that prevents the marbles from continuing onward. As a result, the marbles collide, loose their velocity and accumulate in a stack at the plugged end of the tube. Far ahead of the obstacle, where the marbles still move freely, the line-density of marbles (the number of marbles per unit length) equals $n_1 = 1/L$. The density in the stack equals $n_2 = 1/D > n_1$. The density of the marbles increases when they are added to the stack.

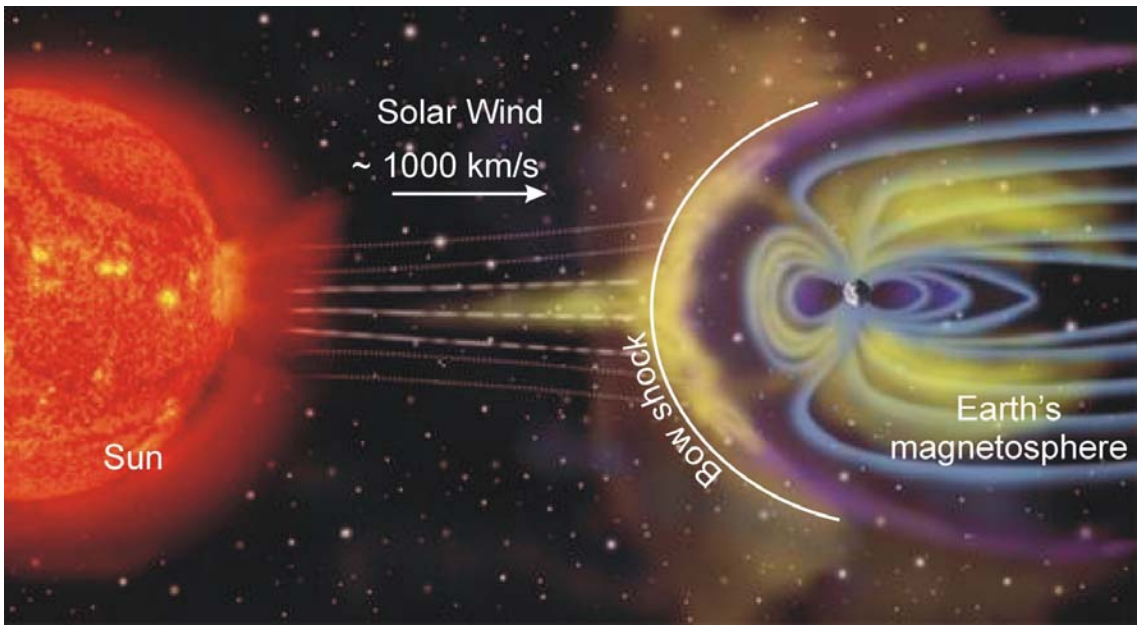

Figure 7.4: *When the Solar Wind impacts the Earth's magnetosphere, the 'sphere of influence' of the Earth's magnetic field, it forms a bow shock. In this bow shock, the incoming Solar Wind material is decelerated, compressed and heated. The properties of the Earth's bow shock can be studied using satellites*

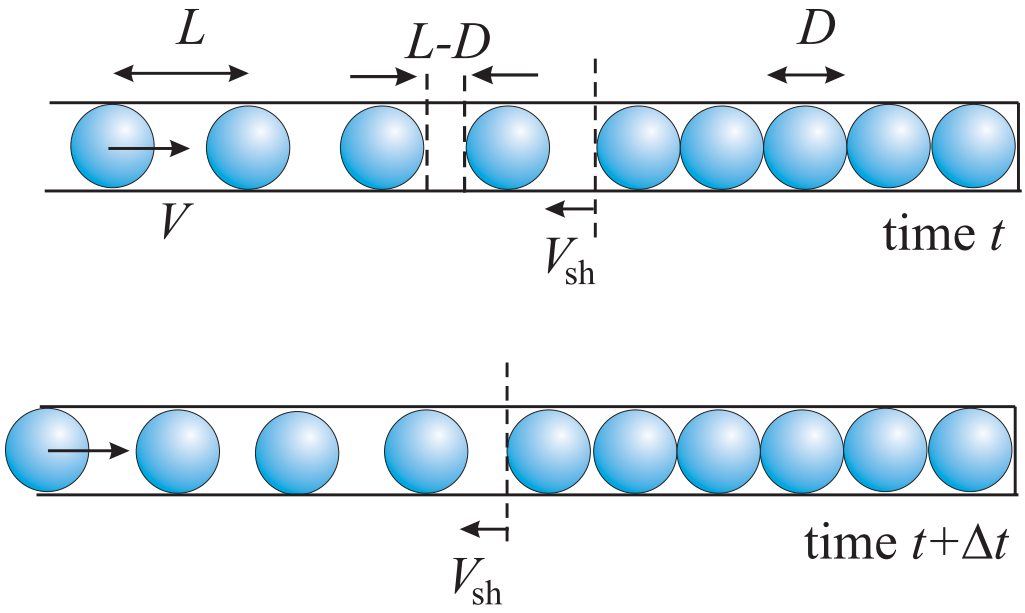

Figure 7.5: *The marble tube as a simple model of shock formation. Marbles collide at the plugged end of the tube, forming a stack that grows as time progresses. The transition between freely moving marbles, and the stationary marbles in the stack, is the analogue of a shock surface. Like a real shock, it marks the transition between a low marble density upstream, and a higher marble density downstream of the transition.*

The growth of the stack is calculated easily. In order to collide, two adjacent marbles have to close the separation distance $\Delta D = L - D$ between their surfaces. The time between two collisions at the front of the stack is therefore

$$\Delta t_{\rm coll} = \frac{L-D}{V} \ . \tag{7.3.1}$$

At every collison, one marble is added to the stack, and the length of the stack increases by D. Therefore, the *average* velocity with which the length of the stack increases equals

$$V_{\rm sh} = -\frac{D}{\Delta t_{\rm coll}} = -V\ \left(\frac{D}{L-D}\right) \ . \tag{7.3.2}$$

Note that this velocity is *negative*: the minus-sign is introduced because this velocity is directed towards the left. This relation defines the 'shock velocity' in this simple model. The imaginary surface at the front end of the stack, the surface that separates a region of low marble density[4] ($n_1 = 1/L$) from the high-density region ($n_2 = 1/D$) in the stack, is the analogue of a hydrodynamical shock.

Let us now transform to a reference frame where the 'shock' is stationary. We neglect the fact that the stack grows impulsively each time a marble is added. In this reference frame, the shock frame, the incoming marbles have a velocity

$$V_1 = V - V_{\rm sh} = V\ \left(1 + \frac{D}{L-D}\right) = V\ \left(\frac{L}{L-D}\right) \ . \tag{7.3.3}$$

The marbles in the stack, which are stationary in the laboratory frame, move away with speed

$$V_2 = -V_{\rm sh} = V\ \left(\frac{D}{L-D}\right) \tag{7.3.4}$$

in the shock frame.

In *any* frame, the *flux* $\mathcal{F}$ of marbles is their line-density $\times$ their velocity. In the shock frame the flux of incoming marbles with density $n_1 = 1/L$ equals:

$$\mathcal{F}_1 = n_1 V_1 = \frac{V}{L-D} \ . \tag{7.3.5}$$

[4]The density is here a *line density*: the number of marbles per unit length¿

The flux of the marbles in the stack with density $n_2 = 1/D$ equals in the shock frame:

$$\mathcal{F}_2 = n_2 V_2 = \frac{V}{L - D} \ . \tag{7.3.6}$$

Comparing this with (7.3.5) one sees that these two fluxes are equal:

$$\mathcal{F}_1 = \mathcal{F}_2 \ . \tag{7.3.7}$$

This equality has a simple interpretation. The number of marbles crossing the shock surface in a time Δt equals $\Delta N = \mathcal{F} \Delta t$. Since an infinitely thin surface can not contain any marbles, as it has no volume, the number of marbles entering the surface at the front must exactly equal the number that leaves in the back:

$$\Delta N_{\rm in} = \mathcal{F}_1 \ \Delta t = \Delta N_{\rm out} = \mathcal{F}_2 \ \Delta t \ . \tag{7.3.8}$$

Equality (7.3.7) follows immediately. As we will see below, many of the concepts introduced here can be immediately transplanted to the physics of shocks in a gas. In particular we will find that the flux of mass, momentum and energy satisfy relations equivalent to (7.3.7): what enters the shock surface in the front must come out in the back.

7.4 Shock waves in a simple fluid

I will consider a simple fluid with density ρ, pressure P and which satisfies the polytropic relation

$$P = \text{constant} \times \rho^{\gamma} \tag{7.4.1}$$

on either side of the shock, but *not* with the same constant on both sides as a result of dissipation (entropy increase) in the shock. I will assume that the shock is planar, located in a fixed position the $y-z$ plane. The flow is from left-to-right so that the pre-shock flow occurs for $x < 0$, and the post-shock flow for $x > 0$ (see figure 7.6). The direction normal to the shock coincides with the direction of the x-axis. The shock-normal, a unit vector pointing into the upstream flow, will be indicated by $\hat{\boldsymbol{n}}_{\rm s}$. In this case $\hat{\boldsymbol{n}}_{\rm s} = -\hat{\boldsymbol{e}}_x$. I will use the subscripts 1 (2) to indicate the values of quantities ahead of (behind) the shock.

The assumption of a *planar* shock in the $x-z$ plane can be realized if the flow properties, such as velocity, density and pressure, depend only on the $x-$coordinate: $\partial/\partial y = \partial/\partial z = 0$. I will also assume that the velocity vector lies in the $x-z$ plane:

$$\boldsymbol{V} = V_{\rm n}\,\hat{\boldsymbol{e}}_x + V_{\rm t}\,\hat{\boldsymbol{e}}_z\,. \tag{7.4.2}$$

Here I have written $V_{\rm n}$ rather than V_x, and $V_{\rm t}$ rather than V_z, in order to stress that these two velocity components are the components of the velocity normal to the shock surface and tangential to the shock surface respectively.

Neglecting the effects of gravity and dissipation in the flow on either side of the shock, the equations describing the fluid are mass conservation, momentum conservation in the x and z-direction and conservation of energy. The set of fluid equations in conservative form (see Chapter 3) in this case reduce to:

$$\begin{aligned}
\frac{\partial \rho}{\partial t} + \frac{\partial (\rho V_{\rm n})}{\partial x} &= 0 \\
\frac{\partial (\rho V_{\rm n})}{\partial t} + \frac{\partial}{\partial x}\left[\rho\, V_{\rm n}^2 + P\right] &= 0 \\
\frac{\partial (\rho V_{\rm t})}{\partial t} + \frac{\partial}{\partial x}\left[\rho\, V_{\rm n}\, V_{\rm t}\right] &= 0 \\
\frac{\partial}{\partial t}\left[\rho\left(\frac{V^2}{2} + e\right)\right] + \frac{\partial}{\partial x}\left[\rho V_{\rm n}\left(\frac{V^2}{2} + h\right)\right] &= 0\,.
\end{aligned} \tag{7.4.3}$$

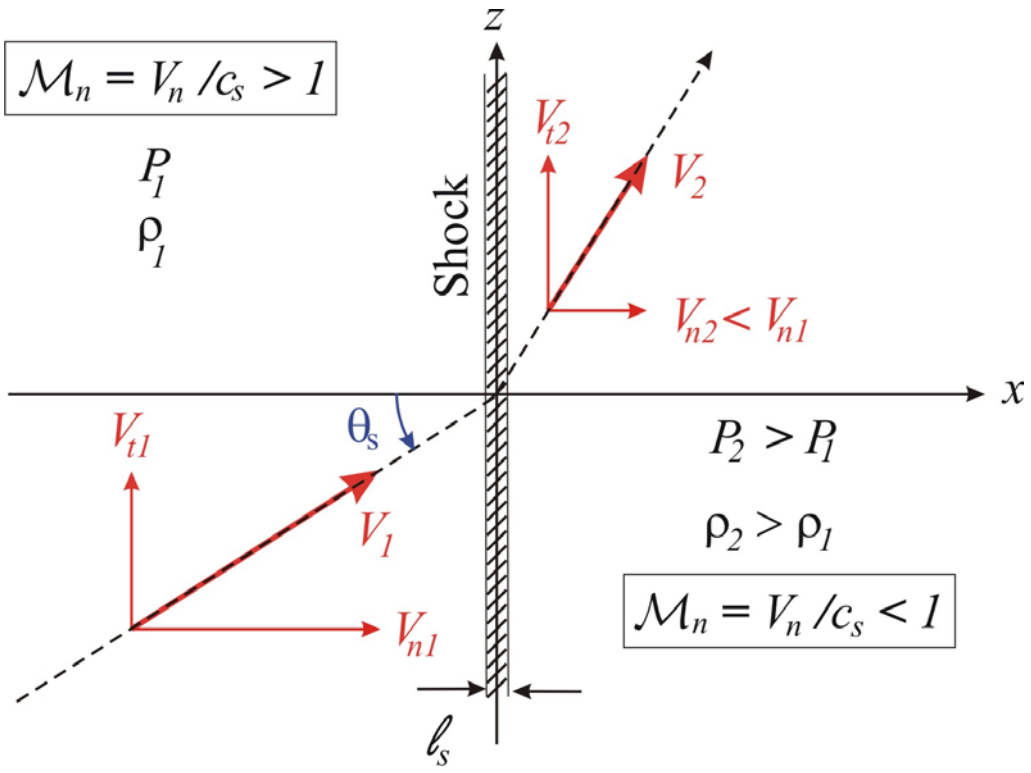

Figure 7.6: *The geometry of the flow at a planar, oblique shock. The shock is a thin transition region in the $x-z$ plane, separating the high-velocity (supersonic) incoming flow ($x<0$) from the shocked outgoing flow ($x>0$). Pre-shock quantities such as density and pressure are labeled with a subscript 1, and post-shock quantities with a subscript 2. The incoming flow has a velocity V_1 at an inclination angle $\theta_{\rm s}$ with respect to the direction normal to the shock surface (the x-axis). In a* normal shock *one has $\theta_{\rm s}=0$.*
The thickness of the shock layer equals $\ell_{\rm s}$. In this Chapter, we we will take the limit of vanishing shock thickness ($\ell_{\rm s}\to 0$) in our calculations, treating the shock as a sudden jump in velocity, density and pressure.
In the shock the flow component normal to the shock is decelerated, so that $V_{\rm n2}<V_{\rm n1}$. The tangential velocity component is unchanged: $V_{\rm t2}=V_{\rm t1}$. The normal Mach number of the flow changes from supersonic ($\mathcal{M}_{\rm n}=V_{\rm n}/c_{\rm s}>1$) ahead of the shock to subsonic ($\mathcal{M}_{\rm n}=V_{\rm n}/c_{\rm s}<1$) behind the shock.

The quantities e and h are the internal energy per unit mass and the enthalpy per unit mass which for a polytropic fluid are given by the usual relations,

$$e = \frac{P}{(\gamma - 1)\,\rho} \quad , \quad h = \frac{\gamma\,P}{(\gamma - 1)\,\rho}\,, \tag{7.4.4}$$

and

$$V^2 = V_{\rm n}^2 + V_{\rm t}^2\ . \tag{7.4.5}$$

All these equations have the same form:

$$\frac{\partial \mathcal{Q}}{\partial t} + \frac{\partial \mathcal{F}}{\partial x} = 0\,. \tag{7.4.6}$$

Here $\mathcal{Q}$ is some quantity like mass density, momentum density or energy density, and $\mathcal{F}$ the flux of that quantity in the $x-$direction. Let us assume that the shock has a thickness $\ell_{\rm s}$ around $x = 0$, so that it extends in the range $-\frac{1}{2}\,\ell_{\rm s} \le x \le \frac{1}{2}\,\ell_{\rm s}$. One can integrate across the shock, from $x = -\ell_{\rm s}/2$ to $x = +\ell_{\rm s}/2$. The integrated version of (7.4.6) reads:

$$\mathcal{F}_2 - \mathcal{F}_1 \equiv \Delta\mathcal{F} = -\frac{\partial}{\partial t}\left(\int_{-\ell_{\rm s}/2}^{+\ell_{\rm s}/2} {\rm d}x\ \mathcal{Q}(x,t)\right)\ . \tag{7.4.7}$$

Here $\mathcal{F}_1 \equiv \mathcal{F}(-\ell_{\rm s}/2)$ and $\mathcal{F}_2 = \mathcal{F}(+\ell_{\rm s}/2)$ are the pre- and post-shock values of the flux. If the shock thickness $\ell_{\rm s}$ is small, and if the quantity $\mathcal{Q}$ changes from an upstream value $\mathcal{Q}_1$ in front of the shock to a downstream value $\mathcal{Q}_2$ behind the shock, one can estimate the integral in (7.4.7) using the mean value of $\partial\mathcal{Q}/\partial t$:

$$-\Delta\mathcal{F} = \int_{-\ell_{\rm s}/2}^{+\ell_{\rm s}/2} {\rm d}x\ \frac{\partial \mathcal{Q}(x,t)}{\partial t} \approx \frac{\ell_{\rm s}}{2}\ \left[\frac{\partial \mathcal{Q}_2}{\partial t} + \frac{\partial \mathcal{Q}_1}{\partial t}\right]\ . \tag{7.4.8}$$

If one now assumes that the shock is infinitely thin, in effect taking the limit $\ell_{\rm s} \to 0$, the integral becomes vanishingly small, $\Delta\mathcal{F} = 0$. In that case the shock is a *discontinuity surface* where the fluid properties change abruptly. Integral relation (7.4.7) in that case reduces to the conservation of flux across the shock:

$$\mathcal{F}_2 = \mathcal{F}_1\,. \tag{7.4.9}$$

This expresses the simple fact that one can not store anything in a infinitely thin surface: there is no volume to store it in. Therefore, the principle 'flux in = flux out' must hold. Exactly the same condition was derived in the marble tube analogy for shock formation treated in the preceding Section.

Let us apply this result to the set of equations (7.4.3), which are the conservation laws for the different fluxes in the problem: the mass flux, the momentum flux that has two components, and the energy flux. For each of these four fluxes condition (7.4.9) holds. As we will see, these flux conservation laws give us the information needed to calculate the state of the gas behind the shock, given its state just ahead of the shock.

Together, the set of four equations (7.4.3) gives the following four flux conservation laws across an infinitely thin shock, the so-called **Rankine-Hugoniot jump conditions**:

$$\begin{aligned} \rho_1 V_{\rm n1} &= \rho_2 V_{\rm n2} \equiv J \\ \left[\rho\, V_{\rm n}^2 + P\right]_1 &= \left[\rho\, V_{\rm n}^2 + P\right]_2 \\ \left[\rho V_{\rm n} V_{\rm t}\right]_1 &= \left[\rho V_{\rm n} V_{\rm t}\right]_2 \\ \rho_1 V_{\rm n1} \left[\frac{V^2}{2} + h\right]_1 &= \rho_2 V_{\rm n2} \left[\frac{V^2}{2} + h\right]_2 \end{aligned} \qquad (7.4.10)$$

The first equation states that the mass flux across the shock, $J = \rho V_{\rm n}$, is constant: you can not 'store' mass in an infinitely thin surface. Since the flow is compressed in the flow (see below, or consider the marble tube analogy) one has $\rho_2 \geq \rho_1$ and

$$V_{\rm n2} = \left(\frac{\rho_1}{\rho_2}\right) V_{\rm n1} \leq V_{\rm n1}\ . \qquad (7.4.11)$$

The second equation is the conservation of the $x-$component of the momentum flux. The third equation is the conservation of $y-$momentum flux. Because the mass flux $J = \rho V_{\rm n}$ does not change across the shock, the conservation of the flux of y-momentum reduces to:

$$V_{\rm t1} = V_{\rm t2}\ , \qquad (7.4.12)$$

provided of course that $J \neq 0$. The component of velocity along the shock surface remains *unchanged*. There is a simple physical reason for this result: by transforming to a frame that moves with velocity $V_{\rm t1}$ along the z-axis towards positive z, you can transform away the perpendicular component of the velocity in the incoming flow. The shock now is a *normal shock*, with the pre-shock flow velocity along the shock normal. (In the laboratory frame, in which we performed the original calculations, the shock is an *oblique shock* provided of course that $V_{\rm t} \neq 0$.) Momentum flux conservation in the new frame of reference then tells you that the post-shock flow must *also* be in the direction normal to the shock, i.e. along the x-axis.

The conclusion of this line of reasoning is as follows: every oblique shock can be tranformed into a normal shock by choosing a new reference frame, and *vice versa* every normal shock can be transformed into an oblique shock. This implies that relation (7.4.12) must be valid.

The two relations (7.4.11) and (7.4.12) together imply that the shock refracts the flow away from the shock normal, see Figure (7.6). The angle between the velocity vector and the normal direction increases as the flow crosses the shock.

The fourth equation gives the conservation of the energy flux across the shock: Since $\rho\, V_{\rm n} = J$ does not change across the shock, this condition is equivalent with

$$\left[\frac{V^2}{2} + h\right]_1 = \left[\frac{V^2}{2} + h\right]_2 . \tag{7.4.13}$$

This is essentially Bernouilli's law applied to a shock. Because of relation (7.4.12) we have $V_{\rm t1}^2 = V_{\rm t2}^2$, and the above relation can also be written in a form involving only $V_{\rm n}$, the normal component of the flow velocity:

$$\left[\frac{V_{\rm n}^2}{2} + h\right]_1 = \left[\frac{V_{\rm n}^2}{2} + h\right]_2 . \tag{7.4.14}$$

This form of the energy conservation law is once again the result of the fact that one can transform away the tangential velocity component $V_{\rm t}$, simply by moving along the shock surface with velocity $V_{\rm t}$. , This procedure leaves $V_{\rm n}$ unchanged but eliminates $V_{\rm t}$ from the equations. In the new reference frame, the kinetic energy per unit mass of the flow is $V_{\rm n}^2/2$.

The conservation of the $x-$momentum flux and the energy conservation law can be written in an alternative form, using as a new variable the *specific volume*, defined as $\mathcal{V} = 1/\rho$. This is the volume that contains 1 gram of gas.

The specific volume takes the following values on the upstream and downstream side of the shock:

$$\mathcal{V}_1 = \frac{1}{\rho_1} \quad , \quad \mathcal{V}_2 = \frac{1}{\rho_2} \, . \tag{7.4.15}$$

The conservation of $x-$momentum can be expressed in terms of $\mathcal{V}$ as

$$P_1 + J^2 \, \mathcal{V}_1 = P_2 + J^2 \, \mathcal{V}_2 \, . \tag{7.4.16}$$

In a similar fashion, the energy conservation law becomes

$$h_1 + \frac{1}{2} \, J^2 \, \mathcal{V}_1^2 = h_2 + \frac{1}{2} \, J^2 \, \mathcal{V}_2^2 \, . \tag{7.4.17}$$

The first equation yields

$$J^2 = \frac{P_2 - P_1}{\mathcal{V}_1 - \mathcal{V}_2} \, . \tag{7.4.18}$$

Expressing the specific enthalpy of an ideal gas in terms of $\mathcal{V}$,

$$h = \frac{\gamma \, P}{(\gamma - 1) \, \rho} = \frac{\gamma}{\gamma - 1} \, P \, \mathcal{V} \, , \tag{7.4.19}$$

one can write the energy flux conservation law as

$$J^2 \left(\mathcal{V}_1^2 - \mathcal{V}_2^2 \right) = \frac{2\gamma}{\gamma - 1} \, \left(P_2 \, \mathcal{V}_2 - P_1 \, \mathcal{V}_1 \right) \, . \tag{7.4.20}$$

Eliminating J^2 from this equation using (7.4.18) one finds the so-called *shock adiabat*:

$$\boxed{\frac{\gamma}{\gamma - 1} \, \left(P_2 \, \mathcal{V}_2 - P_1 \, \mathcal{V}_1 \right) = \frac{1}{2} \, \left(\mathcal{V}_2 + \mathcal{V}_1 \right) \left(P_2 - P_1 \right) \, .} \tag{7.4.21}$$

One defines the *shock compression ratio* r as the density ratio across the shock:

$$r \equiv \frac{\rho_2}{\rho_1} = \frac{\mathcal{V}_1}{\mathcal{V}_2} \,. \tag{7.4.22}$$

Because of $J = \rho V_{\rm n} =$ constant, one also has:

$$r = \frac{V_{\rm n1}}{V_{\rm n2}} \,. \tag{7.4.23}$$

Substituting $\mathcal{V}_1 = r\,\mathcal{V}_2$ in (7.4.21), and solving for the compression ratio, one finds the following relation:

$$r = \frac{\rho_2}{\rho_1} = \frac{\dfrac{\gamma+1}{\gamma-1}\,P_2 + P_1}{\dfrac{\gamma+1}{\gamma-1}\,P_1 + P_2} \,. \tag{7.4.24}$$

The condition $\rho_2 > \rho_1$ implies that $P_2 > P_1$. Let us examine this relation in two important limits. In very weak shocks the fluid properties change only slightly across the shock. One can write

$$P_2 \approx P_1 + \Delta P \quad , \quad \rho_2 = \rho_1 + \Delta\rho \,, \tag{7.4.25}$$

where the pressure jump ΔP and density jump $\Delta\rho$ are small in the sense that $\Delta P \ll P_1$ and $\Delta\rho \ll \rho_1$. Substituting these relations into (7.4.24), and expanding the resulting equation to first order in ΔP and $\Delta\rho$, yields the following relation between the density jump and the pressure jump:

$$\Delta P = \left(\frac{\gamma P}{\rho}\right)_1 \Delta\rho = c_{\rm s1}^2\;\Delta\rho \,. \tag{7.4.26}$$

This relation between the pressure- and density jump is exactly the same as the one found in (small-amplitude) sound waves. For adiabatic sound waves in a gas where the pressure satisfies $P \propto \rho^\gamma$ one has

$$\Delta P = \frac{\partial P}{\partial \rho}\,\Delta\rho = c_{\rm s}^2 \Delta\rho \,. \tag{7.4.27}$$

Therefore *weak* shocks (so that $V_{\rm n1} \gtrsim c_{\rm s}$) can be considered for all intents and purposes as *strong* sound waves.

For very strong shocks on the other hand one expects a large pressure increase across the shock so that $P_2 \gg P_1$. In that case (7.4.24) yields an asymptotic value for the compression across the shock:

$$r \approx \frac{\gamma+1}{\gamma-1} \equiv r_{\rm max} \quad \text{(strong shock)}. \tag{7.4.28}$$

This is the maximum possible compression rate of a shock in an ideal (polytropic) gas. For an ideal mono-atomic gas one has $\gamma = 5/3$, and $r_{\rm max} = 4$.

7.4.1 The Rankine-Hugoniot Relations

One can parametrize the strength of the shock by introducing the *normal Mach number* $\mathcal{M}_{\rm n}$, which is defined for $V_{\rm n} > 0$ as

$$\mathcal{M}_n = \left(\frac{V_{\rm n}}{c_{\rm s}}\right)_1 \ . \tag{7.4.29}$$

It is the ratio of the upstream component of the flow speed along the shock normal, and the sound speed in front of the shock. Defining the inclination angle $\theta_{\rm s}$ of the incoming flow with respect to the direction of the shock normal by

$$V_{\rm n1} = V_1 \ \cos\theta_{\rm s} \ \ , \ \ V_{\rm t1} = V_1 \ \sin\theta_{\rm s} \ , \tag{7.4.30}$$

one can write the normal Mach number in terms of $\mathcal{M}_{\rm s} = V_1/c_{\rm s}$ as

$$\mathcal{M}_{\rm n} = \mathcal{M}_{\rm s} \ \cos\theta_{\rm s} \ . \tag{7.4.31}$$

One can express the compression ratio r and the pressure ratio P_2/P_1 across the shock in terms $\mathcal{M}_{\rm n}$. The resulting expresions are the so-called *Rankine-Hugoniot relations*[5]:

$$\begin{aligned} r = \frac{\rho_2}{\rho_1} &= \frac{(\gamma+1)\,\mathcal{M}_{\rm n}^2}{(\gamma-1)\,\mathcal{M}_{\rm n}^2+2}\,, \\ \frac{P_2}{P_1} &= 1+\frac{2\gamma}{\gamma+1}\,\left(\mathcal{M}_{\rm n}^2-1\right)\,. \end{aligned} \tag{7.4.32}$$

Shocks only exist for $\mathcal{M}_{\rm n} > 1$. If one puts $\mathcal{M}_{\rm n} = 1$, one finds $r = 1$ and $P_2/P_1 = 1$. In such a *infinitesimally weak* shock the flow crosses the shock surface *unchanged*: the density, pressure and velocity in the post-shock flow are equal the density, pressure and velocity in the pre-shock flow. In the limit of a *strong shock* with $\mathcal{M}_{\rm n} \to \infty$ one finds $r \to (\gamma+1)/(\gamma-1)$, and the pressure and temperature increase without bound. For instance: $P_2 \approx 2\gamma\mathcal{M}_{\rm n}^2/(\gamma+1) \to \infty$ as $\mathcal{M}_{\rm n} \to \infty$.

[5] e.g. , L.D. Landau & E.M. Lifshitz: *Fluid Mechanics*, Course of Theoretical Physics Vol. 6, Pergamon Press, Oxford, 1959, §85

7.5 The limit of a strong shock

In many astrophysical applications the normal Mach number is large, $\mathcal{M}_{\rm n} \gg 1$. In this *strong shock limit* the Rankine-Hugoniot jump conditions simplify considerably:

$$\begin{aligned} \frac{\rho_2}{\rho_1} &= \frac{V_{\rm n1}}{V_{\rm n2}} \approx \frac{\gamma+1}{\gamma-1} \; ; \\ \frac{P_2}{P_1} &\approx \frac{2\gamma}{\gamma+1}\,\mathcal{M}_{\rm n}^2 \; . \end{aligned} \tag{7.5.33}$$

Using the definitions (7.4.29) and (7.4.31), one finds that the post-shock pressure can be written as

$$P_2 \approx \frac{2\rho_1 V_{\rm n1}^2}{\gamma+1} = \frac{2\rho_1 V_1^2 \cos^2\theta_{\rm s}}{\gamma+1} \; . \tag{7.5.34}$$

The post-shock temperature follows from the ideal gas law, $P = \rho\mathcal{R}T/\mu$, as:

$$T_2 = \frac{\mu P_2}{\rho_2 \mathcal{R}} = \left(\frac{2\mu(\gamma-1)}{(\gamma+1)^2\mathcal{R}}\right)\,\rho_1 V_1^2 \cos^2\theta_{\rm s} \; . \tag{7.5.35}$$

The sound speed in the shocked gas follows from

$$c_{\rm s2} = \sqrt{\frac{\gamma\mathcal{R}T_2}{\mu}} \approx \left(\frac{2\gamma(\gamma-1)}{(\gamma+1)^2}\right)^{1/2}\,V_1\cos\theta_{\rm s} \; . \tag{7.5.36}$$

From this it is obvious that, as an order of magnitude, one has $P_2 \sim \rho_1 V_{\rm n1}^2$ and $c_{\rm s2} \sim V_{\rm n1} = V_1\,\cos\theta_{\rm s}$. For instance: in an ideal gas with $\gamma = 5/3$ one has $P_2 = 3\rho_1 V_{\rm n1}^2/4$ and $c_{\rm s2} \approx 0.56 V_{\rm n1}$.

These (approximate) relations will be used extensively below, when we consider the physics of Supernova Remnants and Stellar Wind Bubbles that are expanding into the Interstellar Medium.

In the Box below, I will derive these relations directly from the jump conditions for the case of a normal shock.

The infinitely strong normal shock

The algebra that is involved in the solution of the general jump conditions across a shock in an ideal fluid is rather involved. There is one case, however, where the jump conditions can be solved rather simply: the *infinitely strong, normal shock.* This is the case with a vanishing pre-shock pressure, $P_1 = 0$, and with $\mathcal{M}_{\rm s} = \mathcal{M}_{\rm n} = \infty$. The jump conditions (7.4.10) reduce to the following, much simpler set of algebraic relations:

$$\begin{aligned} \rho_1 V_1 &= \rho_2 V_2 \equiv J \ ; \\ \rho_1 V_1^2 &= \rho_2 V_2^2 + P_2 \ ; \\ \tfrac{1}{2} V_1^2 &= \tfrac{1}{2} V_2^2 + \frac{\gamma P_2}{(\gamma - 1)\, \rho_2} \ . \end{aligned} \tag{7.5.37}$$

In the above set of equations I have written simply V_1 and V_2 for the pre- and post-shock flow speeds. Note that we can **not** assume that the post-shock pressure vanishes: if we put $P_2 = 0$ the only solution of this set of relations is the trivial solution: $V_1 = V_2$. There is no shock in the trivial case.

Combining the first two of these relations immediately yields:

$$V_1 - V_2 = \frac{P_2}{J} = \frac{P_2}{\rho_1 V_1} \ . \tag{7.5.38}$$

The last of the three relations of (7.5.37) can be written as

$$V_1^2 - V_2^2 = \frac{2\gamma}{\gamma - 1} \, \frac{P_2 V_2}{J} \ . \tag{7.5.39}$$

Using $V_1^2 - V_2^2 = (V_1 + V_2)(V_1 - V_2)$ and substituting for $V_1 - V_2$ from (7.5.38), this last equation can be written as:

$$\frac{P_2}{J} \ (V_1 + V_2) = \frac{2\gamma \, P_2 V_2}{(\gamma - 1)\, J} \ . \tag{7.5.40}$$

The common factor P_2/J cancels, and the resulting linear equation is easily solved for V_2 in terms of V_1:

$$V_2 = \frac{\gamma - 1}{\gamma + 1}\, V_1 \ . \tag{7.5.41}$$

Substituting this result into (7.5.38) yields the post-shock pressure:

$$P_2 = \rho_1 V_1 \ (V_1 - V_2) = \frac{2}{\gamma + 1}\, \rho_1 V_1^2 \ . \tag{7.5.42}$$

Finally, the continuity of the mass flux, $J = \rho V =$ constant, gives the post-shock mass density:

$$\rho_2 = \left(\frac{V_1}{V_2}\right)\ \rho_1 = \frac{\gamma + 1}{\gamma - 1}\, \rho_1 \ . \tag{7.5.43}$$

This relatively straightforward calculation reproduces the strong-shock jump conditions that follow from the general Rankine-Hugoniot relations in the limit $\mathcal{M}_{\rm n} \to \infty$.

The case of an *oblique* infinitely strong shock with normal velocity $V_{\rm n}$ and tangential velocity $V_{\rm t}$ is easily obtained by making the replacements $V_1 \longrightarrow V_{\rm n1}$, $V_2 \longrightarrow V_{\rm n2}$ in the above expressions, and by adding the jump condition for the tangential velocity component:

$$V_{\rm t2} = V_{\rm t1} \ , \tag{7.5.44}$$

which is valid for *any* hydrodynamical shock for the reasons explained above.

7.6 Dissipation in a shock and the entropy jump

In an ideal polytropic gas the specific entropy (entropy per unit mass) is defined as

$$s = c_v \, \ln\left(P\rho^{-\gamma}\right) . \tag{7.6.1}$$

Since we neglected dissipation in the derivation of our equations, the specific entropy in the flow on either side of the fluid is constant:

$$s(x<0) = \text{constant} \equiv s_1 \quad , \quad s(x>0) = \text{constant} \equiv s_2 \, . \tag{7.6.2}$$

However, from the Rankine-Hugoniot relations (7.4.32) one can calculate s_2, given the upstream state of the gas (including s_1). If one does so one sees immediately that the $s_2 \geq s_1$ *provided* that $\rho_2 > \rho_1$ and (consequently) $P_2 > P_1$ and $V_2 < V_1$. Until now we have assumed that this is indeed the case, with the marble tube analogy as justification. The jump in the specific entropy across the shock is

$$\Delta s \equiv s_2 - s_1 = c_v \, \ln\left[\left(\frac{P_2}{P_1}\right)\left(\frac{\rho_1}{\rho_2}\right)^{\gamma}\right] \geq 0 \, . \tag{7.6.3}$$

One has $\Delta s = 0$ in an infinitely weak shock with $\rho_2 = \rho_1$ and $P_2 = P_1$.

In general, the entropy per particle will *increase* across the shock, a sure sign of some form of dissipation! That there must be some form of dissipation associated with the shock is intuitively obvious: part of the *kinetic* energy $\frac{1}{2}\rho_1 {V_1}^2$ of the directed motion in the upstream flow is irreversibly converted into the thermal (internal) energy of the shock-heated gas downstream. Nevertheless, the *details* of the dissipation mechanism do not enter into the final equations (the jump conditions).

In fact, one can appeal to the laws of thermodynamics in order to show that the *only* possible shock transitions are those where the density, pressure and temperature increase across the shock, and the flow velocity decreases. In that case the entropy jump is positive: $\Delta s \geq 0$. Formally, the jump conditions could also be satisfied if one interchanges the post-shock and the pre-shock flows, and where the flow velocity *increases* across the shock. That would be a transition where the density, pressure and temperature *decrease* across the shock, and where the flow accelerates rather than decelerates. In such a transition the specific entropy *decreases*: $\Delta s < 0$. Thermodynamics tells you that the entropy of the system can only stay equal or increase. $\Delta s \geq 0$. This thermodynamic law specifically *excludes* a shock transition where the flow is accelerated rather than decelerated.

One can think of a shock as a *self-regulating structure* in the following sense: the jump conditions (7.4.10), which were derived assuming an infinitely thin shock, put a strong constraint on the system: *given* the upstream state of the fluid (i.e. ρ_1, $\boldsymbol{V}_1$ and P_1) and the direction of the shock normal $\hat{\boldsymbol{n}}_{\rm s}$, the downstream state is *completely* determined by the Rankine-Hugoniot relations. The detailed (microscopic) structure of the shock, such as it's thickness, will have to adjust in such a way that the dissipation in the shock is exactly at the level required to reach a downstream state where the density, pressure and flow velocity are equal to the values that follow from the jump conditions.

The details of the dissipation only determine the thickness of the layer in which the fluid makes the transition from the upstream state to the downstream state. If the dissipation in the transition layer is due to two-body collisions between molecules or atoms, one can show that the typical thickness of the shock is of similar magnitude as the mean-free-path of the atoms or molecules in the gas. This mean free path is the typical distance an atom or molecule can travel between two collisons. The collisions convert part of the directed kinetic energy of the incoming flow into the kinetic energy of the random thermal motions of the individual atoms or molecules.

7.6.1 Shock thickness and the jump conditions

The formal derivation of the jump conditions in the preceding Sections assumes that the shock transition layer is infinitesimally thin. We derived that this implies that the flux entering the surface from upstream equals the flux exiting the surface into the downstream region. What happens if we allow the shock to have a finite thickness?

The answer to that question is contained in Eqn. (7.4.7): the flux $\mathcal{F}$ of some quantity entering the shock from upstream can only differ from the flux leaving the shock if the associated density $\mathcal{Q}$ of this quantity depends *explicitly* on time:

$$\frac{\partial \mathcal{Q}}{\partial t} \neq 0 \; . \tag{7.6.4}$$

This means that the flow must be time-dependent! In a steady flow, where all flow quantities are independent of time, the jump conditions are also valid in the case of a finite shock thickness.

The reason is simple. Consider two infinite surfaces, with the flow lines crossing both these surfaces. In a steady flow, no mass (and no energy or momentum) can accumulate in (or drain away from) the volume contained between these two surfaces. If it did accumulate (or drain away), the amount of mass (energy, momentum) contained between the two surfaces would grow (decay) in time, and the flow would no longer be steady. This line of reasoning also holds for two surfaces, one at the front and one at the back of a shock transition layer. This implies that the principle *flux in = flux out* also holds for shocks of finite thickness in a steady flow.

7.7 An example: over- and underexpanded Jets

In Chapter 5 we discussed Jet flows: collimated streams of gas which are in pressure-equilibrium with their surroundings. What happens if there is no pressure-equilibrium? If the flow speed inside the jet is supersonic with $\mathcal{M}_{\rm s} > 1$, the attempt of the jet to re-establish pressure equilibrium with the surrounding gas leads to a series of strong shocks in the jet flow, the so-called *Mach Disks*. These Mach Disks are oriented perpendicular to the jet axis, so that these shocks are normal shocks on the jet axis, the axis of symmetry. If the internal pressure $P_{\rm i}$ inside the jet is less than the pressure $P_{\rm e}$ in the external medium, one speaks of an *overexpanded jet* as the jet material has expanded too much, resulting in a low internal pressure. The opposite case (with $P_{\rm i} > P_{\rm e}$) is called an *underexpanded jet*.

What happens in these jets is illustrated in the Figure below. The situation shown there is what typically results in the exhaust jet of a jet engine or a rocket engine. The pressure in such an exhaust is determined by the (chemical) processes ocurring inside the engine, where the fuel is burned. The Mach Disks can actually be observed, as is illustrated below for the case of the Bell X-1 rocket plane, the first plane to break the sound barrier, and for the Space Shuttle.

In an underexpanded jet, the jet material expands sideways, leading to a *expansion fan*: a region where the fluid expands, and pressure and density decrease. These expansion fans, which behave similar to an expansion wave, reflect off the boundary of the jet, and turn (upon reflection) into *compression fans*. Such compression fans steepen into oblique shock waves, and finally cause the formation of the Mach Disk. Material that crosses the Mach Disk is compressed and heated, so that behind the Mach Disk the jet is again underexpanded (and over-pressured) with respect to the surrounding gas that tries to confine the jet. This means that the sequence of events starts anew, and a whole series of expansion fans, compression fans and Mach Disks is possible.

In an overexpanded jet, one starts with a compression fan as the jet material is compressed in response to the higher pressure in the surrounding gas. A Mach Disk is formed, and the shock compression in this Mach Disk raises the jet pressure so that the jet material is now over-pressured (underexpanded) with respect to the surrounding gas. The development of the jet thereafter proceeds as sketched above for an underexpanded jet.

Some astrophysicists believe that the bright 'knots' observed in the jets associated with Active Galaxies, see for example Figure 5.3 for the case of M87, are caused by a similar mechanism. This idea is supported by simulations, which show that the characteristic 'diamond shape' pattern of oblique shocks and Mach Disks indeed occur, as illustrated in the third figure below.

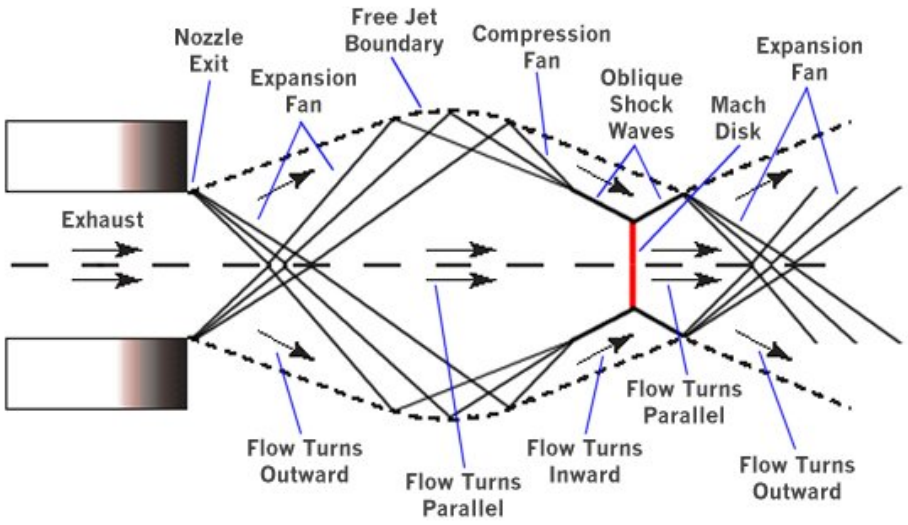

Underexpanded jet: $P_i > P_e$

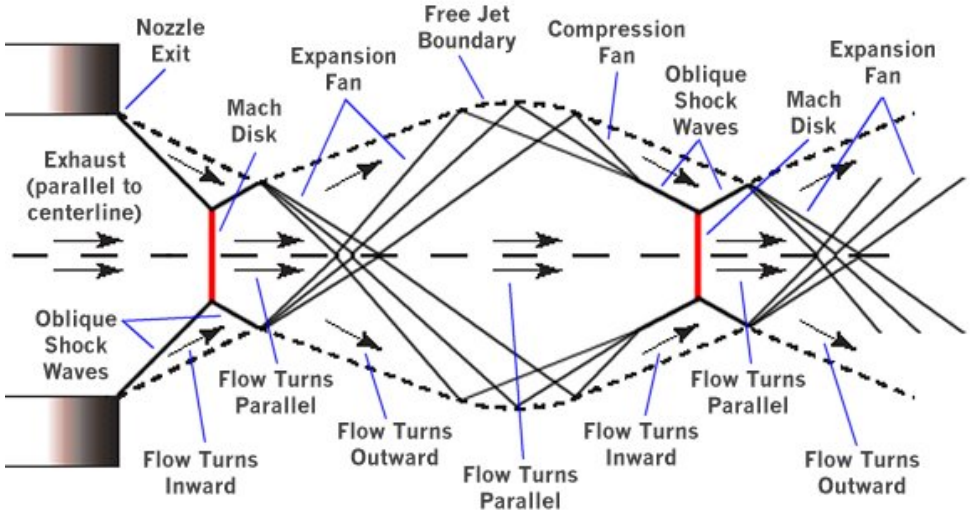

Overexpanded jet: $P_i < P_e$

Figure 7.7: *The flow in an over- and underexpanded jet. The Mach Disks are represented by the red lines perpendicular to the jet axis.*

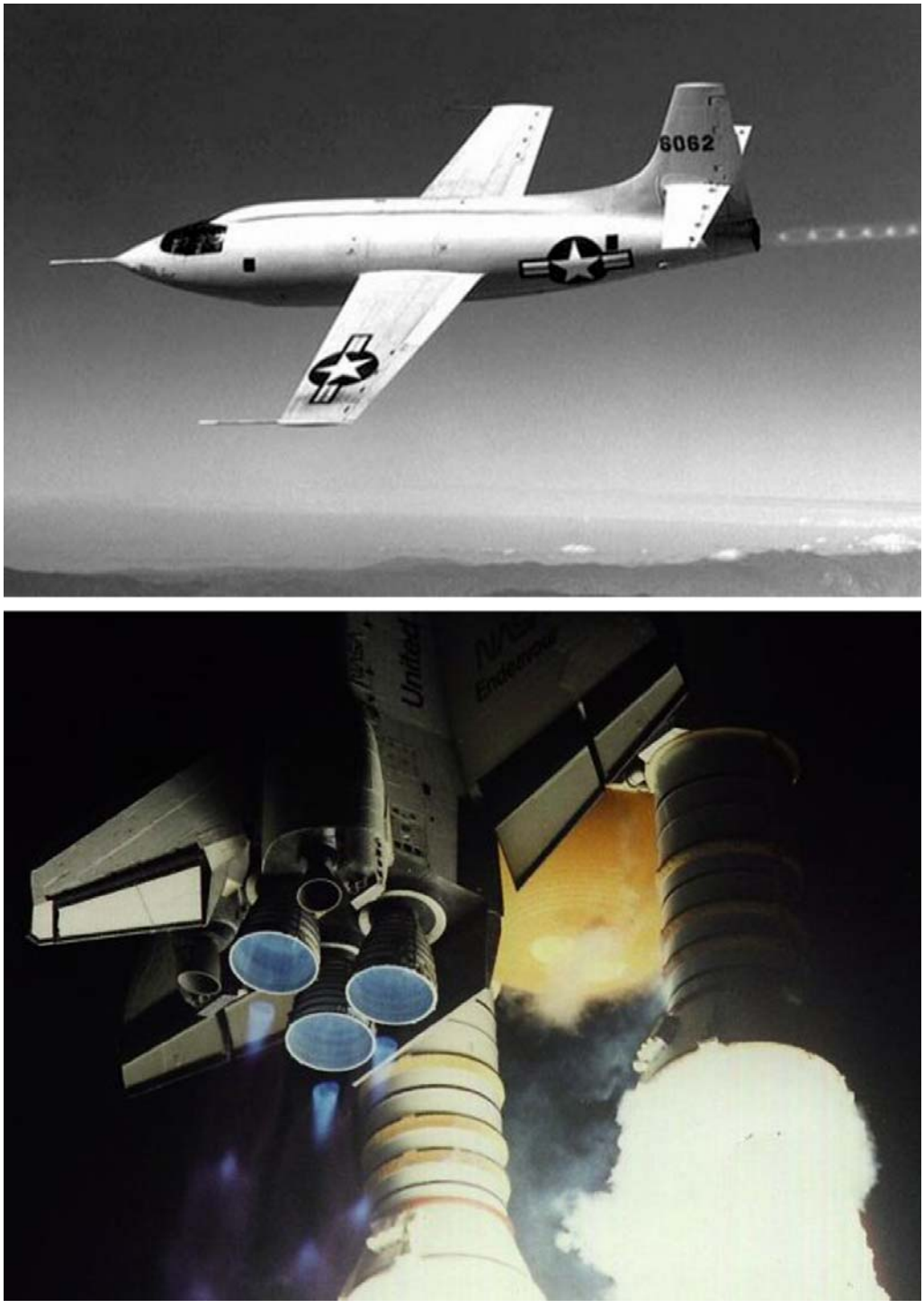

Figure 7.8: *Mach Disks in the exhaust jet of the Bell X-1 rocket plane (top), and behind the three main engines of the Space Shuttle (below). Behind the Bell X-1 a series of bright 'blobs' are visible, which show the location of the series of Mach Disks. Behind the Shuttle engines, only the first Mach Disk is clearly visible, the following disks in the series are less distinct.*

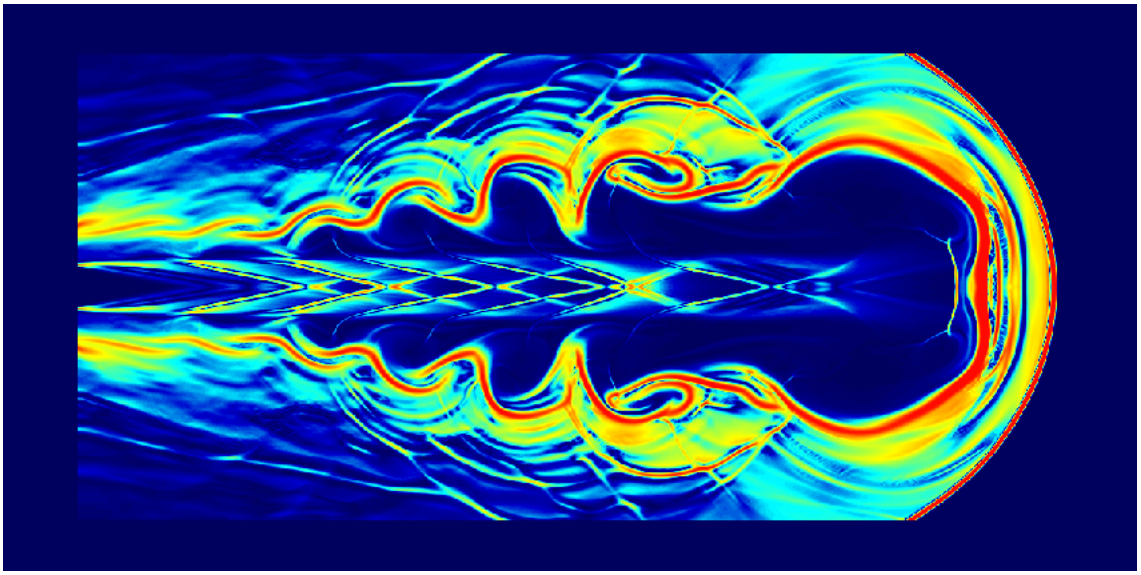

Figure 7.9: *A numerical simulation by P. Hughes, G. Comer Duncan & P. Hardee (University of Michigan) of a relativistic jet. The colors indicate different densities, with the highest densities in red, and intermediate density in yellow. Compressions are therefore colored yellow and red. Note the blunt* bow shock *preceding the jet, and the diamond-shape pattern of shocks inside the jet, just behind the head of the jet where it impacts the shocked intergalactic medium that has just passed through the bow shock. In this case, the shock diamonds are caused by the pressure fluctuations associated with the Kelvin-Helmholz Instability that occurs in the back-flow in the cocoon of shocked jet material near the head of the jet. This distorts the jet boundary and causes the wavy undulations. This instability, which occurs at a* contact discontinuity *between two fluids with a different streaming velocity, is treated in Chapter 9.*

Summary: jump conditions at a shock

The table below summarizes the relevant relations valid at a infinitely thin shock, in the frame where the shock itself is at rest. The normal and tangential components of the incoming flow are $V_{\rm n1} = V_1 \, \cos\theta_{\rm s}$, $V_{\rm t1} = V_1 \, \sin\theta_{\rm s}$.

Definition Mach Number:	$\mathcal{M}_{\rm s} = \dfrac{V_1}{c_{\rm s1}} = \sqrt{\dfrac{\rho_1 V_1^2}{\gamma P_1}}$;
Normal Mach Number:	$\mathcal{M}_{\rm n} = \dfrac{V_{\rm n1}}{c_{\rm s1}} = \mathcal{M}_{\rm s} \, \cos\theta_{\rm s}$;
Density jump:	$\dfrac{\rho_2}{\rho_1} = \dfrac{(\gamma+1)\,\mathcal{M}_{\rm n}^2}{(\gamma-1)\,\mathcal{M}_{\rm n}^2 + 2}$;
Jump normal velocity:	$\dfrac{V_{\rm n2}}{V_{\rm n1}} = \dfrac{(\gamma-1)\,\mathcal{M}_{\rm n}^2 + 2}{(\gamma+1)\,\mathcal{M}_{\rm n}^2}$,
Tangential velocity:	$V_{\rm t2} = V_{\rm t1}$; (7.7.5)
Pressure jump:	$\dfrac{P_2}{P_1} = 1 + \dfrac{2\gamma}{\gamma+1}\,\left(\mathcal{M}_{\rm n}^2 - 1\right)$;
Strong shock limit:	$\mathcal{M}_{\rm n}^2 = \dfrac{\rho_1 V_{\rm n1}^2}{\gamma P_1} \gg 1$
Density jump:	$\dfrac{\rho_2}{\rho_1} \simeq \dfrac{\gamma+1}{\gamma-1}$;
Jump normal velocity:	$\dfrac{V_{\rm n2}}{V_{\rm n1}} \simeq \dfrac{\gamma-1}{\gamma+1}$;
Tangential velocity:	$V_{\rm t2} = V_{\rm t1}$;
Post-shock pressure	$P_2 \simeq \dfrac{2\gamma\mathcal{M}_{\rm n}^2\,P_1}{\gamma+1} = \dfrac{2\rho_1\,V_{\rm n1}^2}{\gamma+1}$.

7.8 Contact discontinuities

The jump conditions of Eqn. (7.4.10) have another solution. Let us assume that no mass crosses the discontinuity surface so that

$$V_{\rm n1} = V_{\rm n2} = 0 \ . \tag{7.8.6}$$

In that case one speaks of a *contact discontinuity*. The conservation of the flux of x-momentum, formally equal to $\rho V_{\rm n}^2 + P$, reduces to a simple pressure-balance equation:

$$P_2 = P_1 \ . \tag{7.8.7}$$

The conservation of the flux of y-momentum and the conservation of the energy flux are both satisfied trivially: both vanish identically as $\rho V_{\rm n} = 0$. This means that in a contact discontinuity the state of the fluid on both sides of the discontinuity is only constrained by the two relations (7.8.6) and (7.8.7). In particular one can have a situation where

$$\rho_2 \neq \rho_1 \ , \tag{7.8.8}$$

and the velocity, which in this case is entirely along the discontinuity surface, is unconstrained. It is not even necessary that the velocity along the contact discontinuity has the same direction on both sides. At a contact discontinuity it is allowed that

$$\boldsymbol{V}_{\rm t2} \neq \boldsymbol{V}_{\rm t1} \ . \tag{7.8.9}$$

We will see however that such a situation, where the two velocities differ across the contact discontinuity, is *unstable*: when the contact surface is warped, the deformations grow as a result of the *Kelvin-Helmholz* instability.

7.9 Supernova remnants and stellar wind bubbles

7.9.1 Blowing high-pressure bubbles into a uniform medium

In the previous Sections we considered the physics of shocks from a reference frame where the shock surface is at rest. The situation in a frame of reference where the shock moves with velocity $\boldsymbol{V}_{\rm s}$ can be obtained (for non-relativistic shock speeds) from a simple Galilean transformation. The Rankine-Hugoniot relations (7.4.32) and the jump conditions (7.4.10) can still be applied, provided one interprets the velocities V_1 and V_2 as the *relative* velocity with respect to the shock, in vector notation:

$$\boldsymbol{V} \implies \boldsymbol{V}_{\rm rel} = \boldsymbol{V} - \boldsymbol{V}_{\rm s} \, . \tag{7.9.1}$$

For a shock propagating with velocity $\boldsymbol{V}_{\rm s}$ into a medium that is at rest, $\boldsymbol{V} = 0$, one has $\boldsymbol{V}_1 = -\boldsymbol{V}_{\rm s}$ and $\theta_{\rm s} = 0$. In this particular case any shock is a normal shock, with $V_{\rm t} = 0$, even when the shock surface itself is not a plane!

Now consider a strong shock, propagating with shock speed $V_{\rm s}$ into a stationary and uniform medium with pressure $P_1 \equiv P_0$ and density $\rho_1 \equiv \rho_0$. This normal shock, with a Mach number $\mathcal{M}_{\rm n} = \mathcal{M}_{\rm s}$, satisfies:

$$\mathcal{M}_{\rm s}^2 = \left(\frac{V_{\rm s}}{c_{\rm s0}} \right)^2 = \frac{\rho_0 \, V_{\rm s}^2}{\gamma P_0} \gg 1 \, . \tag{7.9.2}$$

The strong shock limit of the Rankine-Hugoniot relations (Eqns. 7.5.33 and 7.5.34 with $\cos\theta_{\rm s} = 1$) then give the following result for the pressure P_2 immediately behind the shock:

$$\begin{aligned} P_2 &\approx \frac{2\gamma \, \mathcal{M}_{\rm s}^2}{\gamma + 1} \, P_0 \\ &= \frac{2\rho_0 \, V_{\rm s}^2}{\gamma + 1} \, , \end{aligned} \tag{7.9.3}$$

where I have used (7.9.2). One can invert this relation, and calculate the shock speed in terms of the post-shock pressure P_2, and the pre-shock density ρ_0:

$$V_{\rm s} \approx \sqrt{\frac{\gamma + 1}{2}} \, \left(\frac{P_2}{\rho_0} \right)^{1/2} \, . \tag{7.9.4}$$

This result can be applied for the formation of high-pressure bubbles in a stationary surrounding medium. This is a situation that applies to *supernova remnants* (SNRs) and *stellar wind bubbles* in the interstellar medium.

Consider a spherical bubble containing a low-density, very hot gas with internal pressure $P_{\rm i}$ and internal density $\rho_{\rm i}$. This bubble has a radius R, see the figure below. The bubble is embedded in a cold, dense stationary medium with a low pressure, $P_0 \ll P_{\rm i}$, and a high density $\rho_0 \gg \rho_{\rm i}$. Because of the large pressure difference, the bubble will start to expand rapidly. If the difference between the internal pressure $P_{\rm i}$ and the external pressure P_0 is sufficiently large, the expansion speed will be supersonic with respect to the sound speed in the surrounding medium, $\mathrm{d}R/\mathrm{d}t = V_{\rm s} > c_{\rm s0} = \sqrt{\gamma P_0/\rho_0}$. For instance, the typical (observed) expansion speed of a supernova remant is ~ 1000 km/s. The sound speed in the interstellar medium ranges from 10-100 km/s.

Because of the supersonic expansion velocity, a shock will form at the outer edge of the bubble. This shock is usually called the **blast wave**. The mass that has been swept up by the expanding bubble will collect in a dense 'shell' at its outer rim. If the shock is strong, the typical density in this shell follows from the shock jump conditions. The shocked swept-up material in the shell has a density (see Eqn. 7.5.33)

$$\rho_{\rm sh} \approx \frac{\gamma+1}{\gamma-1}\,\rho_0 \ . \tag{7.9.5}$$

This immediately allows us to calculate the thickness of the shell. If the external medium is uniform, a bubble with radius R has swept a total mass equal to

$$M_{\rm sw} = \frac{4\pi}{3}\,\rho_0 R^3 \ . \tag{7.9.6}$$

This mass is now residing in the dense shell with thickness ΔR and has a density $\rho_{\rm sh}$. So one must have for $\Delta R \ll R$:

$$M_{\rm sw} \approx 4\pi\,\rho_{\rm sh} R^2\,\Delta R \ . \tag{7.9.7}$$

Combining the last to equations, and using (7.9.5), one finds:

$$\Delta R = \frac{(\gamma-1)R}{3(\gamma+1)} = 0.083R \ , \tag{7.9.8}$$

where the numerical value is for $\gamma = 5/3$. So the assumption that the shell is thin is a reasonable one. The swept-up material is separated from the hot material inside the bubble by a contact discontinuity.

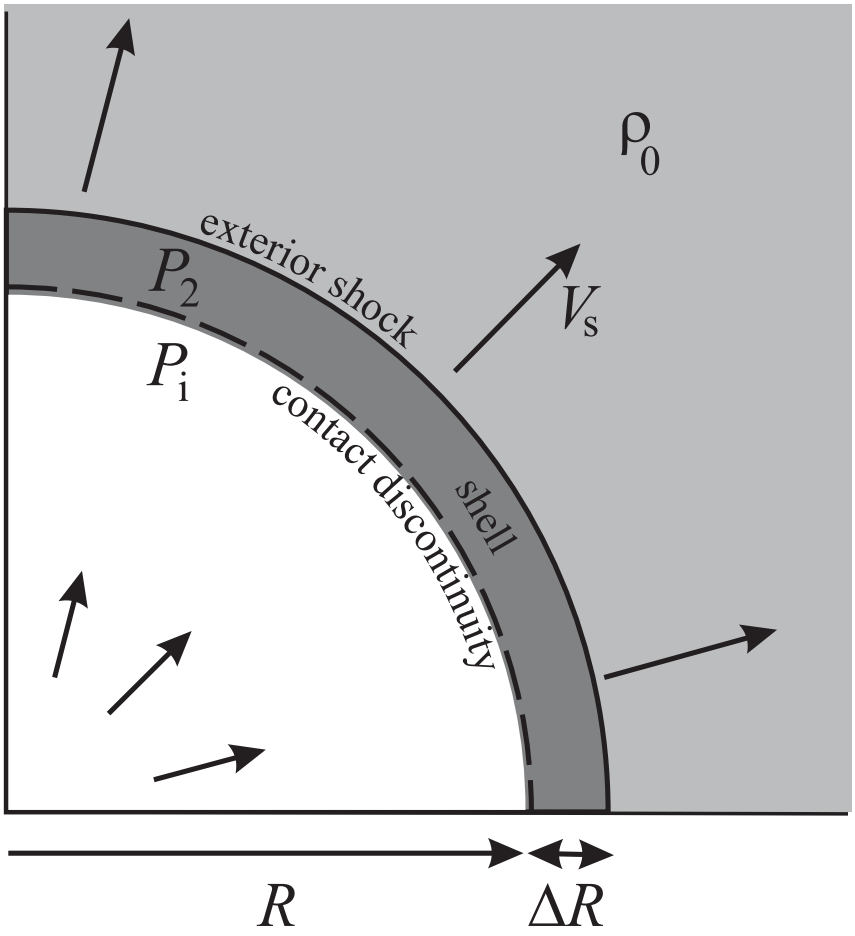

Figure 7.10: *The structure of a tenuous bubble of very hot gas (large internal pressure $P_{\rm i}$ amd small density $\rho_{\rm i}$) expanding with velocity $V_{\rm s} = {\rm d}R/{\rm d}t$ into a low-pressure, high-density medium at rest. The density of the surrounding medium equals ρ_0. If the expansion speed is supersonic with respect to the sound speed in the surrounding medium, the exterior of the bubble is a strong shock, also called a* **blast wave**. *Behind the blast wave, the material that the bubble has swept up in its life time collects in a dense shell. The hot material in the bubble interior is separated from this swept-up material by a contact discontinuity.*

The expansion speed of the bubble can be estimated from shock theory (Eqn. 7.9.4):

$$\frac{\mathrm{d}R}{\mathrm{d}t} \approx V_\mathrm{s} \approx \sqrt{\frac{\gamma+1}{2}} \left(\frac{P_\mathrm{i}}{\rho_0}\right)^{1/2} \tag{7.9.9}$$

This relation also implies that the the expansion is supersonic if $\rho_\mathrm{i} \ll \rho_0$: the material inside the bubble must have a very low density compared with the surrounding medium.

The associated expansion law, which gives the bubble radius $R(t)$ as a function of time, can be obtained from a simple dynamical argument. Let us assume that most of the mass of the expanding bubble is the swept-up material that has been collected over the bubble life time, and which resides in a dense shell at the outer edge the bubble with thickness $\Delta R \ll R$. This immediately gives the mass contained in the bubble as a function of the bubble radius $R(t)$:

$$M(t) \approx M_\mathrm{sw} = \frac{4\pi}{3}\,\rho_0\,R^3(t)\;. \tag{7.9.10}$$

The total energy of the bubble consists of the kinetic energy of the expanding massive shell, and the internal (thermal) energy of the hot, tenuous gas in the bubble interior:

$$E(t) \approx \frac{1}{2}\,M(t)\,\left(\frac{\mathrm{d}R}{\mathrm{d}t}\right)^2 + \left(\frac{4\pi}{3}\,R^3\right)\,\frac{P_\mathrm{i}(t)}{\gamma-1}\;. \tag{7.9.11}$$

Here it is assumed that the internal pressure is almost uniform, which is a reasonable approximation of the expansion speed is less than the *internal* sound speed:

$$V_\mathrm{s} \leq c_\mathrm{si} = \sqrt{\frac{\gamma P_\mathrm{i}}{\rho_\mathrm{i}}}\;. \tag{7.9.12}$$

In that case, the interior pressure must be roughly equal to the post-shock pressure in the shell material:

$$P_\mathrm{i} \approx P_2 \approx \frac{2}{\gamma+1}\,\rho_0\,\left(\frac{\mathrm{d}R}{\mathrm{d}t}\right)^2 \tag{7.9.13}$$

This is simply the pressure-balance condition (7.8.7) applied at the contact discontinuity that separates the bubble interior from the shocked material in the shell. Note that (7.9.13) implies that the ratio of the thermal energy and the kinetic energy of the remnant becomes a constant (equal to $4/(\gamma^2-1) = 2.25$ for $\gamma = 5/3$) when $M(t) \approx M_\mathrm{sw}$.

These relations allow us to find an approximate expression for the total (kinetic + thermal) energy of the expanding, hot bubble. Substituting (7.9.13) into (7.9.11) one finds:

$$E(t) = C_\gamma \, M(t) \, \left(\frac{\mathrm{d}R}{\mathrm{d}t} \right)^2 \, . \tag{7.9.14}$$

Here C_γ is a numerical constant of order unity, which in this simple model is given by

$$C_\gamma = \frac{\gamma^2 + 3}{2(\gamma^2 - 1)} \, . \tag{7.9.15}$$

For an ideal mono-atomic gas with $\gamma = 5/3$ one has $C_\gamma = 1.625$. The value for C_γ is approximate, because of the various approximations made in the derivation (constant interior pressure etc.). However, more exact treatments arrive at the same result, with a somewhat smaller value for C_γ.

If one knows at which rate energy is supplied to the bubble as a function of time, so that $E(t)$ is known, one can use Eqn. (7.9.14) together with Eqn. (7.9.10) to derive the expansion law $R(t)$. We will treat two important cases: that of a point explosion where a fixed amount of energy E_0 is supplied impulsively at $t = 0$ and where no energy losses occur afterwards, so that $E(t) =$ constant $= E_0$. This is a model for a supernova remnant some 100-10,000 years after the explosion of the progenitor star. The other important case is that of a *constant* energy supply at some luminosity L so that $E(t) = Lt$. The latter case can serve as a crude model of the energy of a bubble blown into the interstellar medium by a strong stellar wind.

Another approach gives similar results. Consider the force balance of the dense shell of swept-up material. I will consider the case where of an explosive event where $E(t) = E_0$ is constant. The force balance equation can be written as a relation for the change of the shell momentum $M_{\rm sw} \, V$:

$$\frac{\mathrm{d}(M_{\rm sw} \, V)}{\mathrm{d}t} \approx 4\pi R^2 \, P_{\rm i} \, . \tag{7.9.16}$$

This states that the change of the magnitude of the momentum of the shell is supplied by the push excerted at its inner edge by the pressure of the hot gas inside the bubble. The assumption $P_{\rm i} \gg P_0$ allows us to neglect the force on the shell due to the pressure in the surrounding interstellar medium. If one now uses the expression $M_{\rm sw} = 4\pi\rho_0 R^3/3$, and if one estimates the internal pressure as $P_{\rm i} \sim E_0/4\pi R^3$, which assumes that about half of the total energy resides in the thermal energy in the bubble, one finds an equation of motion that will give the same expansion law as the energy argument used above.

7.10 Supernova explosions and their remnants

In a supernova the core of a massive star ($M \geq 10 M_\odot$) which has exhausted its nuclear fuel collapses under its own weight. Without the constant energy supplied by nuclear fusion, the gas pressure drops and is no longer capable of supporting the outer layers of the star against gravity. The star starts to collapse, a collapse which proceeds most rapidly in the dense inner core. The collapse of the core continues (and accelerates) until it reaches a density comparable to that found in atomic nuclei. In that case a neutron star is left as a 'fossil' of the original exploded star. In a number of supernova remnants, such as the *Crab Nebula* (see figure) this pulsar has been detected. For a recent review about supernovae and their significance for astrophysics see Burrows[6].

The amount of energy liberated when the core collapses into a neutron star is essentially the gravitational binding energy of the core at the moment it 'bounces'. This bounce is due to the change in the equation of state of the material in the collapsing core when it is compressed to nuclear densities ($\rho \simeq \rho_{\rm nuc} = 10^{14}$ g cm^{-3}). Nuclear forces, rather than the pressure of the (degenerate) material start to dominate the pressure. With a core mass $M_{\rm c} \approx 1.5\ M_\odot$ and a bounce radius $R_{\rm b} \approx 10$ km (the typical mass and radius of a neutron star) the binding energy equals:

$$E_{\rm sn} \approx \frac{G M_{\rm c}^2}{R_{\rm b}} \approx 10^{53}\ {\rm erg}\ . \tag{7.10.1}$$

The binding energy is radiated away, mainly in the form of neutrinos. These neutrino's are the product of the reaction

$$p + e^- \ \ \rightarrow n + \nu_{\rm e}\ , \tag{7.10.2}$$

which occurs when protons and electrons 'recombine' into neutrons within the dense, collapsing core. Neutrinos associated with the supernova SN 1987a in the Large Magellanic Cloud were detected on Earth in several experiments set up to measure proton-decay[7]. About 1 % of this energy is transferred from the neutrinos to the stellar envelope, and is used to drive a shockwave that ejects the envelope into the interstellar medium. The mechanical energy of the ejecta is therefore of order

$$E_{\rm snr} \approx 0.01 \times E_{\rm sn} \approx 10^{51}\ {\rm erg}. \tag{7.10.3}$$

This energy fuels the explosive event that ultimately creates a supernova remnant.

[6] A. Burrows, 2000: *Nature* **403**, 727.

[7] e.g.: Hirata, K *et al.*, 1987: *Phys. Rev. Lett.* **58**, 1490; Bionta, R.M. *et al.* 1987: *Phys. Rev. Lett.* **58**, 1494.

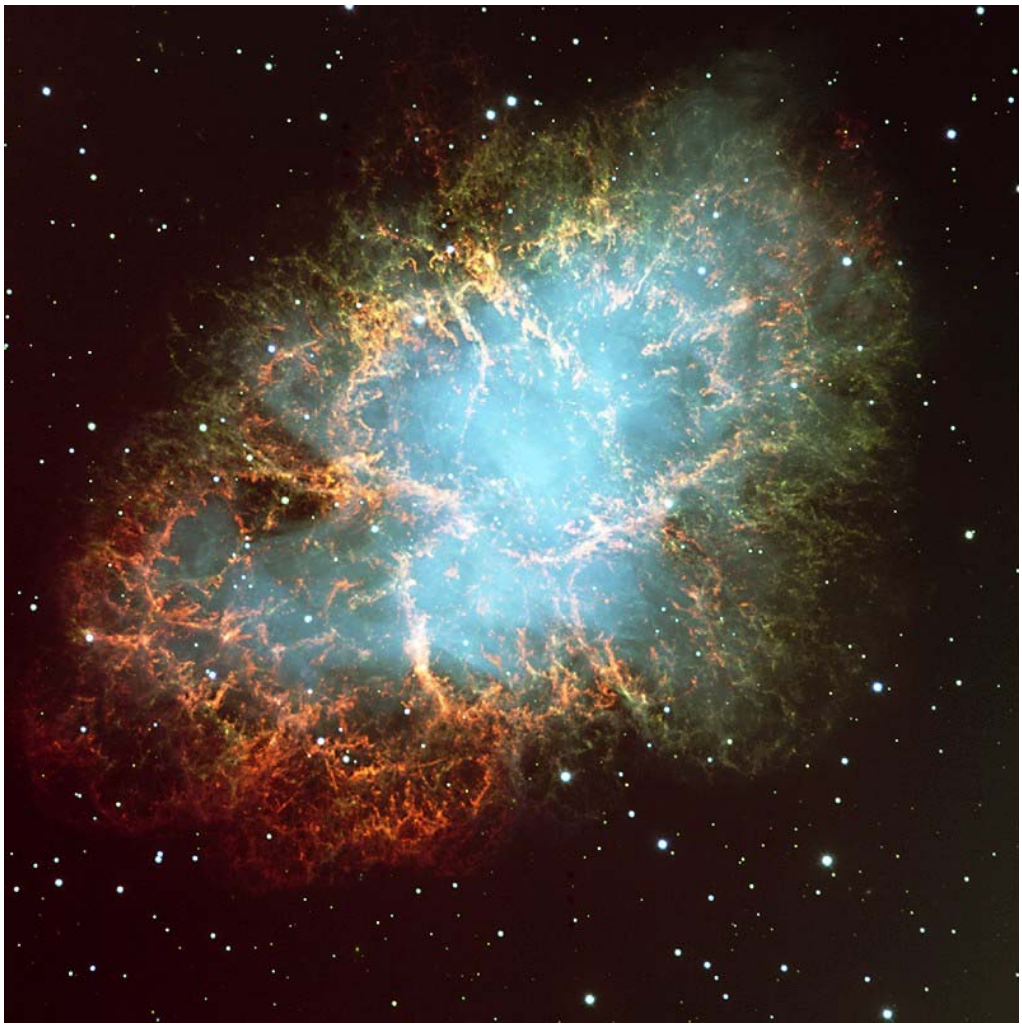

Figure 7.11: *Picture of the* Crab Nebula*, showing the optical filaments and the diffuse glow of optical synchrotron radiation due to relativistic electrons. This nebula is the remnant of the supernova of AD 1054. The actual Sedov blast wave is much larger than the structure shown here, but has as yet not been detected. This emission seen in this picture is largely powered by the* **Crab pulsar***, the first pulsar ever discovered. This rapidly rotating neutron star spinds down slowly Apparently, most of the lost rotational energy is put into an ultra-relativistic wind. Therefore the Crab Nebula is an example of a* **pulsar wind nebula***.*
Photo taken with the VLT, ESO, Chili

The whole sequence of events in a core-collapse supernova (Type II supernova in the astronomical jargon) is illustrated below.

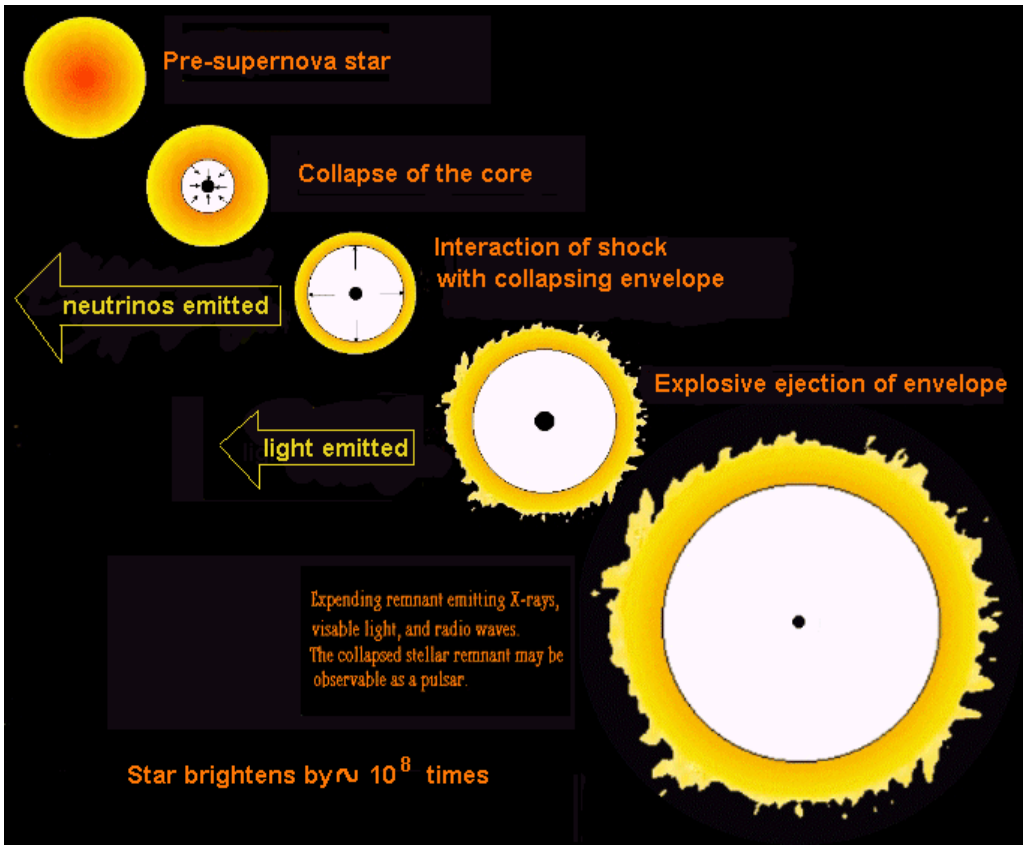

Figure 7.12: *The sequence of events leading to core collapse, and the associated supernova explosion*

A *supernova remnant* consists essentially of the stellar ejecta in a hot expanding bubble, preceded by swept-up interstellar material and an outer blast wave (strong shock) propagating into the interstellar medium. The typical speed $V_{\rm s}$ of this material can be estimated by a simple argument of energy conservation. Let us assume that all the mechanical energy is converted into the kinetic energy of the remnant, $E_{\rm snr} = \frac{1}{2} M_{\rm snr} V_{\rm s}^2$. In that case, the expansion velocity should be of order

$$V_{\rm s} \simeq \sqrt{\frac{2E_{\rm snr}}{M_{\rm snr}}} \, . \tag{7.10.4}$$

The mass $M_{\rm snr}$ is the mass of the ejecta, explosively expelled from the star at the time of the supernova explosion, and the mass $M_{\rm sw}$ (see Eqn. 7.9.6) that is added later as the remnant sweeps up more and more interstellar material.

If the density of the interstellar gas is constant and equal to $\rho_{\rm ism}$, and if the radius of the remnant is $R_{\rm s}$, one has

$$M_{\rm snr} = M_{\rm ej} + \frac{4\pi}{3}\,\rho_{\rm ism}\,R_{\rm s}^3\ . \tag{7.10.5}$$

Since we know the typical energy involved, and the mass of the remnant must be several solar masses, we can estimate the typical expansion velocity:

$$V_{\rm s} \simeq 3,000\,\left(\frac{E_{\rm snr}}{10^{51}\ {\rm erg}}\right)^{1/2}\,\left(\frac{M_{\rm snr}}{10\ M_\odot}\right)^{-1/2}\ {\rm km/s}\ . \tag{7.10.6}$$

Initially, the mass $M(t)$ of the remnant consists almost entirely of the ejecta mass, $M_{\rm ej} \simeq 2 - 10\ M_\odot$. The expansion velocity is nearly constant:

$$V_{\rm s} \simeq (2E_{\rm snr}/M_{\rm ej})^{1/2} = 10,000\ {\rm km/s}. \tag{7.10.7}$$

This expansion velocity is much larger that the sound speed in the interstellar gas ($\simeq 10 - 100$ km/s), so a shock must form at the outer edge of the remnant. This phase in the evolution of the remnant is called the *free-expansion phase*.

As more and more interstellar gas is swept up, the mass of the remnant increases. After a few hundred years, the mass is dominated by this swept-up interstellar material, so that (7.10.4) reduces to:

$$V_{\rm s} \simeq \sqrt{\frac{6E_{\rm snr}}{4\pi\rho_{\rm ism}}}\,R_{\rm s}^{-3/2}\ . \tag{7.10.8}$$

The velocity decreases with increasing radius as $R^{-3/2}$ in this so-called *Sedov-Taylor phase*, the result of the increasing remnant mass: $M_{\rm snr} \propto R^3$. The typical expansion speed remains supersonic for a considerable time (typically 10,000 yr), so the shock at the outer edge of the remnant persists in this evolutionary phase.

The transition between the free expansion phase and the Sedov-Taylor phase occurs gradually when the radius of the remnant reaches the *deceleration radius* $R_{\rm d}$. The deceleration radius is defined as the radius where the ejecta mass equals the mass of the swept-up interstellar gas:

$$\frac{4\pi}{3}\rho_{\rm ism}R_{\rm d}^3 = M_{\rm ej} \iff R_{\rm d} = \left(\frac{3M_{\rm ej}}{4\pi\rho_{\rm ism}}\right)^{1/3} \simeq 2.2\left(\frac{M_{\rm ej}}{M_\odot}\right)^{1/3} n_{\rm ism}^{-1/3}\ {\rm pc}. \tag{7.10.9}$$

Here $n_{\rm ism} \approx \rho_{\rm ism}/m_{\rm p}$ is the *number* density of the interstellar gas, which is typically $n_{\rm ism} \sim 1\ {\rm cm}^{-3}$. It is easily checked that the relation $V_{\rm s} \propto R_{\rm s}^{-3/2}$ leads to an expansion law of the form $R_{\rm s} \propto t^{2/5}$, see below.

Later (typically after $\sim$ 10,000 years) the remnant begins to cool, and the energy is no longer conserved. The figure below gives the typical evolution of a supernova remnant, showing the free-expansion and Sedov-Taylor phase, and the following pressure-driven snowplow phase and the and momentum-conserving phases. Ultimately, a supernova remnant will merge with the general interstellar medium, leaving a Hot-Phase bubble in the interstellar medium. I will now derive the expansion law during the Sedov-Taylor phase, using the results of the previous Section.

7.10.1 The Sedov-Taylor expansion law

In a supernova explosion, the mechanical energy $E_0 \equiv E_{\rm snr}$ that drives the expansion of the bubble is supplied impulsively in a *point explosion* at time $t = 0$. If no energy is lost, for instance through radiation losses, the mechanical energy remains constant for $t > 0$. One can write the energy equation (7.9.11) in this case as:

$$E_{\rm snr} = C_\gamma\, M(t)\, \left(\frac{{\rm d}R}{{\rm d}t}\right)^2 = \text{constant} \tag{7.10.10}$$

The constant C_γ (see Eqn. 7.9.15) is of order unity. Once the remnant has expanded to a radius larger than the deceleration radius, we can use (7.9.10) for the mass of the bubble: $M(t) \approx 4\pi\rho_{\rm ism}R^3(t)/3$. The energy equation can then be written as

$$R^{3/2}\, \left(\frac{{\rm d}R}{{\rm d}t}\right) = \left(\frac{3E_{\rm snr}}{4\pi C_\gamma \rho_{\rm ism}}\right)^{1/2} = {\rm constant}. \tag{7.10.11}$$

This relationship between the velocity and the radius of the bubble, $V_{\rm s} \propto R_{\rm s}^{-3/2}$, is the same one as derived above using a simple conservation law for the kinetic energy. In this derivation we also take account of the thermal energy of the hot bubble material.

Let us try a power-law solution for the radius as a function of time:

$$R(t) = {\rm constant}\ \times\ t^\alpha\,. \tag{7.10.12}$$

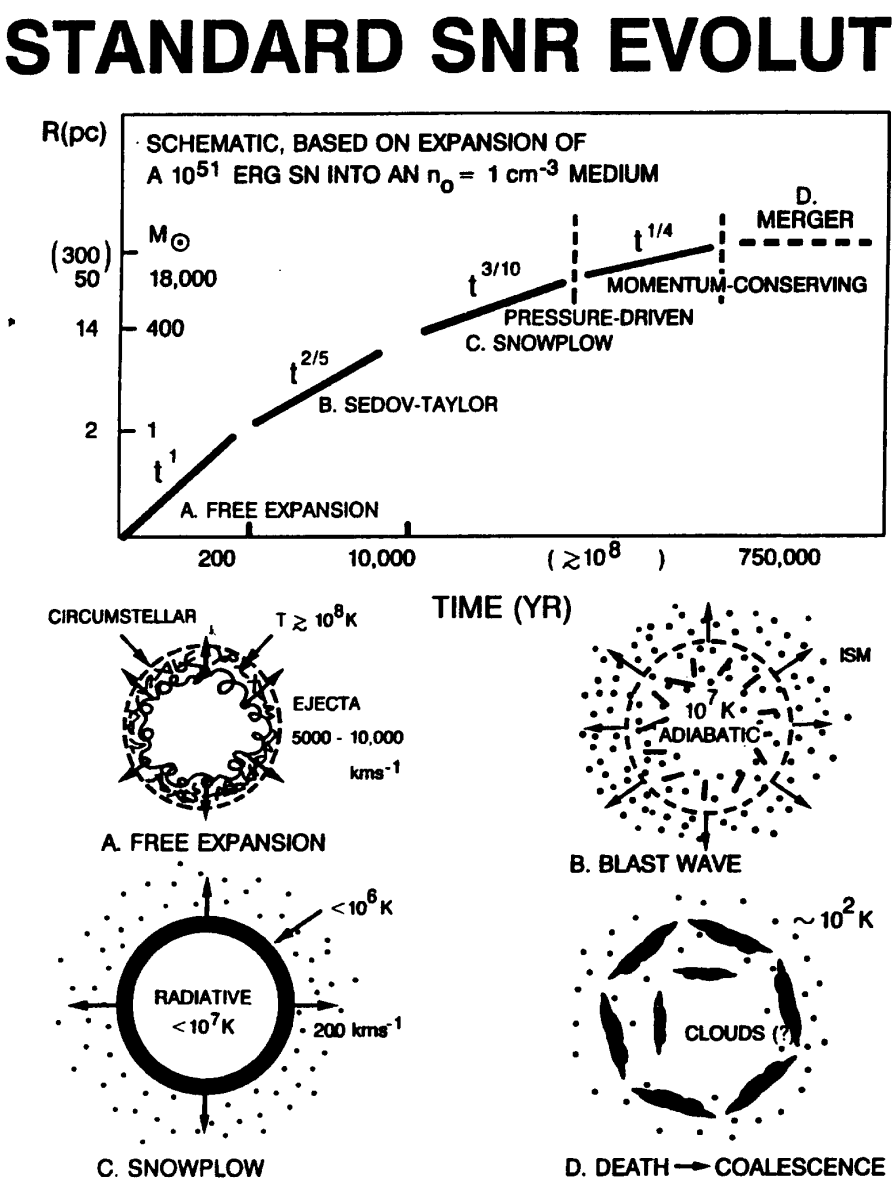

Figure 7.13: *The evolutionary stages in the life of a supernova remnant* From: Cioffi, 1990, in: *Physical Processes in Hot Cosmic Plasmas*, W. Brinkmann, A.C. Fabian & F. Giovannelli (Eds.), NATO ASI Vol. 305, p. 1, Kluwer Academic Publishers.

For an expansion law of this form the velocity is also a power-law in time:

$$V(t) = \frac{\mathrm{d}R}{\mathrm{d}t} = \alpha \, \frac{R}{t} \propto t^{\alpha-1} \tag{7.10.13}$$

Using $V = \alpha R/t$ one sees that this power law for $R(t)$ indeed solves Eqn. (7.10.11), provided that

$$\frac{R^{5/2}}{t} = \text{constant} \iff R(t) \propto t^{2/5} \, . \tag{7.10.14}$$

This solution condition determines the power-law index as $\alpha = 2/5$. Now that the value of α has been determined one can derive the full solution:

$$R(t) = \bar{C} \, \left(\frac{E_{\rm snr}}{\rho_{\rm ism}} \right)^{1/5} t^{2/5} \tag{7.10.15}$$

Here $\bar{C}$ is another constant of order unity, which in our simple theory equals

$$\bar{C} = \left(\frac{75}{16\pi C_\gamma} \right)^{1/5} \tag{7.10.16}$$

For $\gamma = 5/3$ one finds $\bar{C} \approx 0.98$.

The pressure in the bubble decays as the bubble expands. From Eqn. (7.9.3) one has $P_{\rm i} \propto V_{\rm s}^2 \propto t^{-6/5}$. This loss of pressure is simply an expansion loss as the internal pressure is converted into the kinetic energy of the expanding shell.

This energy-conserving Sedov-Taylor solution[8] applies for $R \gg R_{\rm d}$ until the radiation losses from the remnant become important. Radiative cooling makes the pressure inside the hot bubble decay faster, and consequently the remant looses energy, and the expansion slows down more rapidly than in the Sedov-Taylor phase. The cooling-dominated stages of the remnant evolution set in after about 10,000 years.

[8]The Russian physicist Sedov derived this solution analytically. Sedov's method was a very clever use of a mathematical technique known as a *similarity solution*. The British physicist Taylor derived the same expansion law by numerical means. Taylor then used his model to estimate the explosive yield of the first atomic test explosions in the desert of New Mexico in 1945, using the publicly available photographs of the expanding fireball. At the time, the explosive yield of atomic bombs was considered to be classified information by the U.S.

The Sedov-Taylor solution predicts the radius and speed (shock speed) of the remnant to be

$$R_{\rm s} \simeq 3.8 \left(\frac{E_{\rm snr}}{10^{51}\ {\rm erg}}\right)^{1/5} \left(\frac{n_{\rm ism}}{1\ {\rm cm}^{-3}}\right)^{-1/5} \left(\frac{t}{1000\ {\rm yr}}\right)^{2/5} {\rm pc}$$
$$V_{\rm s} \simeq 1580 \left(\frac{E_{\rm snr}}{10^{51}\ {\rm erg}}\right)^{1/5} \left(\frac{n_{\rm ism}}{1\ {\rm cm}^{-3}}\right)^{-1/5} \left(\frac{t}{1000\ {\rm yr}}\right)^{-3/5} {\rm km/s}. \quad (7.10.17)$$

The strong shocks around the supernova remnants are believed to be the source of *cosmic rays*: a tenuous gas of very energetic charged particles (protons, electrons and nuclei) which pervades our whole galaxy. These shocks also accelerate electrons which radiate by the synchrotron mechanism in the weak magnetic field ($B \sim 10^{-4}$ G) inside the remant. This makes supernova remnants strong,non-thermal radio sources, as illustrated by the false-color picture of the radio emisson from Tycho's remnant shown below. The heated gas inside the bubble ($T \sim 10^8$ K) causes emission lines in the optical spectrum of the remant, and X-rays (thermal bremsstrahlung and nuclear lines) which makes them also strong X-ray sources, as illustrated by the picture of Tycho's remnant in X-rays.

7.10.2 The pressure-driven and the momentum-conserving snow-plow phases

I will now briefly consider the two evolutionary phases that follow the Sedov-Taylor phase. If the supernova remnant becomes sufficiently old, radiative cooling becomes important, and the total energy is no longer conserved. In the energy conserving Sedov-Taylor phase, pressure forces accelerate the swept-up interstellar gas, converting thermal energy (which came from the original explosion) into the kinetic energy of the shell of swept-up matter. Since radiative cooling scales with the number density n as n^2, and since the density inside the shell of swept-up matter is much larger than inside the hot interior of the remnant, most of the cooling occurs in the shocked interstellar medium.

In the snow-plow approximation one assumes that all the energy put into the swept-up gas is radiated away, but that the hot interior of the remnant does not cool. This means that the shell of shocked interstellar gas collapses until it becomes very thin, and that the pressure inside the remnant now behaves adiabatically (as no heat is added to, or lost from the interior):

$$P_{\rm i} \propto \rho_{\rm i}^{\gamma} \ . \quad (7.10.18)$$

Since the mass residing in the hot interior is conserved one has:

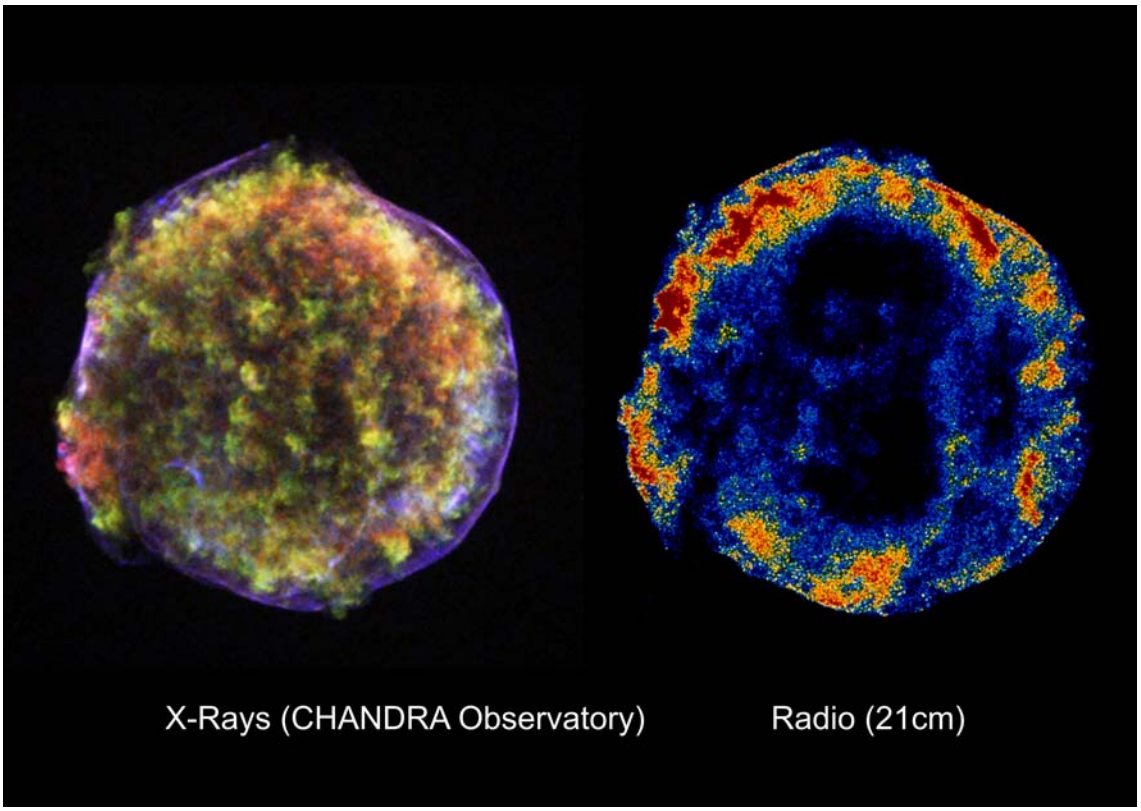

Figure 7.14: *Two pictures of the remnant of Tycho's supernova (AD 1572), a picture in X-Rays (left) , made with the CHANDRA satellite, and a radio picture made with the* Very Large Array *radio synthesis telescope (right). The X-ray picture shows the hot ($T \sim 10^8$ K) gas in the remnants interior in yellow. This is mostly* line emission *from exited nuclei. The blue radiation at the outer rim of the remnant is* synchrotron continuum emission, *caused by relativistic electrons moving in a weak magnetic field. The radio emission is also synchrotron radiation. It is believed that these relativistic electrons are accelerated at the outer shock.*
This is a 'classical' remnant with a nearly perfect spherical shape. It is believed to be entering the Sedov-Taylor phase. Note the sharp outer edge of the remnant, which is believed to coincide with the position of the outer blast wave.

$$\rho_{\rm i} = \frac{M_{\rm ej}}{(4\pi/3)R_{\rm s}^3} \; . \tag{7.10.19}$$

Combining these two relations yields:

$$P_{\rm i} \propto R_{\rm s}^{-3\gamma} \; . \tag{7.10.20}$$

For $\gamma = 5/3$ one finds $P_{\rm i} \propto R_{\rm s}^{-5}$. This behaviour is quite different from the behaviour of the pressure in the Sedov-Taylor phase: there the pressure behaves as $P_{\rm i} \sim \rho_{\rm ism} V_{\rm s}^2 \propto R_{\rm s}^{-3}$. The motion of the collapsed shell, which contains most of the mass, is driven by the pressure of the remnant's interior. The equation of motion of the massive shell can be found by balancing the total pressure force on the shell by the inertial force,

$$\frac{\rm d}{{\rm d}t}\left(M(R_{\rm s}) \, \frac{{\rm d}R_{\rm s}}{{\rm d}t} \right) = 4\pi R_{\rm s}^2 \, P_{\rm i}(R_{\rm s}) \; . \tag{7.10.21}$$

The pressure of the interstellar medium has been neglected. Using the pressure law (7.10.20) together with $M(R_{\rm s}) = 4\pi\rho_{\rm ism} R_{\rm s}^3/3$ one finds that the equation of motion (7.10.21) can be written as:

$$\frac{\rm d}{{\rm d}t}\left(R_{\rm s}^3 \, \frac{{\rm d}R_{\rm s}}{{\rm d}t} \right) = A \, R_{\rm s}^{2-3\gamma} \; . \tag{7.10.22}$$

Here A is a constant, whose value does not concern us here. If one tries to solve this equation with a power-law that gives the radius of the remnant as

$$R_{\rm s}(t) = B \, t^{\alpha} \tag{7.10.23}$$

with B some constant, the condition that both sides of the equation contain the same power of t gives a condition on α. It is easy to check that this condition reads

$$t^{4\alpha-2} = t^{(2-3\gamma)\alpha} \; . \tag{7.10.24}$$

Solving for α one finds:

$$\alpha = \frac{2}{3\gamma+2} = \frac{2}{7} \approx 0.286 \; . \tag{7.10.25}$$

The last value is for $\gamma = 5/3$. So in the pressure-driven snowplow phase the supernova remnant expands as

$$R_{\rm s}(t) \propto t^{2/7} \; . \tag{7.10.26}$$

Numerical simulations of this pressure-driven snowplow phase show that the value of α is actually closer to $\alpha = 3/10 = 0.3$.

Finally, when all the internal energy of the remnant has been radiated away, the internal pressure approaches zero, and the remnant enters the *momentum-conserving snowplow phase*, where

$$\frac{\rm d}{{\rm d}t}\left(M(R_{\rm s})\,\frac{{\rm d}R_{\rm s}}{{\rm d}t}\right) = \frac{\rm d}{{\rm d}t}\left(M(R_{\rm s})\,V_{\rm s}\right) = 0 \; . \tag{7.10.27}$$

This equation implies that

$$V_{\rm s}(R_{\rm s}) \propto M^{-1}(R_{\rm s}) \propto R_{\rm s}^{-3} \; . \tag{7.10.28}$$

The resulting expansion law follows from ${\rm d}R_{\rm s}/{\rm d}t = V_{\rm s} \propto R_{\rm s}^{-3}$:

$$R_{\rm s}(t) \propto t^{1/4} \; . \tag{7.10.29}$$

In the last stages of its life, the supernova remnant dissolves into the general interstellar medium. The figure below shows such an old remnant.

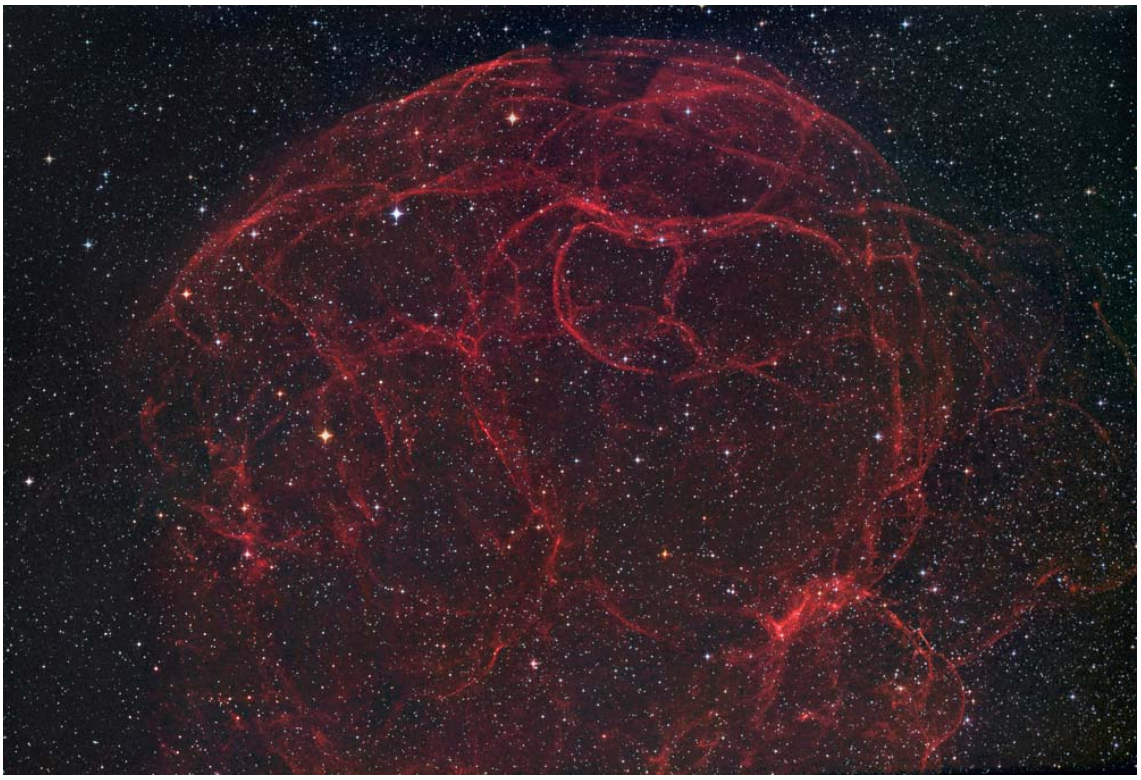

Figure 7.15: *The old supernova remnant S147, which is in the process of dissolving into the general interstellar medium.* Photo credit: Robert Gendler

7.10.3 Stellar wind bubbles

A somewhat more complicated situation is that of the bubble blown into the interstellar medium by a stellar wind. The 'mechanical luminosity' of the wind is roughly given by

$$L_{\rm w} \approx \frac{1}{2}\,\dot{M}\,V_{\rm w}^2 \tag{7.10.30}$$

where $\dot{M}$ is the mass loss in the wind and $V_{\rm w} = V_\infty$ is the terminal velocity of the wind, the velocity it reaches far beyond the critical radius r_c (see Chapter 4). The interpretation of this expression is simple: the kinetic energy per unit mass is $V_{\rm w}^2/2$, and the amount of mass injected by the star into the wind per second equals $\dot{M}$. The thermal energy of the wind far beyond the critical point is small, as the density drops off rapidly with increasing radius: at a distance r from the star it equals

$$\rho(r) = \frac{\dot{M}}{4\pi r^2 V_{\rm w}}\ , \tag{7.10.31}$$

assuming a spherically symmetric wind where $V(r) = V_{\rm w}$ is constant at large radii. Therefore, the energy carried by the wind material far from the star is almost completely kinetic energy, and the mechanical luminosity must be given by (7.10.30).

The wind blows a bubble into the interstellar medium. If the mechanical luminosity of the wind remains constant, the total mechanical energy increases linearly in time:

$$E(t) \approx L_{\rm w} t\ . \tag{7.10.32}$$

Substituting this relation into the energy equation (7.9.11), and using the mass law (7.9.10) and the velocity law (7.9.9), one finds:

$$E = L_{\rm w} t = C_\gamma\,M(t)\,\left(\frac{{\rm d}R}{{\rm d}t}\right)^2 \tag{7.10.33}$$

If the wind is sufficiently long-lived, the bubble becomes so large that most of the bubble mass is in the swept-up interstellar gas: $M(t) \approx M_{\rm sw} = 4\pi\rho_{\rm ism}R^3/3$. In that case the expansion rate follows from Eqns. (7.10.32/7.10.33): one must have

$$R^{3/2}\,\left(\frac{{\rm d}R}{{\rm d}t}\right) = \left(\frac{3L_{\rm w}}{4\pi C_\gamma \rho_{\rm ism}}\right)^{1/2}\,t^{1/2}\ . \tag{7.10.34}$$

The solution for the bubble radius $R(t)$ is again a power-law in time:

$$R(t) = \tilde{C} \left(\frac{L_{\rm w}}{\rho_{\rm ism}} \right)^{1/5} t^{3/5} , \tag{7.10.35}$$

with $\tilde{C}$ a numerical constant of order unity. This same expansion law could have been obtained by directly making the substitution $E_0 \rightarrow L_{\rm w} t$ in the Sedov expansion law (7.10.15).

The detailed structure of such a wind bubble is more complicated than the structure of a supernova remnant (see the figures below). We will look at the structure of a stellar wind bubble by moving to ever larger radii.

The stellar wind is supersonic beyond the critical point. Therefore, it must slow down to a subsonic speed before it impinges on the swept-up interstellar matter. It does so by forming an inner *termination shock*. At this shock the wind material is slowed down, compressed and is strongly heated. Most of the kinetic energy of the incoming wind material is converted into thermal energy, and the pressure in the shocked wind is high. In addition to this termination shock, there is also an outer shock in the interstellar gas around the bubble as long as the expansion velocity is supersonic with respect to the surrounding (cold) medium. Behind that shock the swept-up material collects in a dense shell. In this respect the situation is similar to the one encountered in a supernova remnant.

The shocked interstellar matter and the shocked wind material are separated by a contact discontinuity. Across this contact surface, the shocked wind material and shocked interstellar gas are in pressure-equilibrium. The pressure-equilibrium condition can be used to calculate the radius $R_{\rm ts}$ of the terminantion shock. If the termination shock is strong, the pressure behind the shock follows from the jump conditions for a high-Machnumber shock, Eqn. (7.9.3):

$$P_{\rm 2w} = \frac{2 \rho_{\rm w} V_{\rm w}^2}{\gamma + 1} . \tag{7.10.36}$$

Here the wind density just before the termination shock, $\rho_{\rm w}$, follows from (7.10.31) at $r = R_{\rm ts}$:

$$\rho_{\rm w} = \frac{\dot{M}}{4 \pi R_{\rm ts}^2 V_{\rm w}} . \tag{7.10.37}$$

One can express the post-shock pressure in terms of the wind luminosity, wind speed and termination shock radius:

$$P_{2\mathrm{w}} = \frac{\dot{M} V_{\mathrm{w}}}{2\pi(\gamma+1)R_{\mathrm{ts}}^2} = \frac{L_{\mathrm{w}}}{(\gamma+1)\pi R_{\mathrm{ts}}^2 V_{\mathrm{w}}} \ , \tag{7.10.38}$$

where I have used definition (7.10.30).

In a similar fashion, the pressure of the shocked interstellar gas behind the outer shock is

$$P_{2\mathrm{ism}} = \frac{2\rho_{\mathrm{ism}} V_{\mathrm{s}}^2}{\gamma+1} \ , \tag{7.10.39}$$

with $V_{\mathrm{s}} = \mathrm{d}R/\mathrm{d}t$ the expansion speed of the bubble. Using the energy law (7.10.33) with $M(t) = M_{\mathrm{sw}}$ in the form

$$\rho_{\mathrm{ism}} V_{\mathrm{s}}^2 = \frac{3L_{\mathrm{w}}t}{4\pi C_\gamma R^3} \ , \tag{7.10.40}$$

we have

$$P_{2\mathrm{ism}} = \frac{3L_{\mathrm{w}}t}{2\pi(\gamma+1)C_\gamma R^3(t)} \ . \tag{7.10.41}$$

The pressure-equilibrium condition that must hold across the contact discontinuity, $P_{2\mathrm{ism}} = P_{2\mathrm{w}}$, yields

$$\frac{3L_{\mathrm{w}}t}{2\pi(\gamma+1)C_\gamma R^3(t)} = \frac{L_{\mathrm{w}}}{(\gamma+1)\pi R_{\mathrm{ts}}^2 V_{\mathrm{w}}} \ . \tag{7.10.42}$$

Solving for the termination shock radius one finds:

$$R_{\mathrm{ts}}(t) = \left(\frac{2C_\gamma \, R^3(t)}{3V_{\mathrm{w}}t}\right)^{1/2} \ . \tag{7.10.43}$$

As the stellar wind bubble (and outer shock) expands according to $R(t) \propto t^{3/5}$, relation (7.10.43) gives the expansion law for the termination shock:

$$R_{\rm ts}(t) \propto t^{2/5} \ . \tag{7.10.44}$$

The termination shock radius increases as the wind bubble expands, but the expansion proceeds at a slower rate than the expansion of the outer radius of the bubble. In this way, an increasing volume is available to store the mass injected by the central star.

7.10.4 Expansion into a non-uniform medium

This approach to calculate the evolution of expanding bubbles into a dense, almost pressureless medium can easily be extended to spherical bubbles expanding into a medium with a non-uniform density. The analysis is easy if the external density follows a power-law profile as a function of radius:

$$\rho_{\rm ism}(R) = \text{constant} \times R^{-\mu} \tag{7.10.45}$$

One can show that the swept-up mass now scales with radius as

$$M_{\rm sw}(R) = \int_0^R {\rm d}R 4\pi R^2 \, \rho(R) \propto R^{3-\mu} \ . \tag{7.10.46}$$

Using Eqn. (7.10.10), it is easily shown that a supernova bubble expands (in the Sedov-Taylor limit $M(t) \approx M_{\rm sw}$) with a velocity

$$V_{\rm snr} \sim \sqrt{\frac{2E_{\rm snr}}{M_{\rm sw}}} \propto R^{(\mu-3)/2} \ . \tag{7.10.47}$$

The resulting expansion law is again a power-law in time, with

$$R_{\rm snr}(t) \propto t^{2/(5-\mu)} \ . \tag{7.10.48}$$

The original Sedov-Taylor solution for a uniform medium is recovered if one puts $\mu = 0$.

If one relaxes the assumption of spherical symmetry more complicated techniques must be used[9]. If the bubble becomes old so that the expansion speed becomes *sub*sonic with respect to the sound speed in the interstellar medium (≈ 100 km/s), this derivation is no longer valid as the outer shock disappears.

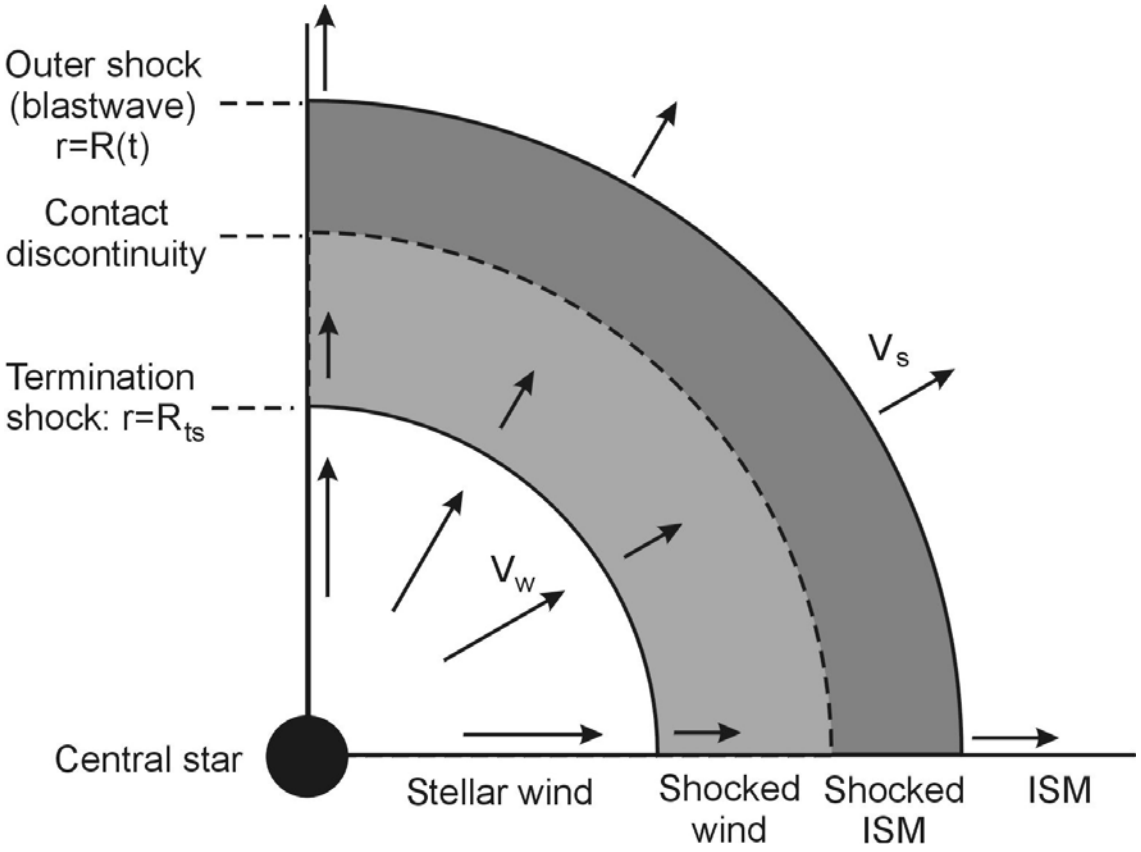

Figure 7.16: *Schematic representation of a stellar wind bubble. Going outwards in radius from the star which acts as a souce of the wind one has [1] the* **stellar wind**, *as described in Chapter 2; [2] a* **wind termination shock** *where the wind is slowed from supersonic to subsonic speeds; [3] a* **contact discontuity**, *separating the shocked stellar wind material from the shocked interstellar gas, and finally [4] the* **outer shock** *which propagates into the undisturbed interstellar medium, and which forms the outer radius of the bubble described by the expansion law $R_{\rm s} \propto t^{3/5}$ derived above. In this idealised picture, there is no mass flow across the contact discontinuity, and the pressure is equal on both sides. This means that the stellar wind material and the shocked interstellar gas do not mix. As soon as one relaxes the assumption of strict spherical symmetry mixing can occur due to instabilities at the contact discontinuity.*

[9] e.g. Icke, V., 1988: *Astron. Astrophys.* **202**, 177.

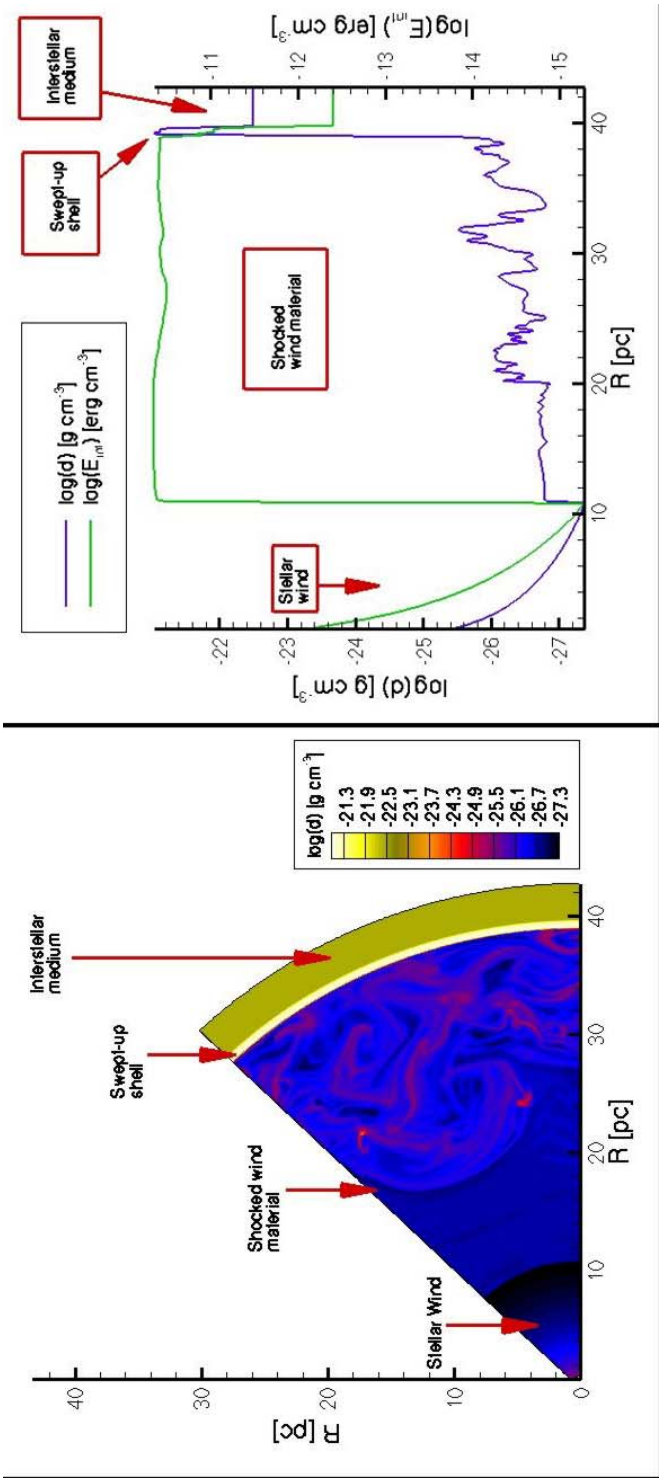

Figure 7.17: *A numerical calculation of a spherically symmetric wind expanding into a constant-density external medium. The left panel gives a false-color picture of the density in a section of the bubble. The right-hand panel plots the density ρ and the thermal energy density e as a function of radius. Note that the thermal energy density makes large jumps at the two shocks: the terminantion shock that ends the free-flowing stellar wind, and the external shock that separates the bubble from the undisturbed interstellar medium.*
Figure courtesy of Allard-Jan van Marle who performed the simulation.

Chapter 8

Rotating flows: rotation and vorticity

8.1 Introduction

In astrophysics and geophysics, one often has to deal with rotating flows. This rotation can be in a large-scale streaming pattern, such as the circulation of matter in an accretion disk around the compact object, or in the form of *vortices*: small swirls, or both. In geophysics and planetary physics one often describes the flow in a rotating reference frame, such as the frame fixed to the Earth's surface. This also has an effect on the description of the flow: centrifugal and Coriolis terms appear in the equation of motion.

In many cases rotation in one way or another is of paramount importance for the flow dynamics. Examples of flows where rotation plays an important role are:

- The flow patterns in the oceans and theatmosphere of the Earth and other planets, in particular the rapidly rotating gas giants Jupiter, Saturn and Uranus;
- The dynamics of accretion disks around compact objects, as found in *X-ray Binaries* containing neutron Stars and Black Holes in an orbit around a normal star that acts as a mass donor, in *Cataclysmic Variables* containing a White Dwarf as the compact object, in *Young Stellar Objects* and in *Active Galactic Nuclei*, which contain massive black holes and an accretion disk in which matter collects from stars that have been tidally ripped apart by the black hole;
- The dynamics of the self-gravitating thin (stellar) disk of *Spiral Galaxies*, well outside the central (quasi-spherical) bulge.

On a much smaller scale, small rotating structures within a flow known as *vortices* can behave as important dynamical entities. The most obvious example are cyclones and (on a smaller scale) the tornadoes which occur in the weather patterns of the (sub)tropics. In planetary physics, the *Great Red Spot* visible on Jupiter is thought to involve cyclonic

motion. Such cyclonic motions are suprisingly stable: once formed, they degrade slowly or, in the case without any friction, not at all. As we will see, the properties of such vortices, and the rotation of the coordinate frame in which one chooses to describe the flow, are closely coupled.

8.2 Vorticity

We start the discussion by looking at small-scale rotational motion in a fluid or gas. The amount of rotation in a flow field $\boldsymbol{V}(\boldsymbol{x}\ ,\ t)$ is quantified in a mathematical way by the *vorticity* $\boldsymbol{\omega}(\boldsymbol{x}\ ,\ t)$, which is formally defined as the curl of the velocity field:

$$\boldsymbol{\omega}(\boldsymbol{x}\ ,\ t) \equiv \boldsymbol{\nabla} \times \boldsymbol{V}(\boldsymbol{x}\ ,\ t)\ . \tag{8.2.1}$$

The action of the rotation or curl operator $\boldsymbol{\nabla} \times$ on any vector $\boldsymbol{V}(\boldsymbol{x}\ ,\ t)$ yields a new vector. In cartesian cordinates the components of this vector are:

$$\boldsymbol{\nabla} \times \boldsymbol{V}(\boldsymbol{x}\ ,\ t) = \begin{pmatrix} \dfrac{\partial V_z}{\partial y} - \dfrac{\partial V_y}{\partial z} \\ \dfrac{\partial V_x}{\partial z} - \dfrac{\partial V_z}{\partial x} \\ \dfrac{\partial V_y}{\partial x} - \dfrac{\partial V_x}{\partial y} \end{pmatrix}\ . \tag{8.2.2}$$

Alternatively[1] one can express it as a 'determinant'. If the three (orthogonal) unit vectors of the cartesian coordinate frame are $\hat{\boldsymbol{x}}$, $\hat{\boldsymbol{y}}$ and $\hat{\boldsymbol{z}}$ one has:

$$\boldsymbol{\nabla} \times \boldsymbol{V}(\boldsymbol{x}\ ,\ t) = \begin{Vmatrix} \hat{\boldsymbol{x}} & \hat{\boldsymbol{y}} & \hat{\boldsymbol{z}} \\ \dfrac{\partial}{\partial x} & \dfrac{\partial}{\partial y} & \dfrac{\partial}{\partial z} \\ V_x & V_y & V_z \end{Vmatrix}\ . \tag{8.2.3}$$

This definition for the vorticity as a curl implies that the vorticity field is divergence-free:

$$\boldsymbol{\nabla} \cdot \boldsymbol{\omega}(\boldsymbol{x}\ ,\ t) = 0\ . \tag{8.2.4}$$

[1] See also the Mathematical Appendix on Internet

It is possible to derive an equation for the vorticity of a fluid directly from the equation of motion. One starts by taking the curl of the equation of motion:

$$\boldsymbol{\nabla} \times \left\{ \frac{\partial \boldsymbol{V}}{\partial t} + (\boldsymbol{V} \cdot \boldsymbol{\nabla})\boldsymbol{V} = -\frac{1}{\rho}\, \boldsymbol{\nabla} P \right\} . \tag{8.2.5}$$

One then uses the vector identity (3.2.13),

$$\begin{aligned} (\boldsymbol{V} \cdot \boldsymbol{\nabla})\boldsymbol{V} &= \boldsymbol{\nabla}(\tfrac{1}{2}V^2) - \boldsymbol{V} \times (\boldsymbol{\nabla} \times \boldsymbol{V}) \\ &= \boldsymbol{\nabla}(\tfrac{1}{2}V^2) - \boldsymbol{V} \times \boldsymbol{\omega} , \end{aligned} \tag{8.2.6}$$

together with the relations

$$\boldsymbol{\nabla} \times \boldsymbol{\nabla} f = 0 \quad , \quad \boldsymbol{\nabla} \times (f \boldsymbol{\nabla} g) = \boldsymbol{\nabla} f \times \boldsymbol{\nabla} g \, , \tag{8.2.7}$$

valid for any function $f(\boldsymbol{x}\,,\, t)$ and $g(\boldsymbol{x}\,,\, t)$. One finds that (8.2.5) reduces to:

$$\frac{\partial \boldsymbol{\omega}}{\partial t} = \boldsymbol{\nabla} \times \, (\boldsymbol{V} \times \boldsymbol{\omega}) + \frac{1}{\rho^2} \boldsymbol{\nabla}\rho \times \boldsymbol{\nabla} P \, . \tag{8.2.8}$$

Finally, by using the vector identity

$$\boldsymbol{\nabla} \times (\boldsymbol{A} \times \boldsymbol{B}) = \boldsymbol{A}\, (\boldsymbol{\nabla} \cdot \boldsymbol{B}) - \boldsymbol{B}\, (\boldsymbol{\nabla} \cdot \boldsymbol{A}) + (\boldsymbol{B} \cdot \boldsymbol{\nabla})\boldsymbol{A} - (\boldsymbol{A} \cdot \boldsymbol{\nabla})\boldsymbol{B} \tag{8.2.9}$$

together with Eqn. (8.2.4), one can write Eqn. (8.2.8) as

$$\frac{\mathrm{d}\boldsymbol{\omega}}{\mathrm{d}t} = (\boldsymbol{\omega} \cdot \boldsymbol{\nabla})\boldsymbol{V} - \boldsymbol{\omega}(\boldsymbol{\nabla} \cdot \boldsymbol{V}) + \frac{1}{\rho^2} \boldsymbol{\nabla}\rho \times \boldsymbol{\nabla} P \, . \tag{8.2.10}$$

Here (as before) $\mathrm{d}/\mathrm{d}t = \partial/\partial t + \boldsymbol{V} \cdot \boldsymbol{\nabla}$ is the comoving time derivative. This is the equation of motion for the vorticity.

It is possible to rewrite this equation of motion in another, more compact form. One can use the continuity equation to eliminate $\boldsymbol{\nabla} \cdot \boldsymbol{V}$:

$$\boldsymbol{\nabla} \cdot \boldsymbol{V} = -\frac{1}{\rho} \left(\frac{\mathrm{d}\rho}{\mathrm{d}t} \right) . \tag{8.2.11}$$

Substituting this relation into (8.2.10), and re-arranging terms, one finds:

$$\boxed{\frac{\mathrm{d}}{\mathrm{d}t} \left(\frac{\boldsymbol{\omega}}{\rho} \right) = \left(\frac{\boldsymbol{\omega}}{\rho} \cdot \boldsymbol{\nabla} \right) \boldsymbol{V} + \frac{1}{\rho^3} \boldsymbol{\nabla}\rho \times \boldsymbol{\nabla} P .} \tag{8.2.12}$$

This last version of the equation of motion for the vorticity shows most clearly how the vorticity changes in response to the motion, and the pressure and density gradients in the fluid or gas.

The only true generation of *new* vorticity occurs when the surfaces of constant pressure and the surfaces of constant density, the so-called *isobaric* and *isochoric* surfaces, do **not** coincide. Using the ideal gas law, $P = \rho \mathcal{R} T/\mu$, this situation occurs whenever[2]

$$\boldsymbol{\nabla}\rho \times \boldsymbol{\nabla} P = \frac{\rho \mathcal{R}}{\mu} \boldsymbol{\nabla}\rho \times \boldsymbol{\nabla} T \neq 0 . \tag{8.2.13}$$

Therefore, the second term on the right-hand side of Eqn. (8.2.12) describes *vorticity generation*: even if $\boldsymbol{\omega} = 0$ initially, the vorticity will grow if condition (8.2.13) is satisfied.

The first term on the right-hand side of Eqn. (8.2.12), which is *linear* in the vorticity, describes the effect of *vortex stretching* due to velocity gradients. This term gives the change of existing vorticity in response to the fluid motions, i.e. *vorticity amplification*. Note that this term can be negative as well as positive, so vorticity may grow as well as decline locally, depending on the properties of the flow. However we will see that, as long as friction is neglected, there is an conserved integral quantity associated with vorticity: the *circulation*.

[2]Strictly speaking one has $\boldsymbol{\nabla} P = (\rho \mathcal{R}/\mu) \boldsymbol{\nabla} T + (T \mathcal{R}/\mu) \boldsymbol{\nabla}\rho$, but since $\boldsymbol{\nabla}\rho \times \boldsymbol{\nabla}\rho = 0$, the second term, involving the density gradient, does not contribute to the vortex-generation term $\propto \boldsymbol{\nabla}\rho \times \boldsymbol{\nabla} P$.

8.2.1 Vortex stretching and vortex tubes

Let us consider the effect of vortex-stretching term a bit more closely, assuming for the moment that the vorticity generation term $\propto \boldsymbol{\nabla} P \times \boldsymbol{\nabla}\rho$ vanishes identically. Consider a curve $\boldsymbol{X}(\ell)$ carried passively by the flow. In chapter 2.4 we derived the equation of motion for this curve (Eqn. 2.6.5): a small section $\Delta\boldsymbol{X}$ of a material curve changes according to

$$\frac{\mathrm{d}(\Delta\boldsymbol{X})}{\mathrm{d}t} = (\Delta\boldsymbol{X}\cdot\boldsymbol{\nabla})\boldsymbol{V}\ . \tag{8.2.14}$$

Equation (8.2.12) for the vorticity, without the generation term, has *exactly* the same form:

$$\frac{\mathrm{d}}{\mathrm{d}t}\left(\frac{\boldsymbol{\omega}}{\rho}\right) = \left(\frac{\boldsymbol{\omega}}{\rho}\cdot\boldsymbol{\nabla}\right)\boldsymbol{V}\ . \tag{8.2.15}$$

This means the following: consider a **vortex line**, which is defined in cartesian coordinates in terms of the vorticity vector components $(\omega_x\ ,\ \omega_y\ ,\ \omega_z)$ by the condition that the relation

$$\frac{\mathrm{d}x}{\omega_x} \;=\; \frac{\mathrm{d}y}{\omega_y} \;=\; \frac{\mathrm{d}z}{\omega_z} \;=\; \frac{\mathrm{d}\ell}{|\boldsymbol{\omega}|} \tag{8.2.16}$$

is satisfied by points along the line. Here

$$\mathrm{d}\ell = \sqrt{\mathrm{d}x^2 + \mathrm{d}y^2 + \mathrm{d}z^2} \tag{8.2.17}$$

is the parameter measuring the length along a vortex line (which in general is actually a *curve* rather than a line). The direction of the tangent vector $\hat{\boldsymbol{l}}$ to a vortex line $\boldsymbol{x}(\ell\ ,\ t)$ is always along $\boldsymbol{\omega}$: from condition (8.2.16) it is easily seen that one has

$$\hat{\boldsymbol{l}} \equiv \frac{\partial\boldsymbol{x}}{\partial\ell} = \frac{\boldsymbol{\omega}}{|\boldsymbol{\omega}|}\ . \tag{8.2.18}$$

Vortex lines give the local direction of the vorticity field, and as such they are the direct analogue of the magnetic field lines in electromagnetic theory[3]. Vortex lines are the field lines of the vorticity field. Note that the field lines of the related field $\boldsymbol{\omega}/\rho$ (vorticity per unit mass) are the same since the density ρ is a scalar. This means that the vorticity can be written as

$$\boldsymbol{\omega}(\boldsymbol{x}\ ,\ t) = \omega(\boldsymbol{x}\ ,\ t)\,\hat{\boldsymbol{l}}\ , \tag{8.2.19}$$

with $\hat{\boldsymbol{l}}$ the unit vector tangent to the vortex line through position $\boldsymbol{x}$ at time t and $\omega \equiv |\boldsymbol{\omega}|$.

Now consider two neighbouring points on a vortex line $\boldsymbol{X}(\ell)$, separated by an (infinitesimal) distance $\Delta\ell \equiv |\Delta\boldsymbol{X}|$. We now follow the motion of these two points. The vortex line is a material curve, carried passively along by the flow. This follows immediately from the fact that the equation of motion for $\boldsymbol{\omega}/\rho$ and of any curve carried by the flow has exactly the same form: they respond in the same way to the flow. This implies that during the motion of the fluid, and the motion of the vortex lines that results from the fluid motion, the condition

$$\frac{\omega(\ell\ ,\ t)}{\rho(\ell\ ,\ t)\Delta\ell} = \text{constant} \tag{8.2.20}$$

must be satisfied at *any* point along a vortex line. Here $\Delta\ell$ is the distance between the original two points on the line at time t. If a vortex line is stretched, so that $\Delta\ell$ increases, this stretching must lead to an associated increase of the vorticity ω/ρ. If one assumes for simplicity that the density ρ remains constant, this means that the vorticity must increase at the same rate as $\Delta\ell$. This explains the term 'vortex stretching'. Of course it is also possible that a vortex line is shortened, in which case ω/ρ must decrease.

The amount of stretching of a vortex line that is built up between some fiducial time t_0 and some later time t, $\lambda(t)$ can be defined formally, by introducing the stretch parameter

$$\lambda(t) \equiv \frac{\Delta\ell(t)}{\Delta\ell(t_0)} = \left|\frac{\partial\boldsymbol{X}(\ell)}{\partial\ell_0}\right|\ . \tag{8.2.21}$$

Here ℓ_0 serves as a 'Lagrangian label': it is the length along the curve at time t_0 so that $|\partial\boldsymbol{X}(t_0)/\partial\ell_0| = 1$.

[3]This 'magnetic analogy' goes further. For instance, the magnetic field $\boldsymbol{B}$ can be defined in terms of a so-called vector potential $\boldsymbol{A}$ as $\boldsymbol{B} = \boldsymbol{\nabla}\times\boldsymbol{A}$ so that $\boldsymbol{\nabla}\cdot\boldsymbol{B} = 0$. For more details see for instance:
A.J. Chorin, 1994: *Vorticity and Turbulence*, Springer Verlag, New York
T.E. Faber, 1995: *Fluid Dynamics for Physicists*, Cambridge Univ. Press, Ch. 7.

This label is carried along by each material point on the vortex line. It serves as an unique identifyer of each point, and defines the initial separation distance $\Delta\ell_0$. Given the amount of stretching λ and the density ρ_0 and vorticity ω_0 at time t_0 one has:

$$\frac{\omega(t)}{\rho(t)} = \lambda(t)\,\frac{\omega_0}{\rho_0}\,. \tag{8.2.22}$$

Remember that different sections of a vortex line can be stretched or shortened by a different amount, i.e. the amount of stretching $\lambda(t)$ in general will be a function of position along the vortex line, and one should write $\lambda(\ell\,,\,t)$.

8.3 Kelvin's circulation theorem

The *circulation* of a flow around an arbitrary *closed* curve C is defined as

$$\Gamma_{\rm c} \equiv \oint_C \boldsymbol{V}\cdot{\rm d}\boldsymbol{r}\,. \tag{8.3.1}$$

From Stokes' theorem,

$$\oint_{\partial\boldsymbol{O}} \boldsymbol{A}\cdot{\rm d}\boldsymbol{r} = \int(\boldsymbol{\nabla}\times\boldsymbol{A})\cdot{\rm d}\boldsymbol{O}\,, \tag{8.3.2}$$

the circulation can also be written as a surface integral of the vorticity over the surface enclosed by the curve C:

$$\Gamma_{\rm c} = \int(\boldsymbol{\nabla}\times\boldsymbol{V})\cdot{\rm d}\boldsymbol{O} = \int\boldsymbol{\omega}\cdot{\rm d}\boldsymbol{O}\,. \tag{8.3.3}$$

Using the last expression, it follows that the time change of the circulation must satisfy (according to the chain rule)

$$\frac{{\rm d}\Gamma_{\rm c}}{{\rm d}t} = \int\left\{\left(\frac{{\rm d}\boldsymbol{\omega}}{{\rm d}t}\right)\cdot{\rm d}\boldsymbol{O} + \boldsymbol{\omega}\cdot\left(\frac{{\rm d}\,{\rm d}\boldsymbol{O}}{{\rm d}t}\right)\right\}\,. \tag{8.3.4}$$

The equation for ${\rm d}\boldsymbol{\omega}/{\rm d}t$ has been derived above. The equation for the time derivative of the surface depends on the choice of that surface. Let us assume that each element of the surface (and therefore also its outer edge as defined by the curve C) is carried along passively by the flow.

Take a small (infinitesimal) oriented surface element (a vector!) defined by two tangent vectors $\Delta\boldsymbol{X}$ and $\Delta\boldsymbol{Y}$:

$$\Delta\boldsymbol{O} = \Delta\boldsymbol{X} \times \Delta\boldsymbol{Y} \ . \tag{8.3.5}$$

If $\Delta\boldsymbol{X}$ and $\Delta\boldsymbol{Y}$ are both carried by the flow, they are infinitesimal sections of a material curve and consequently they both satisfy an equation like (8.2.14). Therefore $\mathrm{d}\Delta\boldsymbol{O}/\mathrm{d}t$ is given by:

$$\frac{\mathrm{d}\Delta\boldsymbol{O}}{\mathrm{d}t} = (\Delta\boldsymbol{X}\cdot\boldsymbol{\nabla})\boldsymbol{V}\times\Delta\boldsymbol{Y} + \Delta\boldsymbol{X}\times(\Delta\boldsymbol{Y}\cdot\boldsymbol{\nabla})\boldsymbol{V} \ . \tag{8.3.6}$$

Let us consider a mathematically convenient special case. Later it will be argued that the result obtained for this special case has in fact general validity: it applies to an infinitesimal surface-element of *arbitrary* shape and orientation.

Choose the coordinate system in such a way that the infinitesimal surface element lies in the x-y plane. Take the shape of the surface element to be a rectangular tile. This means that the two vectors $\Delta\boldsymbol{X}$ and $\Delta\boldsymbol{Y}$ defining the surface-element are mutually orthogonal. We can therefore always orient the coordinate axes in such a way that $\Delta\boldsymbol{X}$ and $\Delta\boldsymbol{Y}$ are along the x-axis and y-axis respectively:

$$\Delta\boldsymbol{X} = \Delta X\,\hat{\boldsymbol{x}} \ , \ \ \Delta\boldsymbol{Y} = \Delta Y\,\hat{\boldsymbol{y}} \ , \ \ \Delta\boldsymbol{O} = \Delta X\,\Delta Y\,\hat{\boldsymbol{z}} \ , \tag{8.3.7}$$

so that

$$(\Delta\boldsymbol{X}\cdot\boldsymbol{\nabla})\boldsymbol{V} = \Delta X\,\frac{\partial\boldsymbol{V}}{\partial x} \quad , \quad (\Delta\boldsymbol{Y}\cdot\boldsymbol{\nabla})\boldsymbol{V} = \Delta Y\,\frac{\partial\boldsymbol{V}}{\partial y} \ . \tag{8.3.8}$$

One can write the right-hand-side of (8.3.6) in determinant form:

$$\frac{\mathrm{d}\Delta\boldsymbol{O}}{\mathrm{d}t} = \Delta X \left\| \begin{array}{ccc} \hat{\boldsymbol{x}} & \hat{\boldsymbol{y}} & \hat{\boldsymbol{z}} \\ \dfrac{\partial V_x}{\partial x} & \dfrac{\partial V_y}{\partial x} & \dfrac{\partial V_z}{\partial x} \\ 0 & \Delta Y & 0 \end{array} \right\| + \Delta Y \left\| \begin{array}{ccc} \hat{\boldsymbol{x}} & \hat{\boldsymbol{y}} & \hat{\boldsymbol{z}} \\ \Delta X & 0 & 0 \\ \dfrac{\partial V_x}{\partial y} & \dfrac{\partial V_y}{\partial y} & \dfrac{\partial V_z}{\partial y} \end{array} \right\| . \tag{8.3.9}$$

Expanding the two determinants one finds:

$$\frac{\mathrm{d}\Delta \boldsymbol{O}}{\mathrm{d}t} = \left(\frac{\partial V_x}{\partial x} + \frac{\partial V_y}{\partial y}\right)\, \Delta X\, \Delta Y\, \hat{\boldsymbol{z}} - \Delta X\, \Delta Y\, \left(\frac{\partial V_z}{\partial x}\, \hat{\boldsymbol{x}} + \frac{\partial V_z}{\partial y}\, \hat{\boldsymbol{y}}\right) . \tag{8.3.10}$$

If one now ads a term $(\partial V_z/\partial z)\Delta X\, \Delta Y\, \hat{\boldsymbol{z}}$ to the first term on the right-hand side of this equation, and then substracts it again by including it with the appropriate sign in the second term, one can write this relation as

$$\begin{aligned} \frac{\mathrm{d}\Delta \boldsymbol{O}}{\mathrm{d}t} \;=\; & \Delta X\, \Delta Y\, \left\{\left(\frac{\partial V_x}{\partial x} + \frac{\partial V_y}{\partial y} + \frac{\partial V_z}{\partial z}\right)\, \hat{\boldsymbol{z}}\right. \\ & \left. - \left(\frac{\partial V_z}{\partial x}\, \hat{\boldsymbol{x}} + \frac{\partial V_z}{\partial y}\, \hat{\boldsymbol{y}} + \frac{\partial V_z}{\partial z}\, \hat{\boldsymbol{z}}\right)\right\} . \end{aligned} \tag{8.3.11}$$

This simple trick, together with $\Delta \boldsymbol{O} = \Delta X \Delta Y\, \hat{\boldsymbol{z}}$, allows one to write the whole equation in vector form,

$$\frac{\mathrm{d}\Delta \boldsymbol{O}}{\mathrm{d}t} = (\boldsymbol{\nabla} \cdot \boldsymbol{V})\, \Delta \boldsymbol{O} - (\boldsymbol{\nabla} \boldsymbol{V})\, \cdot \Delta \boldsymbol{O} . \tag{8.3.12}$$

Here I have introduced the *velocity gradient tensor* $\boldsymbol{\nabla V}$, which is a 3×3 tensor that is defined in cartesian coordinates as:

$$\boldsymbol{\nabla V} = \begin{pmatrix} \dfrac{\partial V_x}{\partial x} & \dfrac{\partial V_y}{\partial x} & \dfrac{\partial V_z}{\partial x} \\ \dfrac{\partial V_x}{\partial y} & \dfrac{\partial V_y}{\partial y} & \dfrac{\partial V_z}{\partial y} \\ \dfrac{\partial V_x}{\partial z} & \dfrac{\partial V_y}{\partial z} & \dfrac{\partial V_z}{\partial z} \end{pmatrix} . \tag{8.3.13}$$

This tensor has as it's nine components all possible spatial derivatives of the three velocity components V_x, V_y en V_z. In a more compact notation one can write this tensor as:

$$(\boldsymbol{\nabla V})_{ij} = \frac{\partial V_j}{\partial x_i} . \tag{8.3.14}$$

This means that the second term in relation (8.3.12) reads in component form

$$\boldsymbol{\nabla V}\cdot\Delta\boldsymbol{O}=\left(\sum_j\frac{\partial V_j}{\partial x_i}\,\Delta O_j\right)\,\hat{\boldsymbol{e}}_i=\Delta X\,\Delta Y\,\left(\frac{\partial V_z}{\partial x}\,\hat{\boldsymbol{x}}+\frac{\partial V_z}{\partial y}\,\hat{\boldsymbol{y}}+\frac{\partial V_z}{\partial z}\,\hat{\boldsymbol{z}}\right)\,, \quad (8.3.15)$$

where the last relation is only true for this particular choice of $\Delta\boldsymbol{X}$, $\Delta\boldsymbol{Y}$ and the coordinate system. This is an example of the contraction of a tensor with a vector, which yields another vector.

One can now make a similar argument as was employed in Chapter 2, when we derived the law for the change of volume of a volume element carried passively by the flow. Relation (8.3.12) is written in **vector** form, without reference to the choice of the coordinate system. It must therefore be true in *any* coordinate system by the principle of covariance. The special choice of $\Delta\boldsymbol{X}$ and $\Delta\boldsymbol{Y}$, while mathematically convenient, does not restrict the validity of this result either. Any surface can be built up of small rectangular 'tiles', each of which satisfying relation (8.3.12) so that the relation must be true for *any* infinitesimal surface, regardless its shape. Another sucessful application of the 'Lego Principle'! One can therefore conclude that the change of an infinitesimal surface-element that is carried (and continuously deformed) by the flow satisfies the generally valid relation

$$\boxed{\frac{\mathrm{d}}{\mathrm{d}t}\mathrm{d}\boldsymbol{O}=(\boldsymbol{\nabla}\cdot\boldsymbol{V})\;\mathrm{d}\boldsymbol{O}-\boldsymbol{\nabla V}\cdot\mathrm{d}\boldsymbol{O}\;.} \quad (8.3.16)$$

An alternative derivation of this relation (and the closely related volume-change law) can be found in the book by Roberts[4].

Using relation (8.3.16) in Eqn. (8.3.4) one finds:

$$\frac{\mathrm{d}\Gamma_\mathrm{c}}{\mathrm{d}t}=\int\mathrm{d}\boldsymbol{O}\cdot\left\{\frac{\mathrm{d}\boldsymbol{\omega}}{\mathrm{d}t}-(\boldsymbol{\omega}\cdot\boldsymbol{\nabla})\boldsymbol{V}+\boldsymbol{\omega}(\boldsymbol{\nabla}\cdot\boldsymbol{V})\right\}\;. \quad (8.3.17)$$

Here I used

$$\boldsymbol{\omega}\cdot\,(\boldsymbol{\nabla V}\cdot\mathrm{d}\boldsymbol{O})=[(\boldsymbol{\omega}\cdot\boldsymbol{\nabla})\,\boldsymbol{V}\,]\cdot\mathrm{d}\boldsymbol{O}\;. \quad (8.3.18)$$

[4]P.H. Roberts, 1967: *An Introduction to Magnetohydrodynamics*, Longmans, Green and Co Ltd., London, Ch. 1.7

Substituting the vorticity equation of motion (8.2.10) in the form

$$\frac{\mathrm{d}\boldsymbol{\omega}}{\mathrm{d}t} - (\boldsymbol{\omega}\cdot\boldsymbol{\nabla})\boldsymbol{V} + \boldsymbol{\omega}(\boldsymbol{\nabla}\cdot\boldsymbol{V}) = \frac{1}{\rho^2}\,\boldsymbol{\nabla}\rho\times\boldsymbol{\nabla}P \tag{8.3.19}$$

into (8.3.17), one finds the following law for the change of the circulation Γ_{c} around a curve that is passively advected by the flow:

$$\boxed{\frac{\mathrm{d}\Gamma_{\mathrm{c}}}{\mathrm{d}t} = \frac{\mathrm{d}}{\mathrm{d}t}\left(\int \mathrm{d}\boldsymbol{O}\cdot\boldsymbol{\omega}(\boldsymbol{x}\,,\,t)\right) = \int \mathrm{d}\boldsymbol{O}\cdot\frac{(\boldsymbol{\nabla}\rho\times\boldsymbol{\nabla}P)}{\rho^2}\,.} \tag{8.3.20}$$

This result leads to *Kelvin's theorem*, which in its original form reads:

In a homogeneous fluid the circulation Γ_{c} around a closed curve carried by the fluid is constant

As one can see from (8.3.20) Kelvin's theorem holds not only in a homogeneous fluid where $\boldsymbol{\nabla}P = 0$ and $\boldsymbol{\nabla}\rho = 0$. The condition $\boldsymbol{\nabla}P\times\boldsymbol{\nabla}\rho = 0$ is in fact sufficient. If Kelvin's theorem holds, the so-called *vortex strength* of a vortex tube, i.e. a tube whose boundary is made up of vortex lines, is constant: $\Gamma_{\mathrm{c}} = \int \mathrm{d}\boldsymbol{O}\cdot\boldsymbol{\omega} =$ constant. This means that the curve bounding the outer edge of the tube always encloses a fixed amount of (surface-integrated) vorticity as it is being progressively deformed by the flow. This is illustrated below.

Kelvin's circulation theorem explains while some structures (vortex tubes) with a strongly localised and large vorticity, such as tornadoes, water sprouts and smoke rings (i.e. a closed vortex tube), are so suprisingly stable, once formed.

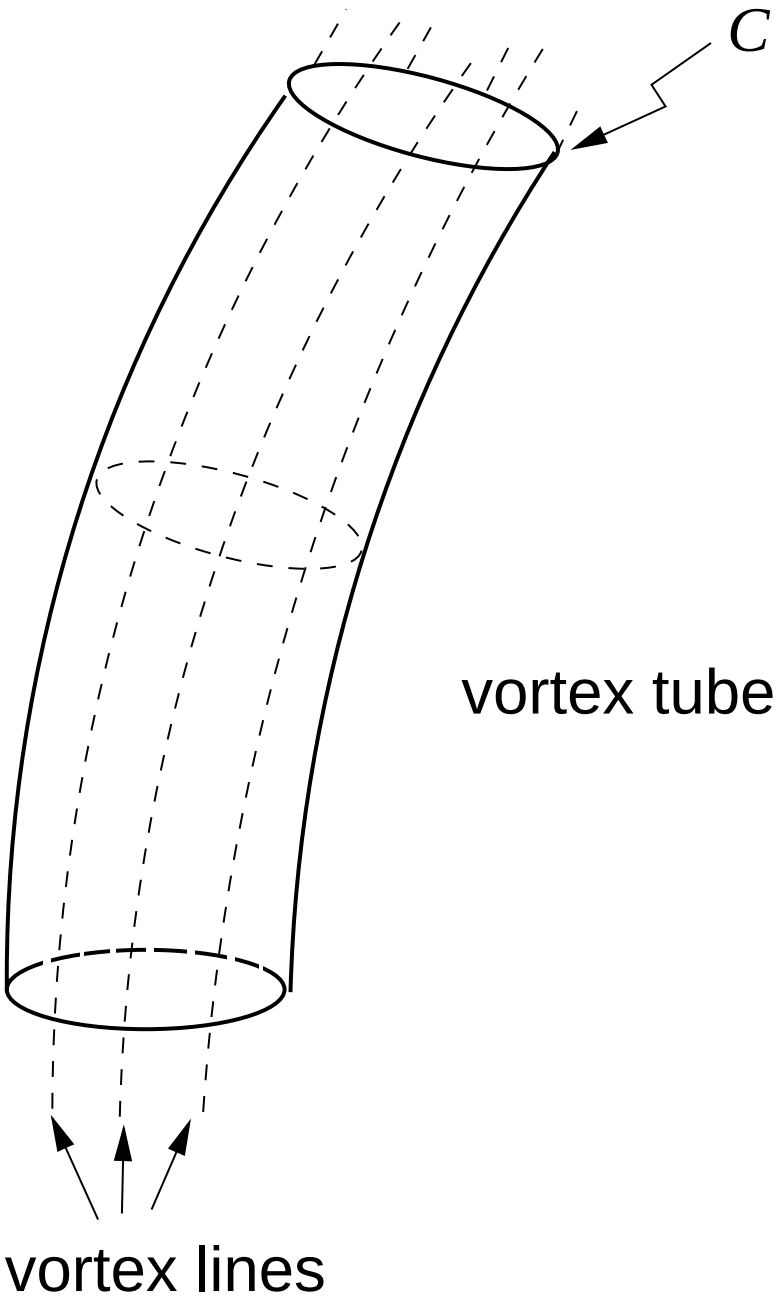

Figure 8.1: *A vortex tube has an outer surface formed by vortex lines. The circulation* $\Gamma_{\rm c}$ *corresponds to the vorticity component along the tube axis, integrated over the tube cross-section. It is the analogue of the magnetic flux in a magnetic flux tube. If Kelvin's theorem holds, the circulation is conserved as the fluid moves and deformes the shape (both length and cross-section) of the tube.*

8.4 Application to a thin vortex tube

Let us consider a thin vortex tube, a bundle of vortex lines, with such a small cross section that the magnitude of the vorticity $\boldsymbol{\omega}$ can be considered constant over its cross section. In that case the circulation associated with the closed curve around the cross section is simply (see figure below)

$$\Gamma_{\rm c} \equiv \int {\rm d}\boldsymbol{O} \cdot \boldsymbol{\omega} = |\boldsymbol{\omega}|\, \mathcal{A} \; . \tag{8.4.1}$$

Here $\mathcal{A}$ is the area of the cross section, and I have used that in this case the vorticity vector is perpendicular to the cross section surface.

As the tube is advected by the flow, it is deformed. But since the outer surface of the tube consists of vortex lines, and since vortex lines are material curves, **no** mass can flow across the cylindrical surface. Consider a small section of the tube with length $\Delta\ell$. The total amount of mass contained in that small section is

$$\Delta M = \rho\, \mathcal{A}\, \Delta\ell \; . \tag{8.4.2}$$

In principle $\mathcal{A}$ is a function of position ℓ along the tube axis, but this is not important for what follows. If we follow this mass-element as the tube is deformed, its mass must be conserved as no mass can flow into or out of the tube across its cylindrical surface:

$$\rho\, \mathcal{A}\, \Delta\ell = \text{constant}. \tag{8.4.3}$$

If $\boldsymbol{\nabla}\rho \times \boldsymbol{\nabla} P = 0$, there is also no production of new vorticity, and the circulation theorem applies so that $\Gamma_{\rm c}$ is a conserved quantity:

$$\Gamma_{\rm c} = |\boldsymbol{\omega}|\, \mathcal{A} = \text{constant}. \tag{8.4.4}$$

To fix the values of the two constants, these two conservation laws can be applied at some reference time t_0, when the density inside the element is ρ_0, the cross section is $\mathcal{A}_0$ and the length of the section of tube equals $\Delta\ell_0$. At an arbitrary (later) time t the conservation of mass and circulation give:

$$\begin{aligned} \rho\, \mathcal{A}\, \Delta\ell &= \rho_0\, \mathcal{A}_0\, \Delta\ell_0 \; , \\ |\boldsymbol{\omega}|\, \mathcal{A} &= |\boldsymbol{\omega}|_0\, \mathcal{A}_0 \; , \end{aligned} \tag{8.4.5}$$

where ρ, $\mathcal{A}$ and $\Delta\ell$ are the density, cross section and length of the mass-element at time t. Combining these two relations by eliminating the tube cross section using

$$\frac{\mathcal{A}}{\mathcal{A}_0} = \frac{\rho_0}{\rho}\,\frac{\Delta\ell_0}{\Delta\ell}\,, \tag{8.4.6}$$

the conservation of circulation yields:

$$\frac{|\boldsymbol{\omega}|}{\rho} = \frac{|\boldsymbol{\omega}_0|}{\rho_0}\,\frac{\Delta\ell}{\Delta\ell_0}\,. \tag{8.4.7}$$

This should look familiar: it is essentially relation (8.2.20)! Therefore, the conservation of circulation (Kelvin's theorem) for thin vortex tubes is equivalent with the vortex stretching law.

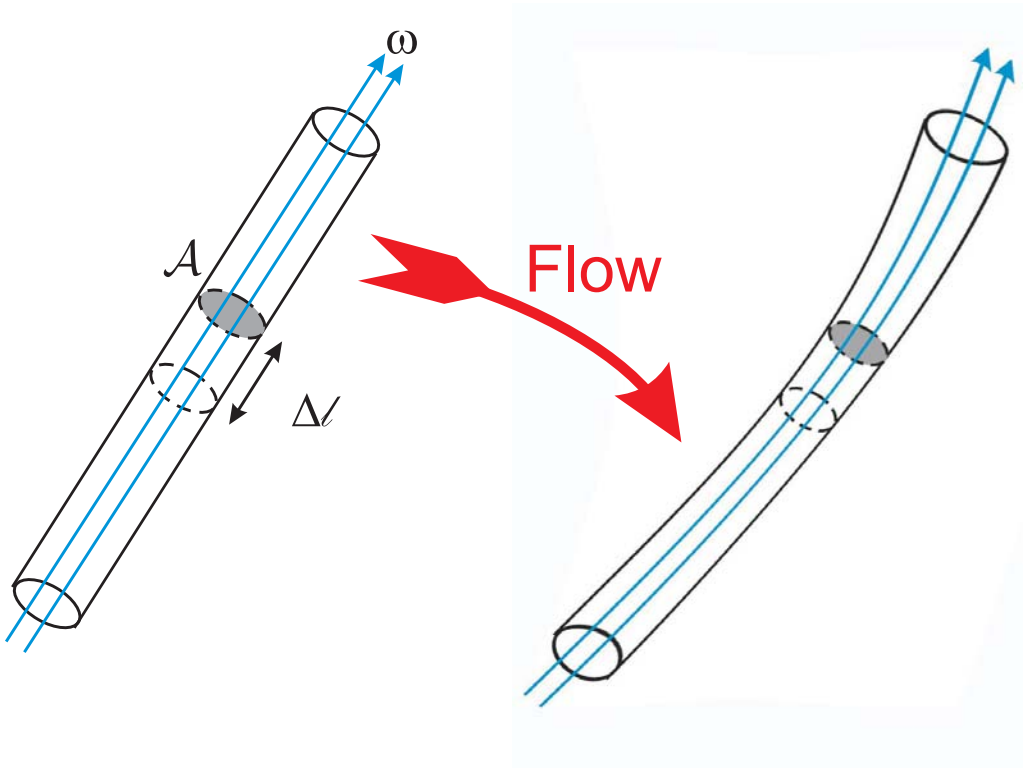

Figure 8.2: *A thin vortex tube, made of a bundle of vortex lines, is deformed by the flow. As a result, the length $\Delta\ell$ and the cross section $\mathcal{A}$ of a small mass-element in the tube changes.*

8.5 Cylindrical and rotating coordinates

In rotating flows in two dimensions, such as the flow in an accretion disk, in the Earth's atmosphere and the motion in disk galaxies, it is convenient to use *cylindrical polar coordinates* R, θ and Z. These coordinates are related to ordinary (cartesian) coordinates x, y and z through the set of relations

$$x = R\,\cos\theta \quad , \quad y = R\,\sin\theta \quad , \quad z = Z\,. \tag{8.5.1}$$

The inverse relations, which give the cartesian coordinates x, y and z as functions of the cylindrical coordinates, read

$$R = \sqrt{x^2 + y^2} \quad , \quad \theta = \tan^{-1}(y/x) \quad , \quad Z = z\,. \tag{8.5.2}$$

The unit vectors of the cylindrical coordinates are given in terms of the unit vectors $\hat{\boldsymbol{x}}$, $\hat{\boldsymbol{y}}$ and $\hat{\boldsymbol{z}}$ of the cartesian coordinate system as (see Figure below)

$$\hat{\boldsymbol{e}}_R = \cos\theta\,\hat{\boldsymbol{x}} + \sin\theta\,\hat{\boldsymbol{y}} \;\; , \;\; \hat{\boldsymbol{e}}_\theta = -\sin\theta\,\hat{\boldsymbol{x}} + \cos\theta\,\hat{\boldsymbol{y}} \;\; , \;\; \hat{\boldsymbol{e}}_Z = \hat{\boldsymbol{z}}\,. \tag{8.5.3}$$

Like the cartesian unit vectors these three vectors are a *orthonormal* set, where the unit vectors $\hat{\boldsymbol{e}}_i$ satisfy:

$$\hat{\boldsymbol{e}}_i \cdot \hat{\boldsymbol{e}}_j = \delta_{ij} = \begin{cases} 1 & \text{when } i = j \\ \\ 0 & \text{when } i \neq j \end{cases} \quad . \tag{8.5.4}$$

The indices i, j can each take the value 1, 2 and 3, where $\hat{\boldsymbol{e}}_1 = \hat{\boldsymbol{e}}_R$, $\hat{\boldsymbol{e}}_2 = \hat{\boldsymbol{e}}_\theta$ and $\hat{\boldsymbol{e}}_3 = \hat{\boldsymbol{e}}_Z$.

An arbitrary vector $\boldsymbol{A}$ has an identity *regardless* the coordinates employed to represent it: it is a arrow with a certain direction and a certain length. In a given coordinate system it can be written in component form,

$$\boldsymbol{A} = A_1\,\hat{\boldsymbol{e}}_1 + A_2\,\hat{\boldsymbol{e}}_2 + A_3\,\hat{\boldsymbol{e}}_3 \equiv A_i\,\hat{\boldsymbol{e}}_i\,, \tag{8.5.5}$$

where the last term on the right-hand side uses the Einstein summation convention.

The components A_1, A_2 and A_3 form a set three *scalar* functions that are defined, **in an orthonormal coordinate system only**, by the projection of $\boldsymbol{A}$ on the unit vector $\hat{\boldsymbol{e}}_i$.

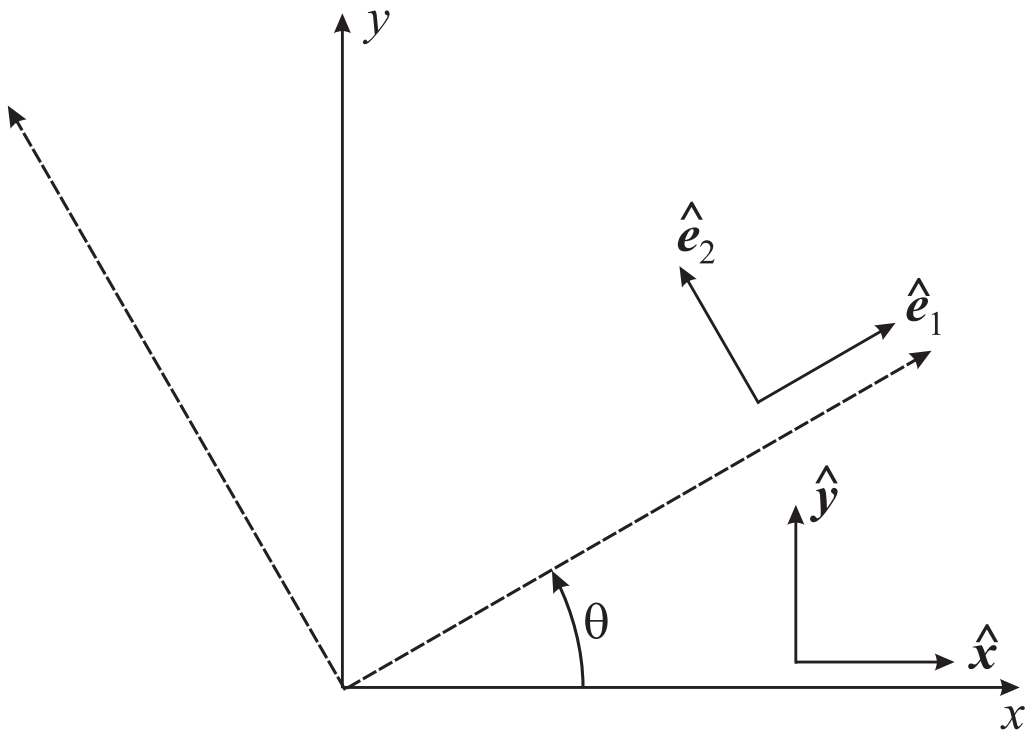

Figure 8.3: *The relation between the unit vectors $\hat{\boldsymbol{x}}$ and $\hat{\boldsymbol{y}}$ of a cartesian coordinate system, and the two unit vectors $\hat{\boldsymbol{e}}_1$ and $\hat{\boldsymbol{e}}_2$ of cylindrical coordinates in the $x-y$ plane. The angle θ is the polar angle*

This projection corresponds to a scalar product:

$$A_i \equiv \boldsymbol{A} \cdot \hat{\boldsymbol{e}}_i = |\boldsymbol{A}| \cos\alpha_i \quad (\text{with } i = 1\ ,\ 2\ ,\ 3)\ . \tag{8.5.6}$$

Here α_i is the angle between $\boldsymbol{A}$ and $\hat{\boldsymbol{e}}_i$. This relation follows immediately from (8.5.4). Using this general recipe for finding vector components, together with definition (8.5.3) that is valid for the particular case of cylindrical coordinates, one finds the components of $\boldsymbol{A}$ in a cylindrical coordinate system:

$$\begin{aligned} A_R &= \boldsymbol{A} \cdot \hat{\boldsymbol{e}}_R = A_x\ \cos\theta + A_y\ \sin\theta\ , \\ A_\theta &= \boldsymbol{A} \cdot \hat{\boldsymbol{e}}_\theta = -A_x\ \sin\theta + A_y\ \cos\theta\ , \\ A_Z &= \boldsymbol{A} \cdot \hat{\boldsymbol{e}}_Z = A_z\ . \end{aligned} \tag{8.5.7}$$

The most important difference between the three cartesian unit vectors $\hat{\boldsymbol{x}}$, $\hat{\boldsymbol{y}}$ and $\hat{\boldsymbol{z}}$ and the three unit vectors $\hat{\boldsymbol{e}}_i$ of cylindrical coordinates, or in any set of orthonormal curvilinear coordinates[5], is that the orientation of the unit vectors is a function of position:

$$\hat{\boldsymbol{e}}_1(\boldsymbol{x}) \quad , \quad \hat{\boldsymbol{e}}_2(\boldsymbol{x}) \quad , \quad \hat{\boldsymbol{e}}_3(\boldsymbol{x})\ . \tag{8.5.8}$$

In this particlular case the unit vectors $\hat{\boldsymbol{e}}_R$ and $\hat{\boldsymbol{e}}_\theta$ rotate as the polar angle θ changes. Cylindrical coordinates form an example of a *curvilinear coordinate system*.

One can also employ a **rotating** frame of reference, for instance a system where two of the coordinate axes rotate with a fixed angular frequency Ω around the z-axis. If one chooses to employ cylindrical coordinates in the rotating reference frame, relation (8.5.1) is replaced by

$$x = R\ \cos(\overline{\theta} + \Omega t) \quad , \quad y = R\ \sin(\overline{\theta} + \Omega t) \quad , \quad z = Z\ . \tag{8.5.9}$$

This definition in effect introduces a new polar angle $\overline{\theta}$ defined by:

$$\theta = \overline{\theta} + \Omega t\ . \tag{8.5.10}$$

[5]See the Mathematical Appendix on Internet

The angle θ is the polar angle as measured by an observer in a fixed frame of reference, while $\overline{\theta}$ is the corresponding angle as measured by an observer in the rotating frame. For such a rotating coordinate frame, the unit vectors $\hat{\boldsymbol{e}}_i(\boldsymbol{x}\ ,\ t)$ as seen from the fixed reference frame are a function of both position **and** time. They are given by:

$$\begin{aligned} \hat{\boldsymbol{e}}_R &= \cos(\overline{\theta}+\Omega t)\,\hat{\boldsymbol{x}} + \sin(\overline{\theta}+\Omega t)\,\hat{\boldsymbol{y}} \\ \hat{\boldsymbol{e}}_{\overline{\theta}} &= -\sin(\overline{\theta}+\Omega t)\,\hat{\boldsymbol{x}} + \cos(\overline{\theta}+\Omega t)\,\hat{\boldsymbol{y}} \\ \hat{\boldsymbol{e}}_Z &= \hat{\boldsymbol{z}}\ . \end{aligned} \tag{8.5.11}$$

Of course, for an observer rotating with the coordinate frame, the unit vectors $\hat{\boldsymbol{e}}_R$, $\hat{\boldsymbol{e}}_{\overline{\theta}}$ and $\hat{\boldsymbol{e}}_Z$ do not change in time!

In both these examples we are dealing with *curvilinear coordinates* since the surfaces of constant radius, say $R = R_0$, are cylinders around the z-axis with radius R_0. The level surface of R is curved, unlike the level surfaces x=constant, y=constant or z=constant of a cartesian coordinate frame. The associated change in the orientation of the unit vectors, which are always perpendicular to a level surface, has an immediate consequence for the differentiation of vectors, and for vector-analysis.

Consider a vector, such as the velocity $\boldsymbol{V}$ or the position $\boldsymbol{x}$ of a fluid element. If we call this vector $\boldsymbol{A}(\boldsymbol{x}\ ,\ t)$, the change $\mathrm{d}\boldsymbol{A}$ of this vector in some time interval $\mathrm{d}t$, or between to close points in space is (remember the summation convention!)

$$\mathrm{d}\boldsymbol{A} = (\mathrm{d}A_i)\,\hat{\boldsymbol{e}}_i + A_i\,\mathrm{d}\hat{\boldsymbol{e}}_i\ . \tag{8.5.12}$$

The second term on the right-hand side of this expression takes account of the change of the unit vectors. Because of the orthonormal condition (8.5.4), the change $\mathrm{d}\hat{\boldsymbol{e}}_i$ of any of the three unit vectors must be orthogonal to itself, e.g.

$$\hat{\boldsymbol{e}}_1\cdot\hat{\boldsymbol{e}}_1 = 1 \iff \mathrm{d}\,(\hat{\boldsymbol{e}}_1\cdot\hat{\boldsymbol{e}}_1) = 2\hat{\boldsymbol{e}}_1\cdot\mathrm{d}\hat{\boldsymbol{e}}_1 = 0\ , \tag{8.5.13}$$

with similar relations for $\hat{\boldsymbol{e}}_2$ and $\hat{\boldsymbol{e}}_3$. For example, the infinitesimal vector $\mathrm{d}\hat{\boldsymbol{e}}_1$ has components that lie in the plane defined by the two other unit vectors $\hat{\boldsymbol{e}}_2$ and $\hat{\boldsymbol{e}}_3$. Relation (8.5.12) implies that the *components* of $\mathrm{d}\boldsymbol{A}$ are given by

$$(\mathrm{d}\boldsymbol{A})_j \equiv \mathrm{d}\boldsymbol{A}\cdot\hat{\boldsymbol{e}}_j = \mathrm{d}A_j + A_i\ (\mathrm{d}\hat{\boldsymbol{e}}_i\cdot\hat{\boldsymbol{e}}_j)\ . \tag{8.5.14}$$

In a curvilinear coordinate system the second term does not vanish in general. Therefore, the components of $\mathrm{d}\boldsymbol{A}$ do in general **not** coincide with *the change of the components* $\mathrm{d}A_i$ $(i = 1\ ,\ 2\ ,3)$ *unless* all three unit vectors are *fixed* so that all $\mathrm{d}\hat{\boldsymbol{e}}_i = 0$. If that is not the case, the change in direction of the unit vectors leads to the other vector components 'mixing' into the expression for the components of $\mathrm{d}\boldsymbol{A}$. This is one of the reasons why differential operators in curvilinear coordinates are more complicated than in cartesian coordinates.

8.6 Distance recipe, gradient, rotation and divergence

8.6.1 Distance, surface and volume

The change of the direction of the unit vectors, and the complication it introduces in the calculation of vector differences in terms of components, leads to more complicated expressions for the gradient, rotation and divergence of a vector. There is however an *additional* reason for these complicated expressions. It has to do with the recipe for calculating physical distances in curvilinear coordinates. Consider two infinitesimally close points, $\boldsymbol{x}$ and $\boldsymbol{x'} = \boldsymbol{x} + \mathrm{d}\boldsymbol{x}$. If we call the first point P and the second P', they are defined by their respective coordinates:

$$P = (x_1\ ,\ x_2\ ,\ x_3) \quad , \quad P' = (x_1 + \mathrm{d}x_1\ ,\ x_2 + \mathrm{d}x_2\ ,\ x_3 + \mathrm{d}x_3)\ . \tag{8.6.1}$$

In curvilinear coordinates, the infinitesimal vector separating these two points is given by

$$\mathrm{d}\boldsymbol{x} = (h_1\,\mathrm{d}x_1)\ \hat{\boldsymbol{e}}_1 + (h_2\,\mathrm{d}x_2)\ \hat{\boldsymbol{e}}_2 + (h_3\,\mathrm{d}x_3)\ \hat{\boldsymbol{e}}_3\ , \tag{8.6.2}$$

which defines the *physical* displacement along each of the three coordinate axes in terms of the coordinate differences. The three so-called *Lamé coefficients* h_1, h_2 and h_3 are scale factors. They are needed because, in general, the three curvilinear coordinates x_1, x_2 and x_3 do **not** have the dimension of [length]. For example: the polar angle θ that is used in cylindrical polar coordinates is a a dimensionless quantity. So a Lamé-factor with dimension [length] is needed to convert the angular separation $\mathrm{d}\theta$ between two points into the corresponding physical distance. In this particular case one has $h_\theta = R$, see below. As soon as at least one of the Lamé-coefficients becomes a function of position[6] at least two of the unit vectors (because of orthonormality) must change their orientation from point to point. In that case one is dealing with a curvilinear coordinate system.

[6] From a geometrical point of view this means: there exists no **global** scale transformation of the form $x_1 \to \alpha x_1$, $x_2 \to \beta x_2$ and $x_3 \to \gamma x_3$ where the constant parameters α, β and γ can be chosen in such a way that the new coordinate system is a system where $h_1 = h_2 = h_3 = 1$ everywhere.

Prescription (8.6.2) implies for orthonormal coordinates that the distance $\mathrm{d}s$ between point P and point P' is given by the recipe

$$\mathrm{d}s^2 \equiv \mathrm{d}\boldsymbol{x} \cdot \mathrm{d}\boldsymbol{x} = h_1^2\,\mathrm{d}x_1^2 + h_2^2\,\mathrm{d}x_2^2 + h_1^3\,\mathrm{d}x_3^2\,. \tag{8.6.3}$$

In the same fashion, the expression for the surface area and of the volume-element is more complicated in curvilinear coordinates.

For instance, consider the surface in the x_1-x_2 plane with edges defined by the two infinitesimal vectors

$$\mathrm{d}\boldsymbol{r}_1 = h_1\,\mathrm{d}x_1\,\hat{\boldsymbol{e}}_1 \quad , \quad \mathrm{d}\boldsymbol{r}_2 = h_2\,\mathrm{d}x_2\,\hat{\boldsymbol{e}}_2\,. \tag{8.6.4}$$

The oriented surface defined by these two vectors is

$$\mathrm{d}\boldsymbol{O} = \mathrm{d}\boldsymbol{r}_1 \times \mathrm{d}\boldsymbol{r}_2 = h_1 h_2\,\mathrm{d}x_1\mathrm{d}x_2\,\hat{\boldsymbol{e}}_3\,. \tag{8.6.5}$$

Here I have used the relation $\hat{\boldsymbol{e}}_1 \times \hat{\boldsymbol{e}}_2 = \hat{\boldsymbol{e}}_3$, valid for a right-handed orthonormal set of unit vectors. The corresponding surface area equals

$$|\mathrm{d}\boldsymbol{O}| = h_1 h_2\,\mathrm{d}x_1\mathrm{d}x_2\,. \tag{8.6.6}$$

Defining a third infinitesimal vector

$$\mathrm{d}\boldsymbol{r}_3 = h_3\,\mathrm{d}x_3\,\hat{\boldsymbol{e}}_3\,, \tag{8.6.7}$$

the volume-element defined by the three infinitesimal vectors is

$$\mathrm{d}\mathcal{V} = \mathrm{d}\boldsymbol{r}_1 \cdot (\mathrm{d}\boldsymbol{r}_2 \times \mathrm{d}\boldsymbol{r}_3) = h_1 h_2 h_3\,\mathrm{d}x_1\mathrm{d}x_2\mathrm{d}x_3\,, \tag{8.6.8}$$

since $\hat{\boldsymbol{e}}_1 \cdot (\hat{\boldsymbol{e}}_2 \times \hat{\boldsymbol{e}}_3) = 1$. This is the fundamental expression for the volume-element in curvilinear coordinates.

8.6.2 gradient, rotation and divergence

Now consider the gradient operator acting on some scalar function $f(x_1\,,\,x_2\,,\,x_3)$ of the three curvilinear coordinates. The components of the gradient can be defined formally by

$$\boldsymbol{\nabla} f \cdot \hat{\boldsymbol{e}}_i = \frac{\text{change of } f \text{ in direction } i}{\text{physical distance}}\,. \tag{8.6.9}$$

The change $\mathrm{d}f$ in f corresponding to a change $\mathrm{d}x_i$ in coordinate x_i is simply

$$\mathrm{d}f = \left(\frac{\partial f}{\partial x_i}\right)\,\mathrm{d}x_i \quad (\textbf{no} \text{ summation over } i!) \tag{8.6.10}$$

The physical distance corresponding to this coordinate interval is (by definition) $\mathrm{d}s = h_i\,\mathrm{d}x_i$. It follows that the i-th component of the gradient is

$$(\boldsymbol{\nabla} f)_i = \frac{(\partial f/\partial x_i)\,\mathrm{d}x_i}{h_i\,\mathrm{d}x_i} = \frac{1}{h_i}\,\frac{\partial f}{\partial x_i}\,. \tag{8.6.11}$$

The gradient of a scalar function in curvilinear coordinates must therefore be a vector that is defined by:

$$\boxed{\boldsymbol{\nabla} f = \frac{1}{h_1}\,\frac{\partial f}{\partial x_1}\,\hat{\boldsymbol{e}}_1 + \frac{1}{h_2}\,\frac{\partial f}{\partial x_2}\,\hat{\boldsymbol{e}}_2 + \frac{1}{h_3}\,\frac{\partial f}{\partial x_3}\,\hat{\boldsymbol{e}}_3\,.} \tag{8.6.12}$$

The rotation and divergence of a vector can be calculated using Stokes theorem for these quantities,

$$\int \mathrm{d}\mathcal{V}\,(\boldsymbol{\nabla}\cdot\boldsymbol{A}) = \int \mathrm{d}\boldsymbol{O}\cdot\boldsymbol{A} \quad , \quad \int \mathrm{d}\boldsymbol{O}\cdot(\boldsymbol{\nabla}\times\boldsymbol{A}) = \oint \mathrm{d}\boldsymbol{r}\cdot\boldsymbol{A}\,, \tag{8.6.13}$$

together with the expressions for the physical distance, the surface element and the volume element derived above. Full details of the derivation can be found in the book by Morse & Feshbach[7], or in the Mathematical Appendix on Internet. Here I simply quote the final results.

[7] P.M. Morse & H. Feshbach, 1953: *Methods of Theoretical Physics*, Vol. I, McGraw-Hill, New York, Ch. 1.3.

The rotation (curl) of some vector $\boldsymbol{A}$ yields another vector that can be represented in determinant form as

$$\boldsymbol{\nabla} \times \boldsymbol{A} = \frac{1}{h_1\, h_2\, h_3} \left\| \begin{array}{ccc} h_1\hat{\boldsymbol{e}}_1 & h_2\hat{\boldsymbol{e}}_2 & h_3\hat{\boldsymbol{e}}_3 \\ \dfrac{\partial}{\partial x_1} & \dfrac{\partial}{\partial x_2} & \dfrac{\partial}{\partial x_3} \\ h_1 A_1 & h_2 A_2 & h_3 A_3 \end{array} \right\| . \tag{8.6.14}$$

The divergence of a vector $\boldsymbol{A}$ (a scalar!) takes the form

$$\boldsymbol{\nabla} \cdot \boldsymbol{A} = \frac{1}{h_1\, h_2\, h_3} \left[\frac{\partial(h_2 h_3\, A_1)}{\partial x_1} + \frac{\partial(h_3 h_1\, A_2)}{\partial x_2} + \frac{\partial(h_1 h_2\, A_3)}{\partial x_3} \right] . \tag{8.6.15}$$

8.6.3 The directional derivative

A final important quantity is the *directional derivative* along some vector. Anticipating our application in fluid mechanics, consider the derivative along a vector $\boldsymbol{V}$, defined formally for a function $f(\boldsymbol{x})$ as the scalar product of $\boldsymbol{V}$ with $\boldsymbol{\nabla} f$ (both vectors!):

$$(\boldsymbol{V} \cdot \boldsymbol{\nabla}) f = \frac{V_1}{h_1} \frac{\partial f}{\partial x_1} + \frac{V_2}{h_2} \frac{\partial f}{\partial x_2} + \frac{V_3}{h_3} \frac{\partial f}{\partial x_3} . \tag{8.6.16}$$

This definition can be generalized to calculate the directional derivatives of vectors and tensors, *provided* one does not forget to take account of the terms which result from the change of orientation of the unit vectors, c.f. Eqn. (8.5.14). One can define the general operator for the directional derivative along $\boldsymbol{V}$ as

$$\boxed{\boldsymbol{V} \cdot \boldsymbol{\nabla} \equiv \frac{V_1}{h_1} \frac{\partial}{\partial x_1} + \frac{V_2}{h_2} \frac{\partial}{\partial x_2} + \frac{V_3}{h_3} \frac{\partial}{\partial x_3} \equiv \frac{V_j}{h_j} \frac{\partial}{\partial x_j} .} \tag{8.6.17}$$

The directional derivative of some vector $\boldsymbol{A}$ then becomes formally

$$(\boldsymbol{V} \cdot \boldsymbol{\nabla}) \boldsymbol{A} = (\boldsymbol{V} \cdot \boldsymbol{\nabla} A_i)\, \hat{\boldsymbol{e}}_i + A_i\, (\boldsymbol{V} \cdot \boldsymbol{\nabla} \hat{\boldsymbol{e}}_i) . \tag{8.6.18}$$

The second term on the right-hand side gives the effect of the change in orientation of the unit vectors. It can be written out as

$$(\boldsymbol{V}\cdot\boldsymbol{\nabla}\hat{\boldsymbol{e}}_i) = \frac{V_1}{h_1}\frac{\partial\hat{\boldsymbol{e}}_i}{\partial x_1} + \frac{V_2}{h_2}\frac{\partial\hat{\boldsymbol{e}}_i}{\partial x_2} + \frac{V_3}{h_3}\frac{\partial\hat{\boldsymbol{e}}_i}{\partial x_3}\ . \tag{8.6.19}$$

If one now calculates the *components* of derivative (8.6.18), using the general rule $B_i = \boldsymbol{B}\cdot\hat{\boldsymbol{e}}_i$ for finding vector components, one finds:

$$\begin{aligned}[(\boldsymbol{V}\cdot\boldsymbol{\nabla})\boldsymbol{A}\,]_i &= (\boldsymbol{V}\cdot\boldsymbol{\nabla}A_i) + \sum_{k=1}^{3} A_k\ [(\boldsymbol{V}\cdot\boldsymbol{\nabla}\hat{\boldsymbol{e}}_k)\cdot\hat{\boldsymbol{e}}_i\,] \\ &= \sum_{j=1}^{3}\frac{V_j}{h_j}\frac{\partial A_i}{\partial x_j} + \sum_{j=1}^{3}\sum_{k=1}^{3} A_k\left(\frac{V_j}{h_j}\frac{\partial\hat{\boldsymbol{e}}_k}{\partial x_j}\right)\cdot\hat{\boldsymbol{e}}_i\ .\end{aligned} \tag{8.6.20}$$

Again one sees how vector components A_k are 'mixed' into this expression when the three unit vectors do not (all) have a fixed orientation, but vary their direction from point to point. By considering the second term one sees that one has to calculate a set of coefficients[8] of the form

$$\Gamma^i_{jk} \equiv \hat{\boldsymbol{e}}_i\cdot\ [(\hat{\boldsymbol{e}}_j\cdot\boldsymbol{\nabla})\hat{\boldsymbol{e}}_k] = \left[\frac{1}{h_j}\frac{\partial\hat{\boldsymbol{e}}_k}{\partial x_j}\right]\cdot\hat{\boldsymbol{e}}_i \quad (\textbf{no}\ \text{summation over}\ j!) \tag{8.6.21}$$

in order to evaluate expression (8.6.20). Note that the orthonormality of the three unit vectors implies that $\Gamma^i_{jk} = 0$ for $i = k$.

These coefficients Γ^i_{jk} contain information about the geometrical properties of the level surfaces $x_i = \text{constant}$ in the coordinate system. Only for cartesian coordinates do they all vanish. In terms of these coefficients the components of the directional derivative of some vector $\boldsymbol{A}$ along the vector $\boldsymbol{V}$ are (using the summation convention)

$$[(\boldsymbol{V}\cdot\boldsymbol{\nabla})\boldsymbol{A}\,]_i = (\boldsymbol{V}\cdot\boldsymbol{\nabla})A_i + \Gamma^i_{jk}\,V_j\,A_k\ . \tag{8.6.22}$$

The formal expressions for the derivatives of the unit vectors $\hat{\boldsymbol{e}}_1$, $\hat{\boldsymbol{e}}_2$ and $\hat{\boldsymbol{e}}_3$, needed to calculate the Γ^i_{jk}, can be found in the Mathematical Appendix on Internet.

[8]The notation here is chosen to conform to the convention used in most textbooks on *General Relativity*, where the corresponding quantities are known as the *connection coefficients* or as the *Christoffel symbols*.

8.6.4 Application to cylindrical polar coordinates

Let us apply these results to cylindrical polar coordinates, formally defining

$$x_1 = R \quad , \quad x_2 = \theta \quad , \quad x_3 = Z \; . \tag{8.6.23}$$

As illustrated in the figure below, the distance recipe in this case reads

$$\mathrm{d}s^2 = dR^2 + R^2 \, \mathrm{d}\theta^2 + \mathrm{d}Z^2 \; . \tag{8.6.24}$$

This corresponds to a set of Lamé coefficients equal to

$$h_1 = h_3 = 1 \quad , \quad h_2 = R \; . \tag{8.6.25}$$

A surface area in the x-y plane is

$$\mathrm{d}O = R \, \mathrm{d}\theta \, \mathrm{d}R \; , \tag{8.6.26}$$

and the volume-element is

$$\mathrm{d}\mathcal{V} = R \, \mathrm{d}R \, \mathrm{d}\theta \, \mathrm{d}Z \; . \tag{8.6.27}$$

The unit vectors $\hat{\boldsymbol{e}}_R$ and $\hat{\boldsymbol{e}}_\theta$, which reside in the x-y plane, vary their direction as θ changes. In contrast, their direction remains the same if one moves in the R- or in the Z-direction. From the figure, or from a direct calculation that uses the definition of $\hat{\boldsymbol{e}}_R$ and $\hat{\boldsymbol{e}}_\theta$ in terms of the fixed unit vectors $\hat{\boldsymbol{x}}$ and $\hat{\boldsymbol{y}}$, one immediately finds that the change of the two unit vectors is given by:

$$\mathrm{d}\hat{\boldsymbol{e}}_R = \mathrm{d}\theta \, \hat{\boldsymbol{e}}_\theta \quad , \quad \mathrm{d}\hat{\boldsymbol{e}}_\theta = -\mathrm{d}\theta \, \hat{\boldsymbol{e}}_R \; . \tag{8.6.28}$$

For example, using definition (8.5.3) one has:

$$\begin{aligned} \mathrm{d}\hat{\boldsymbol{e}}_R &= \mathrm{d}\left(\cos\theta \, \hat{\boldsymbol{x}} + \sin\theta \, \hat{\boldsymbol{y}}\right) \\ &= -(\sin\theta \, \mathrm{d}\theta) \, \hat{\boldsymbol{x}} + (\cos\theta \, \mathrm{d}\theta) \, \hat{\boldsymbol{y}} = \mathrm{d}\theta \, \hat{\boldsymbol{e}}_\theta \; . \end{aligned} \tag{8.6.29}$$

All this implies that the only non-vanishing coefficients entering relation (8.6.22) are due to the change of $\hat{\boldsymbol{e}}_R$ and $\hat{\boldsymbol{e}}_\theta$ as a function of the polar angle θ:

$$\Gamma^R_{\theta\theta} = \frac{1}{R} \quad , \quad \Gamma^\theta_{\theta R} = -\frac{1}{R} \tag{8.6.30}$$

The gradient operator is

$$\boldsymbol{\nabla} f = \frac{\partial f}{\partial R}\,\hat{\boldsymbol{e}}_R + \frac{1}{R}\frac{\partial f}{\partial \theta}\,\hat{\boldsymbol{e}}_\theta + \frac{\partial f}{\partial Z}\,\hat{\boldsymbol{e}}_Z \; . \tag{8.6.31}$$

The derivative of some vector $\boldsymbol{A}$ along a vector $\boldsymbol{V}$ reads

$$\begin{aligned}(\boldsymbol{V}\cdot\boldsymbol{\nabla})\boldsymbol{A} \;\; = \;\; & \left(V_R\,\frac{\partial A_R}{\partial R} + \frac{V_\theta}{R}\frac{\partial A_R}{\partial \theta} + V_Z\,\frac{\partial A_R}{\partial Z} - \frac{V_\theta A_\theta}{R}\right)\,\hat{\boldsymbol{e}}_R \\ & + \left(V_R\,\frac{\partial A_\theta}{\partial R} + \frac{V_\theta}{R}\frac{\partial A_\theta}{\partial \theta} + V_Z\,\frac{\partial A_\theta}{\partial Z} + \frac{V_\theta A_R}{R}\right)\,\hat{\boldsymbol{e}}_\theta \\ & + \left(V_R\,\frac{\partial A_Z}{\partial R} + \frac{V_\theta}{R}\frac{\partial A_Z}{\partial \theta} + V_Z\,\frac{\partial A_Z}{\partial Z}\right)\,\hat{\boldsymbol{e}}_Z \; .\end{aligned} \tag{8.6.32}$$

Finally, the divergence and the rotation of some vector $\boldsymbol{A}$ are given by

$$\boldsymbol{\nabla}\cdot\boldsymbol{A} = \frac{1}{R}\frac{\partial (RA_R)}{\partial R} + \frac{1}{R}\frac{\partial A_\theta}{\partial \theta} + \frac{\partial A_Z}{\partial Z} \; ; \tag{8.6.33}$$

and

$$\begin{aligned}\boldsymbol{\nabla}\times\boldsymbol{A} \;\; = \;\; & \left(\frac{1}{R}\frac{\partial A_Z}{\partial \theta} - \frac{\partial A_\theta}{\partial Z}\right)\,\hat{\boldsymbol{e}}_R + \left(\frac{\partial A_R}{\partial Z} - \frac{\partial A_Z}{\partial R}\right)\,\hat{\boldsymbol{e}}_\theta \\ & + \left(\frac{1}{R}\frac{\partial (RA_\theta)}{\partial R} - \frac{1}{R}\frac{\partial A_R}{\partial \theta}\right)\,\hat{\boldsymbol{e}}_Z \; .\end{aligned} \tag{8.6.34}$$

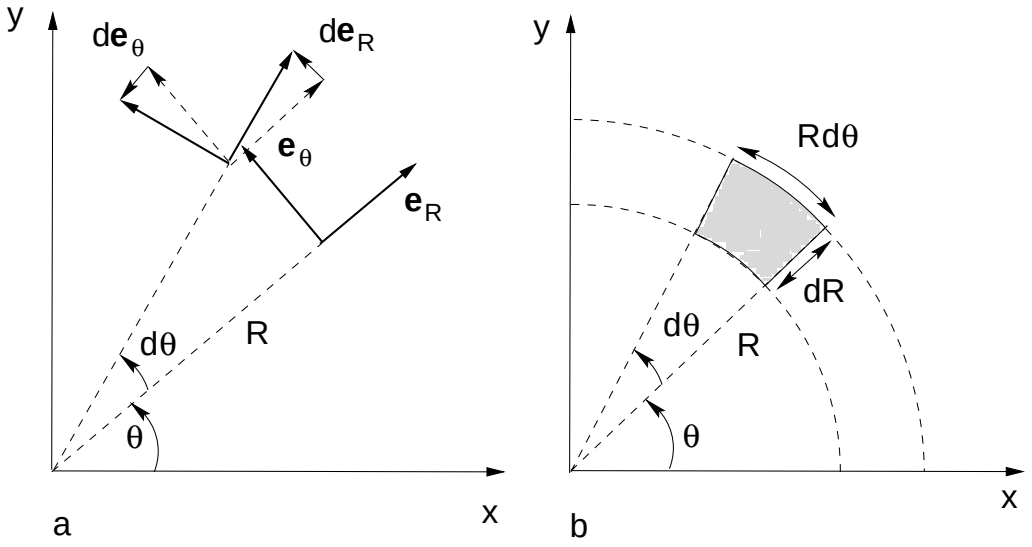

Figure 8.4: *Behaviour of the cylindrical polar coordinates in the x-y plane. Note (figure a) that the direction of the $\hat{\boldsymbol{e}}_R$ and $\hat{\boldsymbol{e}}_\theta$ unit vectors changes with varying angle θ. The surface area (gray in figure b) in this plane has a magnitude* $\mathrm{d}O = R\,\mathrm{d}\theta\,\mathrm{d}R$

8.6.5 The acceleration field in polar coordinates

In Chapter 2 we defined the acceleration associated with the velocity*field* $\boldsymbol{V}(\boldsymbol{x}\ ,\ t)$, which plays such an important role in fluid dynamics. This acceleration, itself a vector*field*, is defined by

$$\boldsymbol{a}(\boldsymbol{x}\ ,\ t) = \frac{\mathrm{d}\boldsymbol{V}}{\mathrm{d}t} = \frac{\partial \boldsymbol{V}}{\partial t} + (\boldsymbol{V}\cdot\boldsymbol{\nabla})\boldsymbol{V}\ . \tag{8.6.35}$$

In ordinary polar coordinates the unit vectors do not depend explicitly on time so that $\partial\hat{\boldsymbol{e}}_i/\partial t = 0$. Therefore the term $\partial\boldsymbol{V}/\partial t$ in the expression for $\boldsymbol{a}$ is simple to evaluate. For the second term $(\boldsymbol{V}\cdot\boldsymbol{\nabla})\boldsymbol{V}$, which involves the *spatial* derivatives of the velocity vector, one must use result (8.6.32) with $\boldsymbol{A} = \boldsymbol{V}$ in order to deal with the changing direction of $\hat{\boldsymbol{e}}_R$ and $\hat{\boldsymbol{e}}_\theta$. This yields the components of the acceleration field in cylindrical polars:

$$\boldsymbol{a}(\boldsymbol{x}\ ,\ t) = \left(\begin{array}{c} \dfrac{\partial V_R}{\partial t} + V_R\,\dfrac{\partial V_R}{\partial R} + \dfrac{V_\theta}{R}\dfrac{\partial V_R}{\partial \theta} + V_Z\,\dfrac{\partial V_R}{\partial Z} - \dfrac{V_\theta^2}{R} \\[2ex] \dfrac{\partial V_\theta}{\partial t} + V_R\,\dfrac{\partial V_\theta}{\partial R} + \dfrac{V_\theta}{R}\dfrac{\partial V_\theta}{\partial \theta} + V_Z\,\dfrac{\partial V_\theta}{\partial Z} + \dfrac{V_R V_\theta}{R} \\[2ex] \dfrac{\partial V_Z}{\partial t} + V_R\,\dfrac{\partial V_Z}{\partial R} + \dfrac{V_\theta}{R}\dfrac{\partial V_Z}{\partial \theta} + V_Z\,\dfrac{\partial V_Z}{\partial Z} \end{array}\right)\ . \tag{8.6.36}$$

One sees how new terms, quadratic in the velocity components, are introduced into the components of the acceleration vector in cylindrical polars due to the curvilinear character of these coordinates.

It is possible to give a simple interpretation to this result. Let us define the angular velocity of the fluid at some point by:

$$\frac{\mathrm{d}\theta}{\mathrm{d}t} \equiv \Omega = \frac{V_\theta}{R}\ . \tag{8.6.37}$$

If one writes $V_\theta = \Omega R$ and substitutes this into (8.6.36) one finds after some algebra[9]:

$$\boldsymbol{a}(\boldsymbol{x}\ ,\ t) = \left(\frac{\mathrm{d}V_R}{\mathrm{d}t} - \Omega^2 R\right)\ \hat{\boldsymbol{e}}_R + \left(R\,\frac{\mathrm{d}\Omega}{\mathrm{d}t} + 2\Omega V_R\right)\ \hat{\boldsymbol{e}}_\theta + \left(\frac{\mathrm{d}V_Z}{\mathrm{d}t}\right)\ \hat{\boldsymbol{e}}_Z\ . \qquad (8.6.38)$$

Here the total time derivative operator $\mathrm{d}/\mathrm{d}t$ is defined in cylindrical coordinates as

$$\begin{aligned} \frac{\mathrm{d}}{\mathrm{d}t} &= \frac{\partial}{\partial t} + \left(\frac{\mathrm{d}R}{\mathrm{d}t}\right)\ \frac{\partial}{\partial R} + \left(\frac{\mathrm{d}\theta}{\mathrm{d}t}\right)\ \frac{\partial}{\partial \theta} + \left(\frac{\mathrm{d}Z}{\mathrm{d}t}\right)\ \frac{\partial}{\partial Z} \\ &= \frac{\partial}{\partial t} + V_\mathrm{R}\,\frac{\partial}{\partial R} + \Omega\,\frac{\partial}{\partial \theta} + V_Z\,\frac{\partial}{\partial Z}\ . \end{aligned} \qquad (8.6.39)$$

From this one can see that the two curvature terms are equivalent with a *centrifugal* acceleration component $\Omega^2 R\,\hat{\boldsymbol{e}}_r$, and a *Coriolis* component $-2\Omega V_R\,\boldsymbol{e}_\theta$.

[9] In particular you must use that $V_R\,(\partial(\Omega R)/\partial R) = R V_R\,(\partial\Omega/\partial R) + \Omega V_R$.

8.6.6 Rotating coordinate systems

In the case of rotating coordinates, where the whole coordinate system rotates with angular velocity $\mathbf{\Omega}$ around the Z-axis, the unit vectors depend *explicitly* on time. This time dependence can be derived immediately from the results of the previous Section.

Consider two unit vectors in the $x-y$ plane that are attached to a point that is fixed in the rotating frame, see the figure below. We use the unit vectors of a cylindrical coordinate system. In a small time interval $\mathrm{d}t$ the two cylindrical unit vectors $\hat{\boldsymbol{e}}_R$ and $\hat{\boldsymbol{e}}_{\overline{\theta}}$, which are attached to the rotating frame, have rotated in the x-y plane. In the fixed frame the polar angle of the point to which these vectros are attached changes from θ to $\overline{\theta} = \theta + \mathrm{d}\theta$, with

$$\mathrm{d}\theta = \Omega \, \mathrm{d}t \; . \tag{8.6.40}$$

The unit vectors therefore coincide in the fixed frame with the corresponding unit vectors of *ordinary* (fixed) polar coordinates at the new angular position $\overline{\theta}$. The change of these two vectors over a time $\mathrm{d}t$ follows immediately from Eqn. (8.6.28):

$$\mathrm{d}\hat{\boldsymbol{e}}_R = \mathrm{d}\theta \, \hat{\boldsymbol{e}}_{\overline{\theta}} = \Omega \mathrm{d}t \, \hat{\boldsymbol{e}}_{\overline{\theta}} \quad , \quad \mathrm{d}\hat{\boldsymbol{e}}_{\overline{\theta}} = -\mathrm{d}\theta \, \hat{\boldsymbol{e}}_R = -\Omega \mathrm{d}t \, \hat{\boldsymbol{e}}_R \; . \tag{8.6.41}$$

This yields the change of the unit vectors per unit time in the fixed frame that results from the rotation of the reference frame to which they are attached:

$$\frac{\mathrm{d}\hat{\boldsymbol{e}}_R}{\mathrm{d}t} = \Omega \, \hat{\boldsymbol{e}}_{\overline{\theta}} \; , \quad \frac{\mathrm{d}\hat{\boldsymbol{e}}_{\overline{\theta}}}{\mathrm{d}t} = -\Omega \, \hat{\boldsymbol{e}}_R \; , \quad \frac{\mathrm{d}\hat{\boldsymbol{e}}_z}{\mathrm{d}t} = \frac{\mathrm{d}\hat{\boldsymbol{z}}}{\mathrm{d}t} = 0 \; . \tag{8.6.42}$$

If one defines the rotation vector

$$\mathbf{\Omega} = \Omega \, \hat{\boldsymbol{z}} \; , \tag{8.6.43}$$

the three equations in (8.6.42) can be captured in a single equation. Writing $\hat{\boldsymbol{e}}_1 = \hat{\boldsymbol{e}}_R$, $\hat{\boldsymbol{e}}_2 = \hat{\boldsymbol{e}}_{\overline{\theta}}$ and $\hat{\boldsymbol{e}}_3 = \hat{\boldsymbol{e}}_Z = \hat{\boldsymbol{z}}$, it is easily seen that the three equations are equivalent with

$$\boxed{\frac{\mathrm{d}\hat{\boldsymbol{e}}_i}{\mathrm{d}t} = \mathbf{\Omega} \times \hat{\boldsymbol{e}}_i \; .} \tag{8.6.44}$$

Of course, for an observer rotating with the reference frame the unit vectors do not change in time.

The rate of change of *any* vector $\boldsymbol{A}$ in an inertial frame can be written as

$$\frac{\mathrm{d}\boldsymbol{A}}{\mathrm{d}t} = \left(\frac{\mathrm{d}A_i}{\mathrm{d}t}\right)\,\hat{\boldsymbol{e}}_i + A_i\,\left(\frac{\mathrm{d}\hat{\boldsymbol{e}}_i}{\mathrm{d}t}\right)\,. \tag{8.6.45}$$

The first term on the right-hand side, involving the change of the *components*, is the change seen by an observer for whom the unit vectors are *fixed*, in this case obviously the observer in the rotating frame. The second term gives the contribution due to the rotation of the coordinate system. These two terms together should always add up to the same answer, *regardless* the coordinate system used!

Using (8.6.44) this means we can write the change of the vector as

$$\left(\frac{\mathrm{d}\boldsymbol{A}}{\mathrm{d}t}\right)_{\mathrm{I}} = \left(\frac{\mathrm{d}\boldsymbol{A}}{\mathrm{d}t}\right)_{\mathrm{R}} + \boldsymbol{\Omega}\times\boldsymbol{A}\,. \tag{8.6.46}$$

Here the subscripts I and R signify that the derivatives are taken in the inertial (laboratory) frame and in the rotating frame respectively. The second term follows immediately, using summation convention, from the linearity of the cross product:

$$A_i\,\frac{\mathrm{d}\hat{\boldsymbol{e}}_i}{\mathrm{d}t} = A_i\,\left(\boldsymbol{\Omega}\times\hat{\boldsymbol{e}}_i\right) = \boldsymbol{\Omega}\times\,\left(A_i\,\hat{\boldsymbol{e}}_i\right) = \boldsymbol{\Omega}\times\boldsymbol{A}\,. \tag{8.6.47}$$

Equation (8.6.46) is a relation between vectors. Therefore it is valid in *any* coordinate system, not just in the cylindrical coordinates used to in the derivation of some of the steps leading to this result.

We can apply relation (8.6.46) immediately to calculate the relation between the velocity assigned by observers to a particle or fluid element in the inertial frame, and the velocity seen by an observer in the rotating frame . Let the position vector of this particle or fluid element be $\boldsymbol{r}(t)$. Defining the velocity in the two frames by

$$\boldsymbol{V}_{\mathrm{I}} = \left(\frac{\mathrm{d}\boldsymbol{r}}{\mathrm{d}t}\right)_{\mathrm{I}}\quad,\quad \boldsymbol{V}_{\mathrm{R}} = \left(\frac{\mathrm{d}\boldsymbol{r}}{\mathrm{d}t}\right)_{\mathrm{R}}\,, \tag{8.6.48}$$

relation (8.6.46) applied to the position vector $\boldsymbol{r}(t)$ implies that the velocities in the two frames are related by

$$\boxed{\boldsymbol{V}_{\mathrm{I}} = \boldsymbol{V}_{\mathrm{R}} + \boldsymbol{\Omega}\times\boldsymbol{r}(t)\,.} \tag{8.6.49}$$

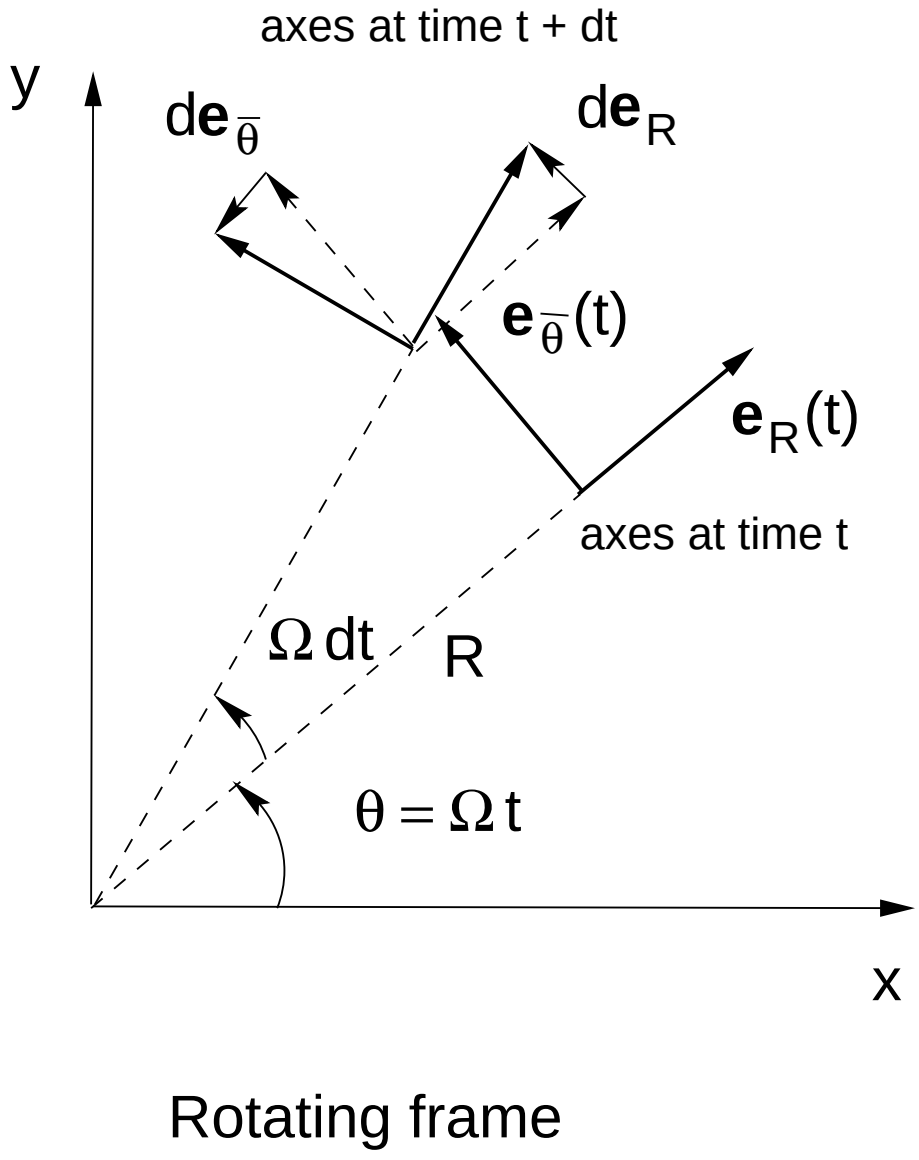

Figure 8.5: *Behaviour of the unit vectors $\hat{\boldsymbol{e}}_R$ and $\hat{\boldsymbol{e}}_{\overline{\theta}}$ in the x-y plane. They change their orientation as a result of the rotation of the reference frame.*

Applying relation (8.6.46) once again, but now putting $\boldsymbol{A} = \boldsymbol{V}_{\mathrm{I}}$, one has

$$\left(\frac{\mathrm{d}\boldsymbol{V}_{\mathrm{I}}}{\mathrm{d}t}\right)_{\mathrm{I}} = \left(\frac{\mathrm{d}\boldsymbol{V}_{\mathrm{I}}}{\mathrm{d}t}\right)_{\mathrm{R}} + \boldsymbol{\Omega} \times \boldsymbol{V}_{\mathrm{I}} \,. \tag{8.6.50}$$

Eliminating $\boldsymbol{V}_{\mathrm{I}}$ in the right-hand side of this equation using (8.6.49) we can rewrite it as

$$\begin{aligned}
\left(\frac{\mathrm{d}\boldsymbol{V}_{\mathrm{I}}}{\mathrm{d}t}\right)_{\mathrm{I}} &= \left(\frac{\mathrm{d}\boldsymbol{V}_{\mathrm{R}}}{\mathrm{d}t}\right)_{\mathrm{R}} + \left(\frac{\mathrm{d}\boldsymbol{\Omega}}{\mathrm{d}t}\right) \times \boldsymbol{r} + \boldsymbol{\Omega} \times \left(\frac{\mathrm{d}\boldsymbol{r}}{\mathrm{d}t}\right)_{\mathrm{R}} \\
&\quad + \boldsymbol{\Omega} \times (\boldsymbol{V}_{\mathrm{R}} + \boldsymbol{\Omega} \times \boldsymbol{r}(t)) \\
&= \left(\frac{\mathrm{d}\boldsymbol{V}_{\mathrm{R}}}{\mathrm{d}t}\right)_{\mathrm{R}} + 2\,\boldsymbol{\Omega} \times \boldsymbol{V}_{\mathrm{R}} + \boldsymbol{\Omega} \times (\boldsymbol{\Omega} \times \boldsymbol{r}) + \\
&\quad + \left(\frac{\mathrm{d}\boldsymbol{\Omega}}{\mathrm{d}t}\right) \times \boldsymbol{r}
\end{aligned} \tag{8.6.51}$$

Here I have allowed for the possibility that the angular rotation vector $\boldsymbol{\Omega}$ changes as a function of time. This relationship gives the connection between the acceleration $\boldsymbol{a}_{\mathrm{I}} = \mathrm{d}\boldsymbol{V}_{\mathrm{I}}/\mathrm{d}t$ as seen by an observer in the inertial (fixed) reference frame, and the acceleration $\boldsymbol{a}_{\mathrm{R}} = \mathrm{d}\boldsymbol{V}_{\mathrm{R}}/\mathrm{d}t$ attributed to the same fluid element or particle by an observer fixed in the rotating frame

8.6.7 Fluid equations in a rotating frame

Newton's equation of motion for a single particle of mass m, moving under the influence of some force $\boldsymbol{F}$, formally only applies in the inertial frame:

$$m \left(\frac{\mathrm{d}\boldsymbol{V}_{\mathrm{I}}}{\mathrm{d}t}\right)_{\mathrm{I}} = \boldsymbol{F} \,. \tag{8.6.52}$$

Substituting for $(\mathrm{d}\boldsymbol{V}/\mathrm{d}t)_{\mathrm{I}}$ from (8.6.51), and re-arranging terms, yields an equation of motion valid for an observer in the rotating frame.

This equation reads

$$m\left(\frac{\mathrm{d}\boldsymbol{V}_{\mathrm{R}}}{\mathrm{d}t}\right)_{\mathrm{R}} = \boldsymbol{F} - 2m\,\boldsymbol{\Omega}\times\boldsymbol{V}_{\mathrm{R}} - m\,\boldsymbol{\Omega}\times(\boldsymbol{\Omega}\times\boldsymbol{r}) - m\,\frac{\mathrm{d}\boldsymbol{\Omega}}{\mathrm{d}t}\times\boldsymbol{r}\;. \qquad (8.6.53)$$

The rotating observer assigns a number of extra 'force terms' to the equation of motion. These are 'fictiteous forces', entirely due to the fact that the rotating observer does not reside in an inertial frame[10]. These extra force terms are:

- The **Coriolis force** $\boldsymbol{F}_{\mathrm{co}} \equiv -2m\,\boldsymbol{\Omega}\times\boldsymbol{V}_{\mathrm{R}}$;
- The **centrifugal force** $\boldsymbol{F}_{\mathrm{cf}} \equiv -m\,\boldsymbol{\Omega}\times(\boldsymbol{\Omega}\times\boldsymbol{r})$;
- The **Euler force** $\boldsymbol{F}_{\mathrm{E}} \equiv -m\,(\mathrm{d}\boldsymbol{\Omega}/\mathrm{d}t)\times\boldsymbol{r}$.

The Euler force only arises if the rotation rate (or the rotation axis) of the coordinate system changes with time. In what follows we will assume that this is not the case, and put $\mathrm{d}\boldsymbol{\Omega}/\mathrm{d}t = 0$.

The obvious generalization of this treatment of a rotating reference frame in single-particle mechanics to the case of fluid dynamics is an equation of motion for the fluid of the form

$$\rho\left(\frac{\mathrm{d}\boldsymbol{V}_{\mathrm{R}}}{\mathrm{d}t}\right)_{\mathrm{R}} = -\boldsymbol{\nabla}P - \rho\,\boldsymbol{\nabla}\Phi - 2\rho\,\boldsymbol{\Omega}\times\boldsymbol{V}_{\mathrm{R}} - \rho\,\boldsymbol{\Omega}\times(\boldsymbol{\Omega}\times\boldsymbol{r}) \qquad (8.6.54)$$

in the rotating frame. Here a centrifugal and a Coriolis terms appear in a completely analogous fashion in the equation of motion. Since we are dealing with a continuum they appear as force densities. Eqn. (8.6.54) can be written as

$$\rho\left(\frac{\mathrm{d}\boldsymbol{V}_{\mathrm{R}}}{\mathrm{d}t}\right)_{\mathrm{R}} + 2\rho\,\boldsymbol{\Omega}\times\boldsymbol{V}_{\mathrm{R}} = -\boldsymbol{\nabla}P + \rho\,\boldsymbol{g}_{\mathrm{eff}}\;. \qquad (8.6.55)$$

The effective gravity $\boldsymbol{g}_{\mathrm{eff}}$ in this expression is defined as the sum of the true gravitational acceleration and the centrifugal acceleration:

$$\boldsymbol{g}_{\mathrm{eff}} = -\boldsymbol{\nabla}\Phi - \boldsymbol{\Omega}\times(\boldsymbol{\Omega}\times\boldsymbol{r})\;. \qquad (8.6.56)$$

[10]For a full discussion of these issues see:
H. Goldstein, 1980: *Classical Mechanics*, Addison-Wesley, Reading, Ch. 4;
J. Pedlosky, 1986: *Geophysical Fluid Dynamics*, Springer Verlag, Ch.1.6.

Here $\Phi(\boldsymbol{x}\,,\,t)$ the Newtonian gravitational potential. In the case of rigid rotation around the Z-axis, where $\boldsymbol{\Omega} = \Omega\hat{\boldsymbol{e}}_Z$, the centrifugal force is

$$-\boldsymbol{\Omega}\times(\boldsymbol{\Omega}\times\boldsymbol{r}) = \Omega^2\,R\,\hat{\boldsymbol{e}}_R = \boldsymbol{\nabla}\left(\tfrac{1}{2}\Omega^2R^2\right) = \boldsymbol{\nabla}\left(\frac{|\boldsymbol{\Omega}\times\boldsymbol{r}|^2}{2}\right)\,, \tag{8.6.57}$$

where the last equality follows from $\boldsymbol{r} = R\,\hat{\boldsymbol{e}}_R + Z\,\hat{\boldsymbol{e}}_Z$ and from $\boldsymbol{\Omega} = \Omega\,\hat{\boldsymbol{e}}_Z$. This means that the effective gravity can also be written in terms of a potential:

$$\boldsymbol{g}_{\rm eff} = -\boldsymbol{\nabla}\left(\Phi - \frac{|\boldsymbol{\Omega}\times\boldsymbol{r}|^2}{2}\right) \equiv -\boldsymbol{\nabla}\Phi_{\rm eff}\,. \tag{8.6.58}$$

This *effective potential* is

$$\Phi_{\rm eff}(\boldsymbol{x}\,,\,t) = \Phi - \frac{|\boldsymbol{\Omega}\times\boldsymbol{r}|^2}{2} = \Phi - \frac{\Omega^2R^2}{2}\,. \tag{8.6.59}$$

This completes the derivation of the equations governing an ideal fluid in a rigidly rotating coordinate frame. Adding for completeness sake the equation of state for an adiabatic medium and the continuity equation, and re-instating the subscript 'R':

$$\begin{aligned}
\rho\left(\frac{{\rm d}\boldsymbol{V}_{\rm R}}{{\rm d}t}\right)_{\rm R} + 2\rho\,\boldsymbol{\Omega}\times\boldsymbol{V}_{\rm R} &= -\boldsymbol{\nabla}P - \rho\,\boldsymbol{\nabla}\Phi_{\rm eff}\,;\\
\frac{\partial\rho}{\partial t} + \boldsymbol{\nabla}\cdot(\rho\,\boldsymbol{V}_{\rm R}) &= 0\,;\\
\Phi_{\rm eff} &= \Phi - \frac{|\boldsymbol{\Omega}\times\boldsymbol{r}|^2}{2}\,;\\
P &= P_0\left(\frac{\rho}{\rho_0}\right)^{\gamma}\,;\\
\left(\frac{{\rm d}\boldsymbol{V}_{\rm R}}{{\rm d}t}\right)_{\rm R} &= \frac{\partial\boldsymbol{V}_{\rm R}}{\partial t} + (\boldsymbol{V}_{\rm R}\cdot\boldsymbol{\nabla})\,\boldsymbol{V}_{\rm R}\,.
\end{aligned} \tag{8.6.60}$$

The last definition corresponds to the comoving time derivative in the rotating frame.

8.6.8 Planetary vorticity and the thermal wind equation

For obvious reasons, geophysicists, oceanographers and planetary physicists use a coordinate system that rotates with the planet: the *corotating frame*. To describe the medium (the ocean, the atmosphere or the magma in the Earth's interior), they have to use the equations outlined in the preceding Section. In many applications, the vorticity of the fluid or gas plays an important role. Since we have transformed the velocities to the corotating frame, something similar must be done for the definition of the vorticity, and the associated equation of motion. This will lead to the definition of the *absolute vorticity*, whose definition includes a contribution from the swirling motions in the corotating frame, and a contribution from the planetary rotation.

One can derive an equation for the vorticity in the rotating frame, $\boldsymbol{\omega}_{\rm R} = \boldsymbol{\nabla} \times \boldsymbol{V}_{\rm R}$, by using the same methods as were employed in Section 8.1. In order to make the notation less cumbersome, I will drop from this point onwards the subscript $\rm R$ in terms like $\boldsymbol{V}_{\rm R}$, $(\mathrm{d}\boldsymbol{V}_{\rm R}/\mathrm{d}t)_{\rm R}$ etc., assuming implicity that all quantities without subscript are the quantities as evaluated by an observer fixed in the corotating frame.

Using the vector identity

$$\begin{aligned}(\boldsymbol{V}\cdot\boldsymbol{\nabla})\boldsymbol{V} &= \boldsymbol{\nabla}(\tfrac{1}{2}V^2) - \boldsymbol{V}\times(\boldsymbol{\nabla}\times\boldsymbol{V}) \\ &= \boldsymbol{\nabla}(\tfrac{1}{2}V^2) - \boldsymbol{V}\times\boldsymbol{\omega},\end{aligned}$$

once again, one can write the equation of motion as

$$\frac{\partial \boldsymbol{V}}{\partial t} + (\boldsymbol{\omega} + 2\,\boldsymbol{\Omega})\,\times\boldsymbol{V} = -\frac{\boldsymbol{\nabla}P}{\rho} - \boldsymbol{\nabla}\left(\frac{|\boldsymbol{V}|^2}{2} + \Phi_{\rm eff}\right)\,. \tag{8.6.61}$$

Taking the rotation $\boldsymbol{\nabla}\times$ in both sides of this relation, one finds the equation of motion for the vorticity $\boldsymbol{\omega} = \boldsymbol{\nabla}\times\boldsymbol{V}$ in the rotating frame:

$$\frac{\partial\boldsymbol{\omega}}{\partial t} = \boldsymbol{\nabla}\times\,\{\boldsymbol{V}\times\,(\boldsymbol{\omega}+2\,\boldsymbol{\Omega})\} + \frac{1}{\rho^2}\boldsymbol{\nabla}\rho\times\boldsymbol{\nabla}P\,. \tag{8.6.62}$$

This equation of motion for $\boldsymbol{\omega}(\boldsymbol{x}\,,\,t)$ shows explicitly how the rotation of the coordinate frame influences the vorticity in the corotating frame an ifluence that can be traced to the Coriolis term $\propto 2\boldsymbol{\Omega}\times\boldsymbol{V}$ in the original equation of motion. One can define the so-called *absolute vorticity* $\boldsymbol{\omega}_{\rm a}$ by

$$\boldsymbol{\omega}_{\rm a} \equiv \boldsymbol{\omega} + 2\,\boldsymbol{\Omega}\,. \tag{8.6.63}$$

If we *assume* that $\mathrm{d}\boldsymbol{\Omega}/\ \mathrm{d}t = \partial\boldsymbol{\Omega}/\partial t = 0$, the vorticity equation can be written as an equation for the absolute vorticity:

$$\boxed{\frac{\partial \boldsymbol{\omega}_{\mathrm{a}}}{\partial t} = \boldsymbol{\nabla} \times \ (\boldsymbol{V} \times \boldsymbol{\omega}_{\mathrm{a}}) + \frac{\boldsymbol{\nabla}\rho \times \boldsymbol{\nabla} P}{\rho^2} \ .} \tag{8.6.64}$$

This equation has exactly the same form as the equation as derived for the vorticity in a non-rotating frame (Eqn. 8.2.8). This result is not suprising once one realises that the absolute vorticity $\boldsymbol{\omega}_{\mathrm{a}}$ in fact coincides with the vorticity $\boldsymbol{\nabla} \times \boldsymbol{V}_{\mathrm{I}}$ of the fluid in the inertial frame. Using

$$\boldsymbol{V}_{\mathrm{I}} = \boldsymbol{V} + \boldsymbol{\Omega} \times \boldsymbol{r} \ , \tag{8.6.65}$$

one can show that for constant $\boldsymbol{\Omega}$ the identity[11]

$$\boldsymbol{\omega}_{\mathrm{I}} = \boldsymbol{\nabla} \times \boldsymbol{V}_{\mathrm{I}} = \boldsymbol{\nabla} \times \ (\boldsymbol{V} + \boldsymbol{\Omega} \times \boldsymbol{r}) = \boldsymbol{\omega} + 2\,\boldsymbol{\Omega} = \boldsymbol{\omega}_{\mathrm{A}} \tag{8.6.66}$$

is valid. According to this relation, the vorticity in the inertial frame can be thought of as the sum of two contributions: the vorticity of the fluid motions ('swirls') in the rotating frame, the *relative vorticity* $\boldsymbol{\omega}$, and the so-called *planetary vorticity* $2\,\boldsymbol{\Omega}$ that is due to the rotation of the reference frame. The circulation can therefore be defined as

$$\Gamma_{\mathrm{c}} = \int \boldsymbol{\omega}_{\mathrm{a}} \cdot \mathrm{d}\boldsymbol{O} = \int (\boldsymbol{\omega} + 2\,\boldsymbol{\Omega}) \ \cdot \mathrm{d}\boldsymbol{O} \ . \tag{8.6.67}$$

Kelvin's circulation theorem still applies, provided one uses the absolute vorticity $\boldsymbol{\omega}_{\mathrm{a}}$:

$$\boxed{\frac{\mathrm{d}\Gamma_{\mathrm{c}}}{\mathrm{d}t} = \frac{\mathrm{d}}{\mathrm{d}t}\left(\oint (\boldsymbol{V} + \boldsymbol{\Omega} \times \boldsymbol{r}) \ \cdot \mathrm{d}\boldsymbol{r}\right) = \int \mathrm{d}\boldsymbol{O} \cdot \frac{(\boldsymbol{\nabla}\rho \times \boldsymbol{\nabla} P)}{\rho^2} \ .} \tag{8.6.68}$$

[11] An interesting exercise in vector analysis, best performed in cylindrical coordinates with the rotation axis chosen along the Z-axis.

This result means that in an ideal (i.e. frictionless) barotropic flow, where $\boldsymbol{\nabla} P \times \boldsymbol{\nabla} \rho = 0$, the circulation $\Gamma_{\rm c}$ is once again conserved:

$$\Gamma_{\rm c} = \int (\boldsymbol{\omega} + 2\boldsymbol{\Omega}) \cdot {\rm d}\boldsymbol{O} = \text{constant}. \tag{8.6.69}$$

In many practical applications the planetary vorticity is much larger than the relative vorticity,

$$2\,|\boldsymbol{\Omega}| \gg |\boldsymbol{\omega}|\ . \tag{8.6.70}$$

In that case, Eqn. (8.6.64) can be approximated. First we write in in the form

$$\frac{{\rm d}\boldsymbol{\omega}}{{\rm d}t} = [(\boldsymbol{\omega} + 2\boldsymbol{\Omega}) \cdot \boldsymbol{\nabla}\ ]\ \boldsymbol{V} - (\boldsymbol{\omega} + 2\boldsymbol{\Omega})(\boldsymbol{\nabla} \cdot \boldsymbol{V}) + \frac{\boldsymbol{\nabla}\rho \times \boldsymbol{\nabla} P}{\rho^2}\ . \tag{8.6.71}$$

Here we once again put $\partial\boldsymbol{\Omega}/\partial t = 0$[12]. If we now assume that the relative vorticity is small compared with the planetary vorticity (Eqn. 8.6.70), we can neglect $\boldsymbol{\omega}$ with respect to $2\boldsymbol{\Omega}$ whever they appear together, as they do in the first two terms on the right-hand side of Eqn. (8.6.71). Therefore, this equation can be approximated by:

$$\frac{{\rm d}\boldsymbol{\omega}}{{\rm d}t} = (2\boldsymbol{\Omega} \cdot \boldsymbol{\nabla})\boldsymbol{V} - 2\boldsymbol{\Omega}\,(\boldsymbol{\nabla} \cdot \boldsymbol{V}) + \frac{\boldsymbol{\nabla}\rho \times \boldsymbol{\nabla} P}{\rho^2}\ . \tag{8.6.72}$$

If, in addition, the timescale for changes in the flow is *long* compared with the planetary rotation period, $P = 2\pi/|\boldsymbol{\Omega}|$, as is the case for instance when one describes large-scale and long-lived planetary circulation rather than a small-scale, short-lived local weather system, one can *also* neglect the time-derivative ${\rm d}\boldsymbol{\omega}/{\rm d}t$ on the left-hand side of this equation. The resulting (approximated) vorticity equation is known as the *thermal wind equation*. It is usually written in the form

$$\boxed{(2\boldsymbol{\Omega} \cdot \boldsymbol{\nabla})\boldsymbol{V} - 2\boldsymbol{\Omega}\,(\boldsymbol{\nabla} \cdot \boldsymbol{V}) = -\frac{\boldsymbol{\nabla}\rho \times \boldsymbol{\nabla} P}{\rho^2}\ .} \tag{8.6.73}$$

[12] $\boldsymbol{\Omega}$ is by definition independent of the spatial coordinates!

A major simplification occurs for *incompressible flows*, with $\boldsymbol{\nabla} \cdot \boldsymbol{V} = 0$. In such flows the density is conserved along flowlines: from the continuity equation one has

$$\frac{\mathrm{d}\rho}{\mathrm{d}t} = -\rho \left(\boldsymbol{\nabla} \cdot \boldsymbol{V} \right) = 0 \; . \tag{8.6.74}$$

This automatically implies that the volume of a fluid element is conserved by the flow, see also Eqn. (2.6.12):

$$\Delta \mathcal{V} = \text{constant.} \tag{8.6.75}$$

In that case equation (8.6.73) can be written as

$$(2\boldsymbol{\Omega} \cdot \boldsymbol{\nabla}) \boldsymbol{V} = -\frac{\mathcal{R}}{\mu \rho} \left(\boldsymbol{\nabla} \rho \times \boldsymbol{\nabla} T \right) \; . \tag{8.6.76}$$

Here I have used the ideal gas law, $P = \rho \mathcal{R} T / \mu$. This equation shows how gradients along the rotation axis in the flow are induced by the action of non-parallel density- and temperature gradients.

8.6.9 A geophysical application: the global eastward circulation in the Zonal Wind

Let us consider the consequence of the thermal wind equation to the dynamics of the Earth's atmosphere. We will assume that the atmosphere is a very thin layer, an excellent approximation. We choose a local *cartesian* coordinate system, in such a way that the z-direction corresponds with the (local) vertical direction, that the x-direction runs from West to East in longitude, and the y-direction runs from South to North in latitude. Finally, the vertical component of the rotation vector of the Earth is $\Omega_z = \boldsymbol{\Omega} \cdot \hat{\boldsymbol{z}}$.

The dominant density gradient in a geometrically thin atmosphere is the vertical gradient due to the gravitational stratification:

$$\boldsymbol{\nabla} \rho \approx \left(\frac{\mathrm{d}\rho}{\mathrm{d}z} \right) \hat{\boldsymbol{z}} \approx -\frac{\rho}{\mathcal{H}} \hat{\boldsymbol{z}} \; . \tag{8.6.77}$$

Here $\mathcal{H}$ is the atmospheric scale height (see Chapter 6.6):

$$\mathcal{H} = \frac{\mathcal{R} T}{\mu g_{\mathrm{eff}}} \; . \tag{8.6.78}$$

Here I assume for simplicity that the atmosphere is isothermal with height: $\partial T/\partial z = 0$. Note that that the gravitational acceleration is taken to be $\boldsymbol{g}_{\rm eff} = -g_{\rm eff}\,\hat{\boldsymbol{z}}$, which is the *effective* gravity in the corotating frame. The dominant temperature gradient is the temperature gradient from the Tropics to the Poles, which runs North-South in the Northern Hemisphere, and in the opposite direction in the Southern Hemisphere:

$$\boldsymbol{\nabla} T \approx \left(\frac{\mathrm{d}T}{\mathrm{d}y}\right)\,\hat{\boldsymbol{y}}\,. \tag{8.6.79}$$

Finally, since most of the large-scale motions must be in the plane of the atmosphere (as there is little room for vertical motions) we assume that the velocity vector $\boldsymbol{V}$ lies in the $x-y$ plane. The thermal wind equation predicts that these density- and temperature gradients induce a circulation along lines of constant latitude, which satisfies:

$$2\Omega_z\,\frac{\mathrm{d}V_x}{\mathrm{d}z} = \frac{\mathcal{R}}{\mu\rho}\,\left(\frac{\mathrm{d}\rho}{\mathrm{d}z}\right)\,\left(\frac{\mathrm{d}T}{\mathrm{d}y}\right)\,. \tag{8.6.80}$$

Here I have assumed that the dominant component of the velocity gradient is in the vertical (z-)direction. Using the relations (8.6.77) and (8.6.78), the thermal wind equation can be written as:

$$2\Omega_z\,\frac{\mathrm{d}V_x}{\mathrm{d}z} = -\frac{\mathcal{R}}{\mu\mathcal{H}}\,\left(\frac{\mathrm{d}T}{\mathrm{d}y}\right) = -g_{\rm eff}\,\left(\frac{1}{T}\,\frac{\mathrm{d}T}{\mathrm{d}y}\right)\,. \tag{8.6.81}$$

Since $\mathrm{d}T/\mathrm{d}y < 0$ in the Northern Hemisphere where $\Omega_z > 0$, and $\mathrm{d}T/\mathrm{d}y > 0$ in the Southern Hemisphere where $\Omega_z < 0$, this induces a global, eastward circulation at high altitude in the atmosphere: the **Zonal Wind**. Near the Earth's surface this eastward velocity is very small, due to friction between the atmospheric motions and the surface of the continents, or the friction between the wind and the surface of the oceans. However, the velocity increases with height according to (8.6.81). At high altitudes only internal atmospheric friction operates, which is much smaller. The resulting flow is an example of a *shear flow*, where the magnitude of the velocity increases in the direction perpendicular to the flow.

The figure below shows a measurement of this global (mean) eastward circulation pattern in the Earth's atmosphere over a period of ten years, from 1990 until 1999. Such a long-term measurement is needed in order to detect this pattern over the strong 'noise' caused by the stronger (but shorter-lived) weather patterns such as high-pressure regions, depressions and tropical cyclones.

The large gas planets in our Solar System, such as Jupiter, Saturn and Uranus, are rotating very rapidly compared to the Earth[13]. As a result, Zonal Winds of these planets are much stronger than those on Earth: they are the cause of the prominent coloured *bands* that are visible in the upper atmospheres of these planets. The photograph below from the Cassini spacecraft illustrates this beautifully. In the gas giants the zonal winds are the dominant weather systems!

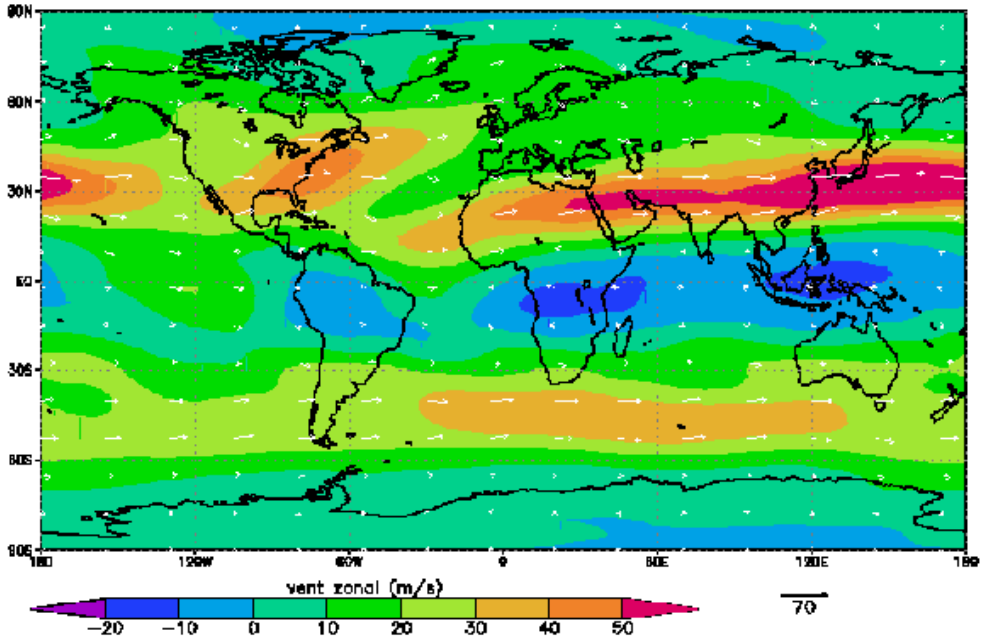

Figure 8.6: *Measurement of the eastward Zonal Wind over the years 1990-1999.*

[13]The rotation periods are for Jupiter: 0.41 day, for Saturn: 0.44 day and for Uranus: 0.65 day.

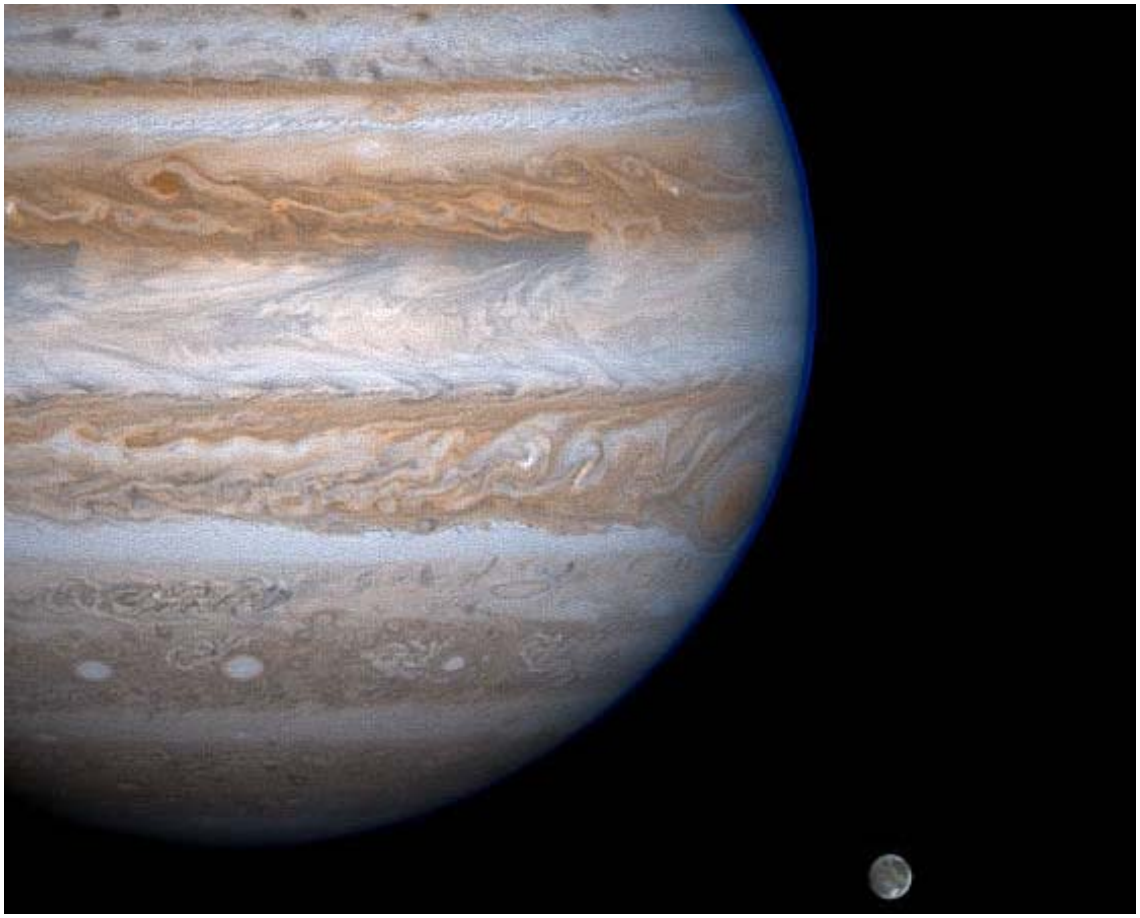

Figure 8.7: *The prominant bands in the atmosphere of Jupiter, as photographed by the Cassini space probe when it passed Jupiter on its way to Saturn. These bands are the visible evidence for strong Zonal Winds, caused by the rapid rotation of Jupiter. Inside these bands, many vortices are seen that are created due to the velocity shear between the different layers in the atmosphere. The large Jovian moon on the right-hand side of this picture is Ganymede*
Photograph: Cassini Imaging Team/NASA.

8.7 The Shallow Water Approximation

In the study of planetary weather systems, both on Earth and in the giant gas planets such as Jupiter and Saturn, one often uses *Shallow Water Theory*. In this theory the motion of the fluid is described as a quasi two-dimensional flow of variable thickness, see the figure below.

The following approximations are made:

1. One assumes that the thickness of the layer is small: if the typical size of the flow in the horizontal direction is L, and if the thickness of the flow layer in the vertical direction is H, then the shallow water theory can be applied provided

$$H \ll L \; . \tag{8.7.1}$$

2. One describes the flow in terms of the thickness of the layer, $H(x\,,\,y\,,\,t)$, and the two components of the velocity in the horizontal $(x-y)$ plane, $\boldsymbol{V}_{\rm h}$;

3. One assumes that the density and horizontal velocity are uniform in the vertical (z-)direction so that

$$\frac{\partial \rho}{\partial z} = 0 \quad , \quad \frac{\partial \boldsymbol{V}_{\rm h}}{\partial z} = 0 \; . \tag{8.7.2}$$

4. The underlying (fully three-dimensional) flow is assumed to be incompressible so that the velocity satisfies $\boldsymbol{\nabla} \cdot \boldsymbol{V} = 0$. If we adopt the notation that is commonly used in the geophysical community[14], and use condition (8.7.2), one can write the velocity as:

$$\begin{aligned} \boldsymbol{V}(\boldsymbol{x}\,,\,t) &= u(x\,,\,y\,,\,t)\,\hat{\boldsymbol{x}} + v(x\,,\,y\,,\,t)\,\hat{\boldsymbol{y}} + w(\boldsymbol{x}\,,\,t)\,\hat{\boldsymbol{z}} \\ &\equiv \boldsymbol{V}_{\rm h}(x\,,\,y\,,\,t) + w(\boldsymbol{x}\,,\,t)\,\hat{\boldsymbol{z}} \; . \end{aligned} \tag{8.7.3}$$

[14] see for instance: J. Pedlosky, 1987: *Geophysical Fluid Dynamics*, Springer Verlag, New York, Ch. 3.

The incompressibility condition then reads:

$$\frac{\partial u}{\partial x} + \frac{\partial v}{\partial y} + \frac{\partial w}{\partial z} = 0 \ . \tag{8.7.4}$$

5. One assumes that there is a uniform gravitational acceleration in the vertical direction,

$$\boldsymbol{g} = -g \, \hat{\boldsymbol{z}} \ , \tag{8.7.5}$$

and that one is working in the corotating frame. The vertical component of the angular rotation vector is

$$\Omega_z \equiv \boldsymbol{\Omega} \cdot \hat{\boldsymbol{z}} \ . \tag{8.7.6}$$

The assumption of an incompressible flow immediately leads to a dynamical equation for the thickness of the layer. In an incompressible flow the volume $\Delta\mathcal{V}$ of a fluid-element is conserved by the flow (see Chapter 2.4):

$$\frac{\mathrm{d}\,\Delta\mathcal{V}}{\mathrm{d}t} = 0 \ . \tag{8.7.7}$$

The conservation of such an infinitesimal volume can be represented as

$$\Delta\mathcal{V} = \Delta O_{\mathrm{H}} \, H(x \ , \ y \ , \ t) = \text{constant} \ . \tag{8.7.8}$$

Here ΔO_{H} is the projected area of the fluid element in the horizontal plane, and H is the layer thickness. The thickness of the layer varies as a function of the position $(x \ , \ y)$ in the horizontal plane, and time. The shallow water approximation (8.7.1) implies that the vertical component of the fluid velocity is much smaller than the horizontal component:

$$|w| \sim \frac{H}{L} \, |\boldsymbol{V}_{\mathrm{h}}| \ll |\boldsymbol{V}_{\mathrm{h}}| \ . \tag{8.7.9}$$

In that case, the deformation of the surface element ΔO_{H} is almost entirely due to the motions in the horizontal plane.

It is therefore described by the z-component of Eqn. (8.3.16):

$$\frac{\mathrm{d}\Delta O_{\mathrm{h}}}{\mathrm{d}t} = \left(\frac{\partial u}{\partial x} + \frac{\partial v}{\partial y}\right) \Delta O_{\mathrm{h}} \; . \tag{8.7.10}$$

Because of (8.7.9), one can approximate the total time derivative here (and in what follows) by

$$\frac{\mathrm{d}}{\mathrm{d}t} = \frac{\partial}{\partial t} + u \, \frac{\partial}{\partial x} + v \, \frac{\partial}{\partial y} \; . \tag{8.7.11}$$

Since the volume is conserved,

$$\frac{\mathrm{d}\Delta \mathcal{V}}{\mathrm{d}t} = 0 = \left(\frac{\mathrm{d}H}{\mathrm{d}t}\right) \, \Delta O_{\mathrm{h}} + H \, \left(\frac{\mathrm{d}\Delta O_{\mathrm{h}}}{\mathrm{d}t}\right) \; , \tag{8.7.12}$$

one can use (8.7.10) to find an expression for the change in the layer thickness $H(x, y, t)$:

$$\begin{aligned} \frac{\mathrm{d}H}{\mathrm{d}t} = \frac{\partial H}{\partial t} + u \, \frac{\partial H}{\partial x} + v \, \frac{\partial H}{\partial y} \quad &= \quad -H \, \left(\frac{1}{\Delta O_{\mathrm{h}}} \, \frac{\mathrm{d}\Delta O_{\mathrm{h}}}{\mathrm{d}t}\right) \\ &= \quad -H \, \left(\frac{\partial u}{\partial x} + \frac{\partial v}{\partial y}\right) \; . \end{aligned} \tag{8.7.13}$$

Re-arranging terms, it is easily seen that this corresponds to

$$\frac{\partial H}{\partial t} + \frac{\partial}{\partial x}(u \, H) + \frac{\partial}{\partial y}(v \, H) = 0 \; . \tag{8.7.14}$$

The $z-$component of the vorticity equation (8.6.71) can be written for $\boldsymbol{\nabla}\rho \times \boldsymbol{\nabla} P = 0$ as:

$$\frac{\mathrm{d}\omega_z}{\mathrm{d}t} = (\boldsymbol{\omega} + 2\boldsymbol{\Omega}) \, \boldsymbol{\cdot} \, \boldsymbol{\nabla} w - (\omega_z + 2\Omega_z) \boldsymbol{\nabla} \boldsymbol{\cdot} \boldsymbol{V} \; . \tag{8.7.15}$$

The second term on the right-hand side vanishes as the flow is incompressible.

Turning our attention to the first term, we can use the fact that the layer is thin: $H \ll L$. In that case we have as an order of magnitude:

$$\frac{\partial w}{\partial z} \sim \frac{w}{H} \gg \frac{\partial w}{\partial x} \, , \, \frac{\partial w}{\partial y} \sim \frac{w}{L} \, . \tag{8.7.16}$$

Therefore, we can approximate the z-component of the vorticity equation by

$$\frac{\mathrm{d}\omega_z}{\mathrm{d}t} = (\omega_z + 2\Omega_z) \, \frac{\partial w}{\partial z} \, . \tag{8.7.17}$$

Using the incompressibility condition (8.7.4) to eliminate $\partial w/\partial z$ from this equation, and defining $\zeta \equiv \omega_z$, one finds:

$$\frac{\mathrm{d}\zeta}{\mathrm{dt}} = -\left(2\Omega_z + \zeta\right) \left(\frac{\partial u}{\partial x} + \frac{\partial v}{\partial y}\right) \, . \tag{8.7.18}$$

If we now use (8.7.14) in the form

$$\frac{\mathrm{d}H}{\mathrm{d}t} = -H \, \left(\frac{\partial u}{\partial x} + \frac{\partial v}{\partial y}\right) \, , \tag{8.7.19}$$

and employ the fact that $\mathrm{d}\Omega_z/\mathrm{d}t = 0$, it is easily seen that these two equations can be combined to yield a conservation law for $(2\Omega_z + \zeta)/H$, a quantity known as the **potential vorticity**:

$$\boxed{\frac{\mathrm{d}}{\mathrm{d}t}\left(\frac{2\Omega_z + \zeta}{H}\right) = 0 \, .} \tag{8.7.20}$$

This equation shows that relative vorticity ζ can be generated by changes in the layer thickness H, even when it is not initially present. If the layer thickness H changes, the relative vorticity must adjust in order to keep the potential vorticity at a constant value. Note that Ω_z never changes: it is a constant set by the rotation of the planet!

This conservation law for the potential vorticity physically corresponds to vortex stretching in Shallow Water Theory. The motions responsible for the change in the layer thickness generate vorticity due to the Coriolis force acting on the flow.

The pressure in the Shallow Water Approximation follows from hydro*static* equilibrium in the vertical direction. This assumes implicitly that the underlying vertical velocities remain small when compared with the horizontal velocities: $|w| \ll |\boldsymbol{V}_{\rm h}|$. The equation of hydrostatic equilibrium reads

$$\frac{\partial P}{\partial z} = -\rho\, g\ . \tag{8.7.21}$$

Since the Shallow Water Approximation assumes a uniform density in the vertical direction, $\partial\rho/\partial z = 0$, the equation of hydrostatic equilibrium can be integrated immediately. If there is a fixed pressure P_0 at the top of the layer, which is located at $z = h(x\,,\,y\,,\,t)$, (see figure) the solution of (8.7.21) reads

$$P(x\,,\,y\,,\,z\,,\,t) = \rho g\ [h(x\,,\,y\,,\,t) - z\,] + P_0\ . \tag{8.7.22}$$

The pressure at depth z is the weight per unit area of the overlying column of fluid, plus the pressure P_0 of the medium at the top of the layer. The pressure P_0 could for instance be the atmospheric pressure at the surface of a body of water.

This relation between the pressure and the height h of the top of the layer implies that the horizontal pressure gradient is **independent** of the z-coordinate. Direct calculation yields:

$$\boldsymbol{\nabla}_{\rm h} P = \begin{pmatrix} \dfrac{\partial P}{\partial x} \\ \\ \dfrac{\partial P}{\partial y} \end{pmatrix} \ = \ \rho g \begin{pmatrix} \dfrac{\partial h}{\partial x} \\ \\ \dfrac{\partial h}{\partial y} \end{pmatrix}\ . \tag{8.7.23}$$

In the Shallow Water Approximation the resulting pressure force in the horizontal plane is completely determined by the variations in the position h of the top of the fluid layer. If the bottom of the layer is at height $z = h_{\rm b}(x\,,\,y)$, where the variation of $h_{\rm b}$ as a function of x and y gives the bottom topography, the thickness H of the fluid layer is simply

$$H(x\,,\,y\,,\,t) = h(x\,,\,y\,,\,t) - h_{\rm b}(x\,,\,y)\ . \tag{8.7.24}$$

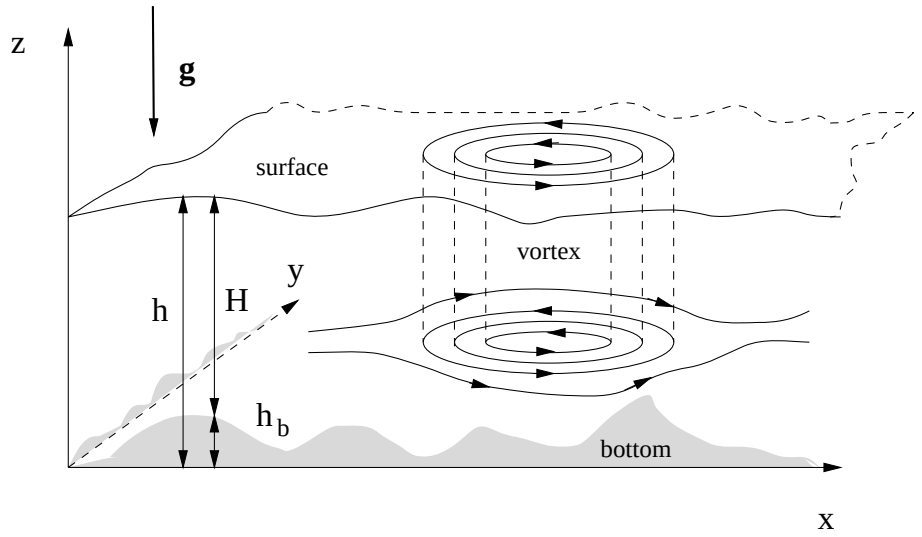

Figure 8.8: *The basic geometry of Shallow Water Theory. The flow is described by the motion in the $x-y$ plane with velocity $\boldsymbol{V}_{\rm h}=(u\,,\,v)$ and the thickness $H=h-h_{\rm b}$ of the fluid layer. The motion is independent of the height in the layer, as illustrated by the vortex column in the figure.*

8.7.1 The Shallow Water Equations

We can now write down the set of equations governing Shallow Water Theory. To facilitate the notation I define the following quantities:

$$\boldsymbol{\nabla}_{\rm h}=\left(\frac{\partial}{\partial x}\,,\,\frac{\partial}{\partial y}\right)\;\;,\;\;\boldsymbol{V}_{\rm h}=(u\,,\,v)\;\;,\;\;\boldsymbol{V}_{\rm h}\cdot\boldsymbol{\nabla}_{\rm h}=u\,\frac{\partial}{\partial x}+v\,\frac{\partial}{\partial y}\,, \tag{8.7.25}$$

where all vectors are two-dimensional entities that reside in the horizontal ($x-y$-)plane. The equations for a fluid in the Shallow Water Approximation are:

1. The **equation of motion** in the horizontal plane:

$$\frac{\partial\boldsymbol{V}_{\rm h}}{\partial t}+(\boldsymbol{V}_{\rm h}\cdot\boldsymbol{\nabla})\,\boldsymbol{V}_{\rm h}+2\Omega_z\;(\hat{\boldsymbol{z}}\times\boldsymbol{V}_{\rm h})=-\frac{\boldsymbol{\nabla}_{\rm h}P}{\rho}\;; \tag{8.7.26}$$

   This equation is simply the general equation of motion for a fluid in a rotating frame (Eqn. 8.6.54), projected onto the $x-y$ plane. Note the presence of the Coriolis term.

2. The **equation for the layer thickness:**

$$\frac{\partial H}{\partial t} + \boldsymbol{\nabla}_{\rm h} \cdot (\boldsymbol{V}_{\rm h}\, H) = 0 \; ; \tag{8.7.27}$$

This equation replaces the continuity equation in ordinary fluid mechanics. It is the result of mass conservation, and of the assumption that the underlying (fully three-dimensional) flow, which the Shallow Water Approximation describes in an approximate fashion, is incompressible.

3. The **constituent relations** for the density ρ, the layer thickness H and the pressure P:

$$\begin{aligned} \frac{\partial \rho}{\partial z} &= 0 \; ; \\ P &= P_0 + \rho g \; [h(x\,,\,y\,,\,t) - z\,] \; ; \\ H(x\,,\,y\,,\,t) &= h(x\,,\,y\,,\,t) - h_{\rm b}(x\,,\,y) \; ; \end{aligned} \tag{8.7.28}$$

The second of this set of equations replaces the equation of state of ordinary gas dynamics: it provides the pressure as a function of the density and the height of the layer. Since we are working in a rotating reference frame, the gravitational acceleration g is really $g_{\rm eff}$.

4. The equation for the **potential vorticity** which follows from the above equations and the equation of motion for vorticity in a rotating reference frame:

$$\left(\frac{\partial}{\partial t} + \boldsymbol{V}_{\rm h} \cdot \boldsymbol{\nabla}_{\rm h} \right) \left(\frac{2\Omega_z + \zeta}{H} \right) = 0 \; . \tag{8.7.29}$$

This equation takes the form of a conservation law.

If one eliminates the pressure from these equations, using relation (8.7.23), one can write the Shallow Water Equations in a form where all explicit reference to pressure and density has disappeared:

The equations of Shallow Water Theory

$$\begin{aligned}
\frac{\partial u}{\partial t} + u\,\frac{\partial u}{\partial x} + v\,\frac{\partial u}{\partial y} - 2\Omega_z\,v &= -g\,\frac{\partial (H + h_{\rm b})}{\partial x}\;; \\
\frac{\partial v}{\partial t} + u\,\frac{\partial v}{\partial x} + v\,\frac{\partial v}{\partial y} + 2\Omega_z\,u &= -g\,\frac{\partial (H + h_{\rm b})}{\partial y}\;; \\
\frac{\partial H}{\partial t} + u\,\frac{\partial H}{\partial x} + v\,\frac{\partial H}{\partial y} &= -H\,\left(\frac{\partial u}{\partial x} + \frac{\partial v}{\partial y}\right)\;; \\
\left(\frac{\partial}{\partial t} + u\,\frac{\partial}{\partial x} + v\,\frac{\partial}{\partial y}\right)\left(\frac{2\Omega_z + \zeta}{H}\right) &= 0\;.
\end{aligned} \tag{8.7.30}$$

Here it is assumed that the bottom topography, as described by the function $h_{\rm b}(x\,,\,y)$, is given.

This form of the shallow water equations is commonly employed in the geophysics community. As such, these equations present a major simplification when they are compared with the full set of equations employed in three-dimensional hydrodynamics. This simplification explains the popularity of the Shallow Water Approximation in the fields of meteorology, oceonography and the study of the atmospheres of the Gas Giants Jupiter, Saturn and Uranus.

Potential vorticity: an alternative derivation

The two main equations leading to the conservation law for potential vorticity can be derived in an alternative manner. I start with the equation for the layer thickness H. The fully three-dimensional flow is assumed to be incompressible:

$$\boldsymbol{\nabla} \cdot \boldsymbol{V} = \frac{\partial u}{\partial x} + \frac{\partial v}{\partial y} + \frac{\partial w}{\partial z} = 0 \; . \tag{8.7.31}$$

This implies that the 'two-dimensional' divergence satisfies

$$\frac{\partial u}{\partial x} + \frac{\partial v}{\partial y} = -\frac{\partial w}{\partial z} \; . \tag{8.7.32}$$

The shallow water approximation assumes that the horizontal velocity components u and v do not vary with height:

$$\frac{\partial u}{\partial z} = \frac{\partial v}{\partial z} = 0. \tag{8.7.33}$$

Integrating equation (8.7.32) from the bottom of the layer, at $z = h_{\rm b}$, to the top, at $z = h_{\rm b} + H$, using (8.7.33) one finds:

$$\begin{aligned} \int_{h_{\rm b}}^{h_{\rm b}+H} {\rm d}z \, \left(\frac{\partial w}{\partial z} \right) \; &= \; - \int_{h_{\rm b}}^{h_{\rm b}+H} {\rm d}z \, \left(\frac{\partial u}{\partial x} + \frac{\partial v}{\partial y} \right) \\ &= \; -H \, \left(\frac{\partial u}{\partial x} + \frac{\partial v}{\partial y} \right) \; . \end{aligned} \tag{8.7.34}$$

The integral on the left-hand side of this relation is trivial: one has

$$\int_{h_{\rm b}}^{h_{\rm b}+H} {\rm d}z \, \left(\frac{\partial w}{\partial z} \right) = w(x \, , \, y \, , \, h_{\rm b} + H \, , \, t) - w(x \, , \, y \, , \, h_{\rm b} \, , \, t) \; . \tag{8.7.35}$$

Since $w = \mathrm{d}z/\mathrm{d}t$, and the fact that it is not possible to draw vacuum bubbles between the bottom and the fluid, one must have:

$$\begin{aligned} w(x\ ,\ y\ ,\ h_{\rm b}\ ,\ t) &= \frac{\mathrm{d}h_{\rm b}}{\mathrm{d}t}\ , \\ w(x\ ,\ y\ ,\ h_{\rm b}+H\ ,\ t) &= \frac{\mathrm{d}(h_{\rm b}+H)}{\mathrm{d}t}\ . \end{aligned} \tag{8.7.36}$$

Substituting these two relations into (8.7.34) one finds:

$$\frac{\mathrm{d}H}{\mathrm{d}t} = -H\left(\frac{\partial u}{\partial x}+\frac{\partial v}{\partial y}\right)\ . \tag{8.7.37}$$

This is equation (8.7.13).

In the shallow-water approximation the only component of the vorticity is the z-component. The *absolute* vorticity (i.e. the vorticity in the laboratory frame that is not corotating) has a z-component

$$\omega_{{\rm a}z} = \zeta + 2\Omega_z\ . \tag{8.7.38}$$

The vortex lines associated with this vorticity are all along the z-axis. The length of these lines varies as the thickness of the layer varies. Since the horizontal velocity components u and v do **not** depend on z, the absolute vorticity also satisfies:

$$\frac{\partial \omega_{{\rm a}z}}{\partial z} = 0\ . \tag{8.7.39}$$

This means that the vorticity is uniform in the z-direction. We can then apply the vortex stretching law Eqn. (8.2.20) in the form

$$\frac{\mathrm{d}}{\mathrm{d}t}\left(\frac{\omega_{{\rm a}z}}{\rho\,\Delta z}\right) = 0 \tag{8.7.40}$$

to the *whole* vortex line, with length $\Delta z = (H+h_{\rm b}) - h_{\rm b} = H$.

The shallow water approximation assumes an underlying incompressible three-dimensional flow, which implies that the density in a given fluid element remains constant:

$$\frac{\mathrm{d}\rho}{\mathrm{d}t} = -\rho\, \boldsymbol{\nabla} \cdot \boldsymbol{V} = 0\ . \tag{8.7.41}$$

Therefore, the vortex stretching law in the shallow water approximation simply reads:

$$\frac{\mathrm{d}}{\mathrm{d}t}\left(\frac{\omega_{\mathrm{a}z}}{H}\right) = 0 \iff \frac{\zeta + 2\Omega_z}{H} = \text{constant}. \tag{8.7.42}$$

This is the conservation law (8.7.20) for the potential vorticity.

8.8 Water waves, cyclones and Jupiter's Great Red Spot

8.8.1 Shallow water waves

The equations of Shallow Water Theory have solutions that describe the small-amplitude waves. Let us assume that the unperturbed fluid is at rest ($\boldsymbol{V}_{\rm h} = 0$), that the bottom is flat so that we can put $h_{\rm b} = 0$. Consider small perturbations in a fluid of unperturbed depth H_0, so that

$$\boldsymbol{V}_{\rm h} = \delta\boldsymbol{V}_{\rm h} = (\delta u\ ,\ \delta v) \quad , \quad H = H_0 + \delta H(x\ ,\ y\ ,\ t)\ . \tag{8.8.1}$$

The Shallow Water equations can be linearised by consistently neglecting all quadratic terms in δu, δv and δH, in their cross-products and in the derivatives. This yields the following set of linear equations:

$$\begin{aligned} \frac{\partial \delta u}{\partial t} - 2\Omega_z\,\delta v &= -g\,\frac{\partial \delta H}{\partial x}\ ; \\ \frac{\partial \delta v}{\partial t} + 2\Omega_z\,\delta u &= -g\,\frac{\partial \delta H}{\partial y}\ ; \\ \frac{\partial \delta H}{\partial t} &= -H_0\left(\frac{\partial \delta u}{\partial x} + \frac{\partial \delta v}{\partial y}\right)\ . \end{aligned} \tag{8.8.2}$$

Let us look for plane-wave solutions of the form

$$\begin{pmatrix} \delta u(x\ ,\ y\ ,\ t) \\ \\ \delta v(x\ ,\ y\ ,\ t) \\ \\ \delta H(x\ ,\ y\ ,\ t) \end{pmatrix} = \begin{pmatrix} \tilde{u} \\ \\ \tilde{v} \\ \\ \tilde{H} \end{pmatrix} \times \exp(ik_x x + ik_y y - i\omega t) + cc.\ . \tag{8.8.3}$$

This is the standard plane wave expansion already introduced in Chapter 6. Substituting this assumption into the set of equations (8.8.2) one finds a set of three linear algebraic equations.

These coupled, linear equations can be written in matrix form as

$$\begin{pmatrix} \omega & -2i\Omega_z & -k_x g \\ +2i\Omega_z & \omega & -k_y g \\ -k_x H_0 & -k_y H_0 & \omega \end{pmatrix} \begin{pmatrix} \tilde{u} \\ \tilde{v} \\ \tilde{H} \end{pmatrix} = 0 \; . \tag{8.8.4}$$

As in the case of sound waves, there are only non-trivial solutions if the determinant of the 3×3 matrix in the above equation vanishes identically. This solution condition yields the dispersion relation for shallow water waves, which includes the influence of the horizontal component of the Coriolis force:

$$\omega^3 - \left[\left(k_x^2 + k_y^2 \right) g H_0 + 4\Omega_z^2 \right] \omega = 0 \; . \tag{8.8.5}$$

Discarding the trivial solution $\omega = 0$, there remain two independent solutions for ω of opposite sign:

$$\omega = \pm \sqrt{k^2 c_H^2 + 4\Omega_z^2} \; . \tag{8.8.6}$$

Here $k \equiv \sqrt{k_x^2 + k_y^2}$ is the horizontal wavenumber. In this dispersion relation appears a characteristic velocity $c_{\rm H}$, which is given by

$$c_H \equiv \sqrt{g H_0} \; . \tag{8.8.7}$$

It is the typical velocity associated with the depth H of the fluid layer, and the strength g of the gravitational acceleration[15]. If there is no rotation (so that $\Omega_z = 0$) the dispersion relation (8.8.6) reduces to $\omega = \pm k c_H$, a dispersion relation that looks exactly the same as the dispersion relation for sound waves: $\omega = \pm k c_{\rm s}$. This velocity $c_{\rm H}$ is analogous to the sound speed $c_{\rm s}$ in the following sense. The pressure at the bottom of the layer equals $P(z = 0) = P_0 + \rho g H_0$, with P_0 the atmospheric pressure. This implies that the speed $c_{\rm H}$ formally obeys the relation

$$c_{\rm H}^2 = \left(\frac{\partial P}{\partial \rho} \right)_{z=0} = g H_0 \; . \tag{8.8.8}$$

[15]There is an analogous velocity in classical mechanics: a pendulum with length ℓ, suspended in a gravity field with a uniform gravitational acceleration g, oscillates with frequency $\omega = \sqrt{g/\ell}$ around the vertical for small-amplitude oscillations. The velocity of the mass at the end of the pendulum equals $v = \omega \ell = \sqrt{g\ell}$.

For sound waves in a polytropic (adiabatic) gas on the other hand, where $P \propto \rho^\gamma$, the characteristic velocity associated with the waves is the adiabatic sound speed, which is also determined by the derivative of pressure with respect to density:

$$c_{\rm s}^2 = \frac{\partial P}{\partial \rho} = \frac{\gamma P}{\rho} \ . \tag{8.8.9}$$

Despite this analogy, there is an important difference between the waves ocurring in Shallow Water Theory, and adiabatic sound waves. Sound waves are *compressible*, with an associated velocity perturbation $\delta \boldsymbol{V} = \partial \boldsymbol{\xi}/\partial t$ that satisfies $\boldsymbol{\nabla} \cdot \delta \boldsymbol{V} \neq 0$. The shallow water equations on the other hand assume *ab initio* that the (three-dimensional) flow is incompressible: $\boldsymbol{\nabla} \cdot \boldsymbol{V} = 0$. As a result, the shallow water waves are *incompressible*! Their existence is entirely due to the variations in the layer thickness and the pressure forces caused by these variations, together with the Coriolis force acting on the fluid.

8.8.2 Cyclones

A cyclone (or hurricane) is a rapid circulation pattern around a compact region of extreme low pressure. They occur in the (sub)tropics above the warm waters of the oceans. (As we will see, the circulation around a high-pressure region is *anti-cyclonic*: the material rotates in the opposite sense). The low pressure in a cyclone is the result of a strong rising motion in the atmosphere. This upward motion is driven by buoyancy, which in turn results from the release of the latent heat by water in the moist air. This heat release occurs when water vapour condenses into droplets. The gas absorbs the energy released by the condensing water vapor, heating the gas. This heating causes the gas to expand in an effort to undo the associated increase in pressure, so that the pressure equilibrium with the surrounding (colder and less moist) air is restored. This lowers the density of the moist gas, and the gas rises due to the Archimedes force. This upward motion lowers the pressure even more, and more moist air from the surface, which carries water from the ocean below, is sucked into the cyclone, keeping the process going.

The two figures below show the circulation pattern and, as an example of cyclonic circulation on the Northern Hemisphere, a satellite image of the tropical Hurricane Katrina, which devastated the South-Eastern coast of the United States in 2005.

The motion of air near the surface into the low-pressure region is deflected by the Coriolis force, leading to a circulation around the low-pressure core.[16] To describe this circulation I will use the so-called *geostrophic limit* of the equations of motion.

[16] Because of mass conservation, the material must flow away again at high altitude, leading to an anti-cyclonic circulation at great height.

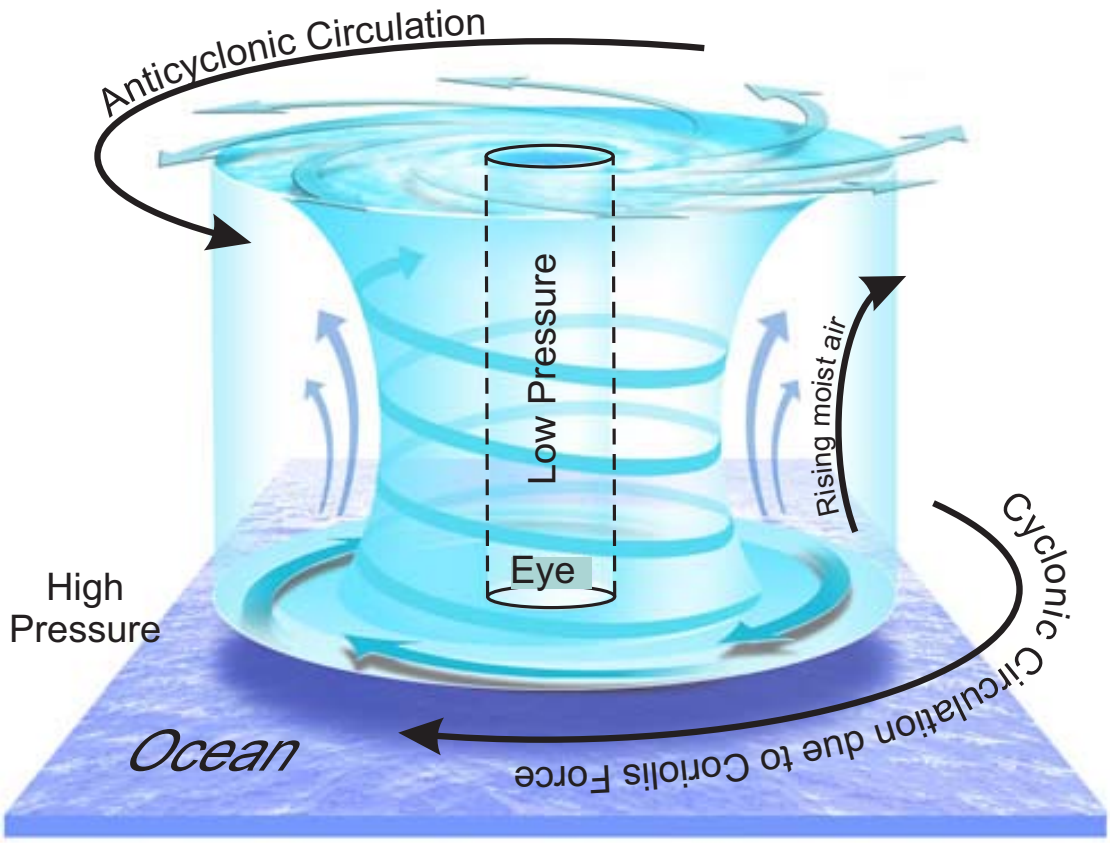

Figure 8.9: *The circulation pattern in a cyclone or a hurricane. Moist air rises due to buoyancy, and the resulting region of low pressure leads to a cyclonic circulation near sea level. At the top of the cyclone, where matter flows away, the circulation is anticyclonic*

In the geostrophic limit one makes a number of approximations. If the typical time for temporal changes in the flow is T, and if the typical length scale for gradients in the horizontal plane is L, one can estimate the typical magnitude of derivatives as

$$\left|\frac{\partial \boldsymbol{V}_{\rm h}}{\partial t}\right| \sim \frac{|\boldsymbol{V}_{\rm h}|}{T} \quad , \quad |(\boldsymbol{V}_{\rm h}\cdot\boldsymbol{\nabla}_{\rm h})\boldsymbol{V}_{\rm h}| \sim \frac{|\boldsymbol{V}_{\rm h}|^2}{L}\,. \tag{8.8.10}$$

The geostrophic limit corresponds to the situation where [1] the intrinsic time dependence of the flow is slow, [2] the flow is very subsonic so that $\rho\, V_{\rm h}^2 \ll P$ and [3] the flow only varies on a sufficiently large length scale, so that:

$$\frac{|\partial \boldsymbol{V}_{\rm h}/\partial t|}{|2\boldsymbol{\Omega}\times\boldsymbol{V}_{\rm h}|} \sim \frac{1}{2|\Omega_z|T} \ll 1 \quad , \quad \frac{|(\boldsymbol{V}_{\rm h}\cdot\boldsymbol{\nabla}_{\rm h})\boldsymbol{V}_{\rm h}|}{|2\boldsymbol{\Omega}\times\boldsymbol{V}_{\rm h}|} \sim \frac{|\boldsymbol{V}_{\rm h}|}{2\Omega_z L} \equiv {\rm Ro} \ll 1\,. \tag{8.8.11}$$

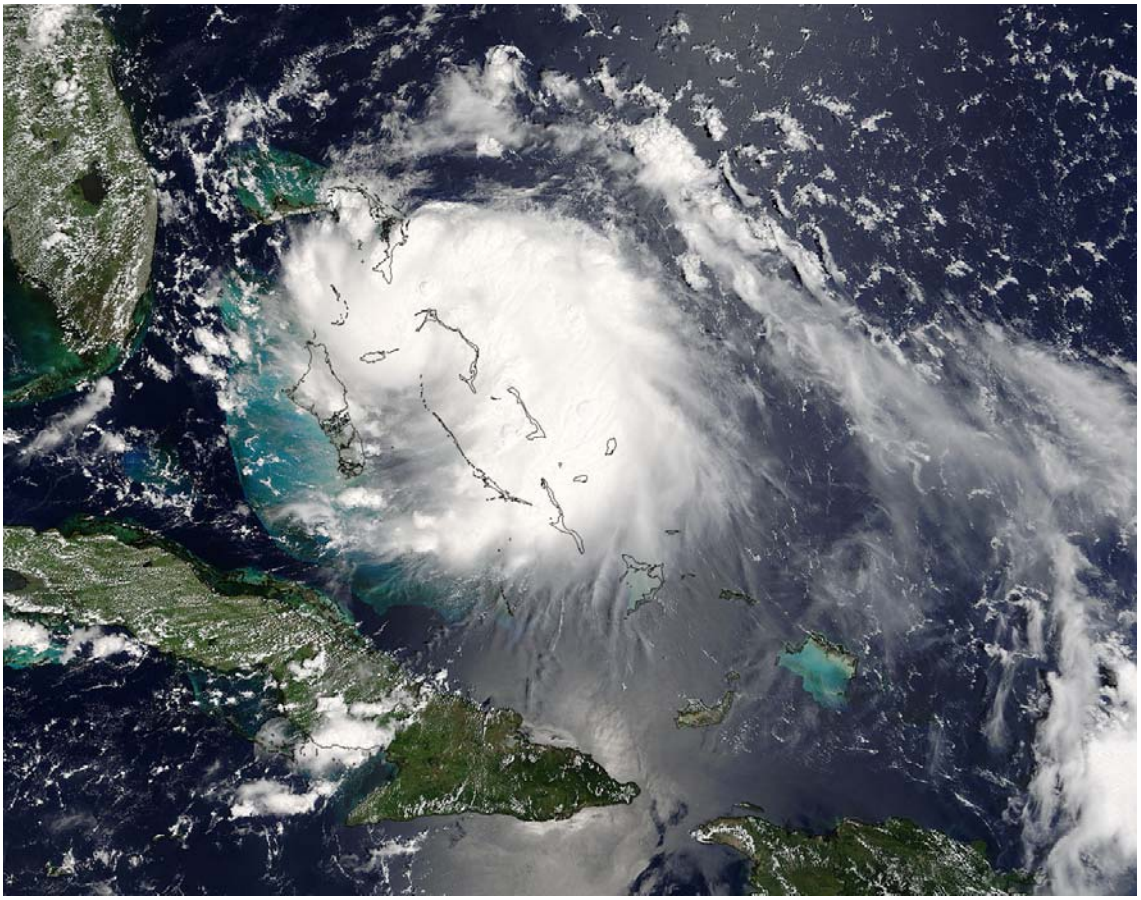

Figure 8.10: *Hurricane Katrina approaching Florida in 2005*

The dimensionless quantity Ro is called the *Rossby Number*, and measures the relative importance of frame rotation for the dynamics of a fluid. If the Rossby number is small, the Coriolis force in the rotating system is dominant over the ordinary inertial force: $|2\boldsymbol{\Omega} \times \boldsymbol{V}_{\mathrm{h}}| \gg |\mathrm{d}\boldsymbol{V}_{\mathrm{h}}/\mathrm{d}t|$. In a flow with $\mathrm{Ro} \ll 1$ one can (as a first approximation) neglect the inertial term $\mathrm{d}\boldsymbol{V}_{\mathrm{h}}/\mathrm{d}t$ in the shallow-water equation of motion. The reduced equation of motion in the geostrophic approximation therefore reads:

$$2\Omega_z \left(\hat{\boldsymbol{z}} \times \boldsymbol{V}_{\mathrm{h}}\right) = -\frac{\boldsymbol{\nabla}_{\mathrm{h}} P}{\rho} \; . \tag{8.8.12}$$

In this limit, the Coriolis force due to planetary rotation balances the pressure force. The unit vector $\hat{\boldsymbol{z}}$ is oriented along the local vertical direction, so its direction (and consequently the vertical component $\Omega_z = \boldsymbol{\Omega} \cdot \hat{\boldsymbol{z}}$) varies with geographical latitude, switching sign at the Equator. Taking the cross product of this equation with $\hat{\boldsymbol{z}}$, using the vector relation

$$\boldsymbol{A} \times \left(\boldsymbol{B} \times \boldsymbol{C}\right) = \left(\boldsymbol{A} \cdot \boldsymbol{C}\right) \boldsymbol{B} - \left(\boldsymbol{A} \cdot \boldsymbol{B}\right) \boldsymbol{C} \tag{8.8.13}$$

for $\boldsymbol{A} = \boldsymbol{B} = \hat{\boldsymbol{z}}$ and $\boldsymbol{C} = \boldsymbol{V}_{\mathrm{h}}$, together with $\hat{\boldsymbol{z}} \cdot \boldsymbol{V}_{\mathrm{h}} = 0$ and $\hat{\boldsymbol{z}} \cdot \hat{\boldsymbol{z}} = 1$, one finds:

$$\boxed{\boldsymbol{V}_{\mathrm{h}} = \frac{\hat{\boldsymbol{z}} \times \boldsymbol{\nabla}_{\mathrm{h}} P}{2\rho\, \Omega_z} \; .} \tag{8.8.14}$$

In the geostrophic approximation, the flow direction is *perpendicular* to the direction of the pressure gradient, exactly at right angles to the flow direction one might naively expect. This implies that the flow lines are *along* the lines of constant pressure: the so-called *isobars*.

Since the projection of the planetary rotation vector on the local vertical, $\Omega_z = \boldsymbol{\Omega} \cdot \hat{\boldsymbol{z}}$, changes sign at the equator, cyclones rotate in opposite directions on the Southern- and Northern Hemisphere. On Earth, the circulation around a region of low pressure region (and around cyclones or hurricanes, which are essentially extreme, compact low-pressure regions) is anti-clockwise on the Northern Hemisphere, and clockwise on the Southern Hemisphere. For high-pressure regions the circulation around the region has the opposite sense.

Of course, if one describes the flow more precisely than is done when one employs the geostrophic limit, the flowlines actually *do* cross the isobars, creating a spiral-like flow pattern with mass flowing into a low-pressure region near the Earth's surface, and mass flowing out of a high-pressure region.

8.8.3 Jupiter's Great Red Spot

Shortly after the invention of the telescope observers noticed a large feature in the atmosphere of Jupiter. This feature, known as the *Great Red Spot* for its reddish color, measures some 14,000 km in the north-south direction, and some 40,000 km in the east-west direction (see figure). The Great Red Spot has persisted until today, some 400 years. Measurements of the motions of the material inside the Great Red Spot, which were done by the Voyager space probes, have shown that this material moves in a counter-clockwise (anticyclonic) direction. The material inside the Great Red Spot is colder than its surroundings. It rotates once per seven days around the core. This rotation corresponds to a wind speed of about 100 m/s. The uppermost clouds of the Great Red Spot rise about 2 tot 5 km above the surrounding Jovian atmosphere.

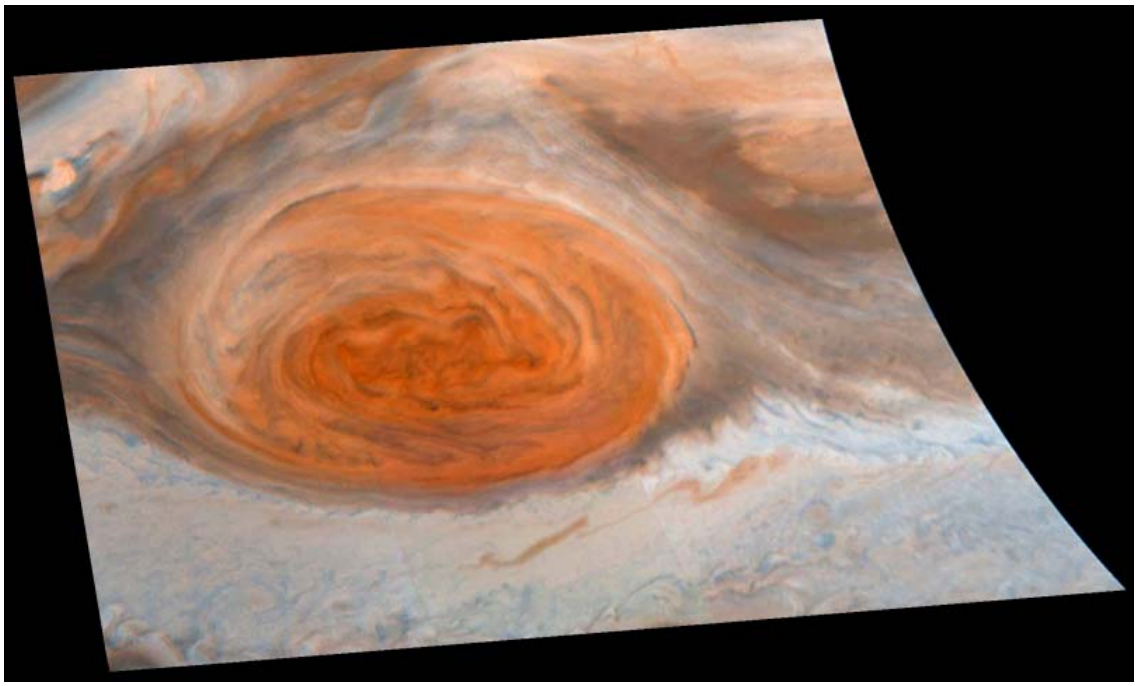

Figure 8.11: *Jupiter's Great Red Spot as observed in 1996 by the Galileo spacecraft at infra-red wavelengths.*

There are many similar (but much smaller) structures visible in Jupiter's atmosphere, the so-called white ovals. Similar structures have been observed in the atmospheres of the other two rapidly rotating gas giants, Saturn and Uranus.

The Great Red Spot (GRS) is the most powerful vortex known in the planetary system. Over the years, a number of different hypotheses have been advanced as to its origin:

- The oldest suggestion, due to Hide (1961), is that the GRS is a so-called *Taylor Column*. Such a column occurs if a planetary wind, (in the case of Jupiter the

strong zonal wind) encounters a solid obstacle, such as a mountain ridge or a large skyscraper. In the lee (the sheltered side) of the obstacle a vortex (or in many cases: a train of vortices) is formed. The thermal wind equation (8.6.73) in the baroclinic limit (where $\boldsymbol{\nabla} P \times \boldsymbol{\nabla} \rho = 0$), reduces to a particularly simple form if one assumes incompressibility $\boldsymbol{\nabla} \cdot \boldsymbol{V} = 0$:

$$(2\boldsymbol{\Omega} \cdot \boldsymbol{\nabla})\boldsymbol{V} = 0 \; . \tag{8.8.15}$$

In this limit, the *Taylor-Proudman theorem* is valid, which states that the velocity does not vary along the direction of $\boldsymbol{\Omega}$. Since the Great Red Spot occurs at rather high latitudes, there is an an appreciable angle between $\boldsymbol{\Omega}$ and the (local) horizontal plane. This means that any fluid motion induced by the obstacle is 'mapped' along the direction of $\boldsymbol{\Omega}$ to higher fluid layers. The fluid moves as if the obstacle were present there also: it is forced to move in 'columns' along $\boldsymbol{\Omega}$. This is illustrated below for a more simpel laminar flow (a flow without vortices) around a cylinder. This hypothesis for the GRS is no longer believed: we know that there is no solid surface on Jupiter[17], and consequently there are no obstacles that a strong zonal wind could hit.

- The Dutch-born planetary scientist Gerald Kuijper proposed in 1972 that the GRS is in fact the top (called the 'anvil' by meteorologists) of the Jovian equivalent of a hurricane. As explained in the previous Section, the motion at the top of a hurricane or cyclone is a diverging flow away from the core, leading to an anti-cyclonic rotation. Such anti-cyclonic motion is indeed observed in the GRS. Although not totally excluded, this hypothesis has gone out of fashion. Wind speed measurements at greater depth do not seem to support the idea of the latent heat release and the associated upward motion that is needed to drive the high-altitute anti-cyclonic circulation.

- Presently, the most popular hypothesis is due to Caltech planetary scientist Andrew Ingersoll. He proposed in 1973[18] that the GRS is a *free atmospheric vortex*. Such a vortex, once formed, is very stable as a result of the conservation of potential vorticity:

$$\frac{2\Omega_z + \zeta}{H} = \text{constant along streamlines.} \tag{8.8.16}$$

In this model, the GRS occurs in a shallow top layer of the Jovian atmosphere which overlies a deeper, strongly turbulent, azimuthal flow (zonal wind) that represents the bulk Jovian circulation.

[17] At great depth, Jupiter probably has a solid core of rocks, surrounded by metallic hydrogen.
[18] Ingersoll, A.P., 1973: *Science* **183**, 1346

Both numerical experiments[19] and experiments in the laboratory using fluids trapped between rotating annuli[20] have shown that such a system can lead to the formation of a single (or a few) large dominant vortices. A phenomenon that contributes to this is *vortex merging*, where smaller vortices merge to form a larger vortex, with a total (potential) vorticity of this larger vortex roughly equal to the total vorticity of all the contributing vortices. Small vortices are created continuously, as a result of the interaction between the shallow top layer in the atmosphere, and the turbulent (disordered) motions in the underlying flow. This deeper flow exhibits a strong *shear*, where the velocity varies in magnitude in the direction perpendicular to the flow lines. In the case of the gas giants, this strong shear is due to the dependence of streaming velocity of the strong zonal winds on the planetary latitude. The colored bands in Jupiter's atmosphere shows convincingly that such a strong shear is present, and the fine-structure in the atmospheric bands consists of many vortices in a range of sizes. Direct measurements of wind speeds by the Pioneer, Voyager and Galileo space probes confirm this picture.

In Ingersoll's theory, the persistence of the GRS over a period exceeding 300 years[21] is explained as the combined result of three factors: [1] the *absence* of an underlying solid surface which would degrade vortices due to friction, [2] the effect of *vortex merging*, where vorticity lost due to internal friction in the gas is replaced by the colaescence of smaller vortices, and [3] the fact that Jupiter has an internal heat source. This heat source is associated with the slow contraction of the planet. That such an internal heat source must be present follows simply from the fact that the amount of energy emitted by Jupiter actually exceeds the amount of energy intercepted by the planet in the form of Solar radiation. Jupiter emits about twice the amount of energy received from the Sun (Saturn emits even three times that amount!). These giant planets are still releasing the energy of their primordial contraction. In fact, they may still be contracting at a rate of about 1mm/year. A more detailed description of the gas giants can be found in the book by Morrison & Owen[22]

[19] P.S. Marcus, 1988: *Nature* **331**, 693

[20] J. Sommeria, S.D. Meyers & H.L. Swinney, 1988: *Nature* **331**, 689

[21] In contrast: the cyclones and hurricanes in the Earth's atmosphere typically last for a period of the order of weeks!

[22] D. Morrison & T. Owen, 1996: *The Planetary System* (Second Edition), Addison-Wesley Publishing Company, Reading, Massachusetts, 1996, Chapter 13.

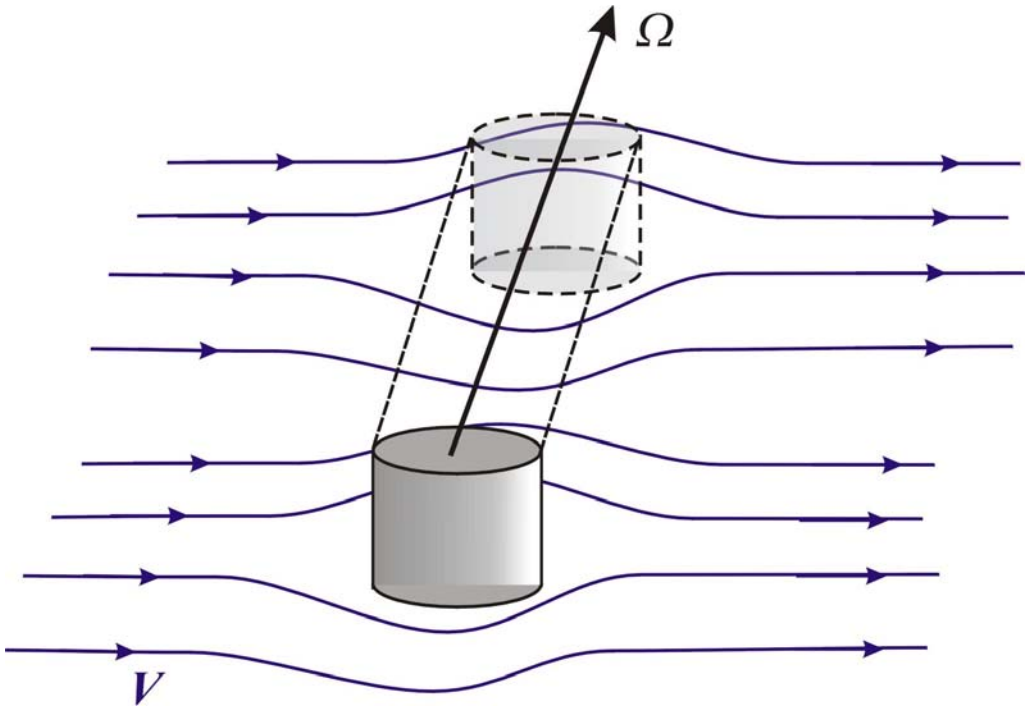

Figure 8.12: *An illustration of the Taylor-Proudman theorem. A cylinder of finite height formes an obstacle in a flow in the horizontal plane. This cylinder serves as a simple model for a skyscraper. The flow lines are forced around the cylinder. Above the cylinder, the flow behaves as if the cylinder is still there, be it at a new position: the flow pattern is mapped without change to larger and larger altitudes in the direction along* $\mathbf{\Omega}$*. The resulting flow pattern exhibits what is known as a Taylor-Proudman column.*

Chapter 9

Theory of diffusion and viscosity

Diffusion processes occur in a fluid or gas whenever a property is transported in a manner resembling a random walk. For instance, consider the spreading of a contaminant in a fluid. The molecules of the contaminating substance get random kicks in collisions with the individual molecules of the fluid. In fact, this is how the random walk was discovered in nature: the historical example of *Brownian motion*. This example looks at the effects of the kicks on the position of the molecule.

Alternatively, one can think of particles subject to a random force with zero mean: in case the 'kick' changes the momentum of a particle. As a result, particles will diffuse in momentum in the sense that a group of identical particles, all starting out with the same initial momentum, will acquire a spread in momentum values after some time. This happens for instance when a beam of charged particles propagates through a plasma: the electrostatic interactions with the plasma particles (called *Coulomb collisions* as they result from the Coulomb interaction) will cause a spread in momentum of the beam particles.

The properties of a diffusion process can be studied using a simple statistical model. More complicated discussions can be found in the book by Zeldovich *et al.*[1] and in the book by Van Kampen[2]

9.1 The one-dimensional random walk

I will start the discussion with a simple example: a one-dimensional random walk in space. Consider a random walk in position x, which starts at a time $t = 0$. For simplicity I put the starting position at $x = 0$. The random walk consists of discrete steps forward and backward, with an equal probability, $P_+ = P_- = \frac{1}{2}$, and a constant step size λ.

[1] Ya.B. Zeldovich, A.A. Ruzmaikin & D.D. Sokoloff, 1990: *The Almighty Chance*, World Scientific Lecture Notes in Physics, Vol. 20, World Scientific, Singapore

[2] N.G. van Kampen, 1981: *Stochastic Processes in Physics and Chemistry*, North-Holland Publ. Company, Amsterdam

I will use a roman index (e.g. i, j etc.) to denote the step number in a sequence of steps.

In this simple random walk, the position shift Δx_i at step number i can be written in the form

$$\Delta x_i = \tilde{\sigma}_i \lambda \, . \tag{9.1.1}$$

A forward step has $\tilde{\sigma}_i = +1$, and a backward step $\tilde{\sigma}_i = -1$, so $\tilde{\sigma}$ is a direction parameter. After N such steps, the position of a participant in the random walk equals:

$$\begin{aligned} x(N) &= \Delta x_1 + \Delta x_2 + \cdots + \Delta x_N \\ &= \lambda \times (\tilde{\sigma}_1 + \tilde{\sigma}_2 + \cdots + \tilde{\sigma}_N) \, . \end{aligned} \tag{9.1.2}$$

An example of two statistically independent realizations of such a simple prescription are shown in the figure below. In order to be able to investigate the statistical properties of this random walk, I will assume that there is large number of participants, the random walkers, which all follow recipe (9.1.1).

Now consider a the whole *group* of random walkers. Each member of the group perfoms his random walk *independently*, without being influenced by the others. All start at the same position $x = 0$, and at the same time, $t = 0$. Let us first calculate the *average* position $\overline{x(N)}$ of that group, the 'center of mass'. In calculating that average position one has to realise that in the sequence of steps that leads to $x(N)$ the values $\tilde{\sigma}_i = +1$ and $\tilde{\sigma}_i = -1$ occur with equal probability, $P_+ = P_- = \frac{1}{2}$. Therefore, the average value of the direction parameter $\tilde{\sigma}_i$, when averaged over a large number of steps, or when averaged over a large group[3], is

$$\overline{\tilde{\sigma}_i} = P_+ \times (+1) + P_- \times (-1) = 0 \, . \tag{9.1.3}$$

As a result, the net value of the sum (9.1.2) vanishes:

$$\boxed{\overline{x(N)} = N \, \overline{\tilde{\sigma}} \, \lambda = 0 \, .} \tag{9.1.4}$$

The average position after N steps is still located at the origin, the point where everybody started.

[3]This interchangebility of a group average and a time average frequently occurs in statistical physics

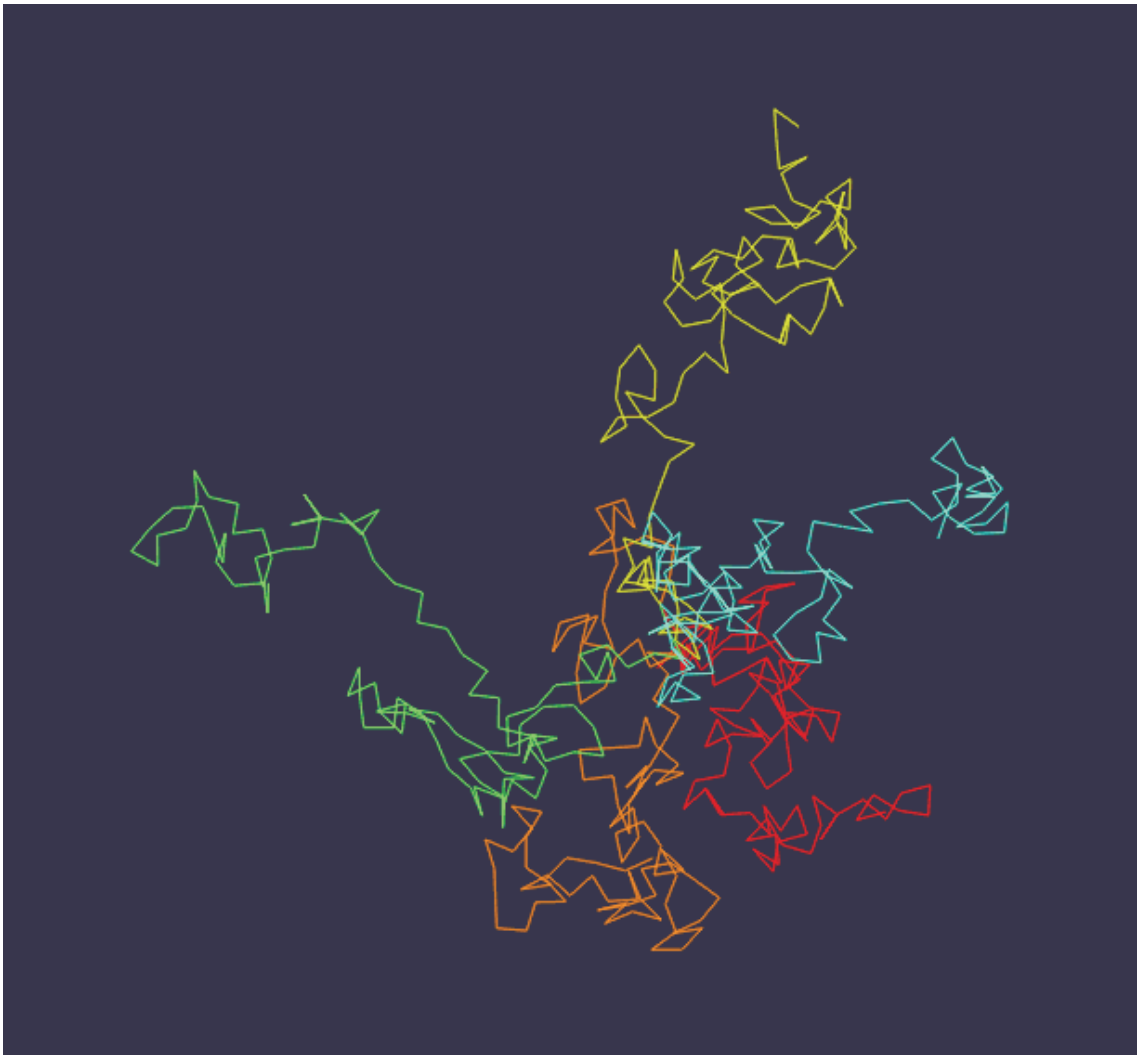

Figure 9.1: *An illustration of a two-dimensional random walk. Five statistically independent realizations (color-coded) of a random walk with the same mean free path are shown.*

This result does **not** imply that all participants are still at $x = 0$! Rather, it takes account of the fact that each *individual* participant will in general not perform an equal number of forward and backward steps. As each participant is statistically independent from the others, the difference between the number of forward steps taken and the number of backward steps taken varies from participant to participant. As a result, they spread out along x with -on average- as many random walkers with a positive value x as with a negative value of x. This difference between the *individual* behaviour of the random walkers and the *mean* behaviour the group as a whole means that the group will spread out around the origin $x = 0$.

The amount of spreading of the random walkers increases with the number of steps. It can be quantified by the so-called *dispersion*, a quantity that follows directly from the average of x^2. From Eqn. (9.1.2) one has

$$\begin{aligned} x^2(N) &= \Delta x_1^2 + \Delta x_2^2 + \cdots \Delta x_N^2 + \\ &\quad + 2\Delta x_1 \Delta x_2 + 2\Delta x_1 \Delta x_3 + 2\Delta x_2 \Delta x_3 + \cdots . \end{aligned} \tag{9.1.5}$$

This sum contains two contributions.

1. The first contribution to $\overline{x^2}$ consists of the squares of the *same* N steps, like Δx_1^2, Δx_2^2 etc. Using Eqn. (9.1.1) it follows for each step i that these terms in the expression for x^2 satisfy $\Delta x_i^2 = \tilde{\sigma}_i^2 \lambda^2 = \lambda^2$. After N steps, there are a total of N such terms, each of which contributes equally to the sum for x^2

2. The second contribution to x^2 comes from the terms that are the product of *different* steps: $\Delta x_i \Delta x_j = \tilde{\sigma}_i \tilde{\sigma}_j \lambda^2$ with $i \neq j$. There are a total of $N^2 - N = N(N-1)$ such terms in the sum for x^2. When $x^2(N)$ is averaged over the whole group, the value $\tilde{\sigma}_i \tilde{\sigma}_j = +1$ occurs as often for as does the value $\tilde{\sigma}_i \tilde{\sigma}_j = -1$. The probability $\mathcal{P}_+$ that $\tilde{\sigma}_i \tilde{\sigma}_j$ takes the value $+1$, and the probability $\mathcal{P}_-$ that it takes the value -1, are equal to:

$$\begin{aligned} \mathcal{P}_+ &= P_+ P_+ + P_- P_- , \\ \mathcal{P}_- &= 2 P_- P_+ . \end{aligned} \tag{9.1.6}$$

   When $P_+ = P_- = \frac{1}{2}$ one automatically has $\mathcal{P}_+ = \mathcal{P}_- = \frac{1}{2}$. Therefore, this second contribution to x^2 vanishes upon averaging as $\overline{\tilde{\sigma}_i \tilde{\sigma}_j} = \mathcal{P}_+ - \mathcal{P}_- = 0$.

These considerations yield a very simple answer: after each of the random walkers has taken N steps, the dispersion of the whole group of random walkers is determined by:

$$\boxed{\overline{x^2(N)} = N \times \lambda^2 \, .} \tag{9.1.7}$$

Therefore, the typical distance $d(N)$ between an individual random walker and his point of origin equals after N steps:

$$d(N) \equiv \sqrt{\overline{x^2(N)}} = \sqrt{N} \times \lambda \, . \tag{9.1.8}$$

This distance $d(N)$ is a measure of the dispersion. Note that it increases as $d(N) \propto N^{1/2}$. This indicates that a random walk is a very inefficient method of getting anywhere! A straight (directed) walk will take the walker a distance $d \propto N$ after N steps.

So far, I have described the random walk as a sequence of discrete steps of equal size. As a result, the number of steps N figures prominently in all equations. Usually however, one is not interested in the average position $\overline{x}$ and dispersion $\sqrt{\overline{x^2}}$ as a function of N, but as a function of time t. The simplest way of achieving this is by assuming that each participant in the random walk takes ν steps every second, with ν the 'step-frequency', so that the time-interval between two successive steps, the collision time, equals $\Delta t_{\rm c} = 1/\nu$. The typical number of steps taken in a time t is

$$N \approx \nu t \simeq t/\Delta t_{\rm c} \, , \tag{9.1.9}$$

where the approximate sign is needed since the number of steps N can only take integer values. This relation allows us to write the dispersion as a function of time:

$$\overline{x^2}(t) = \nu \lambda^2 t \, . \tag{9.1.10}$$

For a one-dimensional random walk, one defines the *diffusion coefficient* $\mathcal{D}$ by the relation:

$$\mathcal{D} \equiv \frac{\overline{x^2}(t)}{2t} = \frac{1}{2} \, \lambda^2 \, \nu \tag{9.1.11}$$

In terms of this diffusion coefficient one can write

$$\boxed{\overline{x^2}(t) = 2\mathcal{D}t \ .} \tag{9.1.12}$$

Note that the diffusion coefficient is completely determined by the *intrinsic* properties of the random walk process: the step size λ and the step frequency ν. These definitions, and the derivation presented above, assume implicitly that the diffusion coefficient $\mathcal{D}$, and also λ and/or ν, do not depend on time or on the position x.

9.2 The isotropic three-dimensional random walk

The principles of the one-dimensional random walk can be generalized easily to the case of an *isotropic* three-dimensional random walk. In this context, 'isotropic' means that the random walk has no preferred direction: the diffusion proceeds equally rapid along the x, y and z axes. In addition, I will use a more realistic model for the individual steps in the random walk. Rather than assuming that each step in the random walk has the same length, $|\Delta \boldsymbol{x}| = \lambda$, I will allow different stepsizes that are drawn from a probability distribution for the step size. This distribution has a well-defined average stepsize $\lambda = \langle |\Delta \boldsymbol{x}| \rangle$.

Let us assume that the random walkers take a step in an arbitrary direction, with a step size equal to Δx_i at the i-th step (see figure below). This implies that the i-th step can be written in vector notation as

$$\Delta \boldsymbol{x}_i = \Delta x_i \, \hat{\boldsymbol{e}}_i \ . \tag{9.2.1}$$

Here $\hat{\boldsymbol{e}}_i$ is a vector of unit length, so that $|\hat{\boldsymbol{e}}_i| = 1$, with a direction that is chosen randomly at each step in tghe random walk. This unit vector plays the same role as the direction parameter $\tilde{\sigma}_i$ in the one-dimensional random walk of the previous Section. The assumption of isotropy implies that the *group average* of the random vector $\hat{\boldsymbol{e}}$ satisfies:

$$\overline{\hat{e}_x} = \overline{\hat{e}_y} = \overline{\hat{e}_z} = 0 \ \ , \ \ \overline{\hat{e}_x^2} = \overline{\hat{e}_y^2} = \overline{\hat{e}_z^2} = \frac{1}{3} \ \ , \ \ \overline{\hat{e}_x \hat{e}_y} = \overline{\hat{e}_x \hat{e}_z} = \overline{\hat{e}_y \hat{e}_z} = 0 \ . \tag{9.2.2}$$

As we compare this with the one-dimensional random walk of the previous section, it is easy to see that the first relation is the equivalent of $\overline{\tilde{\sigma}} = 0$, while the second set of relations replaces $\overline{\tilde{\sigma}^2} = 1$. The second set of relations follows from the fact that $\hat{\boldsymbol{e}}$ is a vector of unit length, and the assumption of isotropy.

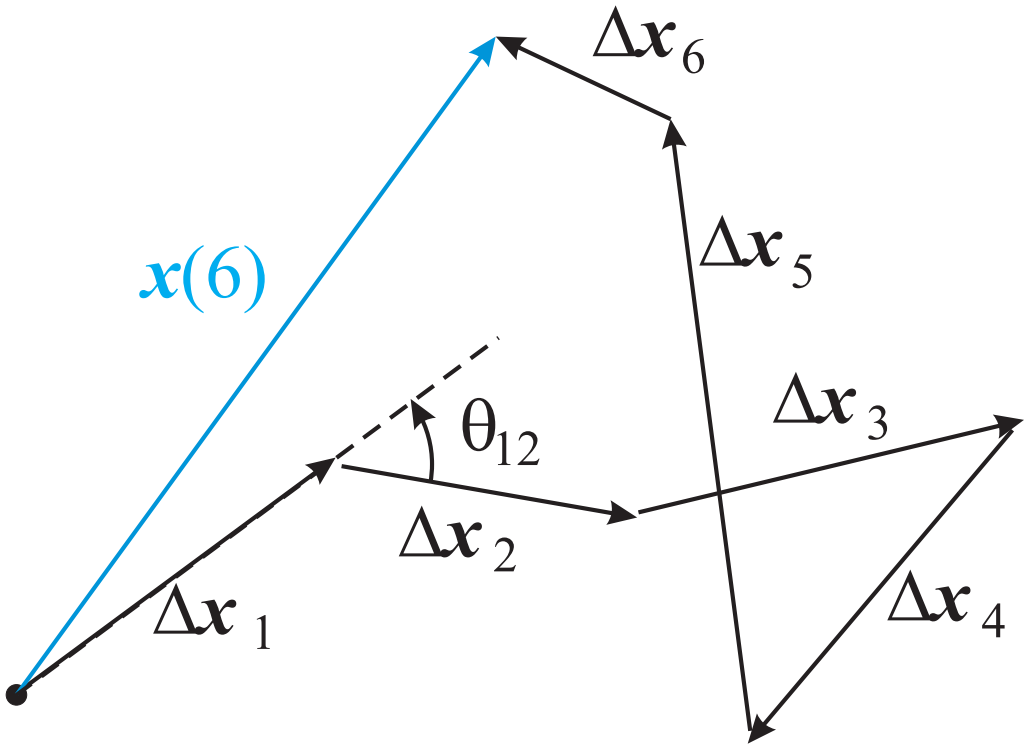

Figure 9.2: *A representation of a three-dimensional random walk with steps of different size. Shown are the first six steps $\Delta\boldsymbol{x}_1$-$\Delta\boldsymbol{x}_6$, and (in blue) the position vector $\boldsymbol{x}(6)$ from the origin to the position of the random walker after these six steps. Also shown is the angle θ_{12} between the direction of the first and the second step.*

The choice of direction of two different steps is arbitrary and, more importantly, uncorrelated. This implies that the *group average* of the step direction satisfies

$$\overline{\hat{\boldsymbol{e}}_i \cdot \hat{\boldsymbol{e}}_j} = \overline{\cos\theta_{ij}} = 0 \;\text{ for } i \neq j. \tag{9.2.3}$$

Here θ_{ij} is the angle between the unit vector of step i and the unit vector of step j. This replaces the relation $\overline{\tilde{\sigma}_i \tilde{\sigma}_j} = 0$ for $i \neq j$ in the one-dimensional random walk.

I will assume that the size of each individual step, $|\Delta \boldsymbol{x}| \equiv \Delta x$, and its direction is determined by some scattering process. The scattering limits the distance that a random walker can travel between two subsequent scatterings. To describe this scattering process, I introduce a *probability distribution* for the step size.

Let the probability $\mathrm{d}P$ that a given step has a length in the range Δx, $\Delta x + \mathrm{d}(\Delta x)$ be given by

$$\mathrm{d}P \equiv \mathcal{P}(\Delta x)\,\mathrm{d}(\Delta x) = \frac{\exp(-\Delta x/\lambda)}{\lambda}\,\mathrm{d}(\Delta x)\;. \tag{9.2.4}$$

The probability distribution $\mathcal{P}(\Delta x) = \mathrm{d}P/\mathrm{d}(\Delta x)$ that is defined in this manner has the following properties:

$$\begin{aligned}
\int_0^\infty \mathrm{d}(\Delta x)\,\mathcal{P}(\Delta x) &= 1\;; \\
\int_0^\infty \mathrm{d}(\Delta x)\,\Delta x\,\mathcal{P}(\Delta x) &\equiv \langle \Delta x \rangle = \lambda\;; \\
\int_0^\infty \mathrm{d}(\Delta x)\,\Delta x^2\,\mathcal{P}(\Delta x) &= \left\langle \Delta x^2 \right\rangle = 2\lambda^2\;.
\end{aligned} \tag{9.2.5}$$

Here the average $\langle \cdots \rangle$ is an average over the step size distribution (9.2.4). The first relation ensures that the probability distribution is properly normalized. The second relation shows that λ is the *mean* distance travelled by a particle between two subsequent collisions. The third relation defines the mean square distance.

One can now repeat the analysis of the previous Section. We will consider the position of a random walker after N steps, and the average distance of the whole group of random walkers to the starting point of the random walk, which I take to be the origin.

The position of a random walker after N steps is

$$\begin{aligned} \boldsymbol{x}(N) &= \Delta\boldsymbol{x}_1 + \Delta\boldsymbol{x}_2 + \cdots + \Delta\boldsymbol{x}_N \\ &= \Delta x_1\hat{\boldsymbol{e}}_1 + \Delta x_2\hat{\boldsymbol{e}}_2 + \cdots + \Delta x_N\hat{\boldsymbol{e}}_N \ . \end{aligned} \tag{9.2.6}$$

We now again take a group average, meaning that we average over all possible directions that the vector $\hat{\boldsymbol{e}}_i$ can take, **and** over all possible step sizes using the distribution (9.2.4). Just as happens in the one-dimensional case, the center-of-mass of the group of random walkers does not change. If all random walkers start at the origin ($x = y = z = 0$), one has after N steps:

$$\overline{\boldsymbol{x}(N)} = \langle\Delta x\rangle \sum_{i=1}^{N} \overline{\hat{\boldsymbol{e}}_i} = \lambda \sum_{i=1}^{N} \overline{\hat{\boldsymbol{e}}_i} = \boldsymbol{0} \ . \tag{9.2.7}$$

Here I have used that the group average of the step size at each step is the same, $\langle\Delta x_i\rangle = \lambda$, and the fact that $\overline{\hat{\boldsymbol{e}}}_i = \boldsymbol{0}$. In component form this means:

$$\overline{x(N)} = \overline{y(N)} = \overline{z(N)} = 0 \ . \tag{9.2.8}$$

The group spreads out in three dimensions. As a result, a calculation similar to the one that leads to Eqn. (9.1.7) in the one-dimensional case can now be performed. For a given random walker one has after N steps, using $\hat{\boldsymbol{e}}_i \cdot \hat{\boldsymbol{e}}_i = 1$:

$$\begin{aligned} |\boldsymbol{x}(N)|^2 &= \Delta x_1^2 + \Delta x_2^2 + \cdots + \Delta x_N^2 \\ &\quad + \sum_{i\neq j} \Delta x_i \Delta x_j \ (\hat{\boldsymbol{e}}_i \cdot \hat{\boldsymbol{e}}_j) \ . \end{aligned} \tag{9.2.9}$$

When we take the group average, the first N terms in this sum contribute equally since the mean value of the square of the step sizes is $\langle\Delta x_i^2\rangle = 2\lambda^2$ for all $1 \leq i \leq N$. All $N(N-1)$ terms in the second group, involving different steps, vanish according to the averaging rule (9.2.3) for the unit vectors. One therefore finds:

$$\overline{|\boldsymbol{x}(N)|^2} = N \left\langle \Delta x^2 \right\rangle = 2N\lambda^2 \ . \tag{9.2.10}$$

The dispersion of the group in a given direction, say the x-direction, follows in an analogous fashion. From

$$\begin{aligned} x^2(N) &= \Delta x_1^2\, \hat{e}_{1x}^2 + \Delta x_2^2\, \hat{e}_{2x}^2 + \cdots + \Delta x_N^2\, \hat{e}_{Nx}^2 \\ &\quad + \sum_{i \neq j} \Delta x_i \Delta x_j\ (\hat{e}_{ix}\, \hat{e}_{jx})\ , \end{aligned} \tag{9.2.11}$$

one finds from (9.2.2) that the group average of $x^2(N)$ equals:

$$\overline{x^2(N)} = \frac{N}{3} \left\langle \Delta x^2 \right\rangle = \frac{2N\lambda^2}{3}\ . \tag{9.2.12}$$

The dispersion in the y and z direction can be calculated in a similar manner, and one has

$$\overline{x^2(N)} = \overline{y^2(N)} = \overline{z^2(N)} = \frac{2N\lambda^2}{3}\ . \tag{9.2.13}$$

It is also easily checked using (9.2.3) that cross terms like $\overline{xy}$ or $\overline{xz}$ vanish. For instance:

$$\overline{x(N)\, y(N)} = 2\lambda^2 \sum_{i=1}^{N} \overline{\hat{e}_{xi}\, \hat{e}_{yi}} = 0\ . \tag{9.2.14}$$

The typical distance travelled still satisfies a relation like Eqn. (9.1.8):

$$d(N) \equiv \sqrt{\overline{x^2} + \overline{y^2} + \overline{z^2}} = \sqrt{N \left\langle \Delta x^2 \right\rangle} = \sqrt{2N}\, \lambda\ . \tag{9.2.15}$$

The only difference is that $\langle \Delta x^2 \rangle = 2\lambda^2$ in this case, whereas in the one-dimensional random walk with a fixed stepsize of the previous Section one has $\Delta x^2 = \lambda^2$ at each step.

9.2.1 The diffusion tensor

In three dimensions one can define a *diffusion tensor*. Formally it is a tensor with components[4]

$$D_{ij} \equiv \frac{\overline{x_i x_j}}{2t} \; . \tag{9.2.16}$$

Here (for cartesian coordinates) one has $x_1 = x$, $x_2 = y$ and $x_3 = z$. Note that this tensor is symmetric: $D_{ij} = D_{ji}$. Now assume that the random walk has a step frequency $\nu = 1/\Delta t_{\rm c}$. In that case one has $N \sim t/\Delta t_{\rm c}$, and the results of the previous Section (Eqn. 9.2.13) show that for isotropic diffusion one must have:

$$D_{xx} = D_{yy} = D_{zz} = \frac{\nu\lambda^2}{3} \;\; , \;\; D_{xy} = D_{xz} = D_{yz} = 0 \; . \tag{9.2.17}$$

One concludes that for isotropic diffusion the diffusion tensor takes a simple (diagonal) form:

$$\boldsymbol{D} = \frac{\nu\lambda^2}{3} \begin{pmatrix} 1 & 0 & 0 \\ 0 & 1 & 0 \\ 0 & 0 & 1 \end{pmatrix} \; . \tag{9.2.18}$$

This means that isotropic diffusion can be characterised with a *single* (scalar) diffusion coefficient,

$$\mathcal{D} \equiv \frac{\nu\lambda^2}{3} \; , \tag{9.2.19}$$

with

$$\overline{x^2}(t) = \overline{y^2}(t) = \overline{z^2}(t) = 2\mathcal{D}t \; , \tag{9.2.20}$$

and by a diffusion tensor that is simply $\boldsymbol{D} = \mathcal{D}\,\boldsymbol{I}$, with $\boldsymbol{I} = \mathrm{diag}(1\;,\;1\;,\;1)$ the unit tensor in three dimensions.

[4] From this point onwards, roman indices (i, j, $\cdots$) are used to denote vector components, **not** step numbers.

The typical distance from the origin of a random walker after a time t equals

$$\overline{|\boldsymbol{x}^2|}(t) = 6\mathcal{D}t \tag{9.2.21}$$

for an isotropic random walk in three dimensions.

Not all diffusion processes are isotropic. Sometimes there are preferred directions. For instance, when charged particles diffuse in a magnetized medium, the magnetic field influences particle motion through the Lorentz force. This force (which is proportional to $\boldsymbol{v} \times \boldsymbol{B}$, with $\boldsymbol{v}$ the particle velocity and $\boldsymbol{B}$ the magnetic field) restricts particle motion in the plane perpendicular to the magnetic field, while leaving the motion along the field unaffected. Without collisons, the particles would 'slide' along the field with velocity $v_{\|} = \boldsymbol{v} \cdot \boldsymbol{B}/|\boldsymbol{B}|$, while gyrating in a circular orbit in the plane perpendicular to the magnetic field. In this case, the diffusion is very anisotropic. As a result, the diffusion tensor has a complicated form. The diffusion along the magnetic field proceeds much faster than diffusion in the plane perpendicular to the field, at least as long as the collision frequency ν is so small that particles make at least one full gyration around the magnetic field between two collisions.

9.3 The diffusion equation

Whenever the carrier particles of some quantity perform a random walk, that quantity obeys a diffusion equation. As a specific example, I will consider diffusion in space, making use of the picture sketched above. However, the type of equation that will be derived for spatial diffusion has a characteristic form that applies to *any* diffusion process.

Let us assume that some quantity $\mathcal{C}$ is carried by particles (molecules or atoms) with a number density $n_{\rm c}(\boldsymbol{x}\,,\,t)$. Due to collisions between molecules with other molecules or atoms in the gas it is diffusively transported in a fluid. For simplicity I will assume that the fluid itself is at rest, so that the mean flow velocity vanishes: $\boldsymbol{V} = 0$. The density $n_{\rm c}$ can represent anything: the concentration of some pollutant in a pool of water, or the density of photons that are propagating diffusively through a scattering medium like the interior of the Sun.

Let us assume that the diffusive propagation is characterised by a mean-free-path (average step size) λ, and that the 'random walkers' that carry (transport) this quantity have a *randomly* directed velocity vector $\boldsymbol{\sigma}$ of magnitude $|\boldsymbol{\sigma}| = \sigma$. If the collision frequency is $\nu = 1/\Delta t_{\rm c}$, with $\Delta t_{\rm c}$ the mean time between collisions, the mean free path λ and the magnitude of the random velocity σ are related by

$$\lambda = \sigma\,\Delta t_{\rm c} = \frac{\sigma}{\nu}\,. \tag{9.3.1}$$

This random velocity could be the thermal velocity of the atoms in a fluid, and equals the velocity of light in the case of diffusing photons.

Let us assume that the quantity $n_{\rm c}(\boldsymbol{x}\,,\,t)$ varies only in the $x-$direction, but not in the $y-$ and $z-$ directions:

$$n_{\rm c}(\boldsymbol{x}\,,\,t) = n_{\rm c}(x\,,\,t) \tag{9.3.2}$$

Consider a flat surface in the $y-z$ plane, which is located at the position $x = x_0$. If no carrier particles are destroyed, the density $n_{\rm c}$ must satisfy a continuity equation of the form

$$\frac{\partial n_{\rm c}}{\partial t} + \boldsymbol{\nabla}\cdot\boldsymbol{F} = 0 \tag{9.3.3}$$

Here $\boldsymbol{F}$ is the flux of the carrier particles, a quantity that is to be calculated shortly.

Let us consider the flux component F_x, the component of the flux that is directed perpendicular to our surface (see the figure below). The number of particles $\Delta N_{\rm c}$ that passes the surface *per unit area* in a time interval Δt is (by definition) related to the flux F_x by

$$\Delta N_{\rm c} = F_x \, \Delta t \; . \tag{9.3.4}$$

On average, a particles arriving at the surface (i.e. at $x = x_0$) within one collision time, with the velocity at an inclination angle $0 \leq i \leq 360^0$ with respect to the normal to that surface, must have originated at a position $x \leq x_{\rm m}$, with

$$x_{\rm m} = x_0 - \Delta x \, \cos i \; . \tag{9.3.5}$$

Here Δx is the size of the last step in the random walk. The quantity $|x_{\rm m}|$ is the maximum distance from the site of the last collison to the surface, measured along the normal. Of course not all particles that cross the surface in a collison time have originated from this maximum distance: *on average*, the normal distance from the site of the last collision and the surface equals for an inclination angle i:

$$|x - x_0| = \tfrac{1}{2} \Delta x \, \cos i \; . \tag{9.3.6}$$

The (infinitesimal) number of molecules that reaches the surface per unit area with a crossing angle in the interval i, $i + {\rm d}i$, and assuming a step size Δx, is equal to the column density of all particles with $x - x_0 \leq \Delta x \, \cos i$ times the fraction of particles ${\rm d}n_{\rm c}(i)/n_{\rm c}$ that have the inclination angle in the interval ${\rm d}i$:

$$\begin{aligned} {\rm d}N_{\rm c} &= \Delta x \cos i \times n_{\rm c}(x_0 - \tfrac{1}{2} \Delta x \, \cos i) \times \frac{{\rm d}n_{\rm c}(i)}{n_{\rm c}} \\ &\approx \left[\Delta x \cos i \, n_{\rm c}(x_0) - \tfrac{1}{2} \Delta x^2 \cos^2 i \, \left(\frac{\partial n_{\rm c}}{\partial x} \right)_{x=x_0} \right] \frac{{\rm d}n_{\rm c}(i)}{n_{\rm c}} \; . \end{aligned} \tag{9.3.7}$$

Note that I have assumed that the average density $n_{\rm c}$ in the column corresponds to the value at the *mean* starting point of the last step in the random walk. Particles reaching the surface from the left side (see the figure below) have $0 \leq i < 90^o$, while particles reaching the surface from the other side have $90^o \leq i \leq 180^o$

The *net* number of particles crossing a unit area on the surface at $x = x_0$ follows from two averages: one average over all possible inclination angles $0 \leq i \leq 2\pi$, *and* an average over all possible step sizes Δx, with the step size probability distribution given by Eqn. (9.2.4). We first perform the average over all possible arrival directions. Assuming that the particles have an isotropic velocity distribution where all values of i are equally probable, the fraction of particles residing in the interval $(i\,,\, i + \mathrm{d}i)$ is simply the fraction of the solid angle 4π that corresponds to this interval:

$$\frac{\mathrm{d}n_\mathrm{c}(i)}{n_\mathrm{c}} = \frac{2\pi \sin i \, \mathrm{d}i}{4\pi} = -\tfrac{1}{2} \, \mathrm{d}\cos i \; . \tag{9.3.8}$$

The average over all possible arrival directions (which is represented by the notation $\langle\langle \cdots \rangle\rangle$) then reduces to a simple integration over $\cos i$ between $\cos i = -1$ and $\cos i = +1$:

$$\langle\langle \cdots \rangle\rangle = \tfrac{1}{2} \int_{-1}^{+1} (\cdots) \, \mathrm{d}\cos i \; . \tag{9.3.9}$$

It is easy to show that $\langle\langle \cos i \rangle\rangle = 0$ and $\langle\langle \cos^2 i \rangle\rangle = 1/3$[5]. One sees that the first term in Eqn. (9.3.7) gives no net contribution, while the second term avergages to:

$$\mathrm{d}N_\mathrm{c} = -\frac{\Delta x^2}{6} \, \left(\frac{\partial n_\mathrm{c}}{\partial x} \right) \; . \tag{9.3.10}$$

If we now average over all possible step sizes, using from (9.2.5) the relation $\langle \Delta x^2 \rangle = 2\lambda^2$, one finds:

$$\mathrm{d}N_\mathrm{c} = -\frac{\langle \Delta x^2 \rangle}{6} \, \left(\frac{\partial n_\mathrm{c}}{\partial x} \right) = -\frac{\lambda^2}{3} \, \left(\frac{\partial n_\mathrm{c}}{\partial x} \right) \; . \tag{9.3.11}$$

If the collision time is $\Delta t_\mathrm{c} = 1/\nu$, one must have

$$\mathrm{d}N_\mathrm{c} = F_x \, \Delta t_\mathrm{c} = -\frac{\lambda^2}{3} \, \left(\frac{\partial n_\mathrm{c}}{\partial x} \right) \; . \tag{9.3.12}$$

[5] One could have derived this result in another way. In this case we have $\cos i = \hat{e}_x$, the x-component of the unit vector $\hat{\boldsymbol{e}}$ along the step in the random walk. For an isotropic random walk we have $\overline{\hat{e}_x} = 0$ and $\overline{\hat{e}_x^2} = 1/3$, see Eqn. (9.2.2) of the previous section.

This relation the immediately gives the flux:

$$F_x = -\frac{\nu\lambda^2}{3}\left(\frac{\partial n_{\rm c}}{\partial x}\right) = -\mathcal{D}\left(\frac{\partial n_{\rm c}}{\partial x}\right) \tag{9.3.13}$$

We conclude that in the diffusion approximation the net flux is proportional to the first derivative of the concentration of the diffusing quantity, with the diffusion coefficient $\mathcal{D}$ as the constant of proportionality.

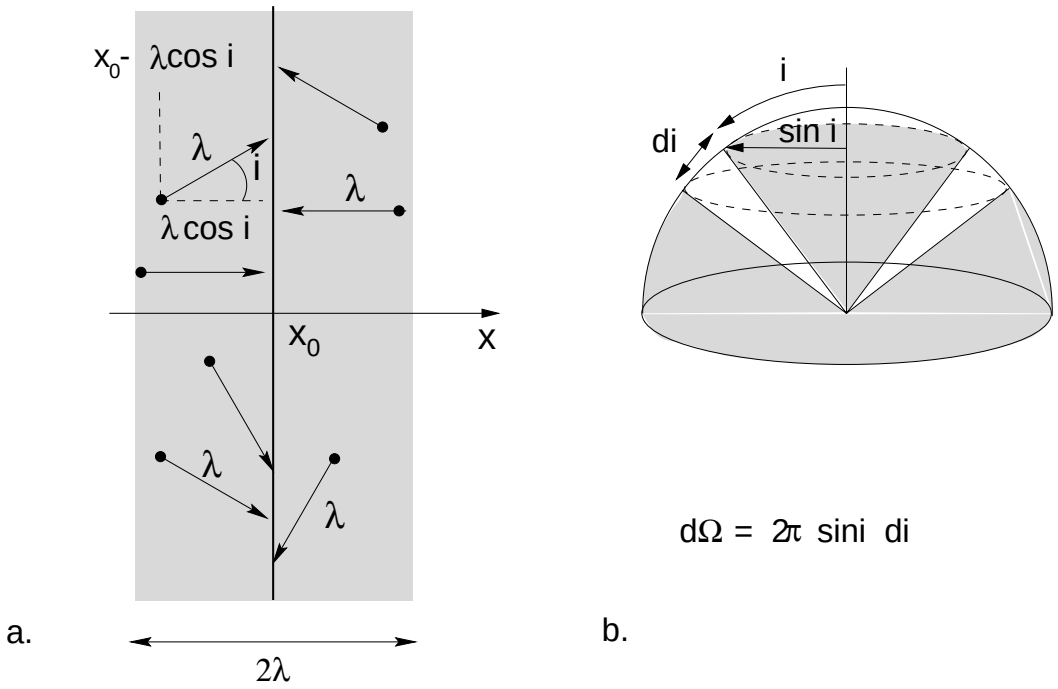

Figure 9.3: *The diffusive transport of some quantity (figure a). Particles originating from the grey region of size 2λ around the plane $x = x_0$, with λ the mean free path, can carry fluid properties to the surface. If the inclination angle between the velocity of the particle and the normal of the surface equals i, the particle carries information about the properties of the fluid at a distance $\lambda\,\cos i$ from the surface.*
If distribution of the random ('thermal') velocities of the particles is isotropic, the number of particles incident on the surface at in some inclination angle interval i, $i + \mathrm{d}i$ is proportional to the solid angle corresponding to that interval (figure b). This solid angle is equal to the surface on a unit sphere between the cones with opening angle i and opening angle $i + \mathrm{d}i$, which equals $\mathrm{d}\Omega = 2\pi\,\sin i\,\mathrm{d}i$.

In the more general three-dimensional case, where n_c also varies in the $y-$ and in the z-direction, the diffusive particle flux in these directions can be calculated in exactly the same way, provided one assumes isotropic diffusion.

The conclusion therefore is as follows: the diffusive flux of some quantity is proportional to the 'concentration gradient'. For isotropic diffusion in three dimensions it is given by

$$\boldsymbol{F} = -\mathcal{D}\,\boldsymbol{\nabla} n_c \,. \tag{9.3.14}$$

The scalar diffusion coefficient is defined as (see Eqn 9.3.1)

$$\mathcal{D} = \frac{\nu\lambda^2}{3} = \frac{\sigma\lambda}{3}\,, \tag{9.3.15}$$

and contains the information about the properties of the random walk that the particles perform. Substituting definition (9.3.14) into the continuity equation, one finds the diffusion equation in three dimensions:

$$\frac{\partial n_c}{\partial t} = \boldsymbol{\nabla}\cdot(\mathcal{D}\,\boldsymbol{\nabla} n_c)\,. \tag{9.3.16}$$

This equation is also known as the *heat conduction equation*: heat in a conducting medium[6] transports diffusively, and the temperature T satisfies an equation of the form (9.3.16). If the diffusion coefficient is uniform ($\boldsymbol{\nabla}\mathcal{D} = 0$), this equation reduces to the simpler form:

$$\frac{\partial n_c}{\partial t} = \mathcal{D}\,\nabla^2 n_c \,. \tag{9.3.17}$$

[6]For instance: in a metal rod the heat is carried by conduction electrons that collide with the atoms.

9.3.1 Fundamental solutions of the diffusion equation

Consider the diffusion equation in one dimension,

$$\frac{\partial n_{\rm c}(x\ ,\ t)}{\partial t} = \mathcal{D}\ \frac{\partial^2 n_{\rm c}(x\ ,\ t)}{\partial x^2}\ . \tag{9.3.18}$$

Let us assume that at $t = 0$ the quantity is concentrated in a sharp spike at $x = 0$. We represent this spike by a *Dirac δ-function*[7] for the concentration $n_{\rm c}$:

$$n_{\rm c}(x\ ,\ 0) = \mathcal{C}_0\ \delta(x)\ . \tag{9.3.19}$$

One can show that the solution of the diffusion equation for $t > 0$ in this case takes the following form:

$$n_{\rm c}(x\ ,\ t) = \frac{\mathcal{C}_0}{\sqrt{4\pi\mathcal{D}t}}\ \exp\left(-\frac{x^2}{4\mathcal{D}t}\right)\ . \tag{9.3.20}$$

The solution has a Gaussian shape, with a width $|\Delta x|$ that increases in time as

$$|\Delta x| \sim \sqrt{2\mathcal{D}t}\ . \tag{9.3.21}$$

The maximum of the density $n_{\rm c}(x\ ,\ t)$ is always at $x = 0$. These last two results clearly show how this fundamental solution reflects the basic properties of the underlying random walk process. The figure below shows a numerical simulation of diffusion in one dimension, together with the analytical solution (9.3.20). One can show that this solution satisfies the condition

$$\int_{-\infty}^{+\infty} {\rm d}x\ n_{\rm c}(x\ ,\ t) = \mathcal{C}_0 \tag{9.3.22}$$

for all t. This reflects the fact the none of the diffusing quantity is lost: diffusion merely spreads it out over a larger and larger volume.

For isotropic diffusion in three dimensions one can immediately guess the fundamental solution if the concentration at $t = 0$ satisfies

$$n_{\rm c}(\boldsymbol{x}\ ,\ 0) = \mathcal{C}_0\ \delta(x)\ \delta(y)\ \delta(z)\ . \tag{9.3.23}$$

[7] e.g. Arfken & Weber, *Mathematical Methods for Physicists*, Ch. Sixth Ed., Ch. 1.15

In that case one has:

$$\begin{aligned} n_{\rm c}(\boldsymbol{x}\ ,\ t) &= \frac{\mathcal{C}_0}{(4\pi\mathcal{D}t)^{3/2}}\exp\left(-\frac{x^2+y^2+z^2}{4\mathcal{D}t}\right) \\ &= \frac{\mathcal{C}_0}{(4\pi\mathcal{D}t)^{3/2}}\exp\left(-\frac{r^2}{4\mathcal{D}t}\right)\ , \end{aligned} \tag{9.3.24}$$

with $r^2 = x^2 + y^2 + z^2$. Apart from the normalization, this three-dimensional solution is simply the product of the three fundamental solutions for diffusion in one dimension: one Gaussian for the x-direction, one for the y-direction and one for the z-direction. This solution reflects the fact that the diffusion proceeds independently in the three directions, but with the same diffusion coefficient, c.f. Eqn. (9.2.20). The three-dimensional analogue of (9.3.22) reads

$$\int_{-\infty}^{+\infty}{\rm d}x\int_{-\infty}^{+\infty}{\rm d}y\int_{-\infty}^{+\infty}{\rm d}z\, n_{\rm c}(\boldsymbol{x}\ ,\ t) = \mathcal{C}_0\ . \tag{9.3.25}$$

Nothing of the diffusing quantity is lost!

9.3.2 Effects of a mean flow: the advection-diffusion equation

If the flow has a mean velocity $\boldsymbol{V}$, and *if* the carrier particles are (apart from the diffusion) carried passively by the flow, the flux $\boldsymbol{F}$ acquires an extra advection term. This term describes how the flow drags the particles along:

$$\boldsymbol{F}(\boldsymbol{x}\ ,\ t) = \underbrace{\boldsymbol{V}n_{\rm c}}_{\rm advection} - \underbrace{\mathcal{D}\,\boldsymbol{\nabla}n_{\rm c}}_{\rm diffusion}\ . \tag{9.3.26}$$

The equation resulting from Eqn. (9.3.3) which describes the changes in the concentration $C(\boldsymbol{x}\ ,\ t)$ now becomes of the *advection-diffusion* type:

$$\boxed{\frac{\partial n_{\rm c}}{\partial t} + \boldsymbol{\nabla}\cdot(\boldsymbol{V}\ n_{\rm c}) = \boldsymbol{\nabla}\cdot\ (\mathcal{D}\boldsymbol{\nabla}n_{\rm c})\ .} \tag{9.3.27}$$

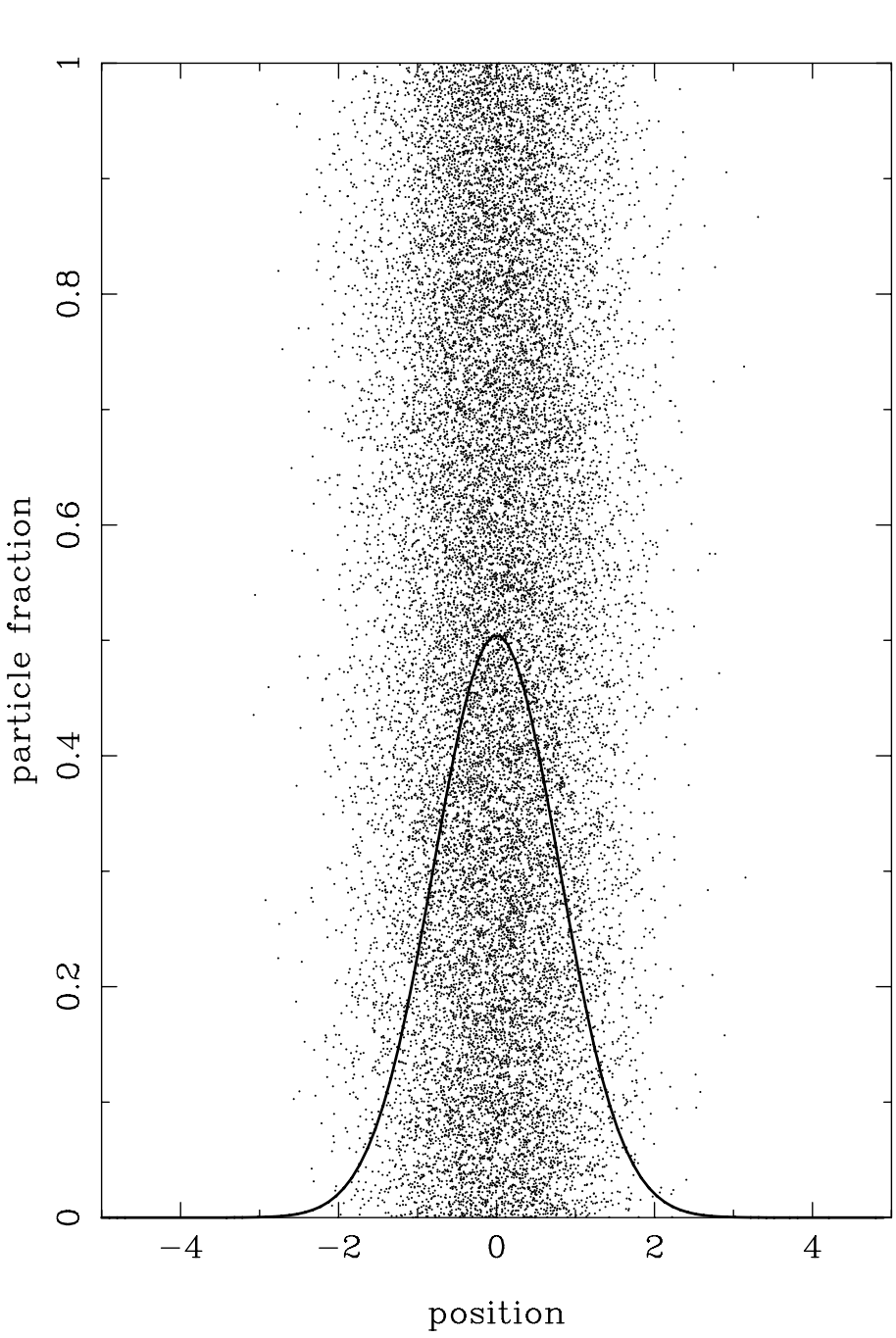

Figure 9.4: *A numerical simulation of a one-dimensional random walk. All particles started at $x = 0$, and have a random (but fixed) position y. The figure shows their position in the $x - y$ plane, together with the analytical solution for their density distribution, expressed in terms of the particle fraction: the number of particles at x divided by the total number of particles.*

More general (and complicated) relations apply when diffusion proceeds at a different rate in different directions. In that case the diffusive contribution to the flux $\boldsymbol{F}$ must be defined in terms of the diffusion*tensor*, which is no longer diagonal. It is equal to

$$(\boldsymbol{F})_{\rm diff} = -\boldsymbol{D}\cdot\boldsymbol{\nabla} n_{\rm c}\ , \tag{9.3.28}$$

or in component form

$$(F_i)_{\rm diff} = -D_{ij}(\frac{\partial n_{\rm c}}{\partial x_j})\ . \tag{9.3.29}$$

If one adds the effects of advection, where the particles are dragged along by the fluid moving with velocity $\boldsymbol{V}(\boldsymbol{x}\,,\,t)$, one has to add the flux component associated with that advection. The resulting advection-diffusion equation reads:

$$\boxed{\frac{\partial n_{\rm c}}{\partial t} + \boldsymbol{\nabla}\cdot(\boldsymbol{V}\,n_{\rm c}) = \boldsymbol{\nabla}\cdot\,(\boldsymbol{D}\cdot\boldsymbol{\nabla} n_{\rm c})\ .} \tag{9.3.30}$$

The corresponding (total) flux of diffusing particles equals

$$\boldsymbol{F} = \boldsymbol{V}\,n_{\rm c} - (\boldsymbol{D}\cdot\boldsymbol{\nabla})\,n_{\rm c}\ . \tag{9.3.31}$$

9.4 Application I: diffusive radiation transport

When a medium is optically thick (opaque), photons will propagate diffusively. The mean free path of the photons is determined by the *opacity* of the medium. If the photons are scattered (or absorbed) by particles with density n, mass m and a cross-section σ, the photon mean-free-path is equal to

$$\ell_{\rm ph} = \frac{1}{n\sigma} = \frac{1}{\kappa\rho} \ . \tag{9.4.1}$$

This quantity plays the same role as λ in the previous Sections. One defines the opacity κ (the cross-section per unit mass) as

$$\kappa = \sigma/m \ . \tag{9.4.2}$$

The probability that a photon travels a path length $s = ct$ without being scattered or absorbed, the 'survival probability', decays with increasing s as

$$\mathcal{P}_{\rm surv}(s) = 1 - \underbrace{\int_0^s {\rm d}(\Delta x)\, \frac{\exp(-\Delta x/\ell_{\rm ph})}{\ell_{\rm ph}}}_{\text{probability for scattering}} = e^{-s/\ell_{\rm ph}} \ . \tag{9.4.3}$$

We will first concentrate on the case where photons are simply scattered, excluding absorption processes where photons are actually destroyed.

Since photons move with the velocity of light, the photon diffusion coefficient, given a mean free path $\lambda = \ell_{\rm ph}$ for scattering, equals

$$\mathcal{D}_{\rm ph} = \frac{c\ell_{\rm ph}}{3} = \frac{c}{3\kappa\rho} \ . \tag{9.4.4}$$

In principle, these quantities depend on the frequency of the photons involved, and the properties (e.g. density and temperature) of the medium. If the photons are in *thermal equilibrium* with the medium, with both the medium and the photons in a thermal distribution[8] with temperature T, the energy density of the radiation equals

$$U_{\rm rad} = a_{\rm r}\, T^4 \ . \tag{9.4.5}$$

Here $a_{\rm r} = 4\sigma_{\rm sb}/c$ is the radiation constant.

[8] For photons the *Planck Distribution*, and for the gas the *Maxwell-Boltzmann distribution*.

If there are temperature gradients, the diffusion of radiation will try to erase these gradients. Photons from hotter regions deposit extra energy, while photons arriving from a colder region have an energy deficit compared with photons originating locally. The resulting net energy flux carried by the radiation is approximated by the diffusion form derived in the previous Section:

$$\boldsymbol{F}_{\rm rad} = -\mathcal{D}_{\rm ph}\,\boldsymbol{\nabla} U_{\rm rad} = -\frac{4ca_{\rm r}T^3}{3\kappa\rho}\,\boldsymbol{\nabla} T\ . \tag{9.4.6}$$

This energy flux will lead to a net loss of energy from hotter regions to cooler regions: a form of *thermal conduction*. The radiation energy density then satisfies the transport equation

$$\frac{\partial U_{\rm rad}}{\partial t} + \boldsymbol{\nabla}\cdot\boldsymbol{F}_{\rm rad} = 0\ . \tag{9.4.7}$$

Using the above definitions for $U_{\rm rad}$ and $\boldsymbol{F}_{\rm rad}$, this equation for the photon energy density can be written as a diffusion equation for the *temperature*:

$$\boxed{\frac{\partial T}{\partial t} = \boldsymbol{\nabla}\cdot\left(\mathcal{K}_{\rm rad}\,\boldsymbol{\nabla} T\right)\ .} \tag{9.4.8}$$

The *radiative thermal conduction coefficient* defined in this equation equals the photon diffusion coefficient:

$$\mathcal{K}_{\rm rad} = \mathcal{D}_{\rm ph}(T) = \frac{c}{3\kappa(\rho,T)\,\rho}\ . \tag{9.4.9}$$

This description simplifies the treatment of radiation transport and the interaction between matter and radiation considerably. For slow speeds ($|\boldsymbol{V}| \ll c$) one can include the advection of photons by a flow approximately by adding an advection term to the photon transport equation as sketched in the preceding section. However, the theory of radiation transfer in moving media is very complicated, and such simple recipes for radiative transfer fail suprisingly fast.

The diffusion approximation for radiative transport has a number of limitations which I will list briefly.

1. As already stated, this diffusion approximation is only valid if the medium is optically thick. Roughly speaking, this means that the size L of the scattering medium (a cloud, a star or an accretion disk) must satisfy the requirement

$$\tau \sim \frac{L}{\ell_{\rm ph}} \gg 1 \ . \tag{9.4.10}$$

   The quantity τ is called the *optical depth* in radiation transfer theory. This condition ensures that the photon is scattered many times before reaching the edge of the medium where it can escape freely.

2. This simple description glosses over the differences between *scattering* and *true absorption*. In scattering a photon changes some of its properties (propagation direction and/or frequency), but remains 'intact'. In absorption the photon is destroyed. In principle, the opacity κ contains a contribution of both these processes:

$$\kappa(\rho, T) = \kappa_{\rm s} + \kappa_{\rm a} \ . \tag{9.4.11}$$

   As long as one assumes thermal equilibrium, this distinction between scattering and absorption is not important. The reason is that in this case a photon with similar properties is emitted for each photon that is absorbed. However, this is only true in an *average* sense. If one wants to calculate the detailed spectrum of the radiation, one has to do a fully-fledged radiation transport calculation in which this distinction *is* important, and where the diffusion approximation need not be true at all wavelengths.

The details of more complicated descriptions of radiation transport can be found in the book by Rybicki & Lightman or the first book in the two-volume set of Shu[9].

In the case of an optically thin medium ($\tau \ll 1$), where the coupling between the photons and the medium in which they propagate is relatively weak, the emerging photons are not necessarily 'thermalized' into a black-body spectrum with a temperature equal to the temperature of the medium. In that case, all kinds of *non-thermal* radiation processes, such as synchrotron radiation or Comptonization, get a chance to put their imprint on the spectrum of the emerging radiation: the spectrum is no longer a Planck spectrum.

[9] G.B. Rybicki & A.P. Lightman, 1979: *Radiative Processes in Astrophysics*, Chapter 1.7 and 1.8, John Wiley & Sons;
F.H. Shu, 1991, *The Physics of Astrophysics*, Volume 1: Radiation, Ch. 2, University Science Books

9.5 Diffusion and viscosity

Diffusive transport is not limited to scalar quantities like the concentration of some contaminant, or the energy density (temperature) of a gas. Vector quantities, such as the momentum density $\boldsymbol{M} = \rho\,\boldsymbol{V}$ of a fluid, can be transported diffusively. Such transport must lead to momentum changes, and therefore to a force. In this case one speaks of *viscous forces*.

The (diffusive) transport of a vector quantity, like the momentum density of a fluid or gas, must be described in terms of a **tensor**. This requirement is already apparant from our discussion of the conservative version of the momentum equation in Chapter 3. The components of such a tensor $\boldsymbol{T}$ are defined as

$$T_{ij} \equiv \text{flux in the } i\text{-direction of the } j\text{-component of momentum density} \tag{9.5.1}$$

The amount of momentum density (a vector!) crossing some oriented surface $\mathrm{d}\boldsymbol{O}$ in a time-interval Δt equals

$$\Delta\boldsymbol{M} = \Delta t\,(\mathrm{d}\boldsymbol{O}\cdot\boldsymbol{T})\;, \tag{9.5.2}$$

or in component form:

$$\Delta M_i = \Delta t\;(\mathrm{d}O_j\,T_{ji})\;. \tag{9.5.3}$$

Now consider a infinitesimally small (closed) volume $\mathcal{V}$. The net amount of momentum $\Delta\boldsymbol{p}$, entering or leaving the volume across it's exterior surface in a time span Δt, equals

$$\Delta\boldsymbol{p} = \Delta\left(\int \mathrm{d}\mathcal{V}\,\boldsymbol{M}\right) = -\Delta t\;\left(\oint_{\partial\mathcal{V}} \mathrm{d}\boldsymbol{O}\cdot\boldsymbol{T}\right)\;. \tag{9.5.4}$$

The extra minus sign introduced in this expression reflects the fact that (by convention) the normal of the oriented surface surrounding the volume is always pointed *outwards*: when $\mathrm{d}\boldsymbol{O}\cdot\boldsymbol{T} > 0$ there is net momentum *leaving* the volume! Using Stokes' theorem (Eqn. 3.1.9) one can rewrite the surface integral into a volume integral,

$$\oint_{\partial\mathcal{V}} \mathrm{d}\boldsymbol{O}\cdot\boldsymbol{T} = \int \mathrm{d}\mathcal{V}\,(\boldsymbol{\nabla}\cdot\boldsymbol{T})\;. \tag{9.5.5}$$

The 'force' on the volume element, which is simply the change in total momentum per unit time, equals:

$$\boldsymbol{F} = \frac{\Delta \boldsymbol{p}}{\Delta t} = -\int \mathrm{d}\mathcal{V}\, (\boldsymbol{\nabla} \cdot \boldsymbol{T}) \; . \tag{9.5.6}$$

This expression gives the force on the whole (infinitesimal) volume as a volume integral. That implies that the force density, i.e. the force per unit volume that is associated with the tensor $\boldsymbol{T}$, must equal:

$$\boldsymbol{f} = -\boldsymbol{\nabla} \cdot \boldsymbol{T} \; . \tag{9.5.7}$$

This relation tells us how to calculate the force from the (tensor-)divergence of the momentum flux tensor. It can be directly applied to diffusive momentum transport.

9.5.1 A simple example: shear flow

As a simple example, consider a pure *shear flow* with straight stream lines. In a shear flow the fluid moves in a fixed direction along straight lines, but the fluid velocity changes in the direction perpendicular to the flow lines, see the figure below. We choose our coordinate system in such a way that the fluid moves along the y-axis, with a velocity that varies in the $x-$direction:

$$\boldsymbol{V} = V(x)\, \hat{\boldsymbol{y}} \; . \tag{9.5.8}$$

Such a shear flow may serve as a rough (local) approximation for the flow in a differentially rotating accretion disk. The momentum density of this fluid only has a y-component:

$$\boldsymbol{M} = \rho \boldsymbol{V} = (0\, ,\; \rho V(x)\, ,\; 0) \; . \tag{9.5.9}$$

To keep things simple, I will assume that the mass density of the fluid is uniform.

Due to diffusion of the atoms or molecules in the fluid or gas, momentum is transported momentum from one position to another. In this specific case this leads to a flux in the x-direction of the y- component of momentum $M_y = \rho V$. This momentum flux is given by the standard expression for a diffusive flux:

$$T^{\mathrm{visc}}_{xy} = -\mathcal{D} \left(\frac{\partial M_y}{\partial x} \right) \sim -\rho \mathcal{D} \left(\frac{\partial V}{\partial x} \right) \; . \tag{9.5.10}$$

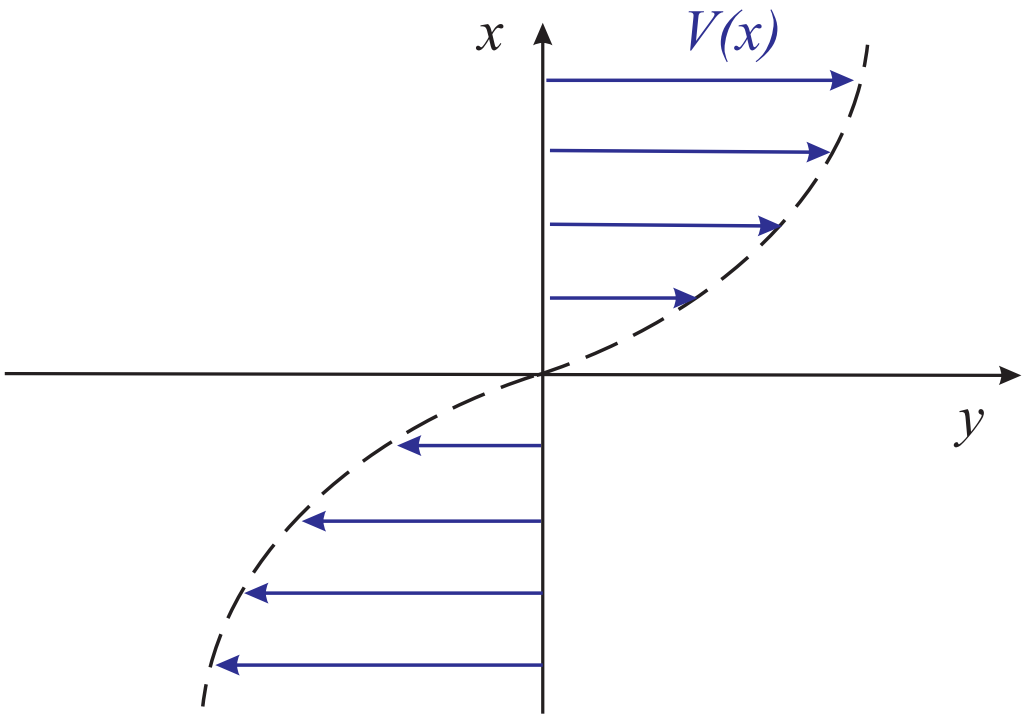

Figure 9.5: *A one-dimensional (linear) shear flow, where the flow velocity is along the y-axis, and the flow speed $V(x)$ varies in the direction perpendicular to the flow lines. In this case we have $V = 0$ at $x = 0$. The thermal motion of the atoms or molecules in the fluid will transport y-momentum in the x-direction, leading to a viscous flux $T^{\rm visc}_{xy} = -\eta\,(\partial V/\partial x)$, and a force density $\boldsymbol{f}^{\rm visc} = -\boldsymbol{\nabla}\cdot\boldsymbol{T}^{\rm visc} = \eta\,(\partial^2 V/\partial x^2)\hat{\boldsymbol{y}}$, with $\eta = \rho\mathcal{D}$ the coefficient of shear viscosity.*

This is the only non-vanishing of the diffusive momentum flux tensor for this flow. The negative divergence of T_{xy} gives the amount of $y-$momentum, deposited by the diffusing particles per unit time and unit volume, and therefore corresponds to a force density: the *viscous force*, which only has an y-component since there is only momentum in the y-direction:

$$f_y^{\rm visc} = -\frac{\partial T_{xy}^{\rm visc}}{\partial x} \sim \eta\left(\frac{\partial^2 V}{\partial x^2}\right) \tag{9.5.11}$$

Here I have defined the *dynamic viscosity coefficient* η as

$$\eta \sim \rho\mathcal{D}\ . \tag{9.5.12}$$

The viscous force is proportional to the second derivative of the velocity. It essentially gives the effect of friction between adjacent fluid layers.

One usually defines the *kinematic viscosity* ν of a fluid by:

$$\nu \equiv \frac{\eta}{\rho} = \tfrac{1}{3}\sigma\ell = \mathcal{D} \; . \tag{9.5.13}$$

This calculation shows, at least in this one-dimensional example, that the kinematic viscosity and the diffusion coefficient of the atoms or molecules involved are the same quantity.

9.5.2 The viscous stress tensor

The full expression for the viscosity tensor in a fully three-dimensional flow is somewhat more complicated. Just like in our simpe example, the tensor $\boldsymbol{T}^{\rm visc}$, the *viscous shear stress tensor*, must depend linearly on the velocity gradients in the fluid as it describes a diffusive flux of momentum. The viscous stress tensor must therefore be a linear function of the components of the *velocity gradient tensor*, which looks like

$$\boldsymbol{\nabla V} = \begin{pmatrix} \partial V_x/\partial x & \partial V_y/\partial x & \partial V_z/\partial x \\ \partial V_x/\partial y & \partial V_y/\partial y & \partial V_z/\partial y \\ \partial V_x/\partial z & \partial V_y/\partial z & \partial V_z/\partial z \end{pmatrix} \tag{9.5.14}$$

in cartesian coordinates. However, it turns out the simplest possible recipe, $\boldsymbol{T}^{\rm visc} = \eta\,\boldsymbol{\nabla V}$, does not work in general, even though it gives the correct answer for the shear flow treated in the previous section.

A simple example shows why the simple recipe fails. Viscous stresses must vanish if a fluid that rotates uniformly, so that

$$\boldsymbol{V} = \boldsymbol{\Omega} \times \boldsymbol{x} \; , \tag{9.5.15}$$

with $\boldsymbol{\Omega}$ some constant angular velocity vector. In that case there is no friction: the rotational velocity in this case corresponds to *solid body rotation*, where the fluid elements at a different distance from the axis of rotation do do not move with respect to each other. This is most easily seen a frame that co-rotates with $\boldsymbol{\Omega}$: in that frame all fluid elements are at rest! Therefore there can be **no** viscous dissipation of momentum for solid body rotation .

If the rotation axis coincides with the $z-$ axis, the velocity for solid-body rotation is in the $x-y$-plane: it equals

$$V_x = -\Omega y \ , \ V_y = \Omega x \ , \ V_z = 0 \ . \tag{9.5.16}$$

The velocity gradient tensor for this case is

$$\boldsymbol{\nabla V} = \begin{pmatrix} 0 & \Omega & 0 \\ -\Omega & 0 & 0 \\ 0 & 0 & 0 \end{pmatrix} \ . \tag{9.5.17}$$

The velocity gradient tensor does not vanish identically for solid-body rotation! There is no viscous force in this case, thus the viscous stress tensor can **not** be directly proportional to the velocity gradient tensor $\boldsymbol{\nabla V}$. However, the components of the *symmetrised* tensor,

$$\boldsymbol{\nabla V} + \boldsymbol{\nabla V}^{\dagger} \ , \tag{9.5.18}$$

do vanish identically for solid-body rotation. Here $\boldsymbol{\nabla V}^{\dagger}$ is the tensor one gets by interchanging the columns and rows of $\boldsymbol{\nabla V}$, i.e. by mirroring the velocity gradient tensor with respect to the diagonal. The components of this symmetrised tensor can be written in index notation as

$$\left(\boldsymbol{\nabla V} + \boldsymbol{\nabla V}^{\dagger}\right)_{ij} \equiv \frac{\partial V_j}{\partial x_i} + \frac{\partial V_i}{\partial x_j} \ . \tag{9.5.19}$$

Therefore, the components of this symmetrised tensor must appear in the general expression for the diffusive momentum flux and in the associated viscous force density.

There is, however, another possible contribution. If the fluid is isotropic so that it's properties are independent of direction, the only other tensor-quantity that can appear in the viscous stress tensor is the unit tensor $\boldsymbol{I}$, which has the components δ_{ij}. Since the viscous stress tensor is linear in the velocity gradients, the unit tensor has to appear in combination with the only scalar quantity that one can form which is linear in the velocity derivatives: the divergence $\boldsymbol{\nabla} \cdot \boldsymbol{V}$. Therefore, the viscous stress tensor in an isotropic fluid must take the general form

$$T_{ij}^{\rm visc} = a \left(\frac{\partial V_j}{\partial x_i} + \frac{\partial V_i}{\partial x_j}\right) + b \left(\boldsymbol{\nabla} \cdot \boldsymbol{V}\right) \delta_{ij} \ . \tag{9.5.20}$$

Note that this expression involves **two** proportionality constants, a and b, yet to be determined! It is always possible to write (9.5.20) in a somewhat different form:

$$T_{ij}^{\rm visc} = -\eta \left(\frac{\partial V_j}{\partial x_i} + \frac{\partial V_i}{\partial x_j} - \tfrac{2}{3} \left(\boldsymbol{\nabla} \cdot \boldsymbol{V} \right) \delta_{ij} \right) - \zeta \left(\boldsymbol{\nabla} \cdot \boldsymbol{V} \right) \delta_{ij} \ . \tag{9.5.21}$$

This expression involves two viscosity coefficients, the *shear viscosity* η and the *bulk viscosity* ζ. It is easily checked that the shear viscosity η is the same quantity as the viscosity coefficient calculated in the one-dimensional example of a shear flow in the previous Section. That pure shear flow is incompressible, with $\boldsymbol{\nabla} \cdot \boldsymbol{V} = 0$, and if one calculates $T_{xy}^{\rm visc}$ from recipe (9.5.21) for the shear flow (9.5.8), it is easily checked that one obtains the correct answer: $T_{xy}^{\rm visc} = -\eta \left(\partial V_y / \partial x \right)$. The coefficient of bulk viscosity ζ is not so straightforwardly calculated in terms of the diffusivity of the flow. In most astrophysical applications one simply puts $\zeta = 0$.

According to the discussion at the beginning of this Chapter the viscous force density equals

$$\boldsymbol{f}^{\rm visc} = -\boldsymbol{\nabla} \cdot \boldsymbol{T}^{\rm visc} \ . \tag{9.5.22}$$

Still using cartesian coordinates, and substituting expression (9.5.21), one finds:

$$f_j^{\rm visc} = -\frac{\partial T_{ij}^{\rm visc}}{\partial x_i} = \eta \left(\frac{\partial^2 V_j}{\partial x_i \partial x_i} \right) + \left(\zeta + \tfrac{1}{3} \eta \right) \frac{\partial (\boldsymbol{\nabla} \cdot \boldsymbol{V})}{\partial x_j} \ . \tag{9.5.23}$$

This implies that the viscous force density can be written in vector form as

$$\boxed{\boldsymbol{f}^{\rm visc} = \eta \nabla^2 \boldsymbol{V} + \left(\zeta + \tfrac{1}{3} \eta \right) \ \boldsymbol{\nabla} (\boldsymbol{\nabla} \cdot \boldsymbol{V}) \ .} \tag{9.5.24}$$

This vector expression is valid in *any* coordinate system by the principle of covariance.

If the flow is incompressible, so that $\boldsymbol{\nabla} \cdot \boldsymbol{V} = 0$, the viscous force density reduces to a more simple form:

$$\boldsymbol{f}^{\rm visc} = \eta \nabla^2 \boldsymbol{V} \ . \tag{9.5.25}$$

The equation of motion for a fluid including viscous forces (but without gravity) becomes

$$\rho \left[\frac{\partial \boldsymbol{V}}{\partial t} + (\boldsymbol{V} \cdot \boldsymbol{\nabla})\, \boldsymbol{V} \right] = -\boldsymbol{\nabla} P + \eta \nabla^2 \boldsymbol{V} + \left(\zeta + \tfrac{1}{3}\eta\right)\, \boldsymbol{\nabla}(\boldsymbol{\nabla} \cdot \boldsymbol{V}) \,. \tag{9.5.26}$$

9.5.3 The Reynolds Number

For order-of-magnitude estimates it is useful to have a measure of the importance of viscous effects on a flow. I will assume that $\zeta = 0$. This measure is provided by a dimensionless number, the *Reynolds number*, which can be defined as:

$$\mathrm{Re} = \frac{\text{magnitude inertial force}}{\text{magnitude viscous force}} \sim \frac{|\rho\, (\boldsymbol{V} \cdot \boldsymbol{\nabla})\boldsymbol{V}|}{|\eta\, \nabla^2 \boldsymbol{V}|} \,. \tag{9.5.27}$$

Let U and L be the typical value of the velocity, and the gradient scale of the velocity field. In that case one may use the estimates

$$|(\boldsymbol{V} \cdot \boldsymbol{\nabla})\boldsymbol{V}| \sim U^2/L \quad , \quad |\eta \nabla^2 \boldsymbol{V}| \sim \rho \nu U/L^2 \,. \tag{9.5.28}$$

This implies that the Reynolds number has a typical magnitude

$$\boxed{\mathrm{Re} \sim \frac{UL}{\nu} \,.} \tag{9.5.29}$$

Here I have used that the shear viscosity satisfies $\eta = \rho\, \nu$. If the Reynolds number is large so that $\mathrm{Re} \gg 1$ one can neglect the viscous effects to lowest order. They become important when $\mathrm{Re} \leq 1$. The viscous forces will dominate the force balance in the flow if $\mathrm{Re} \ll 1$.

9.6 Viscous dissipation

Viscous forces do work on a flow. This work converts the kinetic energy of the flow, the energy of the *bulk motion*, into thermal energy: the kinetic energy of the thermal motion. If there are no losses, such as radiation losses, the internal friction provided by viscosity will heat the fluid.

The amount of viscous dissipation of the kinetic energy can be derived directly from the equation of motion (9.5.26). If one writes this equation as

$$\rho \left[\frac{\partial \boldsymbol{V}}{\partial t} + (\boldsymbol{V} \cdot \boldsymbol{\nabla}) \, \boldsymbol{V} \right] = -\boldsymbol{\nabla} P - \boldsymbol{\nabla} \cdot \boldsymbol{T}^{\rm visc} \; , \tag{9.6.1}$$

one immediately finds from the scalar product of this equation with $\boldsymbol{V}$, c.f. Eqn. (3.2.17):

$$\frac{\partial}{\partial t} \left(\frac{\rho V^2}{2} \right) + \boldsymbol{\nabla} \cdot \left(\rho \boldsymbol{V} \, \frac{V^2}{2} \right) = -(\boldsymbol{V} \cdot \boldsymbol{\nabla}) P - (\boldsymbol{\nabla} \cdot \boldsymbol{T}^{\rm visc}) \cdot \boldsymbol{V} \; . \tag{9.6.2}$$

The last term in this equation is the amount of work per unit volume done by viscous forces:

$$W^{\rm visc} \equiv \boldsymbol{f}^{\rm visc} \cdot \boldsymbol{V} = -(\boldsymbol{\nabla} \cdot \boldsymbol{T}^{\rm visc}) \cdot \boldsymbol{V} \tag{9.6.3}$$

We now use an identity valid for an arbitrary tensor $\boldsymbol{T}$ and vector $\boldsymbol{V}$:

$$\boldsymbol{\nabla} \cdot (\boldsymbol{T} \cdot \boldsymbol{V}) = (\boldsymbol{\nabla} \cdot \boldsymbol{T}) \cdot \boldsymbol{V} + \boldsymbol{T}^{\dagger} : \boldsymbol{\nabla} \boldsymbol{V} \; . \tag{9.6.4}$$

Here $\boldsymbol{T}^{\dagger}$ is the *transpose tensor* of $\boldsymbol{T}$ obtained from interchanging rows and columns so that

$$T^{\dagger}_{ij} = T_{ji} \; , \tag{9.6.5}$$

and the symbol ' $:$ ' is a 'double contraction'[10], defined for two rank-2 tensors $\boldsymbol{T}$ and $\boldsymbol{U}$ as an operation which yields a scalar quantity defined as (remember the summation convention for double indices!)

[10] See the Mathematical Appendix on Internet

$$\boldsymbol{T} : \boldsymbol{U} = T_{ik} U_{ki} \ . \tag{9.6.6}$$

The above identity can be most simply proven in cartesian coordinates where x_i denotes x for $i = 1$, y for $i = 2$ and z for $i = 3$. It is a simple consequence of the chain-rule for differentiation. In component form, using the summation convention, one has:

$$\begin{aligned} \boldsymbol{\nabla} \cdot (\boldsymbol{T} \cdot \boldsymbol{V}) \equiv \frac{\partial}{\partial x_i} (T_{ik} V_k) &= \frac{\partial T_{ik}}{\partial x_i} V_k + T_{ik} \frac{\partial V_k}{\partial x_i} \\ &= (\boldsymbol{\nabla} \cdot \boldsymbol{T})_k V_k + T^{\dagger}_{ki} (\boldsymbol{\nabla} \boldsymbol{V})_{ik} \\ &= (\boldsymbol{\nabla} \cdot \boldsymbol{T}) \cdot \boldsymbol{V} + \boldsymbol{T}^{\dagger} : \boldsymbol{\nabla} \boldsymbol{V} \ . \end{aligned} \tag{9.6.7}$$

Since the viscous stress tensor is symmetric,

$$(\boldsymbol{T}^{\rm visc})^{\dagger} = \boldsymbol{T}^{\rm visc} \ , \tag{9.6.8}$$

this identity allows one to write the amount of work done by viscous forces as

$$\begin{aligned} W^{\rm visc} &= - \underbrace{\boldsymbol{\nabla} \cdot (\boldsymbol{T}^{\rm visc} \cdot \boldsymbol{V})}_{\text{divergence of viscous energy flux}} + \underbrace{\boldsymbol{T}^{\rm visc} : \boldsymbol{\nabla} \boldsymbol{V}}_{\text{kinetic energy loss}} \\ &\equiv -\boldsymbol{\nabla} \cdot \boldsymbol{F}^{\rm visc} - \mathcal{H}^{\rm visc} \ . \end{aligned} \tag{9.6.9}$$

The first term on the left-hand side is the divergence of an energy flux that is associated with the diffusive transport of momentum:

$$\boldsymbol{F}^{\rm visc} \equiv \boldsymbol{T}^{\rm visc} \cdot \boldsymbol{V} \ . \tag{9.6.10}$$

This energy flux can **not** correspond to true dissipation. Like any flux, it simply redistributes energy! The second term, $\mathcal{H}^{\rm visc}$, corresponds to the net loss of kinetic energy per unit volume due to viscous dissipation. This term describes *true* dissipation. It is easily shown that $\mathcal{H}^{\rm visc}$ is a positive definite quantity, as it should be: dissipation is irreversible, and friction always leads to a loss of bulk kinetic energy.

Using (9.5.21) one finds that the amount of kinetic energy **lost** per unit time is

$$\begin{aligned}\mathcal{H}^{\rm visc} &\equiv -\boldsymbol{T}^{\rm visc} : \boldsymbol{\nabla V} \\ &= \eta \left(\frac{\partial V_i}{\partial x_j} + \frac{\partial V_j}{\partial x_i}\right) \frac{\partial V_i}{\partial x_j} + \left(\zeta - \tfrac{2}{3}\eta\right) (\boldsymbol{\nabla \cdot V})^2 \qquad (9.6.11) \\ &= \tfrac{1}{2}\eta \left(\frac{\partial V_i}{\partial x_j} + \frac{\partial V_j}{\partial x_i} - \tfrac{2}{3} (\boldsymbol{\nabla \cdot V})\, \delta_{ij}\right)^2 + \zeta\, (\boldsymbol{\nabla \cdot V})^2 \, .\end{aligned}$$

The last equality follows after some tensor algebra.

The viscous heating $\mathcal{H}^{\rm visc}$ represents the heat generated by internal friction in the fluid or gas. This heating is an irreversible process, which leads to an increase of the entropy density s of a gas or fluid. The entropy increase in an ideal gas with entropy density

$$s = c_{\rm v}\, \ln\left(\frac{P}{\rho^\gamma}\right) \qquad (9.6.12)$$

is described by (see Eqn. 3.2.24):

$$\rho c_{\rm v} T \left(\frac{\partial}{\partial t} + \boldsymbol{V \cdot \nabla}\right) \ln\left(\frac{P}{\rho^\gamma}\right) = \mathcal{H} \, . \qquad (9.6.13)$$

Here I have introduced the total heating rate:

$$\mathcal{H} = \mathcal{H}^{\rm visc} + \mathcal{H}^{\rm ext} \, . \qquad (9.6.14)$$

Here $\mathcal{H}^{\rm visc}$ gives the contribution of viscous dissipation as given by Eqn. (9.6.11), and $\mathcal{H}^{\rm ext}$ includes all *external* sources (or sinks) of heat, such as radiation losses.

9.7 Conservative equations for a viscous fluid

The equations for a viscous fluid can be cast in a conservative form. The derivation is quite analogous to the case without viscosity as treated in Chapter 3, and I will not go through it in great detail. Rather, I will stress the influence of the viscous terms.

The equation of mass conservation is not affected by the presence of viscosity:

$$\boxed{\frac{\partial \rho}{\partial t} + \boldsymbol{\nabla} \cdot (\rho \boldsymbol{V}) = 0 \; .} \tag{9.7.1}$$

The conservation law for the fluid momentum density, $\boldsymbol{M} = \rho \boldsymbol{V}$, is also formally the same as for an ideal fluid, simply because the viscous force can be written as the (negative) divergence of the viscous shear tensor $\boldsymbol{T}^{\rm visc}$. One simply defines the fluid stress tensor in such a way that it includes the contribution of viscosity:

$$\boldsymbol{T} \equiv \rho \boldsymbol{V} \otimes \boldsymbol{V} + P \, \boldsymbol{I} + \boldsymbol{T}^{\rm visc} \; . \tag{9.7.2}$$

The conservative equation of motion therefore takes the same form as for an ideal (non-viscous) fluid:

$$\boxed{\frac{\partial \boldsymbol{M}}{\partial t} + \boldsymbol{\nabla} \cdot \boldsymbol{T} = -\rho \, \boldsymbol{\nabla} \Phi \; .} \tag{9.7.3}$$

Here I have re-introduced the effects of gravity.

The conservative form of the equation for the fluid energy density takes some thought. The equation for the kinetic energy (Eqn. 9.6.2) can be written as

$$\frac{\partial}{\partial t} \left(\frac{\rho V^2}{2} \right) + \boldsymbol{\nabla} \cdot \left(\rho \boldsymbol{V} \, \frac{V^2}{2} + \boldsymbol{T}^{\rm visc} \cdot \boldsymbol{V} \right) = -(\boldsymbol{V} \cdot \boldsymbol{\nabla}) P - \rho (\boldsymbol{V} \cdot \boldsymbol{\nabla}) \Phi - \mathcal{H}^{\rm visc} \; . \tag{9.7.4}$$

Here I have used tensor identity (9.6.4) once again, together with the definition of the viscous heating rate.

If one uses the thermodynamic relations (3.2.21) and (3.2.22),

$$\boldsymbol{\nabla} P = \rho \boldsymbol{\nabla} h - \rho T \boldsymbol{\nabla} s \;\; , \;\; \rho \, \frac{\partial e}{\partial t} = \rho T \, \frac{\partial s}{\partial t} - \frac{P}{\rho} \, \boldsymbol{\nabla} \cdot (\rho \boldsymbol{V}) \tag{9.7.5}$$

together with

$$\rho (\boldsymbol{V} \cdot \boldsymbol{\nabla}) \Phi = \frac{\partial (\rho \Phi)}{\partial t} + \boldsymbol{\nabla} \cdot \, (\rho \boldsymbol{V} \, \Phi) - \frac{\partial \Phi}{\partial t} \, , \tag{9.7.6}$$

one finds that one can write this relationship as an equation for the total (thermal plus kinetic) energy density of the fluid:

$$\begin{aligned} \frac{\partial}{\partial t} \left(\tfrac{1}{2} \rho V^2 + \rho \, e + \rho \, \Phi \right) \;\; + \;\; \boldsymbol{\nabla} \cdot \left[\rho \boldsymbol{V} \left(\tfrac{1}{2} V^2 + h + \Phi \right) + \boldsymbol{T}^{\rm visc} \cdot \boldsymbol{V} \right] = \\ = \;\; \underbrace{\rho T \left(\frac{\partial s}{\partial t} + (\boldsymbol{V} \cdot \boldsymbol{\nabla}) s \right)}_{\text{thermal energy gained}} - \underbrace{\left(\mathcal{H}^{\rm visc} + \rho \, (\mathbf{V} \cdot \boldsymbol{\nabla}) \Phi \right)}_{\text{kinetic energy lost}} \, . \end{aligned} \tag{9.7.7}$$

If we now substitute relation (9.6.13) for the entropy density, one finds shows that the viscous heating term involving $\mathcal{H}^{\rm visc}$ drops out of the equation. This is obvious from a physical point-of-view: the kinetic energy lost due to internal friction, as given in Eqn. (9.7.4), is added to the thermal energy of the gas. Since viscosity is an *internal* process, it can not change the total energy of the gas or fluid! The only viscous effect that remains in the conservative form of the energy equation is the viscous contribution to the energy flux, equal to $\boldsymbol{F}^{\rm visc} = \boldsymbol{T}^{\rm visc} \cdot \boldsymbol{V}$. The final form of the conservative energy equation for a viscous medium reads:

$$\boxed{\frac{\partial}{\partial t} \left(\tfrac{1}{2} \rho \, V^2 + \rho e + \rho \Phi \right) + \boldsymbol{\nabla} \cdot \left[\rho \boldsymbol{V} \left(\tfrac{1}{2} V^2 + h + \Phi \right) + \boldsymbol{T}^{\rm visc} \cdot \boldsymbol{V} \right] = \mathcal{H}_{\rm eff} \, .} \tag{9.7.8}$$

As before, the net heating term $\mathcal{H}_{\rm eff}$ contains only the heat added or removed irreversibly for the system by external processes such as radiation losses, and the violent relaxation term that occurs in a time-dependent gravitational field:

$$\mathcal{H}_{\rm eff} \equiv \mathcal{H}^{\rm ext} + \rho \, \frac{\partial \Phi}{\partial t} \, . \tag{9.7.9}$$

Chapter 10

Axisymmetric, steady flows

10.1 Introduction

In many astrophysical systems one can make the assumption of axial symmetry. Examples are disk galaxies, or of the accretion disks that can be found around compact objects (white dwarfs, neutron stars and black holes) and around proto-stellar objects (proto-planetary disks). If in addition the flow is *steady* one can put

$$\frac{\partial}{\partial t}\,(\text{any flow quantity}) = 0 \quad , \quad \frac{\partial}{\partial \theta}\,(\text{any flow quantity}) = 0 \; . \tag{10.1.1}$$

Here θ is the position angle in the plane perpendicular to the axis of symmetry. In what follows we take the axis of symmetry to be the z-axis, so that θ corresponds with the polar angle in the $x-y$ plane.

In this Chapter, we investigate the global properties of such axisymmetric flows. Once again I will start the discussion by drawing on the analogies between fluid mechanics, and the dynamics of single particles.

In ideal single-particle mechanics in a conservative system with central symmetry, such as the motion of a planet around the Sun under the influence of the Sun's gravitational attraction, the particle angular momentum (a vector!) $\boldsymbol{L}$, defined as

$$\boldsymbol{L} = m\,\boldsymbol{r} \times \boldsymbol{p} \; , \tag{10.1.2}$$

is conserved. This vector conservation law implies that the orbit of a particle must lie in a plane, with the vecor $\boldsymbol{L}$ along the normal to that plane. If we take this orbital plane to be the x-y plane, and if we employ cylindrical coordinates with $R = \sqrt{x^2+y^2}$ and $\theta = \tan^{-1}(y/x)$, we can write the conservation law for angular momentum as

$$L = mRV_\theta \equiv m\lambda = \text{constant} . \tag{10.1.3}$$

Here I have defined the *specific angular momentum* $\lambda = L/m$, the angular momentum per unit mass. The velocity V_θ is the *azimuthal velocity*.

Since we assumed a conservative system, the total (potential + kinetic) energy of the particle is conserved:

$$E = \tfrac{1}{2}mV^2 + m\,\Phi(\boldsymbol{r}) = \text{constant} . \tag{10.1.4}$$

Since the motion is confined to a plane, one can write the kinetic energy as

$$\begin{aligned} \tfrac{1}{2}mV^2 &= \frac{m}{2}\left(V_R^2 + V_\theta^2\right) \\ &= \frac{mV_R^2}{2} + \frac{L^2}{2mR^2} , \end{aligned} \tag{10.1.5}$$

with $V_{\rm R}$ the radial velocity. Here the angular momentum conservation law (10.1.3) has been used to eliminate V_θ. This energy conservation law can be cast in the form

$$\frac{E}{m} \equiv \mathcal{E} = \tfrac{1}{2}V_R^2 + \left(\Phi + \frac{\lambda^2}{2R^2}\right) = \text{constant} . \tag{10.1.6}$$

One can define an *effective potential* $\Psi(\boldsymbol{r})$, a function of the particle position $\boldsymbol{r}$ and the angular momentum that is given by

$$\Psi \equiv \Phi(\boldsymbol{r}) + \frac{\lambda^2}{2R^2} . \tag{10.1.7}$$

In terms of this potential, the conservation of particle energy becomes

$$\mathcal{E} = \tfrac{1}{2}V_R^2 + \Psi(R) = \text{constant} . \tag{10.1.8}$$

The whole problem of particle motion in a central force field can therefore be reduced to an equivalent one-dimensional description in terms of the *radial* motion under influence of the effective potential $\Psi(R)$ [1]. Once the radial problem is solved, yielding $R(t)$, the angular motion follows from the conservation of angular momentum.

I will now show that a similar set of conservation laws can be derived for a axisymmetric steady flow.

10.2 Equations for a steady, axisymmetric flow

The assumption of a steady flow quite generally leads to Bernouilli's law, the conservation of the energy per unit mass $\mathcal{E}$ along flowlines, as derived in Chapter 4:

$$(\boldsymbol{V}\cdot\boldsymbol{\nabla})\mathcal{E} \equiv (\boldsymbol{V}\cdot\boldsymbol{\nabla})\left[\tfrac{1}{2}V^2 + \frac{\gamma P}{(\gamma-1)\rho} + \Phi\right] = 0\,. \tag{10.2.1}$$

The assumption of axial symmetry leads to the conservation of the *specific angular momentum* (angular momentum per unit mass), even for non-steady flows. This can be seen as follows.

The θ-component of the equation of motion can be written as (use Eqn. 8.6.36):

$$\rho\left[\frac{\partial V_\theta}{\partial t} + (\boldsymbol{V}\cdot\boldsymbol{\nabla})V_\theta + \frac{V_\theta V_R}{R}\right] = -\frac{1}{R}\,\frac{\partial P}{\partial\theta}\,. \tag{10.2.2}$$

In this expression the operator $\boldsymbol{V}\cdot\boldsymbol{\nabla}$ must be interpreted as[2]

$$\boldsymbol{V}\cdot\boldsymbol{\nabla} \equiv V_R\,\frac{\partial}{\partial R} + \frac{V_\theta}{R}\,\frac{\partial}{\partial\theta} + V_Z\,\frac{\partial}{\partial Z}\,. \tag{10.2.3}$$

The extra term $V_R V_\theta/R$ is a curvature term due to our use of non-cartesian polar coordinates, and the associated rotation of the unit vectors $\hat{\boldsymbol{e}}_R$ and $\hat{\boldsymbol{e}}_\theta$, as explained in the preceding Chapter. If axial symmetry applies, $\partial/\partial\theta = 0$, the operator $\boldsymbol{V}\cdot\boldsymbol{\nabla}$ reduces to

$$\boldsymbol{V}\cdot\boldsymbol{\nabla} \implies \boldsymbol{V}_{\rm p}\cdot\boldsymbol{\nabla} \equiv V_R\,\frac{\partial}{\partial R} + V_Z\,\frac{\partial}{\partial Z}\,. \tag{10.2.4}$$

[1] See for instance: Goldstein, Poole & Safko, *Classical Mechanics* ($3^{\rm d}$ Edition), Ch. 3, Addison & Wesley, 2003;
José & Saletan, *Classical Dynamics*, Ch. 2.3, Cambridge University Press, 1998

[2] Note that we are working in terms of vector **components**, not in terms of **vectors**!

Here $\boldsymbol{V}_{\rm p} \equiv V_R \hat{\boldsymbol{e}}_R + V_Z \hat{\boldsymbol{e}}_Z$ is the so-called *poloidal velocity*, the velocity in the $R-Z$ plane.

Because of the assumed axial symmetry, the azimuthal component of the pressure force vanishes,

$$\frac{1}{R}\,\frac{\partial P}{\partial \theta} = 0 \; . \tag{10.2.5}$$

This implies that the equation (10.2.2) can be rewritten as:

$$\frac{\partial V_\theta}{\partial t} + V_R\,\frac{\partial V_\theta}{\partial R} + V_Z\,\frac{\partial V_\theta}{\partial Z} + \frac{V_\theta V_R}{R} = 0 \; . \tag{10.2.6}$$

Multiplication of this equation by R, and using

$$R V_R\,\frac{\partial V_\theta}{\partial R} + V_\theta V_R = V_R\,\frac{\partial\,(R V_\theta)}{\partial R} \; ,$$

one can write:

$$\left[\frac{\partial}{\partial t} + (\boldsymbol{V}_{\rm p}\cdot\boldsymbol{\nabla})\right](R V_\theta) \equiv \frac{{\rm d}\lambda}{{\rm d}t} = 0 \; . \tag{10.2.7}$$

This means that the specific angular momentum of the fluid, $\lambda = R V_\theta$, is conserved. This conservation law is the direct analogue of the conservation of angular momentum in single-particle dynamics in a conservative central force field.

We now restrict the attention to steady axisymmetric flows where $\partial/\partial t = 0$. In that case the angular momentum conservation law becomes

$$(\boldsymbol{V}\cdot\boldsymbol{\nabla})\lambda = (\boldsymbol{V}_{\rm p}\cdot\boldsymbol{\nabla})\lambda = 0 \; , \tag{10.2.8}$$

or equivalently

$$\boxed{\lambda = R\,V_\theta = \text{constant along flow lines} \; .} \tag{10.2.9}$$

If one expresses the azimuthal velocity in terms of the specific angular momentum,

$$V_\theta = \lambda/R \,, \tag{10.2.10}$$

one can rewrite the Bernouilli's law (10.2.1) as

$$\tfrac{1}{2}V_{\rm p}^2 + \frac{\lambda^2}{2R^2} + \frac{\gamma P}{(\gamma-1)\rho} + \Phi = \text{constant along flowlines} \,. \tag{10.2.11}$$

Here

$$V_{\rm p}^2 \equiv V_R^2 + V_Z^2 \tag{10.2.12}$$

is the square of the poloidal velocity. By defining an effective potential in exactly the same manner as in the single particle case,

$$\Psi(R\,,\,Z) \equiv \Phi(R\,,\,Z) + \frac{\lambda^2}{2R^2} \,, \tag{10.2.13}$$

one can write Bernouilli's law for an axisymmetric stationary flow as

$$\boxed{\mathcal{E} = \tfrac{1}{2}V_{\rm p}^2 + \frac{\gamma P}{(\gamma-1)\rho} + \Psi(R\,,\,Z) = \text{constant along flow lines} \,.} \tag{10.2.14}$$

This is the direct analogue of the single-particle conservation law (10.1.8).

This effective potential Ψ defined in this Chapter differs from the quantity $\Phi_{\rm eff}$ of the same name introduced in Chapter 8. There the 'effective potential' $\Phi_{\rm eff}$ was introduced to describe the particle motion in a *rotating* frame of reference, casting the eqiation of motion in a form that was closely analogous to the equations valid in an inertial reference frame. In the case considered here the function $\Psi(R\,,\,Z)$ consists of the contribution of the ordinary gravitational potential Φ and the kinetic energy per unit mass $\frac{1}{2}\,V_\theta^2$ of the azimuthal motion in the *inertial* frame.

10.2.1 Fundamental equations for a steady, axisymmetric flow

Let us write down the full set of equations governing an axisymmetric, steady adiabatic flow. These equations are the continuity equation, the equations of motion and the conservation of the specific entropy $s = c_{\rm v} \ln(P\rho^{-\gamma})$ (Eqn. 3.2.24 with $\mathcal{H} = 0$ and $\partial/\partial t = \partial/\partial\theta = 0$). Using Eqn. (8.6.36) one finds:

$$\begin{aligned}
\boldsymbol{\nabla}\cdot(\rho\,\boldsymbol{V}_{\rm p}) &= \frac{1}{R}\,\frac{\partial(\rho R V_R)}{\partial R} + \frac{\partial(\rho V_Z)}{\partial Z} = 0\,,\\
\rho\,(\boldsymbol{V}_{\rm p}\cdot\boldsymbol{\nabla})V_R &= -\frac{\partial P}{\partial R} + \rho\,\Omega^2\,R - \rho\,\frac{\partial\Phi}{\partial R}\,,\\
\rho\,(\boldsymbol{V}_{\rm p}\cdot\boldsymbol{\nabla})(\Omega R^2) &= 0\,, \qquad\qquad (10.2.15)\\
\rho\,(\boldsymbol{V}_{\rm p}\cdot\boldsymbol{\nabla})V_Z &= -\frac{\partial P}{\partial Z} - \rho\,\frac{\partial\Phi}{\partial Z}\,,\\
(\boldsymbol{V}_{\rm p}\cdot\boldsymbol{\nabla})\left[c_{\rm v}\ln(P\rho^{-\gamma})\right] &= 0
\end{aligned}$$

The radial force component includes the centrifugal force $\rho\,\Omega^2 R$ due to the motion in the azimuthal (θ-)direction, where the angular frequency of the motion in the θ-direction is defined in the usual fashion,

$$\Omega \equiv \frac{{\rm d}\theta}{{\rm d}t} = \frac{V_\theta}{R}\,. \qquad (10.2.16)$$

The specific angular momentum of the flow can be written in terms of Ω as

$$\lambda = \Omega R^2\,. \qquad (10.2.17)$$

There is an important difference between the role of the effective potential Ψ in the case of fluid dynamics, and it's role in single-particle dynamics. This difference has to do with the fact that the specific angular momentum is conserved along flow lines, just like the conservation of angular momentum along particle orbits, but that this conservation law does not imply that λ is a **global** constant in the flow. We have seen a similar situation

in Bernoulli's law: the conservation of the specific energy $\mathcal{E}$ along flow lines of a steady flow does *not* imply that $\mathcal{E}$ is globally constant: it's value can differ from flow line to flow line. The same holds for the specific angular momentum λ.

As a result the force density in the R- and Z direction can **not** be derived from the gradient of the effective potential Ψ. A direct calculation of $-\boldsymbol{\nabla}\Psi$ immediately yields

$$\begin{aligned} -\boldsymbol{\nabla}\Psi &= -\boldsymbol{\nabla}\Phi + \frac{\lambda^2}{R^3}\boldsymbol{\nabla}R - \frac{\lambda}{R^2}\boldsymbol{\nabla}\lambda \\ &= -\boldsymbol{\nabla}\Phi + \Omega^2 R\,\hat{\boldsymbol{e}}_R - \Omega\,\boldsymbol{\nabla}\lambda\ . \end{aligned} \tag{10.2.18}$$

Here I have used $\boldsymbol{\nabla}R = \hat{\boldsymbol{e}}_R$. The first two terms on the right-hand side are the required gravitational force and the centrifugal force per unit mass. The last term, the term $\propto \boldsymbol{\nabla}\lambda$, does not correspond to a physical force. Therefore, in fluid mechanics one can only use Ψ to calculate the force if the specific angular momentum is a global constant of the flow, so that $\boldsymbol{\nabla}\lambda = 0$, or equivalently:

$$\partial\lambda/\partial R = \partial\lambda/\partial Z = 0\ . \tag{10.2.19}$$

10.3 An astrophysical example: Accretion Disks

An important application of steady axisymmetric flows is the theory of accretion disks. Accretion disks will occur whenever the material falling onto a compact object (a white dwarf, neutron star or black hole) carries angular momentum. The centrifugal force associated with the rotational motion (which is due to the angular momentum of the material) prevents the matter to approach the compact object arbitrarily close. For instance: for a steady flow, with the gravitational potential determined totally by the mass M_* of the compact object, the effective potential is

$$\Psi(r) = -\frac{GM_*}{r} + \frac{\lambda^2}{2R^2}\ . \tag{10.3.1}$$

Here $r = \sqrt{R^2+Z^2}$ is the spherical radius. Consider the flow close to the equatorial plane (the $x-y$ plane) where $r \sim R$. The net force along flow lines will be directed away from the compact object if

$$-\frac{\partial\Psi}{\partial\ell} = \left(-\frac{GM_*}{R^2} + \frac{\lambda^2}{R^3}\right)\frac{\partial R}{\partial\ell} > 0\ , \tag{10.3.2}$$

assuming $\partial R/\partial \ell = \cos i > 0$, with i the inclination angle between the flow line and the equatorial plane. Here ℓ is the pathlength along a flow line, and I have used that conservation law (10.2.14) implies that $\partial \lambda/\partial \ell = 0$. The conserved angular momentum will prevent material from closely approaching the compact object.

This so-called *centrifugal barrier* prevents an approach much closer than a to radius of order

$$R_{\rm K} \equiv \frac{\lambda^2}{GM_*} \, . \tag{10.3.3}$$

This means that accretion is only possible if the specific angular momentum carried by the flow is somehow lost! However, as we will see the specific details of the loss mechanism are relatively unimportant.

The centrifugal barrier means that in most astrophysical applications the Bondi accretion solution, the solution with purely radial infall that was discussed in Chapter 4, can not be realised in nature. If there is some angular momentum in the infalling material, the flow must deviate strongly from (quasi-)radial infall as the material approaches a radial distance $R \sim R_{\rm K}$. As the material approaches the compact object the azimuthal velocity must increase in order to conserve λ, and the centrifugal force $\rho V_\theta^2/R$ increases, preventing further infall. In the following Section I will discuss the theory of the mode of accretion that must result: *disk accretion*. It will become clear that steady accretion in a flow with angular momentum is only possible if angular momentum is *lost* so that conservation law (10.2.14) no longer applies.

10.3.1 Sources powered by disk accretion: X-Ray Binaries and Cataclysmic Variables

All bright, point-like variable X-ray sources in our galaxy are binaries, where a 'normal' star transfers mass onto a compact object such as a White Dwarf, Neutron Star or Black Hole. This mass transfer is the result of the strong tidal forces excerted on the normal star by its companion, a process known as *Roche Lobe Overflow*. In a binary, where two stars rotate in a plane around their common center-of-mass, Roche Lobe Overflow occurs because of the special shape of the equipotential surfaces in a frame corotating with the binary. If the stars in the system have masses M_1 and M_2, and if the angular rotation vector is $\mathbf{\Omega}$, the equipotential surfaces in the corotating reference frame follow from

$$\Phi_{\rm eff}(\boldsymbol{r}) = -\frac{GM_1}{|\boldsymbol{r}-\boldsymbol{r}_1|} - \frac{GM_2}{|\boldsymbol{r}-\boldsymbol{r}_2|} - \tfrac{1}{2}\,|\mathbf{\Omega}\times\boldsymbol{r}|^2 = \text{constant}. \tag{10.3.4}$$

These surfaces have a 'cusp' at the inner Lagrangian point that is located on the line

connecting the position $\boldsymbol{r}_1$ and $\boldsymbol{r}_2$ of the two stars. The rotation frequency of the binary around their common center-of-mass is given by Kepler's law:

$$|\boldsymbol{\Omega}| = \left[\frac{G(M_1 + M_2)}{a^3}\right]^{1/2} , \tag{10.3.5}$$

with a the semi-major axis of the binary orbit. Mass can be transferred across the inner Lagrangian point if the 'normal' star becomes so large that it completely fills the *Roche lobe*: the volume that is bounded by this special equipotential surface that touches the inner Lagrangian point. Mass that crosses the surface is no longer gravitationally bound to the star, and must ultimately fall on the companion (or leave the system). This situation is illustrated in the figure below.

Such accreting compact stars in a binary have been studied extensively in our Galaxy. With the increasing sensitivity of X-ray satellites they can now also be studied in neighbouring galaxies. Galactic X-ray binaries occur in different classes[3]:

- **Massive X-Ray Binaries**, where the binary system consists of a massive ($M > 10\ M_\odot$) (early type) star and a neutron star or black hole. The emission from some of these systems shows rapid pulsations, which are caused by the combined effect of the rapid rotation of the neutron star, and its strong (roughly dipolar) magnetic field, which guides the accreted material towards the magnetic poles of the neutron star. The accreted material accumulates in 'hot spots' around the magnetic poles. The rotation sweeps these hot spots along the line-of-sight. One then speaks of *X-Ray Pulsars*. The binary character of these systems can be inferred from the eclipses of the X-ray source, or from the Doppler delay of the pulse arrival times.

  Since massive stars evolve rapidly (in about 10^7 years) these must be young objects (Population I stars), and are therefore found close to the Galactic plane where recent star formation has occurred.

- **Low-Mass X-Ray Binaries**, where the binary consists of a late-type (sun-like) star (mass $M < 2\ M_\odot$) and a neutron star. They rarely show eclipses or pulsations. These are much older systems, and can therefore be found at large distances from the galactic plane. This class includes many sources which are located in globular clusters. This suggest they are representative of the older Population II stars.

- **X-ray Bursters**. These systems show irregular or quasi-regular bursts of X-ray emission. There are two types (predictably called *Type I* and *Type II*) where the burst is generated in a different manner.

[3]For an overview see: Frank, King & Raine, *Accretion Power in Astrophysics*, Cambridge University Press, Ch. 4.

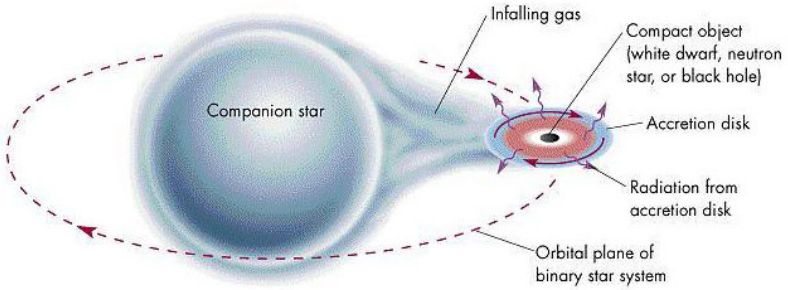

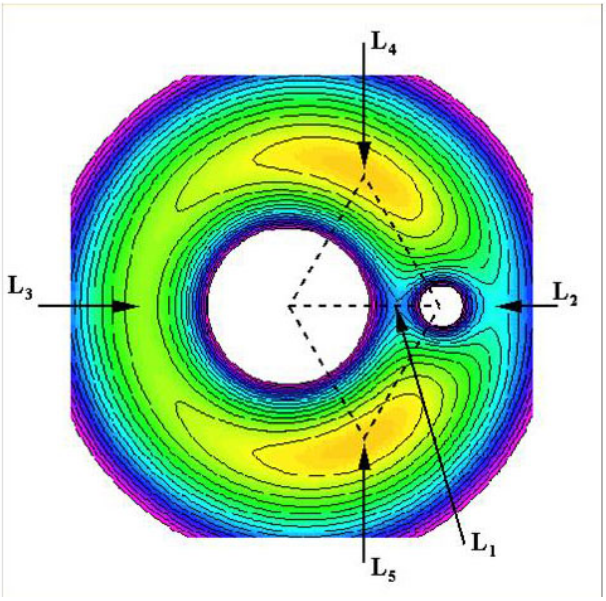

Figure 10.1: *The upper figure shows the typical mass flow leading to the formation of an accretion disk around a compact object (white dwarf, neutron star or black hole) in a binary with a 'normal' star. An accretion disk form as a result of the angular momentum carried by the material pulled from the normal star.*

The lower figure shows the equipotential contours of the potential $\Phi_{\rm eff}(\boldsymbol{r})$ *of Eqn. (10.3.4) in the orbital plane and in a reference frame that is corotating with the binary so that the stars are at a fixed position. Both stars rotate around the center-of-mass. If the heavy star (the larger of the two white areas in the Figure) becomes so large that it fills its Roche Lobe , mass can be transferred to the compact companion star through the inner Lagrangian point* L_1*, which is located between the normal star and the compact star. The other Lagrangian points* L_2 *to* L_5 *are not important for this particular situation.*

In Type I bursters the energy of the bursts is supplied by a *thermonuclear flash*: material accreted on to the neutron star accumulates until the pressure and density are so high that spontaneous nuclear combustion occurs where hydrogen is burned explosively into helium. Between flashes, one sees a persistent luminositty associated with the liberation of the free-fall energy of the material.

In Type II bursts, the bursts are believed to be caused by some form of *spasmodic accretion*, where the mass flow onto the compact object fluctuates strongly. What causes this spasmodic accretion is largely unknown. Only one objects, the *Rapid Burster* is known with these properties.

- **Cataclysmic Variables** are systems where the mass is transferred onto a white dwarf rather than a neutron star. The donor star has a low mass. These systems show large, irregular brightness variations. In non-magnetic CVs there is an extensive accretion disk. In magnetic CVs the formation of such a disk is prevented by the strong magnetic field of the white dwarf, and the accretion flow is chanelled by electromagnetic forces along the magnetic field towards the magnetic poles.

10.3.2 Modes of disk accretion

Disk accretion can proceed in different ways, depending on the circumstances. Theoretically, one can roughly distinguish between the following situations:

- **Geometrically thin disks.** In such disks, the thickness H of the disk is always small compared with the radial distance R to the compact object and the *radial* velocity is assumed to be small compared with the local sound speed: $V_R \ll c_{\rm s}$. As we will see in the next Section, the assumption of a thin disk actually *implies* that the inflow velocity in the disk must be subsonic. This means that pressure forces in the radial direction can be neglected. This assumption leads to a number of important simplifications in the decription of such disks. It is therefore not suprising that most of the theoretical effort has been devoted to thin disks.

- **Slender disks.** In the theory of slender disks, one relaxes the assumption of subsonic inflow, taking account of radial pressure forces. In that case is is possible to obtain solutions where the inflow becomes *supersonic* inside a critical point, just like the case of spherical accretion. This type of theory is usually referred to as an *Advection Dominated Accretion Flow*.

- **Thick disks.** In the theory of thick disks, pressure forces , inertial forces and gravity are of comparable importance, and the disk can have a thickness comparable to its radial extent. This is the most difficult case to describe theoretically. Furthermore, there are some serious doubts about the *stability* of thick disks: they seem to have the tendency to break up on a timescale comparable to their rotation period.

10.4 Thin, quasi-Keplerian disks

Consider a flow in cylindrical coordinates, where the flow is confined to a region of small vertical extent[4] of size $\sim 2H$ around the plane $Z = 0$. The vertical size of the flow region (disk thickness) satisfies

$$H(R) \ll R \, . \tag{10.4.1}$$

This geometrical constraint implies that the flow velocity in the Z-direction must be much smaller than the radial velocity: typically one has

$$|V_Z| \sim \frac{H}{R} \, |V_R| \ll |V_R| \, . \tag{10.4.2}$$

I will also assume that the vertical velocity component is small compared to the azimuthal velocity:

$$|V_Z| \ll |V_\theta| \, . \tag{10.4.3}$$

I will neglect the self-gravity of the disk material, assuming that the gravitational potential is due to the mass of the compact object. As long the thin disk condition (10.4.1) is satisfied one can approximate the gravitational potential near the disk mid-plane $Z = 0$ by

$$\Phi(R, Z) = -\frac{GM_*}{r} \approx -\frac{GM_*}{R} \, \left[1 - \frac{Z^2}{2R^2} \right] \, . \tag{10.4.4}$$

Here I have expanded $1/r = 1/\sqrt{R^2 + Z^2}$ for small values[5] of Z/R.

These assumptions imply that -as a first approximation- the flow velocity is confined to the equatorial plane of the disk (the $R - \theta$ plane), so we can write

$$\boldsymbol{V} \approx -V(R) \, \hat{\boldsymbol{e}}_R + \Omega(R) R \, \hat{\boldsymbol{e}}_\theta \, . \tag{10.4.5}$$

A minus sign has been introduced in the radial velocity component so that *inflow* corresponds to $V(R) > 0$.

[4] From this point on, the vertical direction corresponds with the Z-direction, $r = \sqrt{R^2 + Z^2}$ is the spherical radius, and $R = \sqrt{x^2 + y^2}$ is the cylindrical radius.

[5] Simply use: $1/\sqrt{R^2 + Z^2} = 1/R \times \left(1 + Z^2/R^2\right)^{-1/2} \approx (1/R) \times \left(1 - \frac{Z^2}{2R^2}\right)$

I also use the angular velocity $\Omega(R) = \mathrm{d}\theta/\mathrm{d}t$ to describe the magnitude of the azimuthal flow component. The specific angular momentum of the flow is given by

$$\lambda(R) = RV_\theta = \Omega(R)\, R^2 \ . \tag{10.4.6}$$

Since we will allow for some frictional force, which removes angular momentum from the flow, the specific angular momentum is generally not conserved (see below).

10.4.1 Force balance in a geometrically thin disk

Under these circumstances the equations of motion are enormously simplified. The equations in component form that describe a steady, axisymmetric disk flow read:

$$\begin{aligned}
\rho V\,\frac{\mathrm{d}\,V}{\mathrm{d}R} &= -\frac{\partial P}{\partial R} - \rho\,\frac{GM_*}{R^2} + \rho\,\Omega^2\,R && \text{radial force balance;}\\
-\rho V\,\frac{\mathrm{d}\,(\Omega R^2)}{\mathrm{d}R} &= -\rho V\,\frac{\mathrm{d}\lambda}{\mathrm{d}R} = \dot{l} && \text{angular momentum equation;}\\
0 &= -\frac{\partial P}{\partial Z} - \rho\,\frac{GM_* Z}{R^3} && \text{vertical force balance.}
\end{aligned} \tag{10.4.7}$$

Here I have used (10.4.4), $\boldsymbol{V}_{\mathrm{p}}\cdot\boldsymbol{\nabla} = -V\,\mathrm{d}/\mathrm{d}R$, and introduced a phenomenological angular momentum loss term $\dot{l}$. This quantity corresponds to the change of angular momentum per unit time and per unit volume. It is due to a torque excerted by frictional forces. If this term vanishes, specific angular momentum is conserved: $\lambda = \Omega R^2 =$ constant.

In the vertical direction the pressure force points away from the disk mid-plane, where the density and temperature are presumably highest, and balances the gravitational force, which points towards the mid-plane. This situation corresponds to *hydrostatic equilibrium* in the vertical direction. Let us assume for the moment that the disk is nearly isothermal in the vertical (Z) direction, so that

$$\partial T/\partial Z \approx 0 \ . \tag{10.4.8}$$

From the ideal gas law,

$$P = \rho\,\mathcal{R}\,T/\mu \ , \tag{10.4.9}$$

where $\rho = \rho(R, Z)$ is a function of cylindrical radius and height, and $T = T(R)$ depends only on the radius, it follows that the force balance in the vertical direction (the third equation in 10.4.7) reduces to the following simple equation for the density:

$$\frac{\mathcal{R}T}{\mu}\,\frac{\partial \ln \rho}{\partial Z} = -\frac{GM_*}{R^3}\,Z\ . \tag{10.4.10}$$

The solution is a Gaussian density law of the form

$$\rho(R, Z) = \rho(R, 0)\, e^{-Z^2/2H^2}\ . \tag{10.4.11}$$

The vertical density scale height H in this expression is a function of cylindrical radius, given by:

$$\boxed{H(R) = \left(\frac{\mathcal{R}TR^3}{GM_*\mu}\right)^{1/2} = \frac{s}{\Omega_{\rm K}}\ .} \tag{10.4.12}$$

Here $s(R) = \sqrt{\mathcal{R}T/\mu}$ is the *isothermal sound speed* at radius R. The quantity $\Omega_{\rm K}(R)$ is the *Keplerian angular velocity* appropriate for a circular Keplerian orbit around a mass M_* with radius R:

$$\Omega_{\rm K}(R) = \sqrt{\frac{GM_*}{R^3}}\ . \tag{10.4.13}$$

The assumption of a thin disk implies that one must have $H \ll R$, so that

$$s = \Omega_{\rm K} H \ll \Omega_{\rm K} R = V_\theta\ . \tag{10.4.14}$$

Therefore, the azimuthal flow in a geometrically thin disk is strongly supersonic.

This result allows us to simplify the radial component of the equation of motion even further. It implies that the effect of radial pressure gradients can be neglected in a geometrically thin disk. As an order-of-magnitude estimate for the radial pressure gradient in a disk with a smoothly varying density and pressure distribution as a function of radius, for instance $P(R) \propto R^{-\delta}$, one has using (10.4.12):

$$\left|\frac{1}{\rho}\,\frac{\partial P}{\partial R}\right| \simeq \delta\,\frac{P}{\rho R} = \mathcal{O}\left(\delta\,\frac{s^2}{R}\right) \approx \delta\,\left(\frac{H}{R}\right)^2 \times \frac{GM_*}{R^2}\,. \tag{10.4.15}$$

This means that the radial component of the pressure force is much smaller than the radial component of the gravitational force as long as δ is of order unity. This will be the case if the radial gradient scale at some radius R, the scale on which the pressure, density and velocity varies in the disk plane, is comparable to the radius. One must conclude that the radial pressure force in a thin disk is unable to support the disk against gravity.

A similar conclusion holds for the inertial force, $\rho V\,\mathrm{d}V/\mathrm{d}R$, due to the inflow velocity in the radial direction. It is easily seen that the inertial term due to inflow is of order

$$\left|\rho V\,\frac{\mathrm{d}V}{\mathrm{d}R}\right| \sim \rho\,\frac{V^2}{R}\,. \tag{10.4.16}$$

If we assume that the inflow velocity of the material is much smaller than the rotation speed, $V \ll V_\theta$, this term is much smaller than the centrifugal force $\rho V_\theta^2/R$ that appears in the same equation. We will see below that this assumption is indeed correct.

These two order of magnitude estimates for the pressure and inertial forces lead to the conclusion that a thin disk is *centrifugally supported* in the radial direction:

$$\rho\,\frac{GM_*}{R^2} \approx \rho\,\frac{V_\theta^2}{R} = \rho\,\Omega^2\,R\,. \tag{10.4.17}$$

There is a balance between the two dominant terms in the radial component of the equation of motion: gravity and the centrifugal force. This radial force balance determines the angular velocity of the disk material:

$$\boxed{\Omega(R) = \Omega_{\rm K} = \sqrt{\frac{GM_*}{R^3}}\,.} \tag{10.4.18}$$

One concludes that the angular velocity of the fluid in a geometrically thin disk equals the local Keplerian angular velocity. The force balance in a thin disk is illustrated below.

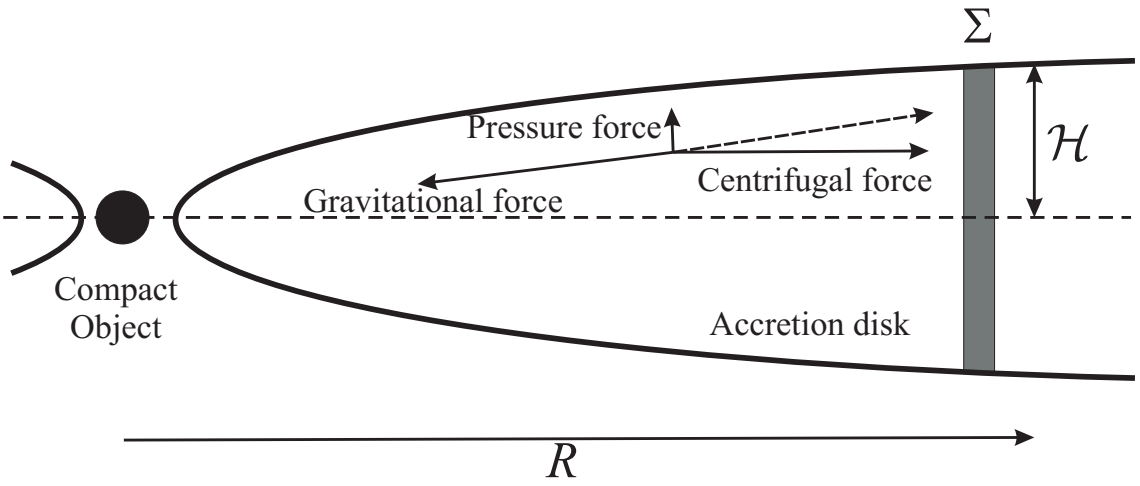

Figure 10.2: *The force balance in a geometrically thin accretion disk around a Compact Object. The figure also shows the definition of the disk thickness and of the column density Σ (gray column).*

10.4.2 Mass flow and angular momentum loss

The *column density* $\Sigma(R)$ of the disk is defined as[6]

$$\Sigma(R) \equiv \int_{-\infty}^{+\infty} \mathrm{d}Z\, \rho(R,Z)\,. \tag{10.4.19}$$

One can integrate the mass conservation law (remember: $V_R = -V(R)$!),

$$\frac{1}{R}\,\frac{\partial}{\partial R}\left[\rho R V(R)\right] - \frac{\partial}{\partial Z}\left(\rho V_Z\right) = 0\,, \tag{10.4.20}$$

across the disk from $Z = -\infty$ to $Z = +\infty$. This yields:

$$\frac{1}{R}\,\frac{\partial}{\partial R}\left[\Sigma(R)\, V(R) R\,\right] = \rho V_Z(Z=+\infty) - \rho V_Z(Z=-\infty) \tag{10.4.21}$$

Using the fact that the density drops exponentially with height above the disk midplane, and assuming that V_Z remains small[7], one concludes that there is no mass flux in the vertical direction at large Z:

[6] Sometimes one works in terms of a *surface density*: the density per unit disk area. Since a thin disk has two sides, the surface density is equal to $\Sigma/2$.

[7] This excludes the possibility that the disk generates a strong wind in the vertical direction, analogous to a stellar wind.

$$\rho V_Z(Z = \pm\infty) = 0 \; . \tag{10.4.22}$$

One then finds an single equation for the surface density:

$$\frac{\partial}{\partial R} \left[\Sigma(R)\, V(R) R \right] = 0 \; . \tag{10.4.23}$$

The total mass flow through the disk therefore satisfies

$$\boxed{\dot{M} = 2\pi R\, \Sigma(R)\, V(R) = \text{constant.}} \tag{10.4.24}$$

The quantity $\dot{M}$ corresponds to the total amount of mass that crosses a cylinder of arbitrary radius R per unit time.

We still need an expression for the radial velocity $V(R)$. This can be found by considering the angular momentum equation. Because of the radial force balance and the resulting Keplerian rotation law (10.4.18), the specific angular momentum $\lambda = \Omega R^2$ must take the Keplerian value:

$$\lambda(R) = \sqrt{GM_* R} \equiv \lambda_{\rm K} \; . \tag{10.4.25}$$

The angular momentum equation (the second equation in the set of equations 10.4.7) gives a relation between the (inward) radial velocity $V(R)$ and the amount of angular momentum loss:

$$-\rho V \, \frac{{\rm d}\lambda}{{\rm d}R} = \dot{l} \; . \tag{10.4.26}$$

Once again integrating vertically over the whole disk one finds:

$$-\Sigma(R) V(R) \left(\frac{{\rm d}\lambda}{{\rm d}R} \right) = \int_{-\infty}^{+\infty} {\rm d}Z \, \dot{l}(R, Z) \equiv \dot{L}(R) \; . \tag{10.4.27}$$

The quantity $\dot{L}$ is the angular momentum loss rate per unit disk area. Using (10.4.25), which implies

$$\frac{\mathrm{d}\lambda}{\mathrm{d}R} = \tfrac{1}{2}\sqrt{\frac{GM_*}{R}} = \tfrac{1}{2}\Omega_{\rm K}(R)\,R\,, \tag{10.4.28}$$

this yields the radial mass flux through the disk,

$$\Sigma\,V(R) = -\frac{\dot{L}}{\mathrm{d}\lambda/\mathrm{d}R} = -\frac{2\dot{L}}{\Omega_{\rm K}R}\,. \tag{10.4.29}$$

This determines the total massflow: using relation (10.4.24) one finds

$$\boxed{\dot{M} = 2\pi R\Sigma V = -\frac{4\pi\dot{L}}{\Omega_{\rm K}(R)}\,.} \tag{10.4.30}$$

This result tells us two important facts about the physics of steady thin accretion disks:

1. In order to accrete onto the compact object ($\dot{M} > 0$) the material must *lose* angular momentum ($\dot{L} < 0$). In view of our discussion at the beginning of this Chapter this is not suprising: if specific angular momentum were conserved the material would never reach the compact object: it would keep orbiting the central object in circular Keplerian orbits. Since the specific angular momentum satisfies $\lambda \approx \sqrt{GM_*R}$ the angular momentum of inflowing material diminishes as it migrates inward.

2. Since we assume a *steady* disk, the total mass flow $\dot{M}$ through the disk must be constant. Its value is set by the boundary conditions at the outer edge of the disk: the amount of material flowing onto the disk from the companion star due to *Roche Lobe Overflow* determines $\dot{M}$. Equation (10.4.30) tells us that, in order to accomodate this mass flow, the angular momentum loss per unit area $\dot{L}$ must take the correct value! This means that the structure of the accretion disk (thickness, density, temperature) must somehow adjust $\dot{L}$ so that the correct amount of mass can flow through the disk at each radius, preventing that mass accumulates (or drains away) anywhere in the disk. The amount of mass entering the outer edge of the disk therefore *determines* $\dot{L}$ and the structure of the disk, and *not* the other way around!

   Note that this conclusion is *independent* of the precise mechanism that is ultimately responsible for the loss of angular momentum. It may be internal friction due to molecular viscosity, it could be magnetic forces (the so-called Maxwell stresses) or the friction could be due to the action of turbulence (turbulent viscosity) or even radiation.

There is a simple analogy that illustrates the fact that a thin accretion disk has to adjust it's internal properties so that it can transfer an amount of mass equal to the amount of mass supplied by the donor star. Consider a bucket, with a number of holes drilled in the bottom (see figure below). A faucet supplies water at a fixed rate of $\dot{M}_{\rm in}$ grams per second. When the faucet is turned on, the water level in the bucket will initially rise. As the water level rises, the pressure at the bottom of the bucket, equal to $P_{\rm b} = P_{\rm atm} + \rho g h$ with h the height of the water column, rises also. As a result, the amount of water pushed out of the holes increases: the outflow rate $\dot{M}_{\rm out}$ is determined by the pressure difference between the water pressure $P_{\rm b}$ at the bottom of the bucket and the atmospheric pressure $P_{\rm atm}$: if the pressure difference $P_{\rm b} - P_{\rm atm} = \rho g h$ increases, so does $\dot{M}_{\rm out}$. The rise of the water level will stop if the amount of water supplied by the faucet is exactly balanced by the amount of water pressed through the holes in the bottom of the bucket: $\dot{M}_{\rm in} = \dot{M}_{\rm out}$. Here, the water level is the analogue for the loss of angular momentum in an accretion disk. It must adjust until a balance is reached between inflow of matter and the outflow.

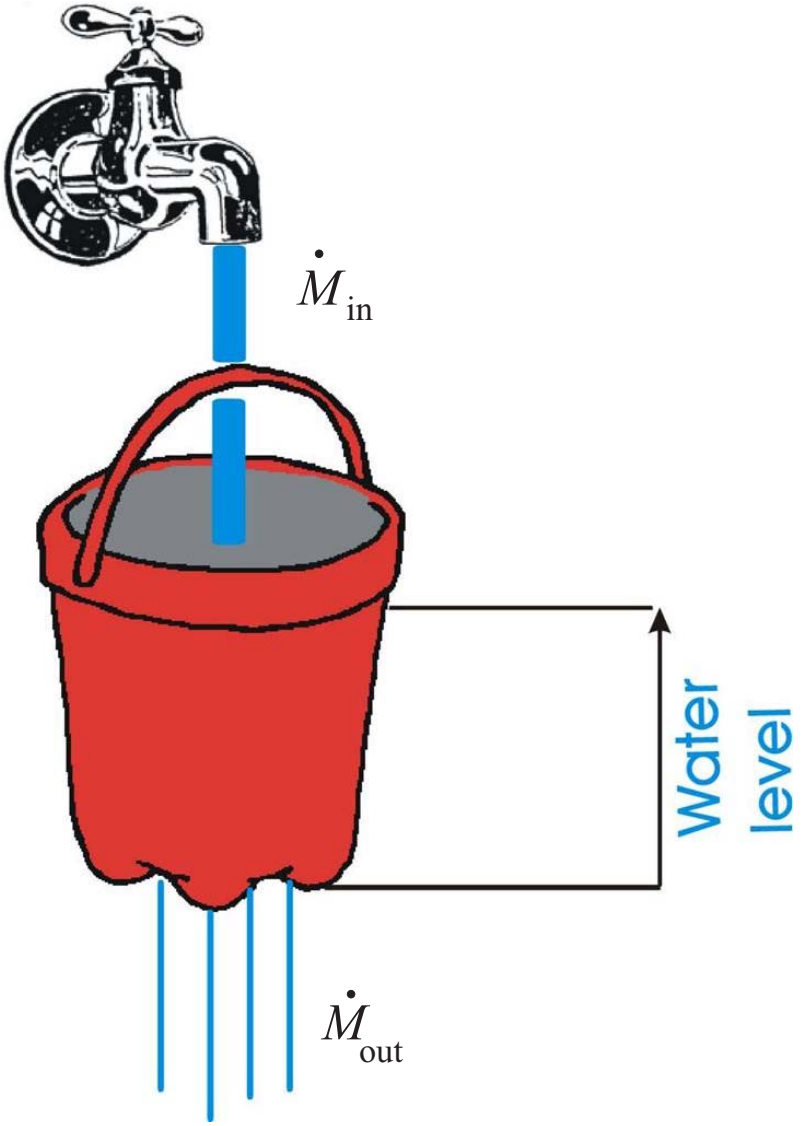

Figure 10.3: *The leaky bucket analogy for mass transport in a geometrically thin accretion disk. The level of water in the leaky bucket must adjust itself in such a way that the amount of water flowing into the bucket from the faucet ($\dot{M}_{\rm in}$) equals the amount of water leaking out through the holes in the bottom ($\dot{M}_{\rm out}$).*

10.5 Viscous angular momentum transport

As we have seen in the preceding Section, the transport of angular momentum is of fundamental importance: mass accretion onto a compact object can not proceed without it! If one assumes that some diffusive process (such as molecular or turbulent diffusion) is responsible for the angular momentum transport, the associated *viscous torque* can be estimated in a relatively straightforward manner.

Consider a fluid rotating on cylinders[8], with an azimuthal velocity

$$V_\theta(R) = \Omega(R)\, R\ . \tag{10.5.1}$$

The angular velocity $\Omega(R)$ is a function of radius, so the disk is not rotating as a solid body but is rotating differentially. The specific angular momentum of the material at radius R equals

$$\lambda(R) = RV_\theta = \Omega(R)\, R^2\ . \tag{10.5.2}$$

Diffusive angular momentum transport, either due to ordinary collisions or due to turbulence, can be treated in the same way as viscosity in the previous Chapter, namely as a process where particles or fluid eddies transport the specific angular momentum of the flow over a typical distance ℓ, the *mean free path*, with typical velocity σ, the random 'thermal' velocity. After travelling one mean free path, the particles or eddies 'deposit' this angular momentum due to an interaction with the local fluid, and the process can start anew. If the typical 'collision time' between interactions equals $\tau_{\rm c}$, the mean-free-path and random velocity are related by

$$\ell \approx \sigma\tau_{\rm c}\ . \tag{10.5.3}$$

At some radius R this diffusive transport will redistribute angular momentum within a layer of thickness $\Delta R \approx \ell$. As long as $\ell \ll R$ the effect of this process can be calculated in a relatively straightforward fashion.

We look at the process from the point of view of an observer rotating with the angular velocity Ω_0 around the Z-axis. The general transformation law (8.6.49) between the velocity in the inertial and the rotating frame (see Figure below),

$$\boldsymbol{V}_{\rm I} = \boldsymbol{V}_{\rm R} + \boldsymbol{\Omega} \times \boldsymbol{r}(t)\ , \tag{10.5.4}$$

[8]Meaning: the angular velocity depends only on the cylindrical radius, and takes a constant value on any cylinder $R = \text{constant}$.

implies that the azimuthal velocity in the corotating frame for $Z \ll R$ is given by

$$(V_\theta)_{\rm R} = (\Omega(R) - \Omega_0)\ R\ . \tag{10.5.5}$$

We choose $\Omega_0 = \Omega(R_0)$ at some fiducial radius R_0 so that observer co-rotates with the flow at R_0. We will consider the effects of diffusive angular momentum transport in a layer of size $\Delta R \sim 2\ell$ around R_0.

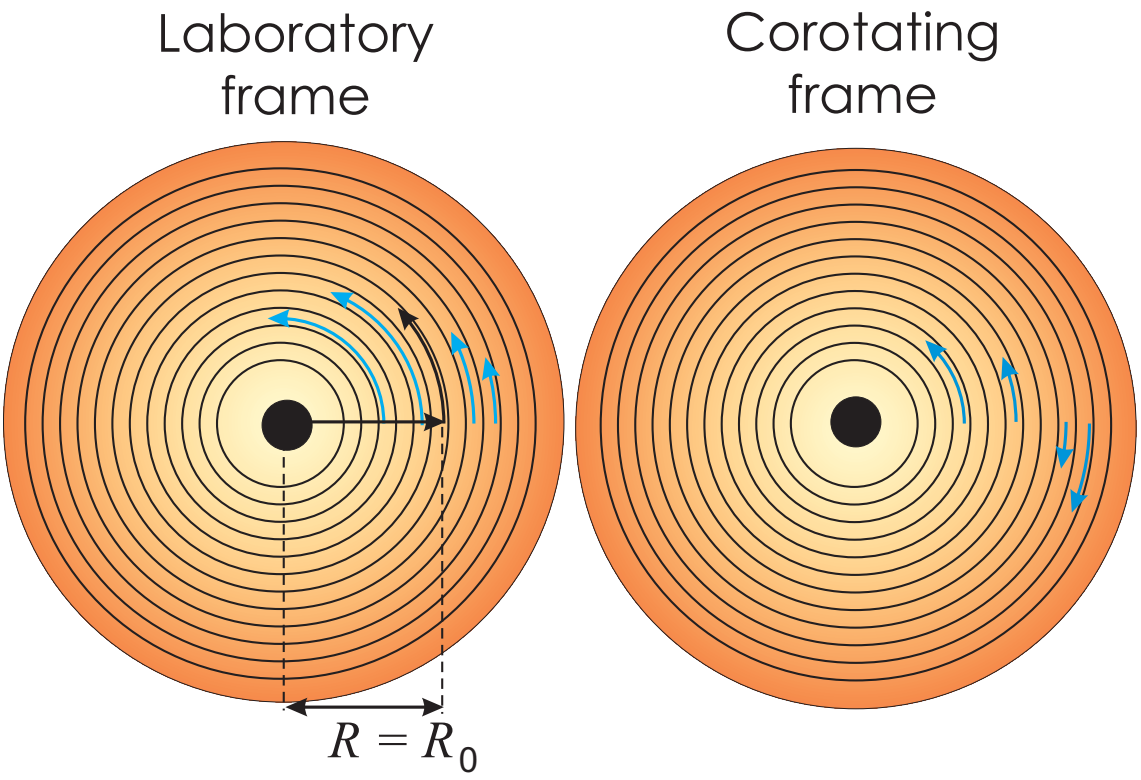

Figure 10.4: *The rotation velocity (the blue arrows) as seen from an inertial frame (left), and in a frame corotating with angular velocity* $\Omega_0 = \Omega(R_0)$ *(right). Shown is the case with* $\mathrm{d}V_\theta/\mathrm{d}R < 0$

Seen from the corotating frame, the azimuthal velocity of material at a neighbouring radius $R_0 + \Delta R$ equals

$$\begin{aligned} \Delta V_\theta &= [\Omega(R_0 + \Delta R) - \Omega(R_0)]\,(R_0 + \Delta R) \\ &\approx \Delta R \left(R \frac{\mathrm{d}\Omega}{\mathrm{d}R} \right)_{R=R_0} . \end{aligned} \tag{10.5.6}$$

Here I have only retained terms to first order in $\Delta R \ll R_0$, neglecting smaller terms $\propto \Delta R^2$. The fact that this velocity difference scales as $\Delta V_\theta \propto \mathrm{d}\Omega/\mathrm{d}R$ can be understood simply once one realizes that for *solid* rotation, where $\mathrm{d}\Omega/\mathrm{d}R = 0$ and $\Omega(R) = \Omega_0$, there is no fluid velocity in the corotating frame.

The associated specific angular momentum of the flow equals, to first order in ΔR,

$$\Delta\lambda = R\Delta V_\theta = \Delta R \left(R^2 \frac{\mathrm{d}\Omega}{\mathrm{d}R} \right) . \tag{10.5.7}$$

Here (and in what follows) I will drop the subscript 0 on R_0, simply writing R. Let us now think of the flow as consisting of particles (or turbulent eddies) which have a velocity dispersion around the mean flow velocity. This dispersion can be due to the thermal motion of the particles (see the discussion in Chapter 2) or, in the case of turbulent eddies, are due to random (macroscopic) motions in the fluid. The velocity of each particle or fluid element can then be written as

$$\boldsymbol{v} = \boldsymbol{V} + \boldsymbol{\sigma} , \tag{10.5.8}$$

with $\boldsymbol{\sigma}$ the random 'thermal' velocity which vanishes on average, and which satisfies the relations introduced in Chapter 2.2:

$$\overline{\sigma}_R = \overline{\sigma}_\theta = \overline{\sigma}_Z = 0 \ , \ \overline{\sigma_R^2} = \overline{\sigma_\theta^2} = \overline{\sigma_Z^2} = \tfrac{1}{3}\sigma^2 \ , \ \overline{\sigma_i\,\sigma_j} = 0 \text{ for } i \neq j . \tag{10.5.9}$$

The corotating observer at radius R assigns a specific angular momentum

$$\Delta\lambda \approx \left(R^2 \frac{\mathrm{d}\Omega}{\mathrm{d}R} \right) \Delta R + R\,\sigma_\theta \tag{10.5.10}$$

to a particle at radius $R + \Delta R$. Here we neglected ΔR with respect to R in the second term. The first term is the angular momentum associated with the mean flow, and the second term is the contribution to the angular momentum in the corotating frame due to the random 'thermal' motion.

If the particle density is $n(R)$, the typical particle flux in the radial direction is entirely associated with the 'thermal' motions, and equals (for given σ_R)

$$\mathcal{F}_R \sim n(R)\,\sigma_R . \tag{10.5.11}$$

If particles deposit their angular momentum after a collision time $\tau_{\rm c}$, the particles arriving at a radius R originated at a radial distance

$$\Delta R = -\sigma_R \, \tau_{\rm c} \tag{10.5.12}$$

from the fiducial radius R (see figure). Between collisions, the particle velocity is unchanged and the specific angular momentum upon arrival at radius R is equal to

$$\Delta\lambda = R \, (\Delta V_\theta + \sigma_\theta) \ . \tag{10.5.13}$$

According to Eqns. (10.5.6) and (10.5.12) this equals

$$\Delta\lambda = \left(R^2 \, \frac{{\rm d}\Omega}{{\rm d}R} \right) \, (-\sigma_R \, \tau_{\rm c}) + R \, \sigma_\theta \ . \tag{10.5.14}$$

Therefore, there is a viscous flux of angular momentum associated with the particle flux. Using that the angular momentum per particle equals $\Delta L = m \, \Delta\lambda$, with m the mass of the molecules or atoms in the gas, this viscous angular momentum flux is

$$\begin{aligned} \mathcal{J} \ &\equiv \ \text{(particle flux)} \times \text{(angular momentum per particle)} \\ &= \ \mathcal{F}_R \, m \, \Delta\lambda \end{aligned} \tag{10.5.15}$$

Collecting results one finds:

$$\mathcal{J} = n(R) m \, \sigma_R \, \left[\left(R^2 \, \frac{{\rm d}\Omega}{{\rm d}R} \right) \, (-\sigma_R \, \tau_{\rm c}) + R \, \sigma_\theta \right] \tag{10.5.16}$$

In order to calculate the *net* angular momentum flux one must average over the isotropic distribution of thermal velocities. Using the above averaging rules one finds :

$$\overline{\mathcal{J}}(R) = -\rho(R) \, \frac{\sigma^2 \, \tau_{\rm c}}{3} \, \left(R^2 \, \frac{{\rm d}\Omega}{{\rm d}R} \right) \ . \tag{10.5.17}$$

Here $\rho(R) = n(R) m$ is the mass density of the gas.

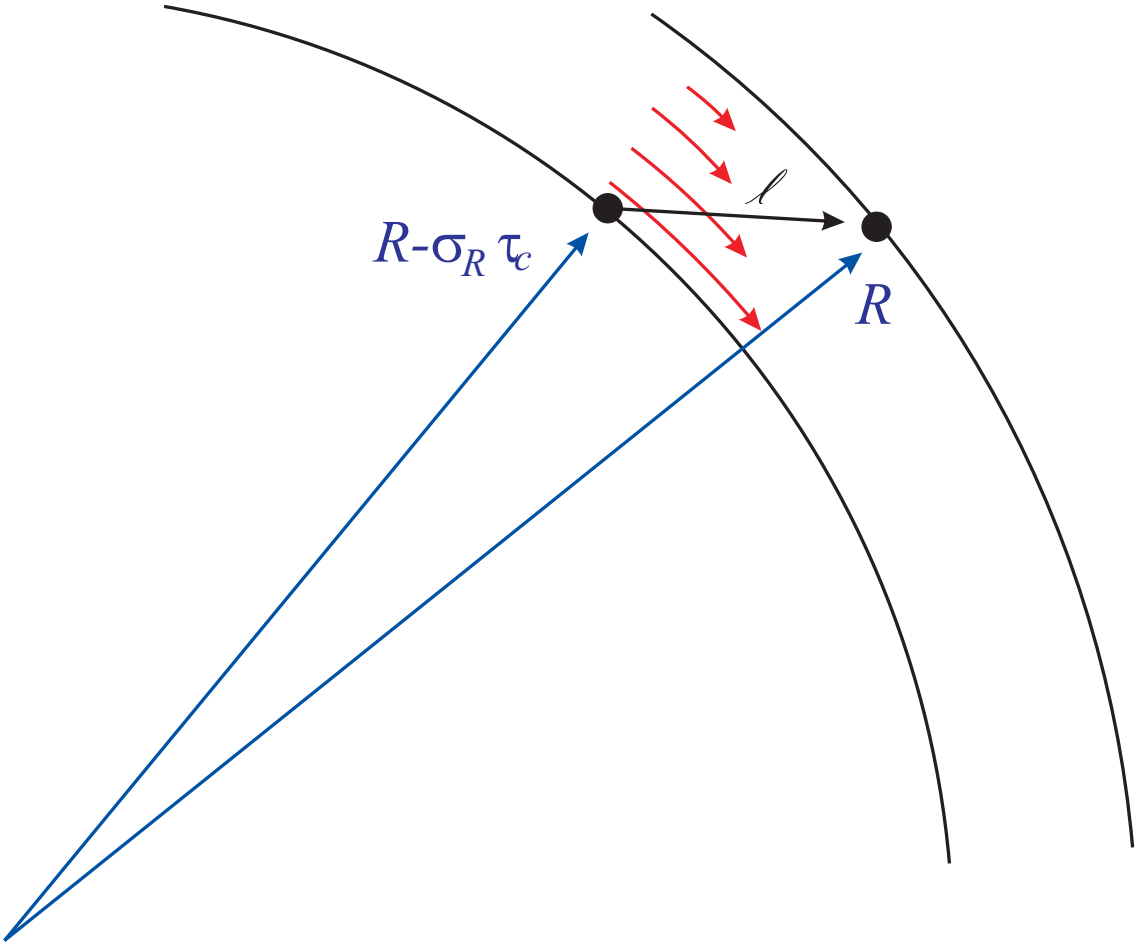

Figure 10.5: *The diffusive transport of angular momentum. The picture shows the situation from the point of view of an observer that corotates with the material at radius R. If the disk rotates differentially, this observer sees a shearing azimuthal velocity (red arrows). A particle originates at a radius $R - \sigma_R\tau_c$, and deposites its angular momentum at radius R. The mean free path between collisions equals $\ell = \sigma\tau_c$ with τ_c the time between two subsequent collisions, and σ_R is the radial component of the random ('thermal') velocity.*

The thermal contribution to the angular momentum in the corotating frame has averaged out completely since $\overline{\sigma_R\,\sigma_\theta} = 0$ for an isotropic distribution of random velocities. Note that this averaging procedure takes account of particles crossing the radius R from both directions.

In Chapter 9 we defined the *kinematic viscosity* ν, which depends only on the 'microscopic' parameters σ, $\tau_{\rm c}$ and ℓ:

$$\nu \equiv \frac{\sigma^2 \tau_{\rm c}}{3} = \frac{\sigma \ell}{3} \ . \tag{10.5.18}$$

This calculation shows that the kinematic viscosity regulates the strength of the angular momentum transport. In terms of this quantity one can write the viscous angular momentum flux as

$$\boxed{\mathcal{J}(R) = -\rho\,\nu\,R^2\,\left(\frac{{\rm d}\Omega}{{\rm d}R}\right)\ .} \tag{10.5.19}$$

Here I have dropped the averaging bar $\overline{\cdots}$. In a Keplerian disk one has ${\rm d}\Omega/{\rm d}R < 0$. This means that $\mathcal{J}(R) > 0$ so that the radial angular momentum flux is *outward* towards larger R. Mass flux and angular momentum flux are in the opposite direction!

The amount of angular momentum crossing some area O perpendicular to $\hat{\boldsymbol{e}}_R$ in a time Δt is simply

$$\Delta J = \mathcal{J}(R)\,O\,\Delta t \ . \tag{10.5.20}$$

Now consider an annulus of material in the disk bounded between a cylinder of radius R and a cylinder of radius $R + \Delta R$ and of unit height $\Delta Z = 1$, with $\Delta R \ll R$. The volume of this annulus is $\mathcal{V} = 2\pi R\,\Delta R$. The *net* change in the angular momentum of this annulus in a time Δt is equal to the difference between the amount of angular momentum entering the inner cylindrical surface at a radius R, (with area $2\pi R$) and the amount leaving the outer cylindrical surface at a radius $R+\Delta R$ (with area $2\pi(R+\Delta R)$):

$$\begin{aligned} \Delta J &= \left[2\pi R\mathcal{J}(R) - 2\pi(R+\Delta R)\,\mathcal{J}(R+\Delta R)\,\right]\,\Delta t \\ &\approx -2\pi\Delta R\,\frac{{\rm d}(R\,\mathcal{J})}{{\rm d}R}\,\Delta t \ . \end{aligned} \tag{10.5.21}$$

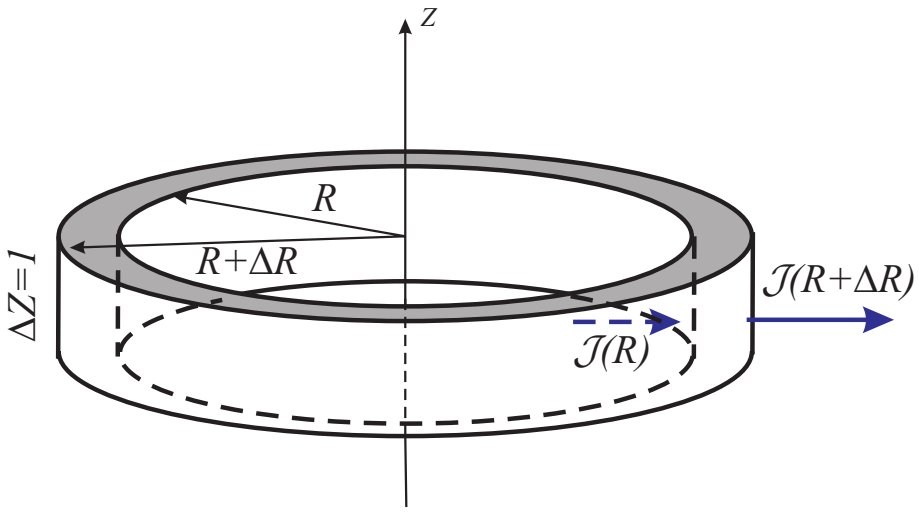

Figure 10.6: *An annulus of unit height $\Delta Z = 1$, with an inner radius R and an outer radius $R + \Delta R$. The angular momentum with flux $\mathcal{J}$ (blue arrows) enters at the inner radius, and leaves the annulus at the outer radius. The net torque on the material is due to the difference in the amount of angular momentum entering the annulus, and the amount leaving the annulus.*

One defines the *torque* as the angular momentum change per unit time and unit volume:

$$\dot{l} = \frac{1}{2\pi R\,\Delta R}\left(\frac{\Delta J}{\Delta t}\right) . \tag{10.5.22}$$

Using expression (10.5.19), this definition gives the viscous torque as

$$\boxed{\dot{l}_{\rm visc} = \frac{1}{R}\frac{\partial}{\partial R}\left[\rho\nu R^3\left(\frac{{\rm d}\Omega}{{\rm d}R}\right)\right] .} \tag{10.5.23}$$

10.5.1 Viscous torque from the viscous stress tensor

The expression for the viscous torque $\dot{l}_{\rm visc}$ was derived in the previous Section using a physical picture. That derivation was a variation on the derivation of viscous momentum transport. This suggests that it should be possible to derive the above results by looking at the viscous stresses in a differentially rotating flow: a flow with ${\rm d}\Omega/{\rm d}R \neq 0$.

This (more formal) derivation starts with the viscous force in terms of the viscous stress tensor, as introduced in the previous Chapter. The θ-component of the equation of motion reads, in the presence of viscosity:

$$\rho\left[\frac{\partial V_\theta}{\partial t}+V_R\,\frac{\partial V_\theta}{\partial R}+\frac{V_\theta}{R}\frac{\partial V_\theta}{\partial\theta}+V_Z\,\frac{\partial V_\theta}{\partial Z}+\frac{V_R V_\theta}{R}\right]=-\frac{1}{R}\frac{\partial P}{\partial\theta}-(\boldsymbol{\nabla}\cdot\boldsymbol{T}^{\rm visc})_\theta\ . \quad (10.5.24)$$

Because of the use of curvilinear cylindrical coordinates, the θ-component of the divergence of some tensor $\boldsymbol{T}$ picks up a number of curvature terms:

$$(\boldsymbol{\nabla}\cdot\boldsymbol{T})_\theta=\frac{1}{R}\,\frac{\partial}{\partial R}\left(RT_{R\theta}\right)+\frac{1}{R}\,\frac{\partial T_{\theta\theta}}{\partial\theta}+\frac{\partial T_{Z\theta}}{\partial Z}+\frac{T_{\theta R}}{R}\ . \quad (10.5.25)$$

Fortunately, in a thin steady disk where $\partial/\partial t=\partial/\partial\theta=0$ the resulting equations are much simpler. Since we will integrate in the vertical direction across the disk, the term with $T_{Z\theta}$ does not contribute after integration. The term with $T_{\theta\theta}$ does not contribute because of axisymmetry. Furthermore, the viscous stress tensor is symmetric so that $T_{R\theta}=T_{\theta R}$. This implies that we only need to consider the term

$$\frac{1}{R}\,\frac{\partial}{\partial R}\left(RT^{\rm visc}_{R\theta}\right)+\frac{T^{\rm visc}_{\theta R}}{R}=\frac{1}{R^2}\,\frac{\partial}{\partial R}\left(R^2\,T^{\rm visc}_{R\theta}\right)\ . \quad (10.5.26)$$

Using all the approximations already introduced above for a steady, axisymmetric and thin disk, we can write the equation of motion in the θ-direction as an equation for the specific angular momentum. After multiplying the whole equation by R one has:

$$\begin{aligned}\rho\,\frac{\mathrm{d}\lambda}{\mathrm{d}t}\approx-\rho V\,\frac{\mathrm{d}(\Omega R^2)}{\mathrm{d}R}\ &=\ -R\,(\boldsymbol{\nabla}\cdot\boldsymbol{T}^{\rm visc})_\theta\\ &=\ -\frac{1}{R}\,\frac{\partial}{\partial R}\left(R^2\,T^{\rm visc}_{R\theta}\right)\ .\end{aligned} \quad (10.5.27)$$

Assuming that we have only shear viscosity (equal to $\eta=\rho\nu$) but no bulk viscosity (so that $\zeta=0$), the viscous stress tensor for the accretion flow is simply

$$\boldsymbol{T}^{\rm visc}=-\eta\,\left(\boldsymbol{\nabla}\boldsymbol{V}+\boldsymbol{\nabla}\boldsymbol{V}^{\dagger}\right)\ . \quad (10.5.28)$$

Here I have used that the flow is incompressible to lowest order in $\mathcal{H}/R\ll1$.

Calculating the $R\theta$-component of the viscous stress tensor, using the fact that $V_\theta = \Omega R \gg V_R$, one finds

$$T^{\rm visc}_{R\theta} = -\eta \left(\frac{\partial V_\theta}{\partial R} - \frac{V_\theta}{R} \right) = -\eta \, R \, \frac{{\rm d}\Omega}{{\rm d}R} \, , \tag{10.5.29}$$

where we pick up yet another curvature term. Substituting this relation into (10.5.27) one finds the final version of the azimuthal component of the equation of motion:

$$-\rho V \, \frac{{\rm d}(\Omega R^2)}{{\rm d}R} = \dot{l}_{\rm visc} = \frac{1}{R} \, \frac{\partial}{\partial R} \left[\rho \nu \, R^2 \, \left(R \, \frac{{\rm d}\Omega}{{\rm d}R} \right) \right] \, . \tag{10.5.30}$$

This expression for $\dot{l}_{\rm visc}$ is exactly the same as the viscous torque derived in the preceding Section.

10.6 Angular momentum transport in a thin disk

We can apply these results to a thin, steady (and therefore quasi-keplerian) disk where $\Omega \approx \Omega_{\rm K} = \sqrt{GM_*/R^3}$. The θ-component of the equation of motion becomes

$$-\rho V \, \frac{{\rm d}\lambda}{{\rm d}R} = \frac{1}{R} \, \frac{\partial}{\partial R} \left[\rho \nu R^3 \, \left(\frac{{\rm d}\Omega}{{\rm d}R} \right) \right] \, . \tag{10.6.1}$$

Integrating this equation across the disk thickness yields

$$-\Sigma V \, \frac{{\rm d}\lambda}{{\rm d}R} = \dot{L} = \frac{1}{R} \, \frac{\rm d}{{\rm d}R} \left[\Sigma \nu R^3 \, \left(\frac{{\rm d}\Omega}{{\rm d}R} \right) \right] \, . \tag{10.6.2}$$

Here ν should be interpreted as the height-averaged viscosity. If one multiplies this equation by $2\pi R$, and uses the mass conservation law

$$\dot{M} = 2\pi R \, \Sigma \, V = \text{constant} \, , \tag{10.6.3}$$

one finds a simple equation:

$$\frac{\rm d}{{\rm d}R} \left[\dot{M} \lambda(R) + 2\pi \Sigma \nu R^3 \, \left(\frac{{\rm d}\Omega}{{\rm d}R} \right) \right] = 0 \, . \tag{10.6.4}$$

This can be integrated immediately:

$$\dot{M}\lambda(R) + 2\pi\Sigma\nu R^3 \left(\frac{\mathrm{d}\Omega}{\mathrm{d}R}\right) = \text{constant} \equiv \dot{J} \; . \tag{10.6.5}$$

This equation states that the *total* angular momentum flow in the radial direction must be constant in the steady state. If this were not the case, angular momentum would accumulate or drain away at some radius. The angular momentum flow consists of two contributions. The first is the specific angular momentum carried by the mass flow, $\dot{M}\lambda(R)$, the angular momentum transport due to the bulk motion of the disk material in the radial direction. The second contribution is the total diffusive (viscous) angular momentum flow, which equals $2\pi\Sigma\nu R^3 \, (\mathrm{d}\Omega/\mathrm{d}R)$. Apart from a minus sign, this is the amount of angular momentum that crosses an infinite cylinder with radius R due to viscous action.

In order to determine the value of the constant $\dot{J}$ one needs a boundary condition at the inner or outer radius of the disk, which sets the value of the net angular momentum flow. It is often assumed that the height-integrated viscous *shear stress*, defined as

$$\text{height-integrated shear stress} = \Sigma\nu R \, \frac{\mathrm{d}\Omega}{\mathrm{d}R} \; , \tag{10.6.6}$$

vanishes at the inner disk radius R_i, essentially because the matter drains out of the disk and falls onto the compact object so that $\Sigma(R_\mathrm{i}) \approx 0$. In a geometrically thin disk the angular momentum is the Keplerian angular momentum: $\lambda(R) = \lambda_\mathrm{K} = \sqrt{GM_* R}$. The assumption of a vanishing shear stress at radius R_i therefore determines the integration constant in Eqn. (10.6.5):

$$\dot{J} = \dot{M} \, \lambda_\mathrm{K}(R_\mathrm{i}) = \dot{M} \, \sqrt{GM_* R_\mathrm{i}} \; . \tag{10.6.7}$$

This means that equation (10.6.5) can be written as

$$\boxed{\nu\Sigma = \frac{\dot{M}}{3\pi}\left[1 - \left(\frac{R_\mathrm{i}}{R}\right)^{1/2}\right] \; .} \tag{10.6.8}$$

This last relation clearly shows how the disk structure (i.e. the product of ν and Σ) must adjust at each radius in order that a steady mass flow $\dot{M}$ results: in a steady disk no material may accumulate at any radius.

10.7 Disk energy balance

The viscous transport of angular momentum through a differentially rotating ($\mathrm{d}\Omega/\mathrm{d}R \neq 0$) disk must lead to an associated dissipation of rotational energy. In a steady state, where the temperature of the disk material at given radius does not change, this energy must be transported out of the disk. In this Section we consider the dissipation due to friction.

How this proceeds is most simply seen by once again using the analogy with single-particle dynamics. There change of angular momentum foolows from the equation of motion for a single particle,

$$\frac{\mathrm{d}\boldsymbol{p}}{\mathrm{d}t} = m\,\frac{\mathrm{d}\boldsymbol{v}}{\mathrm{d}t} = \boldsymbol{F}\ . \tag{10.7.1}$$

The angular momentum $\boldsymbol{L} = \boldsymbol{r} \times \boldsymbol{p}$ follows from

$$\frac{\mathrm{d}\boldsymbol{L}}{\mathrm{d}t} = \left(\frac{\mathrm{d}\boldsymbol{r}}{\mathrm{d}t}\right) \times \boldsymbol{p} + \boldsymbol{r} \times \left(\frac{\mathrm{d}\boldsymbol{p}}{\mathrm{d}t}\right) = \boldsymbol{r} \times \boldsymbol{F} \equiv \boldsymbol{N}\ , \tag{10.7.2}$$

where I have used $\mathrm{d}\boldsymbol{r}/\mathrm{d}t = \boldsymbol{v}$ and $\boldsymbol{v} \times \boldsymbol{p} = m\,\boldsymbol{v} \times \boldsymbol{v} = 0$. The quantity $\boldsymbol{N}$ is the torque[9]. Consider a particle moving in the R-θ plane, subject to a force $\boldsymbol{F} = F_\theta\,\hat{\boldsymbol{e}}_\theta$ in the azimuthal direction. This choice corresponds closely with the situation that occurs in a differentially rotating disk: there the frictional force between fluid rings is also in the θ-direction. The angular momentum is

$$\boldsymbol{L} = \boldsymbol{r} \times \boldsymbol{p} = m\,Rv_\theta\,\hat{\boldsymbol{e}}_z\ , \tag{10.7.3}$$

and the angular momentum change due to the torque $\boldsymbol{N} \equiv N\,\hat{\boldsymbol{e}}_z$ is given by

$$\frac{\mathrm{d}L}{\mathrm{d}t} = N = RF_\theta\ . \tag{10.7.4}$$

This force does work, and leads to a change of the particle kinetic energy $\mathcal{E}$ that is given by

$$\frac{\mathrm{d}\mathcal{E}}{\mathrm{d}t} = \boldsymbol{F} \cdot \boldsymbol{v} = F_\theta v_\theta\ . \tag{10.7.5}$$

[9] e.g. H. Goldstein, C. Poole & J. Safko, 2002: *Classical Mechanics* (Third Edition), Addison-Wesley Publ. Company, Ch. 1

Combining this relation with (10.7.4) and using $V_\theta = \Omega R$, one sees that the energy change and the torque $N = RF_\theta$ are related by

$$\frac{\mathrm{d}\mathcal{E}}{\mathrm{d}t} = \Omega\, N = \Omega\, \frac{\mathrm{d}L}{\mathrm{d}t}\ . \tag{10.7.6}$$

The same principle can be applied to a ring of material in an accretion disk. Consider again a ring of thickness $\Delta R \ll R$, and of unit height, $\Delta Z = 1$. The angular momentum of this ring changes due to viscous angular momentum transport. Given a change ΔJ of the ring angular momentum in a time Δt, the amount of work done by viscous forces is equal to

$$\Delta E = \Omega\, \Delta J\ . \tag{10.7.7}$$

Using Eqn. (10.5.21) for ΔJ one finds

$$\Delta E = -2\pi \Delta R\, \Omega\, \left(\frac{\mathrm{d}(R\mathcal{J})}{\mathrm{d}R}\right)\, \Delta t\ . \tag{10.7.8}$$

Rewriting the right-hand-side of this equation, using

$$\Omega\, \left(\frac{\mathrm{d}(R\mathcal{J})}{\mathrm{d}R}\right) = \left(\frac{\mathrm{d}(R\Omega\, \mathcal{J})}{\mathrm{d}R}\right) - R\mathcal{J}\, \frac{\mathrm{d}\Omega}{\mathrm{d}R}\ , \tag{10.7.9}$$

we can find the rate of change of the energy per unit volume:

$$\dot{e} = \frac{1}{2\pi R \Delta R}\, \left(\frac{\Delta E}{\Delta t}\right) = -\frac{1}{R}\frac{\partial}{\partial R}\left[R\Omega \mathcal{J}\ \right] + \mathcal{J}\, \frac{\mathrm{d}\Omega}{\mathrm{d}R}\ . \tag{10.7.10}$$

Integrating this result across the disk thickness, and using expression (10.5.19), we can calculate the rate of change of the flow kinetic energy per unit disk area due to viscosity at some radius R:

$$\boxed{\dot{\mathrm{E}}(R) \equiv \int_{-\infty}^{+\infty} \mathrm{d}Z\, \dot{e}(Z) = \frac{1}{R}\, \frac{\mathrm{d}}{\mathrm{d}R}\left[\Sigma\nu\, R^3\, \Omega\, \frac{\mathrm{d}\Omega}{\mathrm{d}R}\right] - \Sigma\nu\, \left(R\, \frac{\mathrm{d}\Omega}{\mathrm{d}R}\right)^2\ .} \tag{10.7.11}$$

The first term in this expression for $\dot{\mathrm{E}}(R)$ has the form of the divergence of a flux in the radial direction. From expression (8.6.33) for the divergence in cylindrical polar coordinates it follows that this term can be written as

$$-\boldsymbol{\nabla}\cdot\boldsymbol{\mathcal{F}} \quad \text{with} \quad \boldsymbol{\mathcal{F}}\,(R) \equiv -\Sigma\nu\, R^2\,\Omega\,\left(\frac{\mathrm{d}\Omega}{\mathrm{d}R}\right)\,\hat{\boldsymbol{e}}_R\,. \tag{10.7.12}$$

The flux $\boldsymbol{\mathcal{F}}$ corresponds to the energy flux that is associated with the diffusive angular momentum transport. This flux transports energy through the disk, redistributing the energy over different radii. It does **not** lead to the dissipation of any energy!

The second term in expression (10.7.11) is *negative definite*: it must correspond to an irreversible *loss* of kinetic energy from the azimuthal flow, which has an energy density $\frac{1}{2}\rho\Omega^2R^2$. This kinetic energy is converted into the internal (thermal) energy of the gas. This means that the second term in (10.7.11) describes the *viscous heating* of the gas in the disk. Only this term corresponds to *true* dissipation.

Since the ring under consideration (radius R, thickness ΔR and unit height $\Delta Z = 1$) has two sides, each with an area $2\pi R\,\Delta R$, the amount of viscous dissipation per unit disk area is given by

$$\boxed{\mathcal{D}(R) = \tfrac{1}{2}\Sigma\nu\left(R\,\frac{\mathrm{d}\Omega}{\mathrm{d}R}\right)^2\,.} \tag{10.7.13}$$

Note that this dissipation term vanishes if the disk rotates as a solid body, so that $\mathrm{d}\Omega/\mathrm{d}R = 0$. In that case there is no slippage between adjoining rings of material, and there can be no heating due to friction. Exactly the same argument was used in Chapter 9 to derive the form of the viscous stress tensor in terms of the components of the velocity gradient tensor.

An alternative derivation of the viscous energy flux

In our discussion of the conservative form of the fluid equations in Chapter 9 we already encountered a viscous distribution to the energy flux, equal to $\boldsymbol{T}^{\rm visc} \cdot \boldsymbol{V}$, see Eqn. (9.7.8). This is exactly what we have found here. In this case, the largest contribution to $\boldsymbol{T}^{\rm visc} \cdot \boldsymbol{V}$ is due to the rotational velocity $V_\theta = \Omega R$, and the shear stress $T^{\rm visc}_{R\theta}$, which is due to differential rotation. The dominant contribution to the radial energy flux therefore equals

$$\left(\boldsymbol{T}^{\rm visc} \cdot \boldsymbol{V}\right)_R \approx T^{\rm visc}_{R\theta} V_\theta = -\rho\nu\Omega R^2 \left(\frac{{\rm d}\Omega}{{\rm d}R}\right) . \tag{10.7.14}$$

Here I have used (10.5.29). Integrating this quantity over the disk thickness immediately yields expression (10.7.12) for $\boldsymbol{\mathcal{F}}$:

$$\boldsymbol{\mathcal{F}} = \left(\int_{-\infty}^{+\infty} {\rm d}Z \, T^{\rm visc}_{R\theta} V_\theta\right) \hat{\boldsymbol{e}}_R \approx -\Sigma\nu\Omega R^2 \left(\frac{{\rm d}\Omega}{{\rm d}R}\right) \hat{\boldsymbol{e}}_R . \tag{10.7.15}$$

Here I have used that Ω does not depend on Z in a thin disk.

10.7.1 The effective temperature of a thin disk

In a steady state, the heat added to the gas in a thin disk by viscous friction must be radiated away. Only in that case can the temperature of the disk material remain constant in time. If the disk radiates as a black body, the amount of radiation emitted per unit disk area equals

$$\mathcal{L}(R) = \sigma_{\rm sb} T_{\rm eff}^4 \ . \tag{10.7.16}$$

Here $T_{\rm eff}$ is the effective temperature, and $\sigma_{\rm sb} = 5.6705 \times 10^{-5}\ {\rm erg}/({\rm s\,cm^2\,deg^4})$ is the Stefan-Boltzmann constant.

In a steady state, where heating due to friction is balanced by radiation losses so that $\mathcal{L}(R) = \mathcal{D}(R) = \frac{1}{2}\Sigma\nu\,(R{\rm d}\Omega/{\rm d}R)^2$, one has

$$\sigma_{\rm sb} T_{\rm eff}^4 = \tfrac{1}{2}\Sigma\nu \left(R\,\frac{{\rm d}\Omega}{{\rm d}R} \right)^2 \ . \tag{10.7.17}$$

For a thin Keplerian disk, where relation (10.6.8) is satisfied and where the shear in the azimuthal flow follows from

$$-R\,\frac{{\rm d}\Omega}{{\rm d}R} = \tfrac{3}{2}\,\Omega_{\rm K}(R) \ , \tag{10.7.18}$$

this balance corresponds to

$$\sigma_{\rm sb} T_{\rm eff}^4 = \frac{3GM_*\dot{M}}{8\pi R^3}\ \left[1 - \left(\frac{R_{\rm i}}{R} \right)^{1/2} \right] \ . \tag{10.7.19}$$

Well outside the inner radius ($R \gg R_{\rm i}$) this gives a simple relation for the effective temperature as a function of radius:

$$T_{\rm eff}(R) = \left(\frac{3GM_*\dot{M}}{8\pi\sigma_{\rm sb}\,R^3} \right)^{1/4} \ . \tag{10.7.20}$$

This temperature-radius relation can be written as

$$T_{\rm eff}(R) = T_{\rm d}\ \left(\frac{R}{R_*} \right)^{-3/4} \ . \tag{10.7.21}$$

The characteristic disk temperature $T_{\rm d}$ in this expression is defined as:

$$T_{\rm d} \equiv \left(\frac{3GM_* \dot{M}}{8\pi\sigma_{\rm sb}\, {R_*}^3} \right)^{1/4} \quad . \tag{10.7.22}$$

The temperature $T_{\rm eff}$ is the black body temperature of the radiation emitted by the disk. The typical value of $T_{\rm eff}$ is set, through $T_{\rm d}$, by the typical global parameters of the accretion process: the mass M_* and radius R_* of the compact object and the mass accretion rate $\dot{M}$, and by the radius R.

This effective temperature is a reasonable estimate of the temperature of the visible 'photosphere' of the disk: the thin layer on top of the disk from where all visible radiation originates. However, in practice an accretion disk behaves in many ways that are similar to the behaviour of a star: the emitted radiation does not have a pure black body spectrum. As happens to be the case with a star, the disk spectrum shows absorption and emission lines due to atomic processes that occur in the disk's photosphere.

The table below gives typical values for the temperature $T_{\rm d}$ for observed sources powered by accretion.

Typical temperature in an inner accretion disk

Object	**Mass** ($M_\odot$)	**Radius** R_* (m)	$\dot{M}$ ($M_\odot$/yr)	$T_{\rm d}$ (K)
White Dwarf	≤ 1.4	$\sim 10^7$	$10^{-10} - 10^{-8}$	$10^{4.5} - 10^5$
Neutron Star	~ 1.4	$\sim 10^4$	10^{-8}	2×10^7
Stellar Black Hole	5	5×10^3	10^{-8}	10^8
AGN Black Hole	10^8	3×10^{11}	~ 1	4×10^5

If one relates the typical photon energy ϵ to the effective temperature[10] by $\epsilon = h\nu \approx k_{\rm b}T_{\rm eff}$, then this table shows that the accretion disks associated with accreting white dwarfs and AGN Black holes radiate mostly in the optical/UV (photon energy $\sim 3 - 10$ eV), whereas the disks surrounding accreting neutron stars and stellar-mass black holes radiate mostly in X-rays (photon energy ~ 10 keV).

The temperature $T_{\rm d}$ has a simple physical interpretation. Let us assume that all the mechanical luminosity of an accretion flow hitting the stellar surface at a velocity approaching the free-fall velocity,

$$L_{\rm accr} = \frac{G\dot{M}M_*}{R_*} \, , \tag{10.7.23}$$

is radiated away at the stellar surface. If the material emits this energy as black-body radiation with temperature T, over an area comparable to the surface area of the compact object, one must have:

$$\frac{G\dot{M}M_*}{R_*} \sim 4\pi \, {R_*}^2 \, \sigma_{\rm sb} T^4 \, . \tag{10.7.24}$$

Solving for the temperature one finds:

$$T = \left(\frac{G\dot{M}M_*}{4\pi\sigma_{\rm sb} \, {R_*}^3} \right)^{1/4} \approx 0.9 T_{\rm d} \, . \tag{10.7.25}$$

This shows that the temperature of the inner disk will be close to this characteristic temperature, provided that the inner disk extends almost to the stellar surface so that $R_{\rm i} \approx R_*$.

[10] A good rule of thumb: the temperature corresponding to a thermal energy of 1 eV is 10^4 K.

10.7.2 The central temperature of the disk material

The effective black body temperature of the disk can be related to the typical temperature of the material in the disk mid-plane, provided one knows the details of the radiation transport in the disk. In this sense an accretion disk is like a flat star: in a star, the energy liberated by nuclear fusion 'percolates' to the stellar surface in the form of radiation. This takes a long time since the star is opaque, and the photons are scattered many times, performing a 'random walk' inside the star. As a result, the temperature in the core of a star is much higher than the surface temperature. The temperature difference drives the energy flux carried by photons. This is illustrated in the Figure below.

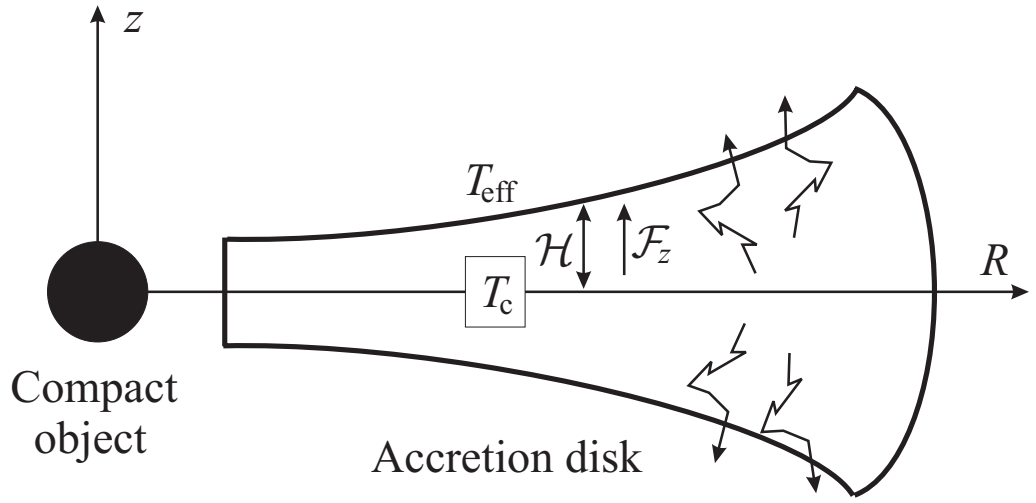

Figure 10.7: *The geometry of a geometically thin ($\mathcal{H} \ll R$) accretion disk around a compact object. Photons diffuse out of the disk, mainly in the vertical direction. This leads to an energy flux $\mathcal{F}_z$, which is driven by the temperature difference between the hot disk interior, with temperature $T_{\rm c}$ in the disk mid-plane, and the (cooler) disc surface that has a temperature $T_{\rm eff}$.*

If an accretion disk is also opaque (*optically* thick) so that

$$\tau_{\rm D} \sim \kappa\rho H \sim \kappa\Sigma \gg 1 \ , \tag{10.7.26}$$

something similar happens. Here the energy is generated by friction rather than fusion, but the radiation transport can still be described as photon diffusion. In this case the energy is transported mainly in the vertical direction as $H \ll R$. This can be seen as follows: the radiative energy flux is given in Eqn. (9.4.6):

$$\boldsymbol{F}_{\rm rad} = -\frac{c a_{\rm r}}{3\kappa\rho}\,\boldsymbol{\nabla}\left(T^4\right) \ . \tag{10.7.27}$$

As an order of magnitude one has

$$\frac{\partial T^4}{\partial R} \sim \frac{T^4}{R} \ , \ \frac{\partial T^4}{\partial Z} \sim \frac{T^4}{H} \ . \tag{10.7.28}$$

This implies that the components of the radiative flux satisfy

$$\frac{(F_{\rm rad})_R}{(F_{\rm rad})_Z} \sim \frac{H}{R} \ll 1 \ . \tag{10.7.29}$$

In view of this estimate, we will neglect the radial component of the flux in what follows.

The vertical radiative flux is

$$F_{\rm rad} = -\frac{ca_{\rm r}}{3\kappa\rho} \left(\frac{\partial T^4}{\partial Z}\right) \ . \tag{10.7.30}$$

If the central temperature in the disk mid-plane equals $T_{\rm c}$, the radiation flux in the vertical direction near the disk surface can be estimated as

$$F_{\rm rad}(z=H) \approx \frac{ca_{\rm r}}{3\kappa\rho H} \left(T_{\rm c}^4 - T_{\rm eff}^4\right) \ , \tag{10.7.31}$$

where I have put $\partial T^4/\partial Z \approx -\left(T_{\rm c}^4 - T_{\rm eff}^4\right)/H$.

The energy flux $F_{\rm rad}(z \approx H)$ coming from the disk interior must equal the black-body energy flux $\sigma_{\rm sb}T_{\rm eff}^4$ that is radiated away per unit area at the disk surface. This requirement yields a relation between the central temperature $T_{\rm c}$ and the effective surface temperature $T_{\rm eff}$. Using $a_{\rm r} = 4\sigma_{\rm sb}/c$ one finds that the effective temperature $T_{\rm eff}$ of the disk surface must satisfy

$$\sigma_{\rm sb}T_{\rm eff}^4 \approx \frac{4\sigma_{\rm sb}}{3\kappa\rho H} \left(T_{\rm c}^4 - T_{\rm eff}^4\right) \ . \tag{10.7.32}$$

This equality allows us to calculate the relation between the central temperature and the surface temperature, which can in principle be determined from observations.

The optical depth from mid-plane to disk edge is of order $\tau_{\rm D} \sim \kappa\rho H$, so one finds:

$$\boxed{T_{\rm c} \approx \left(1 + \frac{3\tau_{\rm D}}{4}\right)^{1/4} T_{\rm eff}\ .} \tag{10.7.33}$$

This is the central temperature that is required to drive the vertical radiation flux through the disk, which is needed to remove the energy that is generated by viscous dissipation.

Expression (10.7.31) for the radiation flux has a simple interpretation that shows it's roots in diffusion theory. The mean-free path ℓ of a photon in the disk, and the associated photon diffusion coefficient $\mathcal{D}$ are given by:

$$\ell = \frac{1}{\kappa\rho} \quad , \quad \mathcal{D}_{\rm ph} = \frac{c\ell}{3} = \frac{c}{3\kappa\rho}\ . \tag{10.7.34}$$

According to diffusion theory, a photon originating in the mid-plane $Z = 0$ travels a net distance $d \sim \sqrt{2\mathcal{D}_{\rm ph} t}$ in a time t. Therefore it takes a time

$$t_{\rm esc} \sim \frac{H^2}{2\mathcal{D}_{\rm ph}} \sim \frac{3\kappa\rho H^2}{2c} \tag{10.7.35}$$

for a photon from the mid-plane to reach the edge of the disk, where it can escape freely. The quantity $t_{\rm esc}$ is the typical photon escape time. The energy density of radiation in thermal equilibrium with the surrounding gas is $U_{\rm rad} = a_{\rm r} T^4$, so the typical rate at which energy leaks away per unit disk volume due to photon escape is

$$\left(\frac{\partial U_{\rm rad}}{\partial t}\right)_{\rm esc} \approx \frac{U_{\rm rad}}{t_{\rm esc}} = \frac{2ca_{\rm r}T^4}{3\kappa\rho H^2}\ . \tag{10.7.36}$$

The total radiative energy flux, the amount of energy radiated away per unit area per second, at the top (or bottom) of the disk is carried by the photons that escape from a column with height $\sim H$. It must therefore be roughly equal to

$$F_{\rm rad} \approx H \times \frac{U_{\rm rad}}{t_{\rm esc}} = \frac{2ca_{\rm r}T^4}{3\kappa\rho H}\ . \tag{10.7.37}$$

Apart from a factor two, this estimate is the same as the expression in Eqn. (10.7.31) in the case where $T_{\rm c}^4 \gg T_{\rm eff}^4$, which occurs when the disk is *optically thick* so that $\tau_{\rm D} \sim \mathcal{H}/\ell \gg 1$.

10.7.3 The luminosity of an accretion disk

The total amount of energy dissipated (and then radiated away) by an accretion disk follows from an integration of the disipation per unit area across the whole disk surface, all the way from the inner radius $R_{\rm i}$ to the outer disk radius $R_{\rm o}$.

This gives the *disk luminosity* L, remembering that the accretion disk has two sides:

$$L_{\rm disk} \equiv 2 \times \int_{R_{\rm i}}^{R_{\rm o}} {\rm d}R\, 2\pi R\, D(R) = \int_{R_{\rm i}}^{R_{\rm o}} {\rm d}R\, 4\pi R\, \sigma_{\rm sb} T_{\rm eff}^4(R)\ . \tag{10.7.38}$$

Of course, typically one can only observe the radiation that comes from one side of the disk. For a thin Keplerian disk that satisfies relation (10.7.21) this integral can be performed simply:

$$L_{\rm disk} = \frac{GM_*\dot{M}}{2}\left(\frac{1}{R_{\rm i}} - \frac{1}{R_{\rm o}}\right)\ . \tag{10.7.39}$$

For a sufficientyly large disk, with $R_{\rm o} \gg R_{\rm i}$, this can be approximated by:

$$\boxed{L_{\rm disk} \approx \frac{GM_*\dot{M}}{2R_{\rm i}}\ .} \tag{10.7.40}$$

The typical luminosity associated with a constant mass flow $\dot{M}$ from infinity to some radius $R_{\rm i}$ is (see Chapter 4, Eqn. 4.3.7)

$$L = \frac{1}{2}\,\dot{M} V_{\rm ff}^2 = \frac{GM_*\dot{M}}{R_{\rm i}}\ . \tag{10.7.41}$$

This means that a thin Keplerian disk, extending all the way to the stellar surface with radius $R_{\rm i} \approx R_*$, radiates about half the maximum possible luminosity associated with the accretion process. The other half of the energy is radiated when the accreted material hits the surface of the star, probably in a hot, thin boundary layer that separates the stellar surface from the accretion disk. Of course, such a boundary layer is will not occur when the accretion disk surrounds a black hole: there is no solid surface in that case, and the remaining half of the available energy is swallowed by the black hole.

The factor $1/2$ that appears in (10.7.40) can be explained in a simple fashion. The specific energy $\mathcal{E}$ of the material in a Keplerian disk at a radial distance R consists almost entirely of the gravitational binding energy, and the kinetic energy due to disk rotation:

$$\mathcal{E} = \tfrac{1}{2}V_\theta^2 - \frac{GM_*}{R} = -\frac{GM_*}{2R} \ . \tag{10.7.42}$$

The second equality follows directly from centrifugal balance (10.4.17) in the disk. This means that, as material migrates from the outer disk (at a radius $R_{\rm o}$) to the inner edge of the disk (at a radius $R_{\rm i}$), the specific energy of the material has changed by an amount:

$$\Delta\mathcal{E} = \frac{GM_*}{2}\left[\frac{1}{R_{\rm i}} - \frac{1}{R_{\rm o}}\right] \tag{10.7.43}$$

For a sufficiently large disk, where $R_{\rm o} \gg R_{\rm i}$, one finds

$$\Delta\mathcal{E} \approx \frac{GM_*}{2R_{\rm i}} \ . \tag{10.7.44}$$

In order to remove it from the disk (so that a steady flow can be maintained) this energy must have been be radiated away. Given a constant mass flow $\dot{M}$ through the disk, the total amount of energy radiated away per second by the disk must equal

$$L_{\rm disk} = \dot{M}\,\Delta\mathcal{E} = \frac{GM_*\dot{M}}{2R_{\rm i}} \ . \tag{10.7.45}$$

This simple estimate agrees with our earlier result, Eqn. (10.7.40).

10.8 Alpha-disks

In order to actually solve the equations for a steady thin accretion disk one must give a prescription which links the specific viscosity ν to the local conditions in the disk, e.g.

$$\nu = \nu(\Sigma\ ,\ T)\ , \tag{10.8.1}$$

the viscosity as a function of the disk temperature and column density. We have already established that the viscosity and the inflow velocity are related. From Eqn. (10.6.8)

$$\nu\Sigma = \frac{\dot{M}}{3\pi}\left[1 - \left(\frac{R_{\rm i}}{R}\right)^{1/2}\right] \tag{10.8.2}$$

together with

$$\dot{M} = 2\pi R\,\Sigma\,V \tag{10.8.3}$$

one finds an estimate for the radial (inflow-)velocity for a radius $R \gg R_{\rm i}$

$$V(R) \approx \frac{3\nu}{2R}\ . \tag{10.8.4}$$

This means that the typical residence time of a parcel of disk material at radius R is

$$t_{\rm res} \equiv R/V(R) \approx R^2/\nu\ , \tag{10.8.5}$$

up to a factor of order unity. This should be compared with the *free-fall time* at the same radius, the time the parcel would take to reach the central object from radius R if it was freely falling under the influence of gravity. The free-fall velocity at some radius R is equal to

$$V_{\rm ff} = \sqrt{\frac{GM_*}{R}}\ . \tag{10.8.6}$$

The free-fall time is of order

$$t_{\rm ff} = \frac{R}{V_{\rm ff}} \approx \left(\frac{R^3}{GM_*}\right)^{1/2} = \frac{1}{\Omega_{\rm K}(R)} \ . \tag{10.8.7}$$

The ratio of the residence time $t_{\rm res}$ and the free-fall time $t_{\rm ff}$ is a dimensionless number equal to

$$\frac{t_{\rm res}}{t_{\rm ff}} = \frac{\Omega_{\rm K}(R) R^2}{\nu} = \frac{R V_\theta}{\nu} \equiv {\rm Re} \ . \tag{10.8.8}$$

The dimensionless number ${\rm Re}$ is in fact the *Reynolds number*, which was already defined in the previous Chapter (Eqn. 9.5.27) as a number that quantifies the importance of viscous forces in a flow:

$$\text{Reynolds number } {\rm Re} = \frac{\text{typical size} \times \text{typical velocity}}{\text{typical viscosity}} \ . \tag{10.8.9}$$

A small viscosity corresponds to little dissipation and a **large** Reynolds number. In the case of the accretion disk, the typical scale is the radius R, and the typical velocity is the azimuthal velocity V_θ which is assumed to be much larger than the radial velocity $V(R)$. Mass spends a long time in the disk when the Reynolds number is large. Another way of putting this is by comparing the inflow speed $V(R)$ with the rotation speed $V_\theta = \Omega_{\rm K} R$:

$$\frac{V(R)}{\Omega_{\rm K} R} \sim \frac{\nu}{\Omega_{\rm K} R^2} \sim \frac{1}{\rm Re} \ . \tag{10.8.10}$$

At large Reynolds numbers, the matter accretes in a very slow trickle.

In an ordinary fluid, the viscosity is the result of the collisions between molecules or, in an ionized gas, between charged nuclei (Coulomb collisions). One then speaks of a *molecular* Reynolds number. For a typical accretion disk in an X-ray-binary, the value of the *molecular* Reynolds number due to Coulomb collisions between charged particles in the ionized gas is very large:

$${\rm Re}_{\rm th} \sim 10^{14}\, n_{15}\, T_4^{-5/2}\, R_{10}^{1/2}\, (M_*/M_\odot)^{1/2} \ . \tag{10.8.11}$$

Here $n_{15} = n/(10^{15}\ {\rm cm}^{-3})$, $R_{10} = R/(10^{10}\ {\rm cm})$ and $T_4 = T/(10^4\ {\rm K})$. An accretion flow that would be governed by such an extremely large value of the Reynolds number would lead to an extremely long residence time for the accreting mass in the disk.

In fact, the residence time would exceed the age of the Universe ($\simeq 1.4 \times 10^{10}$ years) in most accreting binaries! The free-fall time on the other hand is similar to the orbital period of the binary, which in accreting binaries ranges from $\sim$ hours for close binaries to weeks.

This estimate alone is enough to see immediately that the ordinary (molecular) viscosity can not be responsible for the mass transport and angular momentum loss in these objects. The effective Reynolds number in accretion disks must be many orders of magnitude smaller than predicted by ordinary collision theory, and the viscosity must be correspondingly larger.

10.8.1 Turbulent viscosity and the alpha-parameter

Without thinking, any coffee drinker using milk will use a spoon to stirr his cup of coffee. This habit is based on a firm physical basis: the stirring introduces turbulent (random) velocities in the coffee. This turbulence somehow allows a fast mixing of milk and coffee. If one would be able to introduce a small droplet of milk into the coffee without stirring it, ordinary (molecular) diffusion would be responsible for spreading the milk molecules through the coffee, an agonizingly slow process that may take hours.

This everyday experience is an example of what is known as *turbulent mixing* or, somewhat misleadingly, as *turbulent diffusion*. In turbulent diffusion, large-scale fluid motions rather than thermal motions are responsible for spreading some quantity through the fluid. The actual process is quite complicated, and rather difficult to describe.

The viscosity ν that governs the transport of angular momentum in an accretion disk has the form

$$\nu = \frac{\sigma \ell}{3} = \frac{\text{random velocity} \times \text{mean free path}}{3} \ . \tag{10.8.12}$$

From this relationship one can make an educated guess about the value of the *turbulent viscosity* that is associated with random fluid motions.

Let us assume that the turbulence consists of a collection of short-lived and randomly oriented 'swirls' or 'eddies' with a typical size λ and a typical velocity v_λ. If the turbulence is governed only by *internal* parameters (and not by external parameters such as the rotation rate, or the thickness of the disk) the typical life time of an eddy is $\tau_\lambda = \lambda / v_\lambda$. A turbulent eddie can only travel a distance $\sim \lambda$ before it dissolves. This suggests that the turbulent viscosity must have a typical value

$$\nu_{\rm t} \sim \frac{v_\lambda \, \lambda}{3} \ . \tag{10.8.13}$$

Experiments in turbulent fluids confirm the validity of this rough relationship.

This turbulent viscosity can be many orders-of-magnitude larger than the molecular viscosity, reducing the effective Reynolds number and shortening the residence time considerably.

If one applies the above estimate for the turbulent viscosity to a geometrically thin accretion disk, there are obvious limits to the value that $\nu_{\rm t}$ can take:

- The size of turbulent eddies can not be larger than the thickness of the disk:

$$\lambda \leq H \ . \tag{10.8.14}$$

  Larger structures in the disk would have to be highly flattened, and would not be turbulence in the above sense as their properties are influenced by the structure of the disk.

- The velocity of the turbulent motions most be less than the local sound speed [11]:

$$v_\lambda \leq c_{\rm s} \ . \tag{10.8.15}$$

  If this is not the case, so that the turbulence is 'supersonic', shocks would form which rapidly. Dissipation in these shocks would raise the temperature of the disk material, thereby raising the sound speed until the above inequality is satisfied.

On the basis of such considerations, the Russian astrophysicists Shakura and Sunyaev[12] introduced a simple parametrization for the effective (turbulent) viscosity in accretion disks:

$$\boxed{\nu_{\rm eff} = \alpha c_{\rm s} H \quad \text{with } \alpha \lesssim 1 \ .} \tag{10.8.16}$$

The dimensionless parameter α contains all of our ignorance about the precise physics of the processes responsible for this effective value of the viscosity. This *ansatz* has the virtue of being dimensionally correct, and of yielding a simple relation between the value of the viscosity and the local conditions in the disk. In the simplest 'alpha-disk' models one assumes that the value of the parameter α is globally constant so that it does not depend on the radius R. The principles behind the Shakura-Sunyaev model are illustrated below.

[11] In this section I neglect the small difference between the isothermal sound speed $s = \sqrt{P/\rho}$ and the adiabatic sound speed $c_{\rm s} = \sqrt{\gamma P/\rho}$.

[12] N.I. Shakura & R.A. Sunyaev, 1973: *Mon. Not. R. astr. Soc.* **24**, 337.

The effective Reynolds number for this viscosity prescription follows from the relation

$$H \sim c_{\rm s}/\Omega_{\rm K} \ , \tag{10.8.17}$$

which is valid in a thin disk. One finds:

$$\mathrm{Re}_{\rm eff} = \frac{\Omega_{\rm K} R^2}{\nu_{\rm eff}} \approx \frac{1}{\alpha} \left(\frac{R}{H}\right)^2 \ . \tag{10.8.18}$$

With typical values (valid for for thin disks) of $H \sim 0.1 - 0.01R$ and $\alpha \sim 0.1 \ - \ 1$, the effective Reynolds number lies in the range $\mathrm{Re}_{\rm eff} \sim 10^2 - 10^5$. This is considerably smaller than the molecular value (10.8.11), by some 9 to 11 orders of magnitude.

The height-integrated shear stress that is associated with this effective viscosity can be written for a Keplerian disk as

$$\begin{aligned} \int \mathrm{d}Z \, T^{\rm visc}_{R\theta} &= -\Sigma \nu_{\rm eff} \left(R \, \frac{\mathrm{d}\Omega}{\mathrm{d}R} \right) = \tfrac{3}{2} \, \Sigma \nu_{\rm eff} \Omega_{\rm K} \\ &= \tfrac{3}{2} \, \alpha P H \ . \end{aligned} \tag{10.8.19}$$

Here I have used $\Sigma \sim \rho H$ and $\Omega \approx \Omega_{\rm K} \propto R^{-3/2}$, together with the fact that you can write

$$\nu_{\rm eff} = \alpha c_{\rm s} H = \alpha \, \frac{c_{\rm s}^2}{\Omega_{\rm K}} \sim \frac{\alpha P}{\rho \Omega_{\rm K}} \ . \tag{10.8.20}$$

The theory of thin accretion disks has been reviewed by a number of authors[13].

The simple picture behind the alpha-disk model is very attractive. However, the consensus is that simple *fluid turbulence* is not easy to generate in an Keplerian thin accretion disk. For turbulence in Nature one needs either an obstacle in the flow, which is not available in this case, or a *fluid instability*. An instability arises when the equilibrium flow under consideration is unstable. The concept of stability/instability was briefly discussed in Chapter 6, and will be explored further in the next Chapter.

[13] J. Frank, A. King & D. Raine, 1992: *Accretion Power in Astrophysics* (Second Edition), Cambridge University Press, Cambridge, U.K.;
J.C.B. Papaloizou & D.N.C. Lin: 1995, *Ann. Rev. Astron. Astrophys.* **33**, 505;
D.N.C. Lin & J.C.B. Papaloizou: 1996, *Ann. Rev. Astron. Astrophys.* **34**, 703.

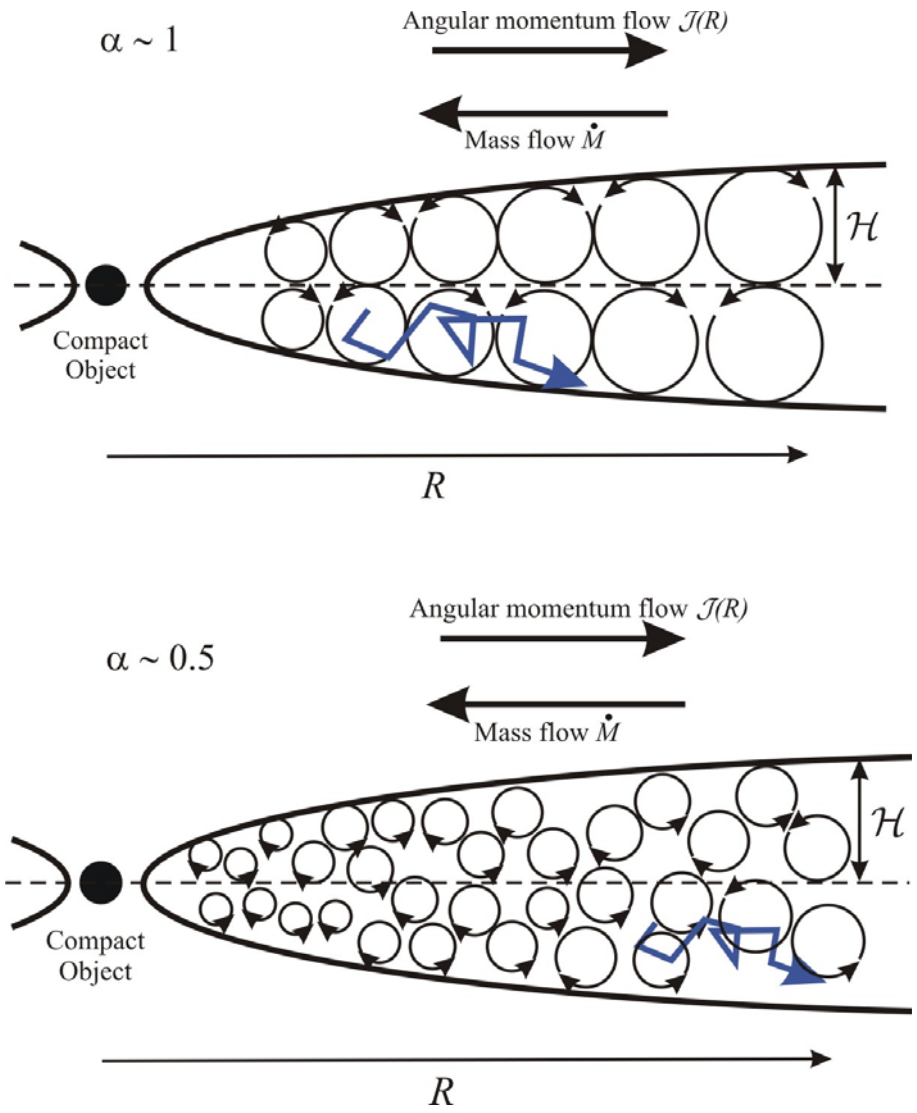

Figure 10.8: *An accretion disk with $\alpha \sim 1$ (top) and $\alpha \sim 0.5$(bottom). The disk is filled with turbulent (convective) eddies, which transport material and angular momentum in the radial (and vertical) direction. A typical fluid element will execute a random walk in the disk with a stepsize that is comparable to the eddy size (the blue trajectories), simply because the eddies are short-lived, and are destroyed and re-formed continuously.* (Adapted from **Los Alamos Science**, Spring 1986)

In a thin Keplerian disk the dominant flow is the rotation, $V_\theta = \Omega R = \sqrt{GM_*/R}$. Such a flow can be shown to be *stable*: it does not spontaneously break up into random small-scale motions. One can show that a differentially rotating flow is stable if the so-called *Rayleigh Criterion* is satisfied[14]:

$$\frac{\mathrm{d}\lambda^2}{\mathrm{d}R} = \frac{\mathrm{d}}{\mathrm{d}R}\left(\Omega R^2\right)^2 > 0\ , \tag{10.8.21}$$

and is *unstable* if the opposite is true:

$$\frac{\mathrm{d}}{\mathrm{d}R}\left(\Omega R^2\right)^2 < 0\ . \tag{10.8.22}$$

Here (as before) λ is the specific angular momentum of the flow. In a Keplerian disk $\lambda^2 = GM_*R$ increases with radius, and therefore the disk is hydrodynamically stable.

The Rayleigh criterion is valid for *small* perturbations: it is a criterion for the *linear* stability of the flow. For many years one has speculated that Keplerian disks are *non-linearly unstable*, i.e. for perturbations with a finite amplitude the flow would still somehow generate turbulence. Numerical simulations seem to indicate that this is not the case.

The present-day consensus is that something extra is needed: in this case the presence of a magnetic field. The hot matter in an accretion disk is an ionized gas (*plasma*), and conducts electricity. In that case magnetic fields can influence the flow and one enters the realm of *magnetohydrodynamics*. In 1992 two American astrophysicists, Steven Balbus and John Hawley, rediscovered a magnetohydrodynamic instability, which had already been described more than thirty years earlier by Chandrasekhar (in 1961) and by Velikov (in 1959) and which apparently had been forgotten. This instability arises when there is a weak magnetic field in the vertical (Z-)direction, and occurs when the angular frequency of the rotation satisfies

$$\frac{\mathrm{d}\Omega^2}{\mathrm{d}R} < 0\ . \tag{10.8.23}$$

It is easily checked that a Keplerian accretion disk indeed satisfies this criterion, in contrast to the purely hydrodynamic criterion (10.8.22) for instability. Therefore, the turbulence in accretion disks is probably some form of magnetohydrodynamic turbulence.

[14]See for instance: S. Chandrasekhar, *Hydrodynamic and Hydromagnetic Stability*, Ch. VII, Dover Publications, 1970

Chapter 11

Fluid Instabilities

In Chapter 6.8 we discussed the *Jeans Instability*, where the amplitude of long-wavelength density perturbations in a self-gravitating fluid grows exponentially in time. This is an example of a fluid instability that occurs when the equilibrium state is unstable. There are a number of such unstable situations in fluid mechanics which have important applications in astrophysics. These include the *Kelvin-Helmholz instability* which arises at contact discontinuities with a different flow speed on either side, the *Rayleigh-Taylor instability* that arises in a stratified fluid in a gravitational field, and *thermal instabilities* that arise as a result of runaway heating or cooling in a dilute gas.

There are different ways of finding out if a flow or a static fluid equilibrium is unstable:

- In **Perturbation Theory** one introduces small perturbations, and then solves the linearized equation of motion for the fluid using the plane-wave assumption. This is exactly the same method as was employed when we calculated the properties of linear waves in a fluid. Assuming that fluid elements are displaced according to

$$\boldsymbol{\xi}(\boldsymbol{x}\ ,\ t) = \boldsymbol{a}\exp\left(i\boldsymbol{k}\cdot\boldsymbol{x} - i\omega t\right) + cc.\ ,$$

  an unstable situation arises when the solution condition for the system yields one or more solutions with an imaginary (or complex) frequency such that

$$\mathrm{Im}(\omega) \equiv \sigma > 0\ .$$

  In that case the linear perturbations grow as

$$|\boldsymbol{\xi}| \propto e^{\sigma t}\ .$$

  The quantity σ is usually called the *growth rate*. Ultimately, this exponential growth of the perturbation amplitude will lead to a break-down of the linear approximation.

- In the **Energy Principle.** one defines some measure of the potential energy of the fluid that is associated with small perturbations so that, due to the perturbations, the total energy W of the fluid changes according to

$$W \implies W + \delta W \ .$$

An instability will occur if

$$\delta W < 0 \ ,$$

i.e. when the presence of the perturbations *lowers* the energy of the fluid. In practice one has to find an expression for δW, which will generally be a quadratic function of the amplitude $\boldsymbol{\xi}$ of the perturbations. The advantage of this method is that it can quickly show under what conditions an instability is present. A disadvantage of this approach is that it generally does not immediately provide the value of the growth rate σ. In order to calculate the growth rate one must usually resort to the first method.

An excellent introduction to the theory of fluid instabilities is the book by Chandrasekhar, a classic in the field[1]. In this Chapter I will treat some of the more important fluid instabilities.

[1] S. Chandrasekhar, 1961: *Hydrodynamic and Hydromagnetic Stability*, Oxford University Press, available in a cheap edition from Dover Publications (1981), ISBN 0-486-64071-X. A small disadvantage of this book is that the notation is rather outdated compared with modern literature on the subject, and therefore not very transparent and cumbersome

11.1 The Rayleigh-Taylor Instability

In Chapter 6.10 we considered the propagation of waves in an atomosphere which is gravitationally stratified in the z-direction. There it was found that such an atmosphere is unstable against convection if the so-called Brunt-Väisälä frequency $N_{\rm BV}$ satisfies

$$N_{\rm BV}^2 = -\frac{1}{\gamma\rho}\left(\frac{{\rm d}P}{{\rm d}z}\right)\,\left(\frac{\rm d}{{\rm d}z}\left\{\ln\left[P\rho^{-\gamma}\,\right]\right\}\right) < 0\ .$$

Here we consider a more simple situation: two stationary, uniform fluids supporting each other in a constant gravitational field with gravitational acceleration

$$\boldsymbol{g} = -g\,\hat{\boldsymbol{e}}_z\ . \tag{11.1.1}$$

The density of the fluid changes abruptly across an interface, an example of a contact discontinuity, which is located at $z = 0$ so that

$$\rho(z) = \begin{cases} \rho_1 & \text{for } z < 0; \\ \\ \rho_2 & \text{for } z > 0. \end{cases} \tag{11.1.2}$$

The pressure must be continuous across the interface, i.e.

$$P(z = 0^+) = P(z = 0^-) = P_0\ . \tag{11.1.3}$$

Here I have introduced the notation 0^+ (0^-) for a position infinitesimally above (below) the plane $z = 0$. Assuming for simplicity that the density is piecewise uniform, the equation of hydrostatic equilibrium reads

$$\frac{{\rm d}P}{{\rm d}z} = -\rho\,g\ , \tag{11.1.4}$$

which is solved by

$$P(z) = \begin{cases} P_0 - \rho_1\,gz & \text{for } z < 0; \\ \\ P_0 - \rho_2\,gz & \text{for } z > 0. \end{cases} \tag{11.1.5}$$

Because of the density jump at $z = 0$ the density gradient is singular:

$$\frac{\mathrm{d}\rho}{\mathrm{d}z} = (\rho_2 - \rho_1)\ \delta(z)\ . \tag{11.1.6}$$

Here $\delta(z)$ is the *Dirac delta function*, which has the following property for any function $F(z)$:

$$\int_a^b \mathrm{d}z\ F(z)\ \delta(z-\zeta) = \begin{cases} F(\zeta) & \text{if } a < \zeta < b; \\ \\ = 0 & \text{if } \zeta \text{ is not in interval } [a,b]. \end{cases} \tag{11.1.7}$$

We now perturb this equilibrium by displacing fluid elements by an amount $\boldsymbol{\xi}$. The linearized equation of motion reads (see Eqn. 6.10.6)

$$\rho\,\frac{\partial^2\boldsymbol{\xi}}{\partial t^2} = -\boldsymbol{\nabla}\delta P + \delta\rho\,\boldsymbol{g}\ . \tag{11.1.8}$$

In order to keep the mathematics simple we limit the discussion to incompressible perturbations, which satisfy

$$\boldsymbol{\nabla}\cdot\boldsymbol{\xi} = 0\ . \tag{11.1.9}$$

This assumption eliminates the effects of sound waves from the discussion, and is a reasonable approximation if $|\omega| \ll kc_{\rm s}$. The general relations for the density- and pressure perturbations then reduce to

$$\delta\rho = -(\boldsymbol{\xi}\cdot\boldsymbol{\nabla})\rho \quad , \quad \delta P = -(\boldsymbol{\xi}\cdot\boldsymbol{\nabla})P\ . \tag{11.1.10}$$

In this case we assumed that the density is piecewise constant for $z > 0$ and $z < 0$, while the pressure satisfies (11.1.4). This implies

$$\delta\rho = (\rho_1 - \rho_2)\ \xi_z\,\delta(z) \quad , \quad \delta P = \rho g\,\xi_z\ . \tag{11.1.11}$$

Substituting the expression for $\delta\rho$ into the equation of motion one finds:

$$\rho\,\frac{\partial^2\boldsymbol{\xi}}{\partial t^2} = -\boldsymbol{\nabla}\delta P - g\ (\rho_1 - \rho_2)\ \xi_z\,\delta(z)\hat{\boldsymbol{e}}_z\ . \tag{11.1.12}$$

First consider the region away from the discontinuity so that $z \neq 0$. In that case the gravity term $\propto g\,(\rho_1 - \rho_2)$ is absent, and the equation of motion reduces to

$$\rho\,\frac{\partial^2 \boldsymbol{\xi}}{\partial t^2} = -\boldsymbol{\nabla}\delta P \qquad (\text{for } z \neq 0)\ .$$

Taking the divergence of this equation, using the incompressibility condition, one finds:

$$\rho\,\frac{\partial^2 (\boldsymbol{\nabla}\cdot\boldsymbol{\xi})}{\partial t^2} = 0 = -\boldsymbol{\nabla}^2\delta P\ ,$$

which implies that the pressure perturbation δP satisfy the harmonic equation

$$\boxed{\boldsymbol{\nabla}^2\delta P = 0 \qquad (\text{for } z \neq 0)\ .} \tag{11.1.13}$$

Because of the jump in the density at $z = 0$, the most general wave-like solution that one can find must take the form

$$\delta P = \tilde{P}(z)\,\exp\left(ik_x x + ik_y y - i\omega t\right) + \text{cc.} \tag{11.1.14}$$

Note that the complex amplitude $\tilde{P}$ depends on z! Substituting this into (11.1.13) one finds that $\tilde{P}(z)$ must satisfy

$$\frac{\partial^2 \tilde{P}}{\partial z^2} - \left(k_x^2 + k_y^2\right)\tilde{P} = 0\ . \tag{11.1.15}$$

The only solution which is physically admissible is one where the amplitude of the pressure perturbation decays exponentially with increasing distance from the interface $z = 0$:

$$\tilde{P}(z) = \begin{cases} \tilde{P}_1\,\exp(kz) & \text{for } z < 0; \\ \\ \tilde{P}_2\,\exp(-kz) & \text{for } z > 0. \end{cases} \tag{11.1.16}$$

Here $k \equiv \sqrt{k_x^2 + k_y^2}$ and $\tilde{P}_1$ and $\tilde{P}_2$ are constant pressure amplitudes. Such a solution corresponds to a **surface wave** because of the rapid decay of the pressure perturbations away from the interface.

We must now somehow connect these two solutions for $z > 0$ and $z < 0$ across the boundary at $z = 0$. The displacement ξ_z must be the same on both sides of the discontinuity. If this where not the case, one would draw 'vacuum bubbles' between the two fluids at the interface! Assuming a similar solution for the displacement as already assumed for the pressure perturbation,

$$\boldsymbol{\xi}(\boldsymbol{x}\ ,\ t) = \boldsymbol{a}(z)\exp\left(ik_x x + ik_y y - i\omega t\right) + \text{cc.}\ , \tag{11.1.17}$$

we must therefore demand that the condition

$$a_z(z = 0^+) = a_z(z = 0^-) \equiv a_z(0) \tag{11.1.18}$$

is satisfied. A second boundary condition can be derived by integrating the z-component of the equation of motion (11.1.12) across the boundary from $z = 0^-$ to $z = 0^+$. This leads to the relation

$$\int_{0^-}^{0^+} \mathrm{d}z\ \left(\rho\,\frac{\partial^2\xi_z}{\partial t^2} + \frac{\partial\delta P}{\partial z} + g\,(\rho_1 - \rho_2)\,\delta(z)\,\xi_z\right) = 0\ . \tag{11.1.19}$$

Because of the continuity of ξ_z across the boundary the first term gives a vanishingly small contribution upon integration. The second term can evaluated using partial integration, while the third term follows directly from the properties of the Dirac delta function. One finds that this equation reduces to a relation connecting the pressure perturbations on both sides of the boundary:

$$\delta P(z = 0^+) - \delta P(z = 0^-) + g\,(\rho_1 - \rho_2)\,\xi_z(z = 0) = 0\ . \tag{11.1.20}$$

This implies that the complex pressure amplitude and the displacement amplitude must satisfy[2]

$$\tilde{P}_2 - \tilde{P}_1 + g\,(\rho_1 - \rho_2)\,a_z(0) = 0\ . \tag{11.1.21}$$

[2]This relationship could also have been found directly from the second relation in Eqn. (11.1.11). This yields $\delta P = -\xi_z(\mathrm{d}P/\mathrm{d}z) = \rho g\,\xi_z$. Using Eqns. (11.1.14) and (11.1.17) it is easily seen that this is equivalent with $\tilde{P} = \rho g a_z$, and thus $\tilde{P}_2 - \tilde{P}_1 = (\rho_2 - \rho_1) g a_z(0)$, which is relation (11.1.21).

The value of $\tilde{P}_{1,2}$ can be found from substituting both (11.1.16) and (11.1.17) into the z-component of the equation of motion for $z \neq 0$. This yields

$$\begin{aligned} \rho_1\,\omega^2\,a_z(z) &= k\,\tilde{P}_1\,e^{kz} \qquad \text{for } z<0; \\ \rho_2\,\omega^2\,a_z(z) &= -k\,\tilde{P}_2\,e^{-kz} \qquad \text{for } z>0. \end{aligned} \tag{11.1.22}$$

Solving for $\tilde{P}_{1,2}$ by taking the limit $|z| \to 0$ leads to

$$\tilde{P}_1 = \frac{\rho_1\,\omega^2 a_z(0)}{k} \quad , \quad \tilde{P}_2 = -\frac{\rho_2\,\omega^2 a_z(0)}{k}\,. \tag{11.1.23}$$

Substituting these relations in the condition (11.1.21) for the pressure difference across the boundary one finds:

$$\Big[(\rho_1+\rho_2)\;\omega^2 - kg\,(\rho_1-\rho_2)\Big]\,a_z(0) = 0\,. \tag{11.1.24}$$

Apart from the trivial solution $a_z(0) = 0$, this condition can only be satisfied if the frequency ω of the surface wave satisfies:

$$\boxed{\omega^2 = kg\,\left(\frac{\rho_1-\rho_2}{\rho_1+\rho_2}\right)\,.} \tag{11.1.25}$$

This is the dispersion relation for the Rayleigh-Taylor Instability.

There are now two possibilities: if the lower fluid is heavier so that $\rho_1 > \rho_2$ the right-hand-side of this dispersion relation is positive, and the wave frequency is real. This corresponds to a *stable, propagating* gravity surface wave. If, on the other hand, the lower fluid is lighter than the upper fluid, $\rho_1 < \rho_2$, the right-hand-side of the dispersion relation is negative, which implies that the solution for the wave frequency is purely imaginary:

$$\omega = \pm i\,\sqrt{kg\,\left(\frac{\rho_2-\rho_1}{\rho_1+\rho_2}\right)}\,. \tag{11.1.26}$$

The root with the positive sign corresponds to an *unstable, non-propagating* [3] solution: the Rayleigh-Taylor instability of a heavy fluid supported by a light fluid in a gravitational field. The amplitude of the unstable surface wave grows exponentially as $e^{\sigma t}$, with $\sigma = \mathrm{Im}(\omega)$.

11.1.1 A Physical explanation of the RT instability

The instability condition $\rho_2 > \rho_1$ for the Rayleigh-Taylor instability can be explained simply using an energy principle. Consider two equal volumes $\mathcal{V}$, placed symmetrically with respect to the boundary surface $z = 0$ (see figure). The corresponding masses are

$$M_1 = \rho_1 \, \mathcal{V} \quad , \quad M_2 = \rho_2 \, \mathcal{V}$$

respectively for the volume located below and the volume above the boundary surface. We now perturb the boundary surface. The resulting surface wave leads to a displacement of the two masses. If these masses are a half-wavelength apart along the undulating boundary, the lower mass (M_1) is displaced upwards, and the other mass is displaced downwards by an equal amount. Note also that their z- position is almost interchanged due to the perturbation if the two masses are initially located close to the contact discontinuity at $z = 0$.

The gravitational potential energy of these masses, measured with respect to the plane $z = 0$, is simply

$$W_{\mathrm{grav}} = Mgz \; , \tag{11.1.27}$$

with g the gravitational acceleration. Before the displacement induced by the surface wave, the gravitational energy associated with both masses is almost zero, since they are located near the boundary $z = 0$. After the displacement, this energy equals

$$\begin{aligned} W^*_{\mathrm{grav}} &= M_1 g\xi - M_2 g\xi \\ &\approx g \, \mathcal{V} \, \xi \, (\rho_1 - \rho_2) \; , \end{aligned} \tag{11.1.28}$$

so that the energy change associated with this displacement is

$$\delta W = W^*_{\mathrm{grav}} \approx g \, \mathcal{V} \, \xi \, (\rho_1 - \rho_2) \; . \tag{11.1.29}$$

[3] Non-propagating because the real part of the frequency vanishes: $\mathrm{Re}(\omega) \equiv \omega_{\mathrm{r}} = 0$.

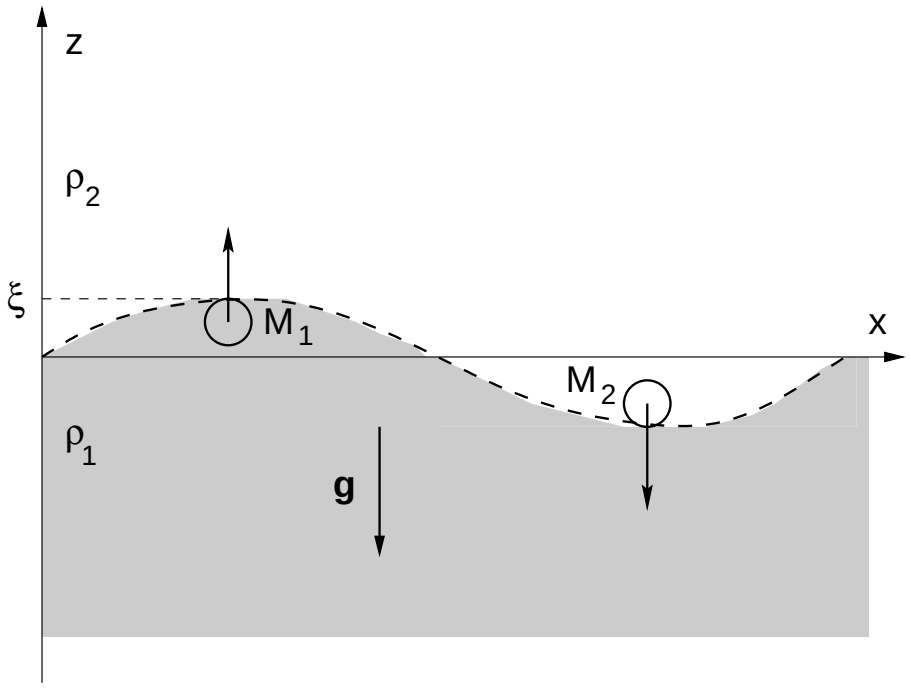

Figure 11.1: *The displacement of two equal volumes of gas located near the interface by a surface wave in the Rayleigh-Taylor instability. The two masses are a half wavelength apart, so that one moves upwards, and the other downwards by an equal amount in such a way that their z-position is almost interchanged.*

If $\rho_2 > \rho_1$ one has $\delta W < 0$: the perturbation lowers the energy of the system, and therefore the equilibrium is unstable in that case. This tells you that a heavier fluid can not be supported by a lighter fluid against gravity.

11.1.2 Astrophysical application of the RT instability

One of the most important applications of the RT instability occurs at the blast waves associated with supernova remnants. Once these waves start to decelerate because they are sweeping up material, an observer travelling with a blast wave material feels a pseudo-force in his non-inertial frame, which feels just like gravity. If the deceleration of the blast wave is $\boldsymbol{a}$ this pseudo-gravity is equal to

$$\boldsymbol{g} = -\boldsymbol{a} \ .$$

In a spherical blastwave $\boldsymbol{g}$ is directed radially outwards (away from the explosion site). If the blast wave material, which is usually of high density, runs into a less dense medium (for instance the remnant of a stellar wind of the progenitor star, the general insterstellar medium or amolecular cloud), a Rayleigh-Taylor instability could occur at the interface (contact discontinuity) separating the blast wave material and the swept-up dense matter. Numerical simulations of supernova explosions have confirmed this expectation.

11.2 The Kelvin-Helmholz instability

We now consider the instability of an interface separating two fluids with different velocities. The interface is located in the plane $z = 0$. The two unperturbed fluids are in pressure equilibrium,

$$P(z<0) = P(z>0) \equiv P_0 \ , \tag{11.2.30}$$

but they have a different velocity and a different density:

$$[\,\rho(z)\ ,\ \boldsymbol{V}(z)\,] = \begin{cases} [\,\rho_1\ ,\ V_1\,\hat{\boldsymbol{e}}_x\,] & \text{for } z<0; \\ \\ [\,\rho_2\ ,\ V_2\,\hat{\boldsymbol{e}}_x\,] & \text{for } z>0. \end{cases} \tag{11.2.31}$$

We neglect the effects of gravity. The equation of motion for small perturbations with displacement $\boldsymbol{\xi}$ and pressure perturbation δP reads for $z \neq 0$

$$\rho\,\frac{\mathrm{d}^2\boldsymbol{\xi}}{\mathrm{d}t^2} = -\boldsymbol{\nabla}\delta P \ . \tag{11.2.32}$$

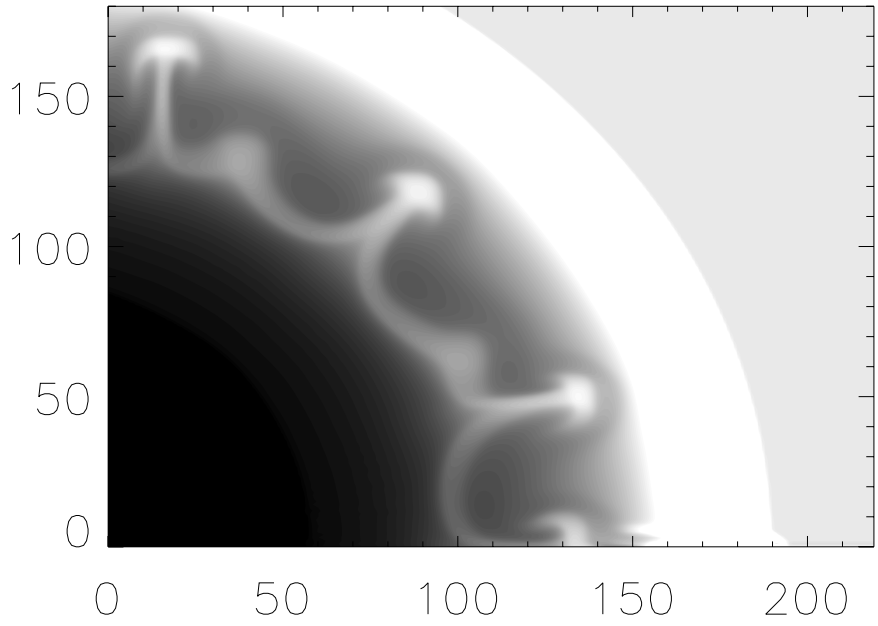

Figure 11.2: *A numerical calculation of the Raleigh-Taylor instability in the decelerating blast wave of a supernova explosion. The interface between the shocked interstellar medium and the stellar ejecta driving the blast wave is unstable to the RT instability. The blast wave is located at the outer interface with the light-gray colored unperturbed insterstellar medium. This RT instability leads to the mushroom-shaped protrusions of heavy stellar ejecta into the light swept-up material. The scale of the numerical grid is such that 1 gridpoint equals 0.01 pc, so that the radius of the blast wave is* $\sim$ *2 pc.* (Figure courtesy Eric van der Swaluw who performed the numerical simulation)

The total derivative $\mathrm{d}/\mathrm{d}t$ should be interpreted differenty on the two sides of the interface:

$$\frac{\mathrm{d}}{\mathrm{d}t} = \begin{cases} \dfrac{\partial}{\partial t} + V_1 \dfrac{\partial}{\partial x} & \text{for } z < 0; \\ \\ \dfrac{\partial}{\partial t} + V_2 \dfrac{\partial}{\partial x} & \text{for } z > 0. \end{cases} \tag{11.2.33}$$

Let us once again consider *incompressible* perturbations that satisfy

$$\boldsymbol{\nabla} \cdot \boldsymbol{\xi} = 0 \; . \tag{11.2.34}$$

Taking the divergence of the equation of motion (11.2.33), one finds that the pressure perturbation must satisfy

$$\nabla^2 \, \delta P = 0 \; , \tag{11.2.35}$$

the same equation as in the case of the Rayleigh-Taylor instability. However, in the absense of gravity the perturbed pressure is the same on both sides of the interface:

$$\delta P(z = 0^-) = \delta P(z = 0^+) \; . \tag{11.2.36}$$

Let us look at pressure perturbations of the form

$$\delta P(z) = \tilde{P}(z) \exp(ikx - i\omega t) + \mathrm{cc}, \tag{11.2.37}$$

where without loss of generality we may assume $k > 0$. This solves the harmonic equation (11.2.35) and satisfies the boundary condition (11.2.36), provided $\tilde{P}(z)$ has the following form:

$$\tilde{P}(z) = \begin{cases} \tilde{P}(0) \exp(kz) & \text{for } z < 0; \\ \\ \tilde{P}(0) \exp(-kz) & \text{for } z > 0. \end{cases} \tag{11.2.38}$$

Again we find a surface wave, where the pressure perturbation decays exponentially with increasing distance $|z|$ from the interface at $z = 0$. For $z < 0$ one can write $\exp(kz) = \exp(-k|z|)$, and for $z > 0$ it is obvious.

The corresponding dispacement perturbation must take the form (compare Eqn. 11.1.17)

$$\boldsymbol{\xi}(\boldsymbol{x}\ ,\ t) = \boldsymbol{a}(z)\exp\left(ikx - i\omega t\right) + \text{cc}. \tag{11.2.39}$$

Substituting this expression into the equation of motion, and using (11.2.38), one finds that the displacement and the pressure perturbations are related by[4]

$$\begin{aligned}
\rho\,\tilde{\omega}^2\,a_x(z) &= ik\tilde{P}(0)\ e^{-k|z|} \\
\rho\,\tilde{\omega}^2\,a_y(z) &= 0 \\
\rho\,\tilde{\omega}^2\,a_z(z) &= -k\left(\frac{z}{|z|}\right)\tilde{P}(0)\,e^{-k|z|}
\end{aligned} \tag{11.2.40}$$

Here the Doppler-shifted frequency $\tilde{\omega}$ is defined by

$$\tilde{\omega} = \begin{cases} \omega - kV_1 & \text{for } z < 0; \\ \\ \omega - kV_2 & \text{for } z > 0. \end{cases} \tag{11.2.41}$$

Note that we can put $a_y = 0$.

As in the case of the Rayleigh-Taylor instability, the displacement component ξ_z must be the same on both sides of the interface so that

$$a_z(z = 0^+) = a_z(z = 0^-) \equiv a_z(0)\ . \tag{11.2.42}$$

[4]Remember that the density ρ takes different values on both sides of the interface!

The pressure perturbation on both sides of the interface follows from the z-component in Eqn. (11.2.40) by taking the limit $|z| \to 0$:

$$\begin{aligned} P(z=0^-) &= \frac{\rho_1 \left(\omega - kV_1\right)^2 a_z(0)}{k} \, , \\ P(z=0^+) &= -\frac{\rho_2 \left(\omega - kV_2\right)^2 a_z(0)}{k} \, . \end{aligned} \tag{11.2.43}$$

The condition that the pressure perturbation is the same on both sides of the interface, $P(z=0^-) = P(z=0^+)$, gives the dispersion relation (solution condition) for the incompressible KH-instability:

$$\rho_1 \left(\omega - kV_1\right)^2 + \rho_2 \left(\omega - kV_2\right)^2 = 0 \, . \tag{11.2.44}$$

Writing out this condition yields a quadratic equation for ω,

$$\left(\rho_1 + \rho_2\right) \omega^2 - 2k \left(\rho_1 V_1 + \rho_2 V_2\right) \omega + k^2 \left(\rho_1 V_1^2 + \rho_2 V_2^2\right) = 0 \, . \tag{11.2.45}$$

A little algebra shows that the two solutions for the frequency are complex conjugates:

$$\boxed{\omega = k \, \frac{\rho_1 V_1 + \rho_2 V_2}{\rho_1 + \rho_2} \pm ik \, \frac{\sqrt{\rho_1 \rho_2} \, \left(V_1 - V_2\right)}{\rho_1 + \rho_2} \, .} \tag{11.2.46}$$

Note that this solution *always* has a root which is unstable (so that $\mathrm{Im}(\omega) > 0$) *regardless* the sign of $V_1 - V_2$! This means that the the interface is always unstable when $V_1 \neq V_2$. This is the so-called *Kelvin-Helmholz instability*.

Such a complex frequency means that the displacement and pressure of the unstable solution behave as

$$\delta P \;\; \text{and} \;\; \boldsymbol{\xi} \propto \cos\left(kx - \omega_{\mathrm{r}} t + \alpha\right) e^{(\sigma t - k|z|)} \, .$$

Here I define

$$\omega_{\mathrm{r}} \equiv \mathrm{Re}(\omega) = k \, \frac{\rho_1 V_1 + \rho_2 V_2}{\rho_1 + \rho_2} \;\; , \;\; \sigma = \mathrm{Im}(\omega) = k \, \frac{\sqrt{\rho_1 \rho_2} \, \left|V_1 - V_2\right|}{\rho_1 + \rho_2} \, ,$$

and introduce a phase angle α which comes from changing from a representation of the pressure perturbation and displacement in terms the complex amplitudes and their conjugate to a representation purely in terms of real quantities.

This representation of the solution shows that the waves travel along the interface with a phase velocity

$$V_{\rm ph} = \frac{\omega_{\rm r}}{k} = \frac{\rho_1 V_1 + \rho_2 V_2}{\rho_1 + \rho_2} \ . \tag{11.2.47}$$

At the same time the amplitude grows exponentially in time as $e^{\sigma t}$ and decays away from the interface as $e^{-k|z|}$. An observer travelling along the interface with velocity $V_{\rm ph}$ will see a pure exponential growth in time of all perturbations.

In practice, there are physical effects that can suppress this instability at short wavelengths, such as surface tension on the interface, or the effects of a magnetic field. We will consider the latter case in some detail later.

11.2.1 A physical picture of the KH-instability

The dispersion relation for the KH-instability can be explained in a relatively straightforward manner. Let us consider the balance of forces on a small fluid element that is centered on the interface between the fluids, seen from the point-of-view of an observer moving with velocity $V_{\rm ph}$ (see figure).

Due to a disturbance, the small region forms a 'bump' on the interface where the fluid is displaced in the z-direction by an amount ξ_z. As a result, the flow lines follow a curved trajectory with a radius of curvature R. The cross-section of the bump perpendicular to the flow is δA, with half of the cross-section in the lower fluid, and half in the upper fluid[5]. The size of the bump in the direction of the flow equals δs, so that the mass contained in the bump is

$$M = M_1 + M_2 \approx \tfrac{1}{2}(\rho_1 + \rho_2)\, \delta A\, \delta s \tag{11.2.48}$$

as long as $\delta s \ll R$. Here M_1 and M_2 are the masses of the two halves of the fluid element.

Let us consider the force acting on this fluid element. Since the flow is forced to move on a curved trajectory, there is a centrifugal force acting perpendicular to the flow, roughly in the z-direction.

[5]This simply reflects the fact that the surface wave decays with the same lengthscale, $L \sim 1/k$ on both sides of the interface.

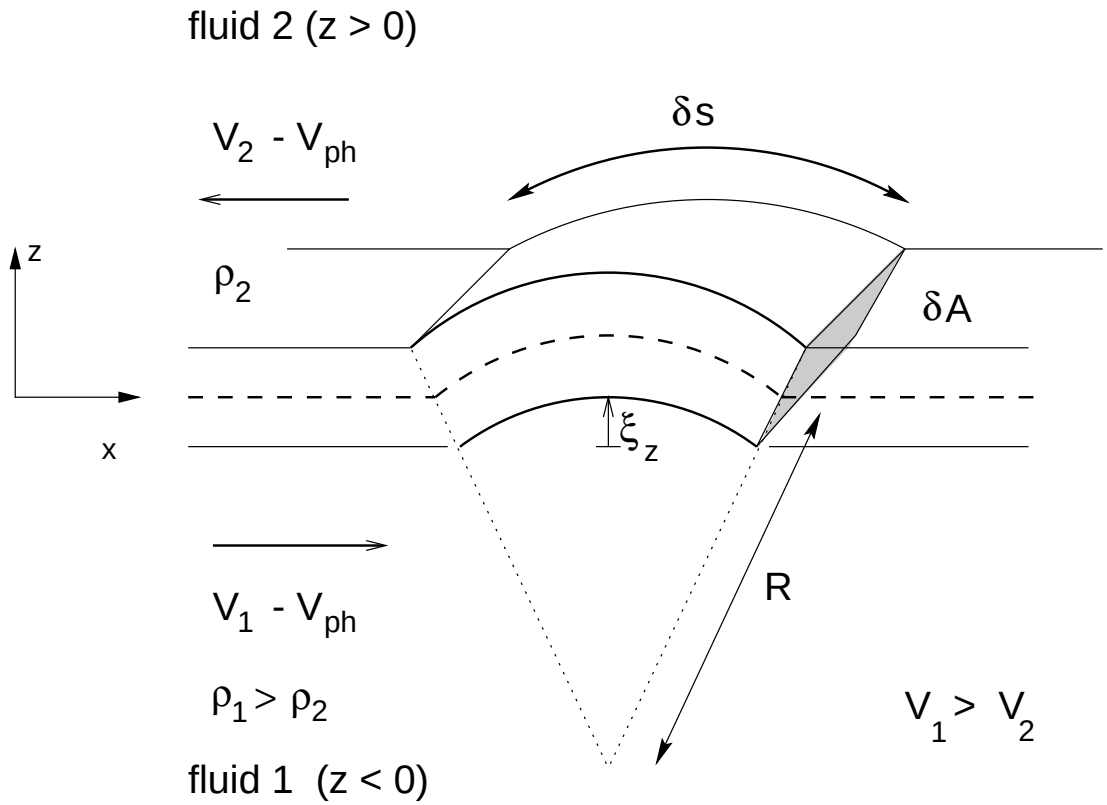

Figure 11.3: *A 'bump' on the interface between two fluids with different density and velocity on both sides. The density of the lower fluid is larger than the density of the upper fluid:* $\rho_1 > \rho_2$ *and* $V_1 > V_2$*. The bump travels at a velocity* $V_{\rm ph}$ *along the interface* $z = 0$*. As a result, the lower fluid moves from left to right, and the upper fluid in the other direction. The bump has an area* δA *perpendicular to the flow (the grey area), with half of that area in the upper, and half in the lower fluid. The radius of curvature of the flow lines equals* R*.*

This centrifugal force equals

$$F_{\rm c} = \frac{M_1\,(V_1 - V_{\rm ph})^2}{R} + \frac{M_2\,(V_2 - V_{\rm ph})^2}{R}\ . \tag{11.2.49}$$

The velocity $V_1 - V_{\rm ph}$ ($V_2 - V_{\rm ph}$) is the velocity of the lower (upper) fluid in the reference frame moving with the bump. There is no net pressure force acting on the fluid element. It is easily checked that the pressure on the lower surface is roughly equal to the pressure on the upper surface, a simple result of the continuity of the pressure across the interface.

This implies that the equation of motion for the displacement ξ_z associated with the bump reads:

$$(M_1 + M_2)\ \frac{{\rm d}^2\xi_z}{{\rm d}t^2} = \frac{M_1\,(V_1 - V_{\rm ph})^2}{R} + \frac{M_2\,(V_2 - V_{\rm ph})^2}{R} \tag{11.2.50}$$

If the amplitude of the displacement remains small, the radius of curvature is related to the displacement by

$$\frac{1}{R} = \left|\frac{\partial^2\xi_z}{\partial x^2}\right| = k^2\,\xi_z \quad \text{(assuming a plane wave)}\ .$$

Using $M_{1,2} = \frac{1}{2}\rho_{1,2}\,\delta A\,\delta s$ this yields an equation of motion of the form

$$\frac{\partial^2\xi_z}{\partial t^2} = \left(\frac{\rho_1(V_1 - V_{\rm ph})^2 + \rho_2\,(V_2 - V_{\rm ph})^2}{\rho_1 + \rho_2}\right)\ k^2\xi_z\ .$$

Substituting

$$V_{\rm ph} = \frac{\rho_1 V_1 + \rho_2 V_2}{\rho_1 + \rho_2}$$

yields after some simple algebra the final version of the equation of motion:

$$\tfrac{1}{2}(\rho_1 + \rho_2)\ \frac{\partial^2\xi_z}{\partial t^2} = \tfrac{1}{2}\,k^2\ \frac{\rho_1\rho_2\,(V_1 - V_2)^2}{(\rho_1 + \rho_2)}\,\xi_z\ . \tag{11.2.51}$$

This equation has an exponentially growing solution where $\xi_z \propto e^{\sigma t}$ with a growth rate

$$\sigma = k\,\frac{\sqrt{\rho_1\rho_2}\ |V_1 - V_2|}{\rho_1 + \rho_2}\ ,$$

exactly the same result for the growth rate of the instability as in the preceding paragraph.

11.2.2 Astrophysical example of the KH instability

One of the most important applications of the KH Instability is in the physics of the jets associated with active galaxies. If a jet propagates through the tenuous intergalactic gas, the interface between the moving jet material and the stationary intergalactic gas is unstable against the KH Instability. As a result, this interface starts to 'ripple' which, in the non-linear regime of the instability, leads to mixing of the jet material with intergalactic gas. As a result, the jet spreads and is slowed down because it has to accelerate intergalactic gas entrained by the jet. Because the interface is now a cylindrical surface, the calculation of the KH Instability is more complicated than in the case of a planar interface considered above. Nevertheless, the conclusions are qualitatively the same. The figure below shows two numerical simulations of a propagating jet which is distrupted by the Kelvin-Helmholz instability. After some distance 'wiggles' appear in the jet, which grow and ultimately lead to rapid mixing and the spreading of jet material over a larger cross-section.

11.2.3 The KH instability in a compressible medium

The calculation of the Kelvin-Helmholz instability performed above assumes from the outset that the medium perturbations are incompressible with $\boldsymbol{\nabla} \cdot \boldsymbol{\xi} = 0$. I now consider the compressible case.

Away from the interface $z = 0$ small perturbations satisfy the equation for moving sound waves, which were derived in Chapter 6.4. If the unperturbed pressure is uniform the pressure perturbation satisfies

$$\Delta P = \delta P = -\gamma P \left(\boldsymbol{\nabla} \cdot \boldsymbol{\xi} \right) . \tag{11.2.52}$$

and the equation of motion takes the standard form

$$\rho \, \frac{\mathrm{d}^2 \boldsymbol{\xi}}{\mathrm{d}t^2} = -\boldsymbol{\nabla} \delta P \, , \tag{11.2.53}$$

with $\mathrm{d}/\mathrm{d}t$ given by Eqn. (11.2.33). With $c_{\mathrm{s}}^2 = \gamma P / \rho$ the equation of motion reads

$$\left(\frac{\partial}{\partial t} + \left(\boldsymbol{V} \cdot \boldsymbol{\nabla} \right) \right)^2 \boldsymbol{\xi} - c_{\mathrm{s}}^2 \, \boldsymbol{\nabla} \left(\boldsymbol{\nabla} \cdot \boldsymbol{\xi} \right) = 0 \, . \tag{11.2.54}$$

This is the equation for sound waves in a moving medium, see Eqn. (6.6.2).

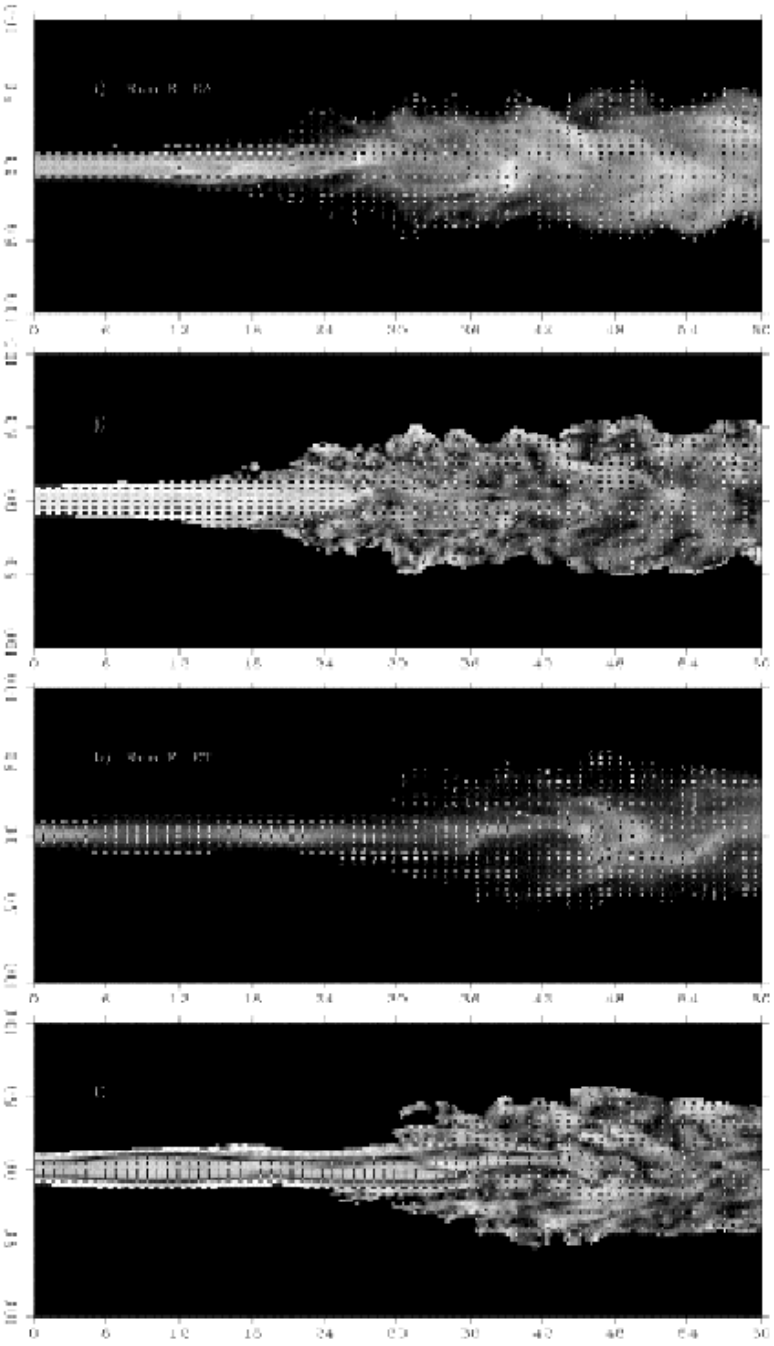

Figure 11.4: *A numerical calculation of the Kelvin-Helmholz instability in a cylindrical magnetized jet. The top two panels show a jet with the magnetic field along the axis of the jet, while the lower two panels show a jet with the magnetic field in 'loops' around the jet axis. Each set of two panels shows the synchrotron emission from the jet, taken to be proportional to the pressure, and the fractional polarization of that emission.* **From:** A. Rosen, P.E. Hardee, D.A. Clarke & A. Johnson, 1999: *Astrophys. J.* **510**, 136.

Taking the divergence of this equation yields for $z \neq 0$

$$\left(\frac{\partial}{\partial t} + (\boldsymbol{V}\cdot\boldsymbol{\nabla})\right)^2 (\boldsymbol{\nabla}\cdot\boldsymbol{\xi}) - c_{\rm s}^2\nabla^2(\boldsymbol{\nabla}\cdot\boldsymbol{\xi}) = 0\ . \tag{11.2.55}$$

Here I have used that the velocity $\boldsymbol{V}$ is constant (but different!) on both sides of the interface. Since $\delta P \propto \boldsymbol{\nabla}\cdot\boldsymbol{\xi}$ this equation can be considered as an equation for the pressure perturbation:

$$\left[\left(\frac{\partial}{\partial t} + (\boldsymbol{V}\cdot\boldsymbol{\nabla})\right)^2 - c_{\rm s}^2\,\nabla^2\right]\,\delta P = 0\ . \tag{11.2.56}$$

A pressure perturbation of the form

$$\delta P(z) = \tilde{P}(z)\exp(ikx - i\omega t) + \text{cc.} \tag{11.2.57}$$

solves Eqn. (11.2.56) provided the amplitude $\tilde{P}(z)$ satisfies the equation

$$\frac{{\rm d}^2\tilde{P}}{{\rm d}z^2} - \left(k^2 - \frac{\tilde{\omega}^2}{c_{\rm s}^2}\right)\,\tilde{P} = 0\ . \tag{11.2.58}$$

Here $\tilde{\omega} = \omega - \boldsymbol{k}\cdot\boldsymbol{V}$ is the Doppler-shifted frequency, which equals $\omega - kV_1$ for $z < 0$ and $\omega - kV_2$ for $z > 0$. The solution of this equation must once again satisfy the requirement that the pressure perturbation is the same on both sides of the interface:

$$\tilde{P}(z = 0^-) = \tilde{P}(z = 0^+) \equiv \tilde{P}(0)\ .$$

Therefore, the amplitude $\tilde{P}$ of the pressure perturbation equals

$$\tilde{P}(z) = \begin{cases} \tilde{P}(0)\exp(q_1 z) & \text{for } z < 0; \\ \\ \tilde{P}(0)\exp(-q_2 z) & \text{for } z > 0. \end{cases} \tag{11.2.59}$$

Here I have defined a quantity $q_{1,2}$ that satisfies

$$q_{1,2}^2 \equiv k^2 - \left(\frac{\tilde{\omega}^2}{c_{\rm s}^2}\right)_{1,2}\ . \tag{11.2.60}$$

This quantity generally takes different values on both sides of the interface, where both $\tilde{\omega}$ and $c_{\rm s}$ are different[6]. The effect of the compressibility is mainly that the length scale on which the surface wave decays away from the interface becomes frequency dependent, and is generally different on both sides of the interface. The earlier (incompressible) results are recovered if one takes the limit $c_{\rm s} \longrightarrow \infty$: in that case $q = k$.

The dispersion relation for the compressible KH instability again follows from the boundary conditions at the interface. We take the displacement vector to be the same as in the incompressible case:

$$\boldsymbol{\xi}(\boldsymbol{x}\ ,\ t) = \boldsymbol{a}(z)\exp\left(ikx - i\omega t\right) + \text{cc.}\ . \tag{11.2.61}$$

The $z-$ component of the equation of motion now gives the following relation between the pressure perturbation and the $z-$displacement:

$$\begin{aligned} \rho_1\left(\omega - kV_1\right)^2 a_z(z) &= q_1\,\tilde{P}(0)\,e^{q_1 z} \qquad \text{for } z < 0; \\ \rho_2\left(\omega - kV_2\right)^2 a_z(z) &= -q_2\,\tilde{P}(0)\,e^{-q_2 z} \qquad \text{for } z > 0. \end{aligned} \tag{11.2.62}$$

Taking the limit $|z| \longrightarrow 0$ on both sides of the interface, together with the condition that the $z-$displacement must be the same on both sides,

$$a_z(z = 0^+) = a_z(z = 0^-) \equiv a_z(0)\ ,$$

yields an equation for the pressure amplitude on both sides of the interface:

$$\tilde{P}(0^-) = \frac{\rho_1\left(\omega - kV_1\right)^2 a_z(0)}{q_1}\ \ ,\ \ \tilde{P}(0^+) = -\frac{\rho_2\left(\omega - kV_2\right)^2 a_z(0)}{q_2}\ . \tag{11.2.63}$$

The condition that the pressure perturbations on both sides are equal, $\tilde{P}(0^-) = \tilde{P}(0^+)$, can only be satsified if the frequency ω satisfies the dispersion relation

$$\boxed{q_2\,\rho_1\left(\omega - kV_1\right)^2 + q_1\,\rho_2\left(\omega - kV_2\right)^2 = 0\ .} \tag{11.2.64}$$

[6]The quantities $q_{1,2}$ may be complex. One must always choose $\mathrm{Re}(q_{1,2}) > 0$ so that the amplitude of the surface wave decays away from the interface at $z = 0$.

Unfortunately, this dispersion relation for the compressible version of the Kelvin-Helmholz instability can not be solved analytically in the general case. The reason is the square root in the definition (11.2.60) for $q_{1,2}$, which complicates the algebra.

Let us look at the most simple case that *can* be solved: the case where the two fluids on both sides of the interface are identical **except** that they stream in opposite directions along the x-axis,

$$P_1 = P_2 \equiv P \ , \quad \rho_1 = \rho_2 \equiv \rho \ , \quad V_1 = -V_2 \equiv V \ . \tag{11.2.65}$$

The first two relations also imply that the sound speed is the same on both sides:

$$c_{\rm s1} = c_{\rm s2} \equiv c_{\rm s} = \sqrt{\frac{\gamma P}{\rho}} \ . \tag{11.2.66}$$

In that case the dispersion relation (11.2.64) can be written as

$$(\omega - kV)^2 \ \sqrt{k^2 - \frac{(\omega + kV)^2}{c_{\rm s}^2}} \ = - \, (\omega + kV)^2 \ \sqrt{k^2 - \frac{(\omega - kV)^2}{c_{\rm s}^2}} \ . \tag{11.2.67}$$

We define the following dimensionless variables:

$$\nu = \omega / k c_{\rm s} \quad , \quad \mathcal{M} = |V| / c_{\rm s} \ , \tag{11.2.68}$$

the wave frequency in units of the sound frequency and the Mach number of the flow. The dispersion relation reads in terms of these variables

$$(\nu - \mathcal{M})^2 \sqrt{1 - (\nu + \mathcal{M})^2} = -(\nu + \mathcal{M})^2 \sqrt{1 - (\nu - \mathcal{M})^2} \ . \tag{11.2.69}$$

Squaring this equation in order to get rid of the two square roots yields (after some straightforward algebra) the following equation for ν:

$$(\nu + \mathcal{M})^4 - (\nu - \mathcal{M})^4 - 4 \mathcal{M} \nu \ \left(\nu^2 - \mathcal{M}^2 \right)^2 = 0 \ .$$

Using

$$(\nu \pm \mathcal{M})^4 = \nu^4 \pm 4 \nu^3 \mathcal{M} + 6 \nu^2 \mathcal{M}^2 \pm 4 \nu \mathcal{M}^3 + \mathcal{M}^4$$

one can write out the dispersion relation.

Because of the high symmetry in the dispersion relation many terms cancel, and one is left with

$$4\mathcal{M}\nu \left[\nu^4 - 2(\mathcal{M}^2+1)\,\nu^2 + \mathcal{M}^2\,(\mathcal{M}^2-2)\right] = 0\,. \tag{11.2.70}$$

There are two the spurious solutions[7] to this equation, $\nu = 0$ and $\mathcal{M} = 0$, which do **not** solve the original equation (11.2.69). The remaining (physical) roots are the solutions of the quadratic equation for ν^2 in the square brackets:

$$\boxed{\nu^2 = \mathcal{M}^2 + 1 \pm \sqrt{4\mathcal{M}^2+1}\,.} \tag{11.2.71}$$

There are two possible situations:

- If $\mathcal{M}^2 > 2$ both roots for ν^2 are positive, and therefore there is **no** instability. In that case the compressibility of the medium stabilizes the Kelvin-Helmholz instability, and the interface between the two fluids is stable when perturbed;
- If $\mathcal{M}^2 < 2$ one of the two roots for ν^2 (the one with the minus sign) becomes *negative*. In that case there are two purely imaginary roots for the frequency ν (i.e. $\nu = \pm i\sigma$) which differ only by a sign, so that there is always a root with $\sigma = \mathrm{Im}(\omega) > 0$. In that case the interface between the two fluids is unstable, and perturbations will grow.

We conclude the Kelvin-Helmholz instability of the interface between two identical and compressible counterstreaming fluids is suppressed if the flow speed on either side satisfies

$$|V| > \sqrt{2}\,c_{\rm s}\,.$$

The figure below shows a graphic representation of the roots of this dispersion relation. The maximum growth rate of the instability occurs for $\mathcal{M} = \frac{1}{2}\sqrt{3} \approx 0.866$ where $\mathrm{Im}(\nu)_{\rm max} = \frac{1}{2}$, which corresponds to

$$|V| = V_* \equiv \sqrt{3}c_{\rm s}/2 \quad , \quad \sigma_{\rm max} = \tfrac{1}{2}kc_{\rm s} = kV_*/\sqrt{3}\,. \tag{11.2.72}$$

[7] These spurious (unphysical) roots occur because we have squared the original equation (11.2.69), a procedure that 'loses' the minus-sign on the right-hand side of that equation. By direct substitution of $\nu = 0$ or $\mathcal{M} = 0$ it is easily checked that they do **not** solve the original (unsquared) equation (11.2.69).

In contrast, the *incompressible* version of the KH instability yields in the case of two identical counter-streaming fluids (Eqn. 11.2.46 with $\rho_1 = \rho_2 = \rho$ and $V \equiv V_1 = -V_2$) a growth rate equal to

$$\sigma_{\rm inc} = k|V|$$

for *all* streaming speeds.

The incompressible solution is in fact contained in the compressible dispersion relation (11.2.71). In the limit of a very subsonic flow, $\mathcal{M}^2 \ll 1$, one can expand the square root, using $\sqrt{1+x} \approx 1 + \frac{1}{2}x$ for $|x| \ll 1$. One finds two approximate solutions for ν^2:

$$\nu^2 \approx 2 + 3\mathcal{M}^2 \quad , \quad \nu^2 \approx -\mathcal{M}^2 \quad (\text{for } \mathcal{M}^2 \ll 1) \; .$$

The second solution contains the unstable case with $\mathrm{Im}(\nu) = \mathcal{M}$, or equivalently $\sigma = k|V|$. One must therefore conclude that the incompressible derivation is only valid for very subsonic flows with $\mathcal{M}^2 \ll 1$. From the figure below one can see that the incompressible approximation $\mathrm{Im}(\nu) = \mathcal{M}$, which corresponds to the diagonal in that figure, is a reasonable one up to $\mathcal{M} \approx 0.4$.

Even though the Kelvin-Helmholz dispersion relation can not be solved analytically in the general case, the conclusion reached in this specific example is generally valid: the interface between flows that move supersonically relative to each other is stable to small perturbations if the Mach number of the flow is sufficiently large.

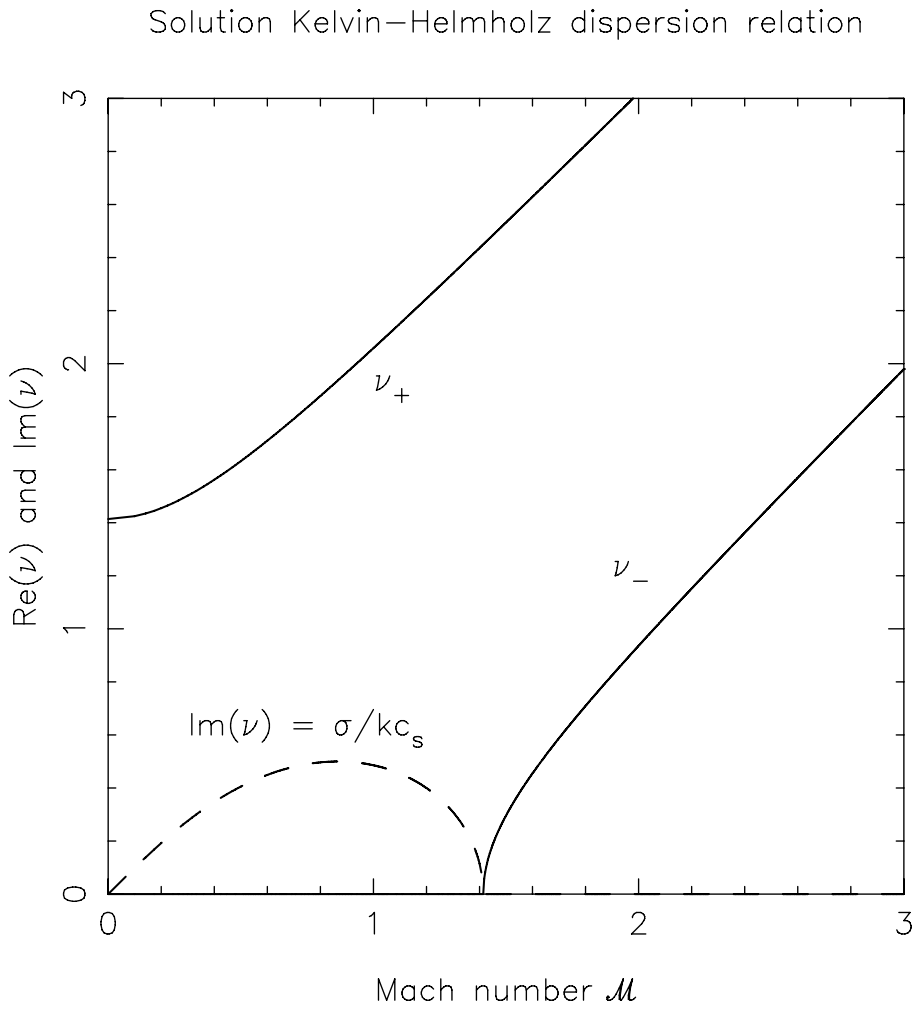

Figure 11.5: *The solution of the dispersion relation for the Kelvin-Helmholz instability in terms of the dimensionless frequency $\nu = \omega/kc_{\rm s}$ and the Mach number $\mathcal{M} = |V|/c_{\rm s}$ of the flow. The solution branch ν_+ corresponds to the plus sign in Eqn. (11.2.71). This root is always real-valued. The solution branch ν_-, which occurs for $\mathcal{M} > \sqrt{2} \sim 1.414$, is the real-valued solution corresponding to the minus sign in Eqn. (11.2.71). The dashed line corresponds to the purely imaginary root with $\sigma = {\rm Im}(\omega) > 0$ which occurs for the minus sign in (11.2.71) for Mach numbers in the range $0 < \mathcal{M} < \sqrt{2}$. The dashed curve corresponds to the unstable branch. There is also a set of roots (not shown) where $\nu_\pm$ and σ are equal in magnitude, but have opposite sign so they are all negative. The solution with ${\rm Im}(\omega) = \sigma < 0$ is damped, and therefore does* **not** *correspond to an instability.*

11.3 The Kelvin-Helmholz Instability of a cylindrical jet

One can extend calculations such as these to non-planar interfaces, such as the cylindrical interface between a jet and the intergalactic medium, or to the case where the velocity between the two fluids does not make a sudden jump, but makes a gradual transition in a boundary layer. In the latter case one finds that the instability only occurs for wavelengths $\lambda = 2\pi/k$ larger than the width of that boundary layer. Here I will consider the stability of a cylindrical jet.

A cylindrical jet has a constant radius a, with the jet axis cincides with the z-axis. The velocicity is constant in the jet, and vanishes in the medium surrounding the jet:

$$\boldsymbol{V} = \begin{cases} V\,\boldsymbol{e}_z & \text{for } R \le a; \\ \\ = 0 & \text{for } R > a. \end{cases} \tag{11.3.73}$$

Here $R = \sqrt{x^2 + y^2}$ is the cylindrical radius. There must be pressure equilibrium between the jet and the surrounding medium: $P_{\rm i} = P_{\rm e}$, where the subscripts 'i' and 'e' respectively stand for the value inside the jet, and in the surrounding (external) medium. The density inside the jet does *not* need to equal the outside density: $\rho_{\rm i} \neq \rho_{\rm e}$ in general. I will assume that the jet and the surrounding medium are both uniform: no density or pressure gradients, except for a density jump at the interface (a contact discontinuity) between the jet and the surrounding medium. I will first consider the incompressible case, where the displacement satisfies $\boldsymbol{\nabla \cdot \xi} = 0$.

In that case the pressure perturbation staisfies (see Eqn. 11.2.35)

$$\nabla^2 \delta P = \frac{1}{R}\,\frac{\partial}{\partial R}\left(R\,\frac{\partial \delta P}{\partial R}\right) + \frac{1}{R^2}\,\frac{\partial^2 \delta P}{\partial \theta^2} + \frac{\partial^2 \delta P}{\partial z^2} = 0\ . \tag{11.3.74}$$

Here I have used the Laplace operator in cylindrical coordinates[8]. A wave-like solution in cylindrical coordinates takes the form

$$\delta P = \tilde{P}(R)\exp\left(im\theta + ikz - i\omega t\right) + \text{cc}. \tag{11.3.75}$$

Here m is the *azimuthal wavenumber*. It equals the number of maxima (or minima) in δP over $\Delta\theta = 2\pi$ (i.e. a full circumference of the jet). Substituting this expression into (11.3.74) one finds that the above wave solution satisfies this equation provided that the function $\tilde{P}(R)$ is a solution of

[8] See the Mathematical Appendix on Internet

$$\frac{1}{R}\,\frac{\mathrm{d}}{\mathrm{d}R}\left(R\,\frac{\mathrm{d}\tilde{P}}{\mathrm{d}R}\right) - \left(\frac{m^2}{R^2} + k^2\right)\,\tilde{P}(R) = 0\;. \tag{11.3.76}$$

If we define the dimensionless variable

$$\varpi = kR\;, \tag{11.3.77}$$

this equation can be written as

$$\varpi^2\,\frac{\mathrm{d}^2\tilde{P}}{\mathrm{d}\varpi^2} + \varpi\,\frac{\mathrm{d}\tilde{P}}{\mathrm{d}\varpi} - \left(m^2 + \varpi^2\right)\,\tilde{P} = 0\;. \tag{11.3.78}$$

The fundamental solutions of this ordinary differential equation are the *modified Bessel functions*[9] $K_m(\varpi)$ and $I_m(\varpi)$. A number of these functions is shown in the figure below. The pressure perturbation should remain finite for $R \downarrow 0$ (the jet axis) and for $R \uparrow \infty$. The behaviour of the modified Bessel functions in these two limits dictates that one must use $I_m(\varpi)$ inside the jet, and $K_m(\varpi)$ outside the jet. Therefore we must have, using $\varpi = kR$:

$$\tilde{P}(R) = \begin{cases} A\,I_m(kR) & \text{inside the jet: } R \le a; \\ \\ B\,K_m(kR) & \text{outside the jet: } R > a. \end{cases} \tag{11.3.79}$$

Just like in the case of the KH-instability for a plane interface between the two fluids, one must demand that the pressure perturbation at the interface (located at $R = a$) is the same on both sides:

$$A\,I_m(ka) = B\,K_m(ka)\;. \tag{11.3.80}$$

This determines one of the two constants[10]:

$$B = A\,\left(\frac{I_m(ka)}{K_m(ka)}\right)\;. \tag{11.3.81}$$

[9] See for instance: Arfken & Weber, *Mathematical Methods for Physicists*, sixth edition, Ch. 11.5, Elsevier Academic Press, 2005.

[10] Since the overal magnitude of the pressure perturbation is arbitrary (but small) only **one** constant can be determined, linking the values of the pressure inside and outside of the jet

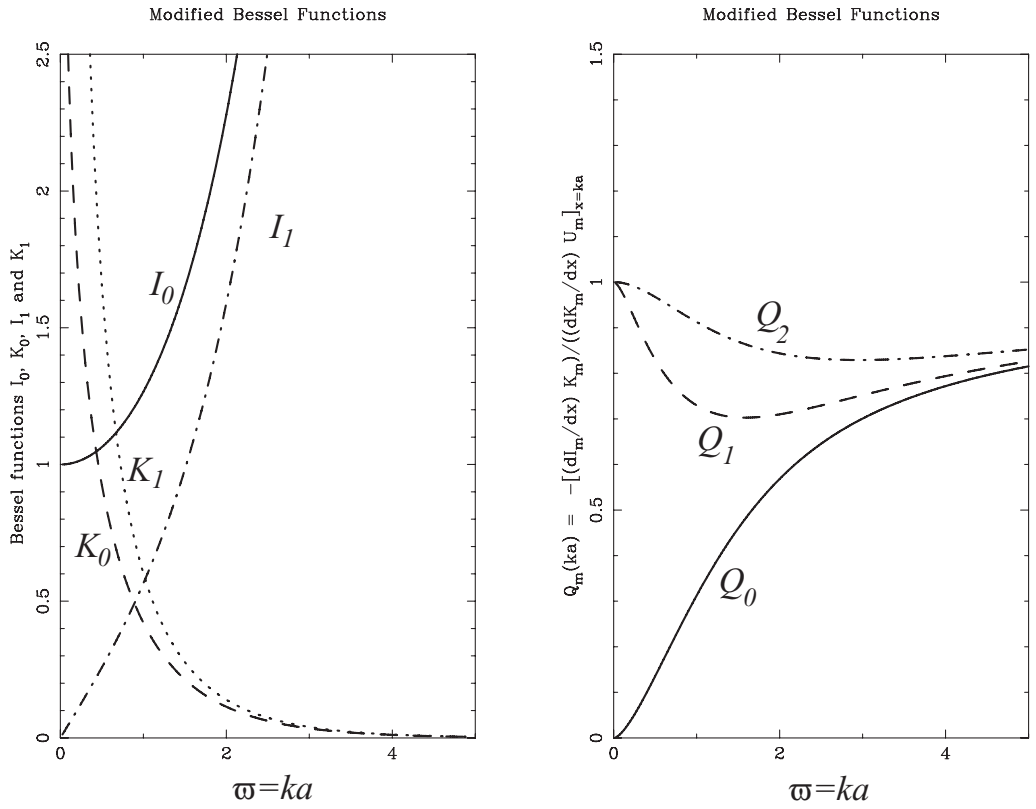

Figure 11.6: *The modified Bessel functions I_0, I_1, K_0 and K_1 as a function of $\varpi = ka$ (left panel). The right panel shows the function $Q_m(ka) = -[(\mathrm{d}I_m/\mathrm{d}\varpi)K_m(\varpi)/(\mathrm{d}K_m/\mathrm{d}\varpi)/I_m(\varpi))]_{\varpi=ka}$ which appears in the KH dispersion relation (11.3.90) for $m = 0, 1$ and 2.*

The pressure perturbation can therefore be written as:

$$\tilde{P}(R) = \begin{cases} A\, I_m(kR) & \text{inside the jet: } R \le a; \\ \\ A\, \dfrac{I_m(ka)}{K_m(ka)}\, K_m(kR) & \text{outside the jet: } R > a; \end{cases} \tag{11.3.82}$$

The second condition at the interface is that the component of $\boldsymbol{\xi}$ perpendicular to the (unperturbed) interface between jet and surroundings should be the same on both sides. If we denote the position just outside the jet by $R = a^+$, and just inside the jet by $R = a^-$, this implies:

$$\xi_R(R = a^+) = \xi_R(R = a^-)\ . \tag{11.3.83}$$

The R-component of the equation of motion,

$$\rho \left(\frac{\partial}{\partial t} + V \frac{\partial}{\partial z} \right)^2 \xi_R = -\frac{\partial \delta P}{\partial R} \tag{11.3.84}$$

with $\rho = \rho_{\rm i}$ for $R \leq a$ and $\rho = \rho_{\rm e}$, $V = 0$ for $R > a$, can be solved by

$$\xi_R = a_R(R) \exp\left(im\theta + ikz - i\omega t\right) + \text{cc}. \tag{11.3.85}$$

Substituting this into (11.3.84) and using the assumption (11.3.75) for the pressure perturbation one finds:

$$\rho \tilde{\omega}^2 a_R(R) = \frac{\partial \tilde{P}}{\partial R} \, . \tag{11.3.86}$$

Here $\tilde{\omega} = \omega - kV$ and $\rho = \rho_{\rm i}$ for $R \leq a$, while $\tilde{\omega} = \omega$ and $\rho = \rho_{\rm e}$ for $R > a$. Using (11.3.82) one finds:

$$a_R(R) = kA \times \begin{cases} \dfrac{I_m'(kR)}{\rho_{\rm i}(\omega - kV)^2} & \text{inside the jet: } R \leq a; \\ \dfrac{I_m(ka)}{K_m(ka)} \dfrac{K_m'(kR)}{\rho_{\rm e}\omega^2} & \text{outside the jet: } R > a; \end{cases} \tag{11.3.87}$$

Here $I_m'(\varpi) = {\rm d}I_m/{\rm d}\varpi$ and $K_m'(\varpi) = {\rm d}K_m/{\rm d}\varpi$ are the derivatives of the modified Bessel functions I_m and K_m.

Condition (11.3.83) implies that $a_R(a^+) = a_R(a^-)$, which is only true if the wave frequency ω satisfies the solution condition

$$\rho_{\rm i} \, (\omega - kV)^2 = \rho_{\rm e}\omega^2 \left(\frac{I_m'(\varpi) \, K_m(\varpi)}{K_m'(\varpi) \, I_m(\varpi)} \right)_{\varpi = ka} \, . \tag{11.3.88}$$

This is the dispersion relation for the incompressible Kelvin-Helmholz Instability in a cylindrical jet of radius a.

If one defines the quantity[11]

$$Q_m(\varpi) \equiv -\frac{I'_m(\varpi)\, K_m(\varpi)}{K'_m(\varpi)\, I_m(\varpi)} \geq 0 \ , \tag{11.3.89}$$

one can write the dispersion relation (11.3.88) as

$$\rho_{\rm i}\ (\omega - kV)^2 + Q_m(ka)\ \rho_{\rm e}\omega^2 = 0 \ . \tag{11.3.90}$$

The function Q_m is shown in the Figure above.

Solving this equation for the frequency ω one finds:

$$\omega = kV\ \left(\frac{\rho_{\rm i}}{\rho_{\rm i} + \rho_{\rm e}\, Q_m(ka)} \pm i\, \frac{\sqrt{\rho_{\rm i}\rho_{\rm e}\, Q_m(ka)}}{\rho_{\rm i} + \rho_{\rm e}\, Q_m(ka)} \right) \equiv \omega(k\ ,\ m) \ . \tag{11.3.91}$$

There is always an unstable solution with $\mathrm{Im}(\omega) \equiv \sigma > 0$ unless $Q_m(ka) = 0$. If we take $kV > 0$ the unstable solution branch corresponds with the $+$-sign in Eqn. (11.3.91).

We can look at two limits: that of a small jet radius and that of a large jet radius compared to the wavelength of the perturbations along the jet axis, which equals $\lambda_{\parallel} = 2\pi/k$.

Small jet radius

If we take $ka \ll 1$, we can approximate the modified Bessel functions by the leading terms of an expansion for small ϖ:

$$\begin{aligned} I_m(\varpi) &\approx \frac{\varpi^m}{2^m m!} \\ K_0(\varpi) &\approx -\ln\varpi \quad , \quad K_m(\varpi) \approx \frac{2^{m-1}(m-1)!}{\varpi^m} \ \ (\text{for } m \neq 0). \end{aligned} \tag{11.3.92}$$

[11] The modified Bessel functions $I_m(\varpi)$ and $K_m(\varpi)$ are always positive, with $I'_m(\varpi) > 0$ and $K'_m(\varpi) < 0$ for all ϖ, see the Figure above. This means that $Q_m(\varpi)$ is positive.

For the derivatives of the modified Bessel functions we can use the relations

$$2I'_m = I_{m-1} + I_{m+1} \ , \ -2K'_m = K_{m-1} + K_{m+1} \tag{11.3.93}$$

for $m \neq 0$, while for $m = 0$ one has

$$I'_0 = I_1 \ , \ K'_0 = -K_1 \ . \tag{11.3.94}$$

In the small-radius limit one finds for $m = 0$:

$$Q_0(ka \ll 1) = \frac{I_1(ka)K_0(ka)}{K_1(ka)I_0(ka)} \approx \frac{(ka)^2}{2} \ \ln\left(\frac{1}{ka}\right) \ . \tag{11.3.95}$$

For $m \neq 0$ and m positive one has:

$$Q_m(ka) \approx 1 \ . \tag{11.3.96}$$

For negative m we can use $I_{-m} = I_m$, $K_{-m} = K_m$.

Large jet radius

In the opposite limit of a large radius, $ka \gg 1$, one can use the asymptotic expansion for the modified Bessel functions[12] and their derivatives:

$$I_m(\varpi) \sim I'_m(\varpi) \sim \frac{e^{\varpi}}{\sqrt{2\pi\varpi}} \ , \ K_m(\varpi) \sim -K'_m(\varpi) \sim \sqrt{\frac{\pi}{2\varpi}} \, e^{-\varpi} \ . \tag{11.3.97}$$

This immediately implies that

$$Q_m(\varpi) \sim 1 \tag{11.3.98}$$

in this limit.

[12] e.g. Abramowitz & Stegun, *Handbook of Mathematical Functions*, p. 377, Dover Publications, 1964.

The behaviour of the growth rate $\sigma = \mathrm{Im}(\omega)$ is illustrated in the figure below. It plots the quantity

$$\frac{\sigma(k\ ,\ m)}{kV} \equiv \frac{\mathrm{Im}(\omega(k\ ,\ m))}{kV} \tag{11.3.99}$$

as a function of the quantity $ka = 2\pi a/\lambda_{\|}$ for three values of the azimuthal wavenumber m: $m = 0$, $m = 1$ and $m = 2$. The curve for $m = 0$ has a growth rate that tends to zero as $k \downarrow 0$. The other curves lie very close to the asymptotic value of the growth rate for large ka (short wavelength $\lambda_{\|}$, or a large radius a), where $Q_m(ka) \to 1$ for all values of m:

$$\sigma_\infty = \sigma(ka \to \infty\ ,\ m) = kV\ \left(\frac{\sqrt{\rho_{\mathrm{i}}\rho_{\mathrm{e}}}}{\rho_{\mathrm{i}} + \rho_{\mathrm{e}}}\right)\ . \tag{11.3.100}$$

This mirrors the behaviour of the function $Q_m(ka)$. This asymptotic value of the growth rate is the same as the growth rate of the incompressible KH Instability of a *planar* interface, as given in Eqn. (11.2.46), with $\rho_1 = \rho_{\mathrm{i}}$, $V_1 = V$, $\rho_2 = \rho_{\mathrm{e}}$ and $V_2 = 0$. In this short-wavelength limit the instability behaves as if the surface separating the jet and the surrounding medium is plane: it does not 'notice' the curvature of the cylindrical surface!

11.3.1 The compressible case

If one allows for the compressibility of the medium, the KH dispersion relation becomes more complicated. We already encountered this in the case of the KH Instability of a plane interface. There we found that, if one allows for compressibility, the equation for the pressure changes to

$$\left[\left(\frac{\partial}{\partial t} + (\boldsymbol{V}\cdot\boldsymbol{\nabla})\right)^2 - c_{\mathrm{s}}^2\,\nabla^2\right]\ \delta P = 0\ . \tag{11.3.101}$$

In cylindrical coordinates, the assumption of a plane-wave solution of the form (11.3.75) leads to an equation for the pressure amplitude of the form (compare Eqn. 11.3.76)

$$\frac{1}{R}\,\frac{\mathrm{d}}{\mathrm{d}R}\left(R\,\frac{\mathrm{d}\tilde{P}}{\mathrm{d}R}\right) - \left(\frac{m^2}{R^2} + k^2 - \frac{\tilde{\omega}^2}{c_{\mathrm{s}}^2}\right)\ \tilde{P}(R) = 0\ . \tag{11.3.102}$$

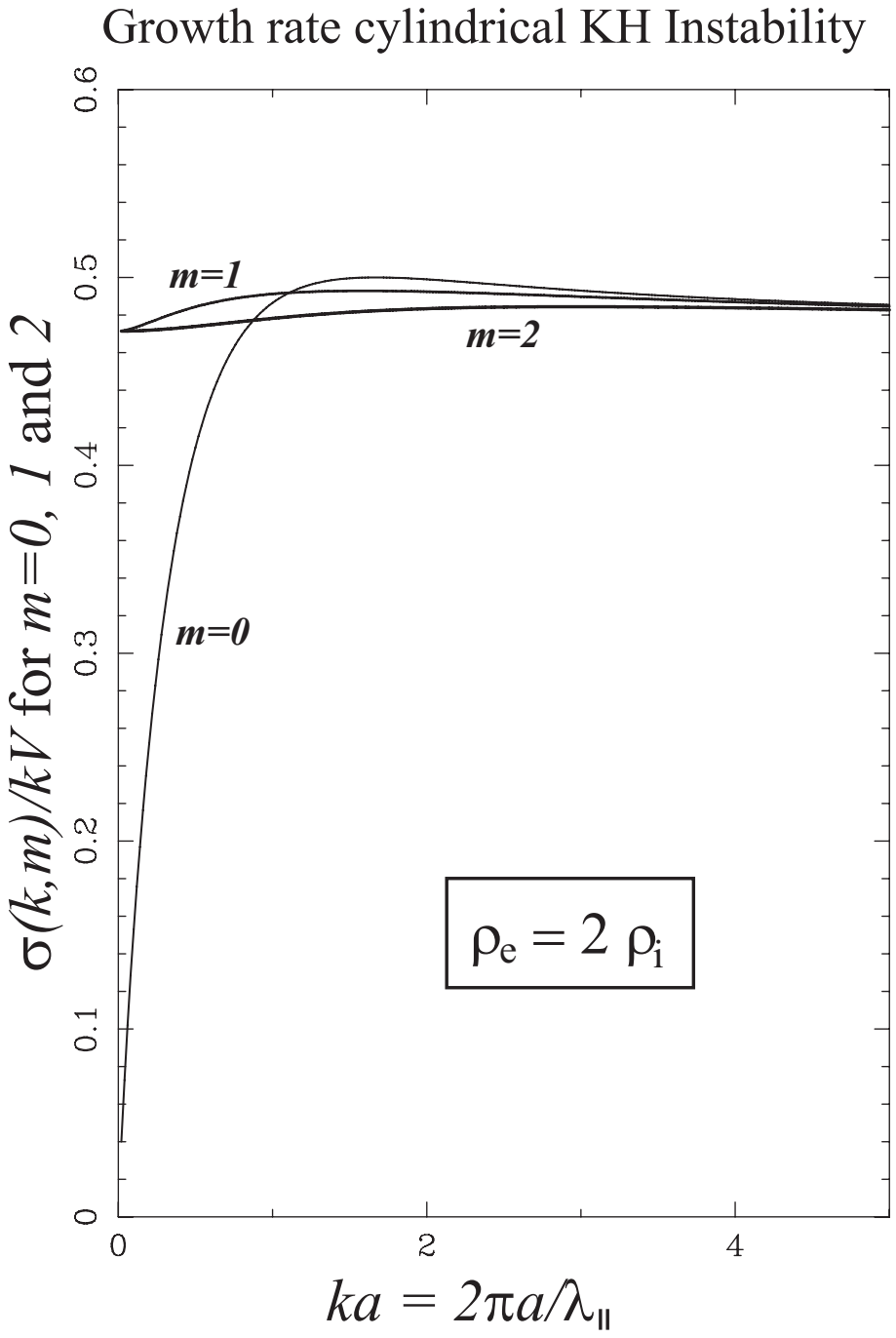

Figure 11.7: *The growth rate of the incompressible Kelvin-Helmholz Instability in a cylindrical jet with radius* a. *Shown is* $\sigma(k\ ,\ m)/kV \equiv \mathrm{Im}(\omega(k\ ,\ m))/kV$ *for* $m = 0$, $m = 1$ *and* $m = 2$, *and for* $\rho_{\rm e} = 2\rho_{\rm i}$. *For large* ka *the curves all go to the same limiting value,* $\sigma_\infty/kV = \sqrt{\rho_{\rm i}\rho_{\rm e}}/(\rho_{\rm i} + \rho_{\rm e}) = \sqrt{2}/3 \approx 0.47$.

This amounts to making the replacement

$$k^2 \implies k^2 - \frac{\tilde{\omega}^2}{c_{\rm s}^2} \equiv q^2 \tag{11.3.103}$$

everywhere, *except* in the definition of the Doppler-shifted frequency, $\tilde{\omega} = \omega - kV$, inside the jet ($\tilde{\omega} = \omega$ in the surrounding medium). Note that $c_{\rm s}$ will be different inside and outside the jet if $\rho_{\rm i} \neq \rho_{\rm e}$. Therefore, the replacement rule (11.3.103) works out differently for the medium inside the jet and for the surrounding medium: $q_{\rm i} \neq q_{\rm e}$!

If one carefully replaces k by q in the preceding derivation, one finds that the pressure perturbation amplitude now satisfies (compare Eqn. 11.3.82)

$$\tilde{P}(R) = \begin{cases} A\, I_m(q_{\rm i} R) & \text{inside the jet: } R \leq a; \\ A\, \dfrac{I_m(q_{\rm i} a)}{K_m(q_{\rm e} a)}\, K_m(q_{\rm e} R) & \text{outside the jet: } R > a; \end{cases} \tag{11.3.104}$$

where

$$q_{\rm i} = \sqrt{k^2 - \frac{(\omega - kV)^2}{c_{\rm si}^2}} \text{ and } q_{\rm e} = \sqrt{k^2 - \frac{\omega^2}{c_{\rm se}^2}}\,. \tag{11.3.105}$$

In this expression $c_{\rm si}$ ($c_{\rm se}$) is the sound speed inside (outside) the jet. Since ω is generally complex, the same holds true for $q_{\rm i}$ and $q_{\rm e}$. One must choose the roots in such a way that $\mathrm{Re}(q) > 0$.

In a similar fashion, the radial component of the displacement vector has an amplitude (compare Eqn. 11.3.87)

$$a_R(R) = \frac{1}{\rho\tilde{\omega}^2}\,\frac{\partial P}{\partial R} = A \times \begin{cases} q_{\rm i}\, \dfrac{I_m'(q_{\rm i} R)}{\rho_{\rm i}(\omega - kV)^2} & \text{inside the jet: } R \leq a; \\ q_{\rm e}\, \dfrac{I_m(q_{\rm i} a)}{K_m(q_{\rm e} a)}\, \dfrac{K_m'(q_{\rm e} R)}{\rho_{\rm e}\omega^2} & \text{outside the jet: } R > a; \end{cases} \tag{11.3.106}$$

As before, the condition that this amplitude has the same value on both sides of the cylindrical interface at $R = a$ yields the dispersion relation for the compressible version of the KH-instability of a cylindrical jet.

In this case the dispersion relation reads:

$$\rho_{\rm i}\ (\omega - kV)^2 + \bar{Q}_m(q_{\rm i}a\ ,\ q_{\rm e}a)\ \rho_{\rm e}\omega^2 = 0\ . \tag{11.3.107}$$

Here the function $\bar{Q}_m \geq 0$ is defined as

$$\bar{Q}_m(q_{\rm i}a\ ,\ q_{\rm e}a) \equiv -\frac{q_{\rm i}}{q_{\rm e}}\ \left(\frac{I'_m(q_{\rm i}a)\ K_m(q_{\rm e}a)}{K'_m(q_{\rm e}a)\ I_m(q_{\rm i}a)}\right)\ . \tag{11.3.108}$$

Like the case of a plane interface that was discussed above, the appearance of the (generally complex-valued) square roots makes an analytical solution of this dispersion relation inpractical. The incompressible case is recovered if one takes the limit $c_{\rm s} \longrightarrow \infty$: in that case $q_{\rm i} = q_{\rm e} = k$, and the dispersion relation (11.3.107) reduces to the simpler relation (11.3.90).

11.4 Stability of a self-gravitating disk

In this Section a very relevant problem for the dynamics of disk galaxies is considered: the stability of a self-gravitating, differentially rotating disk. Ultimately, the calculations in this Section will lead to *Toomre's stability criterion* for such disks, which is an important constraint on the possible properties of spiral galaxies.

Figure 11.8: *A typical example of a 'grand-design' spiral galaxy: the galaxy Messier 101 in the Virgo Cluster.* (Photo: Hubble Space Telescope, NASA/ESA)

11.4.1 A steady, axisymmetric thin disk

Consider a disk galaxy with a disk thickness $\mathcal{H} \ll R$. The stars in the galaxy are rotating around the center with velocity

$$\boldsymbol{V}_{\rm rot} = \Omega(R) R \, \hat{\boldsymbol{e}}_\theta \tag{11.4.1}$$

at a distance R from the center. There is no flow in the radial or vertical direction: $V_R = V_Z = 0$.

The stars in the disk have a velocity dispersion, taken to be isotropic, that satisfies

$$\overline{\sigma_x^2} = \overline{\sigma_y^2} = \overline{\sigma_z^2} \equiv \tilde{\sigma}^2 = \frac{k_{\rm b} T}{m_*} \ . \tag{11.4.2}$$

This is the same relation as used in our discussion of the isothermal sphere in Chapter 2: see Eqn 2.8.2. I will assume that the disk is isothermal in the vertical direction, so that $\tilde{\sigma}$ and T depend only on R. This is usually a good approximation for a real disk galaxy. The pressure associated with the gas of stars equals

$$P(R, Z) = \rho(R, Z) \, \tilde{\sigma}^2(R) \ . \tag{11.4.3}$$

We assume that the unperturbed disk is axisymmetric and steady so that

$$\frac{\partial}{\partial t} (\text{any flow quantity}) = 0 \quad , \quad \frac{\partial}{\partial \theta} (\text{any flow quantity}) = 0 \ . \tag{11.4.4}$$

The rotation law $\Omega(R)$ of the disk is determined by the balance between the pressure gradient, the centrifugal force associated with the rotation and gravity. The radial component of the equation of motion reads

$$\frac{\partial P}{\partial R} = -\rho \, \frac{\partial \Phi}{\partial R} + \rho \, \Omega^2(R) \, R \ . \tag{11.4.5}$$

The unperturbed gravitational potential $\Phi(R, Z)$ follows from Poisson's equation

$$\frac{1}{R} \frac{\partial}{\partial R} \left(R \, \frac{\partial \Phi}{\partial R} \right) + \frac{\partial^2 \Phi}{\partial Z^2} = 4 \pi G \, \rho \ . \tag{11.4.6}$$

If the disk is geometrically thin, a line of reasoning completely analogous to our discussion of thin accretion disks in Chapter 10 quickly shows that the pressure force in the radial direction is small compared with the radial component of the gravitational force:

$$\left|\frac{1}{\rho}\,\frac{\partial P}{\partial R}\right| \approx \left(\frac{\mathcal{H}}{R}\right)\,\left|\frac{\partial \Phi}{\partial R}\right| \ll \left|\frac{\partial \Phi}{\partial R}\right| \quad \text{provided } \mathcal{H} \ll R. \tag{11.4.7}$$

Let us justify this thin-disk assumption.

The thickness $\mathcal{H}$ of an vertically isothermal disk can be estimated by a simple argument. Hydrostatic equilibrium in the plane perpendicular to the disk (i.e. the Z-direction) reads

$$\frac{\partial P}{\partial Z} = \tilde{\sigma}^2(R)\,\frac{\partial \rho}{\partial Z} = -\rho \frac{\partial \Phi}{\partial Z}\,. \tag{11.4.8}$$

This equation implies that the density distribution perpendicular to the galactic plane satisfies

$$\rho(R\,,\,Z) = \rho_0(R)\,e^{-\Phi(R\,,\,Z)/\tilde{\sigma}^2(R)}\,, \tag{11.4.9}$$

with $\rho_0(R)$ the density at $Z = 0$. We assume that $\Phi(R, 0) = 0$, which is always possible *locally* at fixed R as the potential is defined up to an arbitrary constant.

We now once again exploit the assumption $\mathcal{H} \ll R$. This allows us to *approximate* Poisson's equation for the gravitational potential *locally* for given R by neglecting the term with the radial derivatives in ∇^2, writing

$$\frac{\partial^2 \Phi}{\partial Z^2} = 4\pi G\,\rho = 4\pi G\,\rho_0\,e^{-\Phi(Z)/\tilde{\sigma}^2}\,. \tag{11.4.10}$$

Note that we suppress the R-dependence of the density and the potential. The justification for this approximation is that for any smoothly varying potential $\Phi(R\,,\,Z)$ one can estimate

$$\left|\frac{\partial^2 \Phi}{\partial R^2}\right| \sim \frac{\Phi}{R^2} \quad , \quad \left|\frac{\partial^2 \Phi}{\partial Z^2}\right| \sim \frac{\Phi}{\mathcal{H}^2} \sim \left(\frac{R}{\mathcal{H}}\right)^2\,\left|\frac{\partial^2 \Phi}{\partial R^2}\right| \gg \left|\frac{\partial^2 \Phi}{\partial R^2}\right|\,. \tag{11.4.11}$$

As was done in the case of the isothermal sphere one defines a dimensionless height ξ and gravitational potential Ψ:

$$\xi = \frac{Z}{\mathcal{H}} \quad , \quad \Psi = \frac{\Phi}{\tilde{\sigma}^2} = \frac{m_* \Phi}{k_{\rm b} T} \; , \tag{11.4.12}$$

Here $\mathcal{H}(R)$ is the normalizing height at radius R:

$$\mathcal{H}(R) = \left(\frac{\tilde{\sigma}^2(R)}{4\pi G \rho_0(R)} \right)^{1/2} \; . \tag{11.4.13}$$

One can write Poisson's equation in dimensionless form, quite analogous to the dimensionless Poisson equation for the isothermal sphere in Chapter 2.8. (see Eqn. 2.8.13):

$$\boxed{\frac{{\rm d}^2\Psi}{{\rm d}\xi^2} = e^{-\Psi} \; .} \tag{11.4.14}$$

This local approximation for the density distribution perpendicular to the galactic plane is known as the *isothermal sheet model*, the planar analogue of the isothermal sphere, which served as a model for a Globular Cluster in Chapter 2.8. Equation (11.4.14) must be solved subject to the following two boundary conditions:

$$\begin{aligned} \Psi(0) &= 0 \;\; \text{(by choice)} \\ ({\rm d}\Psi/{\rm d}\xi)_{\xi=0} &= 0 \;\; \text{(gravity vanishes in the midplane at } Z = 0) \; . \end{aligned} \tag{11.4.15}$$

The second condition is a consequence of the reflection symmetry of the physical situation around the midplane. The solution for Ψ, when expressed in terms of the density using $\rho(R\,,\,Z) = \rho_0(R)\exp(-\Psi(Z))$, reads[13]

$$\rho(R\,,\,Z) = \frac{\rho_0(R)}{\cosh^2[Z/\sqrt{2}\,\mathcal{H}(R)\,]} \; . \tag{11.4.16}$$

A plot of this distribution is shown in the figure below.

[13] L. Spitzer, 1942: *Astrophys. J.* **95**, 329

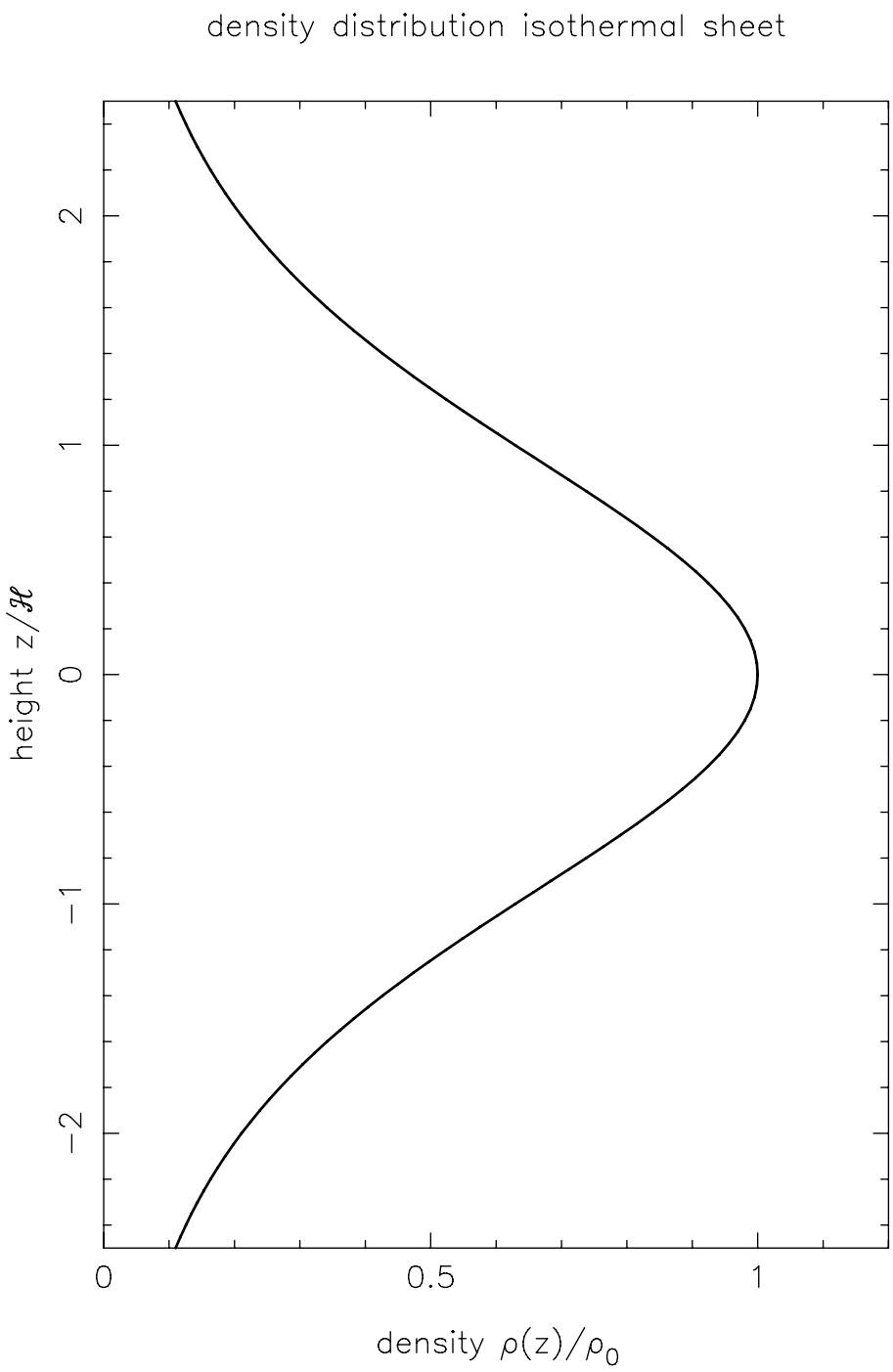

Figure 11.9: *The density distribution $\rho(Z)/\rho_0$ in an isothermal sheet plotted in terms of the dimensionless height $Z/\mathcal{H}$.*

At large distances from the mid-plane, $|Z| \gg \mathcal{H}$, one can use

$$\frac{1}{\cosh^2(Z/\sqrt{2}\,\mathcal{H})} \propto e^{-\sqrt{2}|Z|/\mathcal{H}} \; . \tag{11.4.17}$$

This shows that $\mathcal{H}(R)/\sqrt{2}$ can be considered as the density (and pressure) scale height at radius R.

As an example consider the typical values for these quantities in our own galaxy in the Solar neighbourhood, at a distance $R_\odot \sim 9\,\mathrm{kpc}$ from the Galactic center:

$$\rho_0 \sim 0.1\; M_\odot/\mathrm{pc}^3 \approx 7 \times 10^{-24}\;\mathrm{g/cm}^3 \quad , \quad \tilde{\sigma} \sim 30\;\mathrm{km/s} \approx 3 \times 10^6\;\mathrm{cm/s}\;.$$

The corresponding density scale height of the stellar disk is of order

$$\frac{\mathcal{H}}{\sqrt{2}} = \left(\frac{\tilde{\sigma}^2}{8\pi G \rho_0}\right)^{1/2} \approx 8.8 \times 10^{20}\;\mathrm{cm} \sim 280\;\mathrm{pc}\;.$$

This shows that in the Solar neighbourhood the assumption of a thin disk is a good one: $\mathcal{H}/\sqrt{2}R_\odot \approx 0.03$.

In the thin-disk approximation, one can neglect the radial pressure gradient in Eqn. (11.4.5), and solve directly for the rotation speed of the stars in the disk. This speed now only depends on the radial component of gravity:

$$\Omega(R) = \left(\frac{1}{R}\,\frac{\partial \Phi}{\partial R}\right)^{1/2} \; . \tag{11.4.18}$$

We evaluate the potential derivative $\partial\Phi/\partial R$ in the disk mid-plane $Z = 0$, neglecting the (weak) Z-dependence of the rotation speed.

This means that in a disk galaxy the radial force balance is between the outward centrifugal force due to the rotation, and the inward radial gravitational force. The most important difference between this case and the similar case of a thin accretion disk is that here the gravitational potential must be determined *self-consistently* from the mass distribution in the disk, and is not given a-priori.

11.4.2 Perturbing a self-gravitating disk

In order to investigate the stability of a thin galactic disk, we must solve the linearized equation of motion for a small perturbation $\boldsymbol{\xi}(\boldsymbol{x}\ ,\ t)$ and look for wave-like solutions ($\boldsymbol{\xi} \propto e^{-i\omega t}$). If there are solutions with $\mathrm{Im}(\omega) = \sigma > 0$ the disk is unstable.

The basic equations are

$$\begin{aligned} \frac{\partial \boldsymbol{V}}{\partial t} + (\boldsymbol{V}\cdot\boldsymbol{\nabla})\boldsymbol{V} &= -\frac{\boldsymbol{\nabla} P}{\rho} - \boldsymbol{\nabla}\Phi\ , \\ \boldsymbol{\nabla}^2\Phi &= 4\pi G\,\rho\ , \\ P(\rho) &= \tilde{\sigma}^2\,\rho\ . \end{aligned} \tag{11.4.19}$$

We now perturb the disk by displacing all fluid elements according to

$$\boldsymbol{x} \longrightarrow \overline{\boldsymbol{x}} = \boldsymbol{x} + \boldsymbol{\xi}(\boldsymbol{x}\ ,\ t)\ . \tag{11.4.20}$$

If we assume that the gas of stars behaves isothermally, the pressure and density perturbations follow from the general relations (6.4.37) and (6.4.39) derived in Chapter 6, with $\gamma = 1$ and $P = \rho\tilde{\sigma}^2$:

$$\begin{aligned} \delta\rho &= -\boldsymbol{\nabla}\cdot(\rho\boldsymbol{\xi}) \\ \delta P &= -\rho\,\tilde{\sigma}^2\,(\boldsymbol{\nabla}\cdot\boldsymbol{\xi}) - (\boldsymbol{\xi}\cdot\boldsymbol{\nabla})\left(\rho\,\tilde{\sigma}^2\right) = -\boldsymbol{\nabla}\cdot(\rho\tilde{\sigma}^2\,\boldsymbol{\xi})\ . \end{aligned} \tag{11.4.21}$$

The Eulerian velocity perturbation follows from Eqn. (6.4.12),

$$\delta\boldsymbol{V} = \frac{\partial\boldsymbol{\xi}}{\partial t} + (\boldsymbol{V}\cdot\boldsymbol{\nabla})\boldsymbol{\xi} - (\boldsymbol{\xi}\cdot\boldsymbol{\nabla})\boldsymbol{V}\ . \tag{11.4.22}$$

Writing the displacement and velocity perturbation as

$$\boldsymbol{\xi} = \xi_R\,\hat{\boldsymbol{e}}_R + \xi_\theta\,\hat{\boldsymbol{e}}_\theta + \xi_Z\,\hat{\boldsymbol{e}}_Z \quad , \quad \delta\boldsymbol{V} = u\,\hat{\boldsymbol{e}}_R + v\,\hat{\boldsymbol{e}}_\theta + w\,\hat{\boldsymbol{e}}_z\ , \tag{11.4.23}$$

a straightforward calculation gives the three components of the Eulerian velocity perturbation in terms of the components of the displacement vector:

$$
\begin{aligned}
u &= \left(\frac{\partial}{\partial t} + \Omega\,\frac{\partial}{\partial\theta}\right)\,\xi_{\rm R}\;; \\
v &= \left(\frac{\partial}{\partial t} + \Omega\,\frac{\partial}{\partial\theta}\right)\,\xi_\theta - \left(R\,\frac{{\rm d}\Omega}{{\rm d}R}\right)\,\xi_{\rm R}\;; \\
w &= \left(\frac{\partial}{\partial t} + \Omega\,\frac{\partial}{\partial\theta}\right)\,\xi_{\rm Z}\;.
\end{aligned}
\tag{11.4.24}
$$

The extra term $\propto R({\rm d}\Omega/{\rm d}R)$ in the θ-component results from the use of a curvilinear coordinate system (cylindrical polar coordinates), as explained in Chapter 8.6.4.

The Eulerian perturbation of the acceleration is (see also Chapter 6.8, Eqn. 6.8.56):

$$
\delta\left(\frac{{\rm d}\boldsymbol{V}}{{\rm d}t}\right) \equiv \delta\boldsymbol{a} = \left(\frac{\partial}{\partial t} + (\boldsymbol{V}\cdot\boldsymbol{\nabla})\right)\,\delta\boldsymbol{V} + (\delta\boldsymbol{V}\cdot\boldsymbol{\nabla})\boldsymbol{V}\;. \tag{11.4.25}
$$

Writing this expression in terms of the three components u, v and w of $\delta\boldsymbol{V}$, one finds that the acceleration perturbation $\delta\boldsymbol{a} \equiv \delta a_R\,\hat{\boldsymbol{e}}_R + \delta a_\theta\,\hat{\boldsymbol{e}}_\theta + \delta a_Z\,\hat{\boldsymbol{e}}_Z$ has the components

$$
\begin{aligned}
\delta a_R &= \left(\frac{\partial}{\partial t} + \Omega\,\frac{\partial}{\partial\theta}\right)\,u - 2\Omega\,v\;; \\
\delta a_\theta &= \left(\frac{\partial}{\partial t} + \Omega\,\frac{\partial}{\partial\theta}\right)\,v + \left(2\Omega + R\,\frac{{\rm d}\Omega}{{\rm d}R}\right)\,u\;; \\
\delta a_Z &= \left(\frac{\partial}{\partial t} + \Omega\,\frac{\partial}{\partial\theta}\right)\,w\;.
\end{aligned}
\tag{11.4.26}
$$

Substituting the expressions for the velocity components u, v and w from (11.4.24), one finds the relation between the acceleration and the components of the displacement vector:

$$\begin{aligned}
\delta a_R &= \left(\frac{\partial}{\partial t} + \Omega\,\frac{\partial}{\partial \theta}\right)^2 \xi_{\rm R} + 2\Omega R\left(\frac{{\rm d}\Omega}{{\rm d}R}\right)\,\xi_{\rm R} - 2\Omega\,\left(\frac{\partial}{\partial t} + \Omega\,\frac{\partial}{\partial \theta}\right)\,\xi_\theta\ ; \\
\delta a_\theta &= \left(\frac{\partial}{\partial t} + \Omega\,\frac{\partial}{\partial \theta}\right)^2 \xi_\theta + 2\Omega\,\left(\frac{\partial}{\partial t} + \Omega\,\frac{\partial}{\partial \theta}\right)\,\xi_{\rm R}\ ; \qquad (11.4.27) \\
\delta a_Z &= \left(\frac{\partial}{\partial t} + \Omega\,\frac{\partial}{\partial \theta}\right)^2 \xi_{\rm Z}\ .
\end{aligned}$$

This expression clearly shows the extra terms that are associated with the rotation of the disk: the two Coriolis terms $\propto 2\Omega$ in δa_R and δa_θ, *and* the term $\propto {\rm d}\Omega/{\rm d}R$ in δa_R, which is due to the fact that the disk is rotating *differentially*, and not as a solid body.

The perturbation of the right-hand side of (11.4.19) is simple to evaluate. The pressure term satisfies

$$\delta\left(-\frac{\boldsymbol{\nabla} P}{\rho}\right) = -\frac{\boldsymbol{\nabla}\delta P}{\rho} + \delta\rho\,\left(\frac{\boldsymbol{\nabla} P}{\rho^2}\right)\ . \qquad (11.4.28)$$

Substituting for δP and $\delta\rho$ from Eqn.(11.4.21) one finds:

$$\delta\left(-\frac{\boldsymbol{\nabla} P}{\rho}\right) = \tilde{\sigma}^2\,\boldsymbol{\nabla}(\boldsymbol{\nabla}\cdot\boldsymbol{\xi}) + \frac{1}{\rho}\,\left\{\boldsymbol{\nabla}[(\boldsymbol{\xi}\cdot\boldsymbol{\nabla})P\,] - [(\boldsymbol{\xi}\cdot\boldsymbol{\nabla})\rho\,]\,\left(\frac{\boldsymbol{\nabla} P}{\rho}\right)\right\}\ . \qquad (11.4.29)$$

The first term is the same term that arises in sound waves in a homogeneous medium, with an (isothermal) sound speed s, which in this case equals the velocity dispersion of the stars in the disk:

$$s^2 \equiv \frac{P}{\rho} = \tilde{\sigma}^2\ . \qquad (11.4.30)$$

The second term, the term that involves the pressure- and density gradients in the *unperturbed* disk, gives the effects of the stratification in the radial- and vertical direction. Since we will look at short-wavelength perturbations we can neglect the stratification term, and will approximate the pressure term in the equation of motion by

$$\delta\left(-\frac{\boldsymbol{\nabla}P}{\rho}\right) \approx \tilde{\sigma}^2\,\boldsymbol{\nabla}(\boldsymbol{\nabla}\cdot\boldsymbol{\xi})\;. \tag{11.4.31}$$

The self-gravity term follows straightforwardly from

$$\delta(-\boldsymbol{\nabla}\Phi) = -\boldsymbol{\nabla}\delta\Phi\;, \tag{11.4.32}$$

where $\delta\Phi$ is the solution of the perturbed Poisson equation:

$$\frac{1}{R}\,\frac{\partial}{\partial R}\,\left(R\,\frac{\partial\delta\Phi}{\partial R}\right) + \frac{1}{R^2}\,\frac{\partial^2\delta\Phi}{\partial\theta^2} + \frac{\partial^2\delta\Phi}{\partial Z^2} = 4\pi G\,\delta\rho \approx -4\pi G\rho\,(\boldsymbol{\nabla}\cdot\boldsymbol{\xi})\;. \tag{11.4.33}$$

Here I have neglected the density gradient term $\propto(\boldsymbol{\xi}\cdot\boldsymbol{\nabla})\rho$ in the density perturbation, just like I neglected similar density- and pressure gradient terms in the pressure term (11.4.31).

With these approximations one can write the equation of motion in the form

$$\begin{aligned}
\mathcal{D}_t^2\xi_R + 2\Omega\left(R\,\frac{\mathrm{d}\Omega}{\mathrm{d}R}\right)\,\xi_R - 2\Omega\,\left(\mathcal{D}_t\xi_\theta\right) &= \tilde{\sigma}^2\,\frac{\partial(\boldsymbol{\nabla}\cdot\boldsymbol{\xi})}{\partial R} - \frac{\partial\delta\Phi}{\partial R}\;;\\
\mathcal{D}_t^2\xi_\theta + 2\Omega\,\left(\mathcal{D}_t\xi_R\right) &= \frac{\tilde{\sigma}^2}{R}\,\frac{\partial(\boldsymbol{\nabla}\cdot\boldsymbol{\xi})}{\partial\theta} - \frac{1}{R}\,\frac{\partial\delta\Phi}{\partial\theta}\;;\\
\mathcal{D}_t^2\xi_Z &= \tilde{\sigma}^2\,\frac{\partial(\boldsymbol{\nabla}\cdot\boldsymbol{\xi})}{\partial Z} - \frac{\partial\delta\Phi}{\partial Z}\;.
\end{aligned} \tag{11.4.34}$$

Here I have employed the short-hand notation

$$\mathcal{D}_t \equiv \frac{\partial}{\partial t} + \Omega\,\frac{\partial}{\partial\theta}\;,$$

for the co-moving time derivative in the rotating disk.

The linearized equation of motion must be supplemented with the definition for the divergence in cylindrical coordinates,

$$\boldsymbol{\nabla} \cdot \boldsymbol{\xi} = \frac{1}{R} \frac{\partial (R\, \xi_R)}{\partial R} + \frac{1}{R} \frac{\partial \xi_\theta}{\partial \theta} + \frac{\partial \xi_z}{\partial Z} \, , \tag{11.4.35}$$

and by the linearized Poisson equation (11.4.33).

11.4.3 The self-gravitating sheet approximation

The equations as they stand are still too complicated for a simple analytical solution. The main problem is the stratification of the disk in the radial direction: both $\tilde{\sigma}(R)$ and $\Omega(R)$ are a function of the radius. Also, the density perturbation $\delta\rho$ entering Poisson's equation will depend strongly on both R and Z due to the dependence of the unperturbed density $\rho(R\, ,\, Z)$ on these quantities.

We will deal with the second complication first. If we assume that the wavelength of the perturbation is much larger than the density scale height $\sim \mathcal{H}$ in the vertical direction,

$$\lambda = 2\pi/k \gg \mathcal{H} \, , \tag{11.4.36}$$

we can expect that the disk moves 'as a whole' in the vertical direction. In that case we can 'collapse' the disk into an infinitely thin sheet with a mass surface density Σ, formally defined as

$$\Sigma(R\, , \theta\, ,\, t) = \int_{-\infty}^{+\infty} \mathrm{d}Z \; \rho(R\, ,\, \theta\, ,\, Z\, ,\, t) \, . \tag{11.4.37}$$

For the unperturbed disk the surface density follows from the isothermal sheet solution (11.4.16) as

$$\Sigma(R) = 2\sqrt{2}\mathcal{H}\, \rho_0 = \left(\frac{2\tilde{\sigma}^2(R)\, \rho_0(R)}{\pi G} \right)^{1/2} \, . \tag{11.4.38}$$

In the solar neighbourhood this equals $\Sigma \sim 10^2 \; M_\odot/\mathrm{pc}^2$. In this *sheet approximation* we are no longer able to resolve motions in the vertical direction within the disk, so one must put

$$\xi_Z = 0 \quad , \quad \partial \xi_Z / \partial Z = 0 \, . \tag{11.4.39}$$

The second equality is justified because purely vertical motions (compression) can *never* change the surface density Σ: only horizontal motions in the disk plane will change Σ. The perturbation of the surface density of the disk then equals

$$\delta\Sigma \approx -\Sigma\,(\boldsymbol{\nabla}\cdot\boldsymbol{\xi})_{\rm 2D}\ , \tag{11.4.40}$$

with the two-dimensional divergence defined as

$$(\boldsymbol{\nabla}\cdot\boldsymbol{\xi})_{\rm 2D} \equiv \frac{1}{R}\,\frac{\partial(R\,\xi_R)}{\partial R} + \frac{1}{R}\,\frac{\partial\xi_\theta}{\partial\theta}\ . \tag{11.4.41}$$

This quantity $\delta\Sigma$ (surface density perturbation) is simply the height-integrated $\delta\rho$. I will drop the subscript '2D' from this point on. As before, I neglected the effects of (radial) surface density gradients in the unperturbed disk.

In this self-gravitating sheet approximation one needs only to solve for the components of motion in the disk plane at $Z = 0$:

$$\mathcal{D}_t^2\xi_R + 2\Omega\left(R\,\frac{{\rm d}\Omega}{{\rm d}R}\right)\,\xi_R - 2\Omega\,\left(\mathcal{D}_t\xi_\theta\right) \;=\; \tilde{\sigma}^2\,\frac{\partial(\boldsymbol{\nabla}\cdot\boldsymbol{\xi})}{\partial R} - \left(\frac{\partial\delta\Phi}{\partial R}\right)_{Z=0}\ ; \tag{11.4.42}$$

$$\mathcal{D}_t^2\xi_\theta + 2\Omega\,\left(\mathcal{D}_t\xi_R\right) \;=\; \frac{\tilde{\sigma}^2}{R}\,\frac{\partial(\boldsymbol{\nabla}\cdot\boldsymbol{\xi})}{\partial\theta} - \left(\frac{1}{R}\,\frac{\partial\delta\Phi}{\partial\theta}\right)_{Z=0}\ ;$$

The solution of Poisson's equation (11.4.33) for $\delta\Phi$ needs some discussion. That equation is intrinsically three-dimensional, and must be solved in three dimensions. In the sheet-approximation one should use a density perturbation

$$\delta\rho = \delta\Sigma\,\delta(Z) \tag{11.4.43}$$

in order to relate the density perturbation to the surface density perturbation. Here $\delta(Z)$ is the Dirac delta-function.

We now make a second, important approximation. We assume that the perturbations are wave-like, $\boldsymbol{\xi} \propto e^{ik_R R}$, with a very small radial wavelength so that the radial wavenumber $k_{\rm R}$ satisfying

$$k_R R \gg 1\ . \tag{11.4.44}$$

This means that the wave fronts are separated by a distance $\Delta R = 2\pi/k_R \ll R$ in the radial direction. In that case we can neglect the curvature terms in both Poisson's equation and in the divergence $\boldsymbol{\nabla} \cdot \boldsymbol{\xi}$:

$$\left| \frac{\partial^2 \delta\Phi}{\partial R^2} \right| \gg \left| \frac{1}{R} \, \frac{\partial \delta\Phi}{\partial R} \right| \quad , \quad \left| \frac{\partial \xi_R}{\partial R} \right| \gg \left| \frac{\xi_R}{R} \right| \; . \tag{11.4.45}$$

Assuming these equalities to be satisfied, Poisson's equation for the perturbed potential becomes

$$\left(\frac{\partial^2}{\partial R^2} + \frac{1}{R^2} \, \frac{\partial^2}{\partial \theta^2} + \frac{\partial^2}{\partial Z^2} \right) \, \delta\Phi = 4\pi G \, \delta\Sigma \, \delta(Z) \; . \tag{11.4.46}$$

Let us assume a wave-like disturbance in polar coordinates:

$$\delta\Phi = \tilde{\Phi}(Z) \exp\left(i k_R R + i m \theta - i \omega t \right) + \text{cc.} \tag{11.4.47}$$

Here m must be an integer,

$$m = 0 \; , \; \pm 1 \; , \; \pm 2 \; , \cdots \; , \tag{11.4.48}$$

which ensures that a wave fits exactly m times on a circle between $\theta = 0$ and $\theta = 2\pi$. Assuming a similar form for the surface density perturbation (**without** the Z-dependence for obvious reasons),

$$\delta\Sigma = \tilde{\Sigma} \exp\left(i k_R R + i m \theta - i \omega t \right) + \text{cc.} \; , \tag{11.4.49}$$

Poisson's equation becomes in the short-wavelength approximation

$$\left(\frac{\partial^2}{\partial Z^2} - k_R^2 - \frac{m^2}{R^2} \right) \, \tilde{\Phi}(Z) = 4\pi G \, \tilde{\Sigma} \, \delta(Z) \; . \tag{11.4.50}$$

For $Z \neq 0$ the source term $\propto \tilde{\Sigma}$ vanishes, and the potential perturbation satisfies

$$\left(\frac{\partial^2}{\partial Z^2} - k_R^2 - \frac{m^2}{R^2} \right) \, \tilde{\Phi}(Z) = 0 \; . \tag{11.4.51}$$

The potential must be continuous across $Z = 0$, so the only physically admissible solution is one that decays with increasing distance from the massive sheet,

$$\tilde{\Phi}(Z) = \begin{cases} \tilde{\Phi}_0 \, e^{-kZ} & \text{for } Z > 0; \\ \\ \tilde{\Phi}_0 \, e^{+kZ} & \text{for } Z < 0. \end{cases} \tag{11.4.52}$$

Here I define the magnitude of the wave number as

$$k(R) \equiv \sqrt{k_R^2 + \frac{m^2}{R^2}} \, , \tag{11.4.53}$$

a *positive-definite* quantity.

The value of $\tilde{\Phi}_0$ follows from an integration of (11.4.50) across the sheet from $Z = 0^-$ to $Z = 0^+$. Using the properties of the Dirac delta-function one finds:

$$\left(\frac{\partial \delta\Phi}{\partial Z} \right)_{0^+} - \left(\frac{\partial \delta\Phi}{\partial Z} \right)_{0^-} = 4\pi G \, \delta\Sigma \, . \tag{11.4.54}$$

Substituting the solution for $\delta\Phi$, one gets a relation between the amplitude $\tilde{\Phi}_0$ of the potential perturbations at $Z = 0$ and the amplitude $\tilde{\Sigma}$ of the surface density perturbation:

$$-2k \, \tilde{\Phi}_0 = 4\pi G \, \tilde{\Sigma} \, . \tag{11.4.55}$$

This finally yields

$$\boxed{\tilde{\Phi}_0 = -\frac{2\pi G \, \tilde{\Sigma}}{k} \, .} \tag{11.4.56}$$

With the approximation $k_R R \gg 1$ the density perturbation is

$$\delta\Sigma \approx -\Sigma \, (\boldsymbol{\nabla} \cdot \boldsymbol{\xi}) \approx -\Sigma \left(\frac{\partial \xi_R}{\partial R} + \frac{1}{R} \, \frac{\partial \xi_\theta}{\partial \theta} \right) \, . \tag{11.4.57}$$

The displacement in the disk plane must take the form[14]

$$\begin{pmatrix} \xi_R \\ \\ \xi_\theta \end{pmatrix} = \begin{pmatrix} A_R \\ \\ A_\theta \end{pmatrix} \times \exp\left(ik_R R + im\theta - i\omega t\right) + \text{cc.} \tag{11.4.58}$$

Substituting this into the relation for $\delta\Sigma$ yields:

$$\tilde{\Sigma} = -i(\boldsymbol{k}\cdot\boldsymbol{A})\,\Sigma\;, \tag{11.4.59}$$

where

$$\boldsymbol{k}\cdot\boldsymbol{A} \equiv k_R\,A_R + \frac{m}{R}\,A_\theta\;. \tag{11.4.60}$$

Combining this with (11.4.56) one finds for the perturbation of the gravitational potential:

$$\boxed{\delta\Phi = \frac{2\pi i\,G\,\Sigma\,(\boldsymbol{k}\cdot\boldsymbol{A})}{k}\exp\left(ik_R R + im\theta - i\omega t - k\,|Z|\right) + \text{cc.}} \tag{11.4.61}$$

We are now in a position to solve the equation of motion and find the properties of the waves in the disk. Substituting (11.4.58) and (11.4.61) into the equations of motion (11.4.42) in the sheet-approximation, one finds two algebraic relations for the amplitudes A_R and A_θ:

$$\begin{aligned} \left[\tilde{\omega}^2 - 2\Omega\left(R\,\frac{\mathrm{d}\Omega}{\mathrm{d}R}\right)\right]A_R - 2i\tilde{\omega}\Omega A_\theta &= k_R\left(\tilde{\sigma}^2 - \frac{2\pi G\,\Sigma}{k}\right)(\boldsymbol{k}\cdot\boldsymbol{A})\;; \\ \tilde{\omega}^2\,A_\theta + 2i\tilde{\omega}\Omega\,A_R &= \frac{m}{R}\left(\tilde{\sigma}^2 - \frac{2\pi G\,\Sigma}{k}\right)(\boldsymbol{k}\cdot\boldsymbol{A})\;. \end{aligned} \tag{11.4.62}$$

[14] In this Section I use $\boldsymbol{A}$ rather than $\boldsymbol{a}$ for the amplitude of the displacement vector $\boldsymbol{\xi}$ in order to avoid confusion with the components of the acceleration vector that were introduced in Section 11.4.

Here $\tilde{\omega}$ is the Doppler-shifted frequency of the wave as seen by an observer co-rotating with the flow at an angular velocity Ω:

$$\tilde{\omega} \equiv \omega - m\Omega \; . \tag{11.4.63}$$

It comes from the co-moving time derivative of the wave amplitude,

$$\mathcal{D}_t \boldsymbol{\xi} = -i\tilde{\omega}\, \boldsymbol{A} \exp\left(ik_R R + im\theta - i\omega t\right) + \mathrm{cc.} \tag{11.4.64}$$

Writing out the term $\propto (\boldsymbol{k} \cdot \boldsymbol{A})$, the resulting equation can be written in matrix form as

$$\begin{pmatrix} D_{RR} & D_{R\theta} \\ \\ D_{\theta R} & D_{\theta\theta} \end{pmatrix} \begin{pmatrix} A_R \\ \\ A_\theta \end{pmatrix} = 0 \; . \tag{11.4.65}$$

The matrix components are

$$\begin{aligned} D_{RR} &= \tilde{\omega}^2 - 2\Omega \left(R \, \frac{\mathrm{d}\Omega}{\mathrm{d}R} \right) - k_R^2 \left(\tilde{\sigma}^2 - \frac{2\pi G \, \Sigma}{k} \right) \; ; \\ \\ D_{R\theta} &= -\left[k_R \frac{m}{R} \left(\tilde{\sigma}^2 - \frac{2\pi G \, \Sigma}{k} \right) + 2i\tilde{\omega}\Omega \right] \; ; \\ \\ D_{\theta R} &= -\left[k_R \frac{m}{R} \left(\tilde{\sigma}^2 - \frac{2\pi G \, \Sigma}{k} \right) - 2i\tilde{\omega}\Omega \right] \; ; \\ \\ D_{\theta\theta} &= \tilde{\omega}^2 - \frac{m^2}{R^2} \left(\tilde{\sigma}^2 - \frac{2\pi G \, \Sigma}{k} \right) \; . \end{aligned}$$

Non-trivial solutions of these algebraic equations are only possible if the determinant of the 2×2 matrix vanishes identically:

$$\det(\boldsymbol{D}) = D_{RR} \, D_{\theta\theta} - D_{R\theta} \, D_{\theta R} = 0 \; . \tag{11.4.66}$$

This yields the dispersion relation for these short-wavelength waves in a self-gravitating sheet.

After some algebra one finds that this dispersion relation can be written as:

$$\boxed{\tilde{\omega}^4 - \left[k^2\tilde{\sigma}^2 + \kappa^2 - 2\pi G\,|k|\,\Sigma\right]\,\tilde{\omega}^2 + \left(\frac{m^2}{R^2}\right)\,\left(\tilde{\sigma}^2 - \frac{2\pi G\,\Sigma}{k}\right)\,\left(2\Omega R\,\frac{\mathrm{d}\Omega}{\mathrm{d}R}\right) = 0\;.} \tag{11.4.67}$$

Here the so-called *epicyclic frequency* κ has been defined:

$$\kappa^2 = 2\Omega\,\left(2\Omega + R\,\frac{\mathrm{d}\Omega}{\mathrm{d}R}\right)\;. \tag{11.4.68}$$

This dispersion relation contains a lot of different physical effects. By looking at special (limiting) cases, we can get some insight into the most important of these effects.

- **No rotation:** $\Omega = \kappa = 0$, and $\tilde{\omega} = \omega$:

  In this case the disperion relation (11.4.67) reduces to (remember that $k \geq 0$):

  $$\omega^2\,\left[\omega^2 - \left(k^2\tilde{\sigma}^2 - 2\pi G\,k\,\Sigma\right)\right] = 0\;.$$

  Discarding the solution $\omega = 0$, the remaining solution is

  $$\omega = \pm\sqrt{k^2\tilde{\sigma}^2 - 2\pi G\,k\,\Sigma}\;.$$

  This solution becomes complex for long wavelengths when

  $$k < k_{\mathrm{J}} \equiv \frac{2\pi G\,\Sigma}{\tilde{\sigma}^2}\;.$$

  Since there is one root with $\mathrm{Im}(\omega) > 0$, this corresponds to an instability: the **Jeans Instability** for a self-gravitating sheet. Using the results for the vertical scale height and surface density of an isothermal sheet,

  $$\mathcal{H} = \frac{\tilde{\sigma}}{\sqrt{4\pi G\,\rho_0}} \quad , \quad \Sigma = 2\sqrt{2}\,\rho_0\,\mathcal{H}\;,$$

the condition for the instability can be written as

$$k < \sqrt{2}/\mathcal{H} \quad , \quad \lambda = 2\pi/|k| > \sqrt{2}\pi\,\mathcal{H}\ .$$

Perturbations with a wavelength $\lambda \gtrsim 3.5\mathcal{H}$ are unstable, and will lead to 'clumps' in the disk. In the unstable regime ($k < k_{\rm J}$) the solution for the wave frequency reads

$$\omega = ik\tilde{\sigma}\,\sqrt{\frac{k_J}{k} - 1}\ . \tag{11.4.69}$$

In the opposite limit of very short wavelengths, with $|k| \gg k_{\rm J}$, the solution of the dispersion relation gives a frequency that corresponds to a pure isothermal sound wave: $\omega \sim \pm k\tilde{\sigma}$.

- **Solid rotation:** $\mathrm{d}\Omega/\mathrm{d}R = 0$; $\kappa = 2\Omega$:

  In this case, the dispersion relation reads

$$\tilde{\omega}^2\,\left[\tilde{\omega}^2 - \left(k^2\tilde{\sigma}^2 + 4\Omega^2 - 2\pi G\,k\,\Sigma\right)\right] = 0\ .$$

  The only interesting solution is

$$\omega = m\Omega \pm \sqrt{k^2\tilde{\sigma}^2 + 4\Omega^2 - 2\pi G\,k\,\Sigma}$$

  One sees that the rotation has a *stabilizing* effect: the frequency becomes complex when

$$k^2\tilde{\sigma}^2 + 4\Omega^2 < 2\pi G\,k\,\Sigma\ .$$

  This instability condition can only be satisfied if

$$k_{\rm J} > 4\Omega/\tilde{\sigma} \qquad (\pi G\Sigma > 2\Omega\,\tilde{\sigma})\ .$$

The unstable perturbations have a value of k in the range

$$\tfrac{1}{2}k_{\rm J} - \tfrac{1}{2}\sqrt{k_{\rm J}^2 - \left(\frac{4\Omega}{\tilde{\sigma}}\right)^2} < k < \tfrac{1}{2}k_{\rm J} + \tfrac{1}{2}\sqrt{k_{\rm J}^2 - \left(\frac{4\Omega}{\tilde{\sigma}}\right)^2} \; .$$

If $k_{\rm J} < 4\Omega/\tilde{\sigma}$ (or equivalently $\pi G\Sigma < 2\Omega\,\tilde{\sigma}$) the Jeans instability disappears altogether, and rotation has stabilized the disk against the influence of self-gravity.

- **Axisymmetric perturbations:** $m = 0$, $\tilde{\omega} = \omega$ and $k = |k_R|$:

  If one puts $m = 0$ the perturbations are axisymmetric since $\partial\boldsymbol{\xi}/\partial\theta = 0$ in this case. The axisymmetric dispersion relation is almost the same as in the case of a solidly rotating disk:

$$\omega^2 \left[\omega^2 - \left(k^2\tilde{\sigma}^2 + \kappa^2 - 2\pi G\, k\, \Sigma\right)\right] = 0 \; .$$

  The effect of the differential rotation is included in the epicyclic frequency κ as defined in Eqn. (11.4.68). All the results from the previous case can be transplanted to this case by replacing 2Ω by κ. This means that the rotation again has a stabilizing effect on axisymmetric perturbations. The solution of the dispersion relation now reads

$$\boxed{\omega^2 = k^2\tilde{\sigma}^2 + \kappa^2 - 2\pi G\, k\, \Sigma \; .} \qquad (11.4.70)$$

  The first term on the right-hand side gives the effect of pressure (sound-like), the second of the (differential) rotation, and the last term of the self-gravity of the disk.

  Let us define the *Toomre wave number* [15] as

$$k_{\rm T} \equiv \frac{\kappa^2}{2\pi G\,\Sigma} \; ,$$

  and the *Toomre stability parameter* as

$$Q = \frac{\kappa\,\tilde{\sigma}}{\pi G\,\Sigma} \; .$$

[15] The quantity $k_{\rm T}$ is named after American astrophysicist A. Toomre, who was one of the first to investigate the stability of spiral galaxies: A. Toomre, 1964: *Astrophys. J.* **139**, 1217

In terms of these quantities one can write the dispersion relation for axisymmetric perturbations as

$$\left(\frac{\omega}{\kappa}\right)^2 = 1 + \frac{Q^2}{4}\left(\frac{|k_R|}{k_{\rm T}}\right)^2 - \frac{|k_R|}{k_{\rm T}} \, .$$

An instability will occur if the right-hand side of this equation becomes negative. Stable perturbations have positive ω^2. The boundary between stable and unstable solutions is located at $\omega = 0$. The condition $\omega = 0$ is satisfied at two wavenumbers,

$$\left(\frac{|k_R|}{k_{\rm T}}\right)_1 = \frac{2}{Q^2}\left(1 - \sqrt{1-Q^2}\right) \quad , \quad \left(\frac{|k_R|}{k_{\rm T}}\right)_2 = \frac{2}{Q^2}\left(1 + \sqrt{1-Q^2}\right) \, .$$

Unstable solutions with $\omega^2 < 0$ only occur if $|k_R|$ lies between these two roots, i.e.

$$\frac{2}{Q^2}\left(1 - \sqrt{1-Q^2}\right) < \frac{|k_R|}{k_{\rm T}} < \frac{2}{Q^2}\left(1 + \sqrt{1-Q^2}\right) \, .$$

The gravitational instability is completely suppressed if the condition $\omega = 0$ can not be satisfied for any real $|k_R|$. This occurs when

$$\boxed{Q = \frac{\kappa \, \tilde{\sigma}}{\pi G \, \Sigma} > 1 \, .} \qquad (11.4.71)$$

This condition is known as **Toomre's stability criterion**. If this stability criterion is not satisfied because $Q < 1$, a disk will break up into concentric rings under the influence of self-gravity: the axisymmetric gravitational 'collapse' of a disk.

The fact that the gravitational instability in a rotating disk can be stabilized is due the combined (and competing) effects of the pressure and the rotation:

- At very long wavelengths (small k) the stabilization is due to the effect of rotation. This can be seen by nearly 'switching off' the effect of pressure by taking the limit $\tilde{\sigma} \longrightarrow 0$, keeping all other parameters constant. In this limit the dispersion relation can be approximated by

$$\omega^2 = \kappa^2 - 2\pi G\, k\, \Sigma \ .$$

  The waves are **stable** if

$$k < \frac{\kappa^2}{2\pi G\, \Sigma} = k_{\rm T} \ ,$$

  corresponding to *long wavelength perturbations*.

- If we 'switch off' rotation by taking the limit $\kappa \longrightarrow 0$, we get the dispersion relation valid for a non-rotating and self-gravitating disk that was already discussed above:

$$\omega^2 = k^2\tilde{\sigma}^2 - 2\pi G\, k\, \Sigma \ .$$

  In this limit the perturbations are **stable** if

$$k > \frac{2\pi G\, \Sigma}{\tilde{\sigma}^2} \equiv k_{\rm J} \ ,$$

  corresponding to *short wavelength perturbations* (large k).

In the general case these considerations remain true: pressure stabilises perturbations at the short wavelengths, while rotation stabilises the long wavelength perturbations. If $Q < 1$ there is an intermediate region where neither one of these two stabilizing influences can stabilize the perturbations. If one considers the ratio of the two fundamental wavenumbers $k_{\rm J}$ (pressure effects) and $k_{\rm T}$ (rotation effects),

$$\frac{k_{\rm J}}{k_{\rm T}} = \left(\frac{2\pi G\, \Sigma}{\kappa\tilde{\sigma}}\right)^2 = \frac{4}{Q^2} \ ,$$

it is obvious that near $Q > 1$ (when $k_{\rm T} \gtrsim k_{\rm J}$) the stabilizing effects of pressure and of rotation can overlap sufficiently in wavenumber space so that they completely stabilize

the disk. The figure below gives the wavenumber-frequency diagram for axisymmetric waves in a self-gravitating sheet. The solutions are shown for two values of Q: $Q = 0.75$, where there are unstable waves, and $Q = 1.25$ where all waves are stable. Frequency and wavenumber are shown in terms of the non-dimensional quantities

$$\nu \equiv \omega/\kappa \quad , \quad \ell = |k_R|/k_{\rm T} \; .$$

11.4.4 Spiral density waves and the Lindblad Resonances

We now turn to the general, non-axisymmetric case (i.e. $m \neq 0$). As before I assume the limit $k_R R \gg 1$ applies to the waves under consideration. The general dispersion relation (11.4.67) in this case can be simplified. Assuming that

$$\frac{\tilde{\omega}}{\kappa} = \frac{\omega - m\Omega}{\kappa} = \mathcal{O}(1) \quad , \quad k_{\rm R} R \gg |m|$$

one can neglect the last term $\propto {\rm d}\Omega/{\rm d}R$ in the dispersion relation (11.4.67). These conditions are reasonable for not too large values of $|m|$. Using the dimensionless variables

$$\tilde{\nu} \equiv \frac{\tilde{\omega}}{\kappa} = \frac{\omega - m\Omega}{\kappa} \quad , \quad \ell = \frac{k}{k_{\rm T}} \approx \frac{|k_R|}{k_{\rm T}} \; ,$$

the resulting equation becomes

$$\tilde{\nu}^2 - 1 - \frac{Q^2}{4}\,\ell^2 + \ell = 0 \; . \tag{11.4.72}$$

If we now consider this as an equation for ℓ *given* $\tilde{\nu}$ (rather than as an equation for $\tilde{\nu}$ given ℓ as we did until this point), one finds:

$$\boxed{\ell = \frac{2}{Q^2}\,\left\{1 \pm \left[1 - Q^2\,\left(1 - \tilde{\nu}^2\right)\,\right]\right\} \; .} \tag{11.4.73}$$

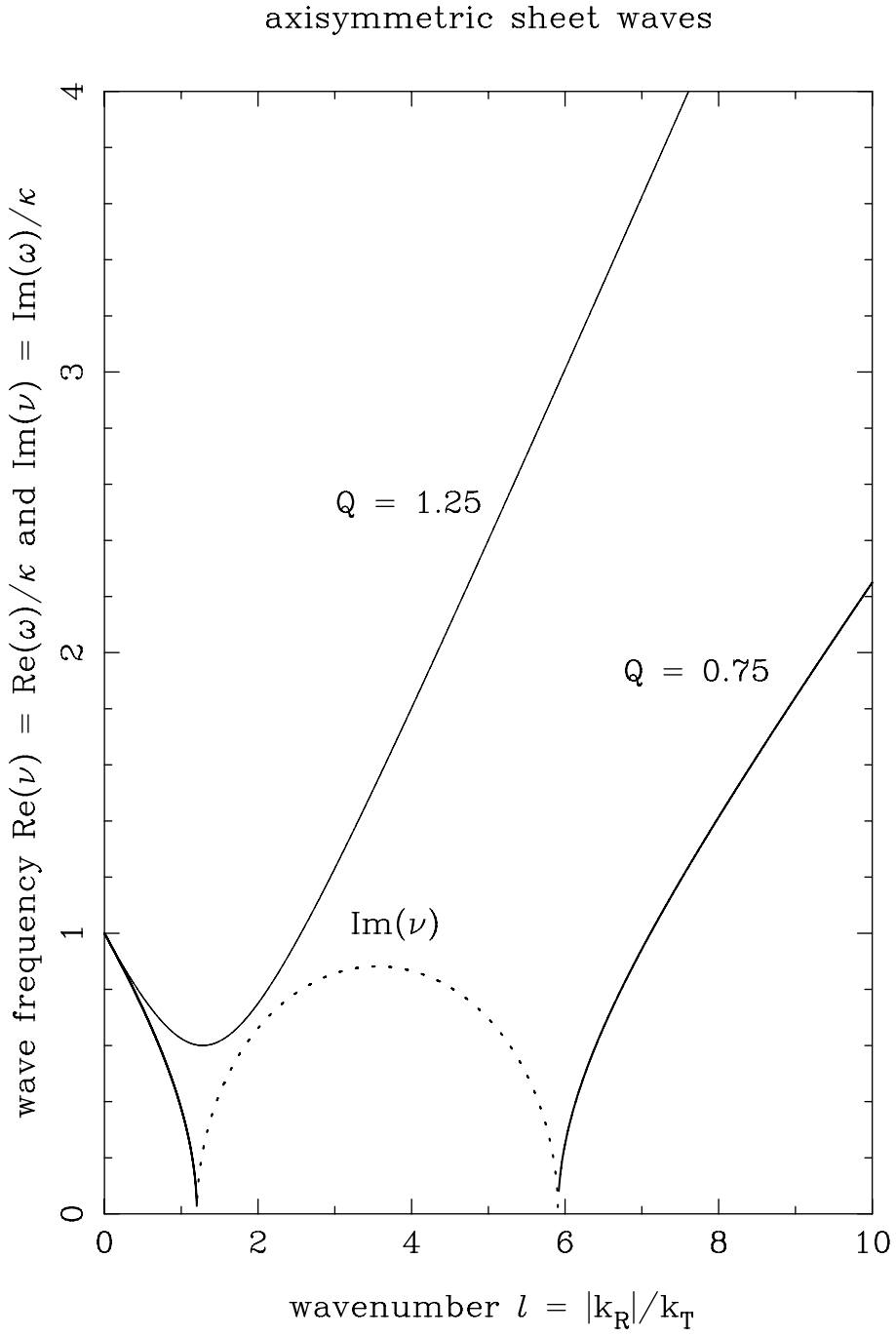

Figure 11.10: *The dimensionless wave frequency $\nu = \omega/\kappa$ as a function of the dimensionless wavenumber $\ell = |k_R|/k_{\rm T}$. The thick solid curve (stable waves), and the dotted curve (unstable waves) correspond to the case with Toomre stability parameter $Q = 0.75$. The unstable waves with purely imaginary frequency (i.e. $\mathrm{Re}(\nu) = 0$) occur in the range $1.203 \lesssim \ell \lesssim 5.907$. There the dotted curve gives the value of $\mathrm{Im}(\nu)$.*
The case $Q = 1.25$ (thin solid curve) has no unstable waves, and the frequency is purely real (i.e. $\mathrm{Im}(\nu) = 0$) for all ℓ.

Let us try to interpret the possible solutions of this equation[16]. The perturbations in surface density behave as

$$\delta\Sigma \propto \cos\left(k_{\rm R}R + m\theta - \omega t + \alpha\right) \ ,$$

with α some constant phase angle. Maxima in this potential occur when the phase S of the wave satisfies

$$S \equiv k_{\rm R}R + m\theta - \omega t + \alpha = 2\pi n \quad \text{(with } n = 0 \ , \ \pm 1 \ , \ \pm 2 \ , \cdots\text{)}, \qquad (11.4.74)$$

Let us consider this condition at some fixed time. At given radius R there are m maxima in the surface density over a full circle of circumference $2\pi R$. These maxima are separated by an angular distance

$$\Delta\theta = 2\pi/m \ .$$

Along a curve with a given value of S (including $S = 0 \ , \ 2\pi \ , \cdots$) one must have at given t

$$\mathrm{d}S = k_{\rm R} \, \mathrm{d}R + m \, \mathrm{d}\theta = 0 \ .$$

This corresponds to a curve of constant phase in the $R - \theta$ plane which follows from

$$\tan i(R) \equiv \frac{1}{R} \frac{\mathrm{d}R}{\mathrm{d}\theta} = -\frac{m}{k_R R} \ll 1 \ .$$

Here $i(R)$ is the angle of inclination between a curve of constant phase and the circle $R = \mathrm{constant}$. Because of our assumptions this angle is small, and the *radial* distance $\Delta R = 2\pi/|k_{\rm R}|$ is also small compared with R: the spirals are **densely wound**. One now distinguishes two cases:

- When $\tan i > 0$ one speaks of **leading spirals**: the radial position of a density maximum increases if θ increases;
- When $\tan i < 0$ one speaks of **trailing spirals**: the radial position of a density maximum decreases if θ increases;

The condition (11.4.74) can be solved for the angle where a maximum in the surface density can be found:

$$\theta_{\rm max}(R \ , \ t) = \frac{\omega t + 2\pi n - k_R R - \alpha}{m} \ .$$

[16] A more general discussion can be found in:
F.H. Shu, 1992: *The Physics of Astrophysics* Vol. II (Gas Dynamics), Chapter 11, University Science Books, Mill Valley CA, USA;
J. Binney & S. Tremaine, 1987: *Galactic Dynamics*, Chapters 5 and 6, Princeton University Press, Princeton, USA

For given t and n this traces out a spiral, and therefore these waves are called *spiral density waves*. Since the inclination angle satisfies $\tan i(R) \propto R^{-1}$, it decreases with increasing R. This means that the spiral pattern of density maxima becomes more and more densely wound as one moves outwards in the disk. In terms of $\tilde{\omega} = \omega - m\Omega$ one can also write

$$\theta_{\max}(R\,,\,t) = \Omega t + \frac{\tilde{\omega}t + 2\pi n - k_R R - \alpha}{m}\,.$$

This shows that the whole spiral pattern rotates with an angular frequency

$$\Omega_{\rm p} \equiv \frac{\partial \theta_{\max}}{\partial t} = \Omega + \frac{\tilde{\omega}}{m}\,.$$

One usually calls $\Omega_{\rm p}$ the **pattern speed**, even though -strictly speaking- it is a frequency. Assuming for simplicity $m > 0$ one sees that positive frequency waves (waves with $\tilde{\omega} > 0$) have a pattern speed that is larger than the local rotation rate of the matter in the disk, while negative frequency waves (i.e. waves with $\tilde{\omega} < 0$) have a pattern speed that is smaller than the matter rotation rate. Note that we make the distinction between positive and negative frequency waves in the frame corotating with the matter where the wave frequency equals $\tilde{\omega}$.

We now apply all this to the solutions of (11.4.73). The possible solutions for $\ell = k/k_{\rm T}$ can be ordered as follows, assuming without loss of generality that $m > 0$:

$$\frac{k}{k_{\rm T}} = \begin{cases} \dfrac{2}{Q^2}\left\{1 - \left[1 - Q^2\,\left(1 - \tilde{\nu}^2\right)\,\right]\right\} & \text{long trailing spiral wave} \\ \dfrac{2}{Q^2}\left\{1 + \left[1 - Q^2\,\left(1 - \tilde{\nu}^2\right)\,\right]\right\} & \text{short trailing spiral wave} \\ -\dfrac{2}{Q^2}\left\{1 - \left[1 - Q^2\,\left(1 - \tilde{\nu}^2\right)\,\right]\right\} & \text{long leading spiral wave} \\ -\dfrac{2}{Q^2}\left\{1 + \left[1 - Q^2\,\left(1 - \tilde{\nu}^2\right)\,\right]\right\} & \text{short leading spiral wave} \end{cases}.$$

Here the nomenclature 'long' and 'short' refers to the *wavelength*, and therefore corresponds to small and large wavenumbers respectively. In this ordering I have now allowed negative values for k. For the disk to be stable against axisymmetric gravitational breakup into rings we must assume that $Q > 1$.

A special case occurs at the so-called **Lindblad Resonances** where $\tilde{\nu} = \pm 1$. At that case the wavelength $\lambda = 2\pi/|k|$ of the long trailing- and leading waves becomes

infinite because $k = 0$. These resonances occur when

$$\omega - m\Omega = \pm\kappa \ .$$

Now consider a long-living spiral wave pattern as observed in disk galaxies. The pattern rotates with the patter speed $\Omega_{\rm p}$. This pattern speed will match the Lindblad resonances when

$$\Omega_{\rm p} = \Omega(R) \pm \frac{\kappa(R)}{m} \ . \tag{11.4.75}$$

In most realistic galactic disks the rotation frequency decreases with increasing radius, for instance

$$\Omega(R) \propto R^{-q} \quad \text{with } q < 2.$$

The corresponding epicyclic frequency is

$$\kappa(R) \equiv 2\Omega \left(1 + \tfrac{1}{2}\,\frac{{\rm d}\ln(\Omega)}{{\rm d}\ln(R)}\right)^{1/2} = (4-2q)^{1/2}\,\Omega(R) \ .$$

In such disks the resonance (11.4.75) with the minus-sign occurs for a given pattern speed $\Omega_{\rm p}$ at a smaller radius and is called the **inner Lindblad resonance**. The one with the plus-sign occurs at a larger radius, and is called the **outer Lindblad resonance**. If the inner Lindblad resonance occurs at $R_{\rm in}$, and the outer resonance at a radius $R_{\rm out}$, the region

$$R_{\rm in} < R < R_{\rm out}$$

in the disk plays a significant role in the theory of long spiral waves: the waves thought to be responsible for the observed spiral structure of galaxies. The fact that $|k| \to 0$ at these resonances means that these are so-called *turning points* where the wave character changes: inside the region they are able to propagate (real k), but outside they become *evanescent* as k becomes purely imaginary. We already encountered the phenomenon of evanescence in our discussion of waves in a stratified atmosphere in Chapter 6.5.

To decribe this properly, one must abandon the simple (asymptotic) analysis of waves in terms of simple plane waves, and actually solve the original differential equations with appropriate boundary conditions, taking account of the fact that the stability parameter Q, the rotational frequency Ω and the epicyclic frequency κ all depend on radius.

Intermezzo: the significance of the epicyclic frequency

In the theory of waves in a differentially rotating self-gravitating sheet the epicyclic frequency $\kappa(R)$, formally defined as

$$\kappa^2 = 2\Omega \left(2\Omega + R\,\frac{\mathrm{d}\Omega}{\mathrm{d}R}\right) ,$$

plays an important role. Its significance can be understood from the dynamics of a single 'test particle' in the gravitational field of the sheet.
Consider a star of mass m_* orbiting in the plane of the galaxy ($Z = 0$). To lowest order its orbit is circular with radius $R = R_0$ with a angular rotation frequency Ω_0 such that the centrifugal force exactly balances the radial component of gravity:

$$m_*\,\Omega_0^2 R_0 - m_*\left(\frac{\partial\Phi}{\partial R}\right)_{R_0} = 0 ,$$

which determines the rotation frequency as

$$\Omega_0 = \left(\frac{1}{R}\,\frac{\partial\Phi}{\partial R}\right)^{1/2}_{R_0}$$

This is the same rotation frequency as was assumed for the matter in the massive sheet.
We now consider the orbit wich results from a small perturbation of this circular orbit. To this end we first transform the a frame rotating with Ω_0 where the unperturbed particle is at rest. In a rotating frame, the motion of a particle can be described by (see the discussion in Chapter 8.3)

$$m_*\,\frac{\mathrm{d}\boldsymbol{V}}{\mathrm{d}t} = -2m_*\,\boldsymbol{\Omega}_0 \times \boldsymbol{V} + m_*\,\boldsymbol{g}_{\rm eff} .$$

The first term on the right-hand side is the Coriolis force, the second term is the effective gravity in the rotating frame, the combined effect of true gravity and the centrifugal force.

The effective gravity can be written in terms of an effective potential:

$$\boldsymbol{g}_{\rm eff} = -\boldsymbol{\nabla}\Phi_{\rm eff} \quad , \quad \Phi_{\rm eff} = \Phi(R\,,\,Z) - \tfrac{1}{2}\Omega_0^2 R^2 \; .$$

The rotation vector $\boldsymbol{\Omega}_0$ is defined as

$$\boldsymbol{\Omega}_0 \equiv \Omega_0\,\hat{\boldsymbol{e}}_Z \; .$$

Since we consider small deviations from a circular orbit, with an excursion in radius $|\Delta R| \equiv |R - R_0| \ll R_0$, we can expand the effective potential around $R = R_0$. Writing $\Delta R = R - R_0$ this yields

$$\begin{aligned}
\Phi_{\rm eff}(R) &\approx \Phi_{\rm eff}(R_0) + \Delta R\,\left(\frac{\partial\Phi_{\rm eff}}{\partial R}\right)_{R_0} + \tfrac{1}{2}\,\Delta R^2\,\left(\frac{\partial^2\Phi_{\rm eff}}{\partial R^2}\right)_{R_0} \\
&= \Phi_{\rm eff}(R_0) + \Delta R\,\left(\frac{\partial\Phi}{\partial R} - \Omega_0^2 R\right)_{R_0} + \tfrac{1}{2}\Delta R^2\,\left(\frac{\partial^2\Phi}{\partial R^2} - \Omega_0^2\right)_{R_0}
\end{aligned}$$

Because of our choice for Ω_0 the linear term $\propto \Delta R$ vanishes identically, and we are left with

$$\Phi_{\rm eff}(R) \approx \Phi_{\rm eff}(R_0) + \tfrac{1}{2}\Delta R^2\,\left(\frac{\partial^2\Phi}{\partial R^2} - \Omega_0^2\right)_{R_0} \; .$$

Note that $\Phi_{\rm eff}(R_0)$ and its derivatives must be treated as *constants*!. This gives the effective gravity in the radial direction at $R = R_0 + \Delta R$ as

$$(\boldsymbol{g}_{\rm eff})_R \equiv -\frac{\partial\Phi_{\rm eff}}{\partial R} = -\frac{\partial\Phi_{\rm eff}}{\partial\,(\Delta R)} = -\Delta R\,\left(\frac{\partial^2\Phi}{\partial R^2} - \Omega_0^2\right)_{R_0} \; .$$

We can now write down the equation of motion for a small displacement $\boldsymbol{\xi}$ from the unperturbed orbit. For motions in the plane of the disk we have

$$\xi_R = \Delta R = R - R_0 \quad , \quad \xi_\theta = R_0\,\Delta\theta = R_0\,\left(\theta(t) - \Omega_0 t\right) \quad , \quad \xi_Z = 0 \; ,$$

and we can use a similar notation as was used in Chapter 6 and this Chapter for the displacement associated with waves.

The velocity in the rotating frame is

$$\boldsymbol{V} = \Delta\boldsymbol{V} = \frac{\mathrm{d}\boldsymbol{\xi}}{\mathrm{d}t} \ ,$$

so the linearized equation of motion (valid for small deviations from the unperturbed orbit) becomes in component form

$$\frac{\mathrm{d}^2\xi_R}{\mathrm{d}t^2} = 2\Omega_0 \frac{\mathrm{d}\xi_\theta}{\mathrm{d}t} - \left(\frac{\partial^2\Phi}{\partial R^2} - \Omega_0^2\right)_{R_0} \xi_R \ ;$$

$$\frac{\mathrm{d}^2\xi_\theta}{\mathrm{d}t^2} = -2\Omega_0 \frac{\mathrm{d}\xi_R}{\mathrm{d}t} \ .$$

By differentiating the R-component of the equation of motion with respect to time, and substituting for the $\mathrm{d}^2\xi_\theta/\mathrm{d}t^2$ term in the resulting equation from the θ-component, one finds a single equation for ξ_R:

$$\frac{\mathrm{d}^3\xi_R}{\mathrm{d}t^3} = -\kappa^2 \frac{\mathrm{d}\xi_R}{\mathrm{d}t} \ ,$$

where the frequency κ is defined as

$$\kappa^2 \equiv 3\Omega_0^2 + \left(\frac{\partial^2\Phi}{\partial R^2}\right)_{R_0} \ .$$

This has a solution of the form

$$\xi_R(t) = a_R \cos(\kappa t + \beta) \ ,$$

with β some arbitrary phase angle set by the initial conditions at $t = 0$. If we substitute this solution for ξ_R back into the original equation for ξ_θ we find that

$$\xi_\theta(t) = -\left(\frac{2\Omega_0}{\kappa}\right) a_R \sin(\kappa t + \beta) \ .$$

The perturbed orbit as seen from the rotating frame is an *ellipse* satisfying

$$\xi_R^2 + \left(\frac{\kappa}{2\Omega_0}\right)^2 \xi_\theta^2 = a_R^2 = \text{constant} \ .$$

This motion in the disk plane is called the *epicyclic motion*, and the frequency κ of the epicyclic orbit is in fact the same frequency as at the beginning of this Intermezzo. To see this we write the relation determining Ω_0 in a general way (i.e. as a relation valid for circular orbits at *any* R):

$$\frac{\partial \Phi}{\partial R} = \Omega^2(R)\, R \; .$$

Differentiating this relationship with respect to R one has

$$\frac{\partial^2 \Phi}{\partial R^2} = \Omega^2(R) + 2\Omega(R) \left(R \, \frac{\mathrm{d}\Omega}{\mathrm{d}R} \right) \; .$$

Subsitituting this result into the above definition for κ yields

$$\kappa^2 \equiv 3\Omega_0^2 + \left(\frac{\partial^2 \Phi}{\partial R^2} \right)_{R_0} = 2\Omega_0 \left(2\Omega + R \, \frac{\mathrm{d}\Omega}{\mathrm{d}R} \right)_{R_0} \; .$$

This matches our original definition of the epicyclic frequency.

The conclusion of this Intermezzo is that the epicyclic frequency κ corresponds to the natural frequency of perturbations, small deviations from the purely circular motion of stars with an angular frequency $\Omega(R)$ in a flat disk.

If we now switch to a fluid description and add other forces, such as the oscillatory pressure forces associated with a wave, it becomes obvious that something must happen whenever these extra forces have a frequency $\tilde{\omega} = \omega - m\Omega_0$ in the rotating frame that matches the natural frequency κ of the epicyclic motion: it is like trying to drive an oscillator resonantly at its natural frequency. This is the main reason for the significance of the Lindblad Resonances in the theory of spiral density waves.

11.5 Couette Flow and the Rayleigh Criterion

In our discussion of Accretion Disks in Chapter 10 we encountered the stability criterion for a flow rotating on cylinders: the *Rayleigh Criterion*. This criterion states that a differentially rotating flow is stable provided the specific angular momentum, $\lambda(R) = \Omega(R)\, R^2$, satisfies:

$$\frac{\mathrm{d}\lambda^2}{\mathrm{d}R} > 0 \; . \tag{11.5.76}$$

It is easily checked that this condition is equivalent with:

$$\kappa^2 = 2\Omega \left(2\Omega + R \frac{\mathrm{d}\Omega}{\mathrm{d}R} \right) > 0 \; . \tag{11.5.77}$$

This relation once again shows the importance of the epicyclic frequency κ.

Consider a flow on cylinders, where $\partial/\partial t = \partial/\partial\theta = \partial/\partial Z = 0$ for all unperturbed flow quantities. Such a axisymmetric flow is called a *Couette flow*. Gravity is absent, and the density in the unperturbed flow is uniform. Small perturbations satisfy the equations of motion (compare Eqn. 11.4.34):

$$\begin{aligned} \mathcal{D}_t^2 \xi_R + 2\Omega \left(R \frac{\mathrm{d}\Omega}{\mathrm{d}R} \right) \xi_R - 2\Omega \, (\mathcal{D}_t \xi_\theta) &= -\frac{1}{\rho} \frac{\partial \delta P}{\partial R} \; ; \\ \mathcal{D}_t^2 \xi_\theta + 2\Omega \, (\mathcal{D}_t \xi_R) &= -\frac{1}{\rho R} \frac{\partial \delta P}{\partial \theta} \; , \\ \mathcal{D}_t^2 \xi_Z &= -\frac{1}{\rho} \frac{\partial \delta P}{\partial Z} \; . \end{aligned} \tag{11.5.78}$$

Here

$$\mathcal{D}_t = \frac{\partial}{\partial t} + \Omega(R) \frac{\partial}{\partial \theta} \tag{11.5.79}$$

is the total (Lagrangian) time derivative in the unperturbed flow.

In the case of *axisymmetric* perturbations, with $\partial/\partial\theta = 0$ and (consequently) with $\mathcal{D}_t = \partial/\partial t$, the second equation in (11.5.78) becomes:

$$\frac{\partial^2 \xi_\theta}{\partial t^2} + 2\Omega \frac{\partial \xi_R}{\partial t} = 0 \; . \tag{11.5.80}$$

This equation can be integrated immediately to[17]

$$\frac{\partial \xi_\theta}{\partial t} + 2\Omega\, \xi_R = 0\ . \tag{11.5.81}$$

Using this to eliminate $\partial \xi_\theta / \partial t$ from the first relation of Eqn. (11.5.78) one finds a single equation for ξ_R:

$$\frac{\partial^2 \xi_R}{\partial t^2} + \kappa^2\, \xi_R = -\frac{1}{\rho}\, \frac{\partial \delta P}{\partial R}\ . \tag{11.5.82}$$

Here I have used definition (11.4.68) of κ^2. Now let us assume that $\boldsymbol{\xi}$ behaves as:

$$\boldsymbol{\xi} = \boldsymbol{a}(R)\, \exp(ikz - i\omega t)\ . \tag{11.5.83}$$

In that case, the two remaining equation can be written as:

$$\begin{aligned} \left(\omega^2 - \kappa^2\right) \xi_R &= \frac{\partial}{\partial R}\left(\frac{\delta P}{\rho}\right)\ , \\ \omega^2\, \xi_Z &= ik\, \left(\frac{\delta P}{\rho}\right)\ . \end{aligned} \tag{11.5.84}$$

The second equation implies

$$\xi_z = \frac{ik}{\omega^2}\, \left(\frac{\delta P}{\rho}\right)\ . \tag{11.5.85}$$

We now assume that the perturbations are *incompressibe*,

$$\boldsymbol{\nabla} \cdot \boldsymbol{\xi} = \frac{1}{R}\frac{\partial}{\partial R}\, (R\xi_R) + ik\xi_Z = 0\ . \tag{11.5.86}$$

[17] The integration constant must vanish, as $\boldsymbol{\xi}$ varies sinusoidally in time, with a vanishing time-average.

If we substitute relation (11.5.85) into this condition we find:

$$\frac{1}{R}\frac{\partial}{\partial R}\left(R\xi_R\right) - \frac{k^2}{\omega^2}\left(\frac{\delta P}{\rho}\right) = 0\ . \tag{11.5.87}$$

This allows us to eliminate $\delta P/\rho$ from the first equation of (11.5.84), and we find a single equation for ξ_R:

$$\left(\omega^2 - \kappa^2\right)\xi_R = \left(\frac{\omega}{k}\right)^2 \frac{\partial}{\partial R}\left[\frac{1}{R}\frac{\partial}{\partial R}\left(R\xi_R\right)\right]\ . \tag{11.5.88}$$

If the flow is confined between two coaxial and rigid cylinders, the inner cylinder with radius R_1 and the outer cylinder with radius $R_2 > R_1$, the radial component of $\boldsymbol{\xi}$ must vanish at the cylinders:

$$\xi_R(R_1) = \xi_R(R_2) = 0\ . \tag{11.5.89}$$

One can rewrite (11.5.88) as

$$\frac{\partial}{\partial R}\left[\frac{1}{R}\frac{\partial}{\partial R}\left(R\xi_R\right)\right] = k^2\left(1 - \frac{\kappa^2(R)}{\omega^2}\right)\xi_R\ . \tag{11.5.90}$$

Multiplying this equation with $R\xi_R$, and integrating the resulting relation from $R = R_1$ to $R = R_2$, yields:

$$\begin{aligned}\int_{R_1}^{R_2} \mathrm{d}R\, R\xi_R \frac{\partial}{\partial R}\left[\frac{1}{R}\frac{\partial}{\partial R}\left(R\xi_R\right)\right] \quad &- \quad k^2\int_{R_1}^{R_2}\mathrm{d}R\, R\xi_R^2 \\ &= \quad -\frac{k^2}{\omega^2}\int_{R_1}^{R_2}\mathrm{d}R\,\kappa^2(R)R\,\xi_R^2\ .\end{aligned} \tag{11.5.91}$$

Here I have stressed that $\kappa(R)$ is a function of the cylindrical radius. By partial integration of the first term, using the two boundary conditions (11.5.89), one finds:

$$\int_{R_1}^{R_2}\mathrm{d}R\left\{\frac{1}{R}\left[\frac{\partial}{\partial R}\left(R\xi_R\right)\right]^2 + k^2 R\,\xi_R^2\right\} = \frac{k^2}{\omega^2}\int_{R_1}^{R_2}\mathrm{d}R\,\kappa^2(R)R\,\xi_R^2\ . \tag{11.5.92}$$

We can interpret this result as an equation for ω^2:

$$\frac{\omega^2}{k^2} = \frac{\int_{R_1}^{R_2} \mathrm{d}R\, \kappa^2(R) R\, \xi_R^2}{\int_{R_1}^{R_2} \mathrm{d}R \left\{ \frac{1}{R} \left[\frac{\partial}{\partial R} (R\xi_R) \right]^2 + k^2 R\, \xi_R^2 \right\}} \,. \tag{11.5.93}$$

The denominator of the term on the right-hand side is positive definite, as is k^2. That means that the sign of ω^2 is determined by the nominator:

$$\mathrm{sign}(\omega^2) = \mathrm{sign}\left(\int_{R_1}^{R_2} \mathrm{d}R\, \kappa^2(R) R\, \xi_R^2 \right) \,. \tag{11.5.94}$$

An instability occurs if $\omega^2 < 0$. It is immediately obvious that this is the case if $\kappa^2(R)$ is negative everywhere. The flow is stable if $\kappa^2(R) > 0$ everywhere, which is Rayleigh's Criterion. One can show that if κ^2 is negative *anywhere* in the flow, that there exist unstable solutions.